RESONANT OVERVOLTAGE PHENOMENA

ASSOCIATED WITH TRANSFORMER FEEDERS

Investigation of transient overvoltages produced by resonance and ferro-resonance phenomena in transformer-terminated single and double circuit feeders operating at high voltage

by

N.L. Diseko, B.Sc. (South Africa), B.Sc. (Strath.)

A Thesis submitted to the University of Strathclyde for the Degree of

Doctor of Philosophy

August 1977

Department of Electrical Engineering
University of Strathclyde
Royal College Building
204 George Street
Glasgow, G1 1XW.

A B S T R A C T

System-generated overvoltages are increasingly becoming a critical factor in determining the insulation level of the system, particularly at the higher transmission voltages. The ability to predict these overvoltages for given system conditions is therefore of paramount importance during the planning stage of a power network. This thesis is concerned mainly with excessive transient voltages generated in composite transformer feeders, particularly due to resonance.

The thesis commences with a comprehensive review of over-voltages produced in power systems (Chapter 1). Power frequency, sustained and transient overvoltages of internal and external origin are discussed, together with measures employed to protect system equipment against their effects. Factors which are critical to system insulation levels at the higher voltages are established. Chapter 2 is concerned more specifically with the modifying influence of a transformer integrally connected to the feeder on switching overvoltages. Particular consideration is given to conditions under which these overvoltages may be accentuated by resonance and ferroresonance effects. The specific aspects of these phenomena which form the basis of the research effort discussed in later Chapters, are identified.

The relative merits of available analogue and digital computer methods which can be used in the study of transients are presented in Chapter 3. The lattice diagram technique adapted for digital computation and the transient network analyser, both of which are utilised in some of the investigations, are described in more detail. Chapter 4 presents the rudiments of an efficient

digital computer method based on the compensation theorem. This method is capable of accurately simulating travelling-wave phenomena in transmission lines as well as the transient response of complex lumped and non-linear sub-networks to switching stimuli.

Single-phase results of investigations utilising the methods described commence in Chapter 5. The effects of system constants and various circuit arrangements on linear resonant energisation overvoltages in transformer feeders are assessed in Chapters 5 and 6 respectively. Conditions potentially onerous in respect of overvoltage magnitudes are identified and simple analytical techniques for their predictions are derived.

A comprehensive mathematical model of three-phase transformer feeder circuits is presented in Chapter 7. This model incorporates mutual effects between the phases of the line and both the electric and magnetic interactions within a transformer of a composite core geometry, including the non-linear saturation characteristics. The compensation method described earlier is extended to three phase circuits and applied to this model to study the effects of sequential pole closure, transformer saturation and winding connections in a resonant network (Chapter 8).

The phenomena of resonance and ferroresonance in double circuit transformer feeders following isolation of one circuit from the rest of the system are dealt with in Chapters 9 and 10, respectively. Analytical methods for predicting the occurrence of linear resonance overvoltages in a reactively compensated circuit which is being dropped, and preventive measures, are suggested in Chapter 9. The fundamental aspects of ferroresonant oscillations, their effects on system equipment and methods for their

suppression, are set out in Chapter 10. The compensation method is used to assess the effects of certain circuit constants and characteristics.

A C K N O W L E D G M E N T S

The author is deeply indebted to E.S. Fairley, B.Sc., Ph.D., ARCTST C Eng FIEE, former Professor and Chairman of the Department of Electrical Engineering, for the facilities which have made this thesis possible and for his encouragement. The author also wishes to express his indebtedness to Mr. J.T. Pender and to Dr. J.P. Bickford, formerly of the Department of Electrical Engineering, for their interest and guidance. Thanks are also due to Mr. T. Arbuckle and laboratory technicians of the department, and to the staff of the Computer Centre, for the assistance they have so readily given. Appreciation is expressed to the secretarial staff of GEC (Power Transmission Division) for typing the text, and to the author's wife, Elizabeth, who has been a constant source of encouragement throughout the preparation of this thesis.

C O N T E N T S

CHAPTER TEN : FERRORESONANCE IN E.H.V. DOUBLE CIRCUIT FEEDERS

C H A P T E R O N E

INTRODUCTION TO POWER SYSTEM OVERVOLTAGES

1.1 Introduction

As system voltage levels continue to increase, the search for a most economical compromise between the system insulation strength and overvoltage level is increasingly becoming a crucial factor in the design of transmission systems. This is particularly the case in extra high voltage (e.h.v.) systems operating at voltages in the range 230 to 765kV, and ultra high voltage (u.h.v.) systems (beyond 765kV) which are presently at an advanced stage of research. The insulation requirements of the system at these transmission voltage levels, particularly those related to the lines, form a significant proportion of the system capital costs. These requirements are set largely by the insulation strengths of the various components of the system as well as air clearances which determine:

(i) the number and size of insulators in a string,

(ii) the physical dimensions of the overhead line configuration, and

(iii) substation layout.

Technical as well as economic factors associated with an attempt to increase the system insulation strength dictate an upper physical limit beyond which the system withstand level cannot be materially influenced by increasing air clearances. The law of diminishing returns begins to apply. A reduction in the insulation level, on the other hand, is economically desirable, provided that it can be achieved without impairing system reliability or exposing expensive items of plant to risk of damage.

Any advantages arising from adopting lower levels of insulation must be measured against the associated increase in the cost of devices required to reduce system overvoltages and protect station equipment against excessive voltages. Optimisation of system insulation strength therefore relies to a great extent on an extensive knowledge of all possible sources of overvoltages, their magnitude, waveshape, frequency of occurance and means of eliminating them or minimising their effects.

Overvoltages may broadly be divided into the following categories:

(a) Transient overvoltages initiated within the system due to some operation or maloperation of system equipment such as switching or system faults, or imposed by some occurrences external to the system such as lightning.

(b) Sustained overvoltages due mainly to malfunctioning of the system and to resonance and ferroresonance phenomena.

(c) Power frequency overvoltages caused mainly by rejection of load from long lines.

Power frequency overvoltages are usually not a critical factor in co-ordinating system insulation provided that line charging requirements are adequately compensated. Overvoltages of a sustained nature are potentially hazardous to system equipment since, in most cases, they are not amenable to control by techniques normally adopted for transient surge protection. Normal practice at present is to design the system, or observe certain operating restrictions, in such a manner that these overvoltages are made consistent with system insulation strength.

The phenomena associated with transient voltage surges in transmission lines are an important consideration in the design, operation and reliability of power systems. At the lower end of transmission voltage levels (less than 230kV), overvoltages of atmospheric origin largely determine the system insulation requirements. In e.h.v. and, in particular, u.h.v. systems, however, overvoltages generated within the system (e.g. by switching and faults) are a predominant factor. These surges occur frequently in power systems and could, when superimposed on the normal power frequency voltages, produce onerous overvoltages. It is therefore essential to employ certain measures to reduce these overvoltages and provide reliable protective devices to reduce the probability of insulation breakdown and possible damage to expensive system equipment.

Generally, overvoltages will be expressed in terms of phase-to-earth (phase-to-phase) per unit overvoltage. This is defined here as the ratio of the peak phase-to-earth (phase-to-phase) overvoltage to the phase-to-earth voltage corresponding to the peak value of the source side voltage.

This chapter contains a brief survey of overvoltages in general and the next chapter will deal in particular with overvoltages occuring in transformer-terminated lines.

1.2 Power frequency overvoltages

The economic incentive to reduce the system insulation level at higher transmission voltage levels makes it necessary to give careful consideration to power frequency overvoltages. This is because the magnitude of these overvoltages can no longer be regarded as insignificant in comparison with switching overvoltages, as is the case at lower voltage levels.

Overvoltages in this category are caused mainly by loss of load and generator overspeeding in long transmission lines linking high reactance sources with busbars of large capacity. Saturation effects in transformers could further intensify these overvoltages. Energisation of series and shunt compensated lines is also a potential source of excessive power frequency oscillations.

1.2.1 Sudden loss of load

In the initial development stage of a system transmitting bulk power from remote sources (e.g. hydro-electric generating station) to a large capacity network, the system usually consists of a long untapped e.h.v. line fed from a source with a high short circuit reactance. When such a system is operated at light or no load conditions following sudden shedding of load, power frequency overvoltages may be produced. The primary cause of these overvoltages is the excessive reactive volt-amp generated on the system. [1-3] If adequate reactive compensation is provided, however, these overvoltages may be significantly reduced. In practice, total compensation of line charging capacitance is not realised and the impedance of the line is effectively capacitive at system frequency for transmission distances up to a quarter wavelength (i.e. 1500 km at 50 Hz).

When load is shed, the voltage rise at the open end of the line is caused mainly by the following factors:

(a) Ferranti effect of the line.

(b) The capacitive line charging current flowing through the inductive reactances of the generators and transformers. This creates a decreasing line voltage profile from the receiving end through the sending end of the line to the generator voltage.

This voltage rise is usually referred to as negative regulation. It persists until automatic voltage regulation on the generator units can accommodate the sudden change in reactive power. The amplitude of the rise is governed by several system variables such as:

(i) the equivalent reactances of the generators and transformer,

(ii) the transformer saturation characteristics,

(iii) the length of line,

(iv) the degree of compensation provided,

(v) the saturation properties of the shunt reactor, and

(vi) the conditions prevailing prior to loss of load.

In general, the voltage rise at both ends of the line increases proportionately as the length of line and equivalent source reactance is increased and inversely with a decrease in the degree of reactive compensation provided.

1.2.2 The effect of machine overspeeds

An additional voltage rise associated with loss of load may be produced by the increase in speed of the generator rotor. This overspeeding is caused by excess accelerating torque made available following load shedding. Such generator overexcitation

persists until the speed generator and exciter mechanism have intervened to decelerate the rotor (usually over a time interval of the order of one second). In addition to the proportional increase in generator voltage which results, (typically 40% increase in voltage behind the generator subtransient reactance for steam turbine generators) this rise in speed also increases the system frequency. As a consequence, the effectiveness of the shunt reactors in limiting the generated overvoltages by compensating reactive current is reduced. Reported investigations have shown that the voltage at the receiving end of the line could increase by up to 7% for a 5% increase in generator speed.

1.2.3 The effect of transformer saturation

The voltage rise following loss of load could be of such a magnitude as to cause saturation of the source-side transformer if the unit is operated close to the knee of its saturation characteristics. Transformers fed from sources with small short circuit capacity (as would be the case during the initial development of a hydro-electric project) are prone to such overexcitation due to the substantial negative regulation which could result. Consequently, harmonic voltages, which are superimposed on the existing power frequency overvoltages, are generated due to the non-linear characteristics of the transformer core. The magnitude of these harmonic voltages depends in part on the impedance which the line presents to the flow of harmonic currents (predominantly the third) which are present in the transformer magnetising current, and also on the extent of saturation obtaining.

1.2.4 Series compensated lines

In long e.h.v. and u.h.v. lines, series capacitors are

normally required to improve system stability and increase the capacity of the lines. Their presence reduces the inductive reactance between the source and load and hence the electrical length of the line. Depending on the location of the capacitor along the line, excessive voltages could be produced when large short circuit currents flow through the capacitor in the event of an earth fault.

Overvoltages could also be produced in series compensated lines which also contain saturable shunt compensating reactors due to ferroresonance phenomenon. When an unloaded line is energised from the source, the inrush current of the reactors sets up harmonic and sub-harmonic voltage oscillations. These ferro-oscillations are a function of the non-linear characteristics of the shunt reactor cores, the value of the series capacitor and the magnitude of the applied system voltage. A marginal increase in the applied system voltage could further intensify the resultant overvoltages.

1.2.5 Limitation of power frequency overvoltages

Conventional means of limiting voltage surges on transmission systems are usually not effective in controlling power frequency overvoltages. Special precautions must be implemented, particularly during the design stage of a transmission project, to ensure that the system insulation level dicated by transient overvoltages is not unduly stressed.

In long e.h.v. and u.h.v. systems operating at light or no load, shunt reactors are essential for absorbing the excess leading reactive power. These reactors, applied at intervals along the line or at the line terminals, also provide one of the most effective measures of reducing the power frequency

overvoltages to which such networks are susceptible. The several types of reactors which could be used for this purpose are described below:

1.2.5.1 Linear shunt reactors

Although linear air-cored or gapped reactors are effective in maintaining the overvoltage within acceptable levels, they have several limitations. Firstly, they lack the capability of self-adjusting their reactance in accordance with reactive power requirements under various load conditions. Secondly, they increase system losses during normal operation. These disadvantages could, however, be overcome by providing expensive switching devices used to take the reactors out of service during normal load conditions.

1.2.5.2 Non-linear shunt reactors

Suitably designed non-linear reactors could be as effective in reducing power frequency overvoltages as linear reactors of a much larger size. Their non-linear properties enable the reactors to provide the requisite reactive power when the system is operating at light or no load, and automatically and instantaneously revert to reduced compensation under normal load conditions. However, these reactors must be designed to withstand prolonged operation in the saturated region to ensure that overheating problems do not arise. The associated problem of harmonic voltage generation needs special attention. These harmonics may be eliminated by using harmonic absorption filters [4].

Further precautionary measures may be necessary when series capacitors are also present, as is usually the case in very long lines, to prevent ferro-oscillations being excited (as previously described in section 1.2.4). These oscillations may

be eliminated by temporarily inserting a damping resistor in parallel with the series capacitor during line energisation. The additional expense of providing these resistors and their related switches could, however, be prohibitive. An alternative method of eliminating or reducing the ferro-oscillations is to design the reactor with a much larger unsaturated range.

1.2.5.3 Static compensator

Most of the limitations associated with linear and non-linear reactors may be overcome by suitably designed static compensators [4]. Basically, a compensator is a polyphase, series-connected, multi-core saturable reactor. When the reactor is used in conjunction with series and shunt connected capacitors, it is capable of automatically maintaining the voltage constant within about 1% of normal system voltage. The series capacitor is used to eliminate the residual slope of the linear portion of the saturated reactor characteristics. While the purpose of the reactor is to absorb reactive power, the function of the shunt-connected capacitor is to provide means of generating reactive power. As a consequence, the device is capable of maintaining constant voltage for both lagging and leading system current. Successful application of the compensator, however, requires that careful consideration should be given to sub-harmonic oscillations generated within the compensator. Such phenomena could be eliminated by using selective damping circuits, connected in parallel, which are designed to produce minimal power dissipation.

1.3 Sustained overvoltages

The most common overvoltages in this category are those caused by maloperation of the system. Resonant and ferroresonant phenomena producing sustained oscillations will be discussed in the next chapter. Sustained overvoltages are sometimes referred to as temporary overvoltages, according to the International Electrotechnical Commission classification of overvoltages [5]. These are defined as oscillatory overvoltages of relatively long duration, which are damped or only lightly damped.

Although, in general, the magnitude of sustained overvoltages is smaller than that produced by switching transients, they may impose severe duty on expensive and sensitive terminal equipment such as surge diverters, due to the repetitive occurrence of maximum voltages. Careful consideration should therefore be given to the sources of these overvoltages and means of controlling them.

1.3.1 System earthing

Sustained overvoltages depend to a large extent on the type of system earthing adopted. In general, a system which is properly earthed is more prone to larger current and lower overvoltages during faults or some maloperation of the system, than is the case when the system neutral is isolated from earth.

At the higher transmission voltage levels, normal practice in Britain and North America is to earth all transformer neutrals directly and all generator neutrals through a resistor to limit stator fault current. The advantage of such practice lies mainly in the fact that :

(i) phase-to-earth overvoltages due to faults are limited to phase-to-phase peak voltage,

(ii) overvoltages associated with arcing ground and intermittent ground faults are eliminated, and

(iii) several types of resonance phenomena are eliminated.

1.3.1.1 Effectively earthed systems

An effectively earthed system is defined, according to international and national specifications [6], as a system in which the coefficient or factor of earthing does not exceed 80%. This factor is defined as the ratio of the highest r.m.s. voltage to earth of the sound phase or phases at a given point during a line to earth fault, to the highest line-to-line r.m.s. voltage, expressed as a percentage of the latter voltage. The system is considered to be effectively earthed if, for all system conditions, the ratio of the zero sequence reactance to the positive sequence reactance (X_o/X_1) is between 0 and +3, and the ratio of the zero sequence resistance to X_1 (R_o/X_1) is between 0 and +1 [6]. These conditions usually pertain in many high voltage systems, and typical values of the coefficient of earthing in e.h.v. and u.h.v. systems lie in the range 70 to 75%.

1.3.1.2 Non-effectively earthed systems

In a non-effectively earthed system, on the other hand, the coefficient of earthing exceeds 80%. This condition applies to systems earthed through resistors or reactors, including ground fault neutraliser or arc suppression coils, and to systems which have some or all neutrals isolated from earth. In this case the factor of earthing may exceed 100% if X_o/X_1 is negative. Such systems are prone to resonance phenomena.

1.3.2 Overvoltages in non-effectively earthed systems

The main causes of overvoltages in systems which are not effectively earthed are those related to arcing ground fault and

resonance phenomena.

1.3.2.1 Arcing ground

An arcing ground fault occurs when the arc produced by a fault on a system with an isolated neutral is sustained by the capacitive current of the healthy phases. Substantial transient voltage oscillations could be produced due to the interchange of energy between the line capacitance and the inductance of the source. This could lead to intermittent clearing and arcing of the fault creating more onerous overvoltages. The process of excessive voltage build-up in such intermittent earth faults is very similar to that which may occur when line charging current is interrupted with restrikes, as discussed in section 1.6.2.

1.3.2.2 Resonance phenomena

Several conditions may arise in which resonant oscillations could be excited. Such a condition could be created by open-circuited phase conductors or single phase inductive faults. Open phase conductors will be discussed in the next chapter. (See section 2.4). An inductive fault could result from an inductive load accidentally taken to earth. The oscillatory circuits formed by the system inductance and the capacitance to earth could produce sustained overvoltages.

1.3.3 Single phase-to-earth fault

Single line to earth faults are by far the most common of all high voltage transmission line faults. The occurance of a fault on one phase causes the voltage on the healthy phases to rise above their normal value. The increase in voltage is attributable to voltage surges injected into the faulty and healthy phases by the sudden collapse of the voltage at the fault location. The power frequency voltages on the healthy phases may

be reinforced at certain instances by these surges to produce excessive voltage peaks.

The overvoltage on the healthy phase or phases is largely dependent on the following factors:

(i) the method of system neutral earthing adopted,

(ii) the impedance through which the fault current flows as determined by the location of the fault along the line, and

(iii) the load flow conditions existing prior to the fault.

Overvoltages as high as 2.1 p.u. are reported to occur on an unfaulted phase in a non-effectively earthed system [7,8]. In general, these overvoltages are a maximum at the midpoint of the unfaulted phases when the fault occurs at the centre of the line. Variation of the fault location by about 67% along the line produces maximum voltages in excess of 1.75 p.u. The voltage rise also tends to intensify with a reduction in the impedances terminating the line.

On the other hand, when the system is effectively earthed, the overvoltages on the unfaulted phases cannot, by definition (see section 1.3.1 above), exceed 80% of the normal phase-to-phase peak voltage (i.e. 1.4 p.u. of normal phase-to-earth peak voltage).

1.3.4 Fault clearing overvoltages

In addition to the overvoltages produced when one phase conductor is suddenly earthed, further voltage rises occur when the fault is being cleared by operation of the circuit breaker. These overvoltages are a maximum near the end of a lightly loaded line or a line from which the load has been rejected following fault

occurance. Hence the equipment and other lines connected to the busbars could be subjected to substantial overvoltages.

One of the problems associated with reduced insulation levels at the higher transmission voltages, is the susceptibility of the system to unacceptable double or multiple line to earth faults when single pole switching is used to clear the original fault, with severe consequences on the stability of the system. The overvoltage caused by the single line to earth fault could be of such a magnitude as to cause the breakdown of insulation on one or two healthy phases. Great care should therefore be exercised if single pole switching is employed.

1.3.5 Limitation of sustained overvoltages

The capability of protective devices such as surge diverters, and conventional type of circuit breakers, in controlling sustained overvoltages is limited mainly by the onerous and repetitive discharge duties to which these devices would be exposed. Pending the development of more durable surge diverters, an effective method of avoiding excessive sustained overvoltages is to earth the system neutrals either directly or through a suitable resistor. This practice predicates elimination of overvoltages created by sequential clearing and restriking (arcing ground faults) and by several resonance phenomena, and ensures that maximum overvoltages will not exceed 80% of the normal peak voltage between phases.

The most effective method of reducing fault clearing overvoltages is the use of opening resistors of a suitable value (typically 300 to 600 ohms), shunting the contacts of the circuit breaker [7,8]. The optimum value of resistance required for this purpose may differ significantly from that normally provided

for other purposes. These conflicting requirements could, however, be overcome by the selective use of a two or multiple step resistors in the circuit breaker.

1.4 Transient overvoltages of external origin

Lightning discharge constitutes the only important external cause of travelling waves on a transmission system, and an extensive literature exists on this subject. The resultant surges may broadly be classified as those arising from:

(i) a direct stroke to a phase conductor,

(ii) a direct stroke to an earth wire or tower, and

(iii) an indirect stroke in the vicinity of an overhead line.

1.4.1 Mechanism of lightning

A thundercloud usually contains positive charges at the top and negative charges at the bottom. These charges set up electric fields not only within the cloud and between clouds, but also between the cloud and earth by induction. When the electric field strength within the cloud exceeds the breakdown level of the medium (typically 10kV/microsec) a negative streamer from the cloud is initiated by an electron avalanche. This initial discharge progresses towards earth in pulsating movements and is usually referred to as a stepped leader stroke. High electric stresses set up above the ground as the leader stroke approaches, initiate an upward streamer of positive charges from the earth to neutralise the charges in the leader stroke. Consequently, an ionised column along which a faster and luminous return streamer travels, is created. Such a discharge usually produces potential unbalance which will initiate further leader and return strokes. Up to 40 of such discharges, known as dart leaders, have been recorded, while the majority of flashes involve 3 or 4 strokes.

The magnitude of the current in the return stroke can be as high as 220kA but, for the majority of lightning flashes, it

ranges between 5 and 100kA, with an average value of about 20kA. Its duration ranges from about 20 microsec. to a few millisec. Short duration flashes usually produce the highest current while long duration strokes of medium current are associated with high energy and consequential incendiary effects known as hot lightning. Rates of rise of current up to 40 kA/microsec. have been reported, with an average of 2 to 5 kA/microsec. for direct strokes. Induced current surges from nearby strokes generally exhibit lower rates of rise.

1.4.2 Direct stroke to a phase conductor

When a lightning stroke terminates in an overhead line conductor, current surges of equal magnitude, emanating from the point of impact, propagate in both directions. Accompanying these current waves are corresponding voltage surges of a magnitude given by the product of half the line surge impedance and the value of lightning current (typically 4000kV for an average value of current (20kA) and a surge impedance of 400 ohms). Such high overvoltages could cause flashover if the breakdown threshold of the overhead line insulation is exceeded, thus imposing a fault on the system.

1.4.3 Direct stroke to an earthwire or tower

A direct stroke to an earth wire or tower sets up voltage and current surges in a manner similar to that described in section 1.4.2 above. The magnitude of the voltage wave is given by the product of the lightning current and the effective surge impedance at the point of impact. For example, a lightning current of 20kA magnitude divided between a tower of surge impedance 120 ohms and two earth wires, each of 400 ohms surge impedance (effective impedance of 67 ohms) injects 1340 kV voltage surges on the earth

wires. Due to partial reflections at points of discontinuities such as neighbouring earth towers, these surges may build up to excessive levels.

By electrostatic and electromagnetic coupling, current surges of similar waveshape will be induced on the phase conductors and the voltage waves set up on these conductors will be superimposed on the power frequency voltages. The resultant potential between the tower or earth wire and a phase conductor may be of sufficient magnitude to cause flashover, particularly across the insulators, producing a phenomenon referred to as back-flashover. However, since the induced surges on the line conductors have the same phase orientation as the earth wire surges, they act to reduce the potential difference and thus the incidence of back-flashover.

1.4.4 Indirect stroke

Indirect strokes are those lightning flashes which do not terminate directly on the system. If a stroke occurs in close vicinity to the line conductors, it could initiate surges on the lines. This is due to the sudden release of bound charges on the line when the polarising charges of opposite polarity on the cloud are neutralised in a lightning stroke. As these charges propagate along the line, voltage surges of relatively moderate amplitudes will be set up.

1.5 Transient overvoltages caused by line energisation

When a line is being energised by closing the circuit breaker at the source end, pre-arcing of the circuit breaker contacts, which is particularly common when pressurised-head circuit breakers are used, subjects the line to a voltage step. The arc drawn by the contacts as they close redistributes, around the system, the voltage which existed across the breaker contacts prior to switching, in accordance with the relative surge impedances on both sides of the breaker. The magnitude of the injected voltage surge depends on this pre-existing voltage and could be equal to the peak of the normal system voltage when an initially quiescent line is being energised. The surge on the line propagates to the remote end of the line where it is doubled if the line is open-circuited, and reflected back to the source as a surge of opposite polarity. Further discussion of this travelling-wave phenomenon will be presented in Chapter 4, together with an outline of Bewley's lattice diagram technique employed to analyse the behaviour of these surges.

The prospective doubling of voltage surges at the receiving end of the line does not represent the worst possible overvoltage produced. Other factors may combine to produce overvoltages in excess of the 2 p.u. Some of the factors which influence the magnitude of the overvoltages are summarised in the following sections.

1.5.1 Residual charge on the line

In order to minimise the prolonged interruption of supply and improve system stability following those transient system faults which do not usually result in permanent damage, it is normal practice to re-energise the line after an interval sufficient

to allow quenching of the fault current through the circuit breaker. A common type of line fault experienced in practice is a single line-to-earth fault. Such a fault could cause considerable residual charge voltage to be trapped on the healthy phases following fault clearance. The process of load rejection followed by disconnecting the line may also result in a trapped charge voltage on the line.

If the line is re-energised before any significant trapped charge leakage has taken place, as would be the case in non-reactively terminated lines switched by means of conventional types of circuit breakers (i.e. breakers without opening or closing resistors), voltage surges of approximately 2 p.u. could be impressed on the line. The extreme case arises if, at the instant of re-energisation, the peak system voltage on the source side of the breaker is in phase opposition to the maximum trapped charge voltage.

For reactively-terminated lines, an oscillation involving interchange of energy between the line capacitance to earth and the transformer or reactor will be initiated when the line is disconnected. In this case, it is still possible for a substantial potential difference to exist across the breaker terminals at the instant of re-energisation, with resultant high voltage surges being impressed on the line.

1.5.2 Mutual effects between phases

In practice, the three poles of high voltage circuit breakers close electrically in sequence within a time span of up to about 6 millisec. depending on the design of the breakers. Before the actual metallic contact of the breaker poles, pre-arcing is likely to occur on one phase at a time depending on

the breaker pole characteristics, the electric strength of the insulation between the poles, and the voltage existing across the terminals of the breaker.

The capacitive coupling which exist between the phases of a line enable charge to be transferred from the energised phase or phases to those not yet energised. The magnitude of the voltage induced in this manner depends on the magnitude of the mutual surge impedance between the phases relative to the self surge impedance of the line (typically 10-30%). If the induced voltage on the second or third phases to close is of such a polarity as to increase the voltage across their respective breaker poles at the instant of closure, voltage surges of magnitudes higher than those arising from simultaneous closure could be impressed on the lines. Consequently, excessive overvoltages may be produced at the receiving end of the line [9]. These overvoltages depend not only on the relative instants at which the breaker poles close, but also on the characteristics of the supply network and the line being energised.

1.5.3 Source and line characteristics

The receiving end overvoltages depend to a great extent on the type of source from which the line is energised. A wide variety of the supply network characteristics exist in practice. These vary from sources consisting mainly of generators and transformers (inductive sources), to those made up of one or more transmission lines, consisting effectively a resistive source. In practice, these two extreme types frequently combine to produce complex supply networks consisting of local generation, transformers, overhead transmission lines and underground cables. Although the effects of the type of source on overvoltages is closely related to

the characteristics of the line being energised, there is an overall tendency to higher overvoltages as the source capacity decreases [9,10]. The critical case is that of a source consisting of a generating or transforming station with a high effective inductance feeding a considerable length of line. The presence of a line on the supply network generally has a mitigating effect on overvoltage magnitude, although in certain cases, it may produce the opposite effect.

The length of line being switched has no effect on receiving end overvoltages if it is energised from an infinite capacity source, except for the Ferranti rise which is length dependent. This is not the case, however, for any other type of source. In this case, the overvoltage depends on the interaction between the following frequency components:

(i) the fundamental system frequency,

(ii) the natural frequencies and phase disposition of the surges on the source-side lines and on the energised line, and

(iii) the natural frequency of the circuit formed by the source inductance and the line charging capacitance.

The possibility of a resonance condition being approached due to (iii) above exists, particularly when a considerable length of line is being energised from a low capacity source.

1.5.4 Composite lines

Energisation of composite lines consisting of two or more sections having different surge impedance characteristics could, under certain circumstances, lead to the production of severe overvoltages at the receiving end of the line [11].

A mixture of overhead lines and short lengths of underground cables with typical surge impedances of 400 and 30 ohms respectively, having identifiable natural frequencies of oscillation, is an example of a composite line. The overvoltage produced at the receiving end depends on the relative positions and lengths of the sections along the line, and on their surge impedances and propogation velocities. It will be shown in section 6.4 that if the sections are arranged in a sequence of increasing surge impedances from the source end, the receiving-end overvoltages are made more onerous, enhanced by a process often referred to as 'surge magnification'. On the other hand, overvoltage magnitudes similar to those obtained when energising an overhead line on its own are produced if the composite line is energised from the other end. The front steepness of the voltage at the end of a cable terminating a composite line is reduced considerably in comparison with the wave-fronts characteristic of overhead lines alone.

1.5.5 Line losses

Losses inherently present in transmission lines modify both the magnitude and waveform of the surges propogating on the lines. The main sources of these losses are:

(i) line series resistance,

(ii) leakage resistance of the line insulation, and

(iii) corona.

Line resistances cause attenuation as well as distortion of the travelling waves. Due to the presence of high frequency components at the front of waves, the reduction in the surge magnitude is enhanced by the increased values of effective resistance, since this parameter tends to increase with frequency. The change in

the waveshape is due to unequal series and shunt leakage energy dissipation which tends to reduce the front steepness and lengthen the tail of the surge as it propogates along the line. Distortion could, in certain cases, increase the magnitude of the transient voltage at a particular point on the line.

Corona also contributes to attenuation and the reduction of the steepness of wavefronts. It only occurs if the line potential exceeds the corona inception voltage level. This means the air surrounding the conductor is subjected to an electric stress to such an extent that it is partially ionised and a corona discharge is established. The ionisation energy is extracted from the system and, as a result, the surges experience attenuation and distortion.

1.5.6 Reactive compensation

Provision of reactive compensation in the form of shunt reactors generally produces lower transient overvoltages if energisation is performed with the reactor integrally connected to the line. The reduction obtained depends on the degree of compensation in relation to the length of line and source reactance and to its location along the line. In the case of reclosing transients, the shunt reactor helps to reduce the trapped charge voltage, although at a much slower rate in comparison with transformers. The rate of discharge is determined mainly by the reactor losses, and, to some extent by the line losses.

The reduction in overvoltages is greater if the reactor is connected at the receiving-end of the line. This is mainly due to the fact that the reactor introduces a finite surge impedance at the receiving end of the line which lowers the

reflection coefficient at this point. As a result, the receiving-end voltage is not as severe as is the case without the reactor.

1.6 Transient overvoltages on circuit interruption

Apart from normal load switching the primary function of a circuit breaker is to interrupt fault current within a time interval sufficiently small to ensure minimum damage to system equipment and continuity of supply. Its functions are not, however, limited to short circuit operation alone. The breaker must also be capable of interrupting low inductive currents such as the magnetising currents of unloaded transformers or reactors, and capacitive currents when switching long unloaded lines cables, or capacitor banks. The sudden disturbance introduced into the system when the breaker operates could, under certain conditions produce excessive voltages across the breaker and at its terminals. Should a restrike occur across the breaker contacts, the voltage across the contacts existing before the restrike divides in proportion to the surge impedances at each end of the breaker terminals and propogates as surges into the system. Repeated restrikes of the circuit breaker could further accentuate the overvoltages produced.

1.6.1 Interruption of fault current

When the circuit breaker is called upon to interrupt fault current, an arc will be established between the separating contacts prior to eventual interruption when the current passes through zero and the arc is extinguished. In the case where the fault current is limited predominantly by the inductance of the supply network, the system voltage will be near a maximum value at the instant of current zero, and the voltage across the breaker will be the relatively small arc voltage drop. When the arc extinguishes, a voltage known as the restriking or transient recovery voltage appears between the parting contacts of the breaker.

This voltage rises from the small arc voltage drop before arc extinction to the normal frequency voltage (known as recovery voltage) across the contacts when open. The capacitance on the supply side of the breaker prevents the recovery voltage from changing instantaneously. As this equivalent capacitance is charged through the supply network inductance, an oscillation at the natural frequency of the circuit will be established. This oscillation is superimposed on the recovery voltage and may produce overswings up to twice the instantaneous value of the recovery voltage. Subsequent to current interruption, the arc will restrike if the rate of rise of restriking voltage (r.r.r.v.) exceeds the rate at which the dielectric strength between the parting contacts builds up. Reignition of the arc will delay interruption of current until the next natural current zero with a possible repetition of events. Severe damage to the circuit breaker and other items of plant could ensue from such repeated restrikes.

The peak amplitude and r.r.r.v depends on the power factor and natural frequency of the supply network, the losses on the system, and on the type and position of the fault.

1.6.2 Interruption of capacitive current

Excessive voltages could result from interruption of capacitive circuits such as switched capacitor banks. These capacitors are usually installed at substations to improve the power factor and on transmission lines to improve the power handling capability of the lines. Such banks are frequently switched in accordance with varying load conditions. Should a restrike occur on the switching breaker, excessive voltage surges may be set up.

At the instant of arc interruption, the capacitor being switched may be charged to peak system voltage (-E),(as shown on Fig. 1.1 (ii))since the charging current leads the voltage by approximately 90 el.deg. When the system voltage attains a peak value of opposite polarity (+E) half a cycle later, a contact gap voltage of +2E could result. If, at this instant, the gap breaks down, an oscillation involving the supply network inductance, L_s, and the capacitance of the bank, C_2, about the voltage across C_1 (see Fig. 1.1 (i))is set up, and the capacitor voltage rises to a peak value of +3E. If the oscillation current is interrupted as it passes through zero,(see Fig.1.1 (iii)) a voltage of +3E will be left trapped on the capacitor. Half a cycle later when the system voltage attains its maximum value (-E), the gap voltage would be -4E. If at this instant the gap breaks down again, the capacitor voltage will rise to a peak value of -5E. Further sequences of clearing and restrikes could result theoretically in an escalation of capacitor voltage. In practice, however, the random nature of the restriking phenomenon is such that there is a high probability of restrikes taking place before the supply voltage reaches its peak value. This factor, together with the effects of system losses, prevents such excessive voltages from being attained in practice.

If the capacitance being switched (C_2 in Fig. 1.1 (i)) comprises the capacitance of long transmission lines or underground cable, much the same phenomena would occur. In this case, the voltage surges which are generated by the repeated restrikes could further accentuate the overvoltages on the line being switched.

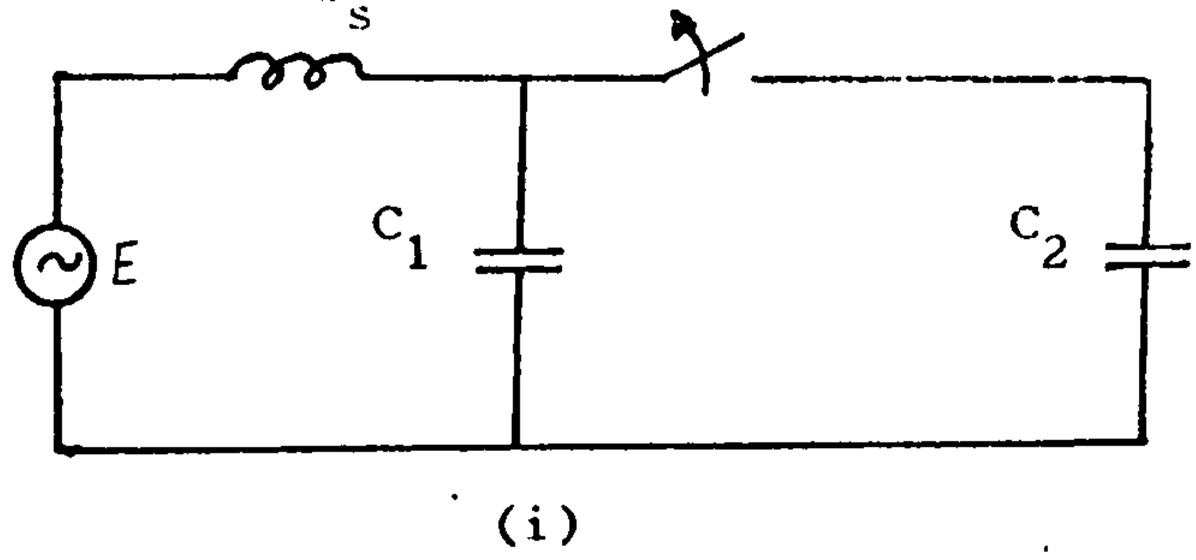

(i)

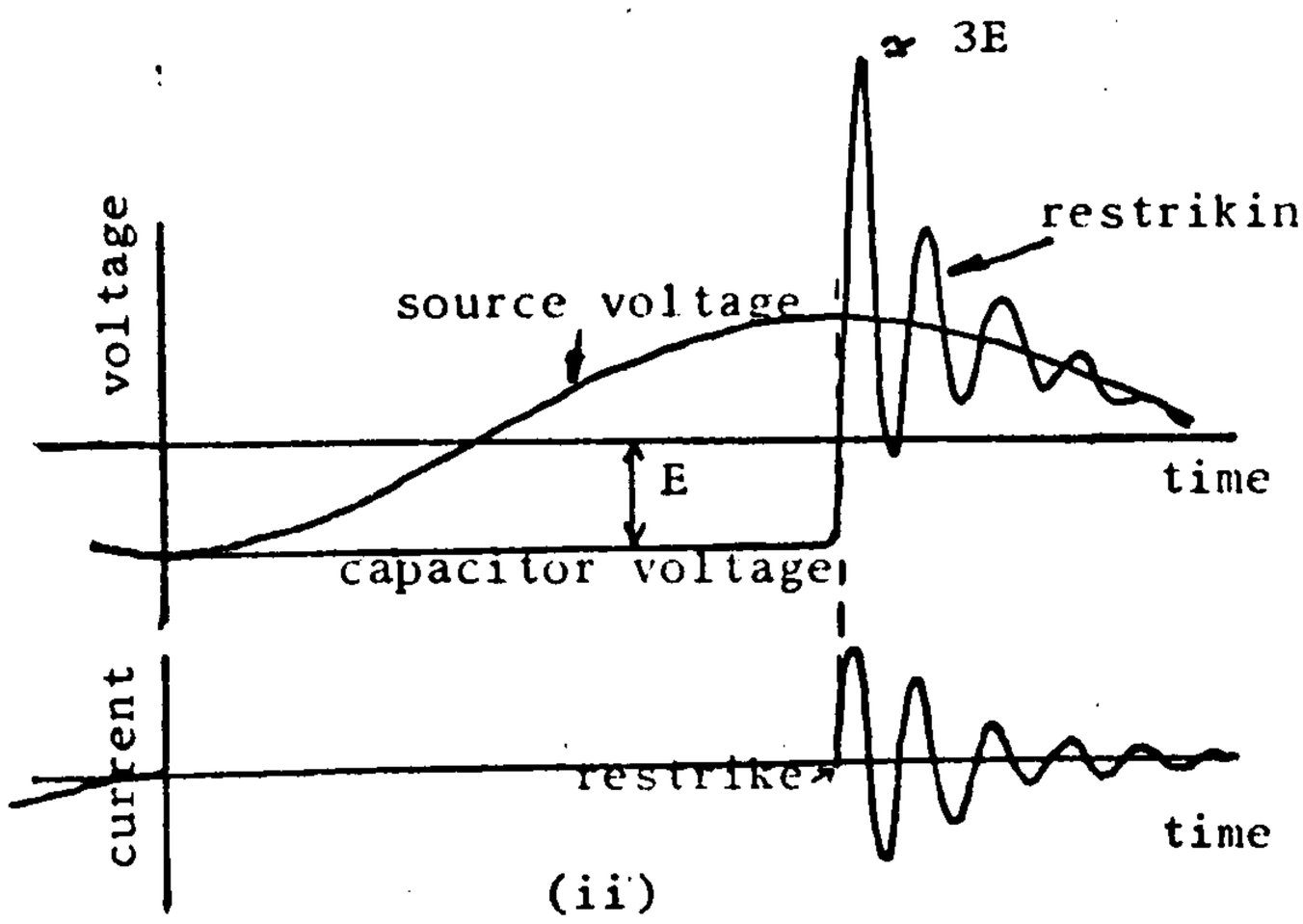

(ii)

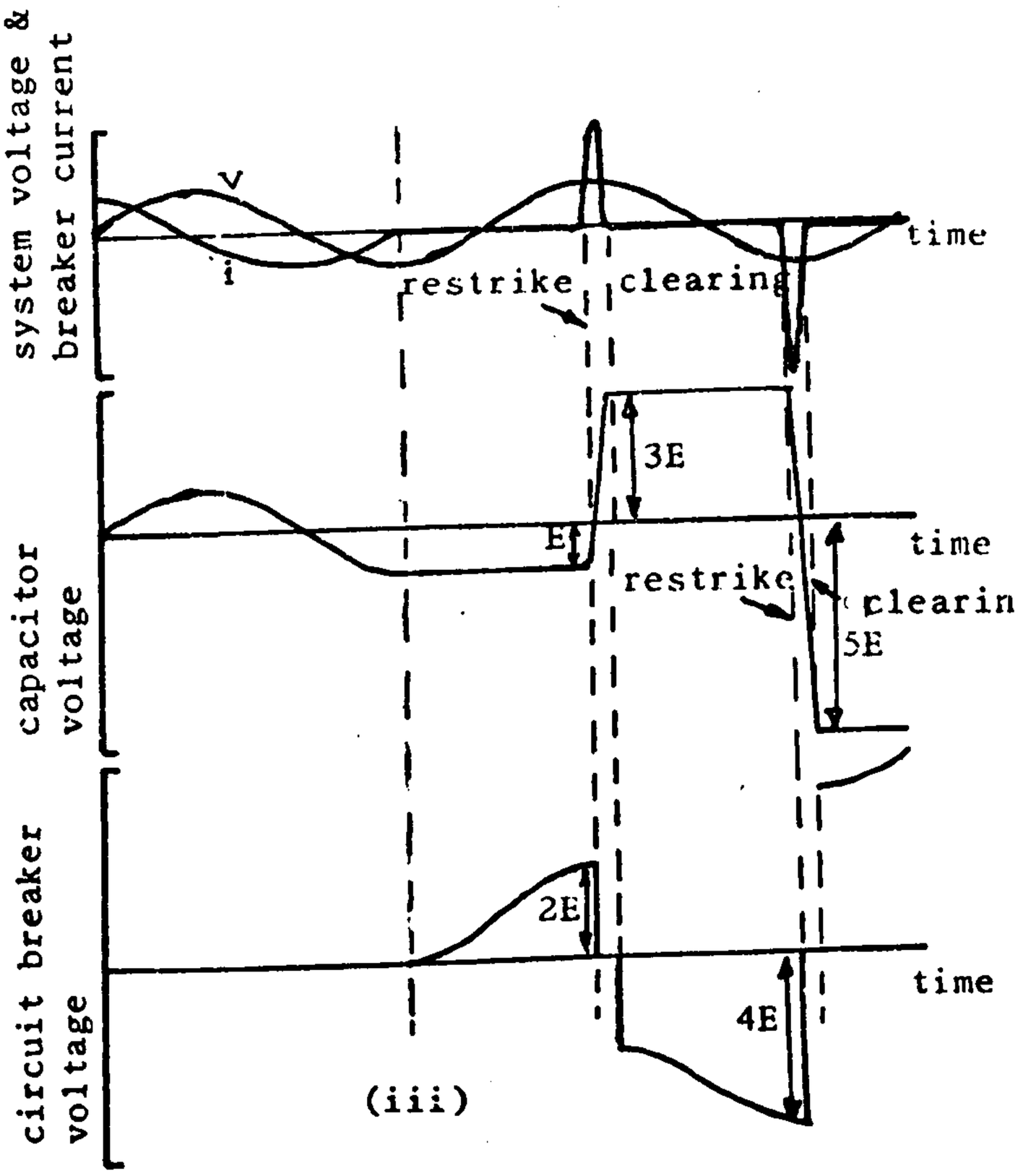

(iii)

Fig.1.1 Interruption of capacitive current
(i) Equivalent circuit
(ii) Restriking voltage and current
(iii) C_2, E and circuit breaker waveforms during multiple restriking.

1.6.3 Interruption of magnetising current

When a transformer or shunt reactor is being de-energised, it is possible for the magnetising current to be forced to zero prematurely before the natural current zero. This is due to the instability of the arc being drawn by the parting contacts of the circuit breaker, and the rapid build-up of arc voltage as the current approaches its normal zero. This instability is caused by the high frequency current oscillation in the arc and stray transformer capacitance. Following such current chopping, some portion of the magnetic energy trapped in the transformer or reactor ($\frac{1}{2}L_m i^2$) will be dissipated in a damped high frequency oscillatory manner involving the effective capacitance of the transformer or reactor and their connections (C). Fig 1.2(i) shows a simplified equivalent circuit under these conditions. The cyclic interchange of magnetic and electrostatic energy ($\frac{1}{2}CV^2$) which results could produce overvoltages across the capacitor and windings and across the circuit breaker contacts. The latter could cause the breaker to restrike. This process may be repeated at subsequent current zeroes, resulting in more onerous overvoltages. However, modern transformers and auto-transformers possess such low magnetising currents which, when interrupted, produce comparatively moderate overvoltages.

Fig.1.2(ii) demonstrates the relation between the instant of current chopping, relative to time at peak current, and the transient overvoltage. The transient voltage peak ranges from a value of 2E, when interruption occurs at the natural current zero, to a value given by the peak current I_o and the surge impedance of the circuit when interruption takes place at peak current. The effects of losses are ignored.

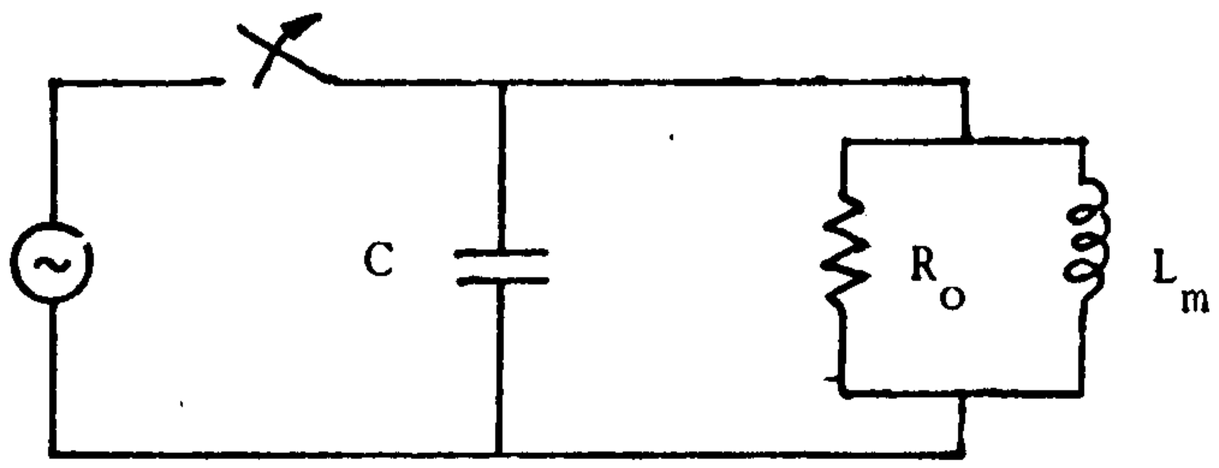

(i)

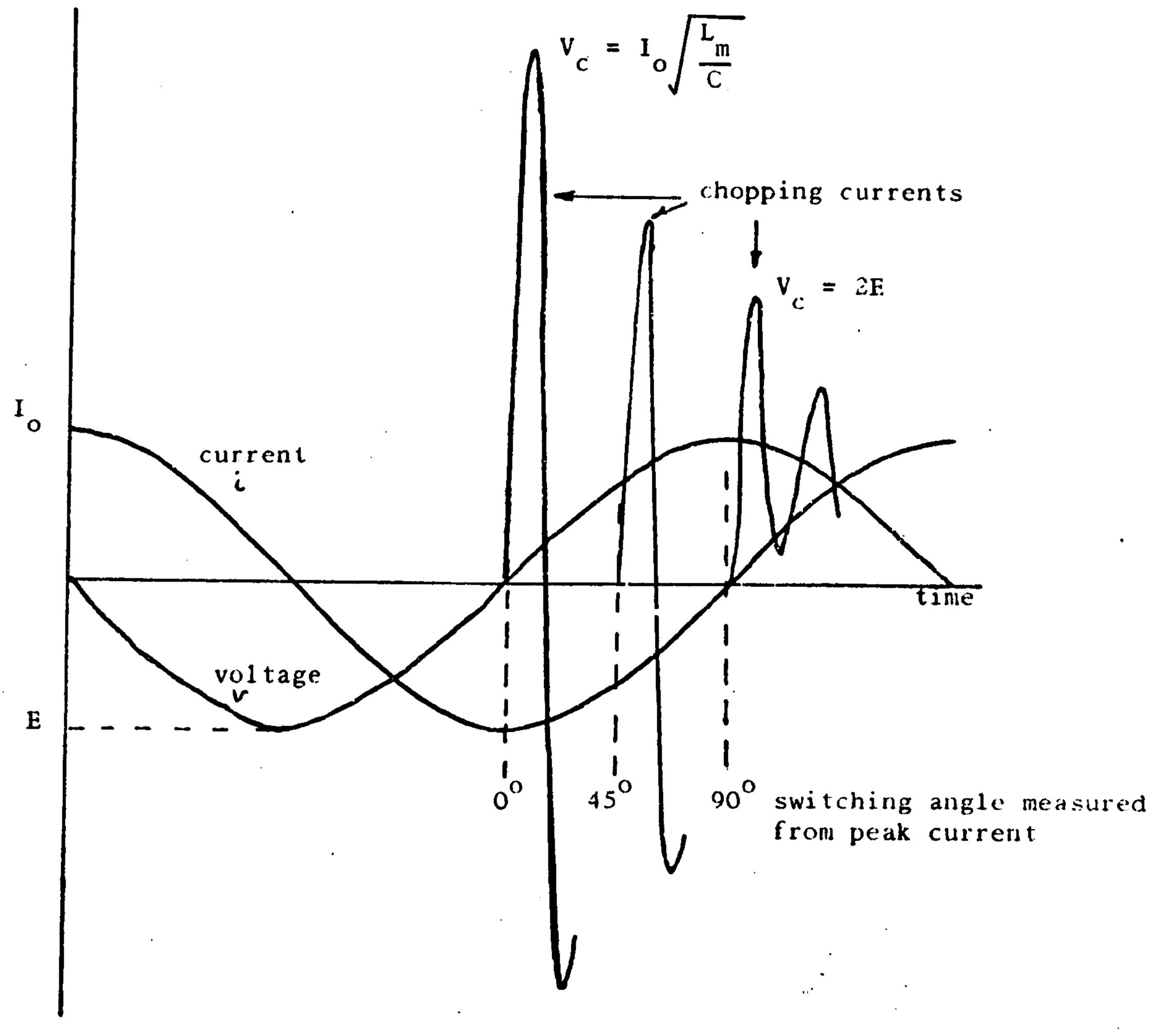

(ii)

Fig.1.2 Interruption of magnetising current
(i) Equivalent circuit
(ii) Effect of angle at which current is interrupted on chopping transients.

1.6.4 Short line fault

When a single line to earth fault only a few kilometers from the circuit breaker is being cleared, severe voltage conditions could be created across the circuit breaker contacts [12]. This could happen at a time before the strength of the insulation between the parting contacts has had time to build up, resulting in the breaker restriking.

A single line diagram and the distribution of voltage along the network prior to circuit interruption is shown on Fig 1.3 (i and ii) respectively. Due to the travelling wave phenomenon established in the short length of line between the breaker and fault, a triangular voltage wave appears on the breaker line-side terminal as shown on Fig 1.3 (iii). This voltage, whose magnitude and frequency depends on the length and characteristics of the line between the fault and the breaker, appears as a component of the transient recovery voltage across the breaker contacts. The other component comprising the transient recovery voltage is the voltage oscillation on the source-side terminal of the breaker. If the initial r.r.r.v., due in particular to the triangular component, is sufficiently large, restriking would result. The rate of rise of the triangular component is given by the product of the line surge impedance and the rate of change of fault current at current zero. The amplitude of its first peak is equal to the product of its rate of rise and twice the transit time of the line [12].

Fig.1.3(iv) indicates how various parameters are related to the distance of the fault from the circuit breaker. As this distance increases, the r.r.r.v., the frequency of the restriking voltage and the fault current being interrupted tend to decrease while the restriking voltage peak increases.

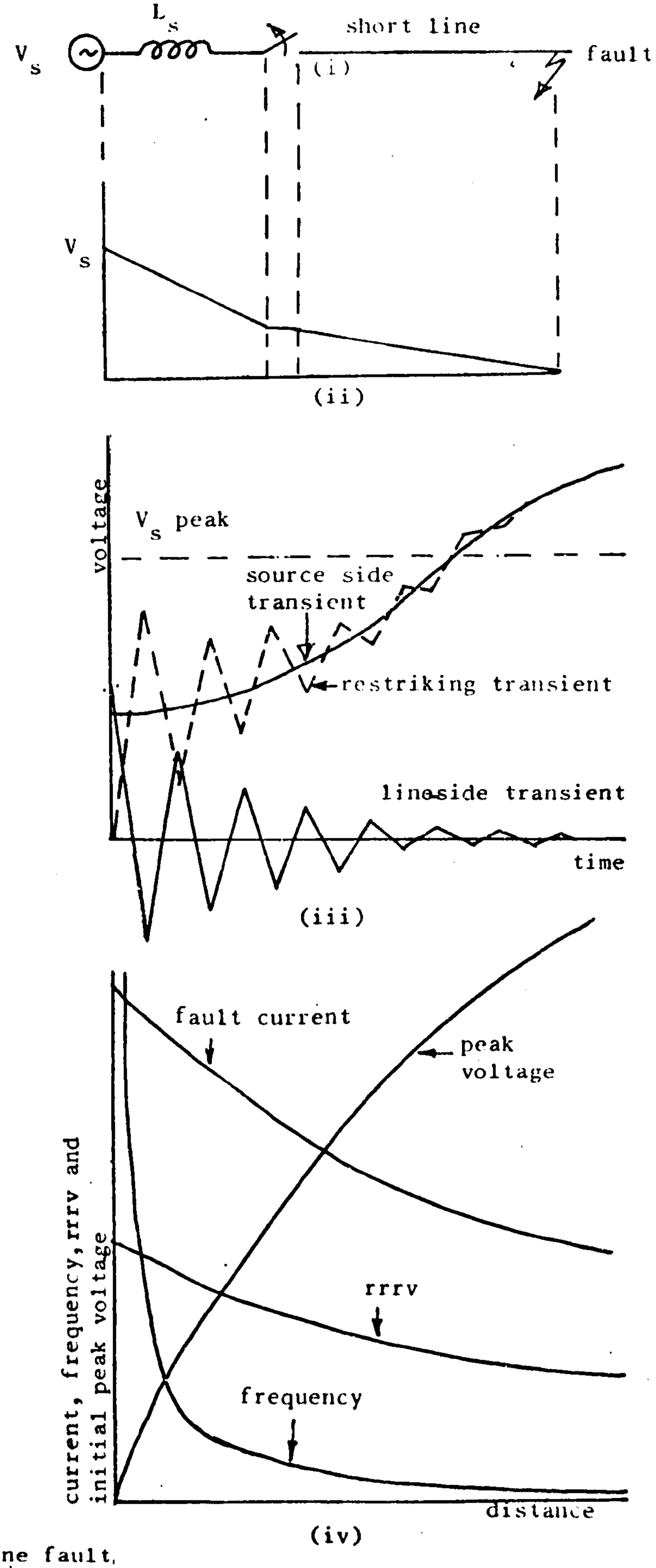

Fig.1.3 Short line fault,
(i) Single line diagram
(ii) Voltage distribution before fault
(iii) Restriking transient waveform and its components
(iv) Variation of current, frequency, r.r.r.v and initial peak voltage with distance to fault.

1.7 Insulation co-ordination

The basic objective of insulation co-ordination at e.h.v. and u.h.v. is to ensure that the characteristics of the protective devices used to limit transient overvoltages are related to the widely varying withstand voltage levels and voltage-time characteristics of all the items of plant, in such a manner as to achieve the required protection and acceptable system reliability. In other words, the system insulation has to be co-ordinated with those transient overvoltages which are likely to cause interruption of supply and, at worst, insulation failure and serious damage to expensive equipment [5]. Although, at high transmission voltage levels, power frequency and sustained overvoltages are usually not critical to insulation co-ordination, it must be ascertained that, under all credible system operating conditions, these overvoltages are within system equipment withstand capabilities as determined from tests.

The insulation level of the various items of plant is a function of several factors such as rise time, duration, frequency and polarity of the transient surges expected at the equipment location. The protective level (i.e. maximum sparkover of the protective devices) is set by the same factors and, in addition, it depends on the characteristics of the protective devices used. The adequacy of the protection afforded to the system is ascertained by the margin by which the insulation level of the system exceeds the protective level. A large margin is usually not economically justifiable, particularly at e.h.v. and u.h.v. transmission levels. In practice, a certain amount of outages may have to be tolerated. The incidence of insulation breakdown leading to permanent damage to equipment, should,

however, be reduced to as low a probability of occurance as is economically practicable. Consideration must also be given to the influence of ageing on internal insulation, and the effect of atmosphere contamination on external insulation.

Overvoltages of atmospheric origin have been, until recently, the controlling factor in co-ordinating system insulation. As transmission voltages increase, however, lightning overvoltages generally become innocuous due to improved insulation, while switching overvoltages assume greater importance. At operating voltages in excess of 400kV, switching overvoltages become a limiting factor in the choice of insulation levels and surge diverter characteristics. This reversal of roles is mainly due to the fact that the magnitude of lightning overvoltages is limited for a particular line, independent of the operating voltage, whereas switching overvoltage magnitudes normally increase with the system voltage.

1.8 Protection against external overvoltages

The occurance of lightning flashover on overhead line systems is not normally accompanied by permanent degradation of the systems insulation. Use of modern auto-reclosure circuit breakers minimises prolonged interruption of supply, and consequently, only a temporary outage is usually experienced. However, to protect expensive equipment at substations from being damaged by excessive lightning surges and reduce the frequency of outages, precautionary measures have to be adopted.

1.8.1 Earth wires

Overrunning earth wires increase the shielding effect provided by the towers. Such earth wires reduce both the incidence of direct strokes terminating on the line conductor by intercepting the strokes, and the frequency of outages if used in conjunction with low tower footing resistances. Earth wires, however, normally increase the incidence of back-flashovers.

Earth wire protection improves with a decrease in the angle between the vertical through the wire and the outermost line conductor, known as the shielding angle. A value of between 35^{o} to 45^{o} has been found, in practice, to be effective in preventing the majority of strokes from reaching the phase conductor. The efficiency of protection could further be improved by providing two horizontally displaced earth wires, particularly where it is most necessary in the approach to substations. Substation shielding wires are sometimes necessary in places of high frequency of potentially severe lightning strokes. According to national specifications [6], shielding is regarded as effective if the probability of shielding failure or back-flashover is so small that the risk is considered acceptable for

the specific application.

1.8.2 Tower footing resistance

In order to minimise the incidence of back-flashovers, tower footing resistances of a sufficiently low value (of the order of tens of ohms) have to be provided. Such resistances prevent large potentials being created at the top of the tower due to the flow of exceptionally large amplitude lightning current. The desired resistance values could be achieved by providing additional earthing electrodes such as driven rods or buried counterpoises.

1.8.3 Voltage limiting devices

Since lightning surges can still reach the substations in spite of adopting an effective shielding system, station equipment has to be protected against overvoltages in case of shielding failures by providing protective devices.

The simplest and cheapest form of voltage limiting devices is a rod gap connected between the terminals of the equipment and earth. The gap breaks down when a certain voltage level, determined by the gap settings, is attained, and the voltage across the protected equipment collapses. This, however, imposes an earth fault on the system, which has to be cleared by operation of the circuit breaker. The wide dispersion in, and the voltage polarity dependence of the breakdown levels associated with rod gaps, constitute further disadvantages of these devices.

The disadvantages of rod gaps are largely overcome in the comparatively more expensive surge diverters or lightning arresters. The essential elements of these devices are non-linear resistors, usually of silicon carbide material, connected

in series with a number of active gaps. The diverter also contains pre-ionising units which, by providing sufficient electrons in the gaps, reduce the dispersion and time lag in flashover values. The gap breaks down when a certain voltage level is reached, and the voltage across the diverter will be set by the product of the diverter current and the resistance of the resistor blocks. During sparkover, the current is limited by the relatively low diverter resistance, while the subsequent power frequency follow current is limited by the high valve block resistance. This power follow current must be interrupted by the series gap elements. In certain types of diverters, arc quenching is assisted by propelling the arc through its own magnetic field in order to achieve elongation and cooling of the arc. The use of silicon carbide discs, which allow relatively small power frequency follow current to flow, also facilitate arc extinction.

The effectiveness of the diverter in limiting the overvoltage is not only governed by the relative impedances of the diverter and the system, and the magnitude of the surge, but it also depends on its ability to cope with the energy involved [13]. This energy is proportional to the magnitude and duration of the impinging surge, and must be absorbed or dissipated by the valve block resistors.

1.8.4 System configuration

Certain features of the system layout may be used to protect expensive equipment against overvoltages. A short length of cable is an example of such an arrangement. By virue of its position and its relatively low surge impedance, the front steepness of the impinging surge is reduced as it passes

through the cable, as explained in Section 1.5.4. The resulting slow fronts enable the co-ordinating gap to operate more effectively.

If several transmission lines are connected to a common junction point such as at a switching station, the co-efficient of reflection at that point will be reduced by a factor depending on the number of lines and their surge impedances. The effect of this is to reduce the magnitude of the overvoltage at this point. The reduction is even more significant if some of the feeders converging at this location are cable circuits, due to the relatively low surge impedance of cables. It is therefore evident that there is less need for protective devices against surges at major substations to which several feeders converge, than on a transformer feeder.

1.9 Protection against switching overvoltages

In practice, several factors exist which act to reduce the magnitude of transient overvoltages. These include resistive and corona losses in the lines and the leakage of residual charge left trapped on the line from a preceeding switching operation, through connected transformers, reactors or through the line insulation. In spite of these mitigating effects, the switching overvoltages produced may still be in excess of the permissible value. Other deliberate measures for reducing these overvoltages may therefore be necessary if the desired reduction in the insulation level at e.h.v. and u.h.v. is to be achieved. An extensive literature exists on these measures [8,9,13,14], some of which are summarised below.

1.9.1 Voltage limiting devices

The basic principles of operation of rod gaps and surge diverters have already been described in Section 1.8.3. The longer rise-times of switching surges in comparison with lightning surges, increases the effectiveness of these devices. The increased discharge duty associated with switching surges, however, requires special attention. Although modern surge diverters may be capable of storing and dissipating such discharge energy, they may not be able to cope with multiple operating requirements due to the frequently occurring switching operations. It is for this reason that they are normally used mainly as a back-up protection at e.h.v. and u.h.v. levels, when other switching overvoltage controlling devices have failed. This requires that the diverter minimum sparkover voltage should be set in such a manner as to make the fequency of diverter operation consistent with its durability.

1.9.2 Resistor switching

Suitably designed circuit breakers equipped with pre-insertion resistors are a most effective method of reducing energisation and re-energisation overvoltages at their source. The line is first energised through a resistor which acts to reduce the voltage impressed on the line. Subsequently, when the resistor is shorted out, another voltage surge will be initiated. With a judicious choice of the resistor value (values of between 0.5 and 2 times the surge impedance of the line are typical) and its insertion time (of the order of 120 elec. deg.), a significant reduction in the overvoltages may be effected. The optimum value is dictated mainly by the length of line being energised and the characteristics of the source-side network. The time of insertion should exceed twice the travel time of the line, since otherwise the resistor would not be effective.

If further reduction of overvoltage magnitudes is necessary, the more complex form of circuit breakers incorporating a two stage closing resistors may be used. The law of diminishing returns applies in this case, however, since subsequent resistor insertions do not produce nearly as much overvoltage reduction as the first resistor.

Overvoltages caused by current interruption may also be reduced by use of opening resistors. The optimum resistor values required for this purpose are usually not consonant with those considered ideal for reducing energisation overvoltages. Opening resistors are inserted during current interruption to reduce the transient recovery voltage by damping the oscillations and, in the case of multibreak circuit breakers, to assist in grading

the recovery voltage across the several breaks. Typical damping resistor values range from 10,000 to 20,000 ohms for magnetising current interruption, from 500 to 5,000 ohms for line charging current interruption, and from 300 to 600 ohms for interrupting short line fault. High resistor values are normally required for grading purposes (10,000 to 200,000 ohms), depending on the effective capacitive reactance across each break, and on the frequency of the recovery transient. Evidently, only in the case of short line fault interruption is the resistance value required consistent with that normally used for energisation. A limited range of resistor value requirements could, however, be met by the use of two or more steps selective opening resistors with one of the stages incorporating resistors of a value required for closing purposes.

In the case where auto-reclosure is employed, opening resistors inserted during interruption provide a path for discharging the line. Consequently, re-energisation overvoltages could be reduced to magnitudes similar to those obtained during energisation, depending on the closing resistor value and its insertion time, the length of line, and the properties of the network supplying the current being interrupted.

1.9.3 Synchronous switching

The magnitude of the voltage surge impressed on the line during energisation and re-energisation depends on the voltage existing across the circuit breaker contacts. If the contacts of the individual phases are closed, or if the closing resistor, if provided, is inserted at the instant when the voltage across the poles is virtually zero, elimination or significant reduction of the surges may be effected. The main disadvantage of this

method, however, is that it requires a rather complex and accurate control system to ensure closure at the most opportune instant for the individual phases. Although the basic concepts of this method have been demonstrated by many authors [14], its practicability has yet to be established.

1.10 Conclusion

Transient switching overvoltages constitute the major criterion for co-ordination of insulation in e.h.v. and u.h.v. systems. In particular, critical overvoltages tend to be generated during line energisation and re-energisation operations [15]. The magnitudes of these overvoltages depend to a large extent on the interactions between the effects of circuit constants and configuration, and the performance characteristics of circuit breakers and voltage limiting devices used. The economic incentive to reduce the insulation level at high transmission voltages requires that :

(i) the development of these overvoltages be inhibited by utilising appropriate circuit equipment such as restrike-free circuit breakers incorporating closing resistors, and

(ii) the magnitude of the surges, once initiated, should be limited by using suitable voltage limiting devices such as rod gaps and surge diverters.

Particular attention need also be paid to the magnitudes of sustained and steady state overvoltages likely to be produced. This is necessary in order to ensure that the advantages of reduced insulation levels, arising from effective control of transient overvoltages, are not compromised due to excessive post-transient overvoltages. This is partularly true at the initial stages of e.h.v. system development. Such systems usually have low short circuit capacity which makes them more prone to higher overvoltages than the more developed systems. In general, the magnitude of most steady state and sustained overvoltages may be reduced by providing:

(i) suitable reactive compensation in the form of shunt reactors or static compensators,

(ii) circuit breakers incorporating multi-stage resistors, and

(iii) system neutral earthing which will ensure that the system is effectively earthed.

The generation of transient, sustained and power frequency overvoltages may further be complicated if the lines are reactively terminated. Such circuits require particular attention since they may, in certain circumstances, produce more onerous overvoltages. In the next chapter, several system conditions which could create overvoltages in transformer-terminated lines are discussed, and those aspects which will be investigated further in subsequent chapters will be identified.

C H A P T E R T W O

SWITCHING OVERVOLTAGES ON TRANSFORMER FEEDERS

2.1 Introduction

In order to avoid the installation of expensive switchgear on high voltage transmission lines, transformers are frequently connected to high voltage lines through disconnect switches. Since the cost of switchgear increases with the increase in transmission voltages, such an arrangement is more common at the higher system voltages. Direct connection of the transformer to the feeder may sometimes be unavoidable during the early stages of superposing a higher transmission voltage on an existing lower voltage level. Interconnection of two high voltage transmission circuits operating at different voltage levels with circuit breakers connected only on the low voltage side of the auto-transformer is also a common arrangement. As a consequence of such composite feeders, the combined transformer and feeder may be switched as a unit by means of circuit breakers located at the transformer secondary side or at the end of the line remote from the transformer. The presence of the transformer would modify the overvoltages initiated by the various switching operations and, in some cases, these may be intensified.

The phenomenon of linear resonance in three-phase transformer feeder circuits arises from the interaction of the inductive reactances of the transformer with the equivalent capacitance. This capacitance may consist of the transformer and bushing capacitances, the capacitance of the lines, cables or capacitor banks connected to the transformer terminals, or some combinations of these components. If such oscillatory circuits are excited resonantly, large overvoltages, limited only by system losses, may be produced. This phenomenon is investigated in Chapters 5, 6 and 8.

If the transformer becomes periodically saturated during unbalanced operation, ferro-resonant oscillations are produced. These oscillations may be sustained if sufficient energy external to the oscillatory circuit is made available to compensate some of the energy dissipated. Such phenomenon is usually initiated by faults or switching operations which cause unbalance in the voltages applied to the transformer. Single phase switching of transformer-terminated lines could, under certain conditions, produce these oscillations.

Dropping one circuit of a double circuit line which is terminated in a transformer while the other circuit remains energised, could create conditions conducive to sustained ferro-oscillations in addition to linear system frequency oscillations. Incidences of ferro-resonance behaviour in such circuits, evidenced by overheating of and increased noise in the transformer, have recently come to light. Chapters 9 and 10 will, respectively, be devoted to such resonance and ferro-resonance phenomena in double circuit feeders.

2.2 Overvoltages caused by circuit interruption

Rejection of load by means of opening the circuit breaker interposed between the line and the transformer has already been discussed in Chapter 1. In the case where such circuit breakers are not provided, however, the feeder and transformer may be de-energised as a unit by opening the low voltage circuit breaker at the secondary side of the transformer, leaving the transformer energised through the line. Such a procedure is usually adopted when shedding load, isolating the transformer feeder circuit for maintenance, or clearing a fault occurring external to the composite feeder.

2.2.1 Secondary-side switching

Overvoltages caused by sudden loss of load from the transformer secondary may, in certain cases, be in excess of those pertaining to rejection of load by means of circuit breakers at the transformer primary side. The latter are discussed in section 1.2 of Chapter 1. It was shown in that section that the overvoltage is mainly due to generator over-excitation and machine over-speeding, negative regulation and Ferranti rise. With the transformer directly connected to the line, however, its interaction with the system could create oscillations which may combine with these effects to produce excessive overvoltages.

As a result of the rise in voltage at the receiving end of the line following load shedding, the transformer may become over-excited. The multiple harmonic components of the excitation current required by the transformer have to be supplied through the line. The over-excited transformer can be visualised as a harmonic current generator feeding the parallel combine of the line capacitive reactance to earth and the source reactance[2]. The harmonic voltage generated would depend on the impedance of this parallel circuit to

the various harmonic current components. This behaviour of the transformer is independent of its position along the line (i.e. at the sending or receiving end of the line). If the transformer windings are connected earthed-star and delta, a low impedance path to the predominantly third harmonic currents would be available and the resultant third harmonic voltages would be relatively small.

For certain line lengths and source reactances, the impedance of the parallel circuit may be high to second, fifth and higher harmonic currents, irrespective of the transformer winding connection. Consequently, high resonant overvoltages will be produced at these harmonic frequencies, and these would be superimposed on the existing elevated power frequency voltages. Since the magnitude of the harmonic current components decreases with the increase in the order of the harmonic, only the second and fifth harmonic voltages are of practical significance. In general, for a given source reactance, fifth harmonic resonance occurs with shorter lengths of line, while resonance in the second harmonic mode is produced with longer line lengths [2,16]. The lengths of line at which these harmonic regions appear tends to increase with increase in the voltage behind the generator subtransient reactance, and decrease with an increase in source reactance.

In addition to the harmonic voltages produced when the load is rejected, sub-harmonic oscillations involving the capacitive reactance of the line and the non-linear magnetising reactance of the transformer may also appear. The presence of such ferroresonant oscillations is evidenced by the low frequency modulation of the voltage waveforms [2]. Their frequencies and amplitudes depend largely on the conditions prevailing during load shedding.

Due to the relatively long duration of these overvoltages (of the order of 1 second), severe discharge duty would be imposed on the surge diverters protecting the transformers. It is therefore necessary to employ measures to prevent or control this phenomenon. For this purpose, several methods have been suggested in the literature. These are summarised below:-

(i) provision of suitable shunt reactors, synchronous condensers or resonant shunt, located at the receiving end of the line (preferably at the transformer delta tertiary winding if available),

(ii) opening the circuit breaker at the sending end of the line within a prescribed interval after opening the breaker at the transformer secondary, to ensure that the transformer is not left energised for a time long enough to permit the overvoltages to build up, and

(iii) automatic tripping of the generator field coil.

In practice, the presence of such dissipative factors as line series and corona losses as well as the transformer core and copper losses act to reduce the severity of these overvoltages.

The overvoltages considered in this section may be eliminated by 'high-side switching'. This, however, introduces overvoltages of a different character to those dealt with here, as discussed in Chapter 1. Even with this method of switching, similar phenomena may occur if a generator transformer is present at the source-end (see section 1.2.3).

2.2.2 Dropping unloaded transformer feeder

If, following the shedding of load by means of transformer low-side switching, the composite feeder and transformer is isolated from the rest of the system by opening the circuit breaker at the sending end of the line, non-linear ferro-oscillations may be set up[15,17]. Similar phenomena occurs if the sequence of opening the two circuit

breakers is reversed, since in both cases, a residual charge voltage is left trapped on the feeder subsequent to the switching operations. Results of field tests [15,18] and transient analyser studies [19], showing the character of these oscillations, have been presented in the literature. These investigations have shown that, in general, the presence of the transformer connected directly to the line being dropped has a mitigating effect on the magnitude and rate of rise of the transient recovery voltage appearing across the interrupting circuit breaker. This reduces the probability of restriking. Overvoltages without restrikes could, however, be higher when the transformer is present.

The problem is essentially a trapped charge voltage oscillation involving the cyclic interchange of energy between the electromagnetic field of the transformer and the electrostatic field of the transmission line. When the leading current is interrupted at successive current zeros , a voltage close to full system voltage will be trapped on the individual phase conductors. It will be shown in section 9.7 of Chapter 9 that there is a finite number of combinations of trapped charge voltage distribution among the individual phases, depending on the instants and phase sequence of current interruption. In general, two phases would exhibit trapped voltage of the same polarity with a magnitude approximately equal to the peak value of system voltage, while a voltage of opposite polarity will be trapped on the third phase.

The magnetising impedance of the transformer provides a path through which the line discharges. This discharge current could be small while the magnetising impedance remains unsaturated. When the time integral of the voltage impressed on the transformer is sufficient to saturate its core, the line discharge current increases

rapidly and the line voltage drops to zero at the peak of current. A voltage of opposite polarity buiids up as the current drops towards zero until the transformer comes out of saturation. At this instant, a voltage of opposite polarity will be left trapped on the line until the transformer volt-second capability is once again exceeded. A repetition of events will then be initiated.

The characteristic trapezoidal voltage waveform and intermittent large current pulses will persist until the losses inherent in the system damp out the oscillations. Since the time integral of the voltage at the transformer required to saturate its core is a constant, successive cycles of the trapped charge voltage oscillations will undergo a gradual reduction in amplitude and a corresponding steady increase in the period of the oscillations.

These oscillations depend largely on the initial conditions obtaining subsequent to switching, the degree of inter-phase magnetic coupling within the transformer and the extent of the electrostatic coupling in the line. These effects will be discussed further in Chapter 10.

If the knee of the saturation curve is high relative to the rated voltage of the transformer, the trapped voltage would take longer to saturate the core. This increases the risk of a restrike occuring due to the possibility of a higher voltage building up across the interrupting breaker contacts. The probability of restriking is further enhanced if the unsaturated impedance of the transformer is large enough to restrain leakage of trapped charge while the transformer is in its unsaturated state.

2.3 Energisation of unloaded transformer-terminated feeders

Energisation of the line with a transformer integrally connected at the receiving end produces a voltage response somewhat different from that pertaining to an open-circuited line. In certain cases, the resulting overvoltages may be more severe as demonstrated by reported field tests [18] and transient analyser investigations[19,20]. In the case of simultaneous closure of the three phases, the over-voltages at the receiving end of the line are generally lower than those obtained when the transformer is omitted. This is not the case, however, when the three phases close non-simultaneously as they do in a practical three phase system. The mutual interactions between the individual phases of the line and of the transformer, which are more pronounced during unbalanced operation when the phases close in sequence, could significantly alter the magnitude of the transient overvoltages. The manner in which the line discharges through the transformer during the circuit breaker reclosing period is a significant factor in determining the magnitude of the reclosing transients.

2.3.1 Sequential closure

The transformer at the end of the line being energised offers a finite impedance to the line surges in comparison with the open-circuited line conditions. The finite surge impedance reduces the coefficient of reflection at the line and transformer junction to a value somewhat below +1. This accounts for the generally lower receiving-end voltages experienced when the transformer is being switched with the line, provided the three phases are energised simultaneously.

In practice, however, when the switch is being closed, the three poles of the circuit breaker do not energise the phase conductors simultaneously but do so in sequence. It will be shown in Section 8.4

that voltage surges will be induced on the still unenergised phases through the following mechanisms:

(a) Electrostatic coupling between the phase conductors induces a voltage in phase with the surge on the first phase to close. Its amplitude is determined by the relative magnitude of the inter-phase and phase-to-earth equivalent line capacitances.

(b) Electromagnetic coupling between the phases within the transformer induces a lower frequency voltage (predominantly the third harmonic). This component is initially in phase opposition to the initial surge on the energised phase. Depending on the instants and sequence of sparkover of the individual circuit breaker poles, it is very likely that the amplitude of the surges injected on the second or third phases to close exceed the corresponding values obtained without the transformer.

In general, coupling within the transformer, often referred to as harmonic backfeed[18], tends to increase with a decrease in the leakage impedance between the primary and delta windings. If the delta tertiary winding is omitted, however, a limited amount of coupling within the transformer will only be present in transformers of three-limb construction due to the core flux circuit. Transient analyser investigations using a core-type transformer with a delta winding[20] have shown that the overvoltages at the transformer tend to increase as the length of line or the transformer zero sequence impedance increases.

2.3.2 Re-energisation of feeders with trapped charge

It has already been mentioned in section 1.5.1 of Chapter 1 that, following certain switching operations, trapped charge voltages of a value approximately equal to peak system voltage could be left on the phases of the line. Re-energisation at the instant when the trapped

charge voltage is of opposite polarity to the source side voltage on the same phase could produce severe overvoltages at the receiving end of an open-circuited line. The presence of the transformer terminating the line does, however, introduce some mitigating effects by reducing the trapped charge during the circuit breaker reclosing period.

When the transformer is unsaturated the trapped charge on the line leaks through its high magnetising impedance. If, on the other hand, the trapped charge voltage is such that the voltage-time capability of the transformer is exceeded, the cyclic saturation of the transformer, in conjunction with the line capacitance, leads to non-linear subharmonic oscillations (as discussed in Section 2.2.2). This voltage will gradually diminish with each successive oscillation as a result of energy dissipation. It will essentially disappear within a few cycles. Consequently, if the reclosing period of the circuit breaker is longer than the duration of these oscillations re-energisation overvoltage magnitudes will be made equal to those pertaining to energisation without trapped charge, provided the interrupting breaker does not restrike. Field tests[18] have shown that an earthed star/delta transformer drains the trapped charge from intermediate lengths of line within approximately 5 cycles.

If the transmission line is shunt compensated, however, the trapped charge oscillations would persist for a much longer period which, in most cases, exceeds the reclosing period of the circuit breaker. In general, shunt compensation tends to reduce energisation overvoltages and increase re-energisation overvoltages when integrally connected feeder and transformer circuits are energised.

2.3.3 Interphase overvoltages

Although the air clearances between the phases of an e.h.v. transmission line are usually adequate to withstand the overvoltages

likely to be experienced in practice, a careful evaluation of the effects of these overvoltages on the direct interphase insulation of the transformer (particularly the composite coretype) and other station equipment, is necessary. Transient analyser studies[21,22] have indicated that surge diverters normally connected phase-to-earth at the transformer, cannot be relied upon to limit the interphase overvoltages. This is because the phase-to-earth components of the interphase over-voltage may fall below the diverter protective level, particularly in the case of maximum interphase overvoltages. The latter could rise as high as twice the phase-to-earth overvoltage. In certain cases, therefore, it may be necessary to adopt a phase-to-phase design over-voltage factor twice as high as the corresponding value between phase and earth.

White[23] has demonstrated from field tests that, when energisation is performed by closing the sequence isolator contacts of an air-blast circuit breaker, simultaneous or near simultaneous prestriking could occur on two phases. Overvoltages some 30% higher compared with single-pole prestriking overvoltages may be produced. This arises when the two phases are energised simultaneously at the instant when their source voltages are in anti-phase. Due to the high surge impedance of the transformer in relation to the line surge impedance, giving a reflection coefficient close to +1, these surges will be nearly doubled at the transformer, producing high interphase overvoltages.

If the pole span of the circuit breaker is sufficiently long in relation to the transit time of the line, harmonic backfeed voltages will develop. Depending on the magnitude, frequency and phase relationship of this component relative to the high frequency voltage on the energised phase, excessive interphase voltages could develop.

2.4 Resonance and ferroresonance phenomena

Interest in the field of resonance when a transformer feeder is being energised with the transformer integrally connected to the line has recently developed due to a number of reported incidents of co-ordinating rod-gap flashover on the low voltage side of the transformer. This probelm has been attributed to resonance phenomena by Czuros, Forman and Glavitsch[24,25]. The occurrence of similar phenomena on the South of Scotland Electricity Board (S.S.E.B.) system has been reported [26,27]. According to Heaton [28], much the same problem arises when a reactor-terminated line is being energised. Incidences of flashover, attributable to resonance conditions, between adjacent low voltage terminals of an auto-transformer when the latter was being energised from the remote end of the high voltage line have also been reported[23]. In most cases, the protection of the surge diverters normally installed at the high voltage terminals of the transformer proved ineffective. This is because when a resonance condition involving the transformer leakage reactances and its associated capacitances exists, the voltage magnitude at the line side of the transformer is normally below the surge diverter protective level. It is therefore necessary to employ certain precautionary measures when such oscillatory circuits are being energised.

Ferroresonance oscillations pertaining to open conductors in transformer-terminated lines have been recognised for many years. Several reports of laboratory or transient analyser studies exist on this subject [2,31,29-33]. Analytical techniques have also been used to study the mechanisms of this phenomenon[2,31,33,34].

Overhead transmission lines of double-circuit configuration are frequently encountered in e.h.v. transmission systems. The phenomenon of resonant excitation of one of the circuits of such a

double-circuit line, reactively terminated, when this circuit is being dropped, has only recently received the attention of the electricity industry. The relative sparcity of information in the literature about this problem to date, is in itself an indication that the potential hazards of such phenomena have not been fully appreciated. With increasing interest in lines of double-circuit configuration, however, this problem will become an important factor in coordinating insulation in double circuit feeders. The safety of workmen when one of the circuits is dropped for maintenance purposes is also of paramount importance.

The oscillations excited on the de-energised feeder circuit of a double-circuit line could be either linear or non-linear in character, depending on the effective terminating reactances. If the predominant reactance at the end of the line being dropped is essentially linear, as would be the case if linear reactors are provided at the end of the line or at the transformer tertiary terminals, the oscillations excited would be linear[34,37]. If on the other hand, the transformer saturation effects are prominent, non-linear ferro-oscillations would be produced[38,39].

2.4.1 Resonant excitation of a transformer

With the transformer omitted, the energisation voltage generated at the receiving end of the line essentially consists of a square waveform. It is caused by the repeated reflections, at the terminals of the line, of the initial voltage step impressed on the line. Its magnitude is twice this voltage step if the effects of attenuation and distortion are neglected. Its frequency is determined by the length of line and is given by $f_L = 1/4T$, where T is the propagation time of the line. In practice, however, the effects of transmission line losses will gradually damp out this oscillatory

component, which is superimposed on the normal system frequency. The natural frequency of the line can be related to the characteristics of the feeder and those circuits connected to the busbar supplying the feeder.

If the transformer is connected directly to the receiving-end of the line, the effective capacitance to earth, C, associated with the transformer, bushing and any length of cable connecting the transformer to the switchgear on the secondary side, forms a series oscillatory circuit with the leakage inductance of the transformer, L. The natural frequency of this circuit is given by $f_T = 1/2\pi\sqrt{LC}$, and will subsequently be referred to as the transformer frequency. Its value depends on the design of the transformer, bushings and the length of cable on the transformer secondary. When the line is energised, there is a possibility of excessive resonance overvoltages being produced across the components of the oscillatory circuit, provided the frequencies defined above are close to each other (i.e., $f_T \simeq f_L$). This is likely to occur when relatively short lengths of feeder are being energised.

When the voltage pulse arrives at the junction between the line and the transformer, the reflected and transmitted pulse fractions will depend on the ratio of the apparent surge impedance of the transformer, defined as $Z_T = \sqrt{L/C}$ (where L and C are as defined above), and the line surge impedance, Z_L. This ratio, Z_T/Z_L, will determine the amount of energy drained from the line to excite the transformer oscillation. A high ratio favours the evolution of large overvoltages since then the energy drawn from the line will be small and the exciting line oscillations will not be significantly affected. Conversely, a low surge impedance ratio involves a drain of relatively large amount of energy from the line which would cause a gradual decay

of the oscillation exciting the transformer. In order to determine the magnitudes, duration and shape of the voltages at the transformer, it is necessary to investigate the effects of those parameters and of such system layout which determine the natural frequencies and surge impedances of the line and the transformer. Chapter 5 will be devoted to the evaluation of the effects of system constants on the over-voltages at the transformer while in Chapter 6, the effects of the configuration of the feeder circuit and the source network from which it is being energised, will be investigated.

2.4.2 Open phase conductors in compensated transformer feeders

Open phase conductors in three phase systems could be brought about by

(i) single phase switching by means of switching isolators or disconect switches,

(ii) three phase switching in which one or two of the poles are mechanically stuck, or

(iii) accidental breaking of phase conductors.

The latter could result in a phase-to-earth fault if the broken conductor falls to ground. Sustained linear resonance oscillations could be produced if linear reactors are connected directly to the terminating transformer for reactive shunt compensation. These oscillations are produced by the excitation of the oscillatory circuit formed by the terminating reactance and the distributed capacitances of the line or cable by unbalanced system frequency voltages. Excessive voltages could occur across the open phase or phases of the feeder and across the reactor of the phase corresponding to the closed phase or phases, depending on the circuit constants.

2.4.2.1 One open phase conductor

If one phase conductor of a transformer feeder is open

while the other two phases are energised, the circuit diagram is as shown on Fig. 2.1 (i). The capacitance shown could represent the distributed capacitance to earth of a line or cable. The compensating reactor, if present, is connected to the transformer secondary and its neutral is isolated from earth. The parallel connection of the sequence network for one phase open is as shown on Fig 2.1 (ii). If the linear reactor is present, S1 and S2 are always closed while X_R is always disconnected from the zero sequence network since the reactor neutral is isolated from earth. Different transformer winding connections are simulated by the state of the switches S3,S4 and S5. For a delta-delta connection, S4 and S5 are closed. S3 is open for the delta-star (earthed or isolated neutral) and star-star (secondary earthed or isolated) connections. S3 and S5 are closed for the earthed star-delta connection while S3 is closed for the unearthed star-delta and earthed star-star (secondary earthed or isolated) connections.

Fig 2.1(iii) (without the dashed connection) represents the simplified equivalent circuit in the case where the reactor is present and the transformer is connected star-delta with the neutral isolated from earth. It is assumed that the sequence magnetising reactances of the transformer (X_{m1}, X_{m2} and X_{m0}) are large in comparison with the reactance of the reactor, X_R, and hence are neglected. It is further assumed that $X_C = X_{C1} = X_{C2} = X_{CO}/n$. The impedance of this circuit as viewed from the source end is given by

$$Z_{in} = j \frac{X_C X_R \left[2X_C - (2n+1)/n \cdot X_R \right]}{(X_C - X_R) \left[X_C - (n+1)/n \cdot X_R \right]}$$

At resonance, (i.e. $Z_{in} = 0$)

$$X_C = (2n+1)/2n \; . \; X_R$$

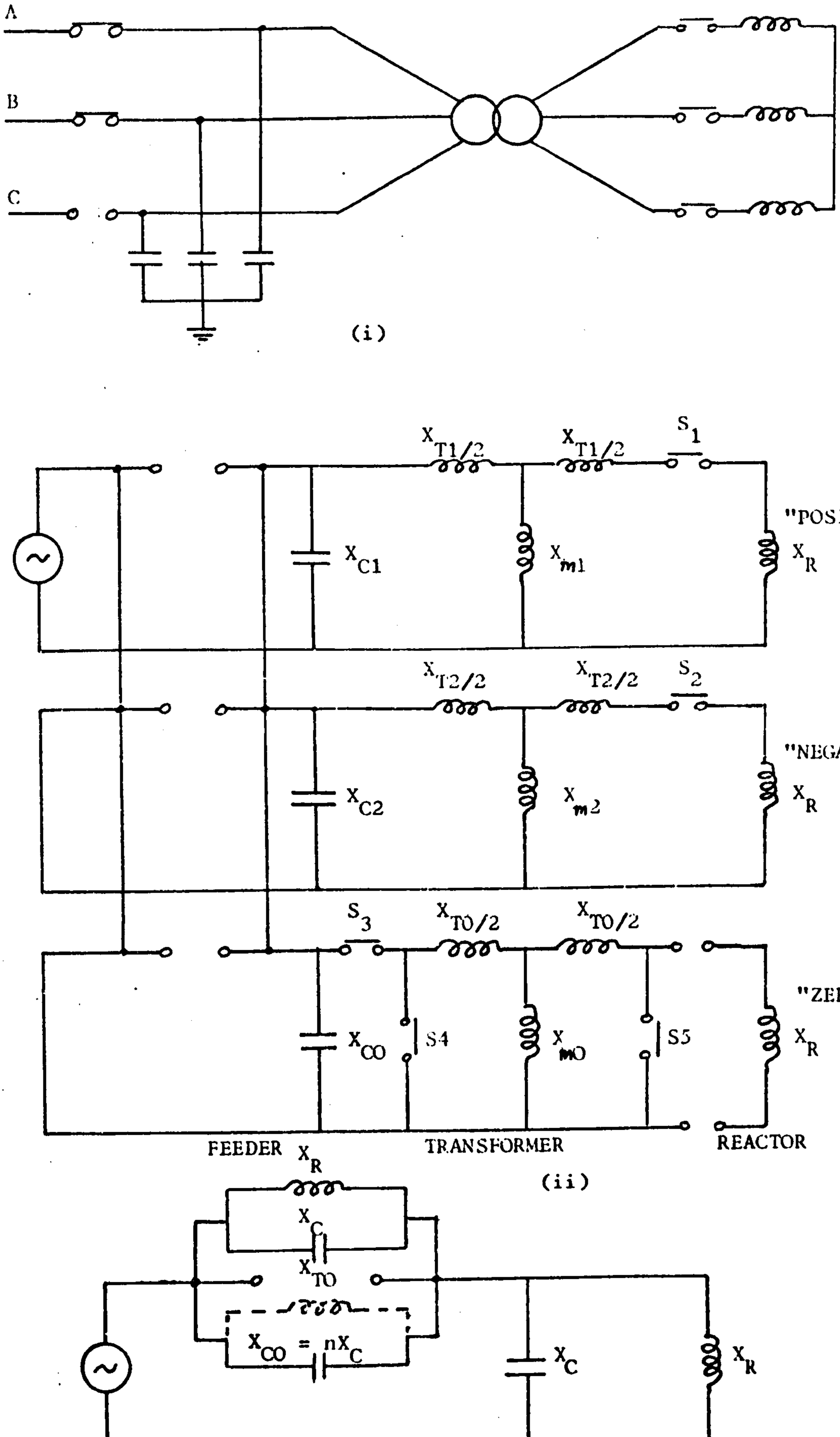

Fig. 2.1 One Phase conductor open
(i) Circuit diagram
(ii) Sequence component network for different transformer connections.
(iii) Simplified equivalent circuit.

Fig 2.2 contains a summary of results of laboratory investigations, using a transformer connected unearthed star-delta. The line or cable was simulated by a bank of three-phase earthed-star capacitors representing the distributed capacitance to earth of the feeders. Each bank was made up of a 7.5 KVAr, 250V, 50Hz Bryce capacitors in steps of 0.125 KVAr and one 100 μF, 300V, 50Hz capacitor in steps of 0.1 μF. The three phase reactor rated 415V, 50Hz had tappings to give from 1.67A to 20A in 12 equal steps. In this case, $X_C = X_{C1} = X_{C2} = X_{CO}$ (i.e. n = 1). For shielded cable, the value of $X_{CO} = X_{C1}$ whereas for overhead transmission lines n is of the order of 2.

The three phase transformer used was an 8.16KVA 50Hz 3-limb core-type Foster transformer with two sections rated 415V and one section rated 240V. A 1:1 transformer turns ratio was used for all tests. For the case of one phase energised, the outer core leg was energised (phase A) while for the case of one phase open, the outer core leg was opened (phase C) in the tests.

A three phase variac was used to supply the system through a 10A switch. The per unit quantities are based on a reference voltage of 240V and base KVA of 2.72 (i.e. transformer ratings). All measured voltages were recorded in per unit of normal r.m.s. phase-to-neutral voltage. The tests were carried out at reduced voltage. As a consequence, the saturation effects of the transformer and reactor do not play any significant role.

It will be seen from Fig 2.2 that, as the capacitive reactance is increased, the reactor and capacitor voltages rise to excessive values when the relation for resonance is satisfied (i.e $X_C = 1.5\ X_R$). Curves (a) and (b) also show the locus of peak resonance voltages as the reactance of the reactor is varied. Maximum capacitor

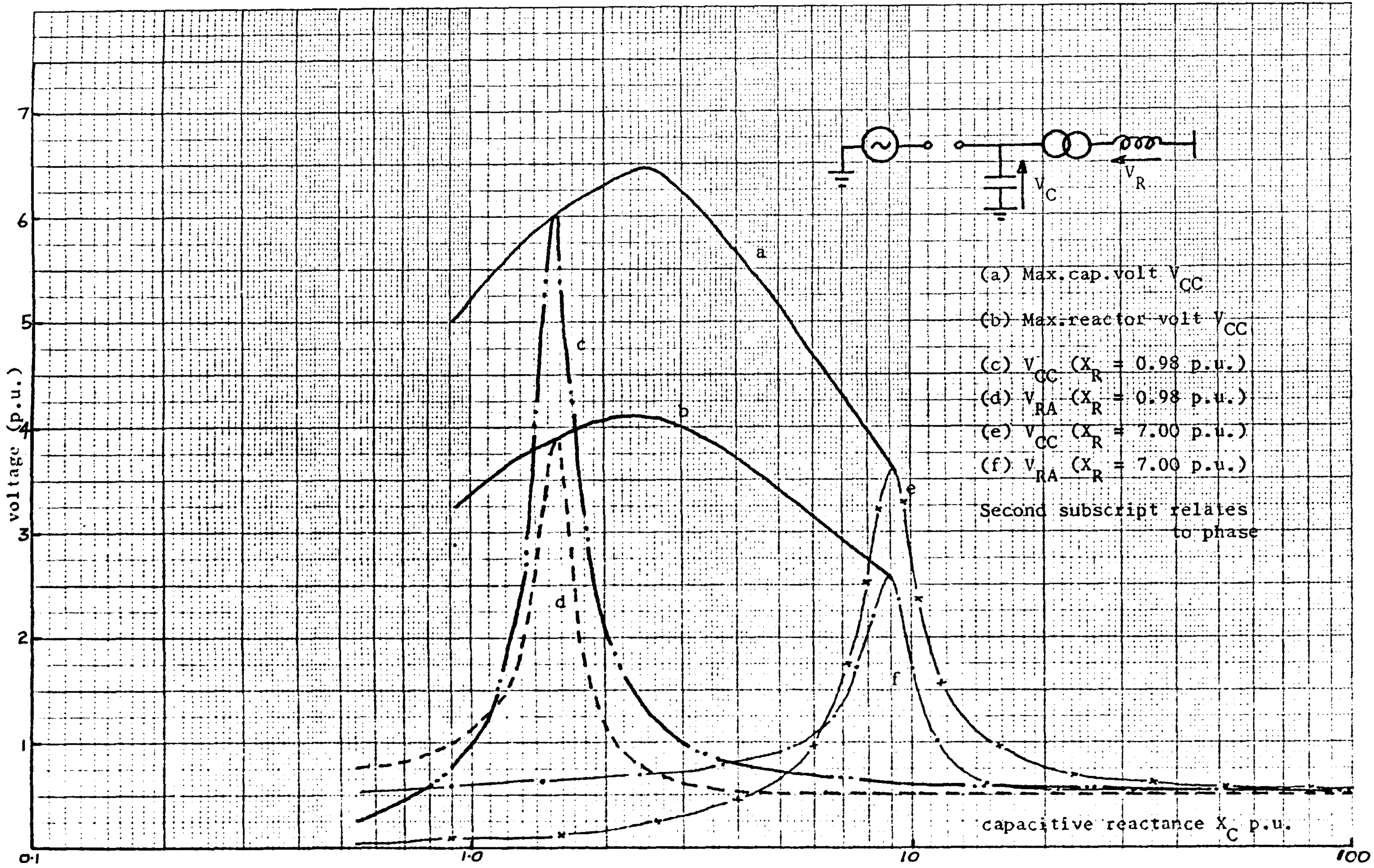

Fig. 2.3 Maximum capacitor and reactor voltages for one phase (C) open and transformer connected star/delta (isolated neutral), as a function of X_C and X_R.

overvoltages occur on the phase which is open, whereas maximum reactor overvoltages are produced on the phases corresponding to the energised conductors.

When the neutral of the star-delta connected transformer is earthed, the equivalent circuit of Fig 2.1 (iii) (including the dashed branch) applies. In this case, the impedance of the circuit is given by

$$Z_{in} = \frac{X_C X_R \left[X_C(X_R + 2X_{TO}) - (2n+1)/n \cdot X_R X_{TO} \right]}{(X_C - X_R) \left[X_C(X_R + X_{TO}) - (n+1)/n \cdot X_R X_{TO} \right]}$$

Hence resonance would occur when

$$X_C = \frac{2n+1}{n} \cdot \frac{X_R X_{TO}}{X_R + 2X_{TO}}$$

If X_R is large in comparison with X_{TO}, as is usually the case, the above relation reduces to

$$X_C = \frac{2n+1}{n} \cdot X_{TO}$$

This expression also holds true if the reactor is omitted from the circuit.

2.4.2.2 Two phase conductors open

The circuit diagram for two phase conductors open and the series connection of the sequence network to simulate this condition are shown in Fig 2.3 (i) and (ii) respectively. The state of the switches is as defined previously. Using the same assumptions as stated in (a), the simplified equivalent circuit of Fig. 2.3 (iii) results. The dashed section is omitted for the case where the transformer is connected star-delta with isolated neutral. Analysis of this circuit will show that a resonance condition is excited if

$$X_C = \frac{2 + n}{n} X_R$$

For the case where n = 1, laboratory investigations revealed the resonance curves of Fig 2.4. Resonant overvoltages of approximately

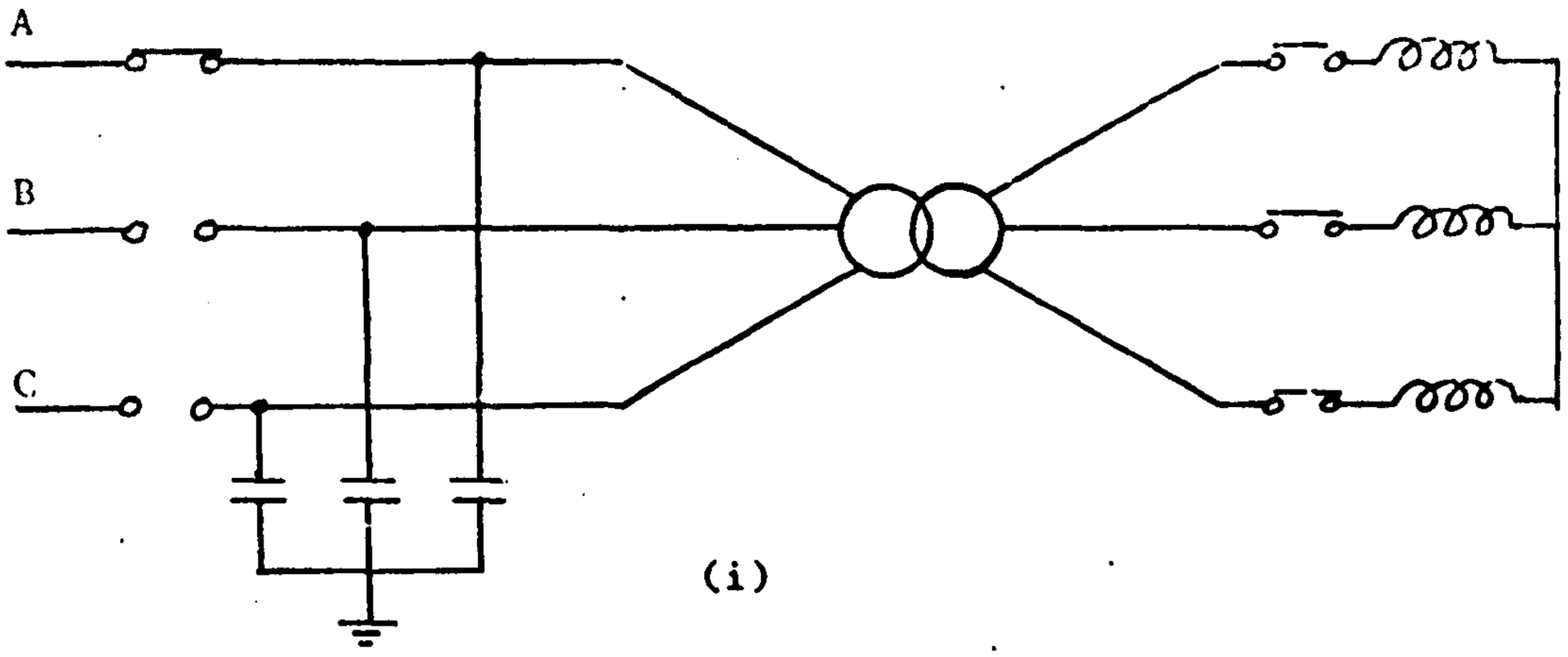

(i)

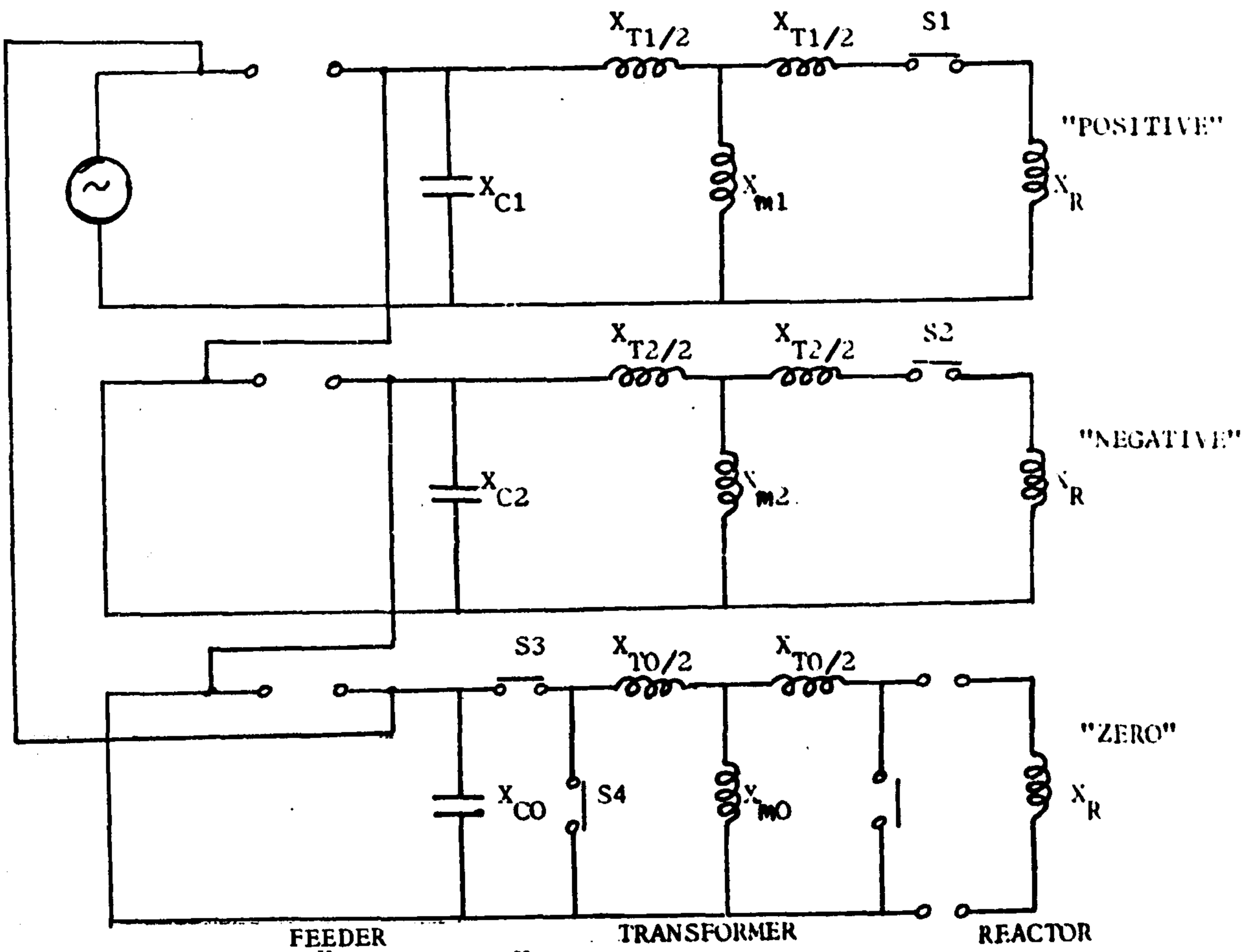

(ii)

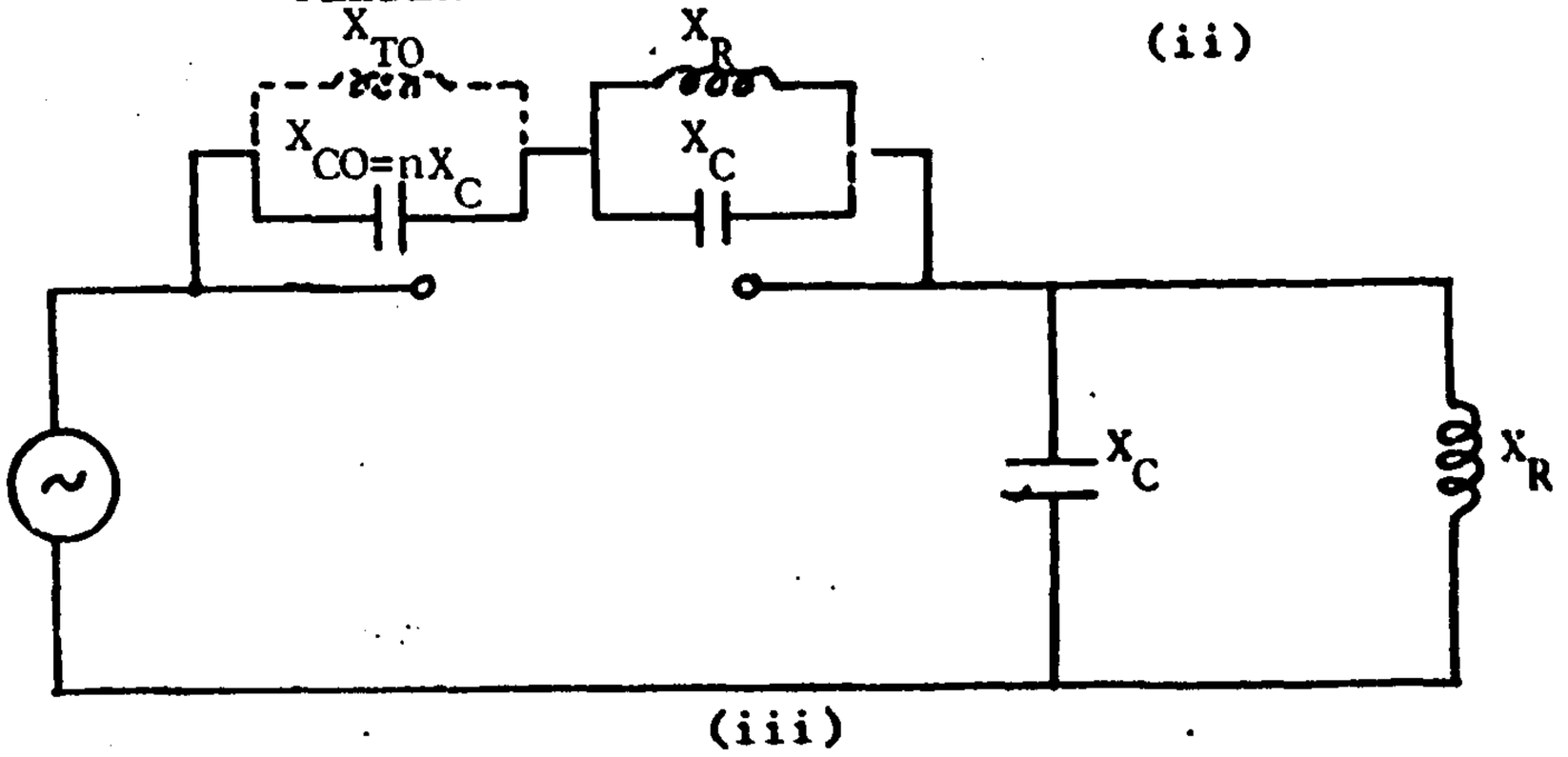

(iii)

Fig. 2.3 Two phase conductors open
(i) Circuit diagram
(ii) Sequence component network for different transformer connections.
(iii) Simplified equivalent circuit.

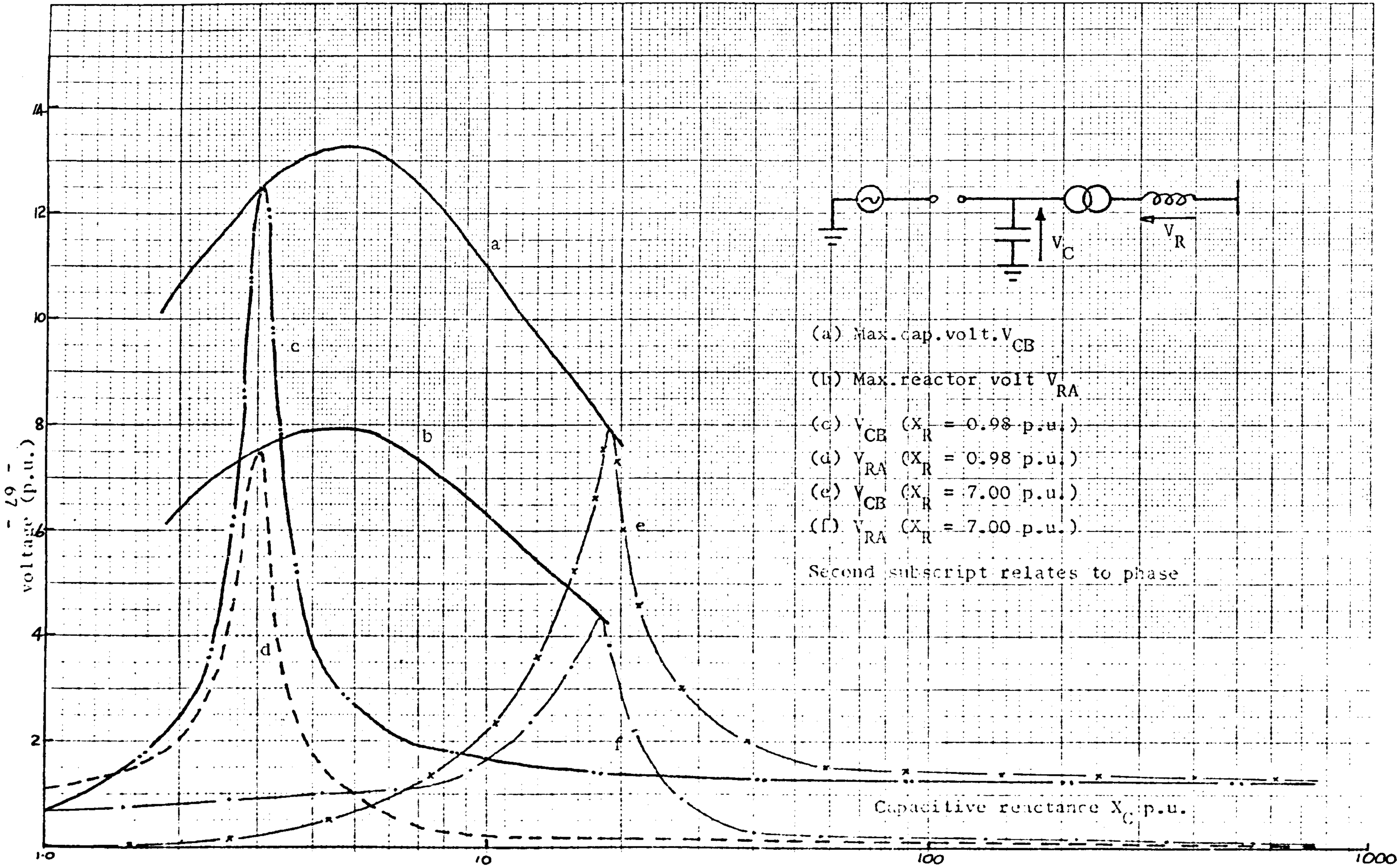

Fig. 7.4 Maximum capacitor and reactor voltages for two phases (B and C) open and transformer connected star/delta (isolated neutral), as a function of X_C and X_R.

twice the values of those obtained when only one phase is open are produced. The relation for resonance ($X_C = (2+n)/n \cdot X_R = 3X_R$ if $n = 1$) is confirmed by these curves. As in the case of one phase open, maximum capacitor overvoltages occur on the open phases while for the reactor, maximum overvoltages are produced on the phase corresponding to the closed phase. The loci of resonant overvoltage peaks again reveal an increase to a peak value followed by a steady decline as the reactance of the reactor increases.

If the neutral point of the transformer is earthed, analysis of the simplified circuit of Fig.2.3 (iii) (including the dashed section) will show that the resonance condition is satisfied by the relation.

$$X_C = \frac{(2 + n)}{n} \cdot \frac{X_{TO} X_R}{2X_R + X_{TO}}$$

In practice, X_R is usually much larger than X_{TO}. The above expression could therefore be reduced to

$$X_C = \frac{2 + n}{2n} \cdot X_{TO}$$

This relation also defines the necessary conditions for resonance in the absence of the compensating reactor.

2.4.3 Ferroresonance caused by open phase conductors

The application of unbalanced voltages at the transformer terminating the line, as a result of open phase conductors, may excite ferro-oscillations between the transformer magnetising reactance and the distributed capacitances of the line. The oscillations depend on the parameters of the circuit, the initial conditions and the characteristics of the transformer and the switching device. This problem is perhaps more prevalent at distribution voltages[2,29-32] where economic considerations favour the use of single phase switching. This is particulatly true where pad-mounted cable-connected distribution transformers are being switched in sequence. This is because

the capacitive reactance of the cable is more likely to be in such a proportion to the transformer magnetising reactance as to produce ferro-oscillations, than would be the case if an equal length of overhead line were used.

This phenomenon is not, however, confined to distribution systems. Certain malfunctioning of the three phase circuit breaker could leave the transformer energised through one or two phases for several cycles. This, together with accidental breakage of one or two phase conductors, could create conditions conducive to ferro-resonance.

The phenomenon described above occurs on an effectively earthed system terminating in a transformer with any winding connections, except the star-star connection with both neutrals earthed. In contrast to the linear resonance case discussed in section 2.4.2., the non-linearity of the transformer magnetising curve produces a resonance curve which is relatively broad and multi-valued. It is therefore not necessary for exact resonance conditions to be satisfied since excessive voltages may still be produced as the peak of the resonance curve is approached. It has been found that suitable secondard loading could eliminate this phenomenon.

Peterson[2] has carried out a detailed investigation of this phenomenon and he has derived certain relations which may be used to predict whether ferro-oscillations would be produced for given circuit constants. His method of analysis is however, based on linear circuit theory and ignores the effects of transformer saturation. Details of the diagrams used to explain this phenomenon are shown on Figs. 2.5 and 2.6 for one and two phases open, respectively.

2.4.3.1 <u>One open phase conductor</u>

The single line and circuit diagrams of the system for one phase open are shown on Fig. 2.5 (i) and (ii) respectively. The vector

(i)

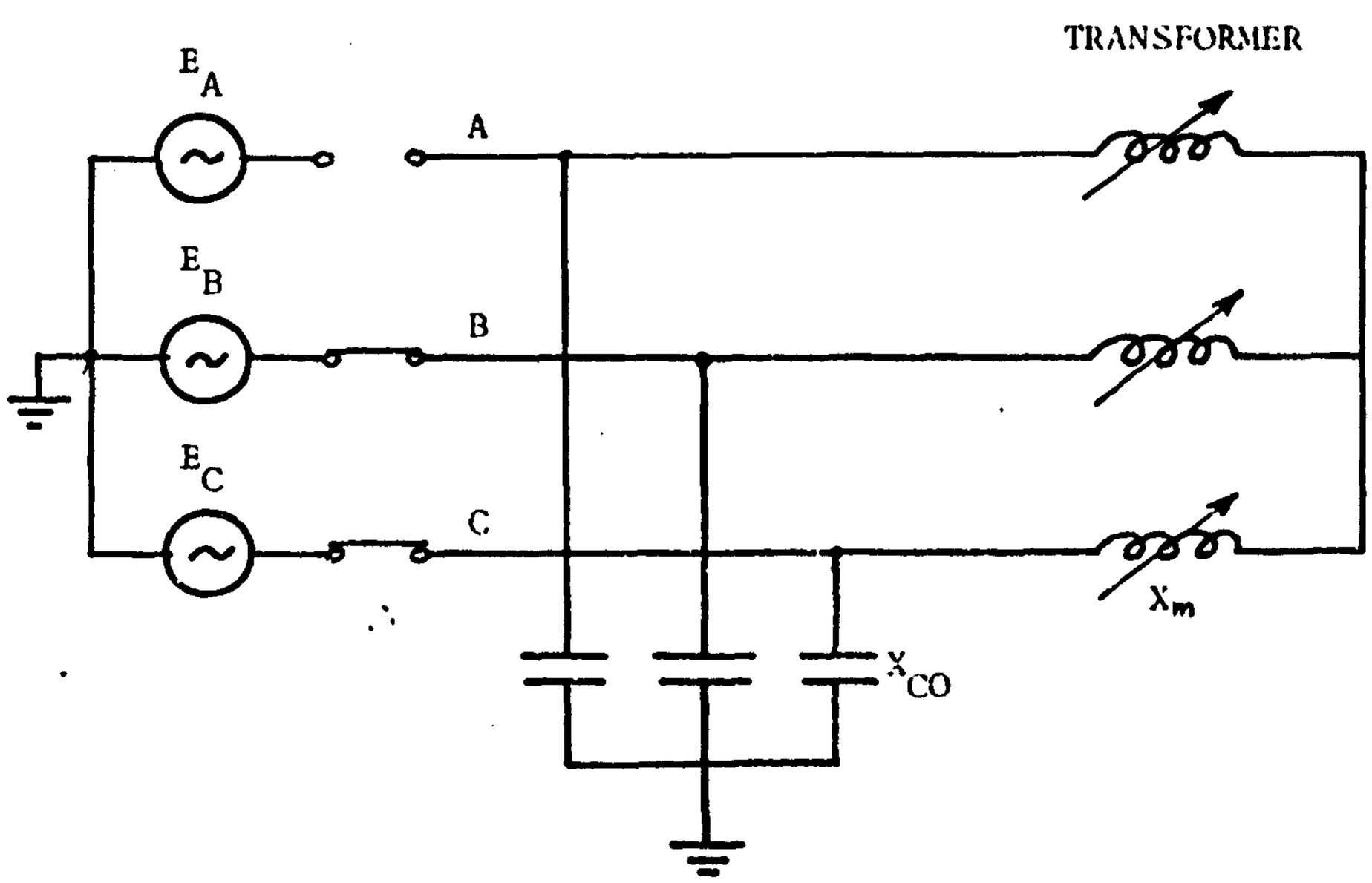

(ii)

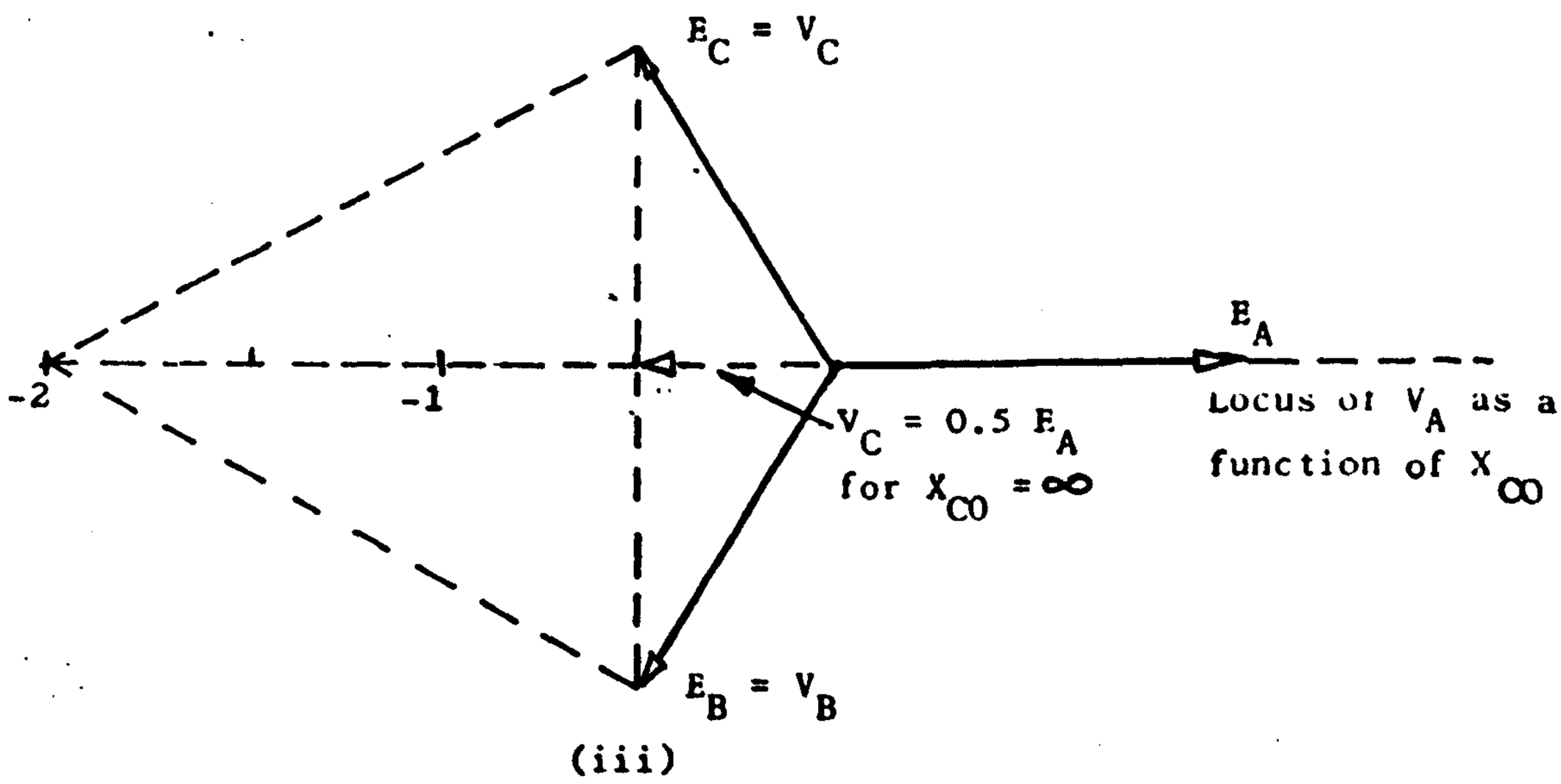

(iii)

Fig.- 2.5 One open phase conductor
(i) One-line diagram
(ii) Circuit diagram
(iii) Vector diagram

diagram of Fig 2.5 (iii) illustrates the behaviour of the voltages across the line capacitances as a result of this abnormality. This diagram shows the balanced source voltages E_A, E_B and E_C of unit value under normal operating conditions which also appear across the corresponding line capacitances (i.e V_A, V_B and V_C). Where phase A is open, V_A moves along the locus indicated and its position is defined by the ratio of X_{CO}/X_m. (X_m is the value of the transformer magnetising reactance at rated voltage). Assuming that X_{CO} is infinite, V_A will attain a value of -0.5 p.u. which is the average of the voltages V_B and V_C. As the ratio X_{CO}/X_m decreases, V_A moves further to the left. When V_A= -2 p.u. for a certain ratio, the vector diagram shows that balanced phase-to-phase voltages of reversed phase rotation would obtain. This condition could cause reversal of the direction of rotation in motors. Further decrease in the ratio X_{CO} could produce large ferroresonant voltages. The non-linear characteristics of the transformer allow more than one mode of oscillation to occur, depending on the initial conditions prevailing following the switching action. As the ratio is decreased even further, the possibility of linear resonance being excited between the saturated reactance of the transformer and the capacitive reactance of the line arises. Voltages in excess of those obtained under ferroresonant conditions, limited only by the system losses, could result.

2.4.3.2 Two open phase conductors

Fig 2.6 shows the one line and circuit diagrams for the case where two phase conductors are open, and the corresponding vector diagram. The latter shows the balanced source voltages when the system is operating normally. With the two phases (B and C) open the voltages V_B and V_C move along the locus indicated, their position being fixed by the ratio X_{CO}/X_m. If the zero sequence capacitive

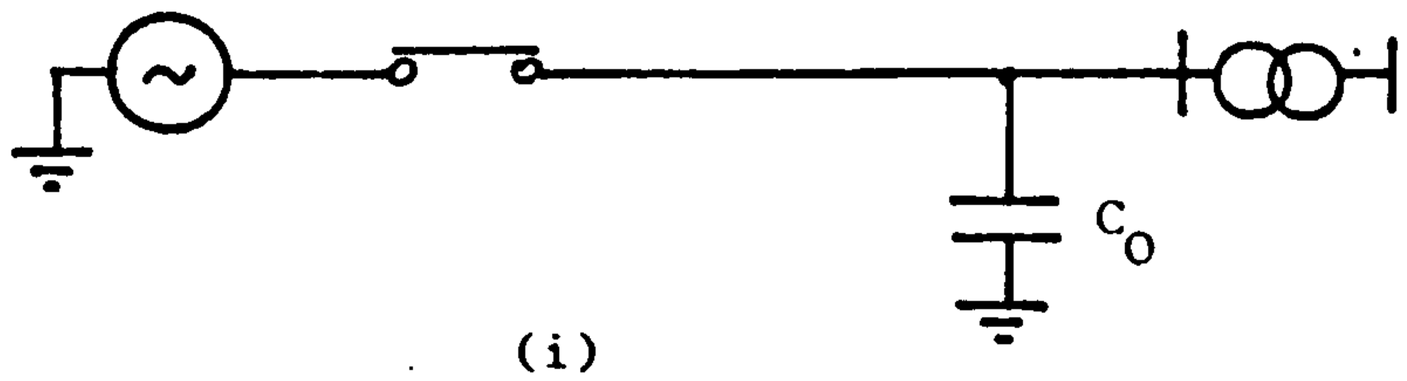

(i)

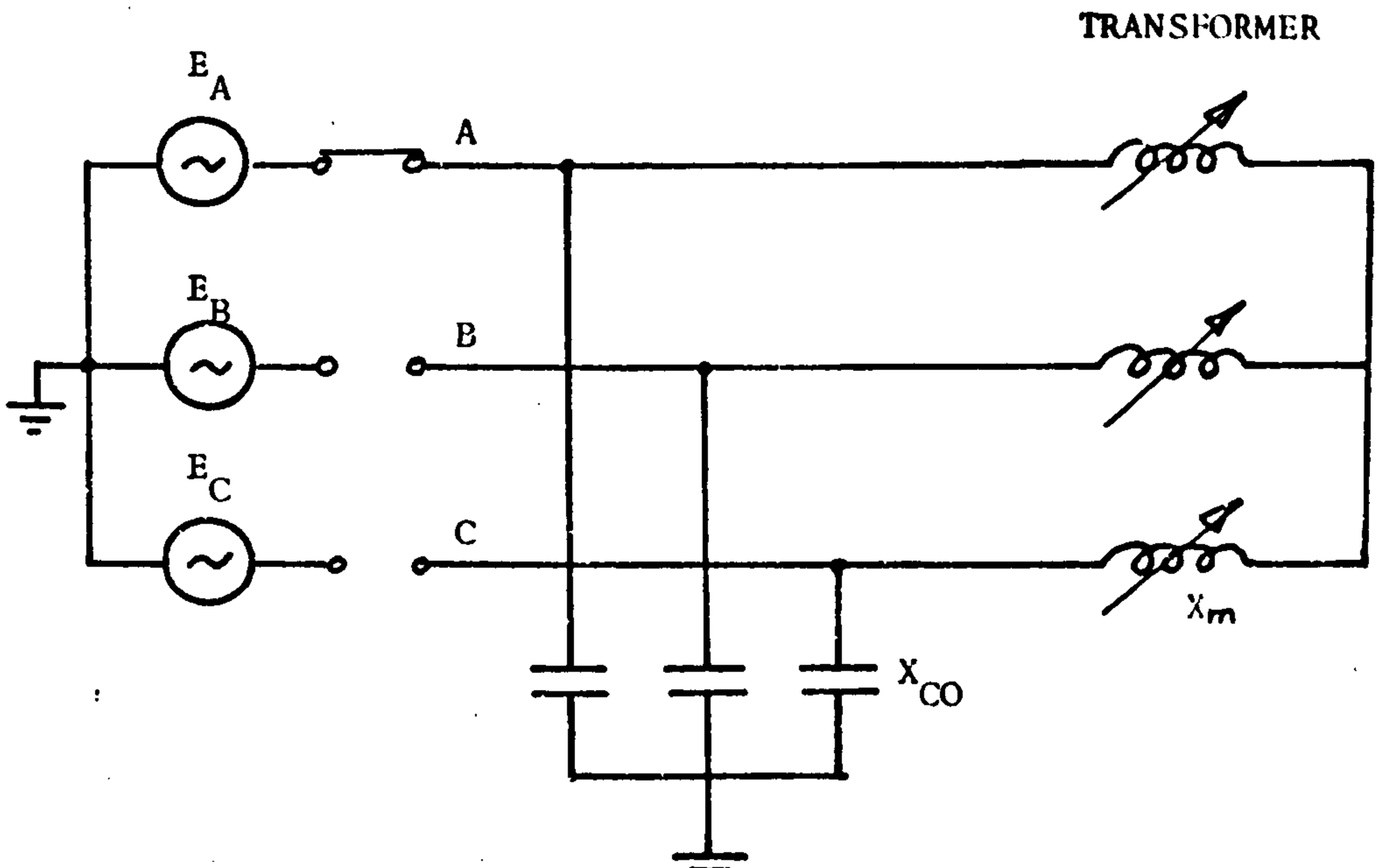

(ii)

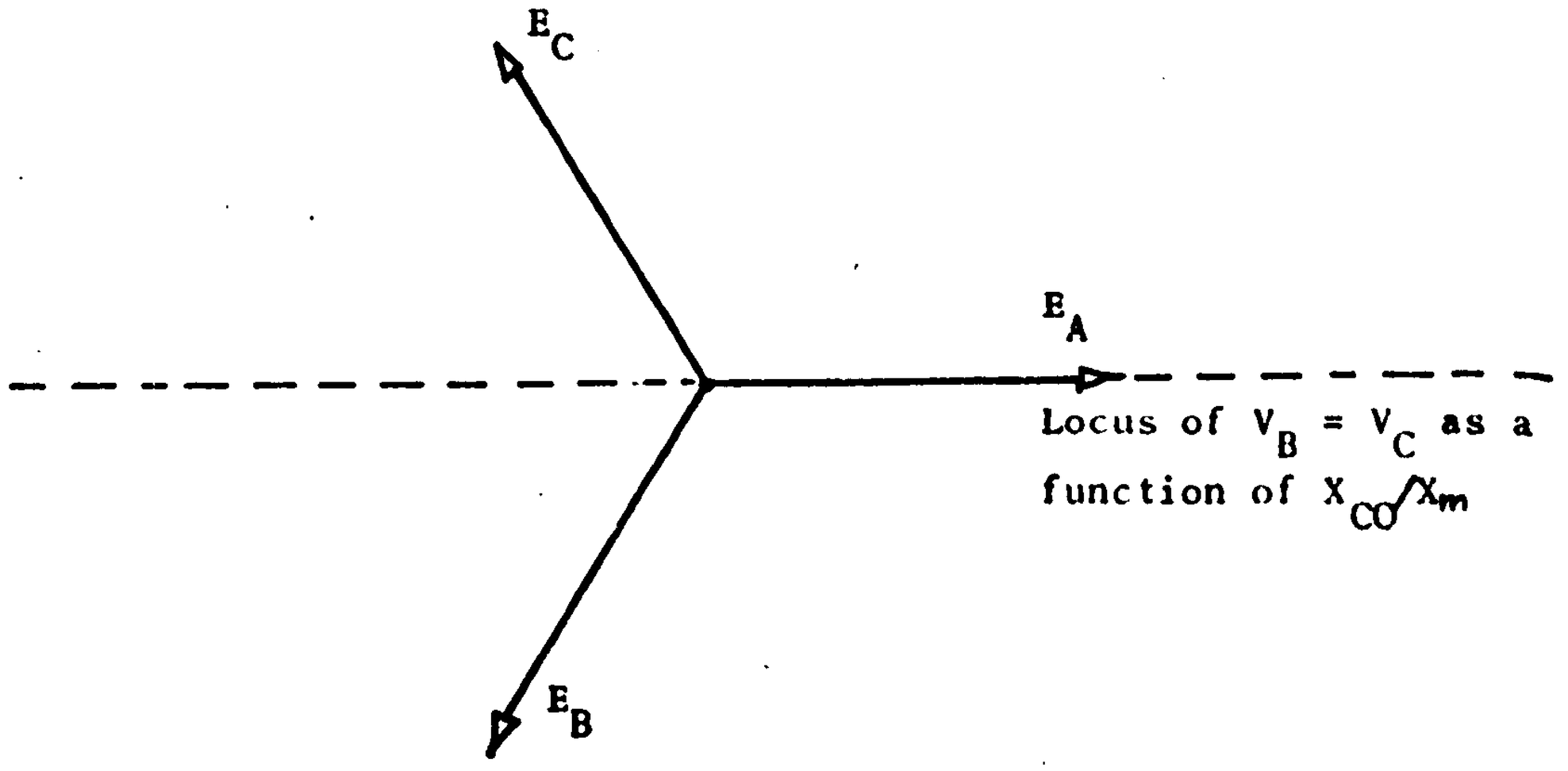

(iii)

Fig. 2.6 Two open phase conductors
(i) One-line diagram
(ii) Circuit diagram
(iii) Vector diagram

reactance of the line is infinite, then $V_B = V_C = V_A = E_A$ since there is no path for current flow. As the ratio X_{CO}/X_m is decreased, the voltages on the open phases, V_B and V_C, will move to the right along the locus shown on the vector diagram and may attain excessive values. Further decrease in the ratio X_{CO}/X_m could again initiate linear resonance oscillations as described above.

2.4.4 Resonant coupling in double circuit feeders

Most transformers in Britain have a tertiary winding which may, among other things, provide a connection for low voltage shunt reactor. Such reactors are normally required to compensate line charging requirements and stabilise voltage at the end of a long transmission line under light or no-load conditions. Where such a transformer and reactor unit terminates one circuit of a closely coupled double circuit line, when this circuit is being dropped, it will form an oscillatory circuit with the effective coupling capacitance between the circuits. If the natural frequency of this circuit is in close proximity to the fundamental system frequency, the resulting oscillations could have severe repurcussions in terms of reclosing transients, and the insulation levels of the line and connected equipment could be violated.

The magnitude of the coupled voltages due to the unbalances in the electrostatic field depends on the characteristics and the physical dimensions of the conductors comprising the double circuit configuration. A value of 15% of the voltage on the energised line is typical. It should be noted, however, that although such induced voltage magnitudes (in the absence of resonance) are of little significance if the two circuits have similar insulation levels, this may not be the case if these voltages are coupled onto a circuit of lower insulation level. This would be the case if the two circuits

on the same tower have different voltage ratings. Analysis of the coupled voltages into sequence components indicates that they usually contain a significant zero sequence component. In addition to the positive sequence resonant oscillations, therefore, resonant excitation in the zero sequence mode is possible. The frequency response of the oscillatory circuit may therefore exhibit two prominent peaks associated with the positive and zero sequence components of the exciting waveform.

The salient features of this phenomenon, and the results of analysis using a mathematical model of the circuit, will be discussed in more detail in Chapter 9. An analytical method for predicting the occurance of such resonant oscillations will be derived, and the several factors which influence the amplitude of these oscillations will also be investigated.

2.4.5 Ferroresonant oscillations in double circuit feeders

The conditions leading to ferroresonance in double circuit feeders are similar to those discussed in section 2.4.5 above. The essential difference is that, in this case, compensating reactors at the transformer tertiary are ommitted. The effective reactance at the end of the line being dropped would therefore essentially consist of the non-linear magnetisation reactance of the transformer. This difference alters the character of the resulting oscillations significantly. The ferroresonant oscillations are produced essentially by the cyclic interchange of the energy initially trapped on the line at the instant the line is dropped, between the electrostatic field of the line and the electromagnetic field of the transformer (as explained in section 2.2.2). In this case, however, since the other circuit of the double circuit line remains energised, electrostatic coupling between the two circuits would provide means of replenishing some of the energy lost. Depending on the balance between the supply

and loss of energy in the oscillatory circuit, these ferro-oscillations may be sustained for a considerable length of time. The resultant repurcussions on transformer overheating, re-energisation overvoltages and safety aspects, could be severe.

This phenomenon depends on a multiplicity of factors. The most prominent are the initial conditions existing subsequent to the line being dropped, the characteristics and geometry of the transformer core, the transformer winding connections, the characteristics and physical configuration of the conductors of the double circuit line and the losses inherent in the system. These effects will be investigated in Chapter 10, with the aid of an analytical technique combining the travelling-wave phenomena on the lines with the state equations representing the electrical and magnetic behaviour of the transformer.

2.5 Conclusion

In this chapter, the many and varied facets of overvoltage generation when transformers connected integrally to the feeder are being switched, have been reviewed. The conditions which are likely to produce excessive or sustained voltages have been identified, and the areas requiring further study have been defined. Some of these factors will be investigated in subsequent chapters.

In particular, the phenomenon of resonant excitation of transformers terminating a feeder will be examined in more detail in Chapters 5, 6 and 8. The effects of linear resonance and ferroresonance in double-circuit feeders will be investigated in Chapters 9 and 10 respectively, using the new compensation method utilising the lattice diagram and lumped parameter techniques.

The presence of a transformer terminating a feeder introduces peculiar phenomena in the response of the composite feeder to certain disturbances. The most prominent feature in the behaviour of such circuits is the interaction between the capacitive reactances of the feeder and the transformer reactances and its magnetisation characteristics. The cyclic interchange of energy between the electric and magnetic fields associated with the feeder and the transformer could, in certain cases, produce resonant voltage oscillations or sustained ferro-oscillations. In the former case, excessive voltage amplitudes could be attained while the effects of the latter are manifest in transformer overheating and increased noise level.

In spite of the mitigating effects of such factors as the inherent system losses which act to damp the oscillations, certain measures may be necessary to prevent such phenomena from being initiated or to alleviate their effects.

These measures include:-

(i) avoidance of those circuit constants and configurations which are potentially susceptible to such oscillations,

(ii) observance of certain operating restrictions, and

(iii) deliberate insertion of resistors of suitable value at appropriate locations in the system to dissipate the energy.

In the case where these oscillations are sustained, the protection of the surge diverters connected at the transformer may not be adequate. On the contrary, the repetitive operation of the diverters under such conditions could lead to the destruction of these devices which would also impose severe stress on the insulation of other station equipment. Until such time when surge diverters of improved durability, capable of withstanding multiple operation, are developed, system designers and operators will continue to rely on the ability to predict and control these overvoltages by some other means. This, of necessity, requires an extensive and thorough knowledge of all the causative factors and the resultant voltage waveforms, magnitudes and frequencies as well as the probability of occurance.

C H A P T E R 3

METHODS OF ANALYSIS

3.1 Introduction

In Chapters 1 and 2, a review of system overvoltages in general and, in particular, overvoltages associated with transformer feeders, was presented. These overvoltages are created by disturbances internal or external to the system, and both experimental and analytical techniques have, in the past, been utilised to study their effects. The purpose of this Chapter is to present a brief description of the methods presently available in studying transients in power systems. The next Chapter will be devoted to the new compensation method combining the lumped parameter and lattice diagram methods to determine the transient response of transformer feeders.

The analogue and digital computers have, for many years been widely used as tools for transient studies. The most commonly used analogue devices are the transient network analyser (TNA) and the electronic differential analyser (EDA). The TNA is essentially a lumped parameter method whereas the EDA in effect solves the equations describing the system. The main advantage of these two aids is their flexibility during operation and the ease with which a particular circuit constant could be optimised to achieve a desired condition. There is, however, a limitation on the size of the model, particularly when greater accuracy is desired.

Digital computers, on the other hand, are fast, versatile and capable of high accuracy. This accuracy is, however, limited by the degree of resemblance achieved between the mathematical model and its actual counterpart.

These two computing aids are frequently used in co-ordination for transient studies. The advantages of the TNA during the preliminary investigations or when minimising certain system conditions may be combined with the higher accuracy capability of the digital computer in specific cases. Digital methods may also be used to provide accurate constants for the TNA components.

The methods used in transient studies may be divided into three basic categories. These are:-

(i) the analogue simulation,

(ii) the transform method, and

(iii) the travelling wave method.

In the analogue simulation, the equations which describe the operation of the artificial system are made analogues to those representing the actual system. While the EDA could incorporate a facility for simulating distributed parameter elements, the TNA is less accurate when applied to such elements.

The second method involves the transformation of the partial differential equations describing wave motion into either the frequency domain (Fourier transformer method) or the complex frequency domain (Laplace transform method). The final solution in the time domain is obtained by an inverse transformation. For all but simple systems, this method is usually economically prohibitive, particularly when used to determine the response at several points on the system. The major advantage of the Fourier transform lies in the fact that the frequency dependence of line parameters may readily be incorporated in the analysis.

The third category includes methods which solve the wave equations such as the Uram and Miller, Schnyder-Bergeron and lattice diagram methods. The latter two methods are digital computer adaptations

of graphical techniques for solving the wave equations. These methods are capable of accurately reproducing the travelling-wave phenomena in lines and cables, provided the variation of inductances, resistances and speed of propagation with frequency is accurately simulated.

3.2 Analogue simulation

The TNA is the most widely used analogue computer. It is basically a scaled electrical model of the actual system. The EDA essentially solves the differential and algebraic equations representing the system. These two computing tools are described below.

3.2.1 Electronic differential analyser

The EDA is a general purpose analogue computer which solves the system equations using electronic units to perform certain basic operations (e.g. summation, multiplication and integration). The system variables are represented by voltages at various points within the model, and the results may be displayed on the cathode ray oscilloscope (CRO) or on recorders. Actual system response to changes in certain system parameters can immediately be determined by variation of resistances and capacitances corresponding to the variable system quantities.

The lumpy constants of the system can be accurately simulated on the EDA. Transmission lines and cables may be represented either by their lumped parameter equivalents or by travelling wave methods. The main disadvantage of the former method is the large number of components, such as integrators, required to produce more accurate results. The travelling wave method requires additional equipment to simulate wave travel times along the lines and reflection effects. This equipment consists of multi-channel pure transport delay time units capable of storing surges of arbitrary waveform and returning these to the computer at a predetermined instant [40]. Although the attenuation effects can be represented, the frequency dependence of attenuation and wave velocity is not included in this method. Component size limitations restrict the application of this method to simple circuit arrangements.

3.2.2 Transient network analyser

The TNA is an established tool for studying electrical transients. It is an adaptation of the well known a.c. network analyser and is basically a scaled electrical analogue of the real system. Transmission lines are simulated by a cascaded series of lumped parameter equivalent π-networks, lumped system elements by their corresponding scaled components and transformers by miniature electromagnetic models or by their equivalent circuits. The accuracy of the TNA depends largely on how closely the model components resemble their actual system counterparts, particularly with regard to those components which are functions of frequency.

The TNA used in studies discussed in later Chapters is a combined steady-state and transient analyser installed at the University of Strathclyde and described by Pender [41]. The analogue of the actual system is constructed from several adjustable resistance, inductance and capacitance decade units, electromagnetic single phase transformer units and transmission line models either built separately or synthesised from the variable decade impedance units. Photographic records of sections of the analyser are shown on Figs. 3.1 and 3.2

The power source is capable of producing a low impedance symmetrical three-phase supply free from harmonic distortion, with adjustable amplitude. Source characteristics may be modelled by addition of appropriate source inductance, capacitance and resistance. Circuit breaker operation or fault occurrence is simulated by a set of electronically controlled point-on-wave switches. These switches are capable of closing and opening repetitively at preselected instants within a period of 10 cycles at model frequency (398Hz). The making and breaking instants are set by positions of the rotary switches shown on Fig 3.1. A set of such switches may also be used to reset

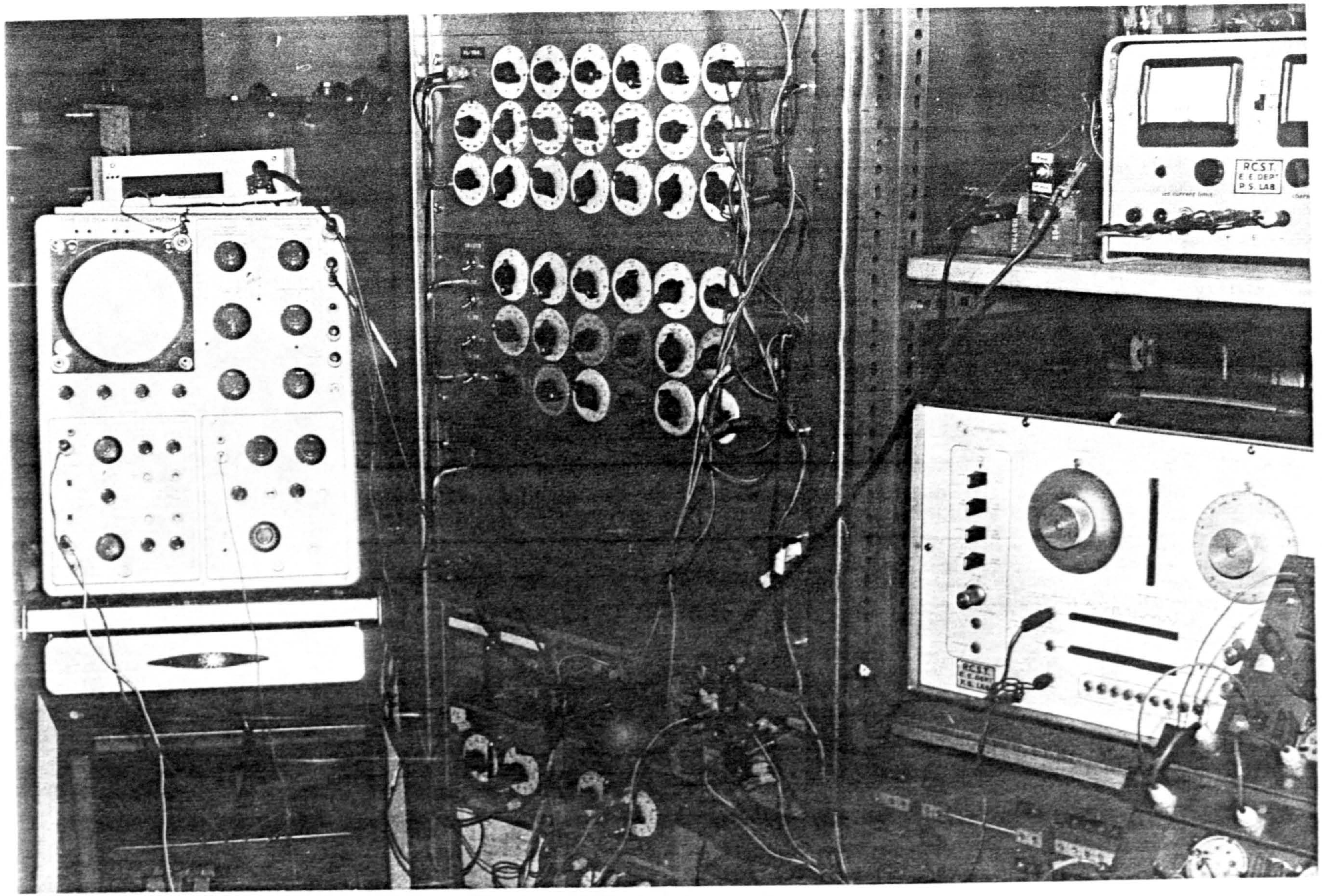
RCST.
E.E. DEPT
P.S. LAB

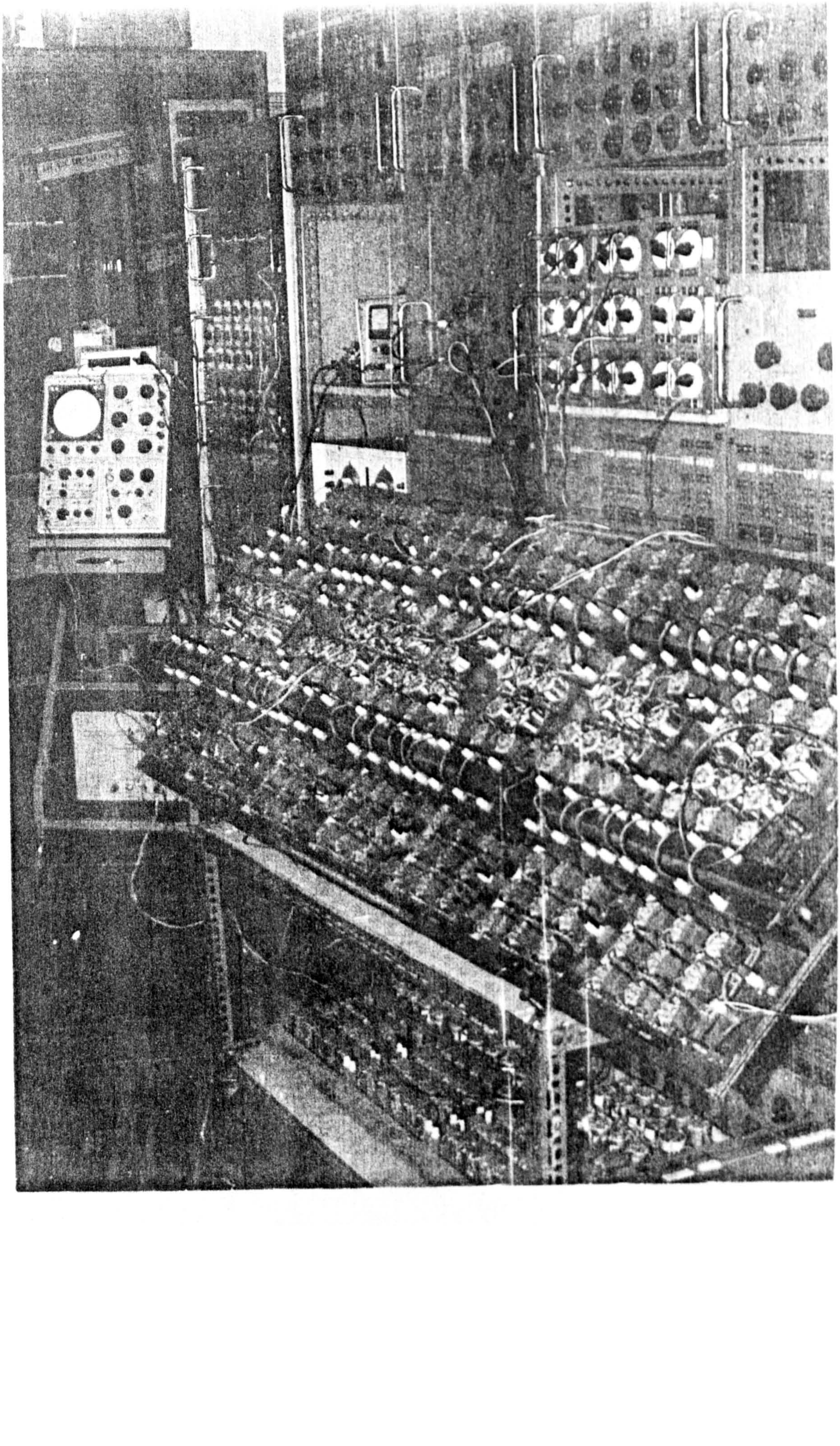

the system after the expiry of the period under investigation, and before the sequence of the main switching operation is restarted. The reset process is achieved by providing means of draining the residual charges on the lines through suitable resistors. The cyclic alternation of energisation and reset periods which results enables the transients to be viewed at ease on the repetitive CRO display. The CRO is triggered synchronously with each recurrent 10-cycle period. Tektronix oscilloscopes type 551 and 564 with pre-amplifier power supply units were used and records of the transients were made with a polaroid oscillographic camera. An integrated peak-reading circuit operating in conjunction with a digital display unit was also incorporated in the instrumentation. This circuit is of great value when certain conditions are to be optimised or when maximised conditions are to be identified over a wide range of variables.

The analyser is designed to operate at 398 Hz (ie ω = 2500 rad/sec). This is approximately 8 times the actual system frequency, and consequently, a time scaling factor of $\frac{1}{8}$ applies.

3.2.2.1 Transmission line models

The available single phase positive sequence model transmission line comprising a cascaded connection of 48 π-sections was originally built to investigate transient recovery voltages on the S.S.E.B. 275 kV network [41]. Each section represets 5 miles of a fully transposed line. Subsequently, a three-phase model of the line consisting of 300 miles of 5 mile π-sections, incorporating the transmission line zero sequence characteristics, was constructed. The earth return path is simulated by inductances and resistances correct at a given frequency. This representation made possible investigations of the system under both balanced and unbalanced operation such as sequential closure of the circuit breaker and fault

occurrence. Fig. 3.2 shows three 100 mile sections of the three-phase line model. Two of these sections may be connected in conjunction with mutual circuit elements to simulate a double circuit line, as shown on the photograph.

Representation of a line by a single π-section reproduces actual system behaviour accurately at one frequency only. This representation may be adequate for steady-state studies, but it is unacceptable for transient investigations. In the latter case, it is necessary to connect several π-sections in cascade. The larger the number of sections used, the more accurate will be the response. The band width in this case will be given by the natural frequency of a single π - section. At frequencies above and well below the cut-off frequency, the performance of the line becomes highly inaccurate. Cables may also be represented by a similar ladder network. For relatively short lengths of cable, however, representation by a capacitor of a value equal to the shunt capacitance of the cable is usually adequate.

Figs 3.3 (a) and (b) show the π-equivalent circuit representation of a single-phase and three-phase line respectively. The subscripts 0 and 1 designate zero and positive sequence quantities respectively. The constants of the line were derived from the physical configuration and parameters of the actual transmission line using a standard digital computer program already available. The effects of earth penetration, earth wires, conductor bundling and conductor sag are included. The program evaluates the surge impedance of the line as well as the positive and zero phase sequence impedances and susceptances. The sequence impedances are then used to calculate corresponding per unit parameters for each 5-mile section of the actual line. The base MVA and kV of the line simulated are 1000 and

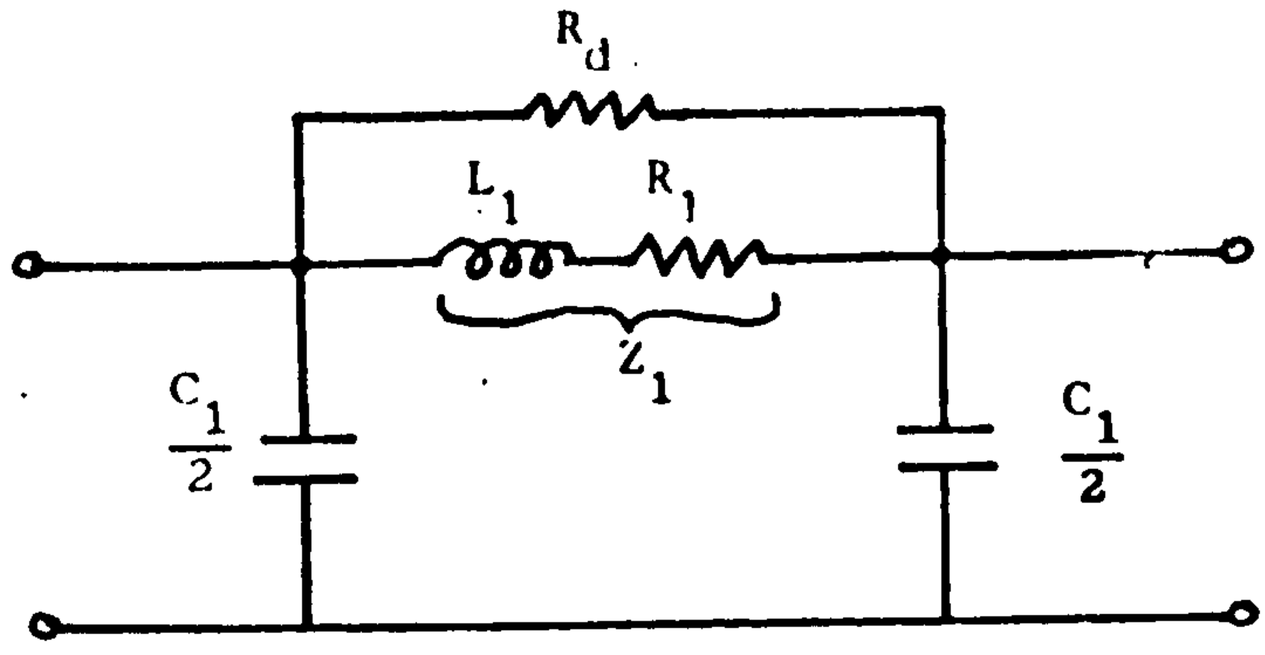

(a)

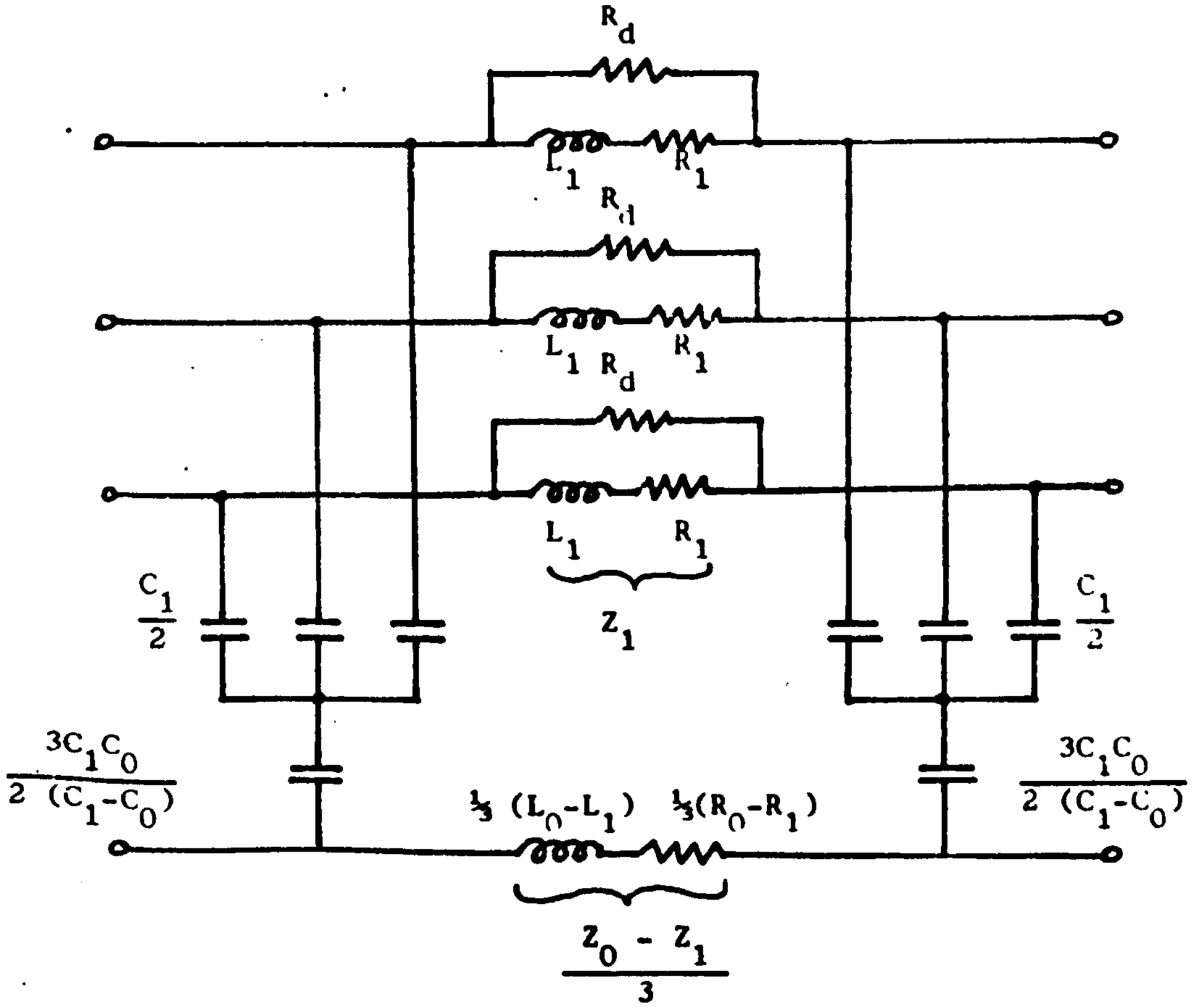

(b)

Fig. 3.3 π -equivalent circuits of compensated transmission lines :
a) Single phase line
b) Three phase line

275 respectively. To obtain model parameters, these per unit impedances are scaled in accordance with the TNA base quantities assumed (i.e. 1000 MVA, 200 ohms and 2500 rad/sec). Consequently, the resistance inductance and capacitance of the actual line will be scaled by the ratios 0.38, 3 and 21 respectively.

Representation of the continuously distributed parameter line with a finite number of π-sections introduces unrealistic oscillations known as Gibbs oscillations. These appear superposed on the line response to a voltage step. The phenomenon is analogous to the spurious oscillations inherent in applications of the Fourier transform method to evaluate the transient response of a system, using a truncation of the infinite range of integrals. In order to achieve a closer correlation between actual system and model response, it is necessary to provide compensation for these oscillations by shunting the series elements of each π-network with an appropriate value of resistor, R_d. In this case, a value of 4700 ohms has been found to be adequate for this purpose.

3.2.2.2 Transformer models

Transformer models for use in conjunction with the TNA may broadly be classified into the following categories [42]:-

(i) the equivalent circuit model,

(ii) the geometrical model, and

(iii) the electromagnetic model.

Several variations of the equivalent circuit representations exist, depending on the type of problem being investigated. In certain studies discussed in later Chapters, the π - equivalent circuit representation was found to be adequate. The series elements of this circuit represents the total leakage reactance of the transformer, and the shunt components consist of the effective transformer capacitance

to earth. The interwinding capacitances are ignored since these are not particularly significant at the frequencies encountered in the investigations. With this representation, simulation of different transformers can readily be achieved by variation of the equivalent circuit components.

In a geometrical model, the linear dimensions of the actual transformer are scaled down by the same factor. The conductivity of the windings and the permeability of the core are also scaled. This model suffers from the disadvantage of large size due to an upper limit on the scale factor, and lack of versatility. The requirement that the resistivity and permeability scale factors should be the same as the linear dimension scale factor cannot, in most cases, be met. The time scale factor must also equal the linear scale factor. This introduces constraints on the applied voltage frequency and wavefront.

The electromagnetic model introduced by Abetti [42] combines the arbitrary time scale attributes of the equivalent circuit representation with the geometric similitude of the geometric model, thus eliminating the shortcomings of the models previously described. The electrostatic behaviour of the transformer is simulated by an equivalent circuit model using variable capacitance decade units, while the electromagnetic properties (including the non-linear characteristics) are simulated by a geometric model. Although the magnetising characteristics are fixed for a given model, the leakage reactances may be increased by addition of linear reactors in series with the transformer. The fact that the resistance of the model tends to be higher than in practice poses a difficult problem. It is, however, possible to compensate the resistance at normal system frequency with the aid of complex electronic negative resistance circuits. Although an accurate simulation of the frequency dependency of the transformer

parameters is possible, it relies to a great extent on an accurate knowledge of the high frequency behaviour of the transformer. This information is not always readily available.

A detailed description of the electromagnetic model used in some of the investigations discussed later, is contained in the Associated Engineering Industry (AEI) departmental engineering report[43]. Each single phase transformer core consists of a high permeability, low loss, 'C' core material, which, although designed to operate at 50Hz, will be run at the TNA frequency of 398Hz. This reduces the relative proportion of the magnetising current and approximates closely the behaviour of the actual transformer. Each unit is rated at 250/25V. Insulated screens are interposed between the windings to reduce the interwinding capacitance. Separate decade capacitor units are provided to permit variation of this component. Further details of the transformer, obtained from experimental tests [43], are summarised on Table 3.1

MEASURED PROPERTIES OF THE ELECTROMAGNETIC MODEL

REFERRED TO THE HIGH VOLTAGE WINDING

Transformer Unit	R-phase	Y-phase	B-phase
D.C. winding resistance (ohms)	16.6	16.7	16.5
Leakage inductance L_s (mH)	24.6	23.0	23.3
Ratio of L_m/L_s at rated current (L_m = magnetising inductance)	450	470	470
Internal Q = wL_s/R at 1000 Hz	9.3	8.6	8.9
Interwinding capacitance (pF)	148	151	158

3.3 Lumped parameter analytical model

This method is a mathematical analogy of the TNA. Lumped and distributed parameter components are represented by lumped, T, L or π -sections consisting of inductances capacitances and resistances. Differential equations of the second order are used to describe each mesh or nodal point. Solution of these equations usually consists of transformation into differential equations of the first order which are then solved simultaneously using techniques such as Runge-Kutta or Kutta-Merson methods. The transient response may also be obtained by first transforming the differential equations into the complex frequency domain using Laplace transforms. The operational solution to a particular excitation is then expressed as a quotient of two polynomials. Inverse Laplace transformation is then applied to evaluate the response in the time domain.

This method can readily accommodate non-linear properties of lumped elements such as transformers, saturable reactors and surge diverters. The non-linear differential equations which define these components are solved simultaneously with the differential equations describing the rest of the network. The main disadvantages of this method are its inability to simulate accurately the distributed parameter elements and its considerable expense in terms of computer memory size and running costs. To a certain extent, network reductions may be used to economise on computation costs at the expense of accuracy.

3.4 Fourier transform method

In order to accommodate the frequency dependence of system parameters due to skin effect and earth penetration, methods based on the Fourier transform have been suggested[44,45]. Basically, the method requires the calculation of system response in the frequency domain and subsequent retrieval of the time domain response by application of the inverse Fourier transform. As a consequence, the frequency dependence of parameters such as mutual coupling, distortion and attenuation, is embodied in the anlaysis provided the relevant value of the parameters is used for calculations in each frequency component. This method is expensive in terms of computation time due to the multiple integrations which have to be performed. Furthermore, it requires a considerable amount of preparatory work on system data, which is not always readily available.

The inverse Fourier transform may be evaluated numerically over the entire range on the digital computer. This method of solution can be economically prohibitive, particularly when waveforms with relatively fast rise times are involved, or when the response is required at several points. A modified method of solution exists [44,45]. This method is designed to minimise the computation time for integration by truncating the infinite range of integrations. A certain smoothing factor is included in the integrand to eliminate the spurious Gibbs-type oscillations which would result.

This method may be extended to three phase systems by first eliminating the mutual coupling between phases. This is achieved by applying a transformation of the phase quantities into another set of modal components free from mutual coupling. The single phase approach may then be used for each independent mode.

3.5 Travelling wave methods

The various travelling wave methods available are based on solutions of the transmission line wave equations given by:

$$\frac{\partial [v]}{\partial x} = - [R] [i] - [L] \cdot \frac{\partial [i]}{\partial t} \qquad 3.1$$

$$\frac{\partial [i]}{\partial x} = - [G] [v] - [C] \cdot \frac{\partial [v]}{\partial t} \qquad 3.2$$

where $[R]$, $[L]$ and $[G]$, $[C]$ are square matrices defining the line series impedances and shunt admittances, and $[v]$, $[i]$ are column matrices of line voltage and current. Since these methods are orientated towards distributed parameter elements, lumpy components are represented by transmission line stubs, or treated as boundary conditions in the solution of wave equations.

3.5.1 Uram and Miller method

Basically, this method applies the Laplace transforms to the partial differential equations representing the line[46]. This operation in effect reduces these equations into ordinary differential equations of voltage (or current), expressed as a function of distance along the line and the Laplace variable, s. Transformation of coordinates further reduces these interdependent equations into a set of independent voltage (or current) modes which are mathematically free from mutual interactions. As these modal components travel down the line, they are delayed and attenuated separately by using appropriate exponential time delay and attenuation functions. The equations are solved at each time increment, using the boundary conditions existing at junctions and terminations. The voltage (or current) at a particular point may be determined by summing the forward and reverse travelling waves, and applying the inverse modal and Laplace transformations.

The main disadvantages of this method, however, are its inability to simulate the frequency dependent parameters and the considerable computation time and computer memory it requires. It is for the latter factor that applications of this method have been limited to relatively simple systems consisting of one or two transmission lines only.

3.5.2 Schnyder-Bergeron method

This method is basically a digital computer adaptation of the Schnyder-Bergeron graphical technique for determining the transient response of a system [47,48]. It uses the method of characteristics and a step-by-step procedure to solve the wave equations at each discrete point for each incremental time interval. For a loss-less single-phase line with inductance L and capacitance C per unit length, the program effectively uses the d'Alembert general solutions to the line equations given by:

$$i(x,t) = f_1(x - vt) + f_2(x + vt) \qquad 3.3$$

$$v(x,t) = Z \cdot f_1(x - vt) - Z \cdot f_2(x + vt) \qquad 3.4$$

where $Z = \sqrt{L/C}$ and $v = 1/\sqrt{LC}$ are the surge impedance and phase velocity of the line, respectively. The functions f_1 and f_2, which may be discontinuous, describe waves travelling in the positive and negative x directions, respectively. The expressions $(x - vt)$ and $(x + vt)$ are constant and represent the characteristics of the differential equations.

This method may be extended to multi-conductor systems by using modal transformation of the phase quantities and applying the inverse transformations at the relevant points of the system. It is particularly suited to cases where voltage and current calculations are required at several points on the system. Attenuation effects are

simulated by constant series resistances, and the total response is, strictly speaking, only accurate at the single frequency at which the line parameters are evaluated.

3.5.3 Lattice diagram method

This method is, like the Schnyder-Bergeron method, a digital computer adaptation of a graphical method. The graphical technique formulated by Bewley[49] essentially solves the transmission-line equations, and is therefore suitable for distributed-parameter elements. The application of this method, described in detail by Bickford and Doepel[50], among others [51,52], is summarised in this section.

In the adapted version, the lattice diagram is replaced by a branch time-table. All circuit elements are represented by lossless lines defined by their surge impedances and line transit-times. The program uses the basic time interval (BTI) specified to partition the circuit elements into integer multiples of the BTI. This information is stored in the branch time table which is a travel time array used to record the progress of each wave along the circuit elements. The BTI is selected such that its value

(i) is less than the shortest travel time

(ii) is less than one third of the smallest circuit time constants, and

(iii) permits adequate representation of the applied voltage wave.

The reflection and refraction coefficients at each point of discontinuity are computed, stored in an array and used for determining the magnitude of the reflected and refracted waves at these points. Incident waves are multiplied by the appropriate entry on the array, and secondary waves are generated away from the junction or termination. A further

array of voltage at points of discontinuity is formed. Its entries are periodically updated by cumulative summation of all incident and reflected voltage waves.

3.5.3.1 Transfer coefficients

The reflection and refraction (or transmission) coefficients at junctions are respectively defined by

$$K_R = \frac{Z_L - Z_o}{Z_L + Z_o} \quad \text{and} \quad K_T = \frac{2Z_L}{Z_L + Z_o} \qquad 3.5$$

where Z_o is the surge impedance of the line on which the incident wave is travelling, and Z_L is the effective surge impedance beyond the junction point, comprising the parallel connection of all other lines and circuits connected at this point. These two coefficients are related by

$$K_R = K_T - 1$$

These equations also apply to multi-conductor systems, in which case their matrix equivalents will be used.

3.5.3.2 Representation of lumped parameter elements

Lumped components such as transformers, reactors and shunt capacitors are usually simulated by distributed elements with surge impedance and travel time given respectively by

$$Z_o = \sqrt{L/C} \qquad 3.7$$

$$\text{and} \quad \tau = \sqrt{LC} \qquad 3.8$$

where L and C represent the inductance and capacitance of the stub line. Shunt capacitors are represented by open-circuited stub lines and shunt inductances by short-circuited stubs. From equations 3.7 and 3.8.

$$Z_o = L/\tau \qquad 3.9$$

$$\text{and} \quad C = \tau/Z_o \qquad 3.10$$

To represent an inductor, the inductance of the stub line is made equal to that of the lumped element. For an accurate simulation, the capacitance of the stub line given by equation 3.10 should be small, and hence τ should also be relatively small.

Similarly, a capacitor is simulated by a stub line having capacitance equal to the lumped capacitor value. In this case, Z_o and L are given by

$$Z_o = \tau / C \qquad 3.11$$

$$\text{and} \quad L = \tau Z_o \qquad 3.12$$

Again L, and hence τ, should be small in order to obtain an accurate representation.

It has been found necessary to make the value of Z_o at least ten times the surge impedance of all other circuits connected to the same busbar. The value of τ is made equal to half the BTI in the case of shunt inductors, series and shunt capacitors, and to the BTI when series reactors are simulated. In the latter case, the stub line is not short-circuited at the remote end, but is connected to other lines. The more complex arrangement for series capacitor representation is described by McElroy and Porter[52].

A linear shunt resistor is simulated by an infinitely long line (i.e. wave reflections from the remote end are ignored) with its surge impedance equal to the resistor value. Representation of series resistors such as circuit breaker closing resistors will be discussed in section 3.5.3.4 below.

3.5.3.3. Representation of non-linear shunt resistor

A technique for representing a non-linear resistor, whose characteristics are approximated by straight line segments, has been incorporated in the program described by Bickford and Doepel[50]. In effect, this method uses a modification of Thevenin's theorem. At each

time interval, the voltage at the busbar to which the non-linear resistor is connected is calculated ignoring the presence of the resistor. This busbar is then represented by a voltage source of a magnitude equal to the voltage just calculated, in series with a source impedance equal to the surge impedance seen looking into the busbar with the resistor removed (Z_E). The circuit comprising this generator in series with the non-linear resistor is then solved at each time interval for resistor currents. This current is deducted from the current similarly calculated during the preceding time interval to obtain the current increment to be injected into the busbar. The busbar voltage may then be obtained by multiplying this incremental current by Z_E.

Surge diverters may be simulated by a non-linear resistor which is switched into the circuit when the voltage of the busbar to which it is connected exceeds the sparkover level. When the resistor current falls below the diverter extinguishing current, the non-linear resistor is switched out of circuit.

3.5.3.4 Representation of switching operations and waveforms

The closing action of a switch is simulated by injecting a voltage equal and opposite to that which existed across the switch before closure, E_{ab}. Consider a circuit breaker with a closing resistor interconnecting two circuit elements having surge impedances Z_a and Z_b connected to terminals (a) and (b) respectively. Assuming that, prior to closure, the closing resistor (R) is connected to terminal (b) in series with Z_b, the current flowing through the switch after closure is given by

$$I = \frac{E_{ab}}{Z_a + Z_b + R} \qquad 3.13$$

Hence the voltages to be injected into terminals (a) and (b) to simulate the closing operation are given by

$$e_a = \frac{-Z_a E_{ab}}{Z_a + Z_b + R} \qquad 3.14$$

$$e_b = \frac{Z_b E_{ab}}{Z_a + Z_b + R}$$

Interruption of current as when the circuit breaker poles open, may be simulated by injection through the switch of a cancellation current of opposite polarity to the current which would exist if the switch were not opened [49].

By using Duhamels theorem , voltage sources of any waveform are synthesised by means of Heaviside step functions of either polarity, occuring at intervals equal to the BTI. The accuracy with which these waveforms are reproduced on the model depends on the value of BTI selected.

In order to minimise computer storage and computation time, electrically remote parts of the system may be simulated by their step responses, provided these parts consists of essentially linear components. It is necessary to calculate these responses before the main computation by applying a unit voltage step to the section at the junction point through a resistor, using the lattice diagram program. The value of this resistor is given by the effective surge impedance of the main part as seen from the section being reduced.

3.5.3.5 Representation of attenuation and distortion

In order to eliminate mutual coupling which exists between the phases of a line, a modal transformation matrix is introduced to diagonalise the matrix equations [53]. This permits the voltage waves in each independent mode to be separately attenuated and retarded. Attenuation in two of the modes, which have velocities approximately equal to the velocity of light, is relatively small. Waves associated

with the third mode (earth mode) are subjected to higher attenuation and retardation due to earth penetration effects.

The effects of frequency dependent parameters may be simulated by combining the lattice diagram method with the Fourier transform technique. The line step response is first determined for each mode using a method based on Fourier transforms. Each voltage step entering the line is modified in accordance with the associated modal step response using the appropriate attenuation constants. The time response at the end of the line is then obtained by application of the inverse transformation from the modal to the real domain.

3.6 Conclusions

This Chapter contains a brief description of the travelling wave, lumped parameter and transform methods used for studying transients, and the main computing tools presently available. The salient details of the particular TNA used in some of the studies have been presented. The lattice diagram method has been described in greater detail as it forms the basis of the compensation method in conjunction with the lumped parameter analytical method also discussed. This combined method, which brings together the best attributes of the individual methods (i.e. capability of accurately simulating distributed and lumped parameter elements) and eliminates their shortcomings, is presented in the next Chapter.

The TNA, although limited in accuracy and size, has proved reasonably adequate for most studies. It is particularly useful when compiling statistical data or when studying the effects of varying one or more circuit elements over a wide range. The digital computer on the other hand, is capable of high accuracy, depending on the fidelity of the model and the reliability of the data. It is also economical, fast, versatile and its ability to cope with extensive systems is limited only by the computer memory core.

C H A P T E R 4

COMPENSATION METHOD FOR SINGLE PHASE SYSTEMS

4.1 Introduction

A review of the various methods available for studying transients in power systems has been presented in Chapter 3. In particular, it was shown that analytical methods may broadly be classified into the following categories:

(i) transform methods,

(ii) lumped parameter methods, and

(iii) distributed parameter methods.

The transform methods, although capable of high accuracy, can only be applied to linear systems or systems including non-linear resistive elements only. Methods based on lumped parameter representation have the advantage of accurately reproducing the response of lumped-parameter elements including non-linear components, but are incapable of high accuracy when applied to distributed-parameter elements. On the contrary, distributed parameter methods are well suited to lines and cables, but their applications to lumped non-linear elements and complicated lumped constant circuits are subject to unacceptable approximations. There is therefore a need for a method capable of representing both distributed and lumped parameter elements, including those which are non-linear functions of either voltage, current or time, to an acceptable degree of accuracy. Such a method is described in this Chapter and is based on the compensation theorem.

Essentially, the compensation method described here combines the attributes of the lattice diagram method when applied to lines and cables, with those of lumped parameter method when used in conjunction with non-linear elements and complex lumped

constant circuits. Both these methods have been described in the last Chapter and will be compared with the compensation method. Extension of this method to three phase systems will be discussed in Chapter 7.

4.2 Compensation method

The compensation technique for solving circuits containing lumped and non-linear elements has been used in conjunction with the Schnyder-Bergeron method of characteristics and the trapezoidal rule for lumped elements, at the Bonneville Power Administration (BPA)[48,54]. This technique essentially separates the non-linear and lumped section of the network from the linear part. The compensation theorem[55] on which this technique is based, states that the branch containing the non-linear element can be excluded from the network and replaced by a current source which must satisfy both the linear system network equations and the equations describing the non-linear branch.

The compensation method presented here is a development of this theorem. The system is decomposed into two sections. One section comprises the linear network of lines, cables and driving functions, and the other, coupled to the linear section at two terminals, may consist of arbitrary complex lumped and non-linear elements. This separation permits the use of the comparatively simple and fast lattice diagram approach for simulating travelling wave phenomena in lines and cables. The linear and non-linear differential equations describing the line terminal equivalent circuit are solved by the Runge-Kutta fourth order numerical integration technique on a step-by-step basis. An appropriate inter-face technique is used for each basic time interval (BTI) to ensure that the terminal voltage and current conditions satisfy the equations relating to both sections of the decomposed network.

4.2.1 Distributed parameter element

The lattice diagram method described in section 3.5 is used to compute the line terminal voltage $V_T(t)$, with the termination equivelant circuit excluded, for each BTI. This voltage is obtained

by cumulative summation of the incident, $v_i(t)$, and reflected, $v_r(t)$, waves.

i.e. $V_T(t) = V_T(t - \Delta t) + v_i(t) + v_r(t) = V_T(t - \Delta t) + 2v_i(t)$ 4.1

where $V_T(t - \Delta t)$ represents the open circuit voltage calculated at the preceding time step. Voltages at the midpoint, $V_T(t + \Delta t/2)$, and at the end $V_T(t + \Delta t)$ of the current time interval are also computed, as these will be required in solving the differential equations using the Runge-Kutta method. These voltages represent the driving function of the line terminal Thevenin equivalent circuit shown on Fig. 4.1. The Thevenin impedance (Z_T) is the effective impedance seen looking into the lines with the termination equivalent circuit excluded. It is given by the reciprocal of the sum of the surge admittances of all lines connected to the terminals of the equivalent circuit.

For lossless lines this method produces accurate results. An error will be introduced, however, if the line travel time is not an integral multiple of the BTI. This error could be minimised if the BTI is chosen sufficiently small, or it could be eliminated by chosing the BTI in such a manner that the line transit time is divisible into an integral number of BTI's. The latter solution may not be possible if the system being studied consists of several lines or cables.

4.2.2 Termination equivalent circuits

The equivalent circuit of the transformer terminating the line and the secondary load circuits is shown on Fig.4.1 The transformer is simulated by a 'T' equivalent circuit. The series elements represent the primary and secondary leakage impedances. The shunt elements, R_o and M_1, simulate eddy current losses and magnetising inductance, respectively. All these quantities are referred to the primary winding turns.

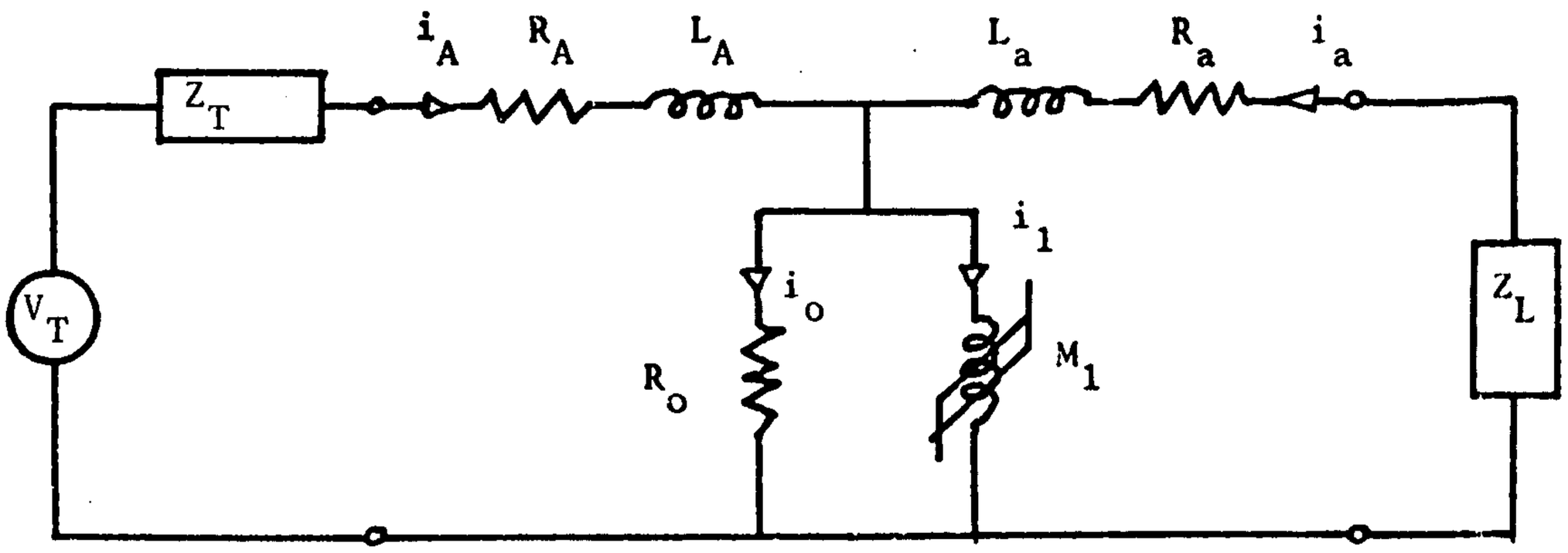

Fig. 4.1 Equivalent circuit for compensation method.

The equations used to describe the state of the termination equivalent circuit at a given instant have been presented in reference[56]. These equations incorporate both the electrical and magnetic properties of the transformer, and are summarised below, with reference to Fig 4.1

$$V_A = R_A i_A + L_A p i_A + N d\emptyset_1/dt \qquad 4.2$$

$$V_a = R_a i_a + L_a p i_a + N d\emptyset_1/dt \qquad 4.3$$

$$0 = -i_o R_o + N d\emptyset_1/dt \qquad 4.4$$

$$i_1 = i_A + i_a - i_o \qquad 4.5$$

where p = d/dt denotes the Laplace variable, $\emptyset$ the magnetic flux, and N the number of turns. The term $Nd\emptyset_1/dt$ can be translated into a form suitable for use in conjunction with the transformer B/H curve by using the relations $\emptyset = BA$ and $B = \mu H$, where

B = magnetic flux density,

H = magnetising force,

μ = differential permeability defined by dB/dH, and

A = cross-sectional area of the core.

Hence $N d\emptyset_1/dt = N A_1 \mu_1 p H_1$ 4.6

Defining the magnetising current for the primary winding limb by $i_1 = H_1 l_1/N$, where l_1 = length of the magnetic circuit, and substituting for H in equation 4.6 gives

$$N d\emptyset_1/dt = \frac{N^2 A_1 \mu_1}{l_1} \cdot \quad p\, i_1 = M_1 p i_1 \qquad 4.7$$

Substituting equation 4.7 into equations 4.2, 4.3 and 4.4 gives

$$V_A = R_A i_A + L_A p i_A + R_o i_o \qquad 4.8$$

$$V_a = R_a i_a + L_a p i_a + R_o i_o \qquad 4.9$$

$$i_o R_o = M_1 p \, (i_A + i_a - i_o) \qquad 4.10$$

These equations may be compounded into a single matrix equation of the form $[V] = [M] \bullet [pi]$ as follows:

$$\begin{bmatrix} V_A - R_A i_A - R_o i_o \\ V_a - R_a i_a - R_o i_o \\ i_o R_o \end{bmatrix} = \begin{bmatrix} L_A & 0 & 0 \\ 0 & L_a & 0 \\ M_1 & M_1 & -M_1 \end{bmatrix} \bullet \begin{bmatrix} pi_A \\ pi_a \\ pi_o \end{bmatrix} \qquad 4.11$$

Any arbitrary secondary load networks may be incorporated in these equations by substituting appropriate expressions for the secondary voltage V_a. For example,

Resistance, R_L : $V_a = - R_L i_a$

Inductance, L_L : $V_a = - L_L pi_a$

Capacitance, C_L : $V_a = - Q/C_L$ and $pQ = i_a$
where Q is the charge on the capacitor

R_L and L_L in series : $V_a = - (R_L i_a + L_L pi_a)$

R_L and C_L in series : $V_a = - (R_L i_a + Q/C_L)$ and $pQ = i_a$

R_L, L_L and C_L in series : $V_a = - (R_L i_a + L_L pi_a + Q/C_L)$ and $pQ = i_a$

If the secondary winding is short-circuited, then $V_a = 0$. For an open-circuited secondary winding (i.e. $i_a = 0$), the equations of 4.11 reduce to

$$\begin{bmatrix} V_A - R_A i_A - R_o i_o \\ i_o R_o \end{bmatrix} = \begin{bmatrix} L_A & 0 \\ M_1 & -M_1 \end{bmatrix} \bullet \begin{bmatrix} pi_A \\ pi_o \end{bmatrix} \qquad 4.12$$

If the non-linearity of the mutual inductance elements of the M matrix are taken into account, solution of the state equations of 4.11 proceeds as follows. The M matrix is first inverted, and, using the fourth order Runge-Kutta routine adapted for non-linear differential equations, current solutions are obtained for each time interval. This procedure will be discussed in Chapter 7 when three

phase and transformer non-linear effects are considered. If, however, the elements of the M matrix are constant, the state equations of 4.11 may be solved directly using stepwise application of the Runge-Kutta method. In this case, the matrix inversion need only be performed once.

i.e. $$\left[pi\right] = \left[M\right]^{-1} \bullet \left[V\right] = f\,(t, i) \qquad 4.13$$

In each step of length Δt, the new value of current, i (t) is calculated using the corresponding value from the previous step, i $(t - \Delta t)$, as follows:

$$i\,(t) = i(t - \Delta t) + \frac{1}{6}\,(K_1 + 2K_2 + 2K_3 + K_4) \qquad 4.14$$

where $$K_1 = \Delta t \cdot f\left[\, t,\ i\,(t - \Delta t)\right]$$

$$K_2 = \Delta t \cdot f\left[\, t + \Delta t/2,\ i(t - \Delta t) + K_1/2\right]$$

$$K_3 = \Delta t \cdot f\left[\, t + \Delta t/2,\ i\,(t - \Delta t) + K_2/2\right]$$

$$K_4 = \Delta t \cdot f\left[\, t + \Delta t,\ i\,(t - \Delta t) + K_3/2\right]$$

The truncation error of this method is of the order of $(\Delta t)^5$. In order to achieve high accuracy and make the solution numerically stable, a small step length should be specified. Although Δt need not necessarily be equal to the BTI, it has been found convenient to use the same step length for both the numerical integration and lattice diagram technique. The choice of this step length is governed by

(i) the smallest time constant or oscillation period of the equivalent circuit,

(ii) the frequency of the applied waveform, and

(iii) the length of the shortest line.

4.2.3 Inter-face technique

For each time step, the transformer primary voltage (V_A) in equation 4.11 is replaced by the open-circuit Thevenin voltage $V_T(t)$, defined by equation 4.1. Matrix equation 4.11 is then solved for currents using the method described in section 4.2.2 above. Thevenin

voltages $V_T(t + \Delta t/2)$ and $V_T(t + \Delta t)$ are required to calculate the auxilliary quantities K_2, K_3 and K_4 of equation 4.14. The calculated current i_A, which satisfy the state equations of the line terminal network, must also satisfy the network equations of the Thevenin equivalent circuit of the lines,

$$\text{i.e.} \quad V_A = V_T(t) - Z_T \cdot i_A \qquad 4.15$$

In other words, the required solution, V_A, is obtained by superimposing the response of the linear Thevenin equivalent circuit to the current source (i_A) representing the lumped constant network, in accordance with the compensation theorem. Even if the termination equivalent circuit contains non-linear elements, this superposition is permissible. because it is applied only to the linear portion of the system.

The injected current is translated into voltage injected into the line, $v_r(t)$, using the relation,

$$v_r(t) + v_i(t) = V_A(t) - V_A(t - \Delta t) \qquad 4.16$$

i.e. the injected voltage is the difference between the voltage calculated from equation 4.15 and that similarly calculated at the preceeding time step, including all incident waves since the previous interval.

4.3 Comparison of methods

Single phase digital computer programs based on the lattice diagram, lumped parameter, and compensation methods were written to enable a comparative study of these methods on a simple transformer feeder circuit. The circuit (shown on Fig. 4.2) consists of a 48.2 km lossless transmission line terminated in a transformer and loaded only with a short length of cable on the secondary side. Voltage waveforms at the transformer obtained when energising this circuit using the methods described are shown on Fig. 4.2.

The transmission line is represented by 15 π-sections on the lumped parameter model. The differential equations describing each section are compounded with those representing the termination equivalent circuit, and solved simultaneously using Runge-Kutta method. The constants of the transformer equivalent circuit used on all mathematical models are the same as the TNA electromagnetic model constants given in section 3.2. The B/H curve is assumed linear and the transformer high frequency losses (estimated from the Q-values) are incorporated in the models used for the compensation and lumped parameter methods. The short length of cable on the secondary side is represented by its total shunt capacitance. On the lattice diagram model, the transformer is represented by its π-equivalent circuit, and its high frequency attenuation effects are not included since the program used was not capable of representing series losses.

Comparison of the transformer secondary voltage waveforms of Fig. 4.2 shows a close correlation in magnitude and frequency between the compensation and lumped-parameter methods. These waveforms also closely resemble those relating to the TNA. The comparatively large oscillations obtained with the lattice diagram method are attributable to the fact that losses have been ignored.

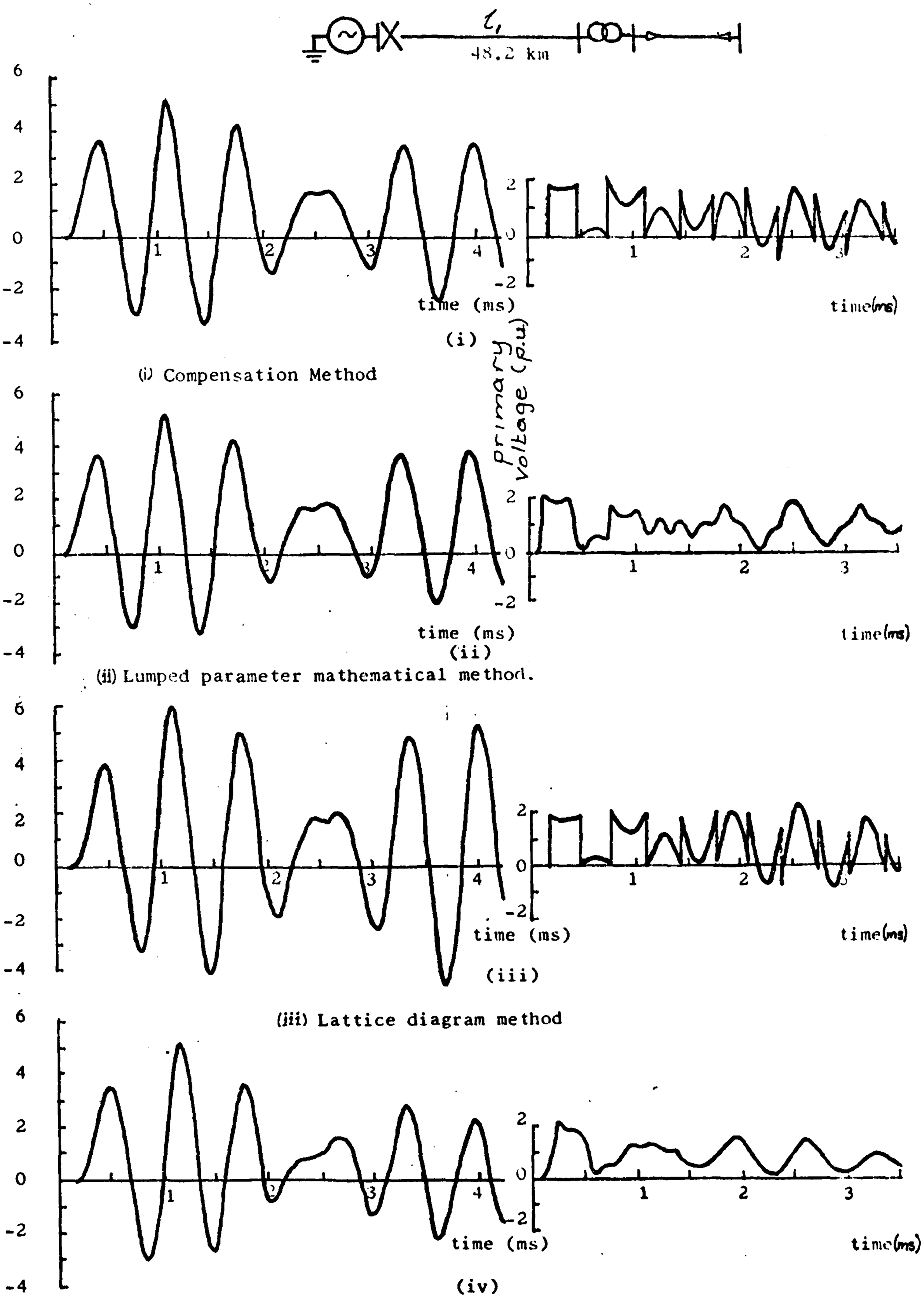

Fig. 4.2 Voltage waveforms at the transformer obtained using different methods.

A significant descrepancy in the transformer primary voltage waveforms exists between methods based on distributed-parameter and lumped constant representation of the line. When transformer losses were disregarded on the compensation model, the resulting primary voltage waveform was almost identical to that obtained with the lattice diagram method.

The close resemblance between the

(i) primary voltage waveforms of the compensation and lattice diagram methods, and

(ii) secondary voltage waveforms of the compensation and lumped parameter methods,

demonstrates the validity of the compensation approach in reproducing both the travelling wave phenomenon and lumped constant response.

Computation time for the compensation method is 0.009 sec/BTI on the ICL 1904S computer. This compares with 0.027 and 0.015 sec/BTI for the lumped parameter method using 15 and 6 π-sections for the line, respectively. This is 300 and 167% greater than the computation time of the compensation method. The lattice diagram program written is a more general purpose program, in contrast with the other programs confined to solution of the simple system studied. Consequently, its computation time (0.195sec/BTI) is much larger than that of the other methods.

4.4 Conclusion

The fundamental precepts of the method based on the compensation theorem have been presented. Although this technique has been used in conjunction with the Schnyder-Bergeron method of characteristics, its application to the lattice diagram method has previously been considered impracticable when non-linear energy storage elements are present. The problem in this case is associated with the difficulty of determining reflection coefficients. This problem is circumvented by introducing an inter-face technique which does not require explicit knowledge of reflection coefficients.

The compensation method makes it possible to use the lattice diagram approach, which allows adequate representation of lines and cables, in combination with the lumped-constant method capable of accurately simulating complex and non-linear termination equivalent circuits. Comparison between methods based on lumped and distributed parameters, and the compensation method, have validated the efficacy of the compensation method in overcoming the shortcomings of the former methods. Both the travelling wave phenomena and lumped constant response are faithfully reproduced.

The compensation program, together with the TNA and a lattice diagram program already available, form the basis of the single phase results discussed in the next two chapters. Extension of this method to three phase and non-linear systems will be presented in Chapter 7.

CHAPTER 5

THE EFFECTS OF SYSTEM PARAMETERS ON LINEAR RESONANT OVERVOLTAGES

5.1 Introduction

The salient features of resonant excitation of a transformer have been discussed in section 2.4 of Chapter 2. It was shown that the phenomenon of linear resonance arises from the near coincidence of the natural frequencies of the feeder and of the oscillatory circuit comprising the leakage reactance of the transformer and its associated capacitances. The overvoltages produced at the transformer depend to a large extend on the natural frequency and surge impedance of the feeder relative to those of the transformer, and on the losses inherent in the system and conditions pertaining at the instant of energisation. These factors are functions of the lengths of feeder and the cable on the transformer secondary, and the characteristics of the line and transformer. The main objective of this Chapter is to identify those circuit parameters which are likely to produce severe overvoltages, using a single phase representation of the circuit. The effects of system layout will be the subject of the next Chapter, and three phase effects are discussed in Chapter 8.

The results presented are obtained from digital computer studies based on the lattice diagram and compensation methods outlined in Chapters 3 and 4 respectively, and from studies carried out on the TNA. It should be noted that, in the digital computer analysis, the effects of line attenuation and distortion as well as losses within the transformer have been ignored (unless otherwise stated). As a consequence, the voltages presented here tend to be higher than those which would occur in practice. The conservatism of such idealised conditions does not, however, affect the basic trends due to

variations in circuit parameters, which this Chapter aims to establish. Methods for predicting whether a resonant condition would occur for given circuit constants will be presented. Some remedial measures to minimise the possibility of excessive voltages are also discussed.

5.2 System representation

5.2.1 Line surge impedance

The single line diagram of the system studied is shown on the circuit diagram of Fig. 5.1. The validity of single-phase results to three-phase systems depends on the value of line surge impedance used in the single-phase simulation. The following two alternative values of single phase surge impedance may be used:

a) Positive sequence impedance of the three-phase system which is defined by

$$Z_1 = Z_{ii} - \tfrac{1}{2} (Z_{ij} + Z_{ik})$$

where Z_{ii} = self surge impedance of phase i

Z_{ij} = mutual surge impedance between phases i and j

Z_{ik} = mutual surge impedance between phases i and k

If this quantity is used, the single-phase representation would then be equivalent to simultaneous closure in a three-phase system.

b) Self impedance of one phase conductor. This is equal to a diagonal term of the three-phase surge impedance matrix (i.e Z_{ii}). In this case the single-phase representation would then be equivalent to closure of one phase of a three-phase system. These equivalences are only true if interphase mutual coupling within the transformer are ignored.

In this study, simultaneous closure of the three phases has been simulated. In the TNA and compensation program models of the single-phase line, the surge impedance of the single-phase line is equal to the positive sequence impedance of the three-phase line (i.e alternative (a) above). In the lattice diagram program, a three-phase model of the system is used with all three phases energised simultaneously.

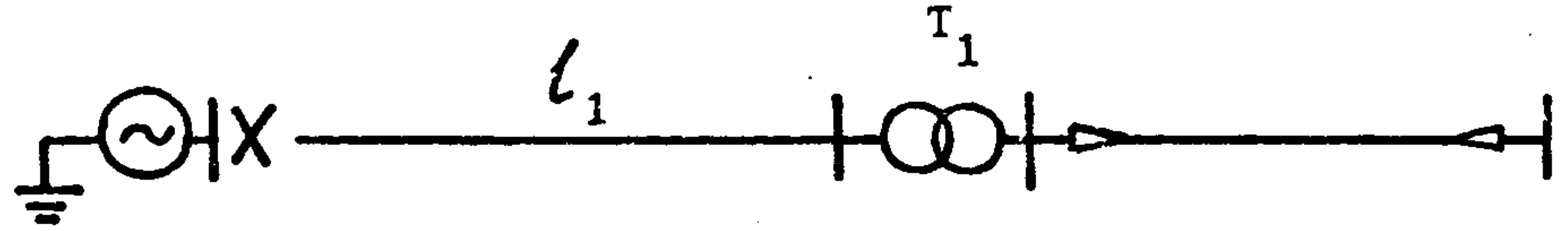

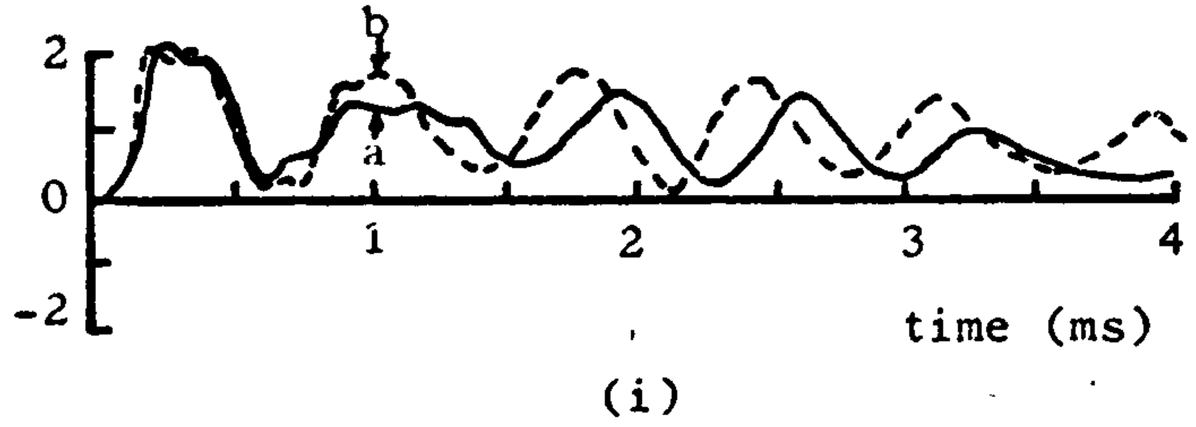

(i)

(a) π-equivalent circuit model
(b) electromagnetic model

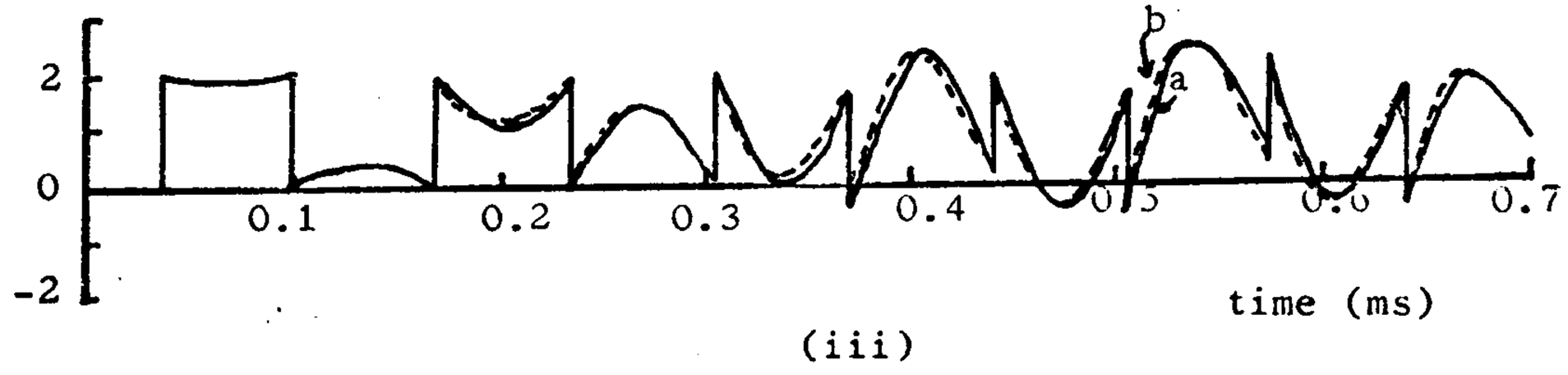

(iii)

Cable represented as
(a) distributed-parameter
(b) lumped constant

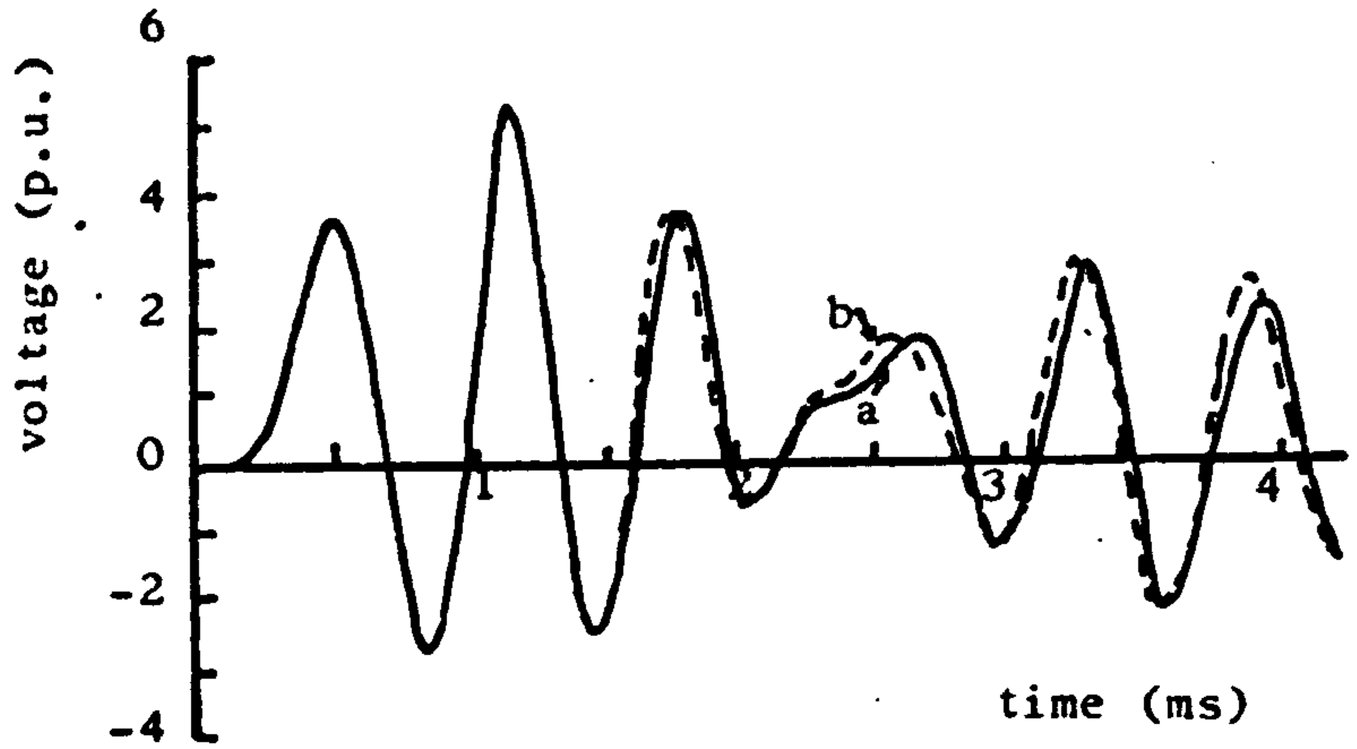

(ii)

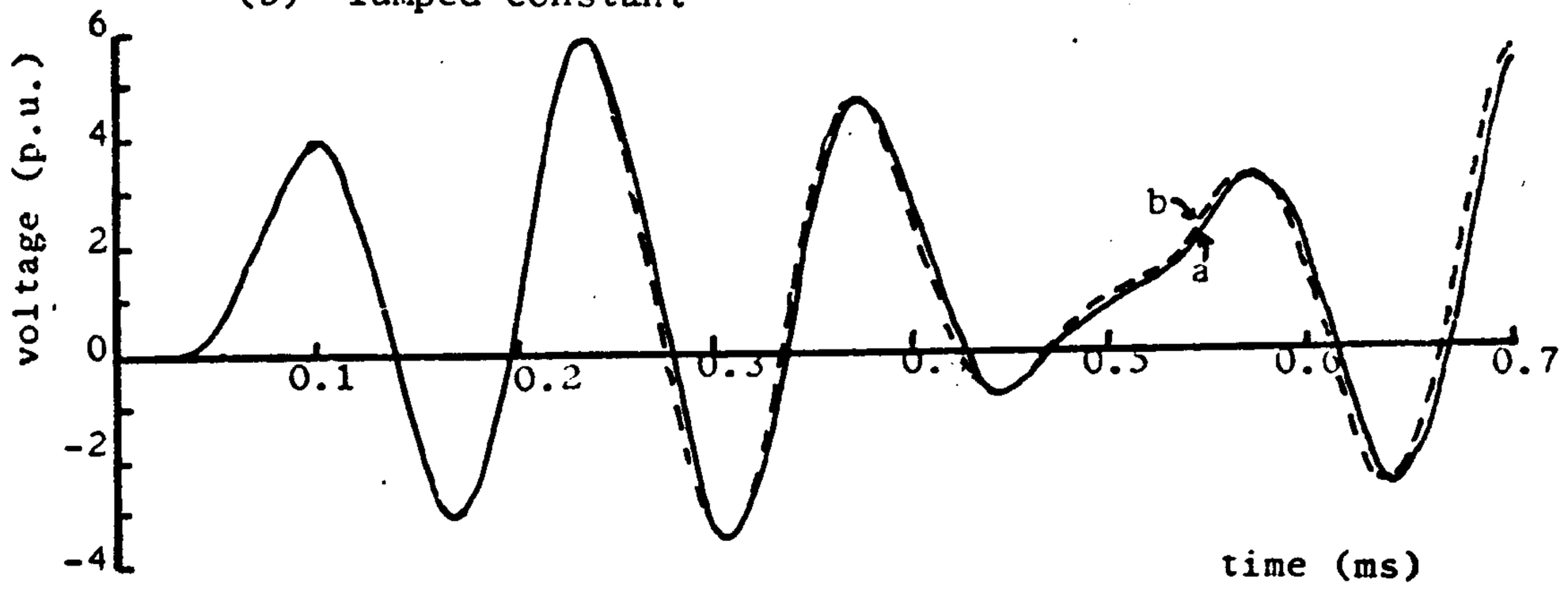

(iv)

Fig. 5.1 The effects of transformer and cable representation
(i) Transformer line-side voltages (TNA)
(ii) Transformer secondary voltages (TNA)
(iii) Transformer line-side voltages (mathematical model)
(iv) Transformer secondary voltages (mathematical model)

The transmission line simulated on the mathematical model consists of a three-phase untransposed, 275kV, twin 0.4 sq. in. conductor line with an earth resistivity of 20 ohm-metre. The constants of this line, calculated at the predominant natural frequency of a 10.2km line used in most studies, are given in section 7.2. A fully transposed line simulated on the mathematical and TNA model has a self surge impedance of 372 ohm and a mutual surge impedance of 75 ohm. In the case of simultaneous closure, this is equivalent to a single-phase line surge impedance of 297 ohm.

5.2.2 Termination constants

The transformer (T_1) simulated on the mathematical model is rated 132/33kV, 60 MVA with a short circuit reactance of 12.5%. The ratings of the second transformer (T_2) used in studies where the feeder is terminated in two transformers, are 132/11kV, 15MVA, with a leakage reactance of 10%.

The details of the electromagnetic transformer model used on the TNA are given in section 3.2.2.

The underground cable associated with transformer T_1 is a 33kV, 193 sq.mm. cable with a surge impedance and transit time given by 21.5 ohm and 6.28 μs/km respectively. Corresponding values for the cable associated with transformer T_2 are 193 sq.mm, 10.2 ohm and 6.35 μs/km.

5.2.3 Transformer representation

Under the conditions pertaining to this study, the mutual impedance effects of the transformer are not significant. This permits a simple but sufficiently accurate representation of the transformer on the TNA by a π-equivalent circuit (see section 3.2.2) The oscillogram traces of Fig. 5.1 (i) and (ii) illustrate the similarity in the voltage waveforms obtained using an electromagnetic

model (curves a) and a π -equivalent circuit model of the transformer. There is, however, a slight frequency shift which is more pronounced on the transformer line-side waveform. This is due mainly to the differences in the loss-factors associated with the transformer models. This will be discussed in Chapter 8.

In order not to exceed the TNA voltage and current limits, a 10V peak-to-peak source voltage was used, which is well below the rated voltage of the electromagnetic transformer model (250V). As a result, the non-linear effects of the transformer are not taken into account. These effects will be investigated using a mathematical model in section 8.2.

The results presented in this Chapter are based on a π -equivalent circuit and an electromagnetic model of the transformer for the digital and analogue models respectively. The leakage inductance of the TNA transformer model is increased from 0.024 to 0.6H by connecting equal linear inductors on either terminals of the transformer, such that its surge impedance is comparable to that of the transformer used on the mathematical model.

5.2.4 Simulation of secondary-side cable

The short length of cable connecting the transformer to the switchgear on the secondary side may, without much loss of accuracy, be represented by a shunt-connected capacitor of a value equal to the total capacitance of the cable. A short section of cable acts like a concentrated capacitance provided that the wave-front of the surge is long relative to the transittime of the cable. This condition is satisfied since the front of waves undergo elongation on being transferred through the transformer to the cable end. The lengths of cable considered in this study are in the region of 1km. The capacitances associated with the transformer and its bushings are

lumped together with the cable capacitances to give the effective value on the secondary. Such a representation on the digital model is found to provide results which are in close agreement with those obtained when the distributed nature of the cable length is taken into account (Fig. 5.1 (iii) and (iv)). In the latter case, the cable is simulated by a length of line with a surge impedance and propagation time equal to those of the cable. This method is, however, expensive in terms of digital computation time since the small transit time of the cable requires a relatively small basic time interval. For this reason, the lumped capacitor model will be preferred on both the digital and analogue models.

5.3 Length of line

In power networks, composite feeders comprising a transformer connected directly to a line are more common when short transmission distances are involved. For long distance transmission, circuit breakers are normally connected at both ends of the line. It will be shown in section 6.2.1 that, in this case, resonance overvoltages are rendered harmless if the transformer is energised from the circuit breaker adjacent to it. This study will therefore be confined to relatively short lengths of line. In addition, the transformer frequencies encountered in practice are such that a resonance state can only exist with short lengths of line.

5.3.1 Fourier analysis of line oscillations

The resonant overvoltages produced at the transformer depend a great deal on the frequency components of the line oscillations in relation to the transformer natural frequency. A frequency spectrum analysis of the voltage waveform appearing at the line side of the transformer can therefore elucidate the mechanism by which resonance is produced.

When the feeder is energised, a surge of voltage travels down the line. Its magnitude could approach the system voltage if pre-arcing of the circuit breaker contacts occurs near the peak of the source voltage. On arrival at the receiving end of the line, it encounters a termination of high surge impedance, Z_T, relative to that of the line, Z_L. The order of Z_T is normally thousands of ohms while the value of Z_L is in the region of 400 ohms. Consequently, it may be assumed for the purpose of this analysis that the surges will be reflected from the transformer as from an open-circuit. The receiving end voltage will be twice the voltage wave at its source, if the effects of attenuation and distortion are ignored.

The time interval to be examined is only a small fraction of the steady state period. As a result, the power frequency changes in the source voltage may be disregarded and a constant voltage source of zero impedance assumed. The transient voltage at the receiving end has a square waveform and may be given symbolically over one period by

$$V = \begin{cases} 0 \text{ when } 0 < t < T \\ 2 \text{ " } T < t < 3T \\ 0 \text{ " } 3T < t < 4T \end{cases} \qquad 5.1$$

where T is the travel time of the line, and t is the time measured from the instant at which the line is energised.

Analysing the voltage given by equation 5.1 into its Fourier series, the following expression results

$$V = 1 + \frac{4}{\pi} \cdot \sum_{n=1}^{\infty} \frac{1}{2n-1} \cos\left[\frac{(2n-1)\pi}{2T} t\right] \cdot (-1)^n \qquad 5.2$$

If $f_L = 1/4T$ is the natural frequency of the line, then

$$\omega_L = 2\pi f_L = \frac{\pi}{2T} ,$$

and

$$V = 1 + \frac{4}{\pi} \cdot \sum_{n=1}^{\infty} \frac{1}{2n-1} \cos\left[(2n-1)\omega_L t\right] \cdot (-1)^n \qquad 5.3$$

Equation 5.3 indicates that, in addition to the fundamental line frequency component, f_L, and the constant term, the waveform is composed of a discrete number of higher frequency harmonics which are odd multiples of the fundamental frequency. The amplitude of the odd harmonics $\left[\frac{4}{\pi(2n-1)}, \text{ where } n = 1,2,3...\right]$, decreases inversely with the harmonic order number,(2n-1).

Each sinusoidal frequency component will produce a transient oscillation in the terminating circuit. Since the system investigated is linear, the complete response to the series of stimuli may be obtained by the superposition of these separate transient

oscillations of the line.

If the natural frequency of the line and that of the transformer are close but not identical, the resulting oscillations at the transformer secondary will be modulated at the relatively low difference frequency which decays slowly. This phenomenon is exemplified by the traces of Fig 5.1. and all subsequent results where the condition of near coincidence of frequency is satisfied. It can be shown that if the frequency of the line ($f_{L)}$ is nearly equal to that of the termination (f_T) the resultant oscillation will have an average frequency $\frac{1}{2}$ ($f_L + f_T$), amplitute modulated at the low difference frequency $\frac{1}{2}$ ($f_L - f_T$).

5.3.2 Line terminated in two transformers

It is very common in practice to energise a line with two transformers solidly connected at the end of the feeder. These transformers will exhibit different natural frequencies dependent on the parameters of the transformers and those of the associated lengths of cable on the secondary sides. There is therefore a possibility of one of these frequencies coinciding with the natural frequency of the line.

The voltage waveforms of Fig. 5.2 (i) relate to a line 5.15km long, whose frequency coincides with that of transformer T_2 (14.5kHz), and Fig 5.2 (ii) shows waveforms for a length of line (10.2km) giving a frequency (7.34kHz) which is the same as that of transformer T_1. The build-up of the secondary voltages under a resonance condition is indicated.

In Appendix 12.1, expressions for the transformer secondary voltage peaks are derived for idealised conditions at the point of resonance. Equation 12.12 of this appendix gives the value of the m^{th} voltage peak as follows:

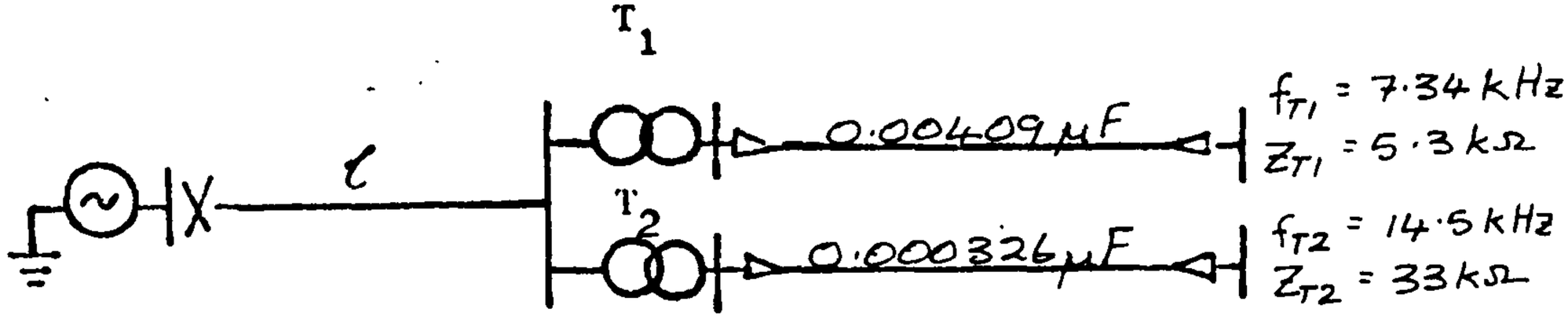

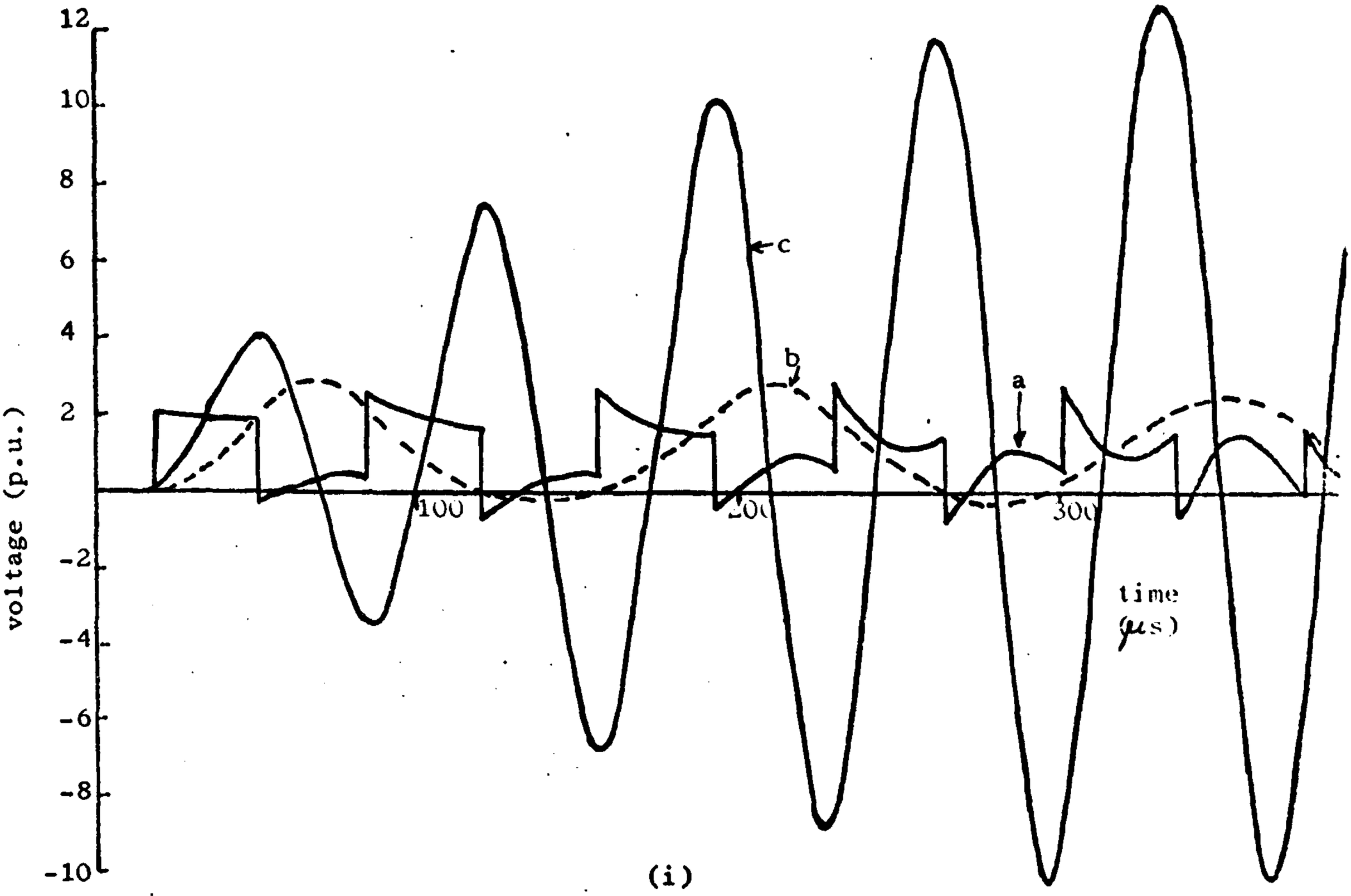

(i)

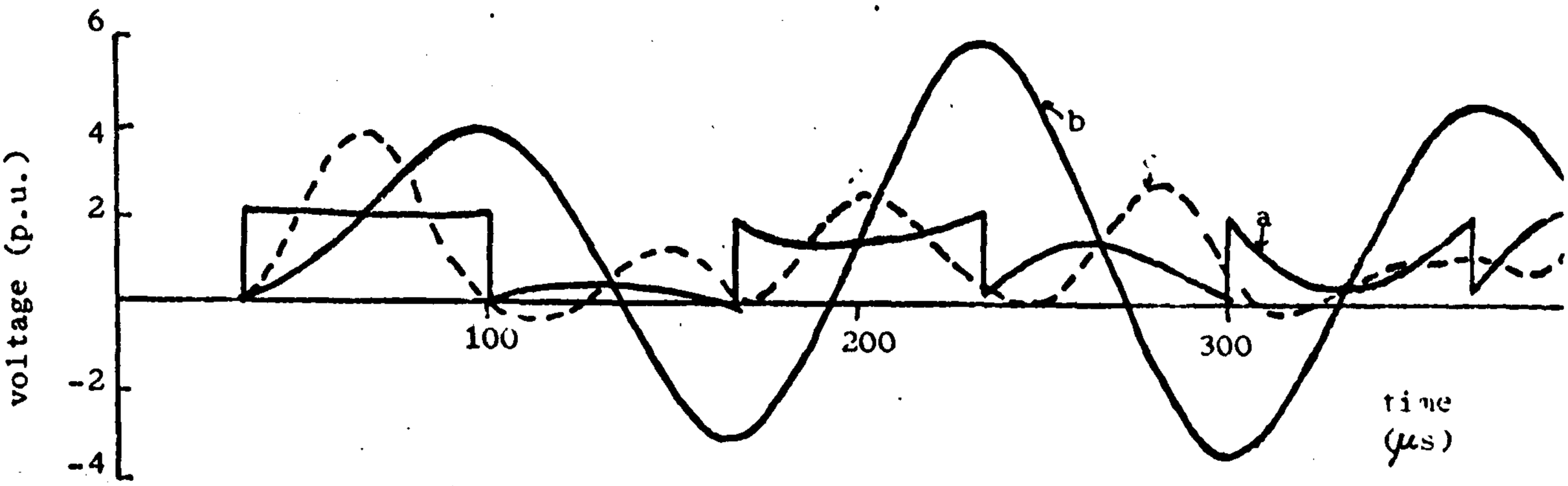

(ii)

Fig. 5.2

The effect of line length on voltage waveforms(digital model)
(i) ℓ = 5.15 km
(ii) ℓ = 10.20 km

(a) Voltage on the line side of the transformers
(b) Secondary voltage of transformer T_1
(c) Secondary voltage of transformer T_2

$$\hat{V}_m = 2\left(\frac{1-k^{m+1}}{1-k}\right) \quad \text{if } m \text{ is odd and } k \neq 1$$

$$= -2\left(\frac{k-k^{m+1}}{1-k}\right) \quad \text{if } m \text{ is even and } k \neq 1 \qquad 5.4$$

where $k = \exp(-Z_L\, T/L)$

$$= (-Z_L/Z_T \cdot \pi/2)$$

In this case, the value of k is 0.895 and 0.981 for transformer T_1 and T_2 respectively. The first three calculated voltage peaks are listed below, with the values measured from the voltage waveforms given within brackets for comparison:

3.8 (3.8), -3.4 (-3.2), 6.9 (5.8) for transformer T_1, and

4.0 (4.0), -3.9 (-3.5), and 7.8(7.3) for transformer T_2.

The measured values tend to be lower in magnitude for second and subsequent peaks of voltage. It will be appreciated that, in the theoretical analysis outlined in the appendix, certain simplifying assumptions were made. These assumptions give conditions which are somewhat more onerous than those obtaining in practice. In a practical system, the effect of system losses become more significant with time, such that, in most cases, the maximum voltage occurs on the first peak. A close approximation of this peak magnitude may be obtained from the equation 5.4 above.

Fig. 5.3 shows the maximum voltage as a function of the line length. The frequency spectrum of the line oscillations is determined by the length of the line. If the length of the line is increased, a point may be reached at which a particular harmonic frequency of the line will resonate with one of the transformer frequencies. According to equation 5.3 this condition will arise if the length of line is an odd multiple of the length at which

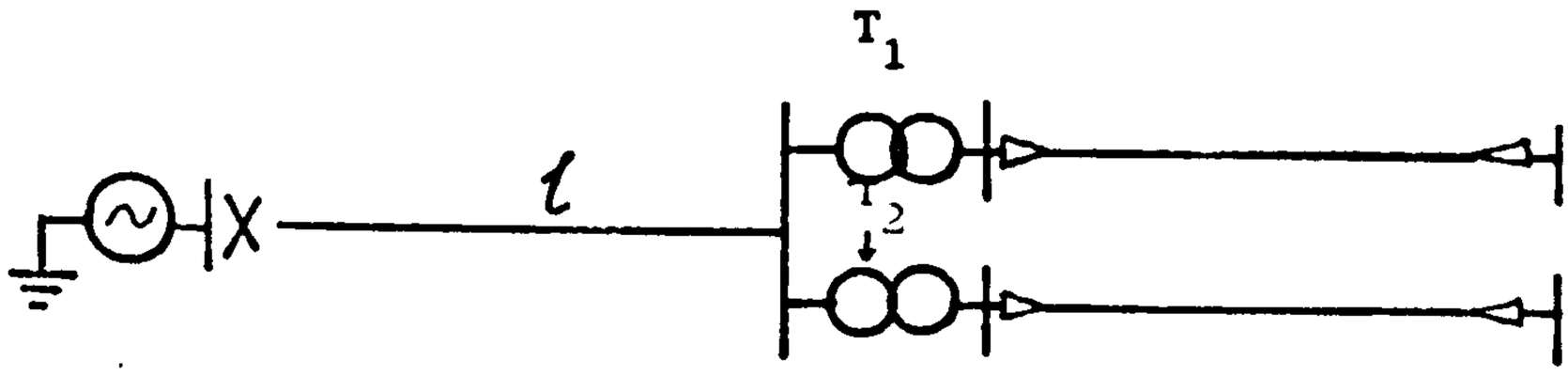

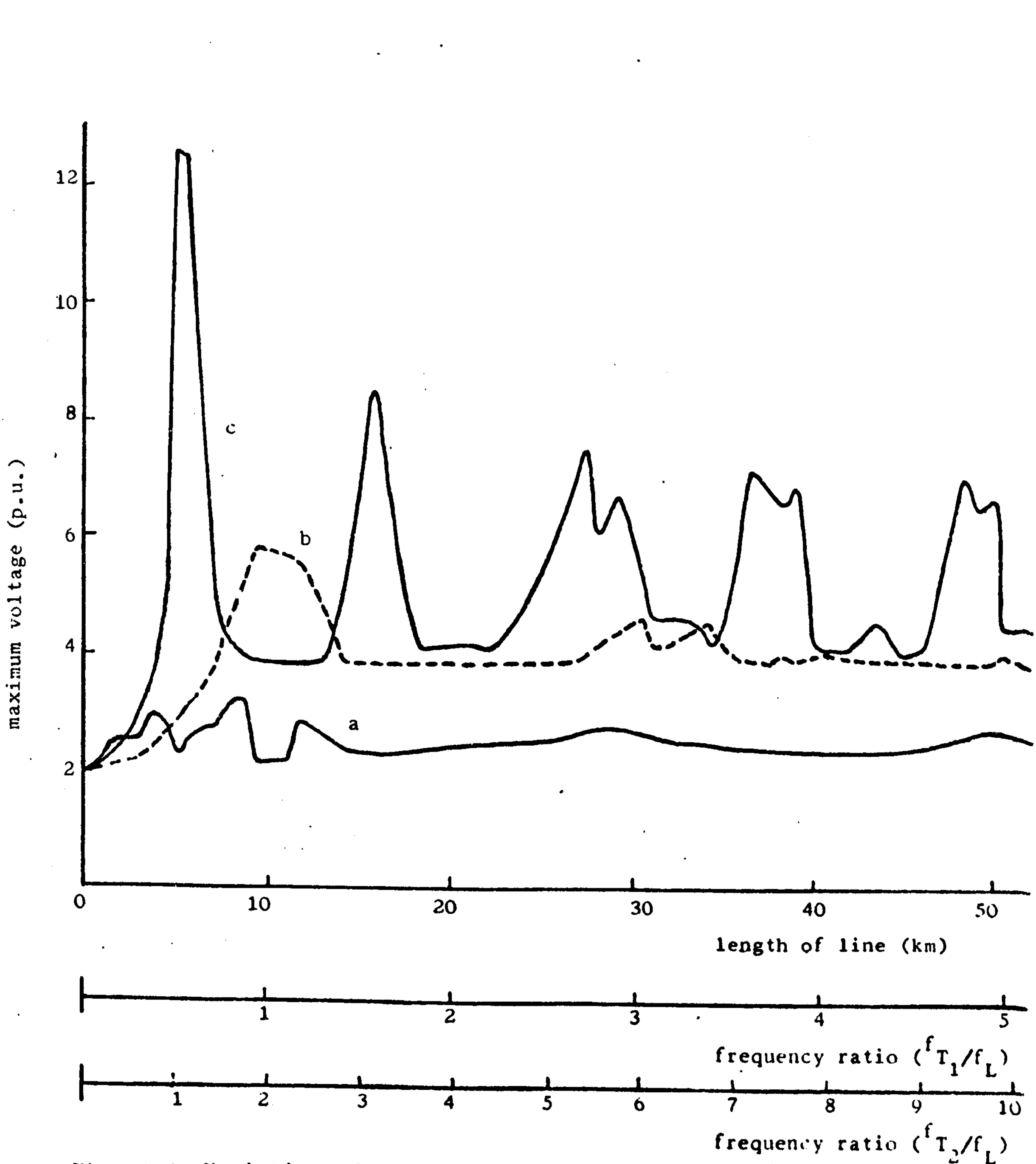

Fig. 1.3 Variation of overvoltage with line length (mathematical model)
(a) Maximum voltage on the line side of the transformers
(b) Maximum secondary voltage of transformer T_1
(c) Maximum secondary voltage of transformer T_2

$f_L = f_T$. The series of overvoltage peaks on Fig. 5.3 confirm the analysis. Examination of these peaks will show a depression at the point where the frequencies coincide ($f_L = f_T$). The amplitude of the harmonic peaks decreaseswith increase in line length. This may be explained with reference to equation 5.3, which shows the inverse relationship between the exciting voltage magnitude and the harmonic number. The vast difference between the magnitudes of the overvoltage peaks of the two transformers investigated can be accounted for by the diffences in the surge impedances of the transformers T_1 and T_2 (5.3 and 33kΩ respectively). The effect of the surge impedance will be dealt with later in section 5.5.

In between the peaks, the overvoltage magnitude is, approximately 4 p.u. This is caused by the overshoot in the secondary voltage to twice the exciting voltage. As shown on curve (c) of Fig 5.3, the overvoltage within this region may exceed 4 p.u. as a result of the influence of transformer T_1. These crests do not exist when transformer T_1 is removed from the circuit. This is shown in Table 5.1 where the overvoltages produced with both transformers present are compared with those obtained with one transformer only in circuit. In general, the influence of one transformer on the overvoltages produced on the other is not significant.

Fig 5.4 A(i, ii and iii) shows the voltage waveforms at the terminals of the two transformers, and B (a and b), the over-voltages obtained as the length of line is varied. The two trans-formers are similar, but transformer T_2 has an equivalent capacitance of 0.044 μF at its secondary terminals. These parameters correspond to a surge impedance of 3.5kΩ and a line frequency of 1.03kHz. As in Fig. 5.3 relating to digital computer studies, the fundamental

TABLE 5.1

THE EFFECT OF ONE AND TWO TRANSFORMERS AT THE END OF FEEDER

Frequency ratio f_L/f_T	Maximum overvoltage on transformer secondary terminal (p.u.)			
	Transformer T_1 only	Transformer T_1 and T_2	Transformer T_2 only	Transformer T_1 and T_2
1	5.75	5.75	12.45	12.55
2	3.83	3.83	4.00	3.84
3	4.62	4.56	8.55	8.46
4	3.84	3.83	4.03	4.12
5	3.84	3.83	7.00	7.30
6	4.07	4.08	4.82	5.44
7	4.00	4.00	6.85	6.70

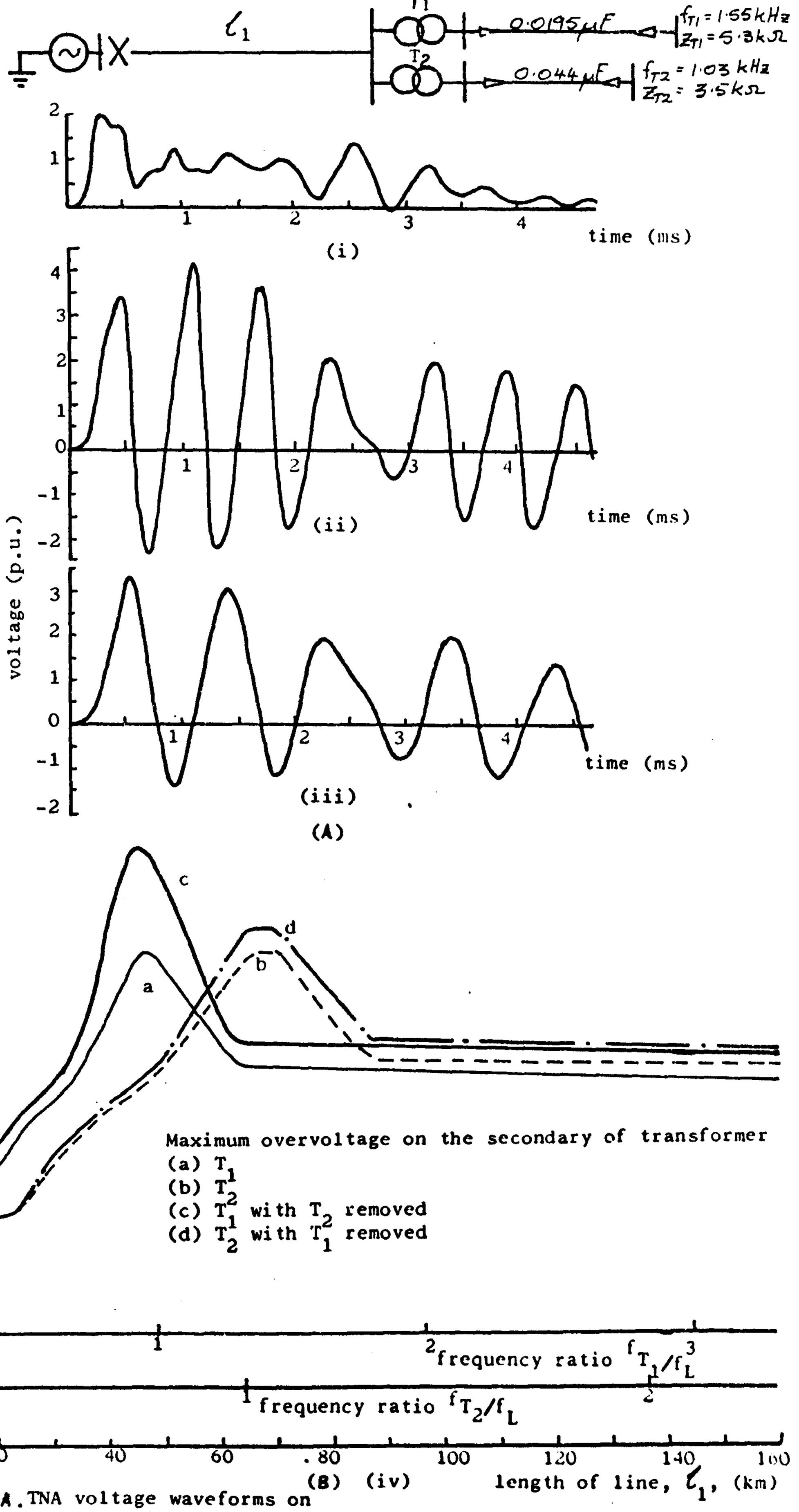

Fig. 5.4 A. TNA voltage waveforms on
(i) line side of transformers
(ii) secondary of transformer T_1.
(iii) secondary of transformer T_2
B. Overvoltage variation with line length.

resonance peaks occur when the line frequency approaches the natural frequency of one of the transformers. Since the surge impedances of the transformers are close (5.3 and 3.5kΩ for T_1 and T_2 respectively), there is no appreciable difference in their secondary overvoltages at resonance.

Curves c and d of Fig. 5.4 B represent overvoltages on one transformer with the other disconnected. In this case there is a significant increase in the overvoltages due mainly to the closeness of the surge impedances of the two transformers.

A significant difference in the overvoltage curves of Fig. 5.3 and Fig. 5.4B is the absence of any harmonic peaks on the T.N.A. waveforms. This may be due to the following reasons:

(a) The damping provided by the transformer and the losses in the line, which were ignored in the digital model, play a significant role in reducing the amplitudes of the harmonic oscillations.

(b) The copper losses of the model transformers used are much higher than the actual transformers they represent.

(c) The length of line can only be increased in discrete steps of 8.05km (5 mi). This means that a resonance peak of small amplitude or bandwidth, occurring within the descrete step length, may not be observed.

5.3.3 Line terminated in one transformer

The effects of length of line on voltage waveforms are shown on the T.N.A. oscillogram traces of Fig.5.5. These relate to the following line frequencies:-

(i) $f_L = f_T$ (ℓ_1 = 48.25km)

(ii) $f_L = \frac{1}{2} f_T$ (ℓ_1 = 96.50km)

(iii) $f_L = \frac{1}{3} f_T$ (ℓ_1 = 144.75km).

It will be noticed that the voltages on the transformer

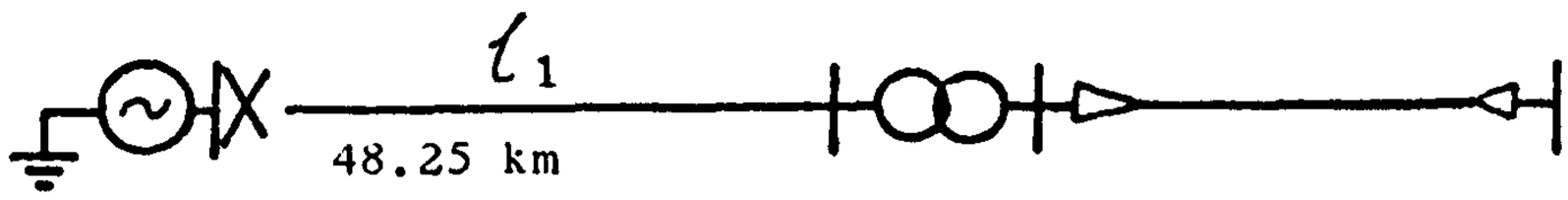

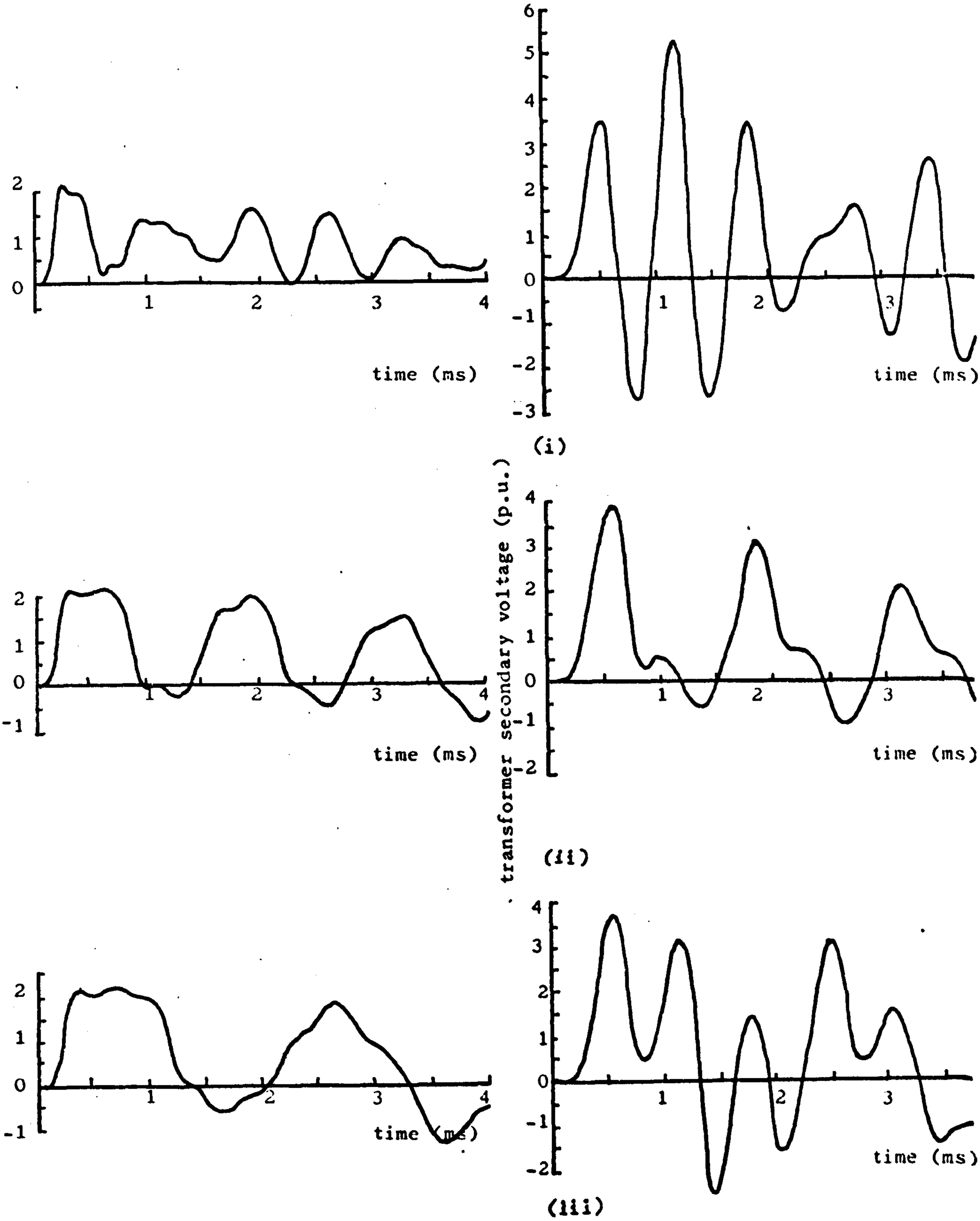

Fig. 5.5 TNA voltage waveforms for various lengths of line
(i) ℓ_1 = 48.25km ($f_L = f_T$)

(ii) ℓ_1 = 96.50km ($f_L = f_T/2$)

(iii) ℓ_1 = 144.75km ($f_L = f_T/3$)

primary are characterised by the slowing-up of the wavefronts due to distortion effects on the line.

Fig. 5.6 shows that if the transformer is energised from a cable, similar resonant overvoltages occur when the fundamental or odd harmonic of the feeder frequency is tuned to the transformer frequency. The overvoltage magnitudes are, however, appreciably higher for a cable feeder due to the larger ratio Z_T/Z_L, as will be explained in section 5.5. Since the transit time of cables (a) and (b) are similar, the overvoltage peaks occur at the same length of cable, but the difference in magnitude is due to the difference in the surge impedance ratio . The voltage waves travel slower on cable (c) with the result that a relatively small length of cable will give a natural frequency equal to that of the transformer.

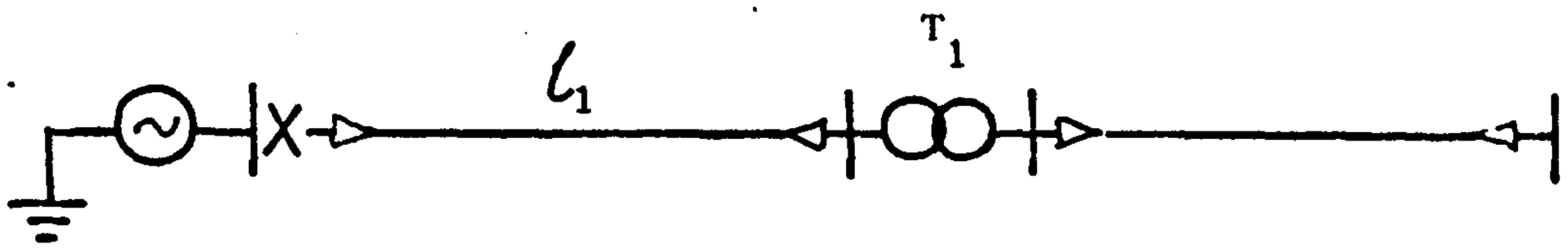

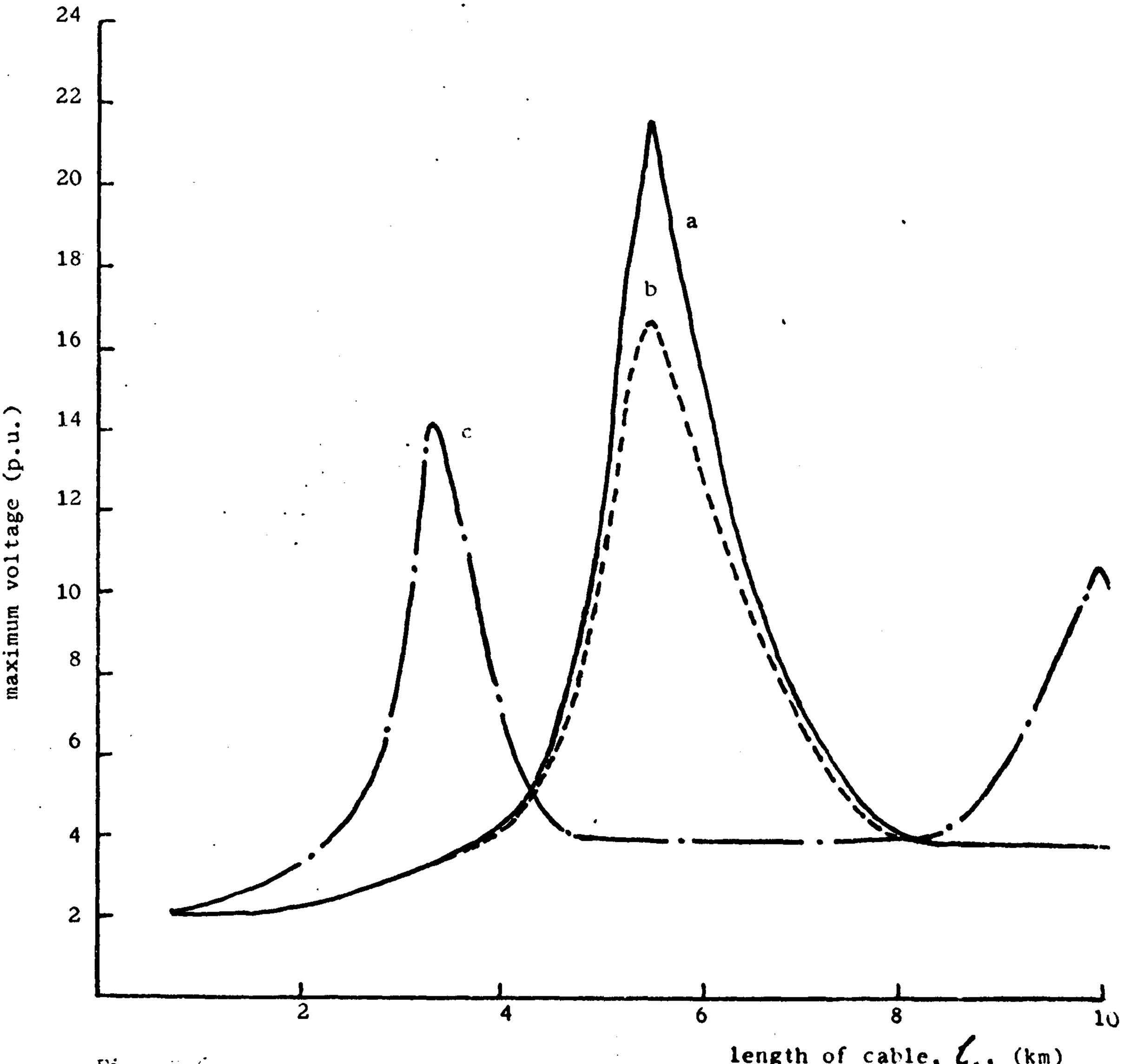

Fig. 5.5

Variation of overvoltage with length of cable

(a) Z_c = 10.2Ω ; τ = 6.28 μsec/km (10.1 μsec/mile)
(b) Z_c = 21.5Ω ; τ = 6.28 μsec/km (10.1 μsec/mile)
(c) Z_c = 32.4Ω ; τ = 10.32 μsec/km (16.6 μsec/mile)

5.4 Length of line or cable on transformer secondary

The length of cable beyond the transformer determines not only the transformer natural frequency, $f_T = 1/2\pi\sqrt{LC}$ but also its apparent surge impedance, $Z_T = \sqrt{L/C}$. The effect of varying the cable length on maximum voltages at the transformer is shown in Fig.5.7 for a fixed length of line ℓ_1. As in the previous section, the curves relating to digital computation are characterised by a series of overvoltage peaks in the proximity of an odd frequency ratio (Fig.5.7(i)). In this case, however, the magnitudes of the resonance peaks increase as the frequency ratio f_T/f_L increases. This is because C is inversely proportional to the squares of f_T and Z_T. The high surge impedance ratio associated with shorter lengths of cable favours higher overvoltage peaks.

Fig 5.7 (ii) relating to TNA results shows only the resonance peak near unity frequency ratio. The reasons for the absence of subsequent harmonic peaks given in section 5.3.2 also apply in this case.

If a short overhead line is connected in place of the secondary cable, Fig. 5.8 (i) and (ii) show the voltage waveforms for different line lengths. It can be shown that when the length of line on the transformer secondary is 5.5km, the natural frequency of the termination will equal that of the feeder. This figure is based on a line capacitance of 0.0112 μF/km on the 33kV system. Referred to the 132kV side the effective capacitance of this length of line is 0.00409μF. Fig 5.8 (iii) shows that a resonace peak is produced when the length of line ℓ_2 approaches this value. The depression occurring when lengths ℓ_2 and ℓ_1 are nearly equal (10.2km) may be caused by the destructive interference of the surges on both lines at the transformer secondary.

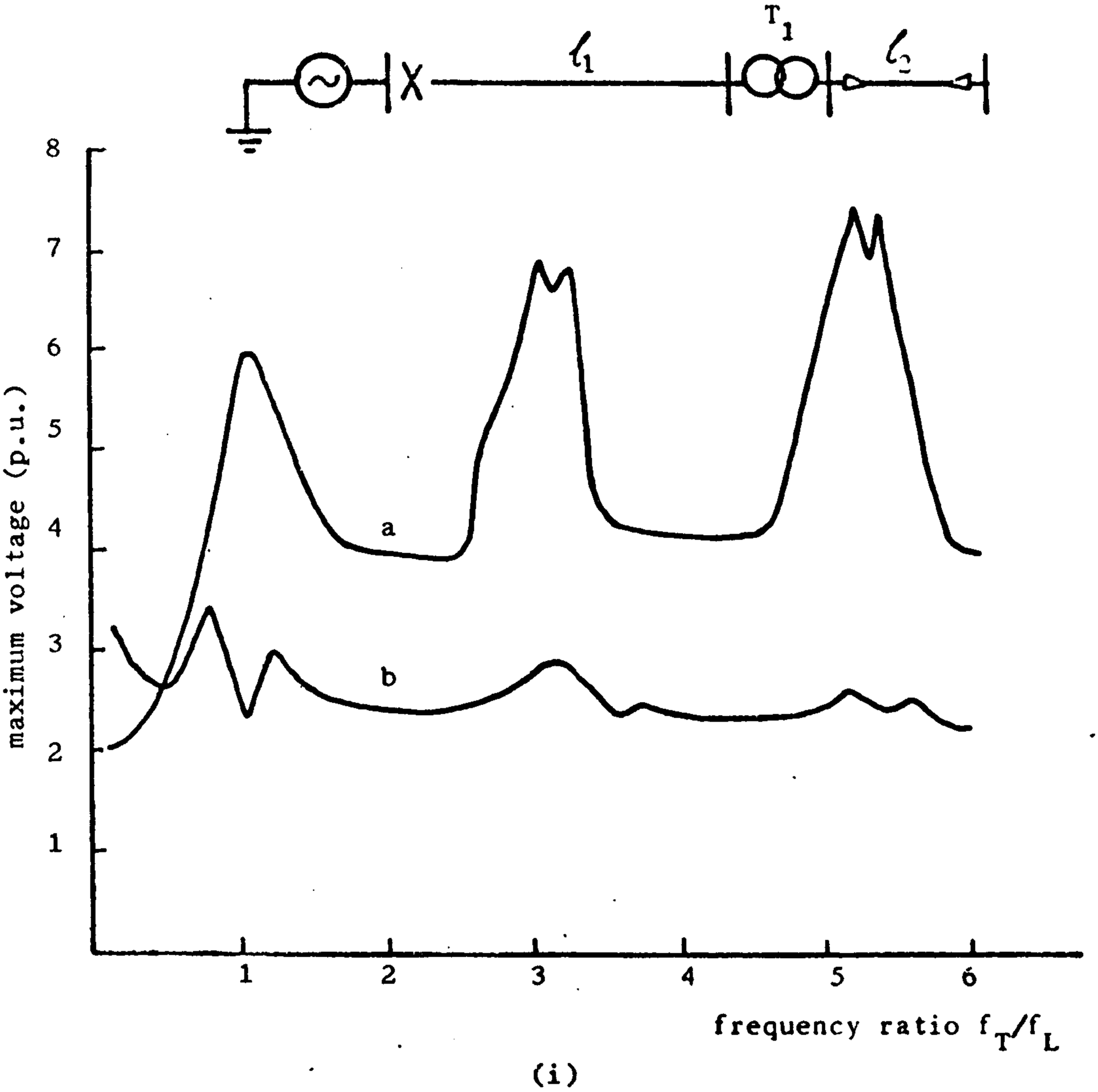

(i)

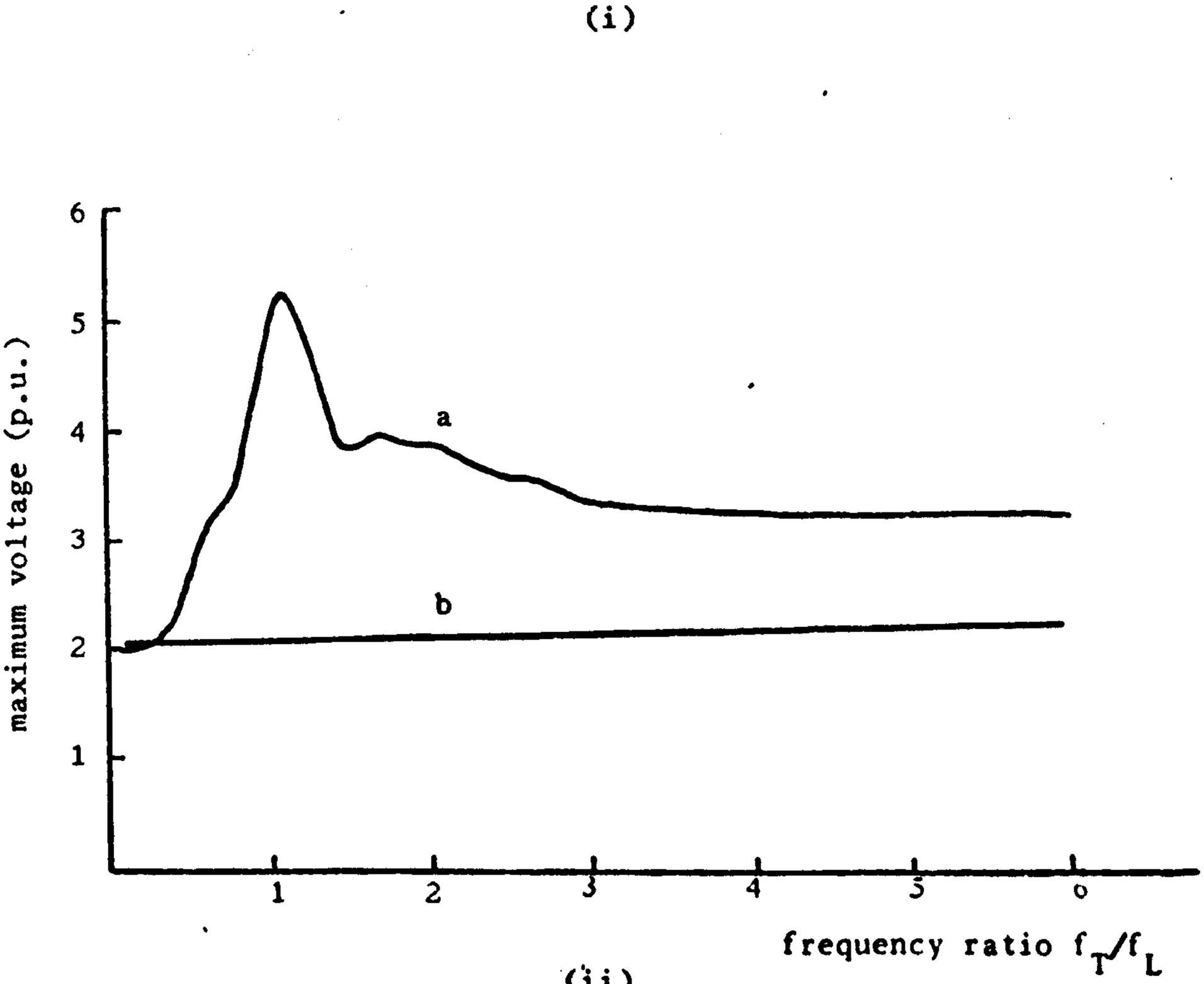

(ii)

Fig. 5.7
Variation of maximum voltage with length of cable ℓ_2
(i) Digital computer results, f_L = 7.54kHz.
(ii) TNA results, f_L =1.55 kHz.
(a) transformer secondary overvoltage
(b) transformer primary overvoltages

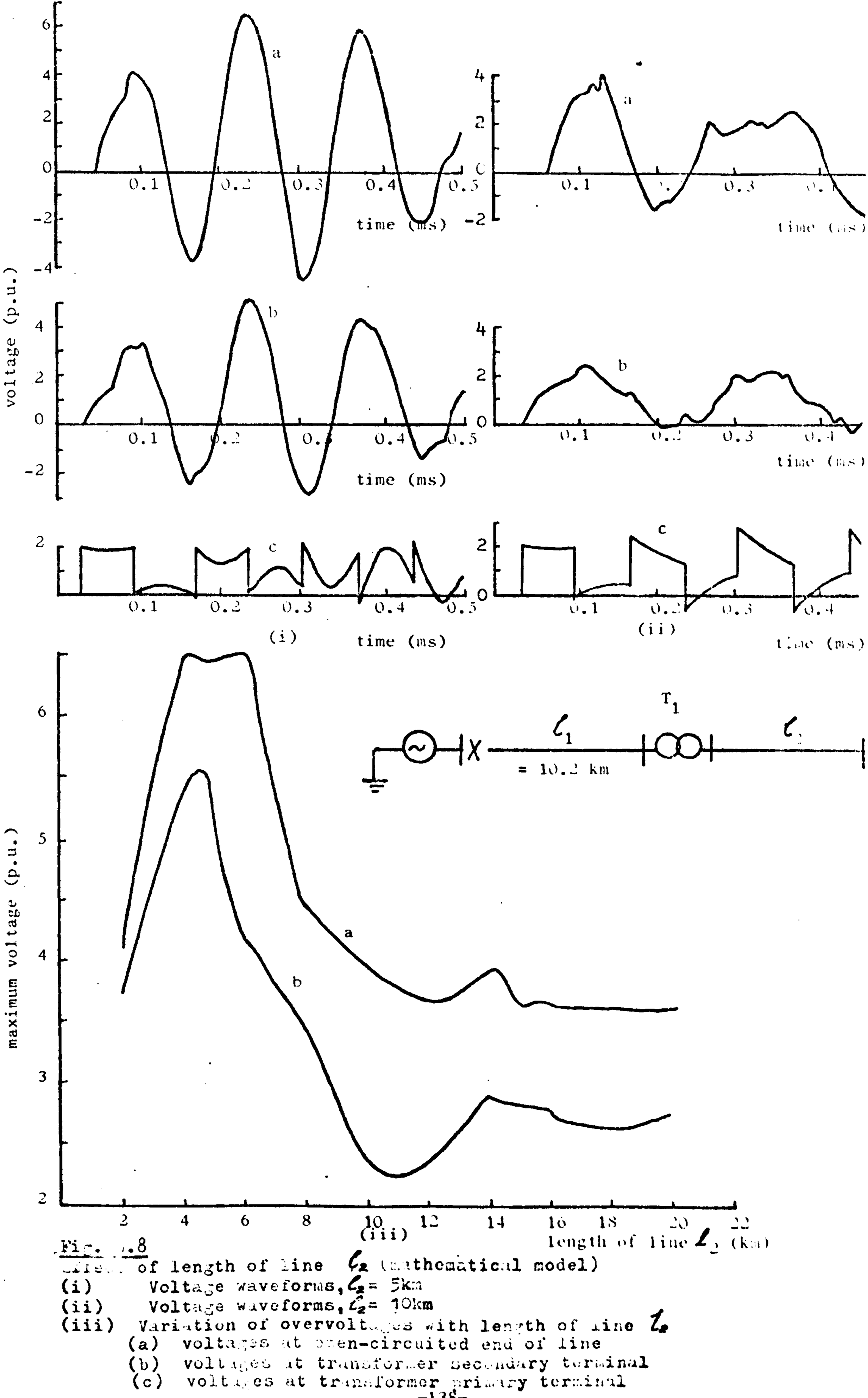

Fig. 4.8
Effect of length of line ℓ_2 (mathematical model)
(i) Voltage waveforms, ℓ_2 = 5km
(ii) Voltage waveforms, ℓ_2 = 10km
(iii) Variation of overvoltages with length of line ℓ_2
(a) voltages at open-circuited end of line
(b) voltages at transformer secondary terminal
(c) voltages at transformer primary terminal

Similar digital computer results obtained using transformer T_2 are presented in Fig. 5.9. The harmonic resonance peaks are clearly shown. These occur when length ℓ_2 is close to 4.2 km and to three times this value. A line 4.2km long corresponds to a capacitance of 0.047 μF on the 11kV system, giving an effective capacitance of 0.000326μF referred to the 132kV side.

Results of a simular study carried out on the TNA are presented on Fig. 5.10. The voltage waveforms are for a length of line ℓ_2 equal to 80.4 and 40.2km. The maximum voltages plotted as a function of line length are shown on curves of Fig.5.10 (iii). It can be seen from this figure that a high resonance peak occurs only at the remote end of line ℓ_2 when its length is in the region of 40km.

In all the above cases, the secondary line behaves as if its entire capacitance were concentrated at the end of the line. The capacitance of the line may be determined from its surge impedance defined as $Z = \sqrt{L/C}$ and the velocity of propagation of the waves along the line given by $v = 1/\sqrt{LC}$, where L and C are expressed in henry and farad per unit length respectively. Hence $C = 1/Zv$ F.

For the line with a surge impedance of 297 Ω the line capacitance is calculated as 0.0112μF/km based on 33kV (or 11kV in the case of transformer T_2) side of the transformer. Referred to the 132kV system the line capacitance is 0.0007 μF/km (or 0.0000777 μF/km for transformer T_2).

Fig. 5.11 (i) shows voltage waveforms computed when length of line ℓ_1 = 10.2km and ℓ_2= 5.8 km. Curves (ii) d and e show the variation with length of feeder ℓ_1 of maximum voltages at the remote end of line ℓ_2 and at the transfomer secondary terminal respectively. Because of the high surge impedance of the transformer relative to that of the

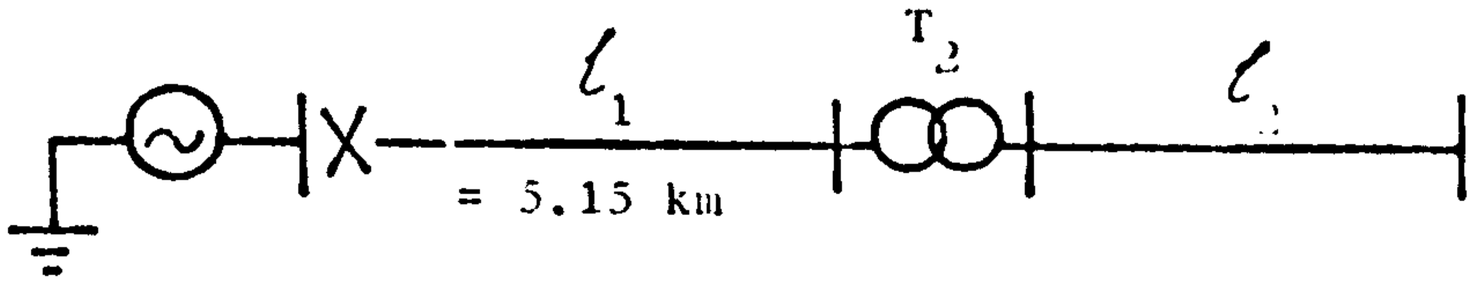

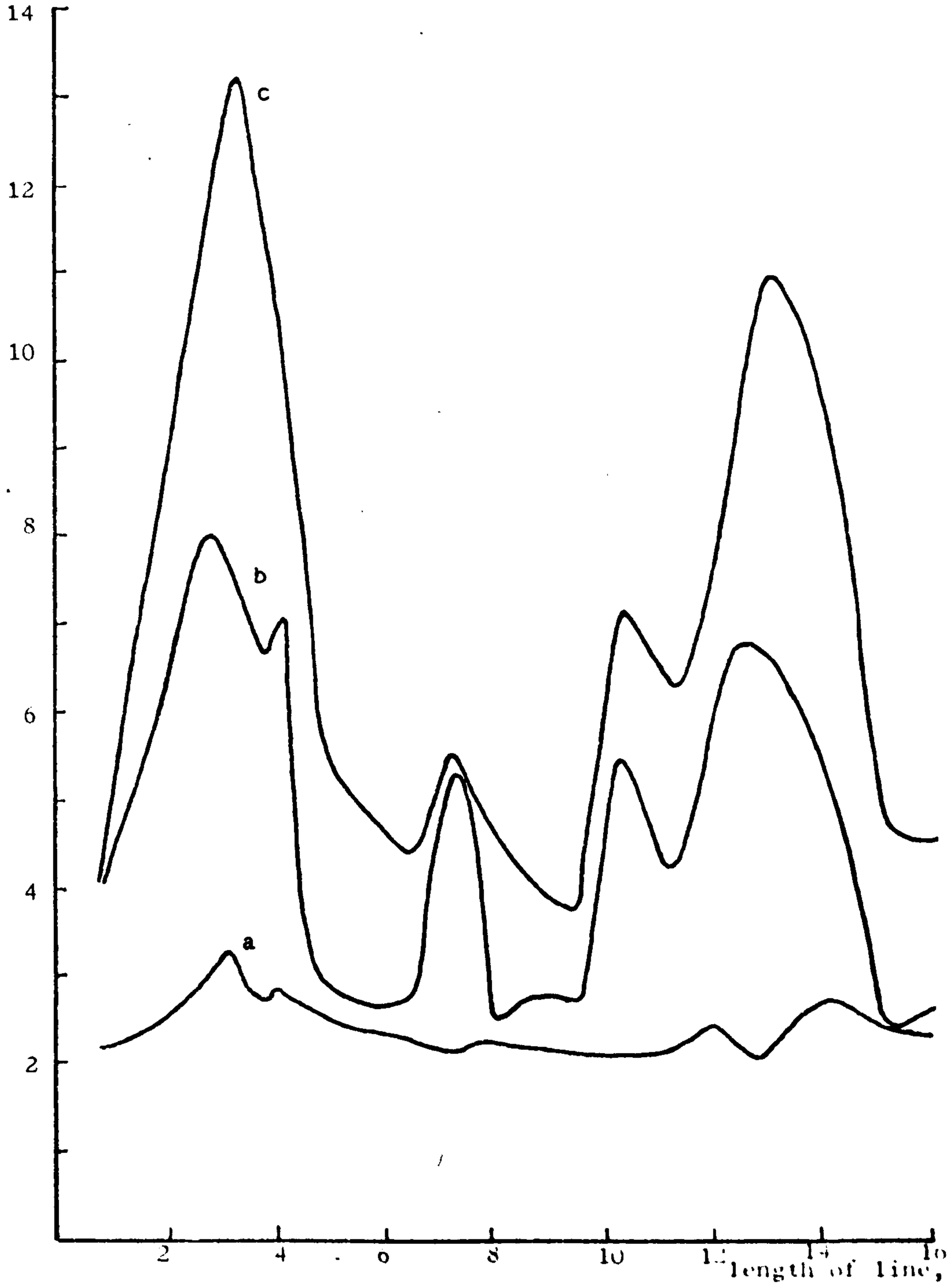

Fig. 5.9
Variation of overvoltages with length of line ℓ_2 (mathematical model)
(a) maximum voltages at open-circuited end of line ℓ_2
(b) maximum voltages on transformer secondary terminal
(c) maximum voltages on transformer primary terminal

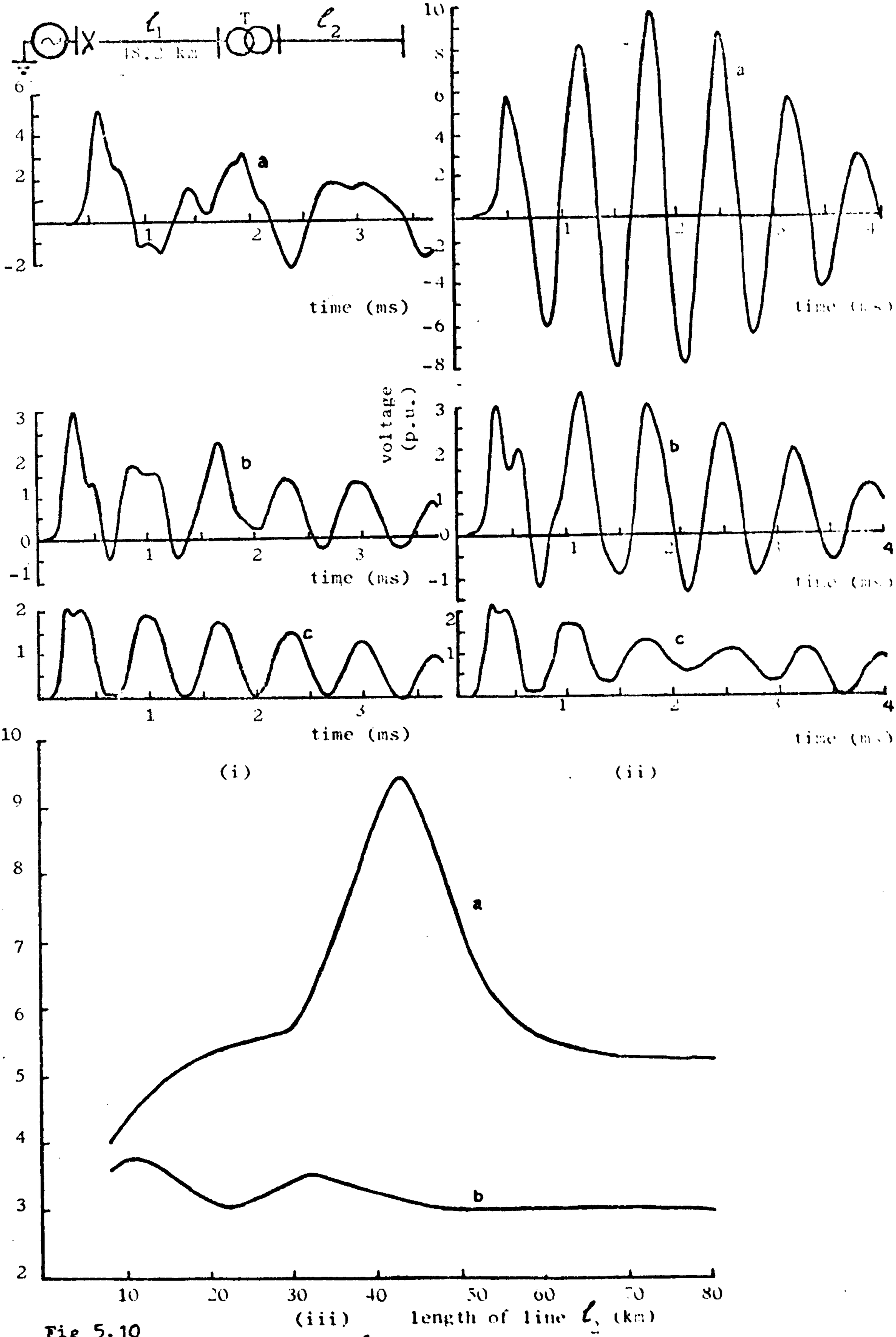

Fig 5.10
Effect of length of line ℓ_2 (Thévenin model)
(i) Voltage waveforms, ℓ_2 = 30.4km
(ii) Voltage waveforms, ℓ_2 =40.2km
(iii) Variation of overvoltages with length of line
(a) voltages at open-circuited end of line ℓ_2
(b) voltages on transformer secondary terminal
(c) voltages on transformer primary terminal

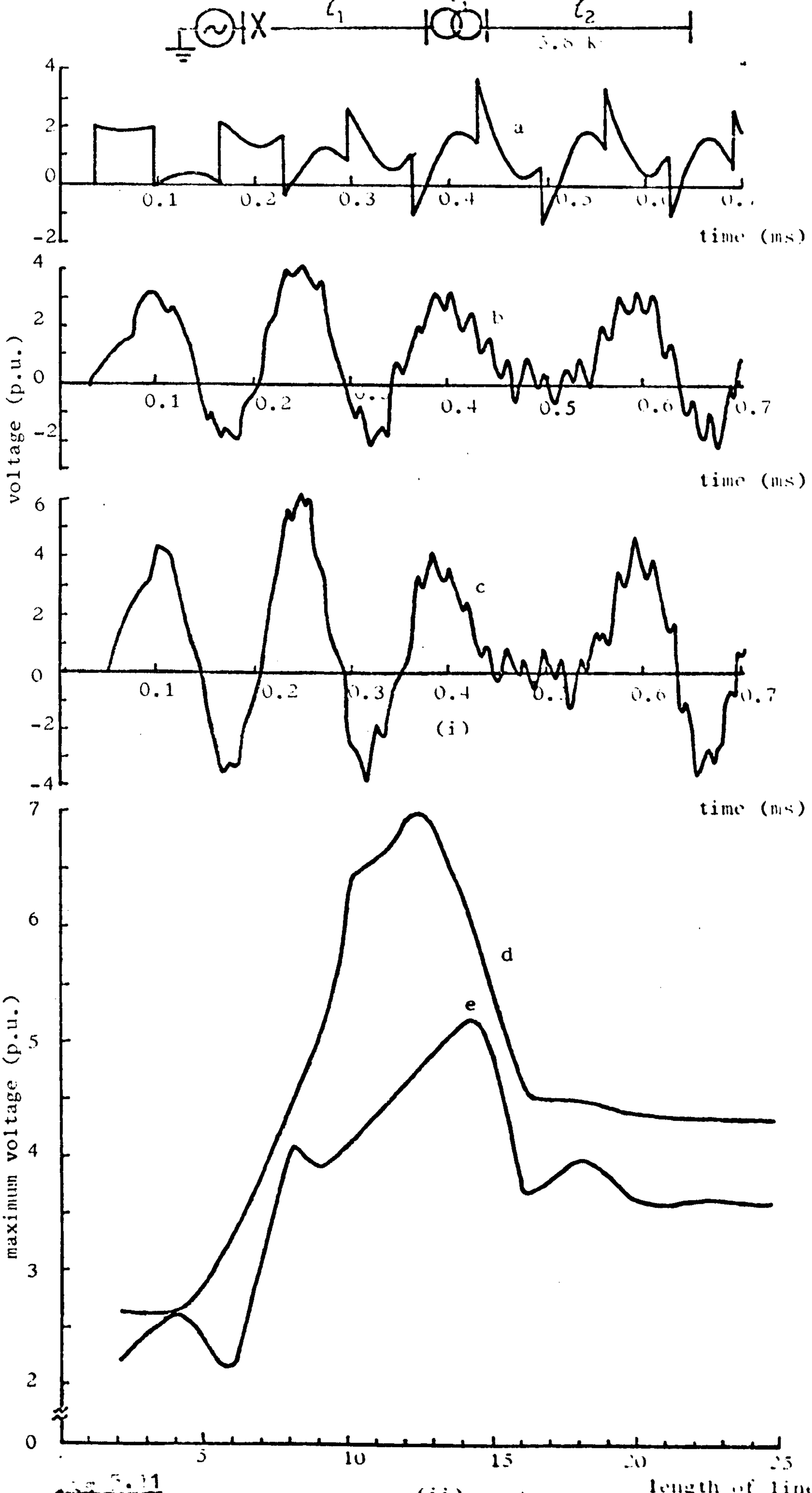

Fig. 5.11

The effect of varying length of line ℓ_1 (ℓ_2 = 5.1 km) on computed
(i) voltage waveforms at the (a) transformer line side
(b) transformer secondary
(c) remote end of line ℓ_2
(ii) maximum voltages at (d) remote end of line ℓ_2
(e) transformer secondary

feeder ℓ_1, the magnitude of the voltage surges transferred to the secondary line is initially a small fraction of the incident wave. The transformer leakage inductance temporarily stores the magnetic energy drawn from the sharp positive and negative step fronts of the surges transferred to the secondary side. The result is that the square-wave voltage incident along the feeder enters the secondary line, not abruptly, but with a voltage that rises gradually. This exponential rise of the voltage wave is evident on the curves of secondary voltages (Fig. 5.11 (i) b and c). The point of inflection on the initial slope of these curves is due to the arrival of the wave reflected from the other end of the line ℓ_2. The train of pulses on the feeder are also modified somewhat. Each positive or negative voltage step is followed by an exponential decay and the square waveform degenerates into a train of pulses consisting of very sharp spike pulses, as shown on curve (a).

If transformer T_2 and a 3.7km line replace transformer T_1 and the secondary line, Fig. 5.12 (b and c) shows that the essential character of resonance peaks is preserved as the length of feeder is varied. Overvoltage peaks occur at both ends of the secondary line when the length of feeder is close to 4.9km and three times this value (14.7km). The crest between the overvoltage peaks, occurring when the length of ℓ_1 (11.1km) is approximately three times the length of ℓ_2, is caused by a resonance condition. The phenomenon arises because the frequency of line ℓ_1 approaches the third harmonic frequency of line ℓ_2. The overvoltage tends to rise again when length of line ℓ_1 is reduced below 2km. In this region, the frequency of line ℓ_2 is near to the third harmonic frequency of line ℓ_1. These frequencies will coincide when

$$\ell_1 = \tfrac{1}{3}\ell_2 = 1.2\text{km}.$$

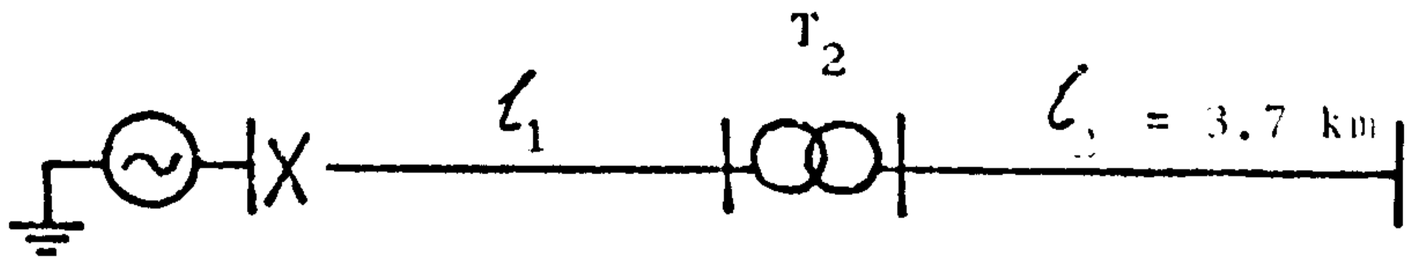

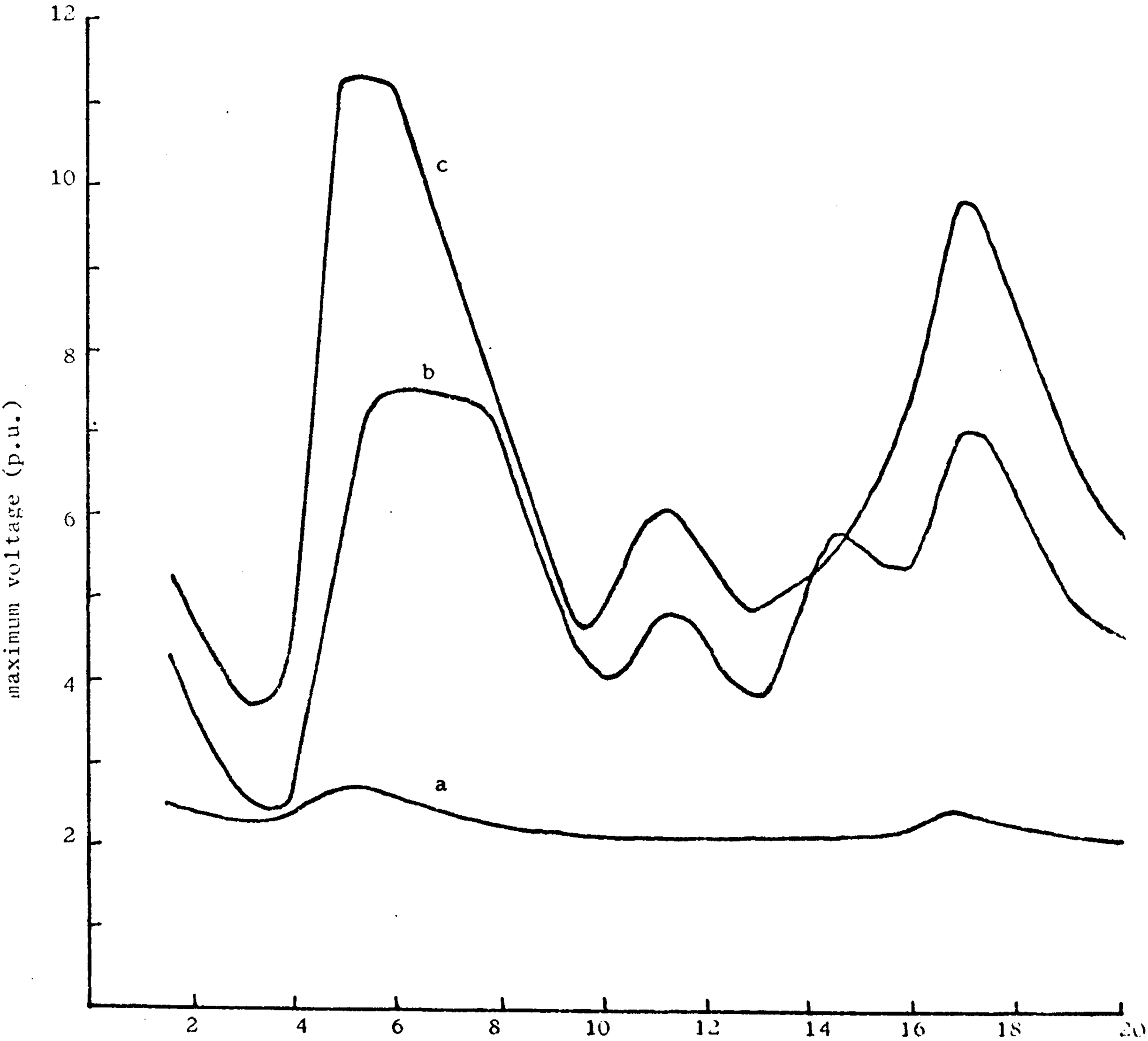

Fig 5.12

The effect of varying length of line ℓ_1 (ℓ_2 =3.7km) on computed maximum voltages at the
(a) transformer line side
(b) transformer secondary
(c) remote end of line ℓ_2

5.5 Surge impedance

The resonant oscillations developed at the transformer terminating a feeder are largely governed by the exchange of energy at the transformer junction. The amount of the energy which penetrates the transformer depends mainly on the surge impedance ratio, Z_T/Z_L, which is normally high. Such a high ratio permits only a small amount of energy to be extracted from the line, leaving the energy contained in the exciting oscillations essentially constant. This allows high resonant overvoltages to develop if the line frequency is such that a resonant mode is excited in the transformer.

In Appendix 12.1 equation 12.11 gives the magnitude of the mth voltage peak at resonance

$$\hat{V}_m = 2 \cdot \sum_{n=1}^{m+1} \left[1 - (-k)^{m-n+1} \right] \cdot (-1)^{n+1} \qquad 5.5$$

where, according to equation 12.14

$$k = \exp(-\pi/2 \cdot Z_L/Z_T)$$

This equation shows that, at a given frequency, the magnitude of the overvoltage is dependent on the surge impedance ratio.

Fig. 5.13 shows overvoltages at the transformer as a function of the surge impedance ratio while the frequency of the oscillatory circuit and that of the line is kept constant. This is achieved by increasing the leakage inductance of the transformer by a certain factor, and decreasing the equivalent capacitance on the transfomer secondary by the same factor. A fixed length of feeder maintains the line frequency constant. The overvoltages increase somewhat exponentially as the surge impedance ratio increases. This exponential relationship may be explained with the aid of equation 5.5. The magnitude of the mth peak isshown to increase with the value of k, and k is exponentially related to the surge impedance ratio Z_T/Z_L.

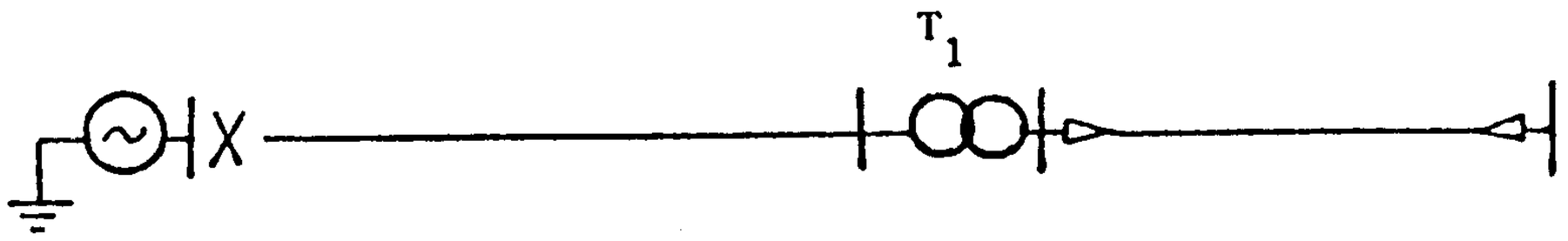

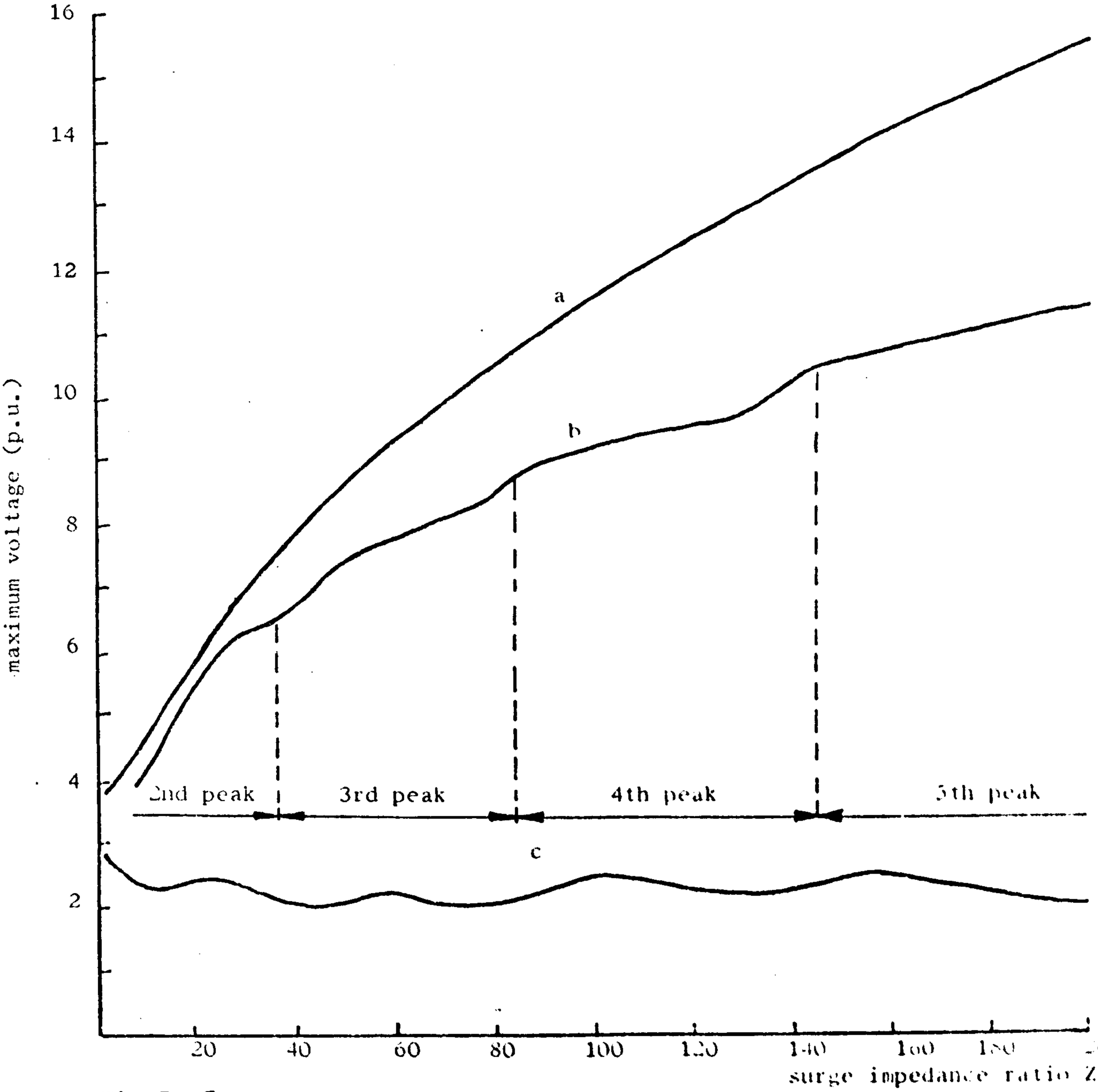

Fig 5.13
Effect of surge impedance ratio on overvoltages at the transformer
(a) transformer secondary overvoltage factor (mathematical model)
(b) transformer secondary overvoltage factor (..... model)
(c) transformer primary overvoltage factor (mathematical model)

As this ratio increases, the value of k approaches unity, resulting in overvoltages of increasing severity.

The overvoltage curve obtained from T.N.A. results (Fig. 5.13 b) consists of a series of displaced exponential curves. The transition points as defined on this figure correspond to the change in the number of cycle at which the maximum voltage occurs. For a particular peak with maximum voltage, the increase in the overvoltage is initially high after the point of transition, and becomes less as the surge impedance ratio increases. These changes of slope on the curve are not evident on curve (a) of this figure relating to digital computer results.

It may be seen from Fig 5.13 (a) that the maximum voltage on the transformer primary range between 2 and 3 p.u. The corresponding overvoltages recorded from the T.N.A. barely rise above 2 p.u. due to the effects of losses and attenuation on the line.

In Fig. 5.14 (curves a and b) a comparison of voltage waveforms at the transformer is made for surge impedance ratios (Z_T/Z_L) of 15.7 and 84.8. It may be seen that the transformer line-side voltage for the higher impedance ratio tends to maintain its 'squareness' longer than that recorded for the lower surge impedance ratio. The secondary overvoltage factor shows a marked increase from 5.3 to 8.8 when the impedance ratio is increased from 15.7 to 84.8.

A reduction of the line impedance will have the same effect on the overvoltage factor as the increase in the transformer surge impedance. Curves c and d of Fig 5.14 show the effect of a 50% reduction in the line impedance. The maximum secondary voltage increases from 5.3 to 6.1 p.u. Fig 5.6 relating to digital computer results, also shows that if the line feeder is replaced by a cable of surge impedance 10.2Ω, the secondary overvoltage factor increases

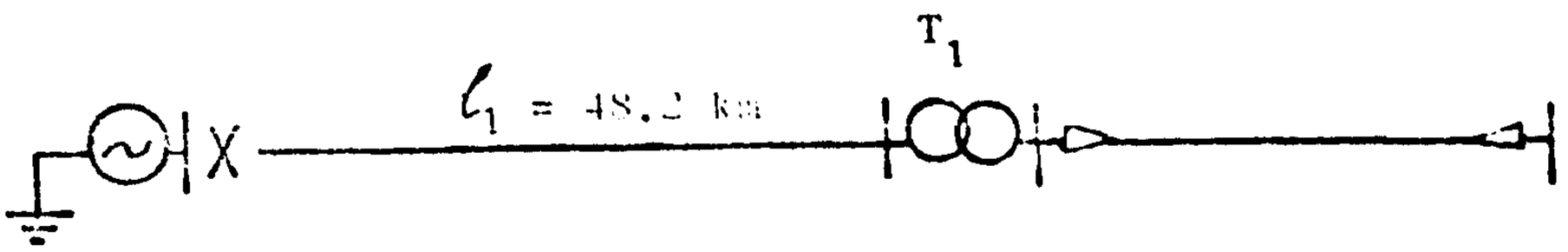

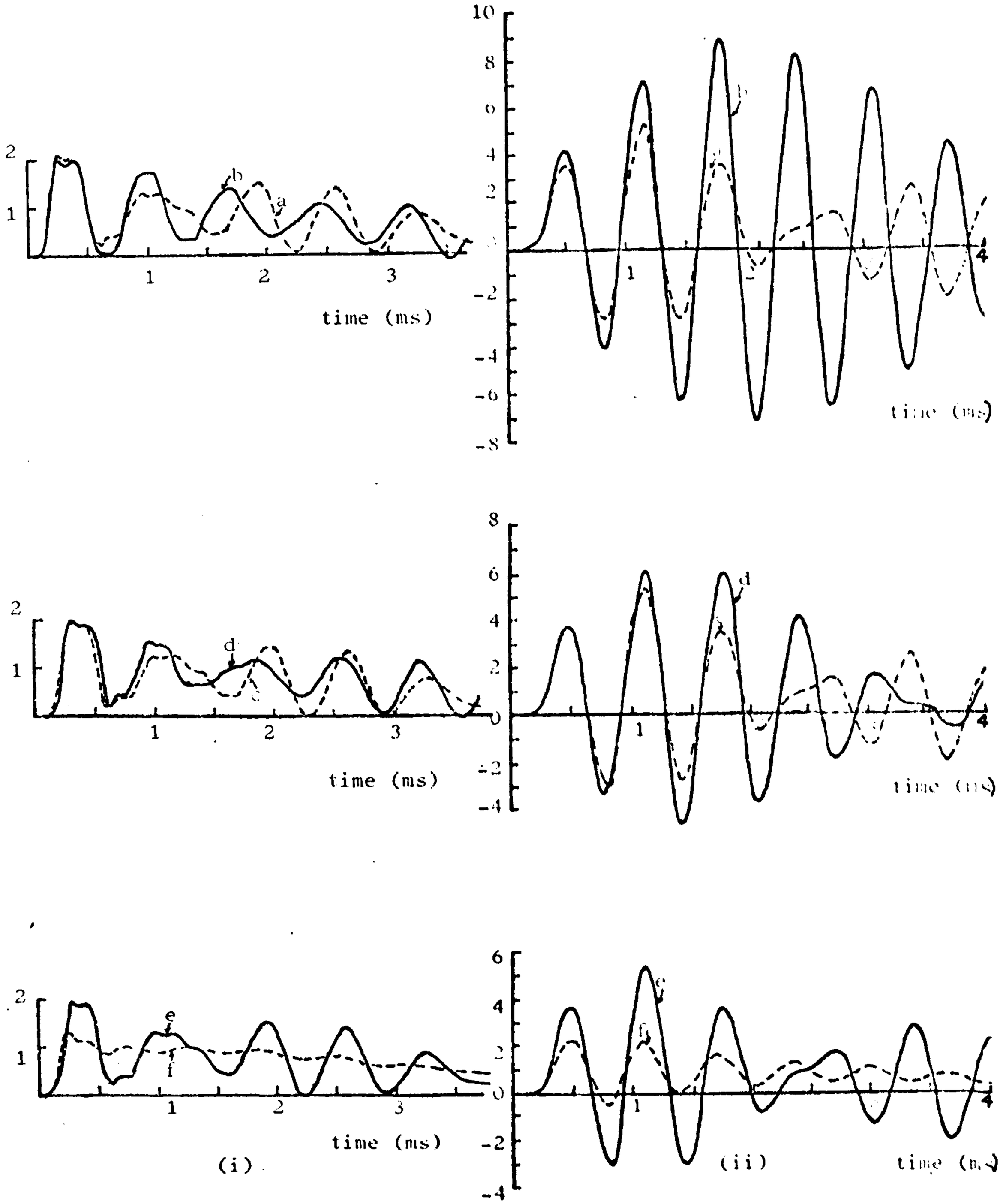

Fig 5.14
Effect of surge impedance ratio on voltage waveforms (T.N.A. model)
(i) Transformer primary voltage
(ii) Transformer secondary voltage
(a) Z_T/Z_L = 15.7
(b) Z_T/Z_L = 34.8
(c) Z_L = 297.0 Ω
(d) Z_L = 148.5 Ω
(e) transformer energised without infinite line
(f) infinite line connected at transformer primary

from 5.75 to 21.65 at resonance. For the 21.5 and 32.4Ω surge impedance cables, the corresponding overvoltages are 16.70 and 14.16 p.u. respectively. In each case, the length of the cable is such that its propagation time gives a frequency equal to that of the transformer. Table 5.2 gives the overvoltage factors obtained from digital computation as a function of line surge impedance. The difference in the maximum line-side voltages is not significant. The secondary overvoltages increase sharply at first with increase in the ratio Z_T/Z_L, and subsequently gradually.

A transformer may, in practice, be energised together with a line connected in parallel to the same busbar. If the transit time of this line exceeds the time of observation, the line may be considered infinite. This line has the effect of significantly reducing the ratio Z_T/Z_L. A considerable amount of energy from the line oscillations will drain into the infinite line. This is illustrated on Fig.5.14, curve f, which shows only a small ripple of oscillations at line frequency. Hence the significant reduction in the secondary over-voltage factor when the infinite line is switched with the transformer (curves e and f) from 5.3 to 2.0. If the surge impedance ratio of this infinite line is reduced, the maximum voltage at the transformer decrease further as shown on Table 5.3.

TABLE 5.2

EFFECTS OF THE SURGE IMPEDANCE OF FEEDER (DIGITAL COMPUTER STUDY)

Surge Impedance ratio (Z_T/Z_L)	Maximum Transformer Voltage (p.u.)	
	Line side	Secondary side
18	2.45	5.75
36	2.38	7.55
54	2.34	8.82
72	2.30	10.10
90	2.23	11.00
108	2.21	11.80
126	2.20	12.64
144	2.19	13.37
162	2.17	13.94
180	2.41	14.53

TABLE 5.3

EFFECT OF THE SURGE IMPEDANCE OF THE INFINITE LINE CONNECTED AT THE TRANSFORMER PRIMARY (DIGITAL COMPUTER STUDY).

Surge Impedance ratio (Z_T/Z_L)	Maximum Transformer Voltage (p.u.)	
	Line side	Secondary side
18.00	2.45	5.75
1.00	1.05	1.96
0.50	1.01	1.42
0.33	0.99	1.27
0.25	0.98	1.18
0.20	0.97	1.14

5.6 Losses

In the preceding sections the mathematical models used for digital computation do not take account of system losses. These losses are however inherent in the electromagnetic TNA models used. In practice, the losses in the system act to reduce the magnitude of the overvoltages by damping the travelling pulses in the lines and the oscillations in the transfomer.

When energising a transformer through a line, with a short length of cable connected on the secondary side, the flux in the transformer is mainly the leakage flux carried by air. The iron losses due to the flux in the core are not in this case significant. Damping of the transformer oscillations is provided principally by the ohmic series resistance of the windings. At system frequency, this resistance is very small and may be of the order of 0.1 p.u. However, at the high frequencies of oscillations encountered in this study, the effective resistance increases considerably due to both skin and proximity effect. The resistance in this case could be several times more than the resistance at system frequency (typically of the order of 100 p.u.)

The tendency of the current in the conductors to flow in greater density in the outer layers of the conductors increases as the frequency increases. It is this non-uniform distribution of current in the conductor which increases its effective resistance. When this distribution of current across the cross-section is affected by the field of a neighbouring conductor, the phenomenon referred to as proximity effect contributes to the apparent resistance which provides substantial damping of the transformer oscillations.

Fig 5.15 presents digital computer results showing that the maximum resonance voltages at the transformer secondary decrease

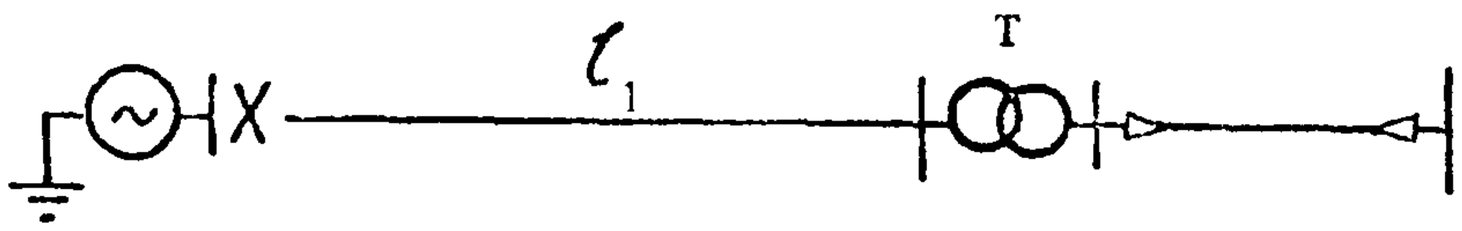

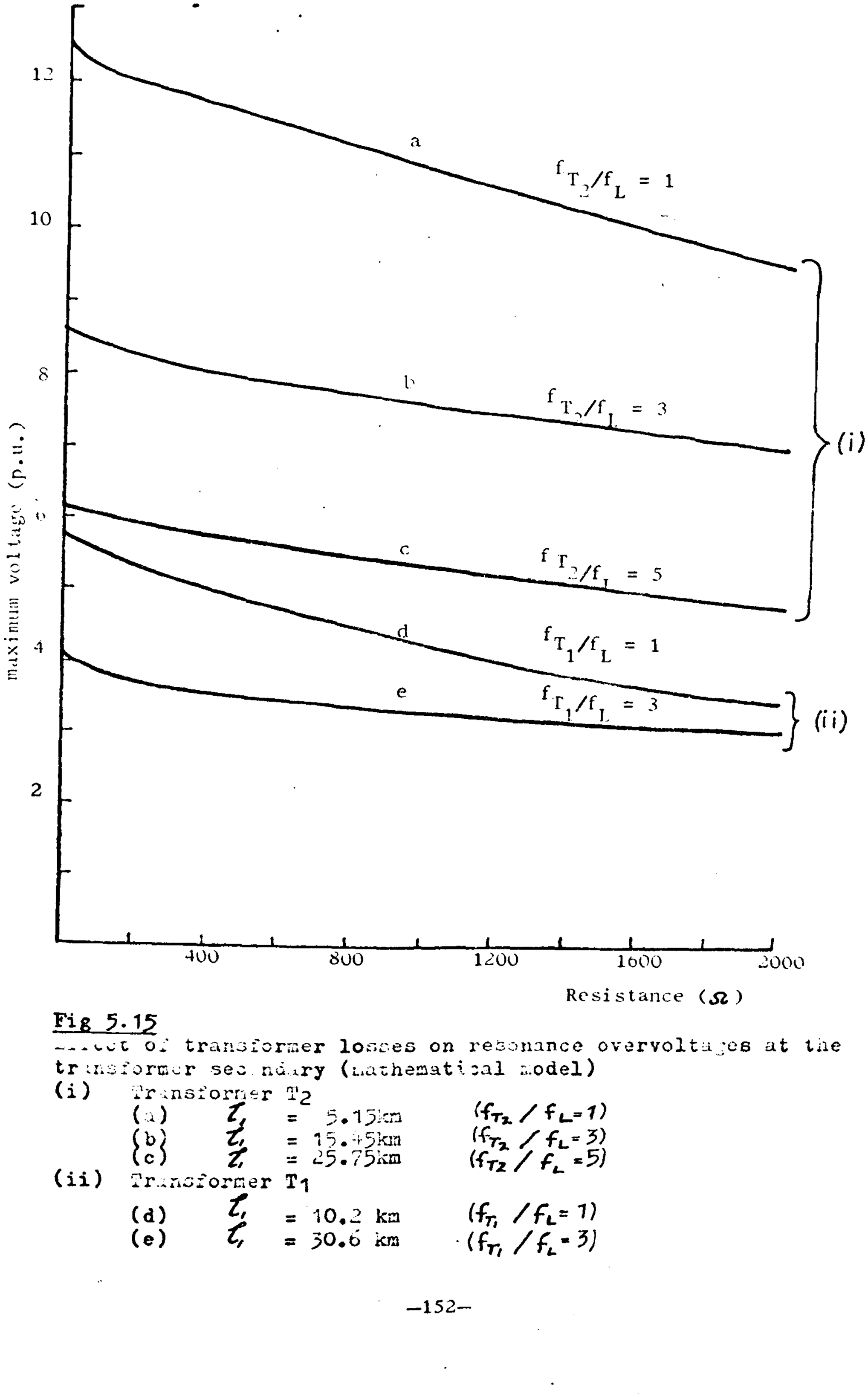

Fig 5.15

Effect of transformer losses on resonance overvoltages at the transformer secondary (mathematical model)

(i) Transformer T_2
- (a) ℓ_1 = 5.15km $(f_{T_2}/f_L = 1)$
- (b) ℓ_1 = 15.45km $(f_{T_2}/f_L = 3)$
- (c) ℓ_1 = 25.75km $(f_{T_2}/f_L = 5)$

(ii) Transformer T_1
- (d) ℓ_1 = 10.2 km $(f_{T_1}/f_L = 1)$
- (e) ℓ_1 = 30.6 km $(f_{T_1}/f_L = 3)$

as the transformer resistance is increased. This decrease is more significant for equal line and transformer frequencies than when the line frequency is equal to an odd harmonic of the transformer frequency.

The overvoltage magnitudes are also affected by the attenuation and distortion of the travelling waves as they propagate along a line. This is caused mainly by the losses in the energy of the wave due to line and insulation resistance and corona loss. Owing to the high frequency components contained in the steep front of the exciting waveform, the apparent resistance of the line conductor is increased considerably by the skin effect. Since the ground provides the return currents of the surges propagated between the phase conductor and earth, ground losses also increase the effective resistance. These losses are dependent on the conditions of the soil. The conductivity of the soil is attributable almost entirely to the moisture contained in it and the minerals dissolved in this mositure. It is shown in the literature that the resistance of the line conductor and ground is proportional to the square root of the frequency. The line losses also depend on the distance travelled by the waves along the line. The wave-front decays exponentially as it proceeds along the line because of the greater attentuation of the high frequency components comprising the front of wave. The fronts become less steep and the tails become elongated, leading to distortion of the travelling wave. The slower velocity of propagation of the earth mode compared to that of the aerial modes introduces a time lag in the transient voltage at the end of the line. This also distorts the waveform, but does not necessarily decrease the magnitude of the voltage wave. The time delay in the slower earth mode may alter the phase relationship between the travelling waves on the line. As a result, portions of the waves may undergo an increase in voltage.

Energy may also be expended in the vicinity of line conductors through a discharge known as corona. When the voltage wave amplitude exceeds a critical value, the air surrounding the conductors is partially ionised and a corona discharge current flows from the conductor surface to the air insulation. The effect is to reduce exponentially the amplitude of portions of the voltage wave whose magnitude exceeds the corona threshold voltage. The lower amplitude waves are not affected. Corona, therefore, attenuates the voltage peaks and distorts the waveform.

5.7 Residual charge on line

Conditions may arise where the feeder being energised is charged to a voltage of opposite polarity to the system voltage due to a previous switching operation. The initial voltage surge applied to the line may be of the order of 2.0 p.u. This may arise if the contacts of the circuit breaker close at peak system voltage, when the charge retained on the line is of opposite polarity. The resulting 2.0 p.u. voltage across the switch sets up a large amplitude oscillation on the line.

In practice, however, the residual charge on the line decays due to leakage through the insulation. The rate of discharge increases considerably if transformers (or shunt reactors to some extent) are connected at the end of the line. The magnetising impedance of the transformer provides a path through which the residual charge trapped in the electrostatic field of the line discharges in an oscillatory manner. The time constant of the discharge is generally much greater than the 'dead' time of high-speed auto-reclosure circuit breakers normally used. It is dictated mainly by the transformer losses, and, to a less extent by line losses. Even with the transformer connected at the end of the line, a considerable residual charge may be present at the instant of re-closure.

Table 5.4 shows how the maximum resonance voltages at the transformer increase with the increase in the trapped charge on the line, when the feeder is energised at a positive peak system voltage. The relationship between charge and overvoltage is approximately linear. If the polarity and amplitude of the voltages at both ends of the circuit breaker are the same, a sharp reduction in the resonance overvoltages results, as may be seen from the last line of this table.

TABLE 5.4

THE EFFECT OF TRAPPED CHARGE ON THE LINE ON OVERVOLTAGE AT THE TRANSFORMER

Trapped Charge p.u.	Maximum voltages (p.u.)	
	Line-side voltage	Secondary voltage
0	2.25	5.75
-0.25	2.60	7.00
-0.33	2.68	7.40
-0.50	2.91	8.25
-0.67	3.15	9.08
-0.75	3.25	9.50
-0.85	3.39	10.00
-1.00	3.60	10.75
+1.00	1.48	2.43

5.8 Conclusions

Although the computation results presented here do not take account of system losses, the phenomenon of resonance and consequent overvoltage is potentially hazardous enough to warrant consideration during the design stages of a power system. This chapter established the system parameter values which are likely to aggravate the resonance overvoltages produced. A necessary condition for the occurrenceof this phenomenon is that the waveform produced at the line side of the transformer must contain a frequency component approximately equal to that of the transformer. Since the ratio of the surge impedances Z_T/Z_L, is normally high, an analysis of the open circuit voltage at the end of the feeder may provide sufficient information to determine whether resonance would occur. If necessary, a change in one of the parameter values of the system may alter either the line or the transformer frequencies, effectively taking the system out of resonance. As an example, a change in the length of the cable or line on the transformer secondary, or connection of a shunt capacitor on the secondary, detunes the oscillatory circuit. Consequently, resonant oscillations will not develop.

Use may also be made of pre-insertion resistors of the circuit breaker to reduce the amplitude of the initial voltage step applied to the line. If high-speed auto-reclosure employing switching resistors are used, these resistors also help to reduce the amount of residual charge on the line.

Although the parameters of the transformers used in the T.N.A. and digital computer studies are different, these two methods produce results which are in close correlation with respect to general trends of overvoltage due to variations of system parameters. In this single phase study, the transformer non-linear and mutual effects have

not been considered. This will be the subject of Chapter 8. Further methods used to reduce these overvoltages will be discussed in that Chapter.

Although the probability of exact coincidence of line and transformer frequencies under service conditions is small, the curves of maximum voltages against frequency show that a difference of up to 30% in the two frequencies is sufficient to cause large overvoltages at the transformer secondary.

C H A P T E R 6

THE EFFECTS OF SYSTEM CONFIGURATION ON RESONANT OVERVOLTAGES

6.1 Introduction

In the previous chapter, resonance overvoltages arising from energisation of a line with an integrally connected transformer, are discussed. Transient voltages in excess of those obtaining when energising unterminated lines are found to occur. For certain values of system parameters, the severity of these overvoltages may be increased considerably. This study will now be extended to include the effects of system configuration on overvoltages at the transformer.

It has been established that the resonant overvoltages depend on the frequency spectrum of the transient voltage on the line-side of the transformer. A study of the factors which could modify this voltage is therefore crucial in predicting the occurrence of this phenomenon. These multiple reflections will depend, among other things, on the physical layout of the feeder circuit, the characteristics of the circuits connected to the circuit breaker terminal remote from the transformer, and the relative arrangement of overhead lines, cables and circuit breakers. These factors may, in certain cases, intensify the overvoltages at the transformer secondary.

6.2 Transformer feeder configuration

The transformer feeder very often consists of an integrated system of lines having a wide variety of physical arrangements. These lines may be switched as a unit with the transformer. The effect of the oscillations set up in these lines and the position of the breaker along the line, on transformer overvoltages, will now be investigated.

6.2.1 Position of circuit breaker

It is possible in practice, for a feeder to be energised from a circuit breaker separated from an infinite source by a length of line. In this case, the line on the source side of the breaker is in the steady state before the breaker closes. It will be assumed that the natural frequency of the transformer equals that of the combined source-side line and feeder.

When the breaker is positioned at the source, it has been shown in section 5.3 that a voltage wave of twice the input step voltage is generated at the remote end of the line. If, on the other extreme, the breaker is placed adjacent to the transformer, this is not the case. When the switch operates, the voltage across it (E) divides into two surges injected into the transformer and the source-side system in accordance with the surge impedances on both sides of the breaker. The voltage surge impressed on the line is given by

$$V_L = \frac{Z_L}{Z_L+Z_T} E \qquad 6.1$$

and the surge applied to the transformer is

$$V_T = \frac{Z_T}{Z_L+Z_T} E \qquad 6.2$$

where Z_L and Z_T are the surge impedances of the line and transformer, respectively. Since the ratio Z_T/Z_L is normally large, the oscillations set up on the line will have a relatively small amplitude, and hence

the overvoltages will be minimised.

For an intermediate location of the breaker, the surge impedances on both sides of the breaker are equal. Equations 6.1 and 6.2 show that voltage surges of half the voltage across the breaker will be set up on each line section. Overvoltages developed at the transformer will be less severe than those resulting from energisation at source.

By making the surge impedance of the transformer infinite, the magnitudes and frequencies of the voltage components may be estimated by Fourier analysis of the waveform. Referring to the circuit diagram of Fig 6.1, it can be shown from lattice diagram considerations that the voltage at the end of line ℓ_2 is given by

$$V = \begin{cases} 0 \text{ when } 0 < t < T_2 \\ 1 \text{ when } T_2 < t < 2T_1 + T_2 \\ 2 \text{ when } 2T_1+T_2 < t < 2T_1 + 3T_2 \\ 1 \text{ when } 2T_1+3T_2 < t < 4T_1 + 3T_2 \\ 0 \text{ when } 4T_1+3T_2 < t < 4T_1 + 4T_2 \end{cases} \qquad 6.3$$

for the first period, where

T_1 = travel time of line ℓ_1, and

T_2 = travel time of line ℓ_2.

This is an even periodic function with period $4(T_1 + T_2)$.

Fourier analysis of this wave gives

$$V = \sum_{n=1}^{\infty} \left[\frac{2}{n\pi} \left\{ \sin \frac{n\pi T_2}{2(T_1+T_2)} + \sin \frac{n\pi (2T_1+T_2)}{2(T_1 + T_2)} \right\} \cdot \cos \frac{n\pi t}{2(T_1+T_2)} \right] \qquad 6.4$$

Using the trigonometric relation

$$\sin A + \sin B = 2 \sin \frac{A+B}{2} \cdot \cos \frac{A-B}{2} \qquad 6.5$$

then

$$V = 1 - \frac{4}{\pi} \sum_{n=1}^{\infty} \left[\frac{1}{n} \sin \frac{n\pi}{2} \cos \frac{n\pi\, T_1}{2(T_1+T_2)} \right] \cos \frac{n\pi}{2(T_1+T_2)}\, t \qquad 6.6$$

But $\sin n\pi/2 = 0$ when n is even

$= \pm 1$ when n is odd

and $\omega_L = 2\pi f_L = \dfrac{\pi}{2(T_1+T_2)}$

where ω_L and f_L relate to the frequency of the line of length $l_1 + l_2$

$$V = 1 + \frac{4}{\pi} \sum_{n=1}^{\infty} \left[\frac{1}{2n-1} \cos (2n-1)\, \omega_L T_1 \cdot \cos(2n-1)\omega_L t \right] \cdot (-1)^n \qquad 6.7$$

If the breaker is placed at the source, then $T_1 = 0$ and

$$V = 1 + \frac{4}{\pi} \sum_{n=1}^{\infty} \left[\frac{1}{2n-1} \cos (2n-1)\omega_L t \right] \cdot (-1)^n \qquad 6.8$$

which is identical toequation 5.3 derived for this case.

For the case where the breaker is positioned adjacent to the transformer, $T_2 = 0$

i.e $\omega_L T_1 = \pi/2$

equation 6.7 gives

$$V = 1 \qquad 6.9$$

A comparison of equations 6.7 and 6.8 will show that, for breaker locations along the line, the surge amplitude will be reduced by a factor

$\cos (2n-1)\omega_L T_1$ where n=1, 2, 3 ....

If the breaker is located midway between the source and the transformer, then $T_1 = T_2$

$$\text{ie. } \omega_L = \frac{\pi}{4T_1}$$

Equation 6.7 becomes

$$V = 1 + \frac{4}{\sqrt{2}\pi} \sum_{n=1}^{\infty} \left[\frac{1}{2n-1} \cos (2n-1)\, \omega_L t \right] \cdot (-1)^{n(n-1)/2} \qquad 6.10$$

from which it may be seen that the amplitude is reduced by a factor of $1/\sqrt{2}$.

Oscillogram traces of the three cases considered above are shown in Fig. 6.1. The dependence of the transformer primary voltages on breaker location is demonstrated. The reduction of secondary voltage magnitudes as the breaker is moved closer to the transformer. is clearly shown. When the transformer is energised directly from the breaker with no intermediate line (Fig.6.1(iii)) the line side voltage barely exceeds 1 p.u. as is also illustrated by equation 6.9. The amplitude of the line frequency component is relatively small. Consequently the secondary voltage oscillations do not develop.

The envelopes of maximum secondary voltages for different breaker locations are shown in Fig. 6.2. The close agreement in the tendencies of these overvoltages obtained from the digital and analogue methods, is demonstrated.

6.2.2 Length of line beyond the transformer

It is sometimes possible for a transformer to be energised from either of two feeders teed together at the transformer, as shown on the circuit diagram of Fig. 6.3. It is assumed that the frequency of the line used to energise the transformer is maintained constant at the transformer frequency. The length of the other line, open-circuited at its remote end, is varied.

When the surges initiated on the energised line arrive at the transformer, they will see a surge impedance given by the transformer and line surge impedances in parallel. A considerable amount of the incident energy will drain into the line ℓ_2, and the resulting oscillations set up in this line will influence the transformer overvoltages.

Fourier analysis may again be used to determine the

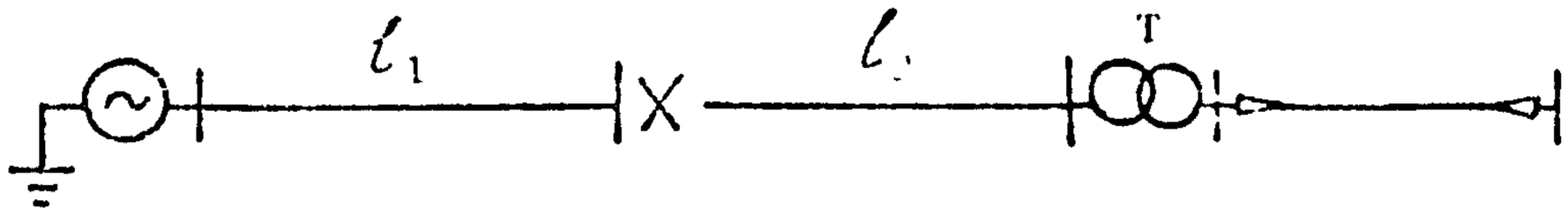

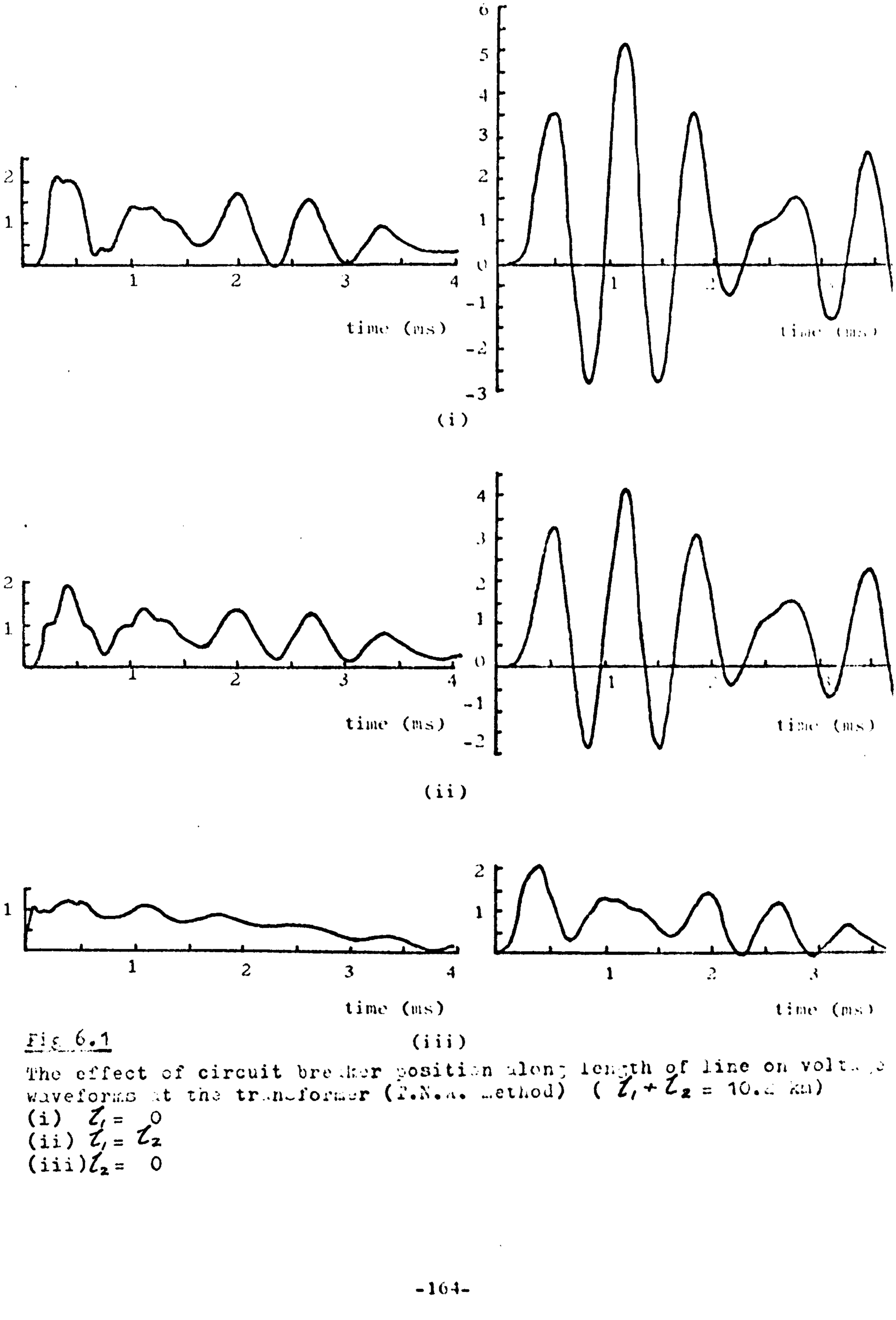

Fig 6.1

The effect of circuit breaker position along length of line on voltage waveforms at the transformer (E.M.A. method) ($\ell_1 + \ell_2$ = 10.4 km)

(i) ℓ_1 = 0

(ii) $\ell_1 = \ell_2$

(iii) ℓ_2 = 0

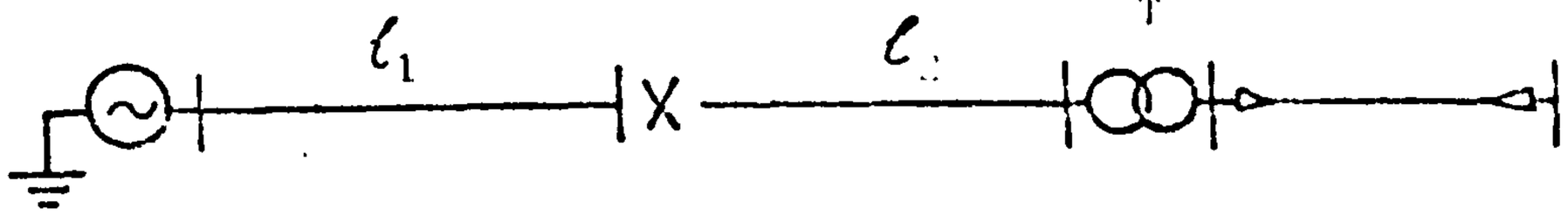

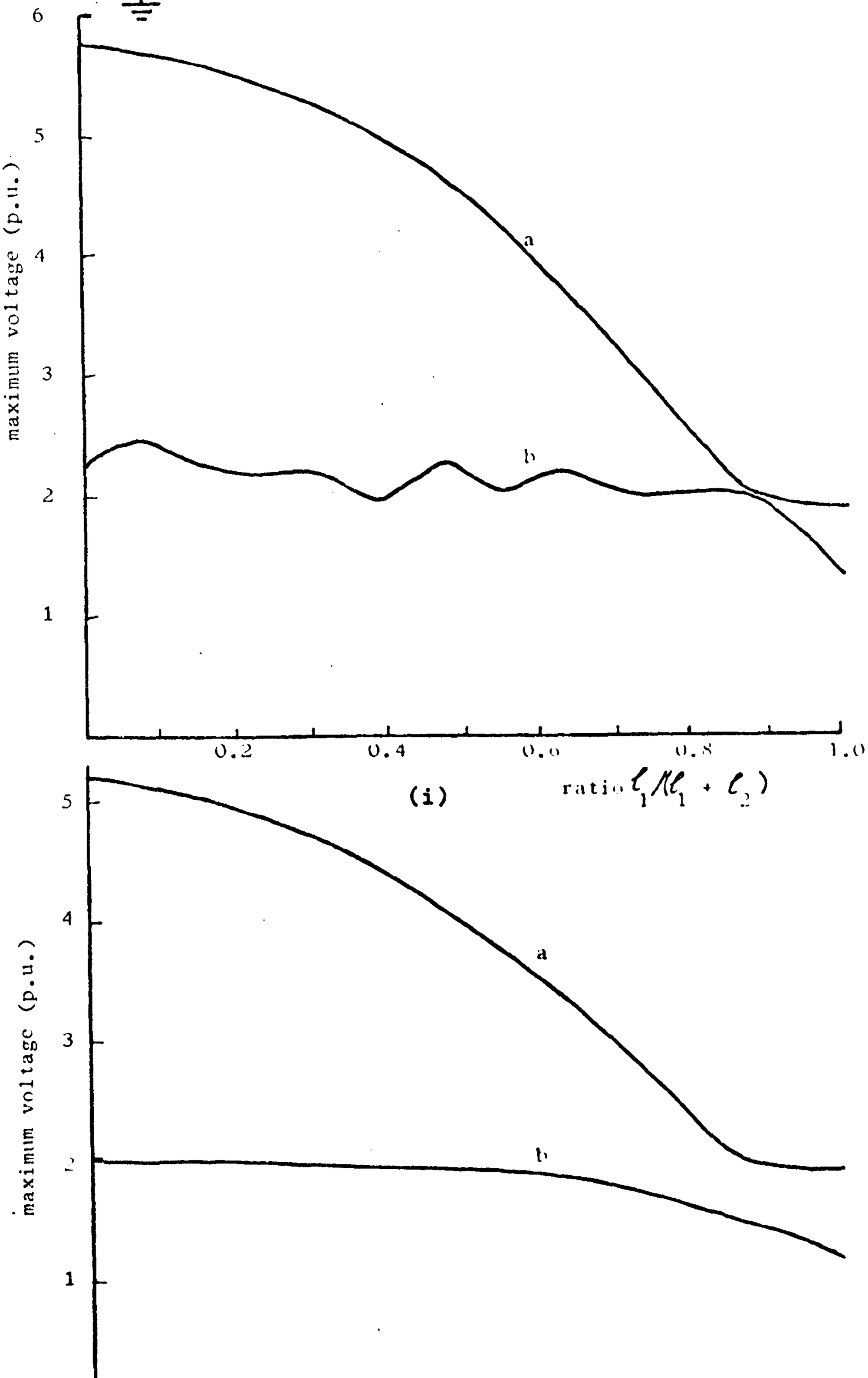

Fig 5.2

Variation of overvoltage with the position of the circuit breaker along the line (i) Digital computer method ($\ell_1 + \ell_2$ = 10.2 km)
(ii) T.N.A. method ($\ell_1 + \ell_2$ = 10.2 km)
(a) maximum voltage at the line side of the transformer
(b) maximum voltage at the transformer secondary

combined influence of oscillations on both lines at the transformer primary. Assuming an infinite transformer surge impedance, the voltage at the tee busbar is given by an equation similar to equation 6.3 with T_1 and T_2 interchanged. Application of Fourier analysis to this voltage leads to the following equation.

$$V = 1 - \sum_{n=1}^{\infty} \left[\frac{2}{n\pi} \left\{ \sin \frac{n\pi T_1}{2(T_1+T_2)} + \sin \frac{n\pi (T_1+2T_2)}{2(T_1+T_2)} \right\} \cdot \cos \frac{n\pi}{2(T_1+T_2)} t \right] \quad 6.11$$

Expressing ℓ_2 as a multiple of ℓ_1

$$\ell_2 = k\ell_1$$

$$\text{i.e} \quad T_2 = kT_1$$

$$V = 1 - \sum_{n=1}^{\infty} \left[\frac{2}{n\pi} \left\{ \sin \frac{n\pi}{2(k+1)} + \sin \frac{n\pi(2k+1)}{2(k+1)} \right\} \cdot \cos \frac{n\pi}{2(k+1)T_1} t \right] \quad 6.12$$

By simplifying this equation further and substituting,

$$\omega_L = 2\pi f_L = \pi/2T_1$$

leads to

$$V = 1 + \frac{4}{\pi} \sum_{n=1}^{\infty} \left[\frac{1}{2n-1} \cos \frac{(2n-1)\pi k}{2(k+1)} \cos \frac{(2n-1)\omega_L}{k+1} t \right] \cdot (-1)^n \quad 6.13$$

A resonance condition would occur if the voltage, V, contains a function whose frequency is equal to that of the transformer ($f_L = f_T$)

$$\text{Hence} \quad \frac{2n-1}{k+1} = 1$$

$$\text{i.e} \quad k = 2(n-1) \quad 6.14$$

where n = 1,2,3,4 .....

k must therefore be an even integer.

i.e For a resonance condition to occur, ℓ_2 must be an integral multiple of ℓ_1. This is verified by Fig. 6.3 which shows a series of overvoltage peaks occuring when the ratio $k = \ell_2/\ell_1$ is an even integer. The amplitude of these peaks decreases with increasing values of k. This may be explained with the aid of equation 6.13. As the value of k is increased, the value of n increases according to the relation 6.14.

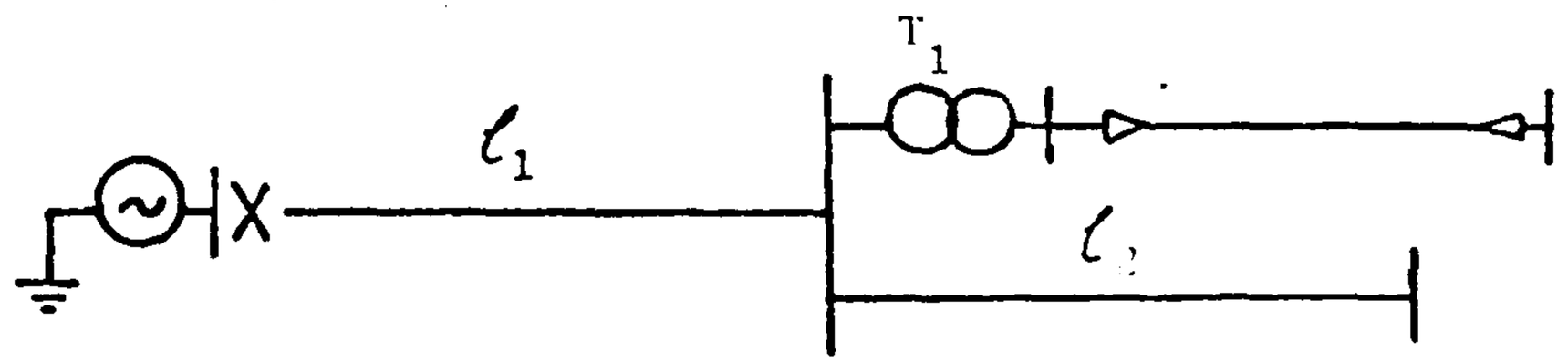

a) Voltage at the line side of the transformer(mathematical method)
b) Voltage at the transformer secondary (mathematical method).
c) Voltage at the transformer secondary (TNA method)

Fig 6.3 The effect of length of line beyond the transformer (ℓ_2) on overvoltages.

Hence the amplitude of the n^{th} component of V,

$$\frac{4}{(2n-1)\pi} \cos \frac{(2n-1)\pi}{2(k+1)} \cdot k$$

will decrease.

Fig 6.4 (i) shows the voltage waveform for the condition where ℓ_2=0 (i.e k=0). If k = 2 (i.e $\ell_2 = 2\ell_1$), Fig 6,4 (iii) shows that a resonant oscillation of lower amplitude exists. In this case, the voltage at the line side of the transformer contains a harmonic component whose frequency equals that of the transformer.

If k is an odd integer, the condition for resonance given by equation, 6.14 cannot hold. This accounts for the troughs shown in Fig. 6.3 at odd values of k. The oscillograms of the voltage at the transformer for this case are shown on Fig.6.4 (ii).

In the limit, if the line beyond the transformer is considered to be infinitely long and represented by its surge impedance, the secondary overvoltage reduces to 2.0 p.u.

The close correlation of the maximum voltage envelopes obtained using the analogue and digital methods is again demonstrated by the overvoltage loci of Fig. 6.3.

6.2.3 Position of tee along the feeder

The tee-point referred to in section 6.2.2 may be located anywhere along the length of the feeder, as shown by the circuit diagram of Fig. 6.5. This system may be energised as a whole by operating the circuit breaker at the source with no breakers adjacent to the tee. In this case, the transformer overvoltages will not only be influenced by the length of the tee-off line, ℓ_2, but also by the position of the tee along the feeder. The effect of varying the position of the tee along the feeder for various lengths of the tee-off line is investigated in this study. The total length of line

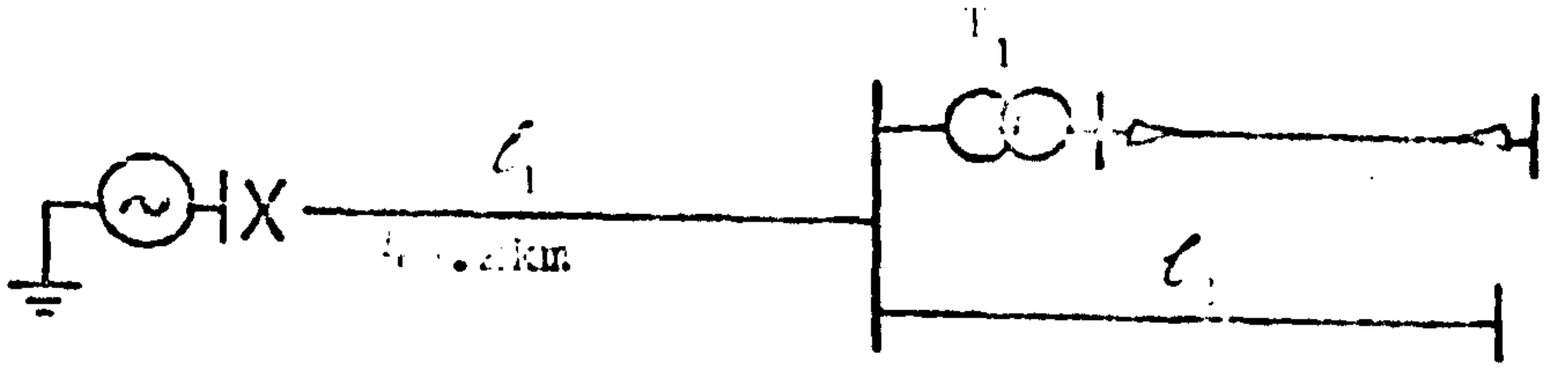

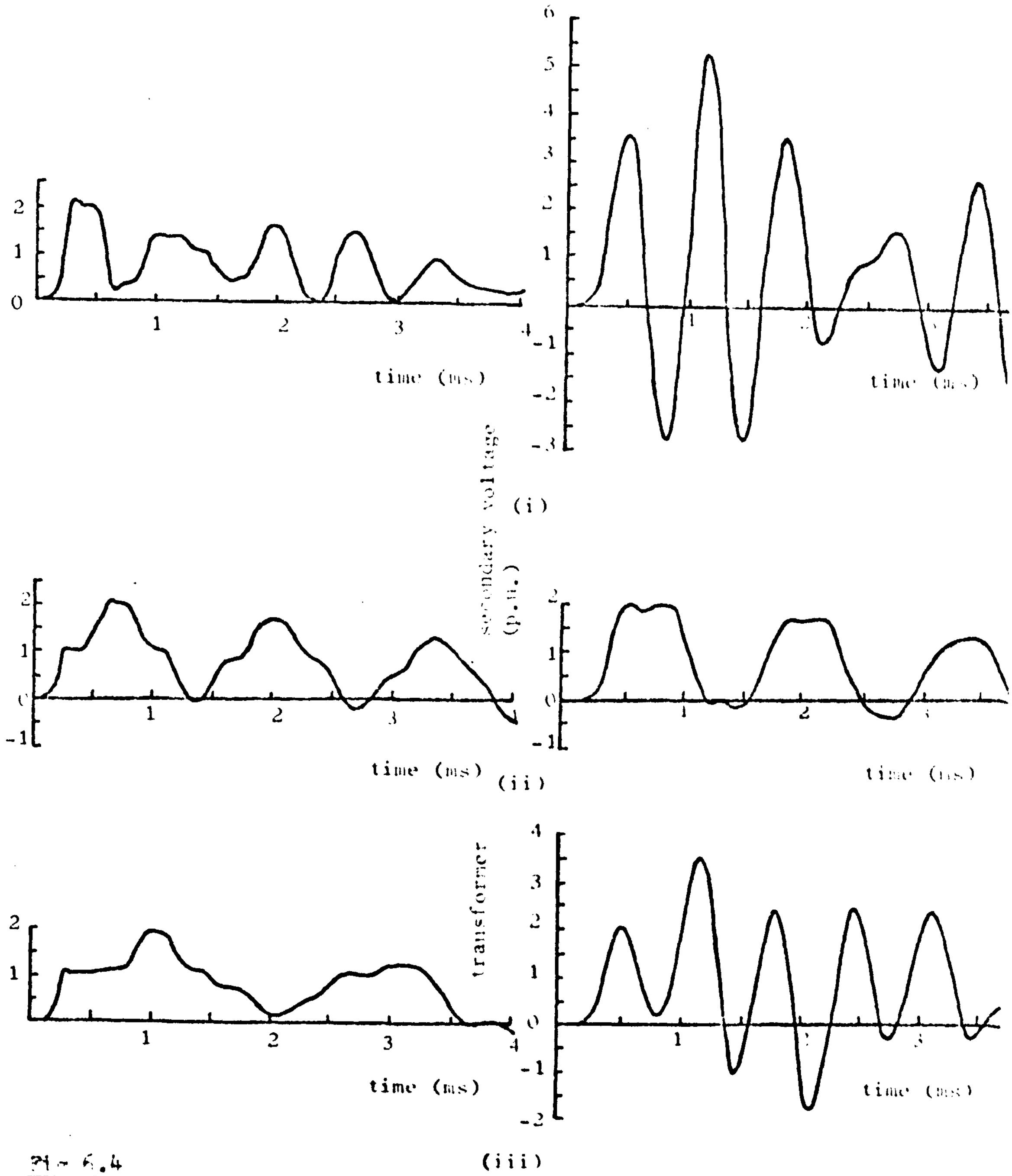

21 - 6.4

The effect of length of line, l_2, beyond the transformer (F.M.A. method)

(i) $l_2 = 0$
(ii) $l_2 = l_1$
(iii) $l_2 = 2l_1$

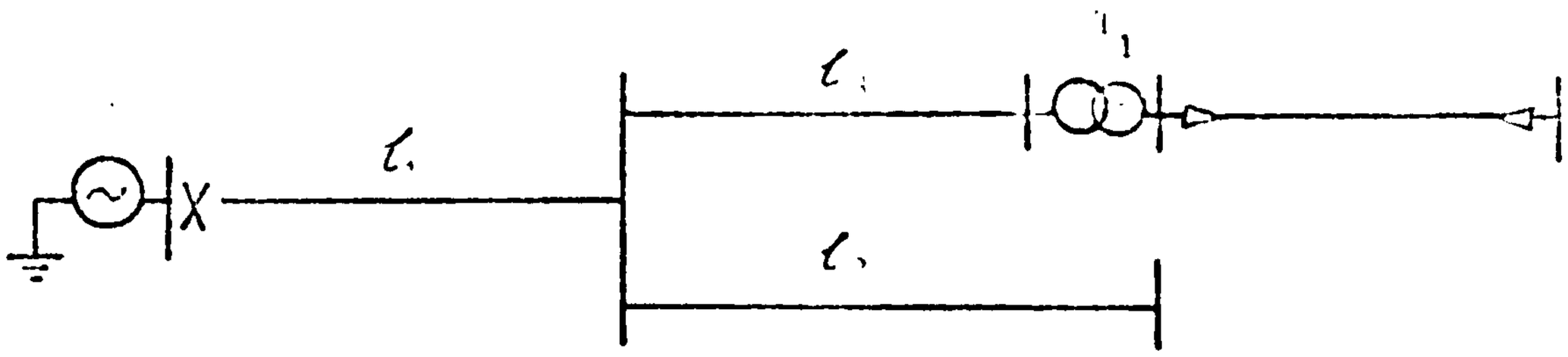

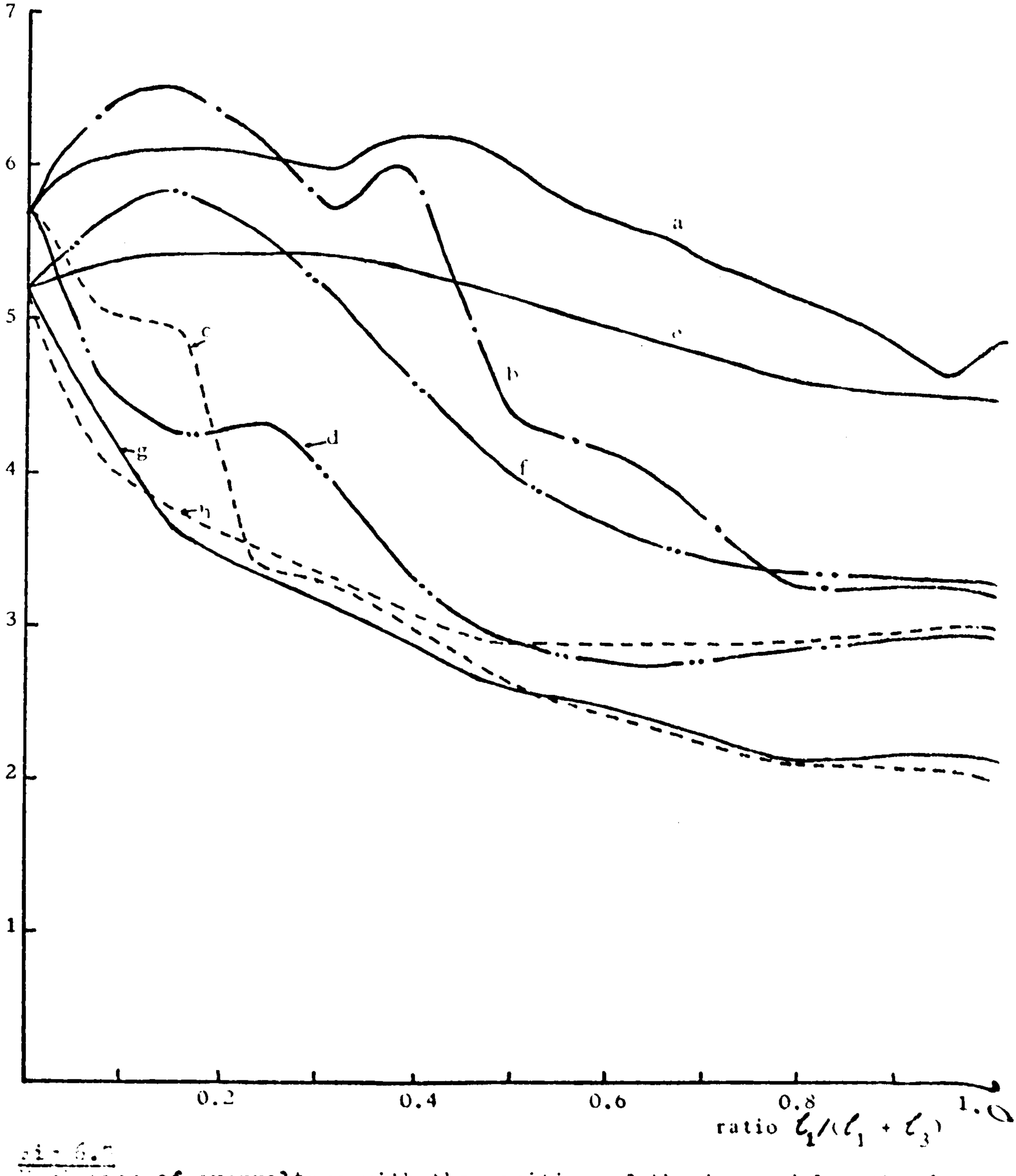

Fig. 6.7

Variation of overvoltage with the position of the tee and length of the tee-off line ($\ell_1 + \ell_3$ = constant)

(i) Mathematical method ($\ell_1 + \ell_3$ = 10.2 km)
- (a) $\ell_2 = 0.05\ (\ell_1 + \ell_3)$
- (b) $\ell_2 = 0.5\ (\ell_1 + \ell_3)$
- (c) $\ell_2 = \ell_1 + \ell_3$
- (d) $\ell_2 = 1.5\ (\ell_1 + \ell_3)$

(ii) T.N.A. method ($\ell_1 + \ell_3$ = 13.2 km)
- (e) $\ell_2 = 0.107\ (\ell_1 + \ell_3)$
- (f) $\ell_2 = 0.5\ (\ell_1 + \ell_3)$
- (g) $\ell_2 = \ell_1 + \ell_3$
- (h) $\ell_2 = 1.5\ (\ell_1 + \ell_3)$

between the source and the transformer, $\ell_1 + \ell_3$, is maintained constant and has the same frequency as the transformer. In spite of this constraint, the increase in the number of variable lengths of the system makes an analysis of the line oscillations a rather cumbersome process.

In Fig 6.5, the position of the tee is specified by the ratio $\ell_1/(\ell_1+ \ell_3)$, where $\ell_1+\ell_3$ is constant. Overvoltage curves are drawn for various lengths of the tee-off line, ℓ_2, rationalised as $\ell_2/(\ell_1+ \ell_3)$. The T.N.A. results are superimposed on those of the digital computer for comparison.

The curves show that, for both methods used, the overvoltage magnitude tends to increase initially, when the position of the tee is nearer the source for lengths of ℓ_2 less than or equal to 0.5 $(\ell_1+\ell_3)$, before falling off again (curves a,b and e,f). A peak value of 6.5 p.u. is obtained for the case ℓ_2= 0.5 $(\ell_1 +\ell_3)$ and ℓ_1 = 0.13 $(\ell_1+\ell_3)$ for the mathematical method (curve b). The corresponding T.N.A. overvoltage (curve f) is 5.75 p.u. at the point where $\ell_1$and ℓ_2 bear the same ratio to $\ell_1 +\ell_3$ as above.

For values of ℓ_2 greater than 0.5 $(\ell_1 + \ell_3)$, on the other hand, the overvoltage magnitude tends to decrease as the tee point is moved further away from the source. The decrease is at first considerable, and then gradual as the tee gets closer to the transformer.

The T.N.A. and the digital computer methods show a close correlation in the overvoltage trends, although the curves derived from the T.N.A. are smoother. The reason is that fewer points are used to plot these curves since the lengths of lines on the T.N.A. can only be increased in relatively large steps.

6.3 Type of source

Previously, it has been assumed that the transformer feeder is energised from a source with an infinite capacity, with the exception of section 6.2.1, where effectively a transmission line source is used. A zero impedance source is only one example of the wide variety of source characteristics. In practice, the source side network terminating at the circuit breaker from which the feeder is energised may be very complex. On the one hand, the line may be energised from a switching station at which a number of transmission lines originating at remote points of the network terminate. In this case the source appears as a resistance equivalent to the combined surge impedance of the lines on the source network. On the other hand, the feeder may be energised directly from a generating station with no transmission lines connected between the generating station and the energising circuit breaker. The source would appear as a pure inductance for this condition. Between the two extremes, a wide variety of combinations is possible. These different physical arrangements of the source have a profound effect on the shape of the travelling waves set up on the feeder, and the oscillations which these waves may excite at the transformer.

6.3.1 Source inductance

If the feeder is energised from a localised generation source, the equivalent inductance of the source may be derived from the short-circuit MVA and system voltage at the source.

$$\text{i.e} \quad L = \frac{(kV)^2}{\omega\ MVA}$$

For example, an inductance of 0.5H corresponds to a fault level of about 110MVA at 132kV.

The effect of the inductive source is examined under conditions where the line natural frequency equals that of the

transformer. The lattice diagram technique put forward by Bewley will be used to study the nature and significance of the effects of source inductance on the oscillations set up on the line. In order to simplify the analysis, the transformer surge impedance will be assumed infinite in relation to that of the line.

In the case of the zero impedance source the incident waves are reflected at the source with a coefficient of -1. On the other hand, a source with an inductance L has a reflection coefficient given by

$$K_R = \frac{pL - Z_L}{pL + Z_L} \qquad 6.15$$

where $p = \frac{d}{dt}$, and

Z_L is the surge impedance of the line. When the circuit breaker closes, the voltage impressed on the line does not rise instantaneously as with an infinite busbar source, but rises exponentially and is given by

$$V_L(p) = \frac{E}{p} \frac{Z_L}{pL + Z_L} \qquad 6.16$$

where E is the step voltage applied.

Taking the inverse Laplace transform of 6.16 gives

$$V_L(t) = E\,(1 - e^{-Z_L t/L}) \qquad 6.17$$

Heaviside Shifting Theorem, defined in Appendix 12.1, shows that the voltage at the receiving end of the line due to multiple reflections may be expressed as

$$V_R(p) = 2V_L(p) \cdot \sum_{n=1}^{\infty} (K_R)^{n-1} e^{-(2n-1)pT} \qquad 6.18$$

where T is the line transit time.

Substituting 6.15 and 6.16 in 6.18 gives

$$V_R(p) = \frac{2EZ_L}{p(pL+Z_L)} \cdot \sum_{n=1}^{\infty} \left[\left(\frac{pL - Z_L}{pL + Z_L} \right)^{n-1} \cdot e^{-(2n-1)pT} \right] \qquad 6.19$$

Considering only terms up to 5T, equation 6.19 may be expressed as

$$V_R(p) = \left[\frac{2EZ_L}{p(pL+Z_L)}\right] \cdot \left[e^{-pT} + \frac{pL-Z_L}{pL+Z_L} \cdot e^{-3pT}\right] \qquad 6.20$$

Expanding equation 6.20 and taking the inverse Laplace transform gives

$$V_R(t) = 2E\ (1-\exp\{-(t-T)Z_L/L\})\ H(t-T) - 2E\ (1-\exp\{-(t-3T)Z_L/L\}) \cdot (1 + \frac{2Z_L}{L}(t-3T))\ H(t-3T) \qquad 6.21$$

where $H(t-T) = 0$ for $t \leqslant T$

$= 1$ for $t > T$

and $H(t-3T) = 0$ for $t \leqslant 3T$

$= 1$ for $t > 3T$

Equation 6.21 shows that the receiving end voltage wave is synthesised from exponentially varying curves displaced from one another in time.

Fig. 6.6 illustrates the variations in voltage waveforms as the source inductance is increased from zero. The initial slope of the voltage waveform at the line side of the transformer is determined by the time constant L/Z_L. When the time constant is such that the voltage is near its peak value before the arrival of the waves reflected from the source, a hump occurs on the waveform (Fig 6.6 (ii)). This increase is caused by the reflection at the source inductance. The inductance initially acts as an open circuit with a positive reflection coefficient, and subsequently as a short circuit to incident waves. These humps are less evident when the time constant is large as shown at (iii) of Fig. 6.6.

As the source inductance increases, the frequency of the primary voltage waveform departs further from the natural frequency of the line. This means that the conditions for resonance no longer

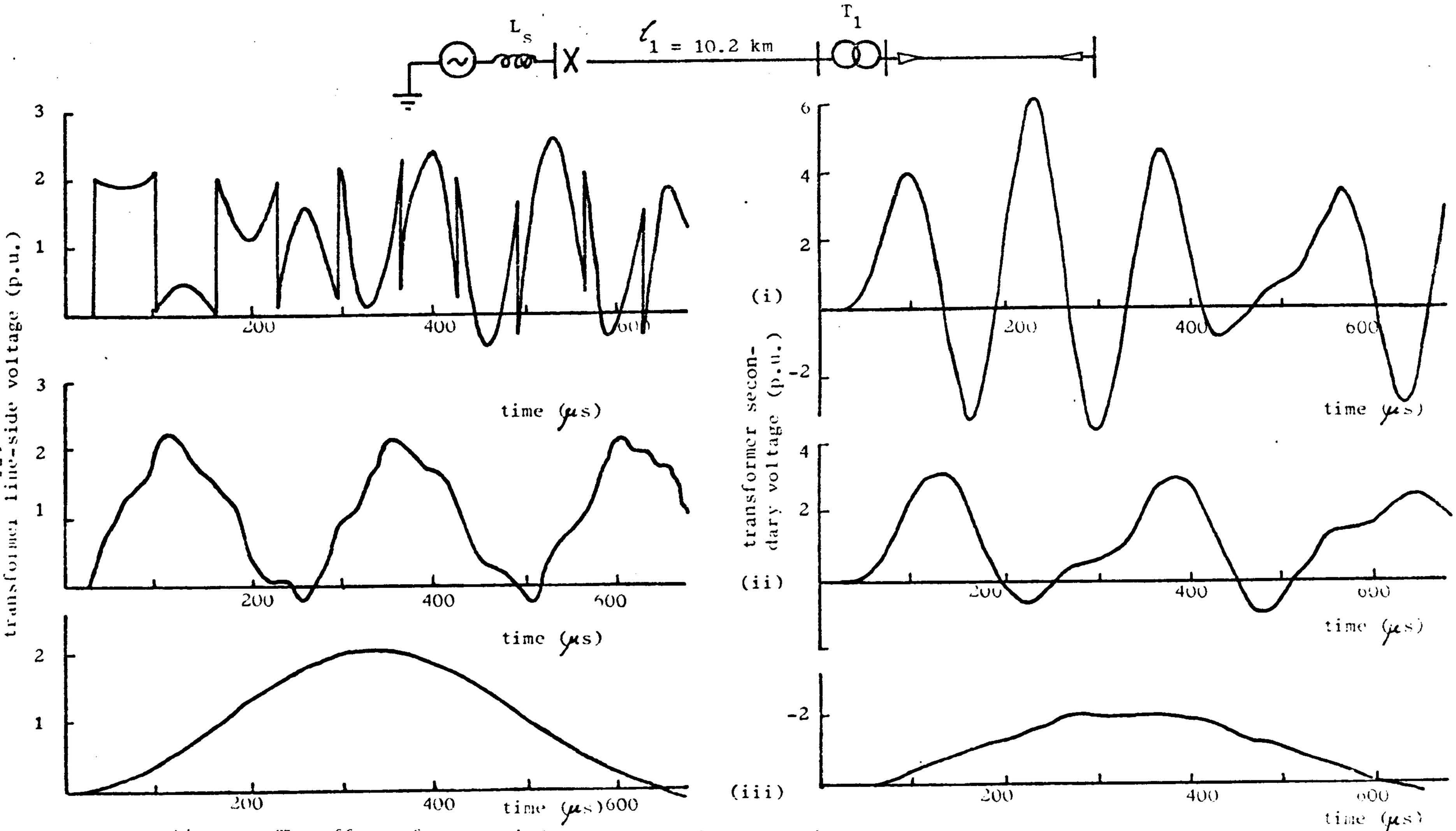

Fig 6.6 The effect of source inductance on voltage waveforms (mathematical method).

(i) $L_s = 0$

(ii) $L_s = 0.01$H

(iii) $L_s = 0.1$H

prevail. Hence the transformer secondary voltages are reduced considerably (from 5.8p.u. for the zero impedance source, to 3.1 and 2.0 p.u. for a 0.01 and 0.1H source inductance respectively).

The corresponding oscillogram traces obtained from the T.N.A. investigation are shown in Fig. 6.7. The detuning effect of the inductive source due to a decrease in line frequency with increasing values of source inductance, is again demonstrated. It will be noticed that the peak voltage on the transformer secondary is only reduced by 13% from 5.3 to 4.6 p.u. when the zero impedance source is replaced by a 0.01H inductive source. The corresponding percentage decrease obtained from the digital computer study is 47. This vast difference is mainly due to the differences in the parameters of the system simulated on the T.N.A. and on the mathematical model. For the purpose of comparison, results obtained from the T.N.A. system modelled on the digital computer, are presented in Fig. 6.8. In this case, the percentage reduction is 10, giving reasonable agreement with the T.N.A. results.

Fig. 6.9 shows a sharp fall in maximum voltages on the transformer secondary initially as the source inductance is increased from zero. At lower source ratings, the overvoltage approaches a value of 2 p.u. This decrease is less sharp for the overvoltage envelope derived from the T.N.A. results (Fig. 6.9 (ii)) as compared with that obtained from computation(Fig 6.9 (i)). Although the time constants are equivalent in both models used, the length of the line simulated on the T.N.A. is 48.2km, and the mathematical model line length is 10.2km. Hence, in the former case, the voltage wave on the line side of the transformer will rise closer to its peak value before the arrival of the reflection from the source.

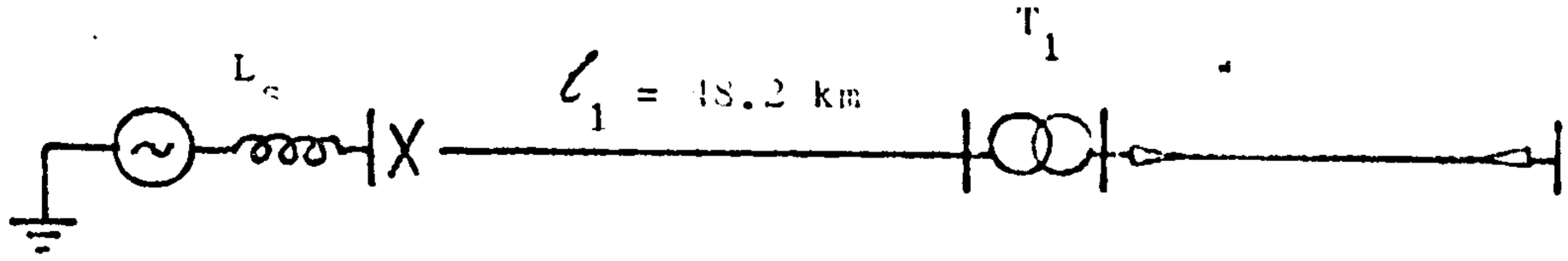

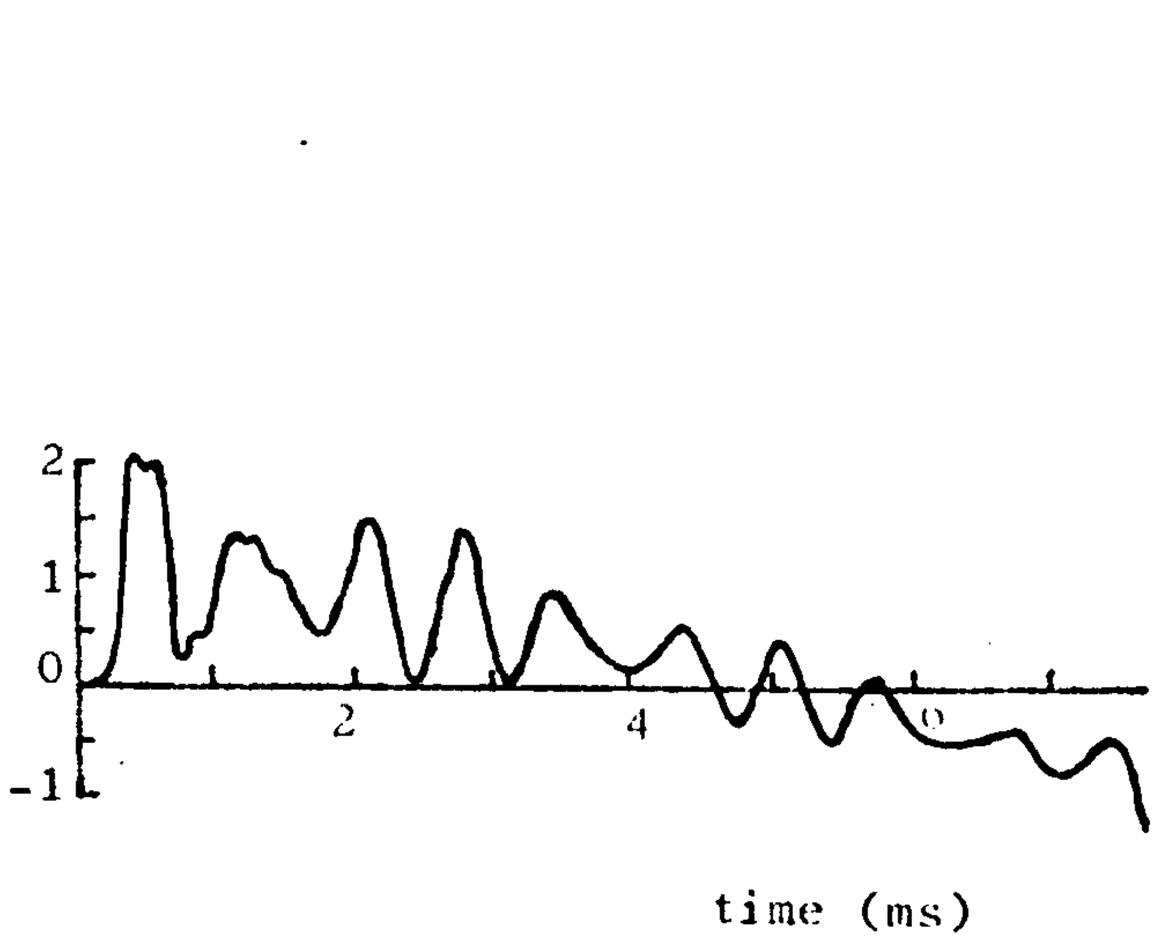

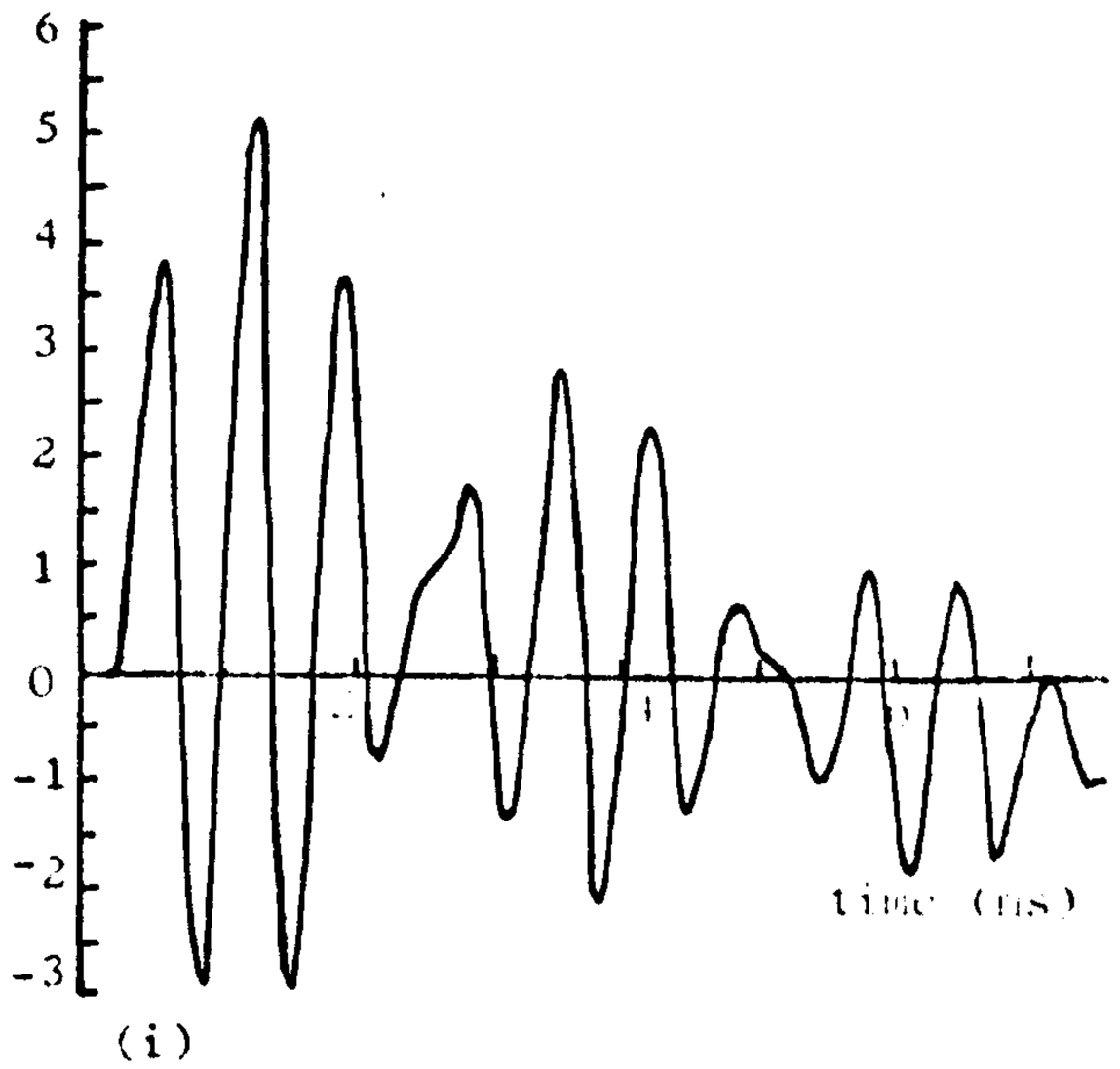

(i)

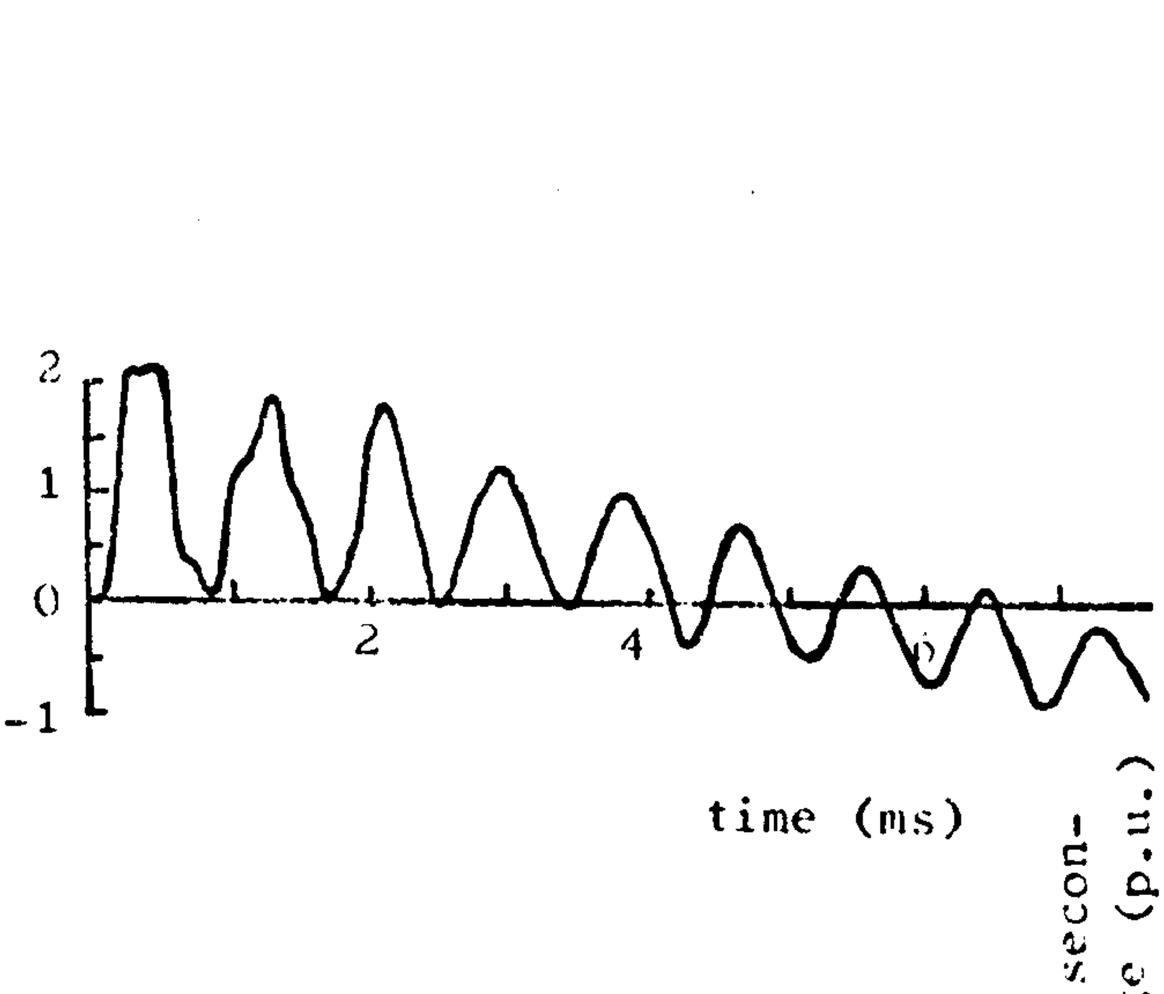

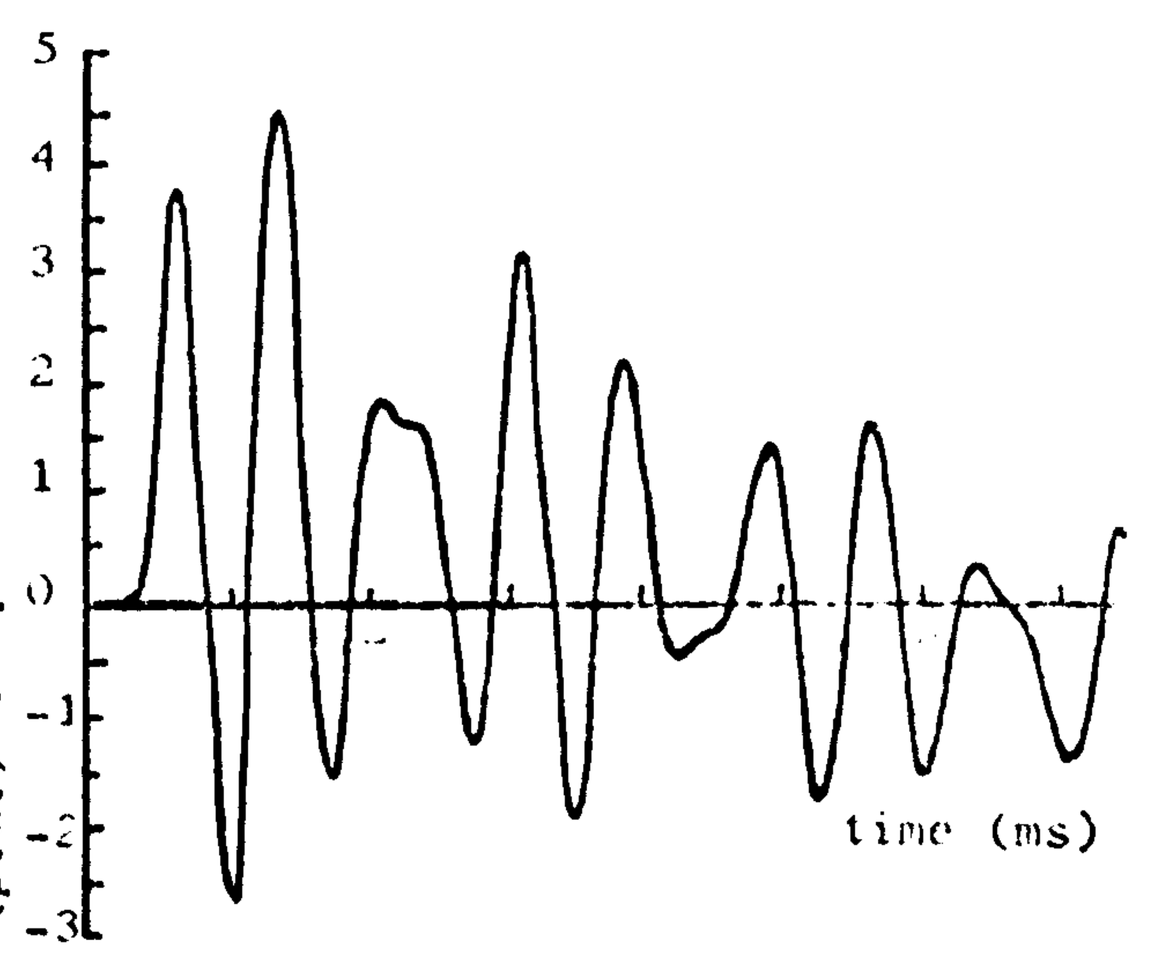

(ii)

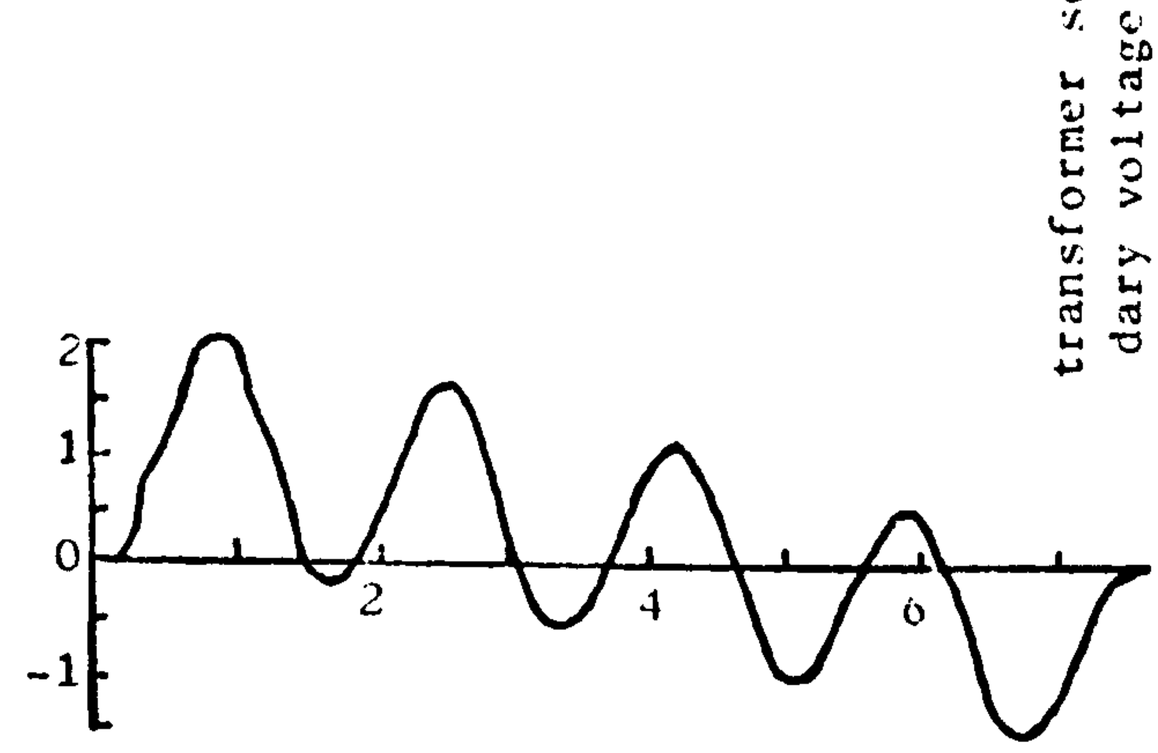

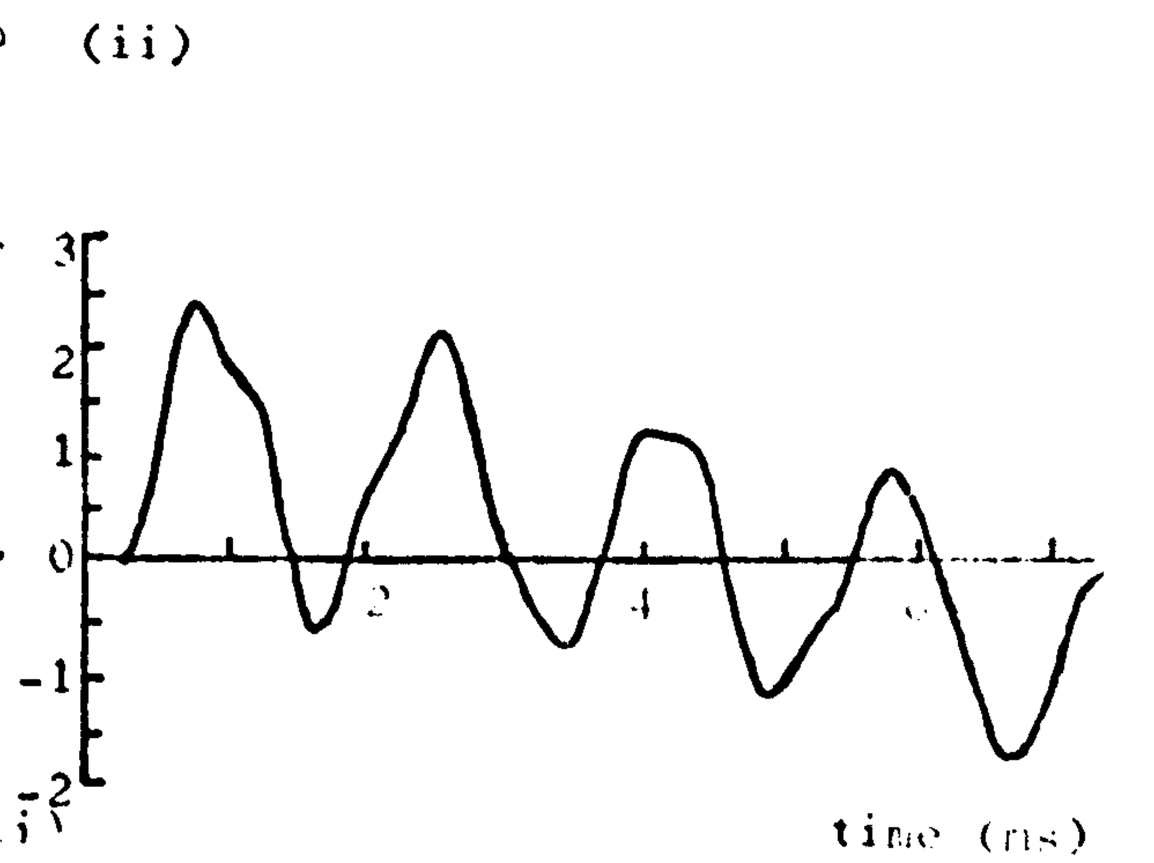

(iii)

Fig. 6.
Effect of source inductance on voltage waveforms (T.L.A. method)
(i) $L_s = 0$
(ii) $L_s = 0.01H$
(iii) $L_s = 0.1H$

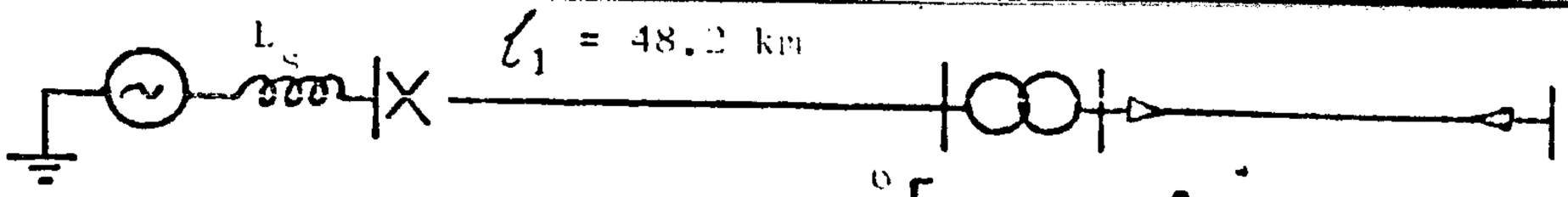

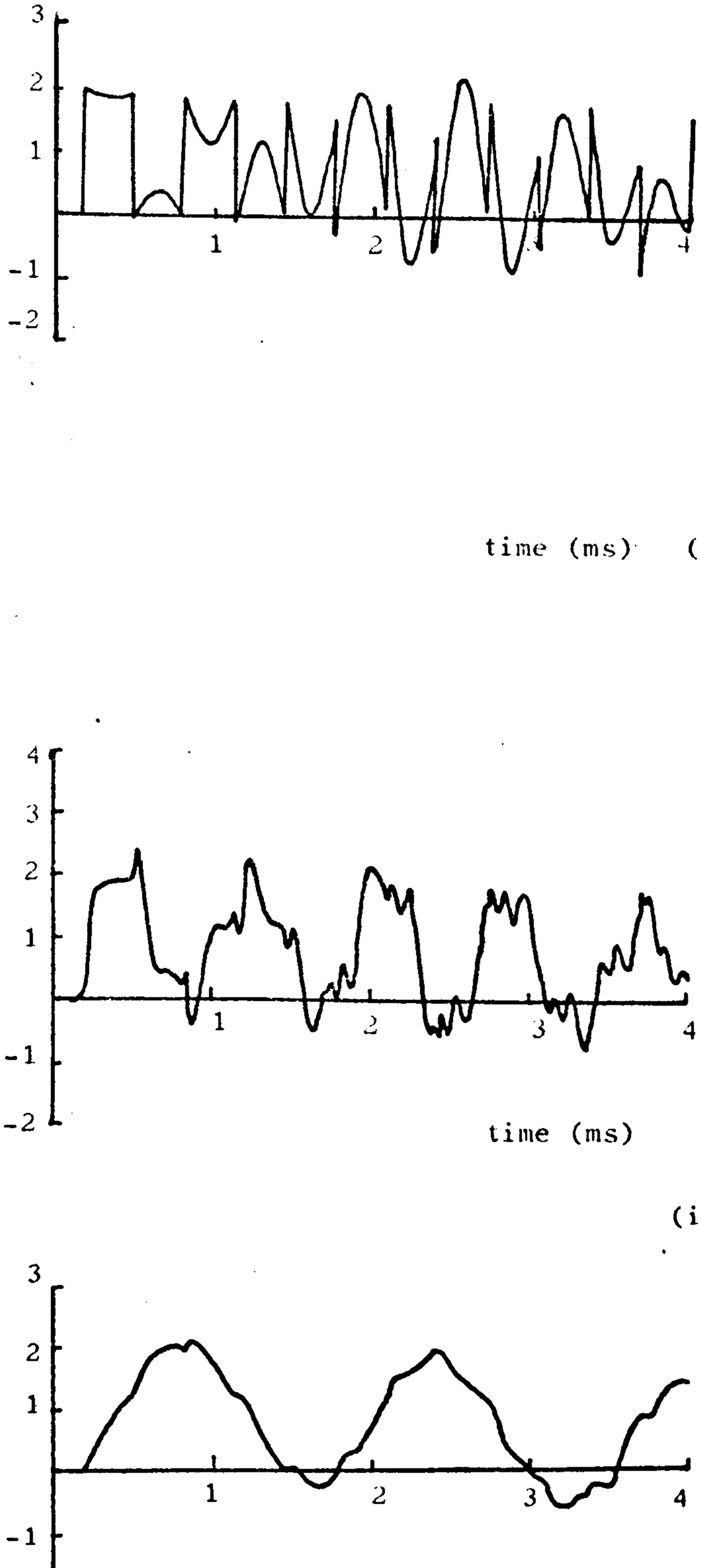

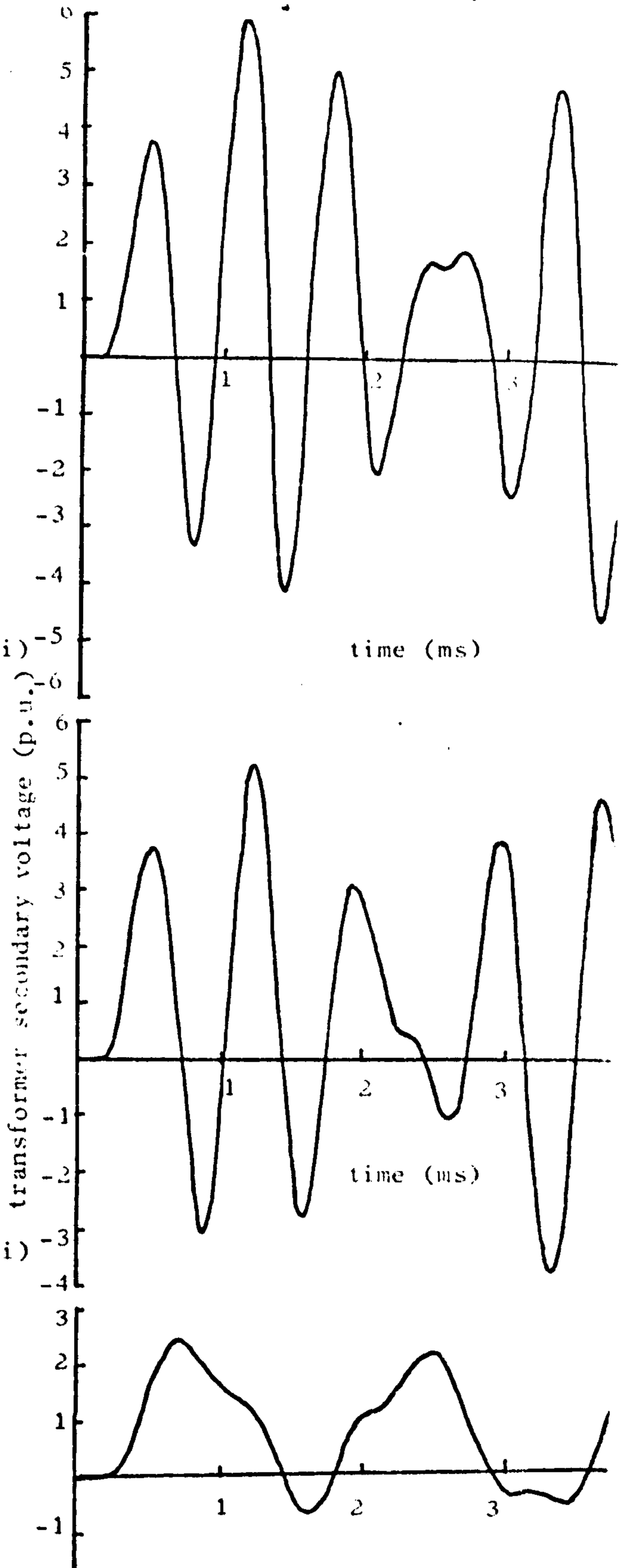

Fig. 6.8 Effect of source inductance on voltage waveforms (mathematical method)

(i) $L_s = 0$

(ii) $L_s = 0.01H$

(iii) $L_s = 0.1H$

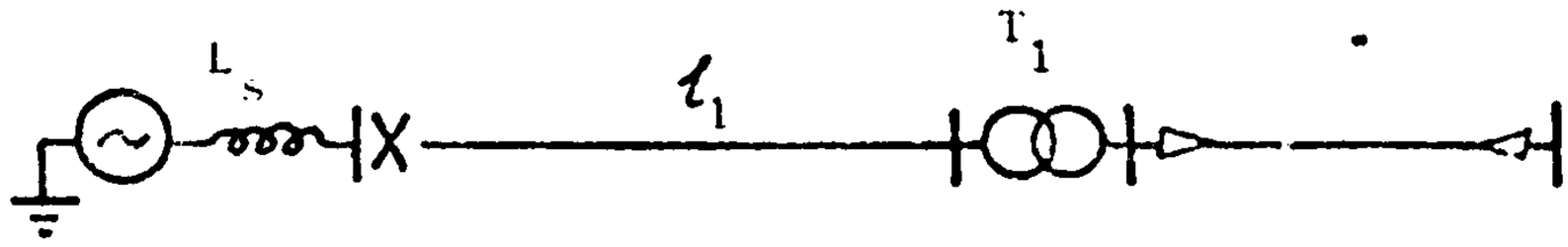

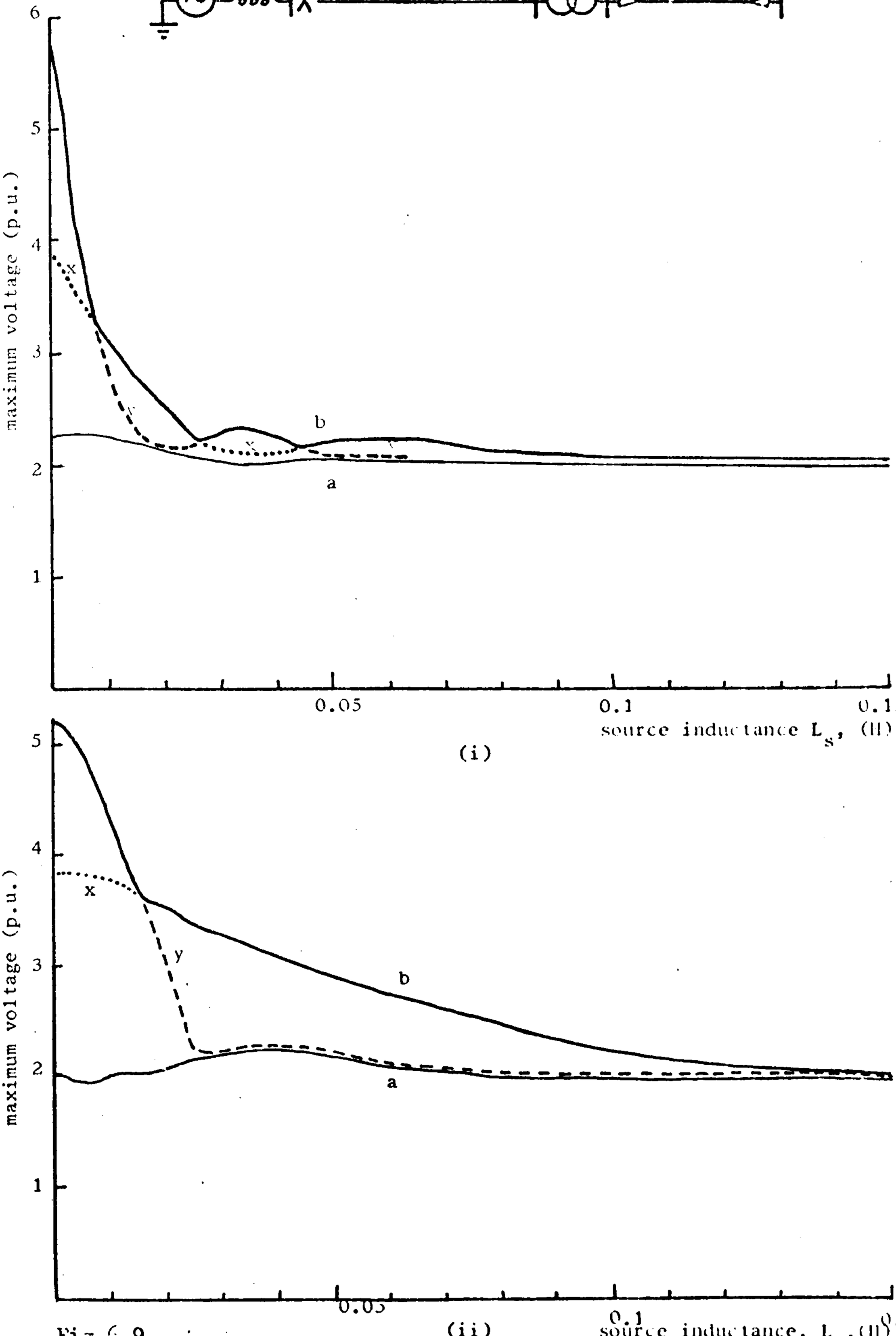

Fig 6.9
Variation of overvoltage with source inductance
(i) Mathematical method (ℓ_1 = 10.2 km)
(ii) T.N.A. method (ℓ_1 = 48.2 km)
(a) Voltage on the transformer primary
(b) Voltage on the transformer secondary

The sharp changes of slope shown on these curves correspond to a change in the number of the half cycle on which the maximum voltage peak occurs. Initially, the peak amplitude occurs on the third half cycle, but as the source inductance increases, the second half cycle peak exceeds that of the third half cycle, as illustrated on both curves. Due to the hump on the voltage waveform on the line side of the transformer, the maximum voltages at this point show a slight increase for low values of the time constant.

6.3.2 Effect of length of feeder energised from inductive source.

When the feeder is energised from a low fault impedance source, a resonance condition may still arise in spite of the difference in the transformer frequency and that of the line as determined by its length.

In Fig 6.10, the variations of secondary overvoltages with line length are compared for different values of source inductance. The feeder is terminated in two transformers T_1 and T_2, whose constants are given in section 5.2. If the infinite busbar source is replaced by a 0.01H inductive source corresponding to a fault level of 5500MVA at 132kV, resonance peaks of lower amplitude are shown to occur (curves iii) on the secondary side of the transformers. The maximum over-voltages are reduced from 8.5 and 12.5 p.u. to 4.5 and over 4.8 p.u. respectively. These peaks are horizontally displaced from their original positions. This is because the line oscillation frequency is reduced due to the inductance at source. Consequently the length of line has to be decreased to obtain line and transformer frequency equivalence necessary for resonance to occur. It may be seen from curve (ii)b that a resonance condition is approached as the length of line is reduced towards zero.

For the 0.1H source corresponding to a 550MVA fault level

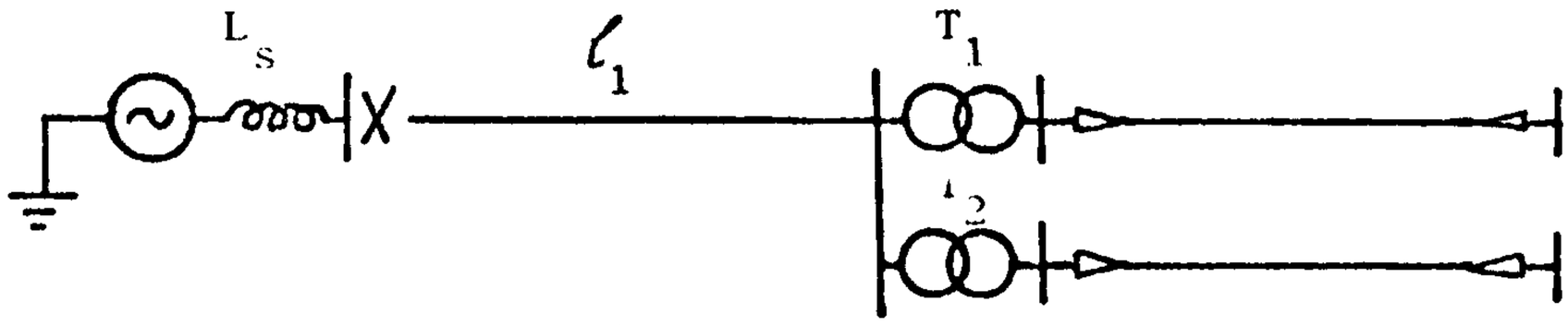

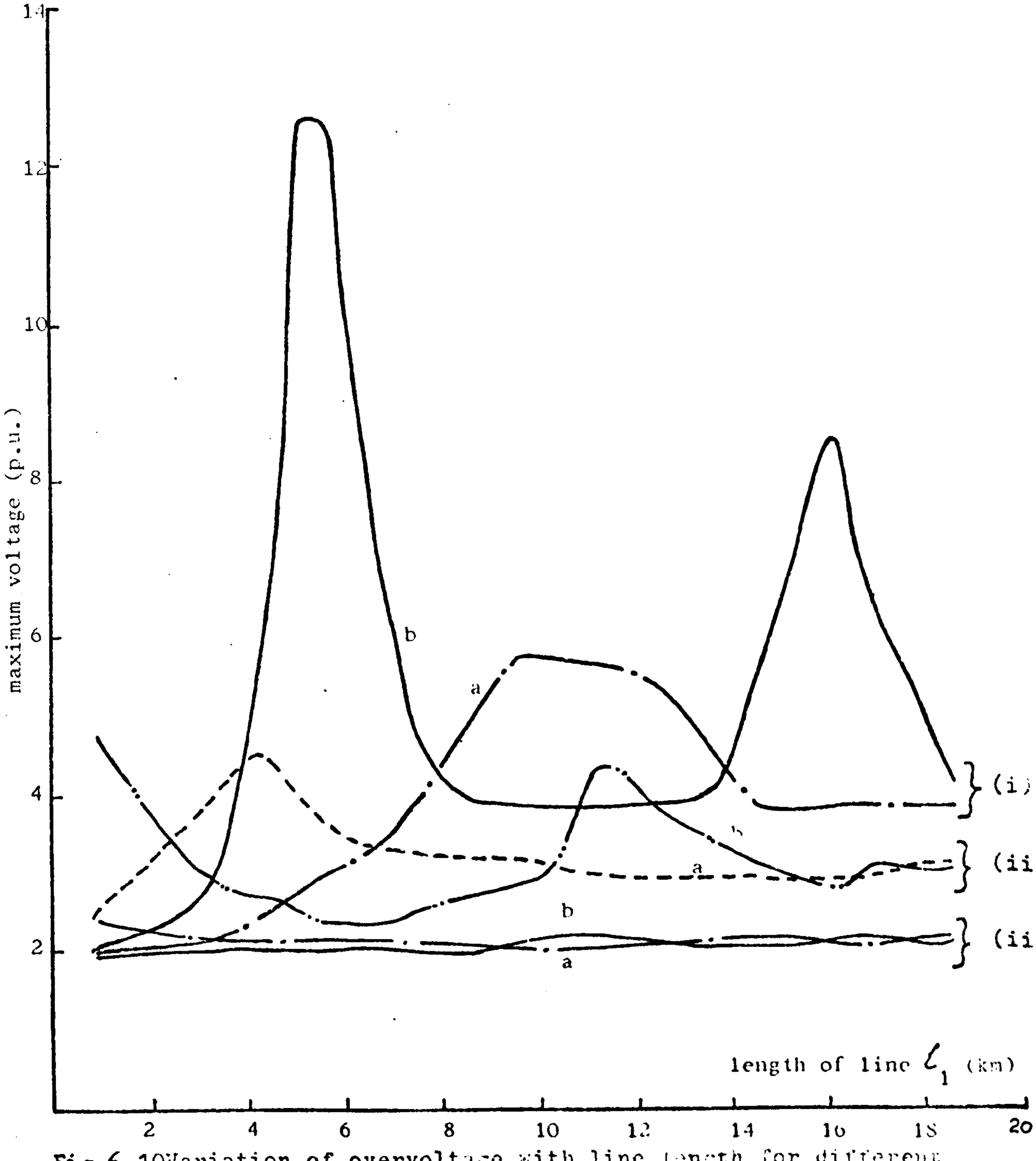

Fig 6.10 Variation of overvoltage with line length for different values of source inductance (mathematical method)

(i) $L_S = 0$
(ii) $L_S = 0.01H$
(iii) $L_S = 0.1H$
(a) Secondary voltage of transformer T_1
(b) Secondary voltage of transformer T_2

at 132kV, the length of line has to be decreased further for a resonance condition to exist. The magnitude of the overvoltage peaks becomes smaller. Curve (iii)d shows an upward trend in the maximum voltage below 2km. The third harmonic peak of the secondary overvoltage at the transformer T_2(curve (iii)b) is just visible when the length of line is approximately 11km.

6.3.3 Source inductance and transmission line

It is common in practice for a transformer feeder to be energised from a switching station fed by a transmission line, which in turn is fed from a generating station. In this case, the resulting transient surges will be influenced by the characteristics of the source and the line connecting the source to the energising circuit breaker. It will be assumed that the length of feeder is maintained constant at the length giving a natural frequency equal to the transformer frequency, so that the effects of the source characteristics may be determined.

If a source having an equivalent inductance of 0.1H energises the feeder through a length of line, ℓ_1, equal to that of the feeder, ℓ_2, the voltage on the line side of the transformer is as shown in Fig. 6.11 (i). Since the surge impedances of the lines on both sides of the circuit breaker are equal, voltage surges which are equal in magnitude but with opposite signs will be impressed on the lines when the breaker closes. Both the inductive source and the transformer have positive reflection coefficients. This accounts for the steep fronts of alternating polarity on the waveform at the transformer primary shown at (i) of Fig 6.11. Assuming, for the sake of simplicity, that the reflection coefficient at the transformer and at the source is +1, Fig 6.12 (ii) shows how the waveform evolves from the lattice diagram analysis. Because of the equal lengths of

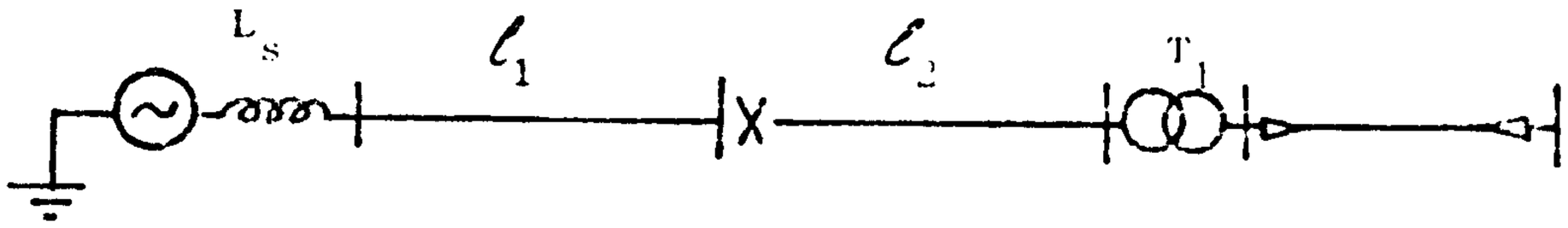

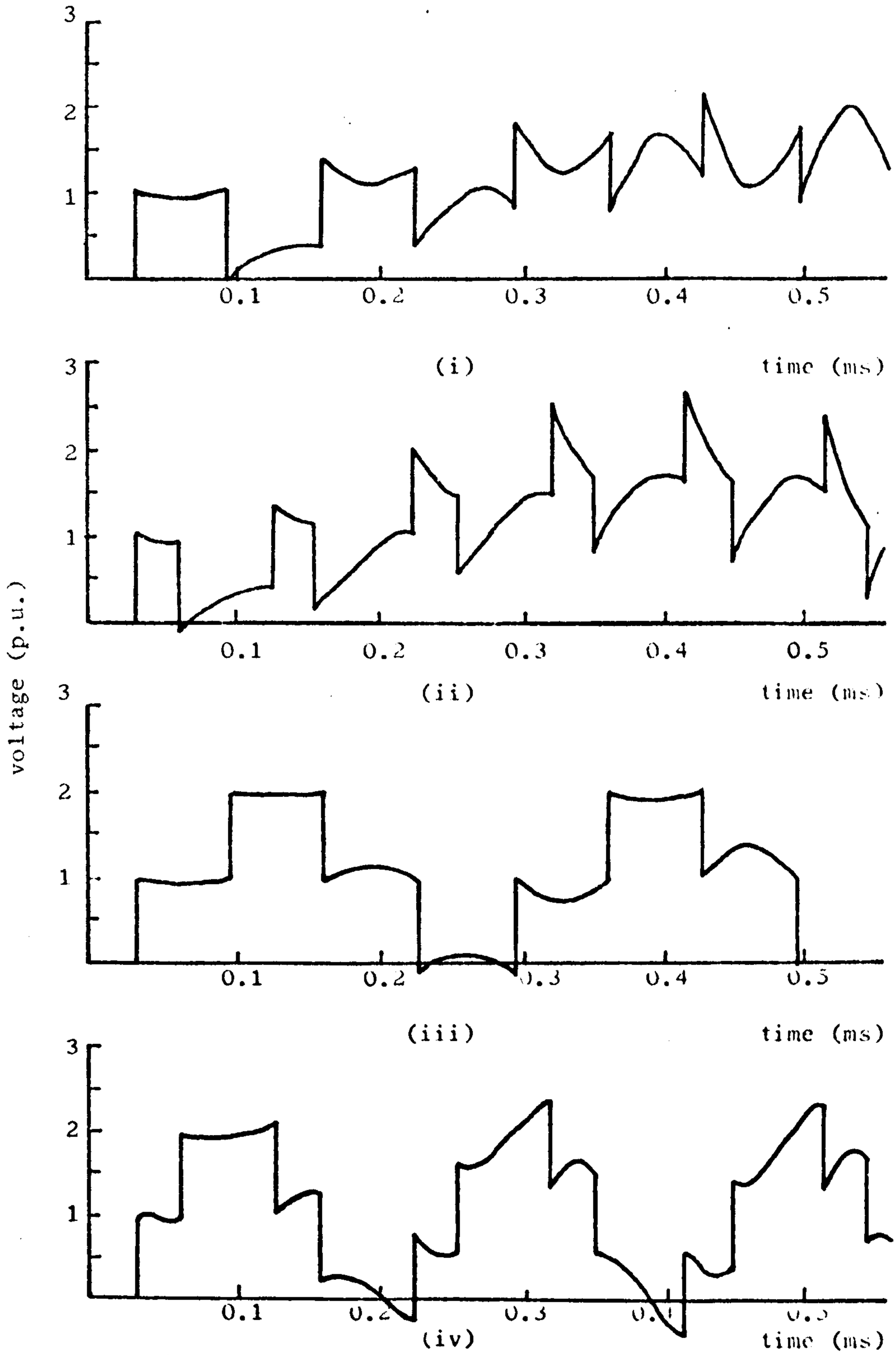

Fig 6.11
Voltage waveforms at the line side of the transformer when energised from a second transmission line. Length of ℓ_2 = 10.2 km (mathematical method)
(i) $L_S = 0.1H$, $\ell_1 = \ell_2$
(ii) $L_S = 0.1H$, $\ell_1 = 0.5\ell_2$
(iii) $L_S = 0$, $\ell_1 = \ell_2$
(iv) $L_S = 0$, $\ell_1 = 0.5\ell_2$

line on both sides of the breaker, the mark to space ratio is equal. The waveform will therefore contain a frequency component equal to the transformer frequency which is sufficiently large to produce an overvoltage of 4.5 p.u.

If the length of the source-side line is not equal to that of the feeder, the overvoltages produced decrease in magnitude. In this case, that frequency component in the waveform which is equal to the transformer frequency, is no longer predominant due to the unequal mark to space ratio. This is illustrated at (ii) of Fig 6.11 where the length of the source-side line is half that of the feeder.

If the inductive source is replaced by an infinite busbar source, the reflection coefficient at the source becomes -1. In this case, lattice diagram considerations give the waveform shown in Fig.6.12 (i) where $\ell_1 = \ell_2$. Fig 6.11 (iii) and (iv) relate to the condition where $\ell_1 = \ell_2$ and $\ell_1 = 0.5\ell_2$ respectively. The frequency spectrum of these waveforms is such that resonance will not be excited in the transformer. If however, the length of the source side line is reduced towards zero, the successive step pulses of the same polarity tend to coincide and the frequency component of the waveform necessary to excite transformer resonance is reinforced.

The corresponding T.N.A. waveforms with the same source characteristics as those described above, are shown in Fig. 6.13. The waveforms at the line-side of the transformer, do not contain the steep fronts which are characteristic of curves obtained from digital computation. The overvoltage recorded at the transformer secondary for the case of equal lengths of source-side line and feeder with a 0.1H inductive source is 3.8 p.u. (Fig 6.13 (i)). This maximum voltage is reduced to 2.9 p.u. when the length of the source-side line is

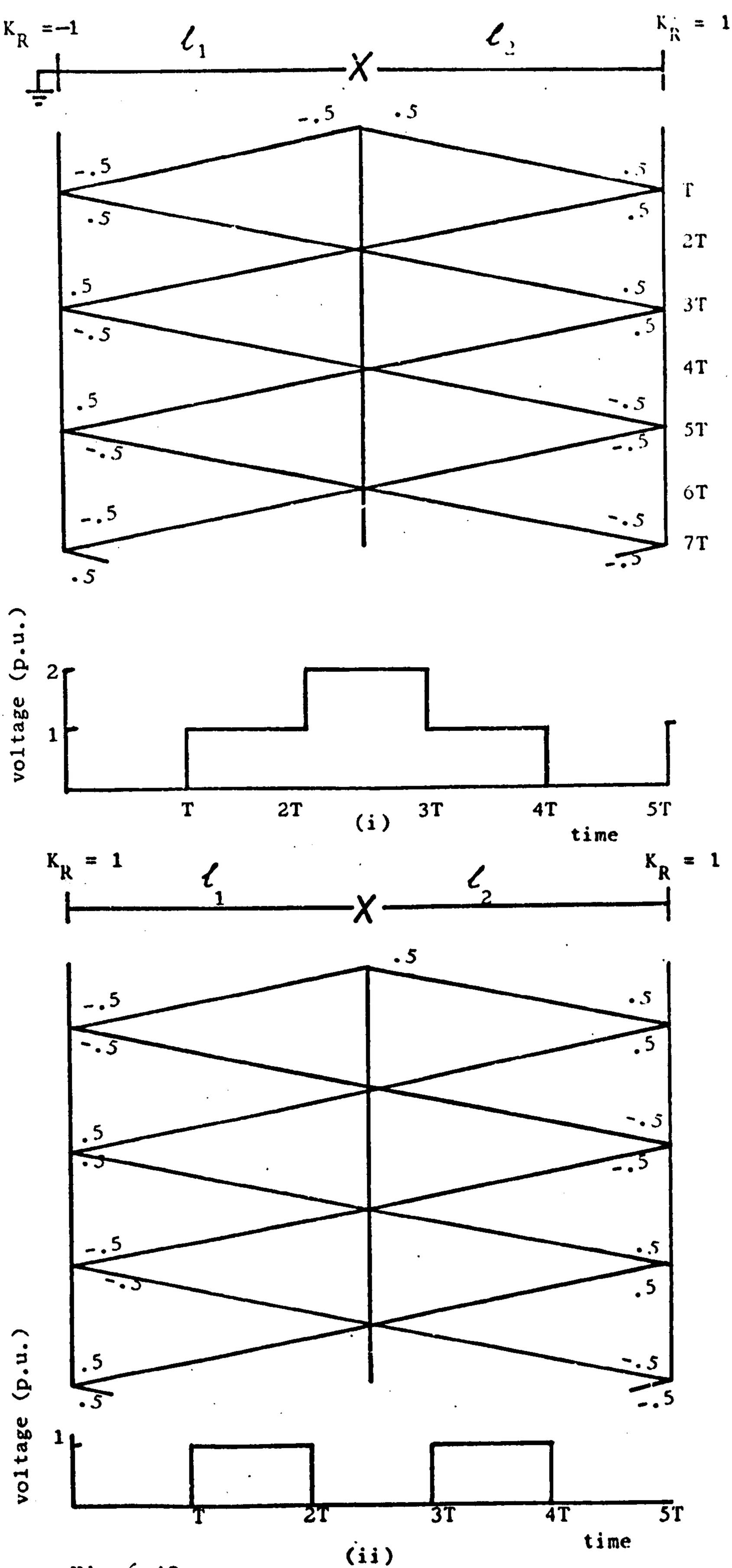

Fig.6.12
Lattice diagram analysis ($\ell_1 = \ell_2$)
(i) Infinite source
(ii) Inductive source

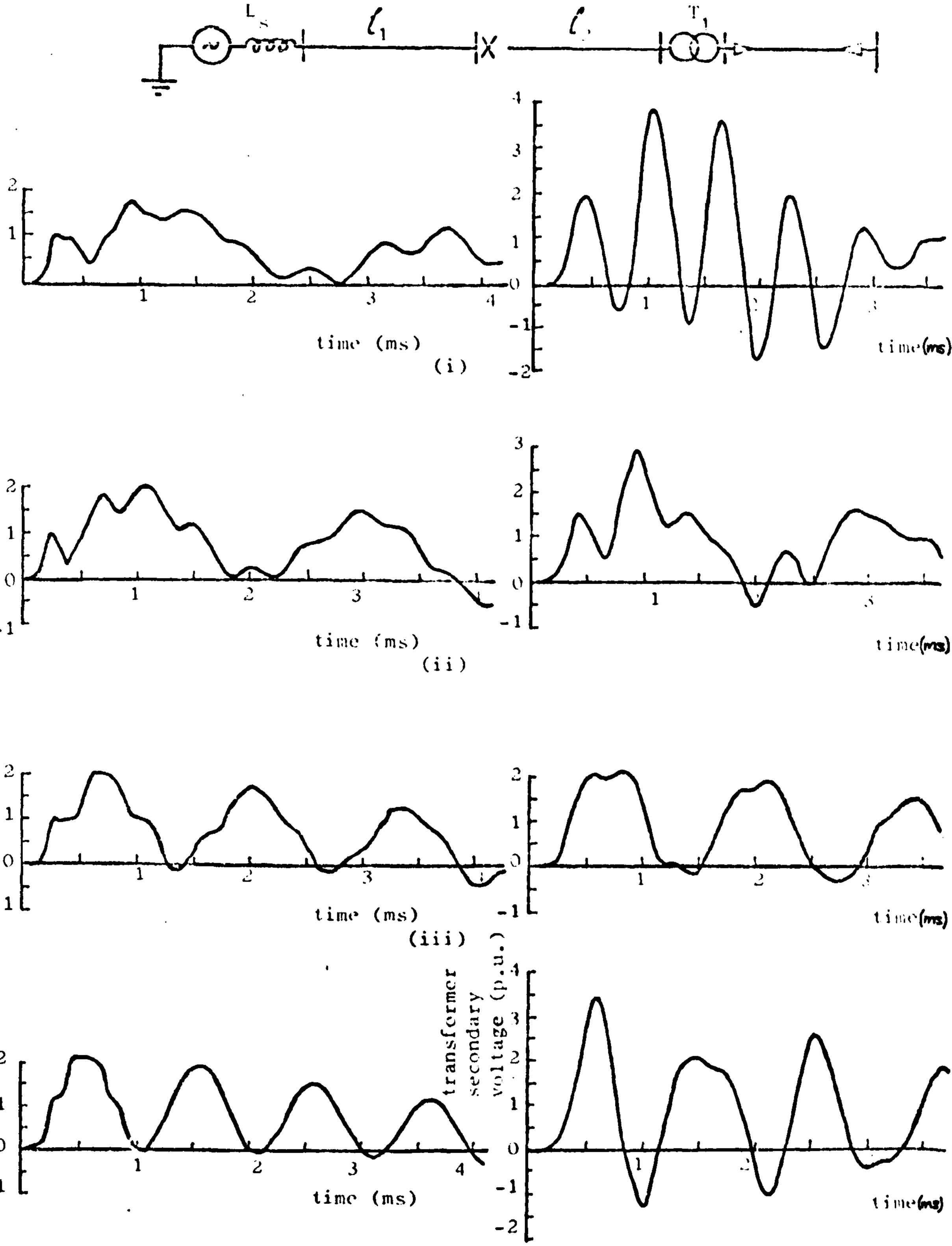

Fig.6.13
Voltage waveforms at the transformer when energised from a second transmission line. Length of ℓ_2 = 46.2 km. (T.N.A. method)
(i) L_S = 0.1H, $\ell_1 = \ell_2$
(ii) L_S = 0.1H, $\ell_1 = 0.5\ell_2$
(iii) L_S = 0 , $\ell_1 = \ell_2$
(iv) L_S = 0 , $\ell_1 = 0.5\ell_2$

halved (Fig 6.13 (ii)). Fig 6.13 (iii) and (iv) show that for the zero impedance source, the overvoltage increases from 2.1 to 3.4 p.u. when the length of the source-side line is halved.

Because of the difference in parameters of the systems represented on the T.N.A. and on the digital computer, the resulting waveforms are not similar. The waveforms of Fig. 6.14, obtained from computation of the T.N.A. system, provide a direct comparison with waveforms of Fig. 6.13 which are superimposed as discontinuous surves. The close agreement between the two methods is again demonstrated.

The voltage waveforms for the condition of zero impedance source may be analysed using Fourier analysis as in section 6.2. Equation 6.6 will also apply in this case.

$$\text{i.e } V = 1 - \frac{4}{\pi} \sum_{n=1}^{\infty} \left[\frac{1}{n} \sin \frac{n\pi}{2} \cos \frac{n\pi T_1}{2(T_1+T_2)} \right] \cdot \cos \frac{n\pi}{2(T_1+T_2)} t \quad 6.15$$

Let $\ell_1 = k\ell_2$

$$\text{i.e } T_1 = kT_2$$

$$V = 1 - \frac{4}{\pi} \sum_{n=1}^{\infty} \left[\frac{1}{n} \sin \frac{n\pi}{2} \cos \frac{n\pi k}{2(1+k)} \right] \cos \frac{n\pi}{2T_2(1+k)} t \quad 6.16$$

Substituting $\sin n\pi/2 = 0$ when n is even

$= \pm 1$ when n is odd

and $\omega_L = 2\pi f_L = \pi/2T_2$

in equation 6.16, where ω_L and f_L relate to the frequency of the line length, ℓ_2.

$$V = 1 + \frac{4}{\pi} \sum_{n=1}^{\infty} \left[\frac{1}{2n-1} \cos \frac{(2n-1)\pi k}{2(1+k)} \cos \frac{(2n-1)\omega_L t}{(1+k)} \right] \cdot (-1)^n \quad 6.17$$

This expression is similar to that given by equation 6.13, except that in this case, ω_L refers to the frequency of line ℓ_2, which is kept constant. An analysis of this equation will again show that a resonance condition would exist if the value of k satisfies the relation.

$$k = \ell_1/\ell_2 = 2(n-1)$$

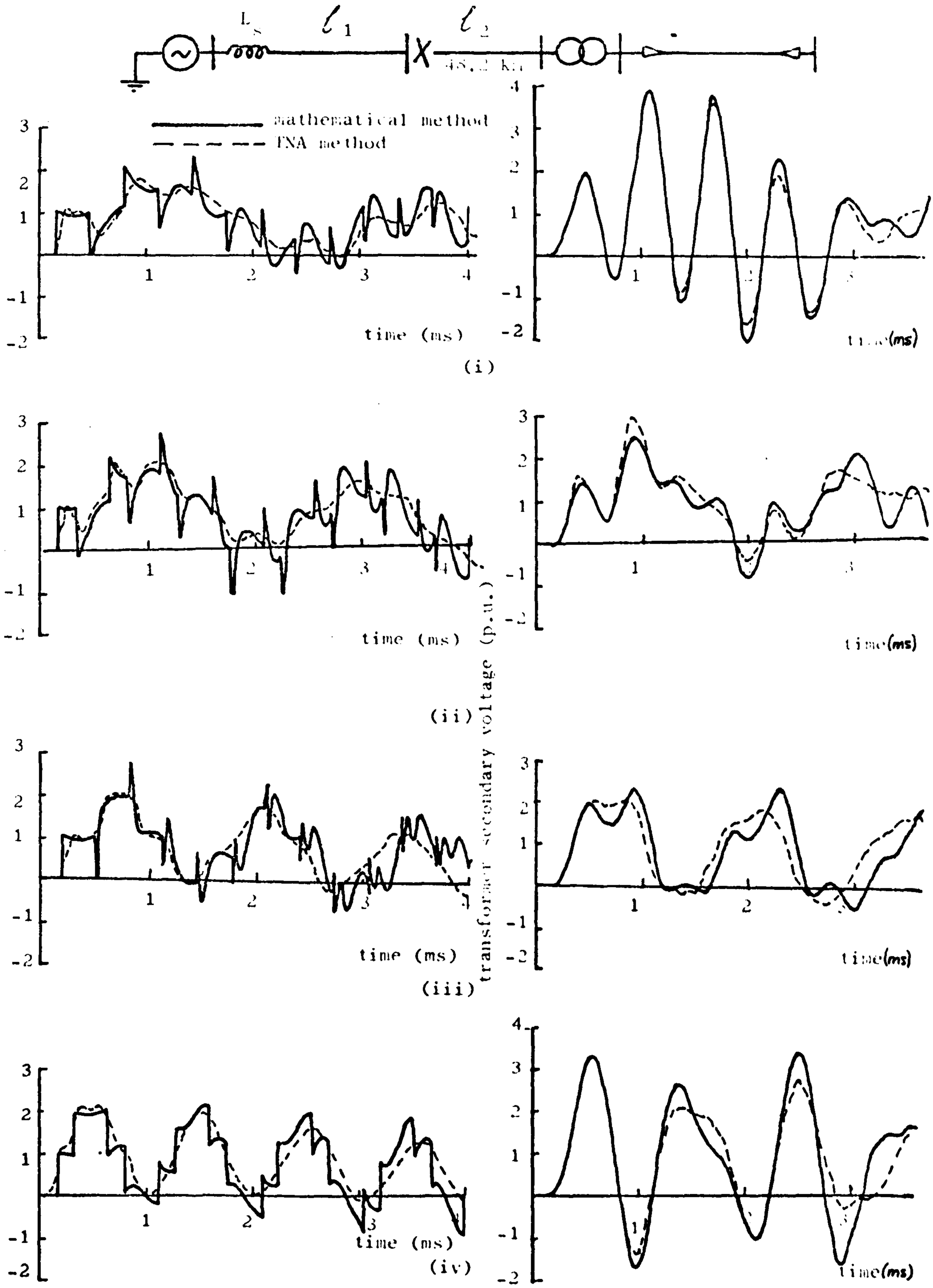

Fig. 6.14 Voltage waveforms at the transformer when energised from a second transmission line. Length of ℓ_2=48.2km

(i) L_s= 0.1H, $\ell_1=\ell_2$ (ii) L_s= 0.1H, $\ell_1=0.5\ell_2$

(iii) L_s= 0, $\ell_1=\ell_2$ (iv) L_s=0, $\ell_1=0.5\ell_2$

where n = 1, 2, 3, 4 ....

i.e ℓ_1 must be an even integral multiple of ℓ_2 for resonance to occur. The overvoltage curves of Fig 6.15 (i) a and c, obtained using mathematical and analogue methods respectively, confirm this relation. Curves b and d of this Figure indicate that when the source is inductive the converse is true. i.e a necessary condition for resonance is that ℓ_1 must be close to an odd integral multiple of ℓ_2.

The overvoltage envelopes similar to curve b of Fig 6.15 (i) relating to different values of source inductance, may be summarised by the contour curves of Fig 6.16. These curves are drawn for source inductance in the range 0 to 0.5H, and for lengths of line between the source and the circuit breaker of up to twice the length of the transformer feeder.

Examination of these curves shows that the overvoltages become more severe in the region where the length of the source-side line is in the neighbourhood of that of the transformer feeder (10.2km) for all values of source inductance considered. The maximum overvoltage of 4.64 p.u. is obtained when the source inductance is 0.08H and the length of line on the source side is 11.8 km.

If the source is separated from the circuit breaker by a length of underground cable instead of an overhead line, conditions similar to those described above occur, as may be seen from Fig.6.15(ii). In this case, however, the propagation time of the cable must be close to that of the feeder in order to produce the maximum voltage in the secondary of the transformer for the zero impedance source. Under this

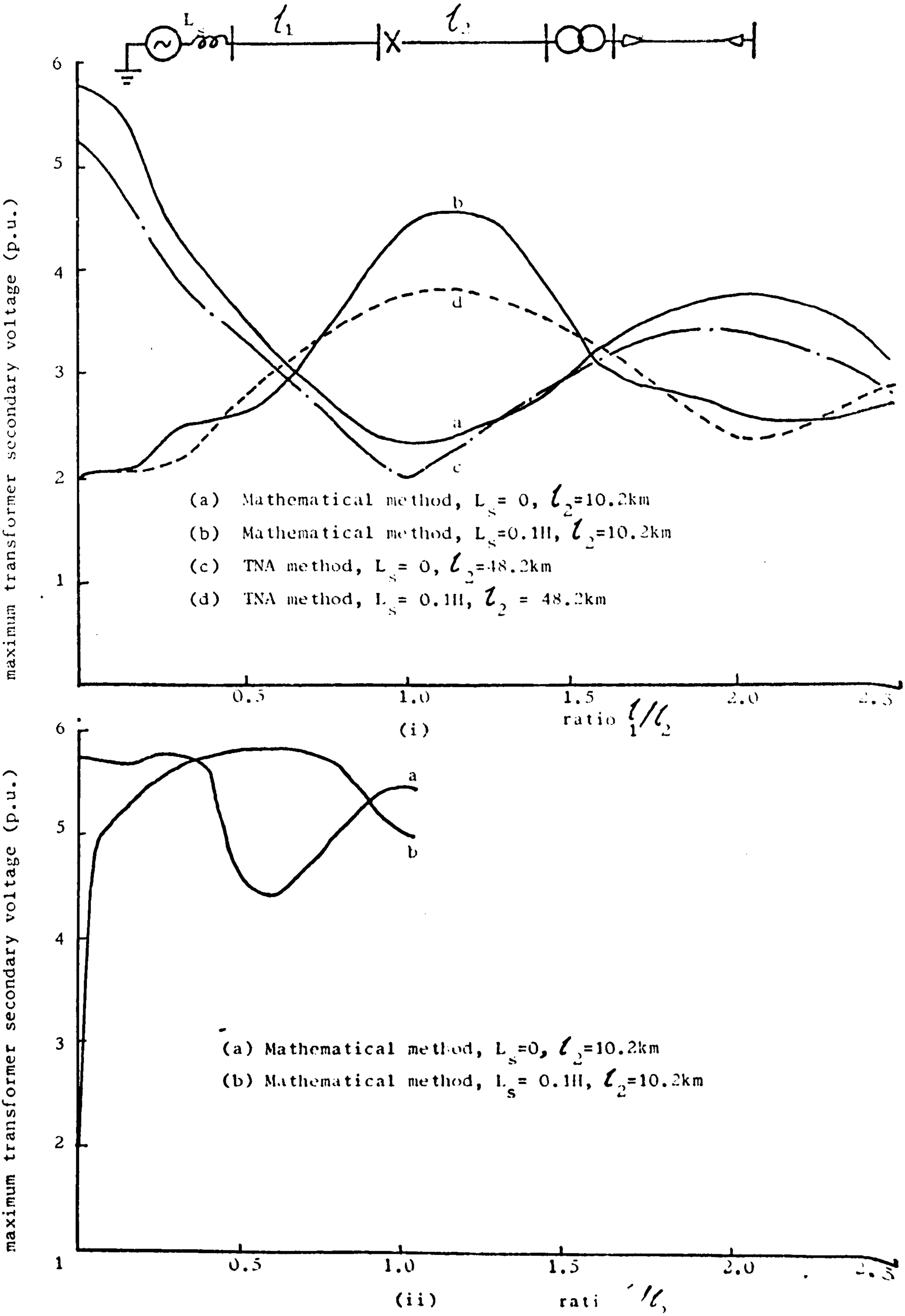

Fig. 6.15 Effect of energising transformer under from :

(i) an overhead line

(ii) an underground cable

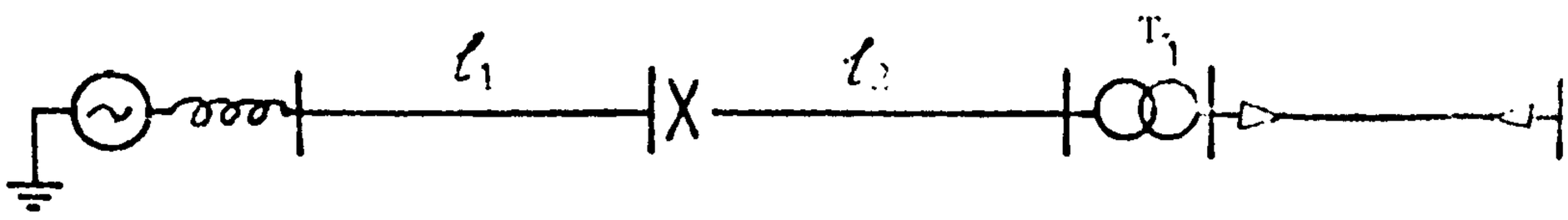

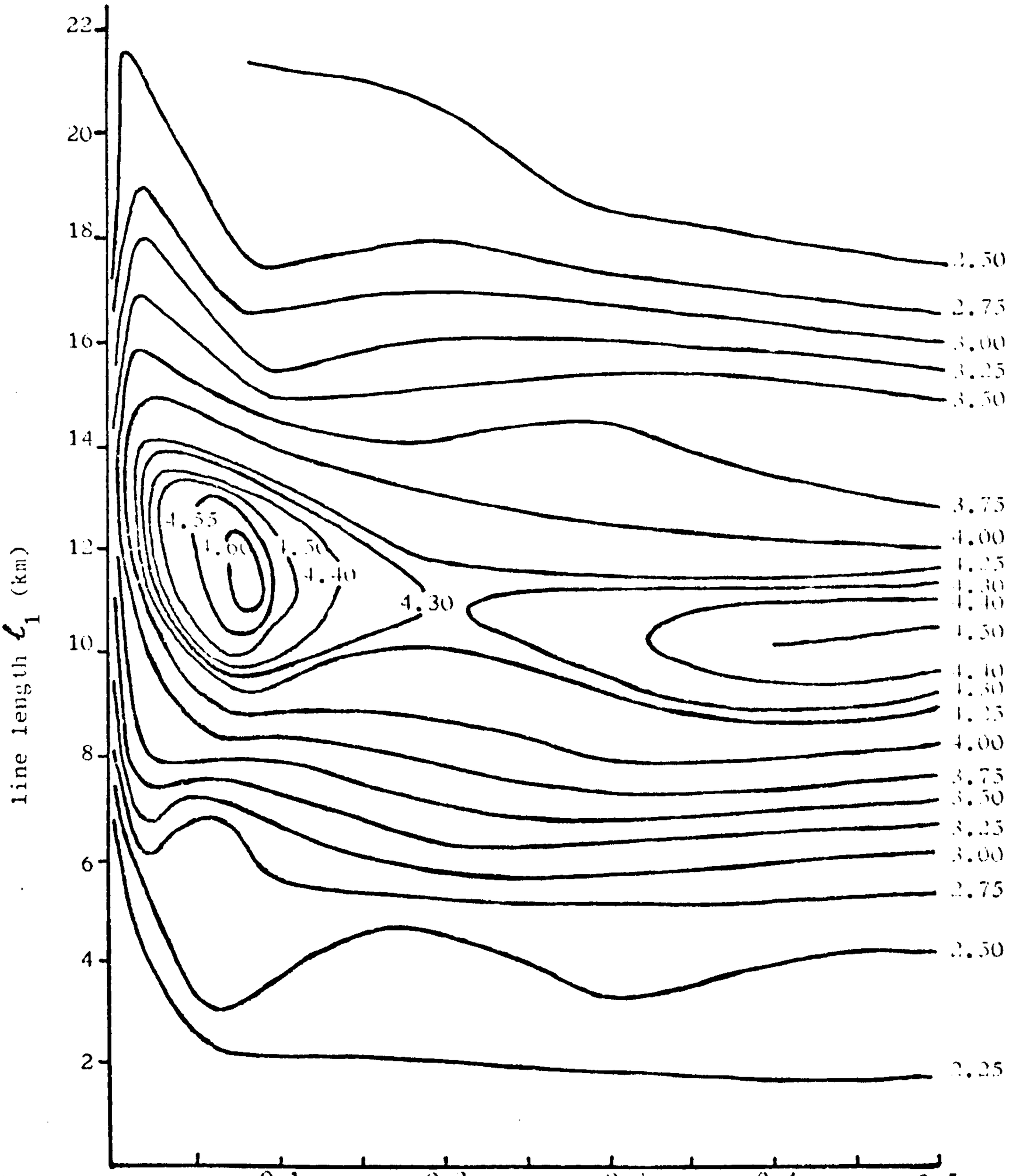

Fig 6.16
Contours of maximum transformer secondary voltage with variation in source inductance and length of source-side overhead line. (ℓ_2 = 10.2km) (mathematical method)

condition, a minimum overvoltage occurs if the source has an inductance. The overvoltages occur over a wider range of cable lengths than in the previous case due to the effects of the cable adjacent to the source. This condition will be examined further in the next section.

6.4 Mixed line and cable transformer feeder

The use of overhead transmission lines may sometimes prove unacceptable for aesthetic or technical reasons, or in cases where wide stretches of water have to be crossed. If this is the case, underground cables are used for power transmission and interconnection at all voltage levels inspite of the high capital costs involved. Very often, a length of cable is used at transmission voltages to connect the end of an overhead line to equipment in a substation for instance, as in an underground power station. The length of such a cable may vary from a few metres to a few kilometres. At the highest voltage levels, however, the length of the cable is usually short in comparison with that of the overhead line connected in series with it. At lower voltage levels the converse may be true. In such cases of mixed feeders, the overvoltages produced at the transformer may be made more onerous depending on the individual lengths and physical arrangement of cables and lines which comprise the feeder.

6.4.1 Position of length of cable along the transformer feeder.

Bewley[49] and Rudenberg[57] have, among others, examined the behaviour of travelling waves on a mixed line and cable transmission system when the composite feeder is energised from either end. The nature of these line oscillations will determine whether resonance will be excited at the transformer.

When a voltage wave arrives at a junction of two lines of different surge impedances Z_1 and Z_2, the reflected and transmitted waves will be governed by the reflection and transmission coefficients given by

$$V_r = \frac{Z_1 - Z_2}{Z_1 + Z_2}$$

and $$V_t = \frac{2Z_2}{Z_1 + Z_2}$$

respectively. For the case of an underground cable joined to an overhead line, the ratio Z_2/Z_1 is of the order of ten. Hence the amplitude of the voltage wave is increased on transmission into the line. In the limiting case when Z_2 becomes very much larger than Z_1, a twofold increase in the amplitude of the voltage penetrating into the line may be produced. When the wave arrives at the end of the line, a voltage approaching twice the amplitude of the incident wave may occur depending on the ratio of the terminating surge impedance to that of the line. In the limit, a four-fold increase in the voltage impressed on the cable may be obtained at the end of the line remote from the junction. The voltage waveform at the transformer primary for this condition is shown in Fig. 6.17 (i). In this study, the length of cable is held constant at 0.81km and the lengths of the overhead line sections are always such that the composite frequency of the mixed feeder is constant at 7.34 kHz (i.e equal to transform frequency).

Fig 6.18 (i) shows how the waveform at the receiving end of the line is derived from Bewley's lattice-diagram technique, assuming an infinite transformer surge impedance. Comparison of this waveform with that of Fig 6.17 shows a close resemblance. There is, however a slight discrepancy in the frequencies of oscillations. This could be accounted for by the rounding-up error inherent in the digital computer method when the length of line is expressed in terms of an integral number of basic time intervals.

It may be seen from Fig 6.17 (i) that although the waveform is dominated by that frequency component due to oscillations in the cable, there is also present in this waveform a component of frequency determined by the travel time of the line sections. Hence a large overvoltage will be excited at the transformer.

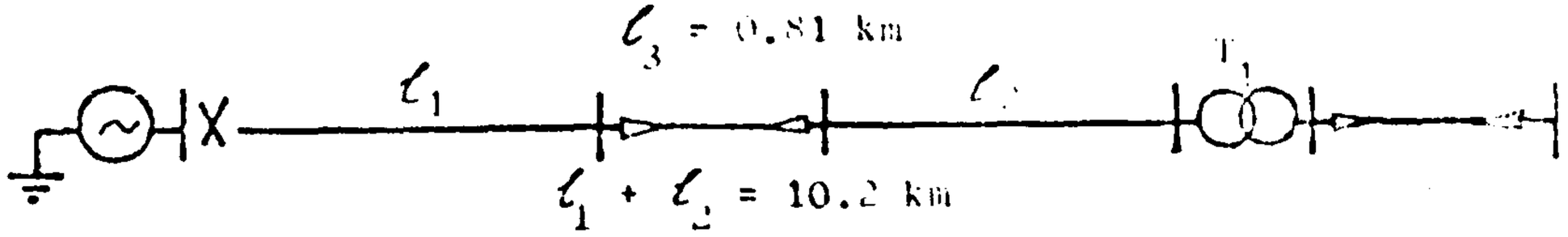

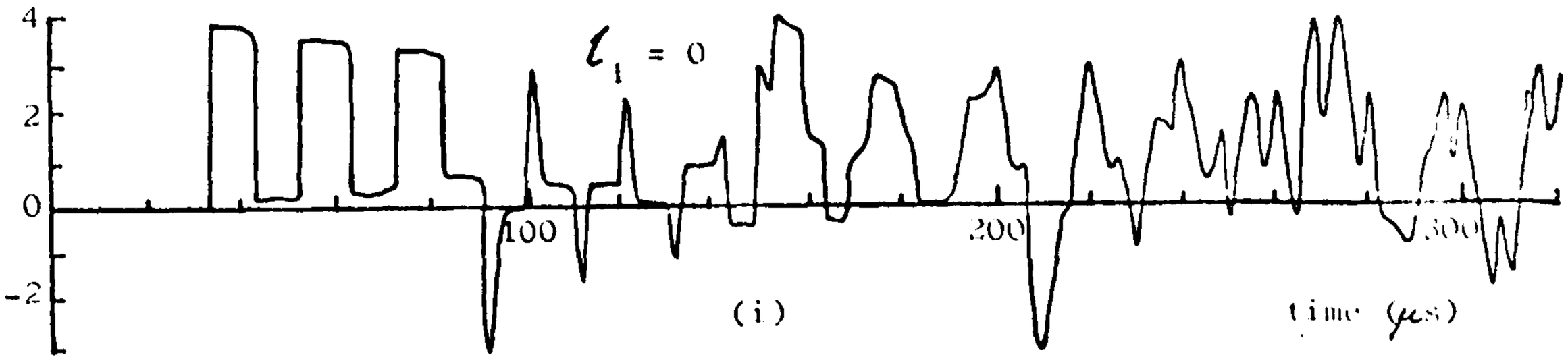

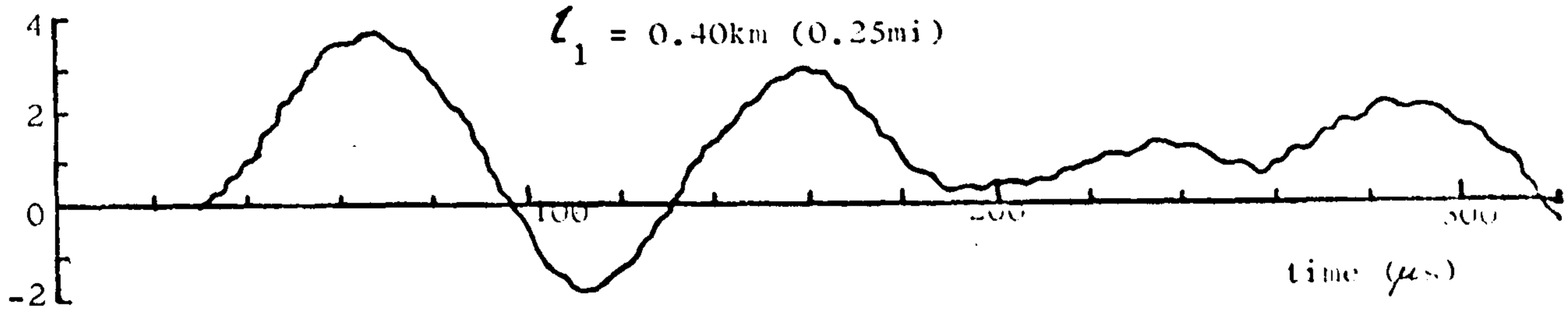

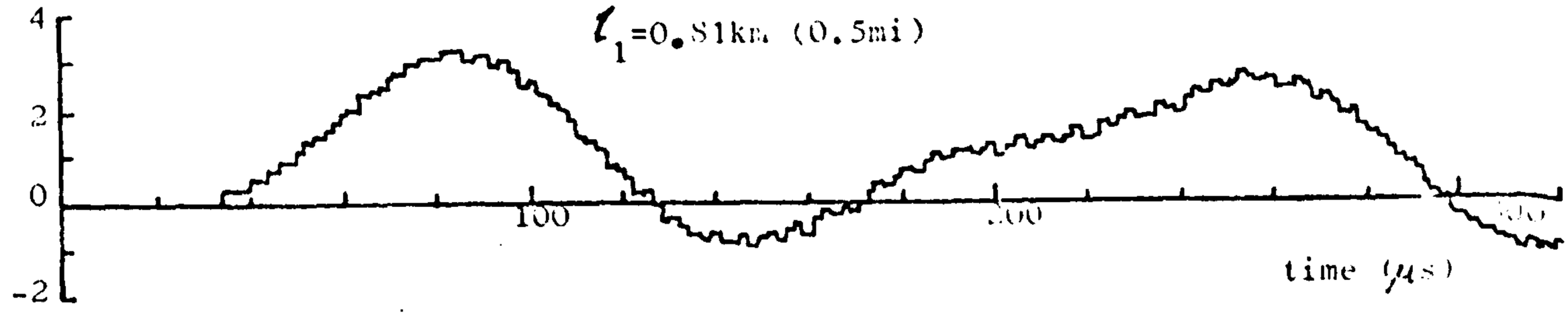

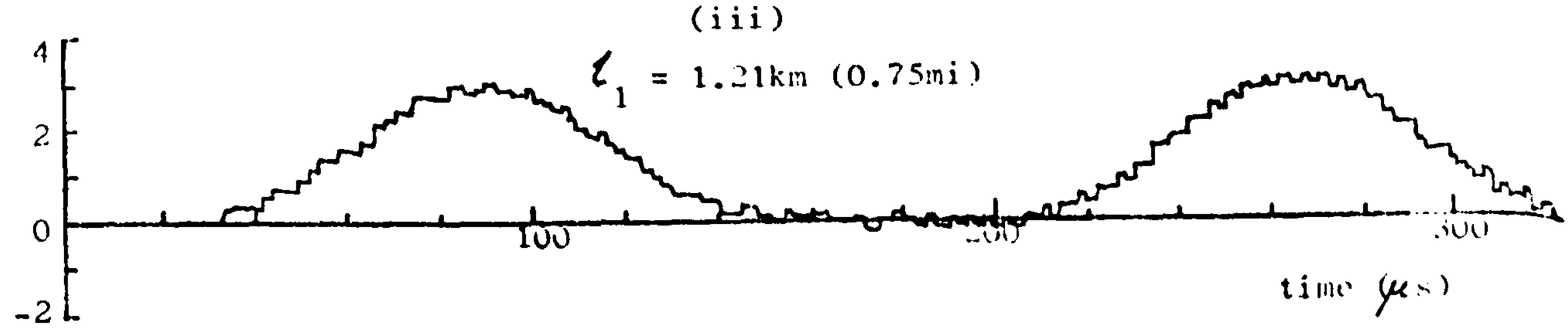

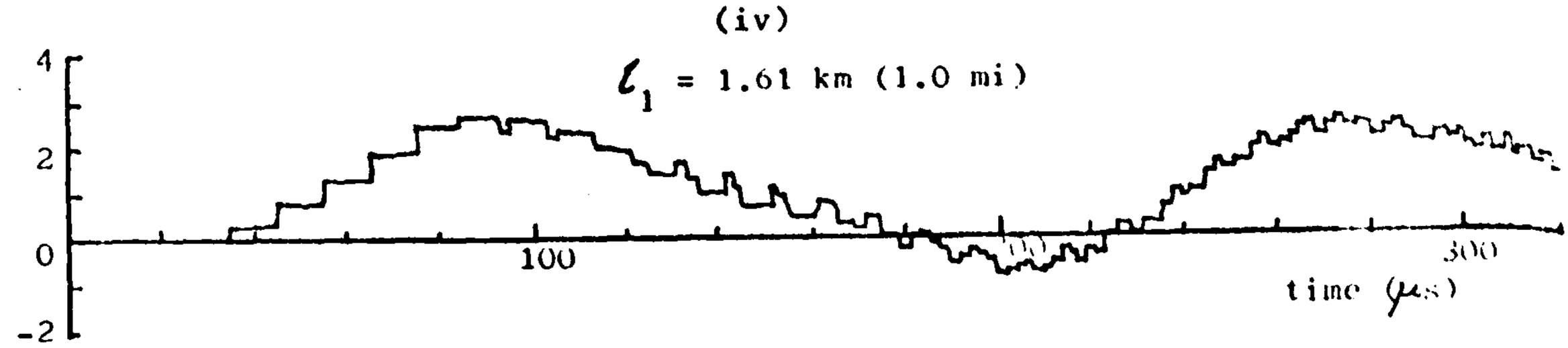

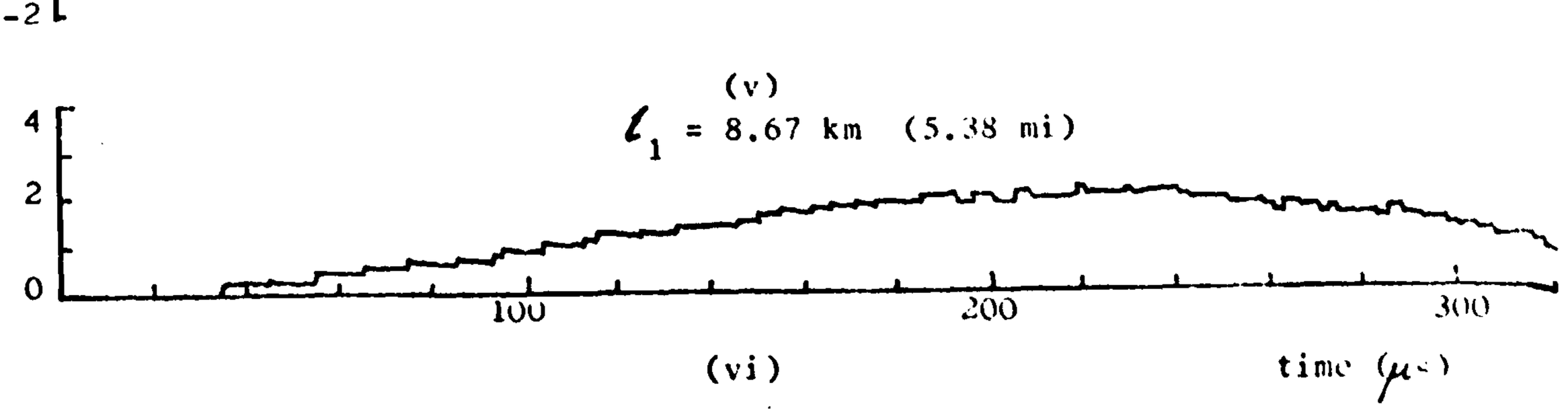

Fig. 6.17 Voltage waveforms on the line-side of the transformer

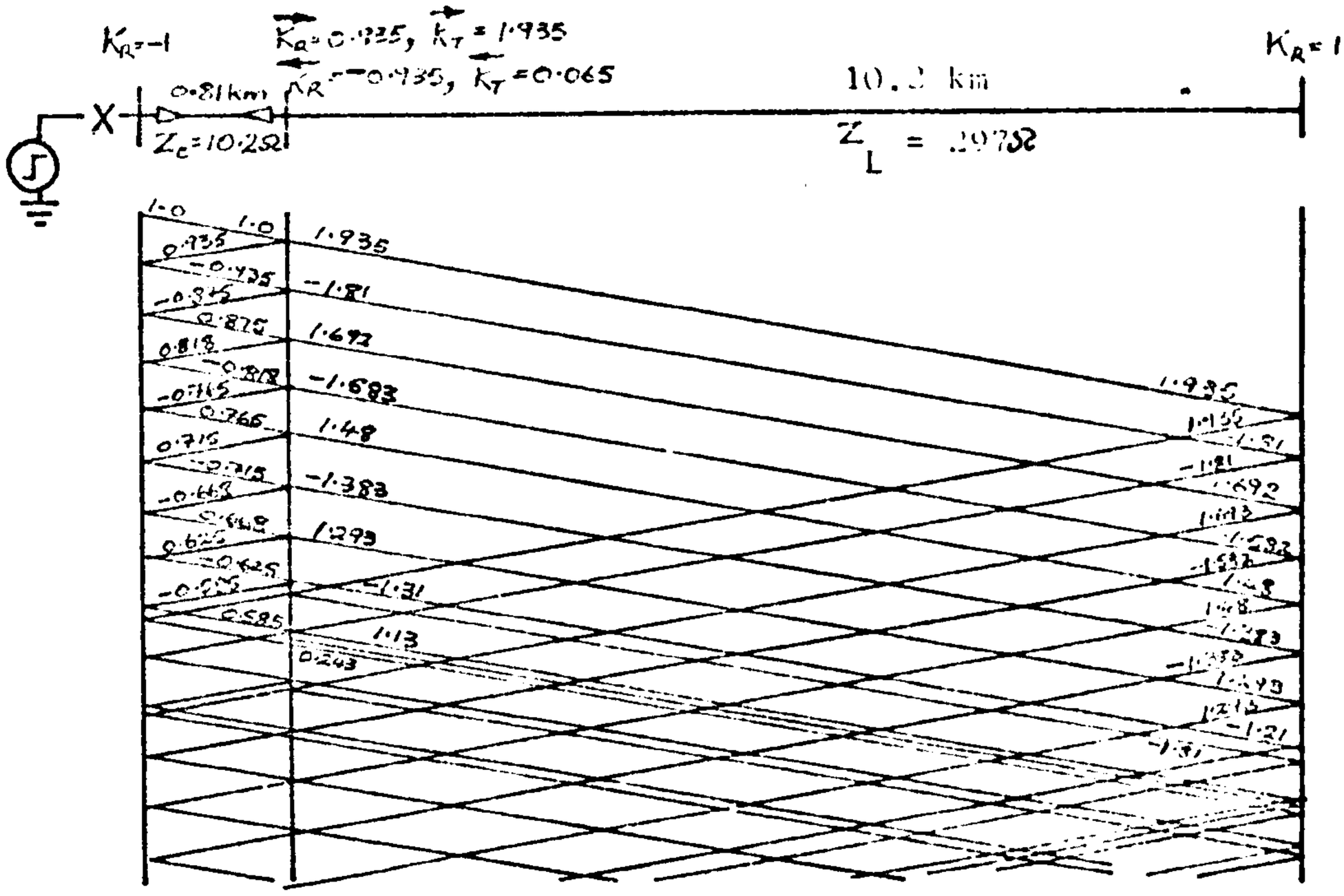

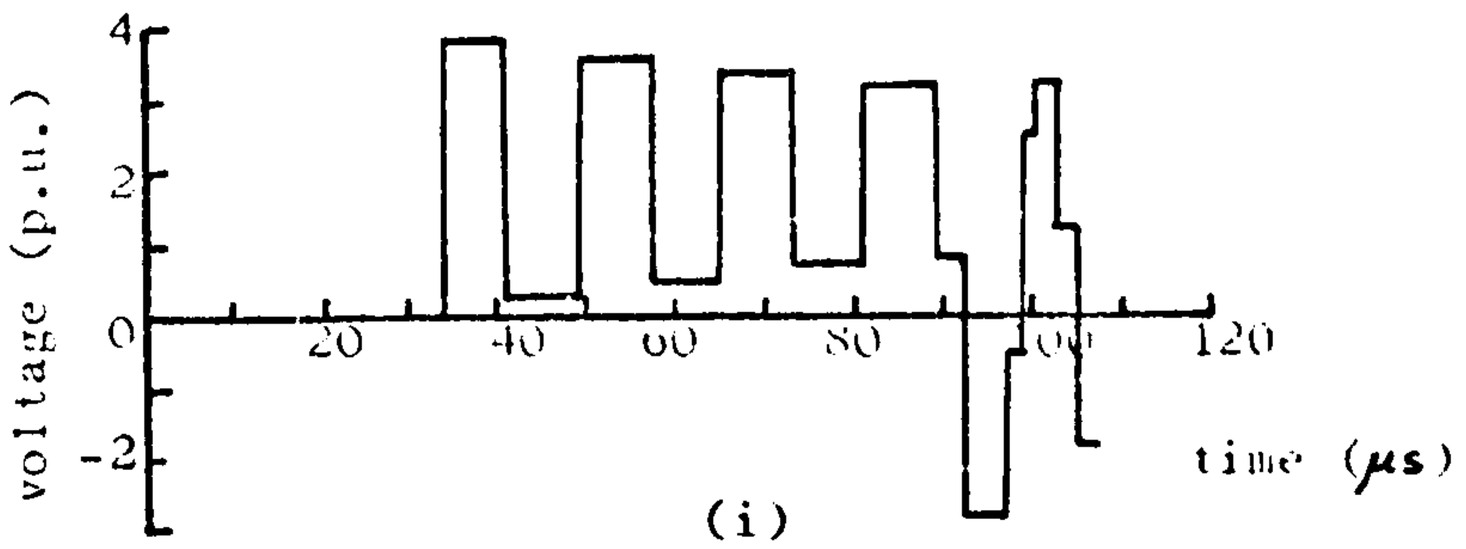

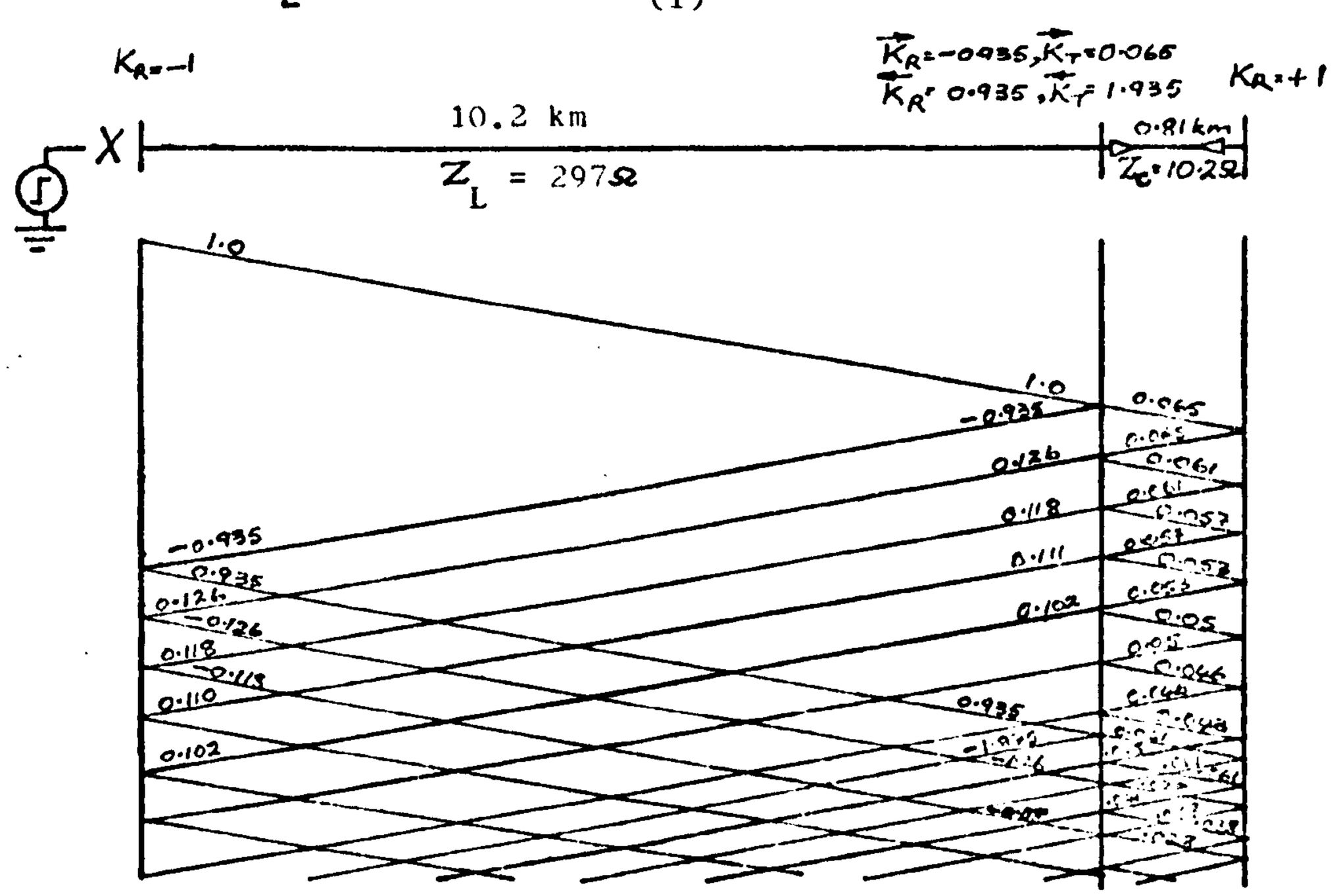

Fig. 6.18 Lattice diagram analysis
(i) cable adjacent to energi . circuit breaker
(ii) cable adjacent to trans: r

As the length of the cable is moved away from the energising circuit breaker, the voltages on the line side of the transformer no longer exhibit a dominating cable frequency component. This is shown by the remaining waveforms of Fig. 6.17. When the cable is situated 0.81km from the circuit breaker (i.e $\ell_1 = 0{\cdot}081\ (\ell_1 + \ell_2)$, Fig 6.17 (iii) shows that the voltage at the transformer contains a large component at the transformer frequency (f = 7.34kHz, T = 136 μs). This accounts for the large peak in the overvoltage at the transformer secondary as shown in Fig 6.19. As the cable is moved further away from the circuit breaker (see Fig 6.17) this component decreases causing a reduction in overvoltage.

If the length of the cable is located adjacent to the transformer, the wave that penetrates the cable is reduced considerably due to the low transmission coefficient at the junction. The voltage at the cable ends builds up by successive reflections of the waves oscillating in the cable, as shown in Fig 6.17 (vi). If the transformer surge impedance is considered infinite compared with that of the cable the voltage waveform at the end of the cable may be computed with the aid of Bewley's lattice diagram, as shown on Fig 6.18.

The cable is charged in successive steps to a voltage tending asymptotically to twice the amplitude of the incident wave. It is clear that the cable does not limit the overvoltage at its end, but causes a substantial reduction of the steepness of the incident waves. The extent of the reduction depends on the charging time constant, $Z_L C$, where Z_L is the line surge impedance and C, the total cable capacitance to earth.This is because for times far exceeding the cable travel time, the cable behaves like a lumped capacitance.

In the analogue method, the cable is represented by its equivalent capacitance. This may be obtained from the characteristics

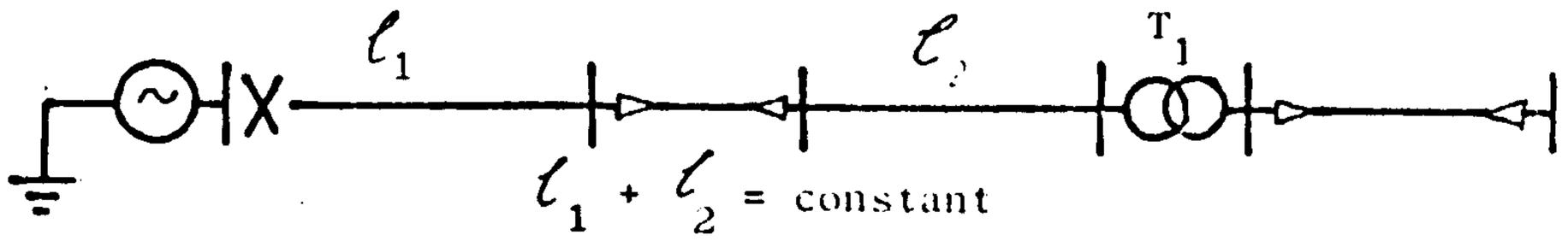

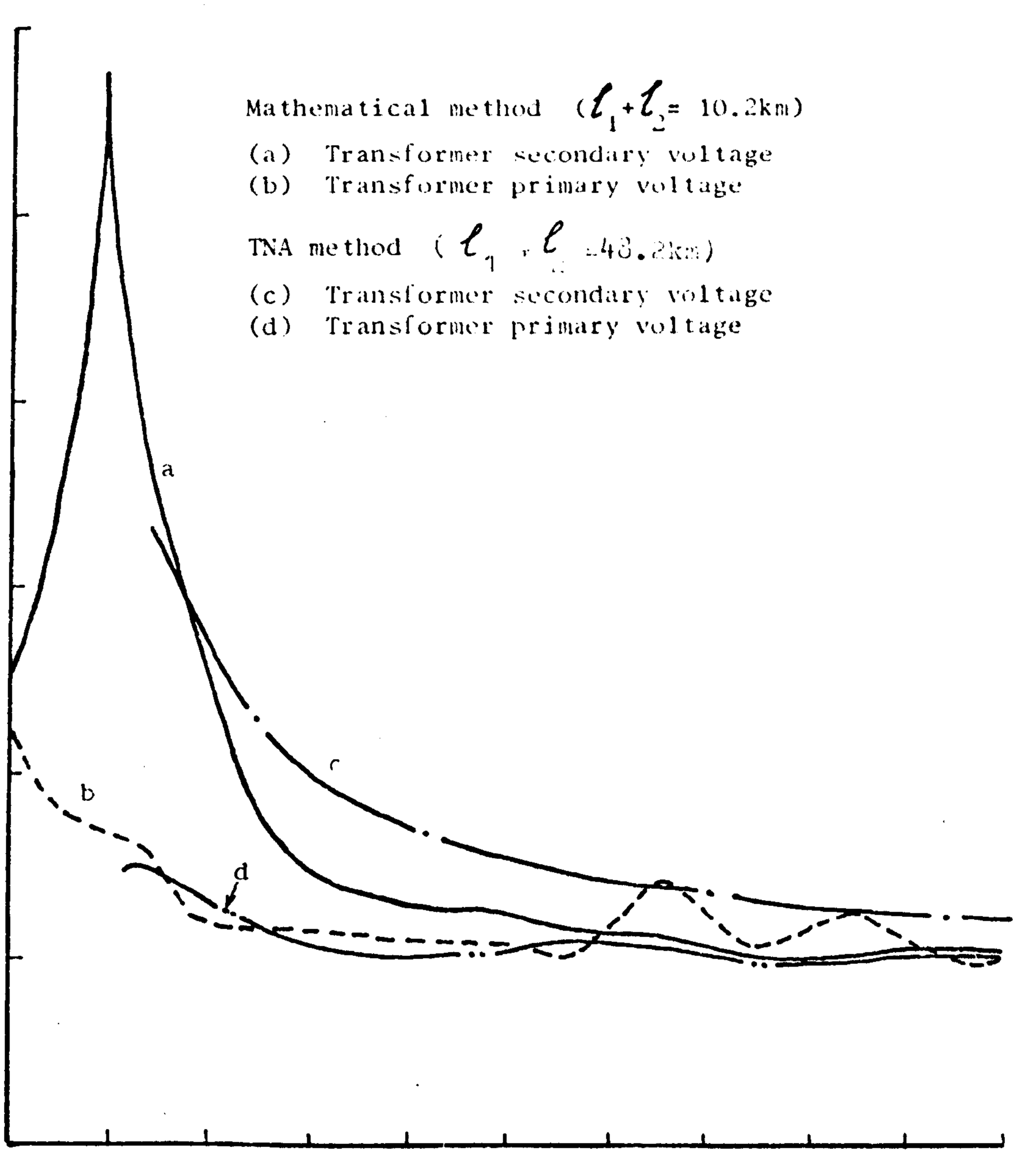

Mathematical method ($\ell_1 + \ell_2 = 10.2$km)

(a) Transformer secondary voltage
(b) Transformer primary voltage

TNA method ($\ell_1 + \ell_2 = 48.2$km)

(c) Transformer secondary voltage
(d) Transformer primary voltage

Fig. 6.19 Effect of varying the position of a 0.81km (0.5mi) cable along the length of transformer feeder.

of the cable

$$\text{i.e} \quad C = \tau / Z_c \qquad \mu F/m$$

where Z_c = cable surge impedance (ohms),

and τ = transit time of cable (sec/m.).

In this case, Z_c = 10.2 ohm and τ = 6.15×10^{-9} sec/m. Hence

$$C = 0.000615 \ \mu F/m.$$

The 0.84 μF capacitance used on the TNA therefore represents 1.37km of cable. The oscillograms of Fig 6.20 relate to the case where the sum of the lengths of the overhead line sections is held constant ($\ell_1 + \ell_2$ = 48.2km), giving a line frequency equal to that of the transformer. (f_L = 1.55kHz, T = 0.65 ms).

Since the cable is represented as a lumped capacitance, the distributed effects of the cable are not present on the oscillograms of Fig. 6.20. However, the decrease in the frequency of the transformer line-side voltage as the length of cable is moved nearer to the transformer, is again illustrated. The resulting voltage waveforms on the transformer secondary are shown to depend on the frequency spectrum of the transformer primary voltage.

6.4.2 Length of cable

When the underground cable is positioned adjacent to the transformer, the overvoltage decreases as the length of cable is increased (Fig. 6.21). In this case the frequency of the mixed feeder is kept constant at the transformer frequency. The sharp changes of slope shown on the overvoltage curves result from the change in the half cycle on which the maximum voltage occurs. Initially the maximum voltage occurs on the third half cycle, but as the length of cable increases the second half cycle peak exceeds that of the third half cycle. The dotted and dashed curves represent the voltage peak on the second and third half cycles respectively.

On the other hand, if the underground cable is located

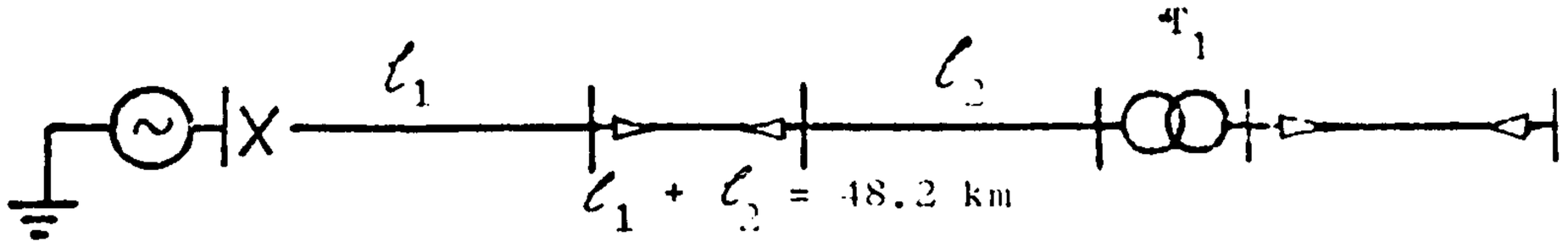

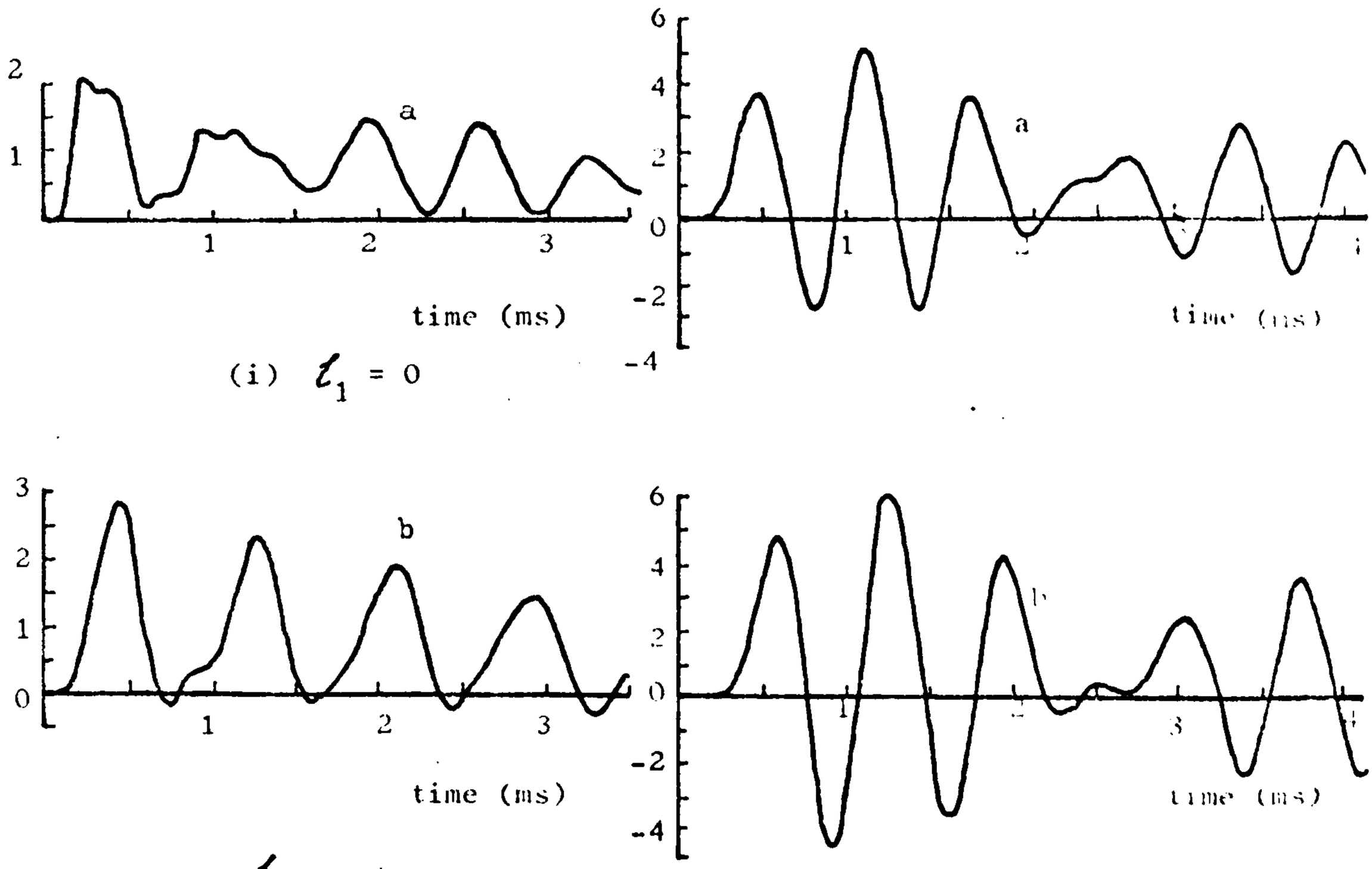

(i) $\ell_1 = 0$

(ii) $\ell_1 = 8.0$km

(iii) $\ell_1 = 24.1$ km

(iv) $\ell_1 = 48.2$km

Fig. 6.20 TNA voltage waveforms on the

(i) line-side of the transformer
(ii) secondary side of the transformer

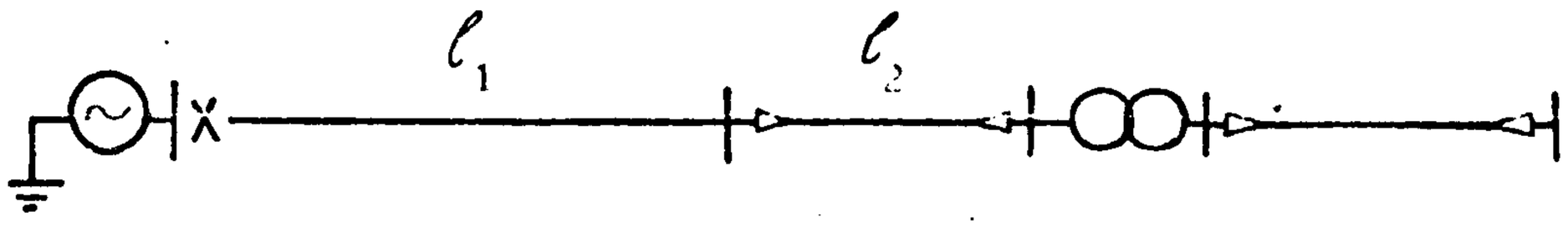

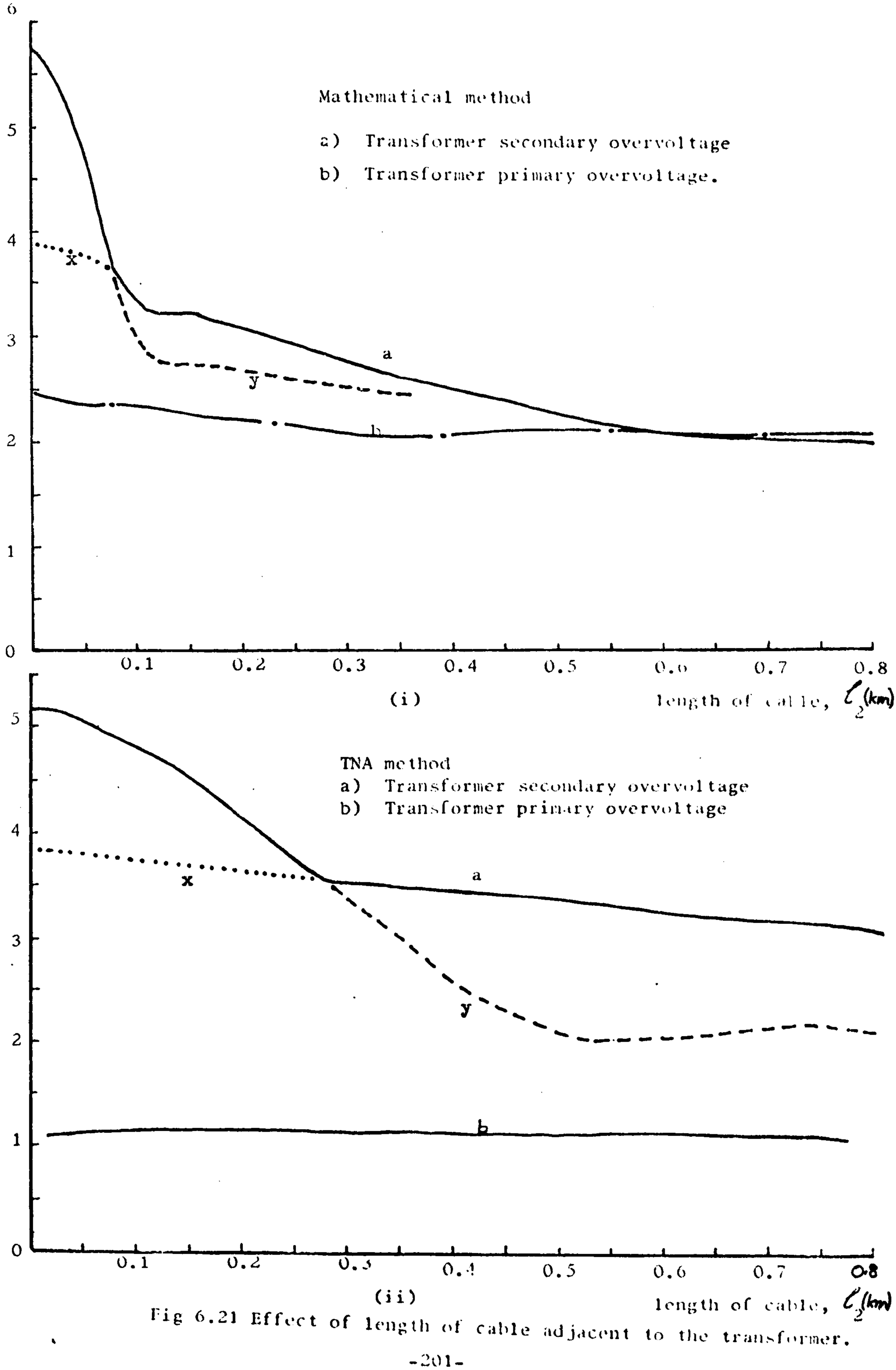

Fig 6.21 Effect of length of cable adjacent to the transformer.

adjacent to the energising circuit breaker and its length varied, the overvoltages vary as shown in Fig. 6.22. Again the mixed feeder frequency is maintained constant at the transformer frequency. When the cable length is increased to a value where the transit time of the cable is equal to that of the line, the voltage on the line side of the transformer increases from 2.5 p.u. (its value when the cable is not present) to 6.8 p.u. Since the transit time of the cable used is 1.88 times that of an equal length of line, this point will be reached when the length of cable is 2.7 km. This increase is accounted for by the interference of the oscillations on the line and cable. The oscillations may add up to give voltage spikes in excess of the approximate quadrupling of the initial voltage step travelling through sections of increasing surge impedances. Fig. 6.23 (ii) indicates a peak value of 6.5 p.u. on the primary waveform. The waveform is distorted and the component with frequency equal to that of the transformer does not dominate the resultant feeder oscillations as is the case when no cable is present (Fig. 6.23 (i)). Hence large resonant oscillations do not develop on the transformer secondary.

Increasing the length of cable further until its travel time is twice that of the line, the transformer line side over-voltage decreases to 4.4 p.u. and the secondary peak voltage increases steadily to 5.4 p.u. (Fig. 6.22). The voltage waveforms pertaining to the two to one ratio of cable and line travel times are shown on Fig. 6.23 (iii). Assuming that the transformer surge impedance is infinite and the line surge impedance is very much greater than that of the cable, lattice diagram considerations will show that the voltage waveform at the end of the line will consist of a train of pulses of 2T/6T mark-space ratio (T = travel time of line) and

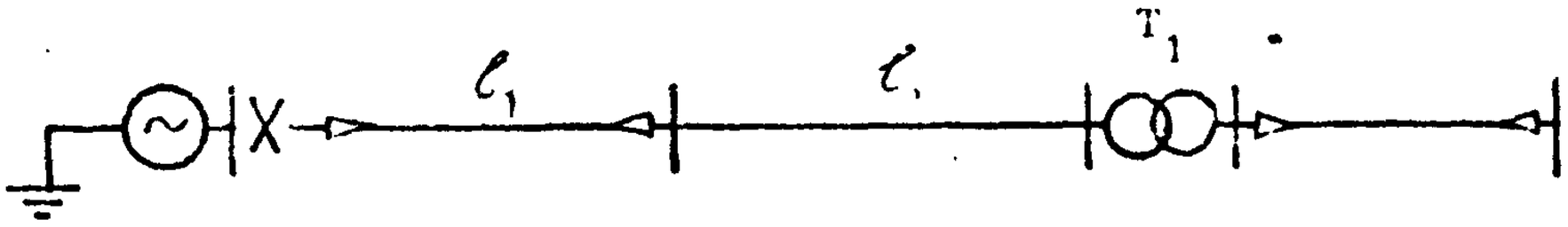

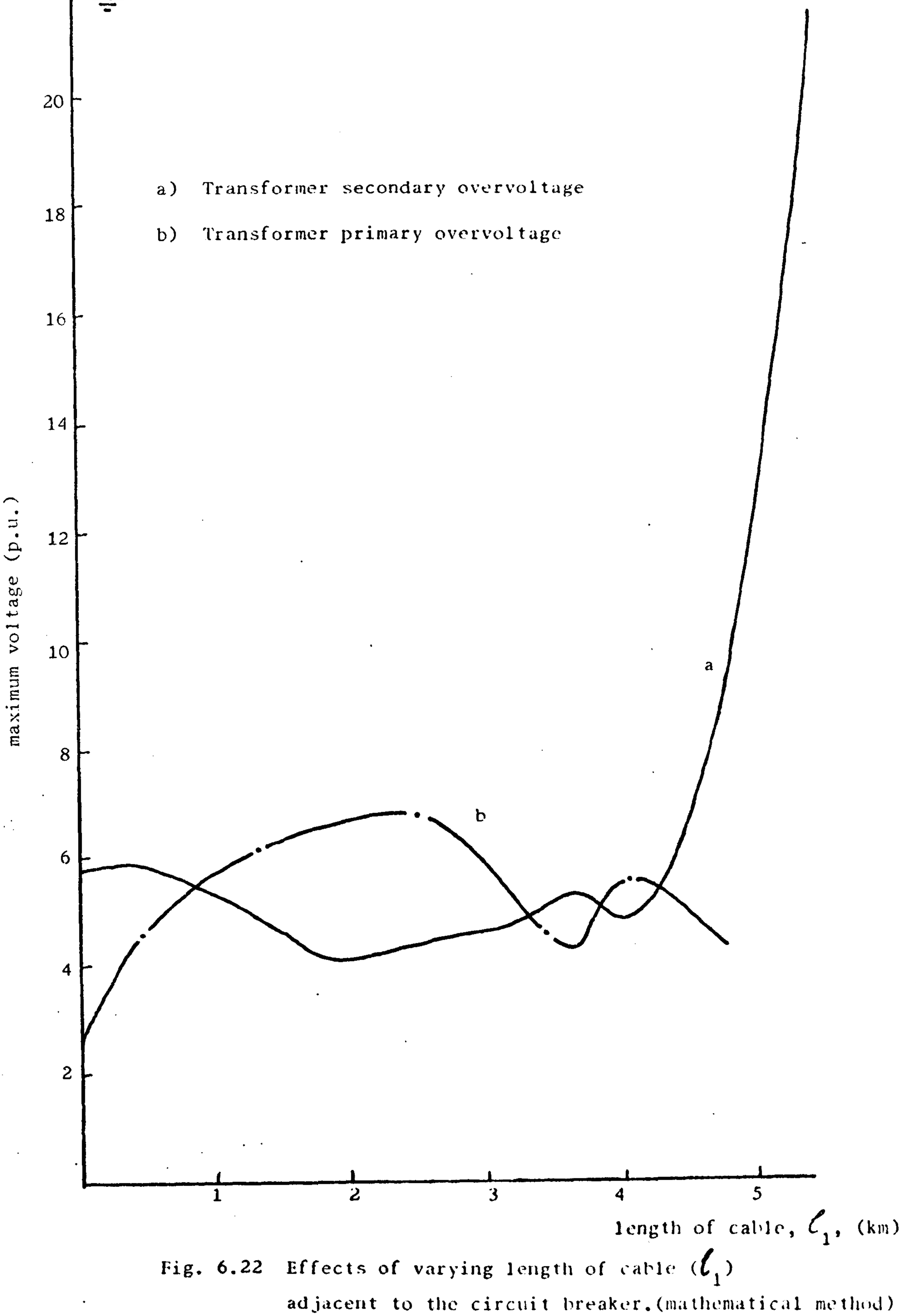

Fig. 6.22 Effects of varying length of cable (ℓ_1) adjacent to the circuit breaker.(mathematical method)

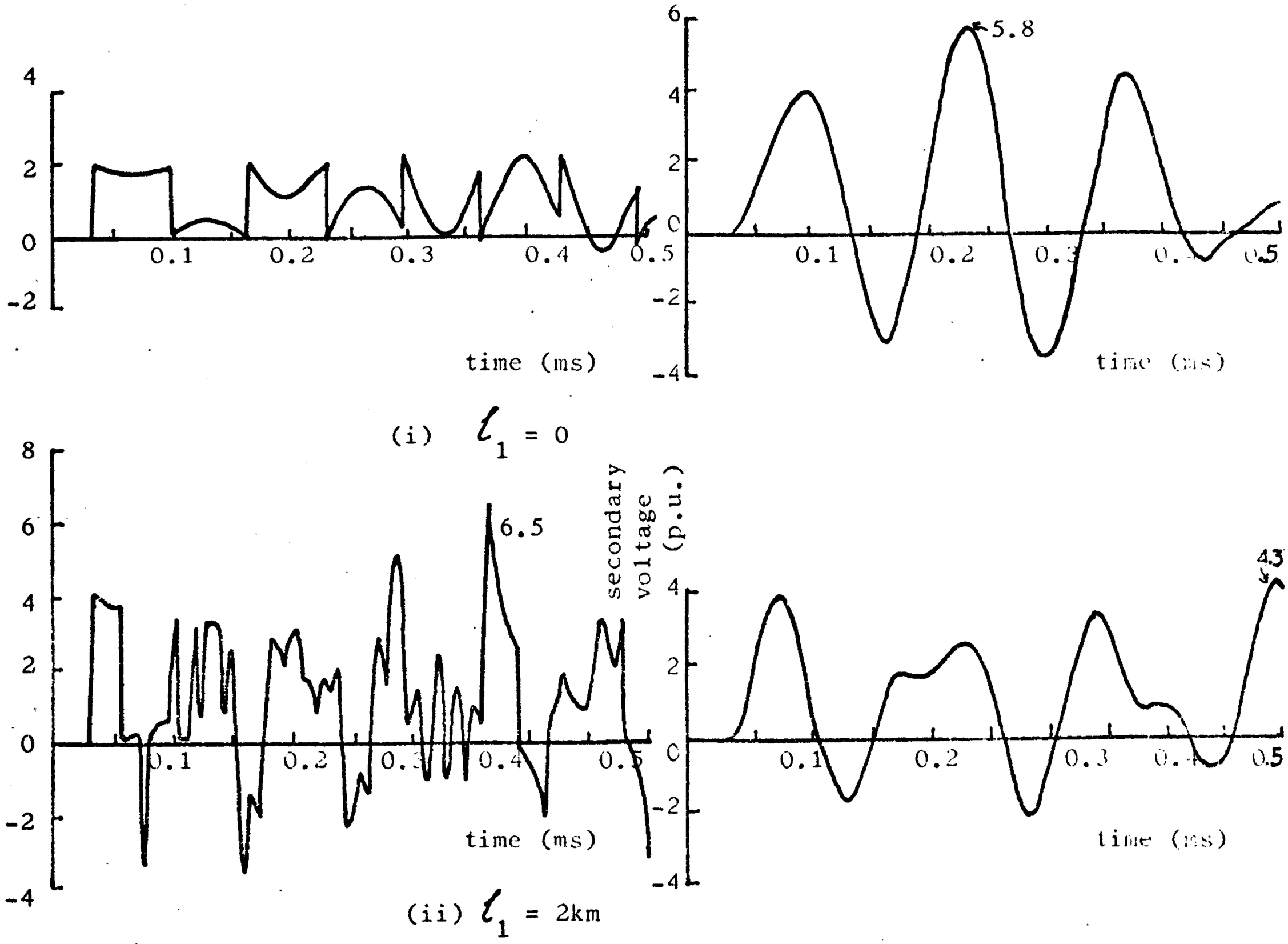

(i) $\ell_1 = 0$

(ii) $\ell_1 = 2$km

(iii) $\ell_1 = 3.6$km

Fig. 6.23 The effect of varying the length of cable (ℓ_1) on computed voltage waveforms.

magnitude 4 p.u. The waveform displayed in Fig. 6.23 (iii) is essentially of this form, with modifications due to finite line and transformer surge impedances. In spite of the approximate 4 p.u. amplitude of the exciting waveform, curve (iii) shows that the secondary overvoltage is 5.4 p.u. compared with 5.8 p.u. obtained in the case when no cable is present. This is because the predominant feeder oscillations frequency is not close to that of the transformer.

As the length of line approaches zero, the oscillations on the cable dominate the voltage waveform on the transformer primary. The cable frequency approaches that of the transformer and large resonant overvoltages are obtained (Fig. 6.22). The low surge impedance of the cable relative to that of the transformer produces the excessive overvoltages shown.

6.5 Conclusion

For transmission at the medium and high voltage levels, economic considerations may preclude the installation of circuit breakers at the high voltage side of the transformer. However, it is normal to instali switching isolators adjacent to the transformer instead. These are used to connect or disconnect circuits and, unlike normal isolators, are capable of making or breaking normal load and transformer magnetising currents. In this case, the resonance phenomenon investigated here could be eliminated by first energising the feeder until steady state conditions obtain before closing the switching isolators at the transformer.

When the feeder is energised with the tee-off line at the transformer line-side busbar as a unit, the overvoltages produced are less than 4 p.u. These overvoltages may be reduced further if the ratio of the length of the tee-off line to that of the feeder is odd. If the tee-off point is nearer the energising circuit breaker, large overvoltages may result when the length of the tee-off line is less than or equal to half the total length of line between the circuit breaker and the transformer. If this condition arises, it is possible to eliminate or reduce the overvoltage by energising the circuit from the breaker at the remote end of the tee-off line.

The conditions in the network supplying the energy to the feeder have a marked influence on the evolution of the transient voltages. The effect of an inductive source is to increase the transformer primary overvoltage at the higher ratings of the source capacity, but the maximum voltages on the transformer secondary are reduced considerably. If the feeder is energised from a line originating at a generating station, the overvoltage excited at the transformer may be made more severe if the length of the source-side

line is close to that of the feeder.

The main source of danger in mixed line and cable feeders is a system where the elements are connected in a sequence of monotonically increasing surge impedances. This is the case if a length of cable connects the energising circuit breaker to an overhead line terminating in a transformer. On the other hand, a length of cable interposed between the overhead line and the transformer may be a mitigating factor. Although the presence of the cable does not limit the voltage at the cable ends, it reduces the front steepness of the incident waves considerably. This reduction of the rate of rise of voltage at the transformer reduces the stress on the insulation of the transformer. A reduction in the magnitude of the crest voltage applied to the transformer can only be effected if the travel time of the cable is comparable to the duration of the surge. In this case the crest would be reduced by an amount depending on the ratio of the transit time of cable to twice the propagation time of the overhead line feeding the cable. It is apparent that if a feeder contains a cabled section at either end, there is a best end from which the feeder may be energised.

It will be appreciated that in practice, particularly at lower voltage levels, the system configuration may be more complex. The feeder may consist of a number of intermediate sections of cable and may also include fault limiting reactors, while the circuit on the source side may contain any one of several combinations of local and distant generation. In such cases, the overvoltages produced will depend on the physical arrangements, characteristics and lengths of the components comprising the network. An individual investigation of such a system would be necessary in order to establish conditions likely to produce severe resonant oscillations.

C H A P T E R 7

MATHEMATICAL MODEL OF THREE-PHASE TRANSFORMER FEEDER CIRCUITS

7.1 Introduction

The single-phase compensation method, on which the analytical results discussed in the last two Chapters is based, has been described in Chapter 4. The need for a method capable of faithfully reproducing travelling wave phenomena in lines and cables, and accurately simulating the termination equivalent circuit response was pointed out. The compensation method was found to achieve both these objectives. Its validity was demonstrated by comparison with established methods based on the lattice diagram and lumped parameter approaches, as well as with the TNA.

In this Chapter, this compensation method will be extended to include three-phase effects. A more detailed equivalent circuit of the transformer, simulating both the electrical and non-linear properties, will be presented. The efficacy of this method will be demonstrated in subsequent Chapters in investigating the transient and dynamic response of three-phase transformer feeder circuits under certain operating conditions.

7.2 System constants

7.2.1 Transmission line constants

The particulars of the 275 kV, twin 0.4 sq.in. conductor, three-phase transmission line used in the analytical studies discussed in Chapter 8, are summarised on Table 7.1. These constants are calculated at a frequency of 8 kHz using an existing computer program. This frequency was selected because it is close to the natural frequency of a 10.2 km line used in most of the studies. Ignoring line attenuation effects, the line is defined by its surge impedance matrix in the lattice diagram and compensation methods.

The constants of the twin and quadruple double circuit lines simulated in studies discussed in Chapters 9 and 10, are presented in Tables 7.2 and 7.3. From the physical configurations of the lines shown on Fig. 7.1, a standard computer program evaluates the surge impedance matrix, line series, shunt and mutual phase and symmetrical component sequence impedance matrices. Data required for the mathematical model consist of the 6 x 6 surge impedance matrix.

7.2.2 Transformer constants

The transformer simulated is a 275/132/33 kV 1000 MVA auto-transformer connected star/star/delta with the neutral earthed. The physical dimensions of the five-limb auto-transformer core are shown on Fig. 7.2 (i). The core is composed of Unisil 46 material with an operating flux density of 1.7 Tesla. The magnetisation characteristics of the core will be discussed in section 7.4.

In the absence of data relating to a three-limb transformer, the core structure assumed in simulating three-limb transformers is similar to that shown on Fig. 7.2 (i) with the outer

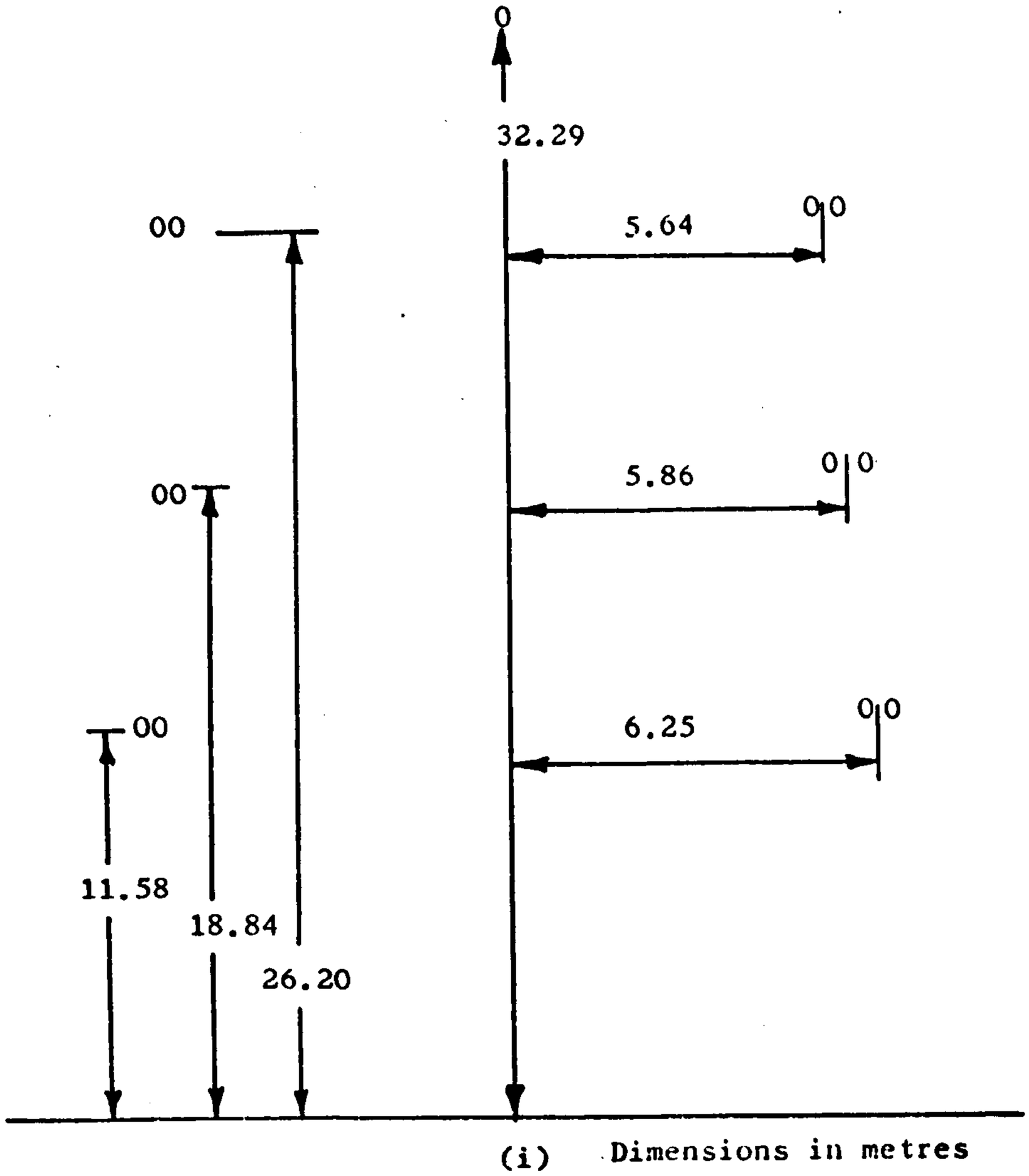

Fig. 7.1 Double circuit line configurations
(i) 275 kV Twin conductor line
(ii) 400 kV Quadruple conductor line

Table 7.1

275 kV TWIN CONDUCTOR SINGLE CIRCUIT LINE CONFIGURATION CONSTANTS

Frequency = 8000 Hz

Earth resistivity = 20 ohm - meter

Upper triangular matrix elements

Series resistance R (ohm/km)	Series reactance X_L (ohm/km)	Shunt reactance X_C (Mohm/km)	Surge impedance Z (ohm)
1.8204	66.8806	0.002233	386.4811
2.1648	18.9035	0.000550	101.9551
2.5479	12.2278	0.000282	58.7186
2.6852	67.9876	0.002209	387.5539
3.1558	19.0142	0.000474	94.8878
3.8382	67.3054	0.002078	373.9597

Table 7.2

275 kV TWIN CONDUCTOR DOUBLE CIRCUIT LINE CONFIGURATION CONSTANTS

Frequency = 50 Hz

Earth resistivity = 0 ohm - meter

Upper triangular matrix elements :

Series resistance R(ohm/km)	Series reactance X_L (ohm/km)	Shunt reactance X_C (Mohm-km)	Surge Impedance Z (ohm)
0.0424 0.0041 0.0024 0.0063 0.0041 0.0023	0.4060 0.0988 0.0508 0.0757 0.0636 0.0390	0.35533 0.08795 0.04511 0.06560 0.05586 0.03432	380.94 93.23 47.88 70.45 56.63 36.58
0.0387 0.0015 0.0041 0.0026 0.0015	0.3995 0.0839 0.0636 0.0703 0.0500	0.35343 0.07576 0.05586 0.06273 0.04486	375.76 79.74 56.63 66.42 47.39
0.0369 0.0023 0.0015 0.0009	0.3754 0.0390 0.0500 0.0480	0.33247 0.03432 0.04486 0.04334	353.30 36.58 47.39 45.62
0.0424 0.0041 0.0024	0.4060 0.0988 0.0508	0.35533 0.08795 0.04511	380.94 93.23 47.88
0.0387 0.0015	0.3995 0.0839	0.35343 0.07576	375.76 79.74
0.0369	0.3754	0.33247	353.30

Z_1 = positive sequence impedance = 0.0347 + j 0.3144 ohms/km

Z_0 = zero sequence impedance of one circuit = 0.0439 + j 0.5458 ohms/km

Z_{mo} = zero sequence mutual impedance between circuits = 0.0100 + j 0.1601 ohms/km

B_1 = positive sequence susceptance = 3.644 μS/km

B_0 = zero sequence susceptance of one circuit = 2.274 μS/km

B_{mo} = zero sequence mutual susceptance between circuits = -0.679 μS/km

Table 7.3

400 kV QUADRUPLE CONDUCTOR DOUBLE CIRCUIT LINE CONFIGURATION CONSTANTS

Frequency = 50 Hz

Earth resistivity = 30 ohm - meter

Upper triangular matrix elements :

Series resistance R(ohm/km)	Series reactance X_L(ohm/km)	Shunt reactance X_C(Mohm-km)	Surge impedance Z (ohm)
0.0441 0.0279 0.0285 0.0271 0.0279 0.0285	0.4405 0.1765 0.1463 0.1494 0.1390 0.1316	0.33290 0.07812 0.03972 0.06789 0.04661 0.02951	377.15 117.44 76.23 100.70 80.50 62.32
0.0461 0.0301 0.0279 0.0291 0.0300	0.4645 0.2036 0.1390 0.1490 0.1532	0.31398 0.07039 0.04661 0.04139 0.03182	381.88 119.73 80.50 78.55 69.80
0.0480 0.0285 0.0300 0.0310	0.4734 0.1316 0.1532 0.1708	0.28706 0.02951 0.03182 0.03099	368.65 62.32 69.80 72.74
0.0441 0.0279 0.0285	0.4405 0.1765 0.1463	0.33290 0.07812 0.03972	377.15 117.44 76.23
0.0461 0.0301	0.4645 0.2036	0.31398 0.07039	381.88 119.73
0.0480	0.4734	0.28706	368.65

Z_1 = positive sequence impedance = 0.0172 + j 0.2840 ohms/km

Z_0 = zero sequence impedance of one circuit = 0.1037 + j 0.8105 ohms/km

Z_{mo} = zero sequence mutual impedance between circuits = 0.0838 + j 0.4389 ohms/km

B_1 = positive sequence susceptance = 4.138 µS/km

B_0 = zero sequence susceptance of one circuit = 2.515 µS/km

B_{mo} = zero sequence mutual susceptance between circuits = -0.680 µS/km

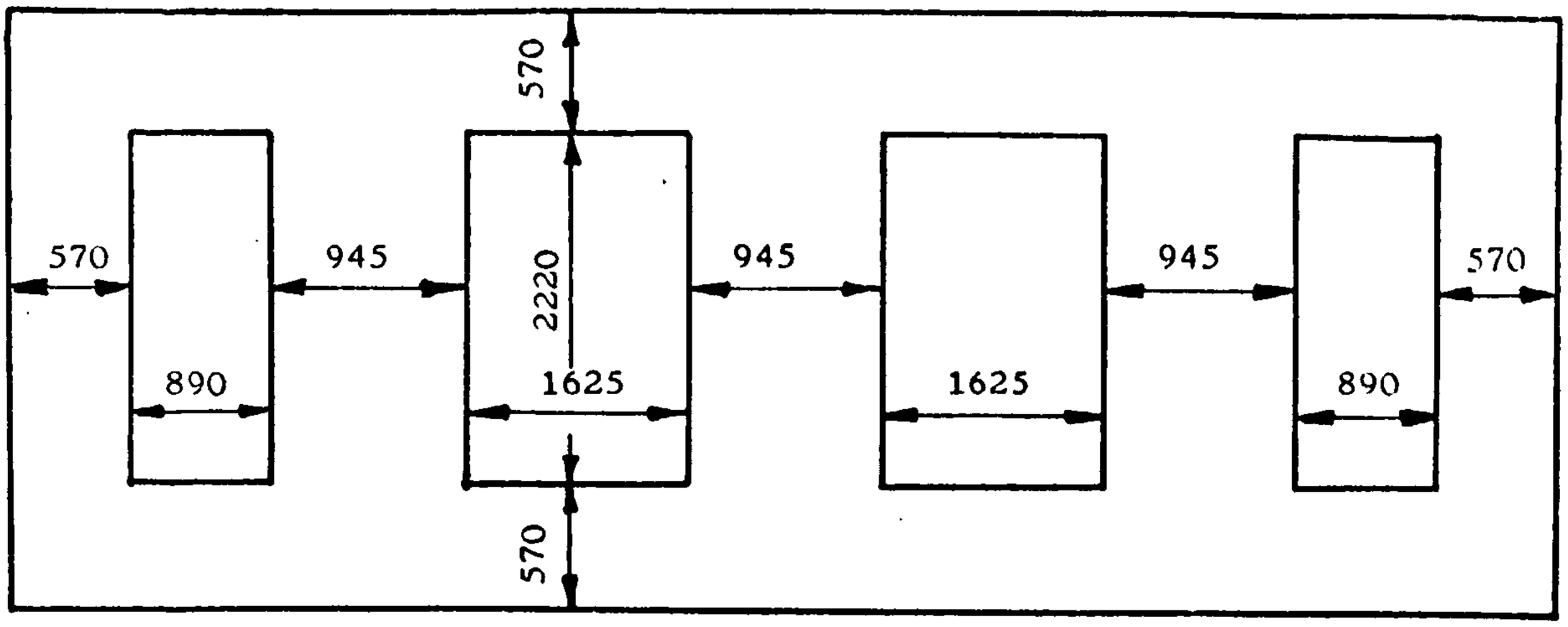

Fig. 7.2 (i) Five-limb auto-transformer core dimensions
(ii) Magnetic flux paths and reference directions

core limbs excluded.

The measured impedances per phase of the transformer are as follows :

(a) Positive sequence leakage reactances at full load and $75^{o}C$:

X_{H-L} = 0.170 p.u. where X_H = 31.0 ohm

X_{H-T} = 1.215 p.u. X_L = -3.8 ohm

X_{L-T} = 0.995 p.u. X_T = 163.1 ohm

The subscripts H, L and T relate to the high voltage, low voltage and tertiary windings, respectively. All values are referred to the 400 kV winding.

(b) Zero sequence reactances :

X_{H-L} = 0.163 p.u. where X_H = 30 ohm

X_{H-T} = 0.908 p.u. X_L = -4 ohm

X_{L-T} = 0.693 p.u. X_T = 115 ohm

referred to 400 kV turns.

(c) Copper losses :

I^2R losses corrected to full load on 400 kV at $75^{o}C$ are given by :

W_{H-L} = 1400 kW at 1442A i.e. R_{H-L} = 0.68 ohm

W_{H-T} = 74.5 kW at 86.7A R_{H-T} = 10.00 ohm

W_{L-T} = 81.5 kW at 126.0A R_{L-T} = 5.14 ohm

To obtain series resistances appropriate to the T-equivalent circuit of the transformer, the resistance values calculated above are divided in proportion to the measured d.c. winding resistances. The measured d.c. winding resistances corrected to $75^{o}C$ are 1.0, 1.7 and 6.64 ohms for the 400, 275 and 33 kV windings respectively. Hence

R_H = 1.31 ohm and R_T = 8.69 ohm

for an unloaded transformer, and

$$R_H = 0.252 \text{ ohm and } R_L = 0.428 \text{ ohm}$$

for a two-winding transformer.

(d) Core losses :

No-load losses measured on the 33 kV winding = 15.65 kW. Hence the equivalent conductance, $G_0 = 9.78 \times 10^{-7}$ Siemen, referred to the 400 kV winding.

The equivalent shunt resistance, R_0, used to simulate the core losses, is given by

$$R_0 = 1/G_0 = 1.022 \text{ M-ohm}$$

Owing to the unavailability of similar data for transformers of three-limb construction, the above constants were assumed to apply also in this case. Although this assumption is not strictly valid, particularly in respect of magnetic circuit core dimensions, it was necessary to use the same constants in order to demonstrate the potential applications of the compensation method.

7.3 Transformer state equations

Transformer simulation is based on a method described in reference (56) for a two-winding three-limb transformer. This method has been extended to model a three-winding five-limb transformer with a delta tertiary winding. The method combines the equations describing the electrical characteristics of the transformer with the magnetic circuit equations, including magnetic interactions and non-linearities, to form a composite and potentially accurate electromagnetic model with extensive potential applications. The reliability of available transformer data is, however, crucial to the overall fidelity of this model. Such detailed and accurate data is not readily available, particularly in respect of h.v. and e.h.v. transformers which cannot be subjected to detailed laboratory tests. In this case it is necessary to rely on the information made available by the manufacturers which, in most cases, is not adequate for the purpose of this model.

The equations describing the mathematical model are derived in Appendix 12.2 with the aid of Fig. 7.2 (ii), showing the windings and magnetic flux paths for a five-limb three-winding transformer. The flux paths are split up into sections associated with the winding limbs, outer limbs, yoke sections, and phase leakage paths, as shown on the diagram. The magnetising currents producing these fluxes are denoted by corresponding suffixes.

The resultant matrix equation expressed in the form $V = [M] . [pI]$ is presented in Table 12.1 of Appendix 12.2. For a two winding transformer without a tertiary winding, the tenth row of all matrices and the tenth column of the inductance matrix, are excluded. This reduces the order of the matrices from 10 to 9. In the case of unloaded secondary windings, the 7th, 8th and 9th

rows of all matrices and the corresponding columns of the inductance matrix are removed. In this case, the order of the matrices is reduced to 7 or 6, depending on whether the tertiary winding is present or not.

The matrix equations relating to a three-limb transformer differs from that given in Table 12.1 by the exclusion of inductances associated with the outer core limbs (M_9 and M_{10}).

7.4 Magnetic circuit characteristics

7.4.1 Phase leakage flux

In Appendix 12.3, the assumed phase leakage inductances associated with flux paths ϕ_6, ϕ_7 and ϕ_8 (see Fig. 7.2 (ii)), are expressed in measurable quantities. These inductances are assumed to be constant on the model, since the paths are predominantly in air. However, since data required to calculate these inductances were not available, the transformer zero sequence inductance, which is a close approximation of this quantity, was used instead.

7.4.2 Non-linear magnetisation characteristics

The method used to simulate the B/H curve is based on the exponential series representation outlined in reference(59). Three exponential terms have been found to be sufficiently adequate in accurately simulating both the flux density and differential permeability. A constant term is included to take account of large magnetisation forces when the associated fluxes are predominantly air-borne and essentially constant. The expression used is :

$$B = \sum_{i=1}^{3} C_i \left[1 - \exp(-D_i H) \right] + \mu_o H \qquad 7.1$$

where C_i and D_i are constant coefficients determined by an iterative procedure. The computer program requires six co-ordinates from the B/H curve to solve for the six unknown constants. In addition, co-ordinates of a point corresponding to the start of the core saturation region of the B/H curve is required to restrain the curve within pre-determined limits in the saturated portion.

The program proceeds first by evaluating the coefficients C_1 and D_1 using the first term of the exponential series and the first two co-ordinates of the B/H curve. In a similar manner, the expression containing the constants previously

derived, and the flux density increments are then used to evaluate the remaining coefficients. Considerable simplification of the curve-fitting technique can be achieved by selecting a constant ratio of successive pairs of field strength values (i.e. $H_2/H_1 = H_4/H_3 = H_6/H_5$). The co-ordinates generated by the expression derived are compared with the data points from the B/H curve. If the differences at these pivotal points exceed a predetermined value, the entire procedure is repeated until the error is acceptable. Fig. 7.3 shows a comparison of the actual B/H curve and the curve generated by the exponential expression. After 20 iterations, the maximum error at the pivotal points was 0.01%. The curves indicate a close correlation between both the flux densities and differential permeabilities defined by the slopes of the curves. The latter is important since it is the quantity used in solving the transformer state equations.

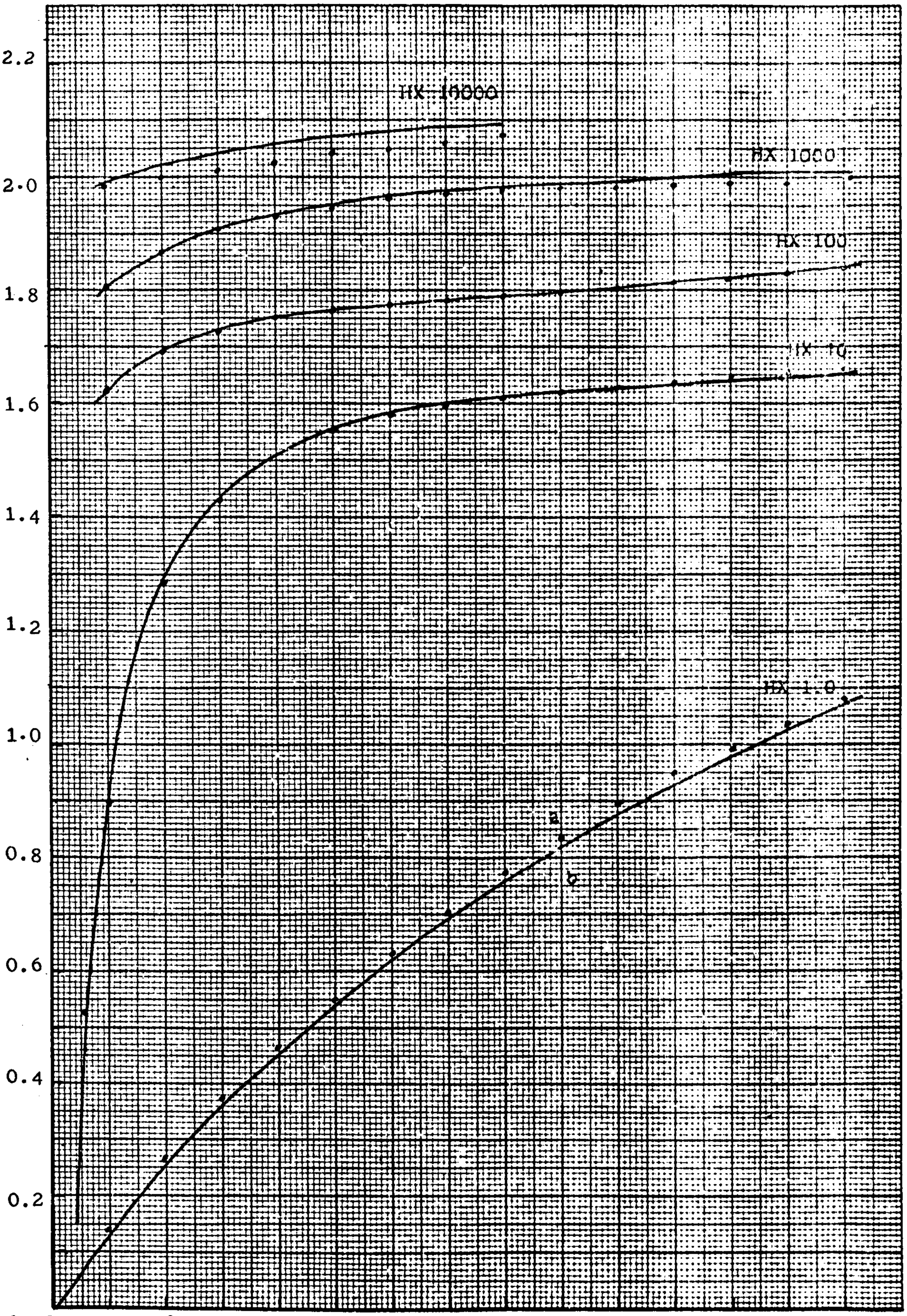

Fig. 7.3 Transformer magnetisation characteristics
(a) Transformer B/H curve for UNISIL 46
(b) B/H curve generated by exponential series

7.5 Three-phase compensation method

The three-phase compensation method is an extension of the single-phase method described in Chapter 4. This method is essentially an application of the compensation theorem which allows a subdivision of the system into several network components. Methods of solution appropriate to each sub-network can then be independently applied. In this case, the termination equivalent circuit is separated from the lines and replaced by an equivalent hypothetical current source of such a magnitude and sense that the voltage across the removed equivalent circuit is the same as the voltage across the same terminals in the original network. This theorem also forms the basis upon which the equations of diakoptics are formulated[60]. The lattice diagram technique is applied to the linear line networks, while the lumped parameter method is used to solve the non-linear lumped constants. This compensation method will be described with the aid of the flow diagram shown on Fig. 7.4.

7.5.1 System set-up and matrix modification

Data required consist of the constants of the single or double circuit line, initial conditions, switching operations, transformer and B/H equation constants, and the secondary load conditions. After initialisation, the system is decomposed into a linear section and a non-linear network comprising the transformer and secondary load circuits. Voltage surges initiated on the lines by switching operations are computed and the Thevenin equivalent circuit formulated. The B/H equation is used to determine the relevant differential permeabilities for currents pertaining to the previous time step (or initial conditions). This information is used to calculate the inductances associated with the magnetising currents as discussed in Appendix 12.2. The time and current-

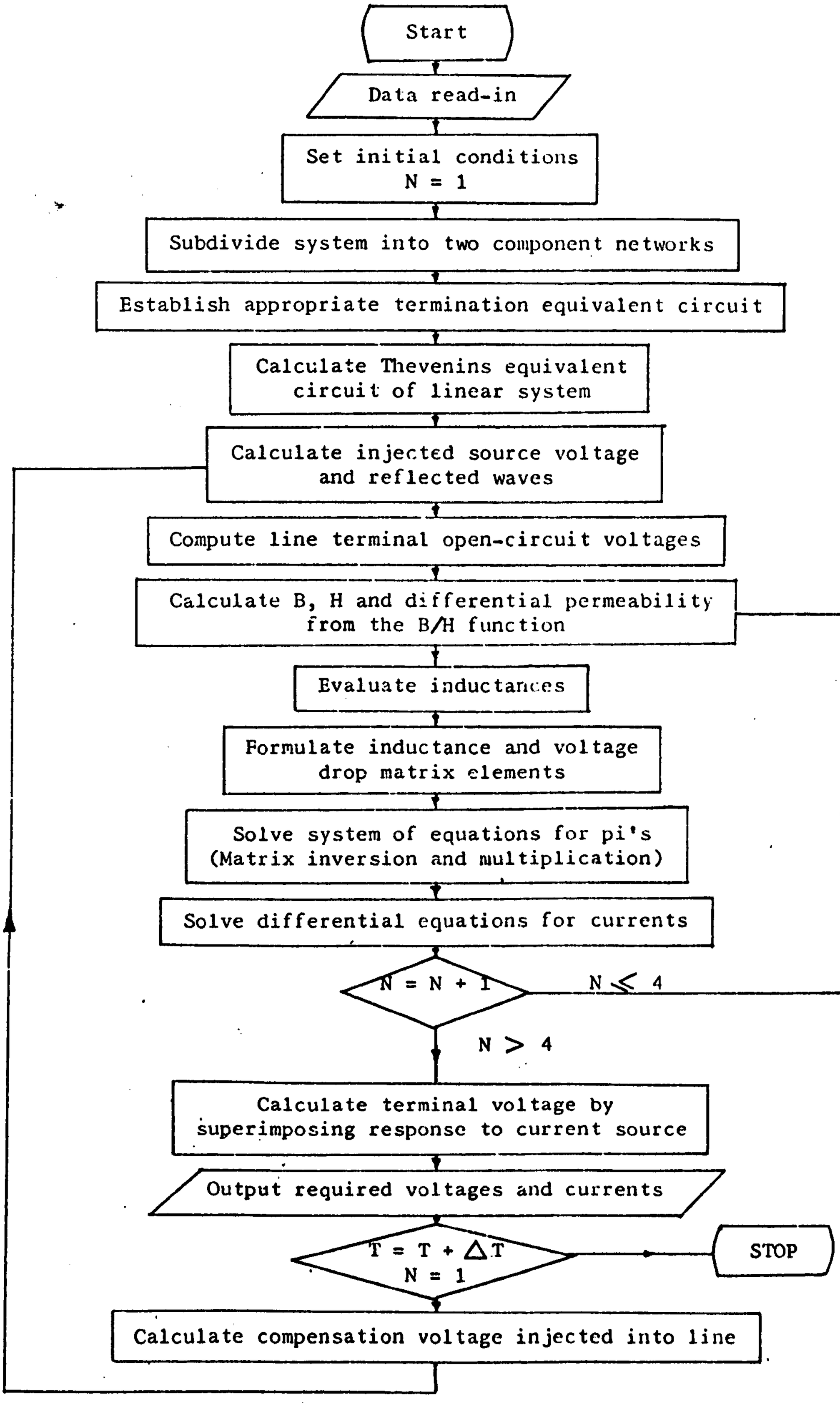

Fig. 7.4 Flow diagram for the compensation program

dependent elements of the voltage drop and inductance matrices of Table 12.1 are substituted to formulate matrices appropriate at a given time.

7.5.2 Solution of differential equations

To solve the system of differential equations represented by the matrix equation of Table 12.1, it is first necessary to solve the equations for pi's (where p = d/dt). This requires an implicit inversion of the inductance matrix. This procedure is repeated four times within each basic time interval, if the termination equivalent circuit includes non-linear elements. For matrices of a relatively large order, this process can be time-consuming. Considerable reduction in computational effort (approximately 50%) can be achieved by exploiting the symmetry of the inductance matrix. Since the inverse of a symmetrical matrix is also symmetrical, calculations need only be performed for the upper triangular matrix.

Under extreme saturation conditions, the determinant of the matrix could be numerically small in relation to some of the elements of the inductance matrix. This could create an ill-conditioned matrix extremely sensitive to round-off errors in calculations, particularly if the elements of the principal diagonal are small in comparison with the off-diagonal terms. Formulating the system of differential equations in such a manner that most inductance elements are concentrated along the leading diagonal to provide relatively large diagonal elements helps to minimise the errors which would otherwise be present. At the start of the saturation region, however, small changes in transformer voltages produce relatively large changes in currents. This tends to accentuate the ill-conditioning of the equations. In this case, errors can only be avoided by reducing the basic time interval.

Application of iterative methods of matrix inversion to the non-linear differential equations proved unsatisfactory. Several sub-routines, available as standard library programs, based on both iterative and direct methods, produced at best highly inaccurate results. A method which proved successful in dealing with problems of this nature is a form of direct method based on diakoptics [60]. The steps in the inversion of an n'th order matrix M_{ij}, where i and j denote the matrix row and column respectively, are summarised below :

(i) Select any one element on the principal diagonal as pivot and replace it by its reciprocal

$$M^{1}_{pp} = 1/M_{pp}$$

(ii) Replace the elements of each i'th row, except the one containing the pivotal element (i.e. i = 1, 2, ... n and $i \neq p$) as follows :

$$M'_{ip} = M_{ip} \cdot M'_{pp}$$

$$M'_{ij} = M_{ij} - M'_{ip} \cdot M_{pj} \quad \text{(where } j = 1, 2, \ldots n \text{ and } j \neq p\text{)}$$

(iii) Replace the elements of the p'th row (i.e. containing the pivotal element) by

$$M_{pj} = - M'_{pp} \cdot M_{pj} \quad \text{(where } j = 1, 2, \ldots n \text{ and } j \neq p\text{)}$$

(iv) Repeat the process for all diagonal terms using the matrix previously derived.

The resulting matrix is the inverse of the original matrix. Selection of the pivotal elements in descending order of magnitudes increases the accuracy of this method considerably, and minimises errors arising from multiplication by numerically large values.

It will be observed from Table 12.1 that the inductance matrix contains many zero elements. This sparsity of the matrix can be taken advantage of to economise further on computation time. Calculations are confined only to cases involving non-zero element multipliers in steps (ii) and (iii) above.

Solution of the differential equations for currents is performed using fourth-order Runge-Kutta technique described in section 4.2.2. The inter-face technique outlined in section 4.2.3 is then applied to determine the transformer voltages.

7.6 Conclusion

The basic logic used in formulating the mathematical model of three-phase transformer feeders has been described. The model incorporates the mutual effects which exist between the phases of the line and within the transformer, as well as the non-linear characteristics of the core. Transformers of various winding connections and core geometry may be simulated. In the transformer model, the equations of state representing the transformer electrical characteristics have been compounded with the equations describing the transformer magnetic circuit.

A powerful method based on the compensation theorem and capable of accurate simulations of distributed and lumped-parameter effects has been described. This method allows independent solution of sub-networks and intermittent compounding to ensure consistency of voltage and current conditions at the point of severance, using an inter-face technique at each time interval. Lattice diagram techniques are applied to the line while the transformer equations are solved by the fourth-order Runge-Kutta method. An efficient matrix inversion method based on diakoptics and suitable for ill-conditioned matrices is used. This method incorporates algorithms designed to take advantage of the inductance matrix symmetry and sparsity in order to economise on computation time.

The method described here is used in the investigations discussed in the following three Chapters. The non-linear and mutual effects in lines and in transformers are studied in Chapter 8 when a single-circuit transformer-terminated line is energised. Chapters 9 and 10 consider resonance and ferroresonance phenomena in double-circuit feeders when one of the circuits is isolated from the system. The action of opening switches to isolate the circuit is

simulated by specifying initial trapped charge voltages on the line and transformer. Calculations are then initiated by closing the circuit breaker at the source end of the still energised line. This technique saves a considerable amount of computation time, since otherwise the program would have to be run for a relatively long time until steady-state conditions obtain, before opening the switches.

This method is not, however, restricted to the subjects investigated in the following Chapters. These serve to demonstrate the potential applications of this method which could easily be extended to include several other facilities. For example, multi-valued B/H curves could be incorporated. This, however, can only be a useful addition if realistic data for the particular transformer being investigated is available. Such information is not readily available, however, and this has proved a considerable handicap even when single-valued characteristics are assumed. Although the computer program described can only deal with one transformer feeder, it can readily be extended to cope with more complex feeder networks including more than one transformer. The effects of transmission line attenuation and distortion, and frequency dependent parameters, can also be incorporated.

CHAPTER 8

NON-LINEAR PHENOMENA IN THREE PHASE TRANSFORMER FEEDER CIRCUITS

8.1 Introduction

In this chapter, the study of resonance phenomena in transformer feeders, discussed in Chapter 5 on a single phase basis, is extended to include three phase effects. The mathematical models outlined in Chapter 7 and the three phase transient analyser model of the system presented in Chapter 3 will be used to assess the effects of mutual coupling between phases of transmission lines and of transformers. The influence of transformer saturation will be investigated using the mathematical model.

During the reclosing period of the circuit breaker, coupling of the surge component on the energised phase to the un-energised phases is dictated by the electrostatic field distribution of the lines. Interphase coupling within the transformer, on the other hand, is determined by the transformer magnetising characteristics, geometry of the core and the manner of connecting the phase windings. Depending on the magnitude, frequency and phase relationship of these coupled components in relation to the system voltage on the busbar side of the circuit breaker, excessive voltage waves may be impressed on the phases when they are energised.

8.2 Transformer magnetising characteristics

8.2.1 Non-linear effects in single phase transformers

At the high frequencies encountered in this study, the unsaturated reactance of the magnetising branch is so high that its shunting effect may be neglected. This is particularly so if the reclosing period is sufficiently long to permit the residual charge trapped on the system to decay to negligible amount. This insensitivity of the transient voltages to the magnetising impedance is confirmed by the oscillograms of Fig.8.1 (i). These traces show a close correlation between waveforms arising from simulating the transformer on the T.N.A. by its electromagnetic equivalent and by its constant short circuit inductance. Saturation effects were not represented in this case. In Fig.8.1 (iv), similar comparison between waveforms computed using a linear inductance and a more detailed transformer simulation (including the magnetising impedance but disregarding saturation effects) reveals close agreement in the waveforms. The overvoltage magnitude is reduced from 5.26 to 5.12 when the mutual effects between windings are taken into account.

Fig.8.1 (ii) shows T.N.A. and computed waveforms when the saturation characteristics are neglected. In order to obtain better correlation between the waveforms, it was found necessary to incorporate the frequency dependent losses of the transformer in the digital model. These losses are represented by a series resistance estimated from the model transformer Q - value as 350 ohms. Unless otherwise stated, these losses have been included in all computed waveforms. The oscillograms show that the voltages at the transformer secondary are similar in waveform but differ only slightly in frequency. This difference will be explained later in this

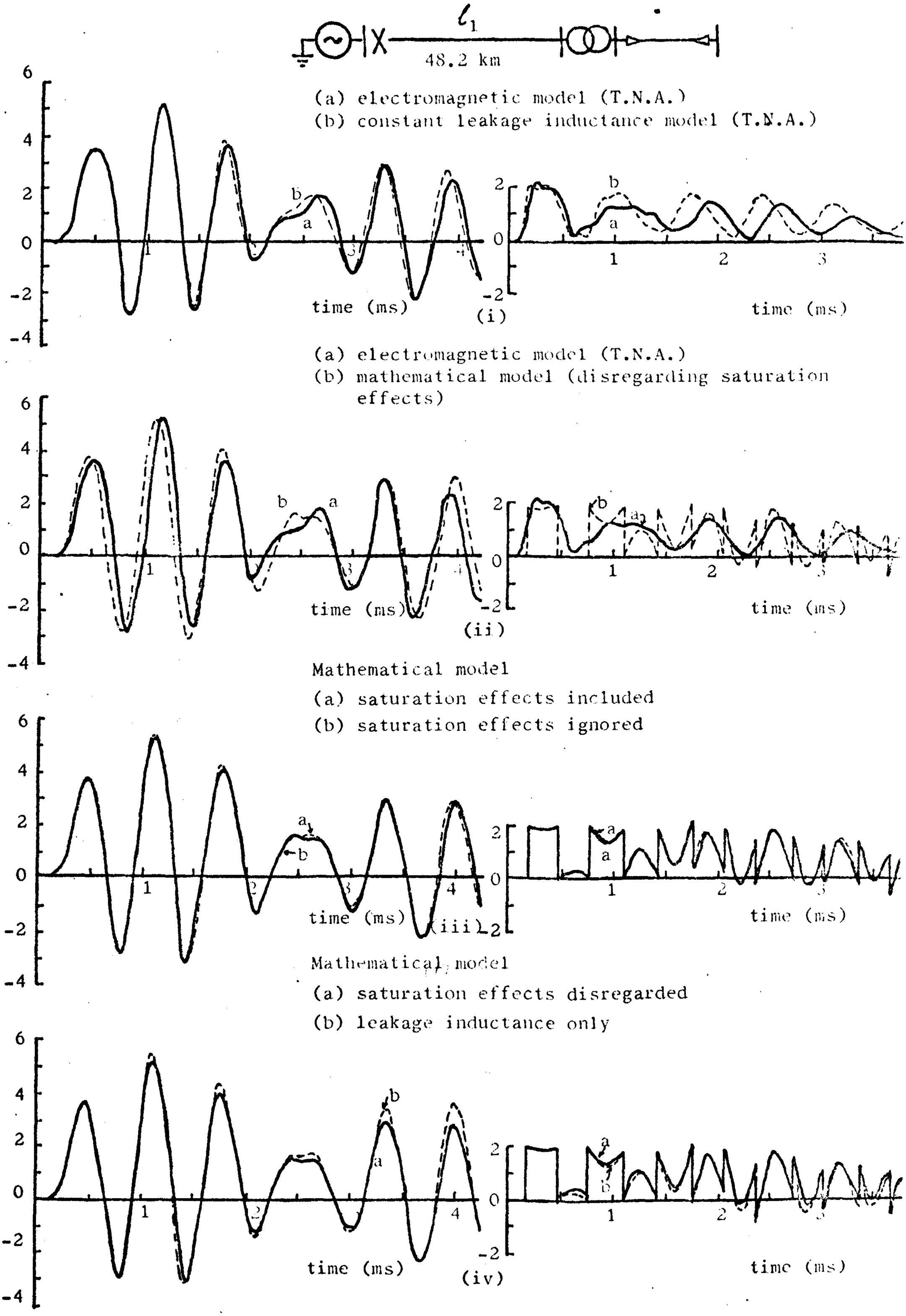

Fig.8.1 Effect of different transformer simulations

section. On the line side of the transformer, the T.N.A. waveform does not display the sharp voltage changes which are typical of the computed waveforms. On the T.N.A. these sharp voltage discontinuities are rounded and damped by the effects of internal capacitances and high frequency dissipation phenomena in both transformer windings. This difference does not, however, materially affect the voltage oscillations at the transformer secondary.

The effects of saturation could not be investigated on the T.N.A.since the model transformer was operated at reduced voltage. The voltage at the knee point of the model characteristics was far in excess of the maximum voltage at which the T.N.A. could safely be operated, taking into account the current ratings of the switches. A comparison made using the linear and non-linear representations of the transformer magnetising characteristics is presented in Fig.8.1 (iii). The insignificant effects of saturation are demonstrated by the similarities in waveforms. At the relatively high frequencies involved, the transformer does not saturate. The magnetic flux in the core does not respond to the exciting surge sufficiently fast to influence the high frequency oscillations appreciably. This, however, is based on the assumption of negligible flux in the core at the instance of energisation. It may be possible for the transformer to be already under saturation as in the case of fast reclosing operations. It has been reported, however, that the reclosing period of modern circuit breakers is sufficiently long to enable the magnetic energy in the transformer to dissipate to a negligible amount [18,20].

The effects of saturation become significant in the dynamic state following the transient. Harmonic currents are generated when the transformer core saturates and the resulting

harmonic voltages may increase the dynamic voltage magnitude due to the superposition of these harmonics on the fundamental frequency component of voltage. These voltage magnitudes may be made even more severe if a resonance condition exists between the transformer saturated inductance and the line capacitance. These effects have been considered in more detail in Chapter 2.

8.2.2 Validity of single phase results

Fig.8.2 (i) and (ii) shows oscillograms of the voltages at the transformer using single phase and three phase representations of the system on the T.N.A. In the three-phase case the three poles of the circuit breaker close simultaneously and the waveform shown is that of the R-phase closing at peak system voltage. The transformer consists of a bank of three single phase units connected in star-star with the neutrals solidly earthed. The difference in the waveforms is marginal. This confirms that the single phase treatment of the resonance phenomenon gives results which are valid in a three phase system in which the transmission line is transposed and the three phases are energised simultaneously. This is to be expected because in such a case of earthed transformer neutrals, each phase is independant of the others.

8.2.3 Non-linear effects in three phase transformers

In Fig.8.2 (iii) and (iv) the oscillograms relating to the electromagnetic model (curves a) are compared with those obtained when the transformer is simulated with a constant short-circuit inductance (curve b). The similarity of the waveform on the transformer secondary is evident. The slight deviation in the magnitude and frequency of the primary voltage waveforms may be due

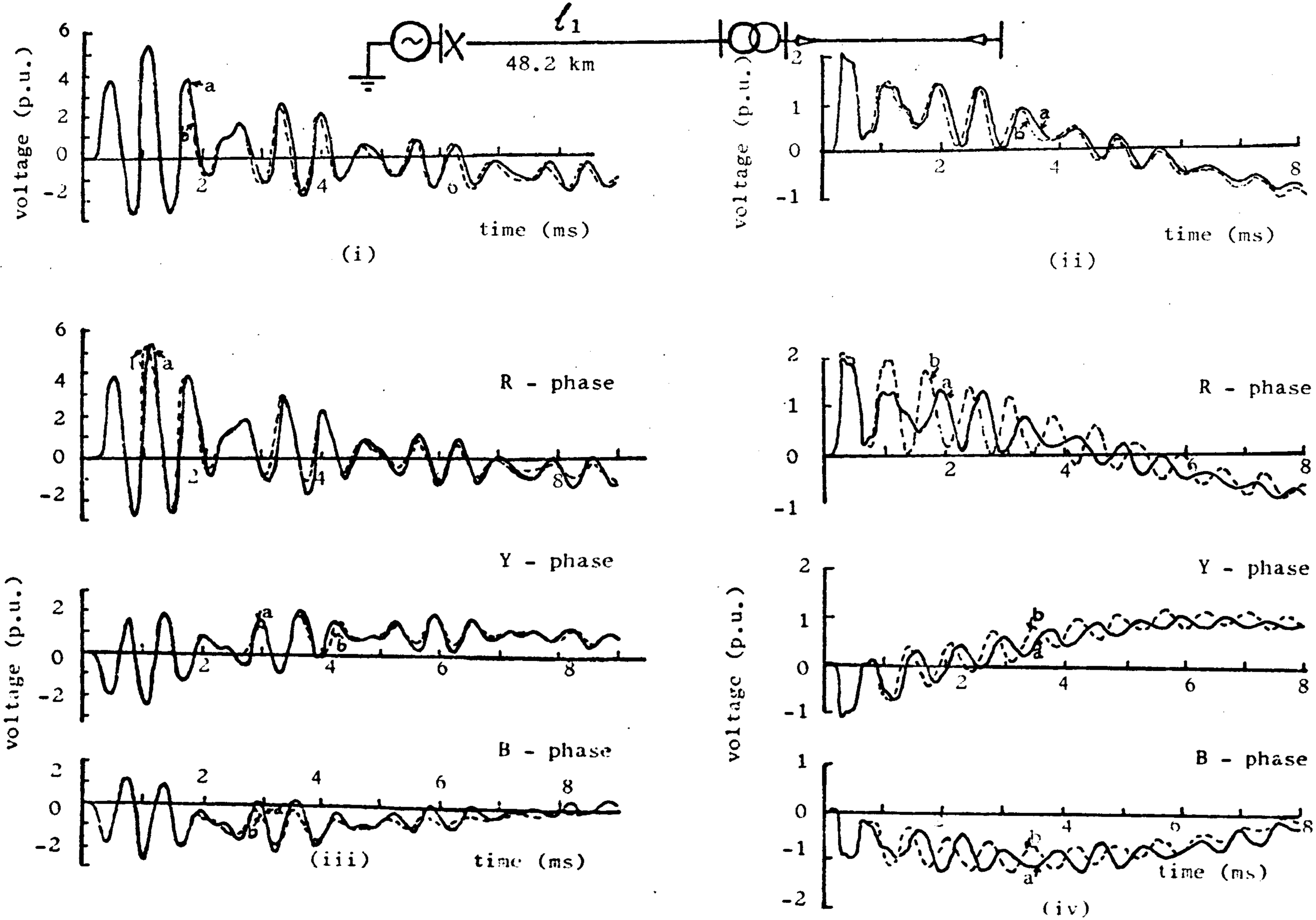

Fig.8.2 Comparison of T.N.A. waveforms at the transformer primary (i and iii) and secondary (ii and iv)
(i) (ii) (a) single phase electromagnetic model (b) three phase electromagnetic model
(iii) (iv) (a) electromagnetic model (b) constant short circuit inductance model

to differences in series resistances and leakage conductances to earth which may be present in the individual transformer models. The Q - values of the inductors used to simulate the transformer are high, typically 50 at 1kHz for a 20 mH coil, compared with 9 for the electromagnetic model. The higher losses associated with the electromagnetic model account for the increase in attenuation, distortion and decrease in oscillation frequency of the primary waveforms as demonstrated on Fig.8.2 (iv).

By using the three phase program incorporating a more detailed simulation of the transformer, the effect of the non-linearity in the transformer magnetising impedance is illustrated in Fig.8.3. Simultaneous closure is assumed. As in the single phase treatment discussed in section 8.2.1, it is evident that the influence of saturation is too small to change the character of the oscillations appreciably over the relatively short period of observation. The complications introduced by taking into account the effects of variable permeability cores of transformers are therefore not justified in this analysis.

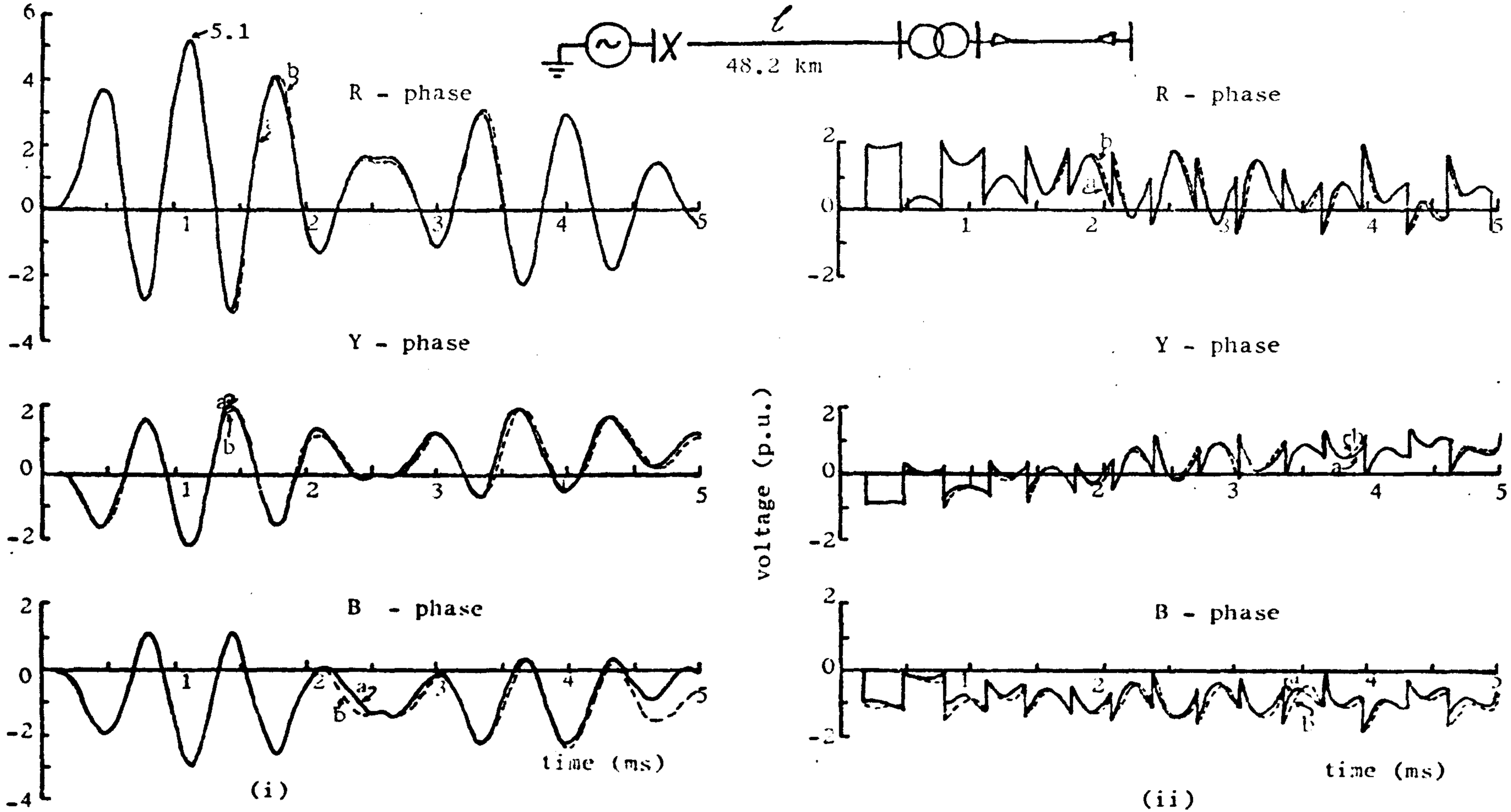

Fig.8.3 The effects of transformer saturation (using mathematical model)

(a) saturation effects simulated
(b) saturation effects disregarded

8.3 Transformer winding connections

Fig.8.4 shows oscillogram traces of the transformer secondary voltages for different transformer phase connections, assuming that the system is completely de-energised prior to switching. In all these cases, the transformer leakage reactance, the turns ratio and the capacitive reactances of the cables as seen from the primary side were maintained constant. The transformer models used in this T.N.A. study are banks of three single phase electromagnetic units, details of which are given in section 5.2.

Comparison of the waveforms of Fig.8.4 (i) and (ii) indicates the minimal effect of earthing the transformer neutral on the peak voltage magnitudes of phase R. There is, however, a slight difference in the phase distribution of the oscillations. In particular, the amplitudes of oscillations on phases Y and B when at least one neutral is isolated, are not the same as in the case when both transformer neutrals are solidly earthed. This dissymmetry of waveforms is mainly due to the neutral instability inherent in such an isolated neutral connection involving three single phase units. Any unbalance that may exist in the secondary circuits and the inequalities of the excitation characteristics of the individual units composing the transformer enhances the instability of the neutral. The fact that the capacitive and inductive reactances of the three phases are not balanced is indicated by the difference in the beat frequencies of the phase oscillations as observed in Fig.8.4 (ii).

If the transformer is now connected in star/delta, while maintaining the same turns ratio, leakage inductance and cable capacitance referred to the primary, the voltage oscillations on the

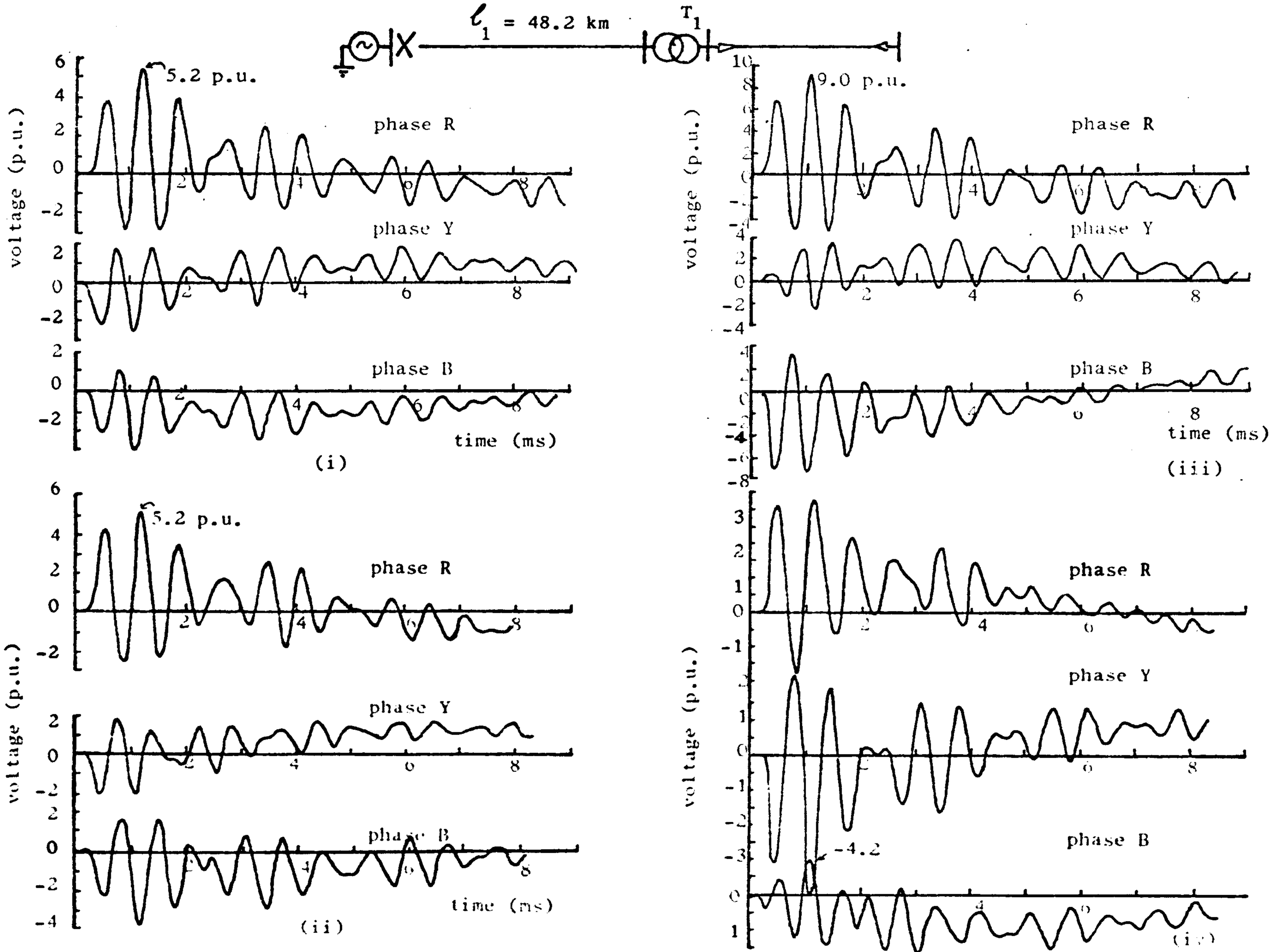

Fig.8.4 The effect of transformer phase connection (i) star/star with both neutrals earthed, time (ms) (ii) star/star with either or both neutrals isolated (iii) star/delta (iv) delta/star

secondary are as shown on Fig.8.4 (iii). In this case, the peak amplitude of the oscillations on the R phase is 9.0 p.u. of normal phase to earth voltage. In absolute terms the magnitude is identical to that recorded when the transformer is connected star/star. In the case of the star/delta transformer, the base voltage on the secondary is reduced by a factor of $\sqrt{3}$.

A delta/star connection (Fig.8.4 iv) on the other hand, gives a peak amplitude of -4.2 p.u. For this case the base voltage is $\sqrt{3}$ times that of a star/star connected transformer.

When a delta winding is present, the waveforms were found to be independent of whether the neutral of the star connected winding was earthed or not.

8.4 Sequential pole closure

Previous analysis of the resonant overvoltages was based on either single phase representation of the system or simultaneous closure of the circuit breaker poles in three-phase simulation. This form of representation precludes the mutual effects which exist between the phases of a transmission line and within the transformer. In practice, when the switch is closed, the three poles of the circuit breaker do not energise the phase conductors at the same instant. Even if the contacts are driven by the same mechanism, pre-arcing of the gap between poles occurs frequently at or near peak system voltage. This means that one phase is likely to close before the other two phases. This is particularly the case when a rotating-arm type air-blast circuit breaker is used. The incidence of sparkover is, however, minimised if pressurised-head type air-blast circuit breaker is employed. In this study, it will be assumed that the time displacement between the closing of the three poles is within 5 ms. This pole span is sufficiently adequate for modern pressurised-head breakers, but it may be exceeded when rotating-arm breakers are used.

When an unterminated transmission line is energised sequentially, the resulting transient overvoltage at the receiving end may be higher than that obtained in the case of simultaneous closure [9,20]. This overvoltage is influenced by the instant of closure of the second and third phases, the impedance of the line, and the type of source from which the line is being energised. The mechanism of voltage surge transfer is mainly electrostatic, and it is predominantly due to line parameters.

When a transformer is present at the end of the line, the oscillations on the secondary side may be magnified due to the

increased magnitude of the exciting voltage waves [18,23,24,25].

In addition to the electrostatic coupling, field tests have shown that mutual coupling within the transformer may contribute to the increase in the magnitude of the line oscillations on the second and third phases to close. If the source-side voltage of the unenergised phase is of opposite polarity to the induced voltage at the instant of closure it is possible to initiate a voltage surge in excess of peak system voltage.

8.4.1 Electromagnetic and electrostatic coupling

The magnetic coupling within the transformer is influenced predominantly by the zero sequence impedance of the transformer. This is dependent on the manner in which the transformer windings are connected and the method of construction of the core. In this study, however, mainly solidly earthed star-star connected transformers were investigated. The absence of a delta-connected winding in the analogue model used and the fact that the core is not of a composite design implies minimal coupling within the transformer. Although the mathematical model used in the analogue study has a composite core structure, the degree of electromagnetic coupling between the phases of the transformer is minimised by the omission of the delta tertiary winding.

Electrostatic coupling from one phase conductor to the other is dictated by the values of the mutual surge impedances existing between the phases relative to the self surge impedance of the line conductors. These mutual impedances are derived from the line conductor configuration and spacing. Translated in terms of symmetrical components, it may be shown that for a symmetrical transmission line, the capacitance between phase conductors is given

by $(C_1 - C_0)/3$, ignoring the effects of inductive leakage. The capacitance of each conductor to earth is given by C_0 where C_0 is the zero sequence line capacitance. C_1 is the positive sequence capacitance. The coupled voltage surge, $V_C(t)$, to the floating phase conductor due to the wave on the closed phase, $V_E(t)$, is therefore given by:

$$V_C(t) = \frac{C_1 - C_0}{C_1 + 2C_0} V_E(t)$$

For a typical high voltage line, the amplitude of a coupled surge lies within the range 10 to 30% of the surge on the closed phase.

In this study, it will be assumed that the first phase (R) is closed at the peak of system voltage, and that no precharge exists on the line prior to it being energised. The reference angle in each phase is the angle when the system voltage on phase R is a positive peak. The T.N.A. line model used is premised on transposed line parameters.

8.4.2 Saturation effects

It was shown in section 8.2 that for zero pole span, the voltage waveforms at the transformer are not sensitive to the transformer saturation characteristics over the period considered. Saturation effects do, however, become more pronounced with time and will affect particularly those oscillations arising from closure of the second and third phases if the pole span is sufficiently long.

The results contained in this section are based on a three-limb star-star connected transformer with both neutrals solidly earthed. The computed waveforms of Fig.8.5 relate to the case when

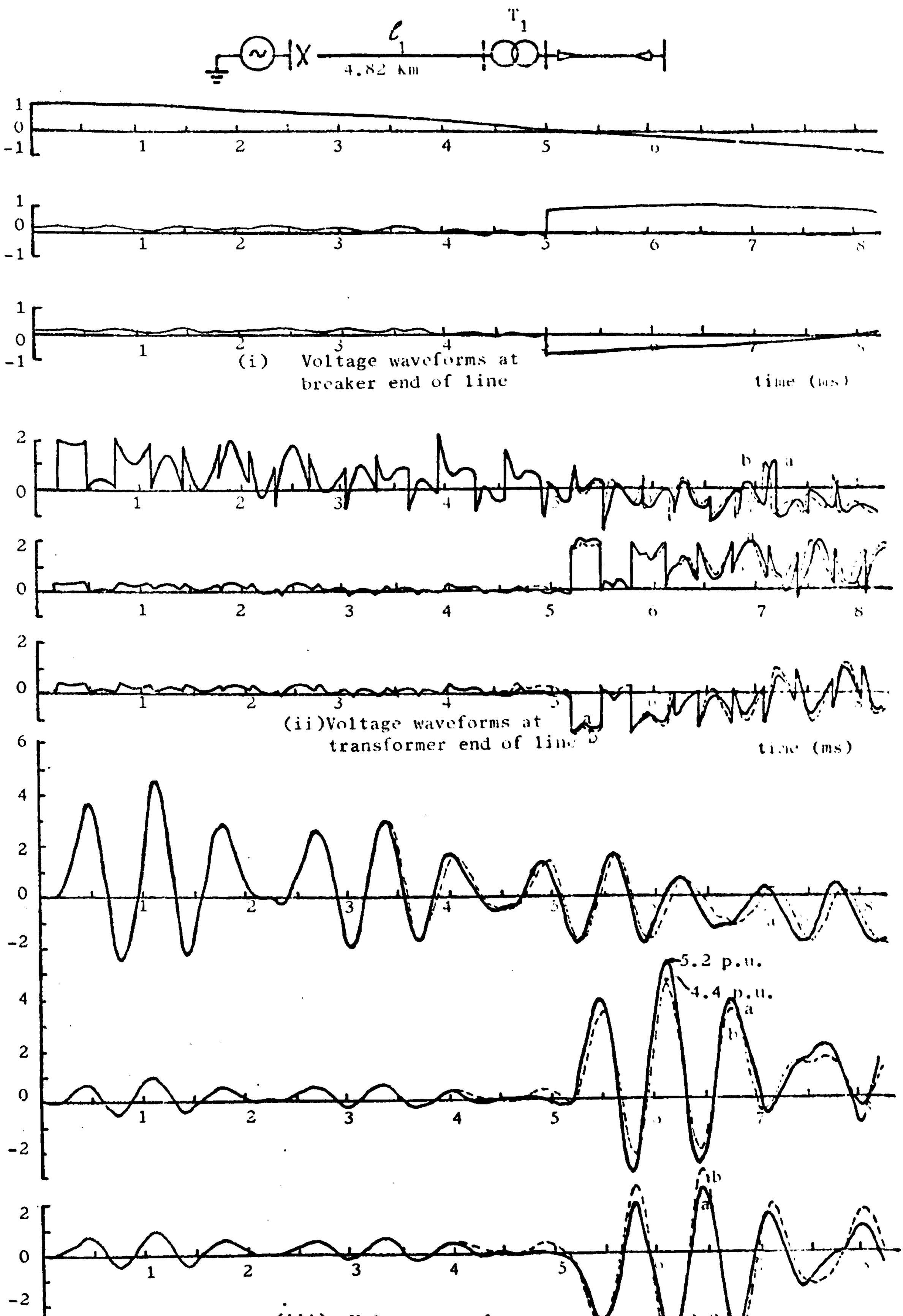

Fig.8.5 Computed waveforms for sequential closure (R = 0°, Y = 90°, B = 90°)

the Y and B phases are closed 90 electrical degrees (5 ms) after closure of phase R (curve i) and show the effects of transformer non-linearity. It may be seen from the oscillations at the transformer (curves ii and iii) that if the saturation characteristics are incorporated in the mathematical model, these begin to have some influence on the waveforms from about 4 ms after closure of the first pole. In particular, differences will be observed on the secondary voltage oscillations on phases Y and B beyond this time. The over-voltage on phase Y is increased from 4.4 to 5.2 p.u. while that on phase B is reduced from -4.3 to -3.8 p.u. when saturation effects are taken into account. The maximum voltage on phase R (4.8 p.u.) remains the same since this occurs much earlier in time before the effects of saturation begin to assert themselves.

The occurrence of the maximum overvoltage on phase Y is accounted for by the large initial voltage step impressed on its phase conductor when energised (curve i). At this instant, the voltage induced on phase Y by the surge on R is of opposite polarity to the breaker source side voltage. Consequently, the surge sent down the line has a magnitude which in this case exceeds the initial voltage step on the first phase energised. The surge amplitude on phase B is smaller since the voltage across its breaker contacts is lower at the moment this phase is closed.

A detailed computation of the overvoltages arising from varying the instants of closure of the three poles over the complete span of say 5 m_S in steps minute enough to take into account all the possible closing angles is very uneconomical in terms of computation time. However, results of a limited number of computations are presented in Table 8.1. The system studied consists of a 5.5km

TABLE 8.1 Maximized phase-to-earth overvoltages, at the transformer secondary as a function of phases Y and B delay angles relative to phase A closure (computed)

Phase B Delay Angle (Deg.) \ Phase Y Delay Angle (Deg.)	0			12			24			36		
Phase	R	Y	B	R	Y	B	R	Y	B	R	Y	B
0	4.42	-2.24	-2.22	4.27	-1.57	-2.32	4.27	0.46	-2.32	4.27	0.47	-2.32
12	4.37	-2.41	-2.98	4.10	-1.86	-3.18	4.10	0.97	-3.25	4.10	1.00	-3.27
24	4.37	-2.41	-3.75	4.10	-2.00	-3.18	4.10	0.98	-3.58	4.10	0.97	-3.63
36	4.37	-2.41	-4.18	4.10	-2.00	-3.38	4.10	0.98	-6.03	4.10	0.98	-4.22

transmission line terminating in a transformer with a leakage reactance of 0.0778H and an equivalent transformer secondary capacitance of 0.00175 μF. The transformer model used is similar to that used in the ferro-resonance analysis presented in Chapter 10, and it includes saturation effects.

Phase R closes first at peak system voltage and closure of the poles of the other two phases is varied in steps of 12 degrees (666 μS) up to 36 degrees. Owing to the rather large closing angle variations, it is possible that larger overvoltages may occur within the intervals selected. The Table shows that when phases Y and B close 24 and 36 degrees, respectively, after energisation of phase R, an overvoltage of -6.03 p.u. is obtained. This value exceeds the zero pole span overvoltage (4.42 p.u.) by 37%.

8.4.3 T.N.A. study of sequential closure

Economic considerations favour analogue methods for studying the effects of non-simultaneous closure as compared with the digital computer method. On the T.N.A., at least one closing angle can be varied continuously making it easier to detect the maximum possible overvoltage between the fixed intervals selected.

Fig.8.6 shows oscillogram traces of the waveform at the source side (curve i) and transformer side (curve ii) of the line, and the oscillations at the transformer secondary (curve iii) when the Y and B phases close 90 degrees after phase R energisation. An overvoltage of 5.5 p.u. on phase Y at the transformer secondary is obtained. This maximum voltage can be related to the voltage existing across the breaker contacts of this phase at the moment it closes, Curve (ii) shows an abrupt voltage jump on the Y phase with a

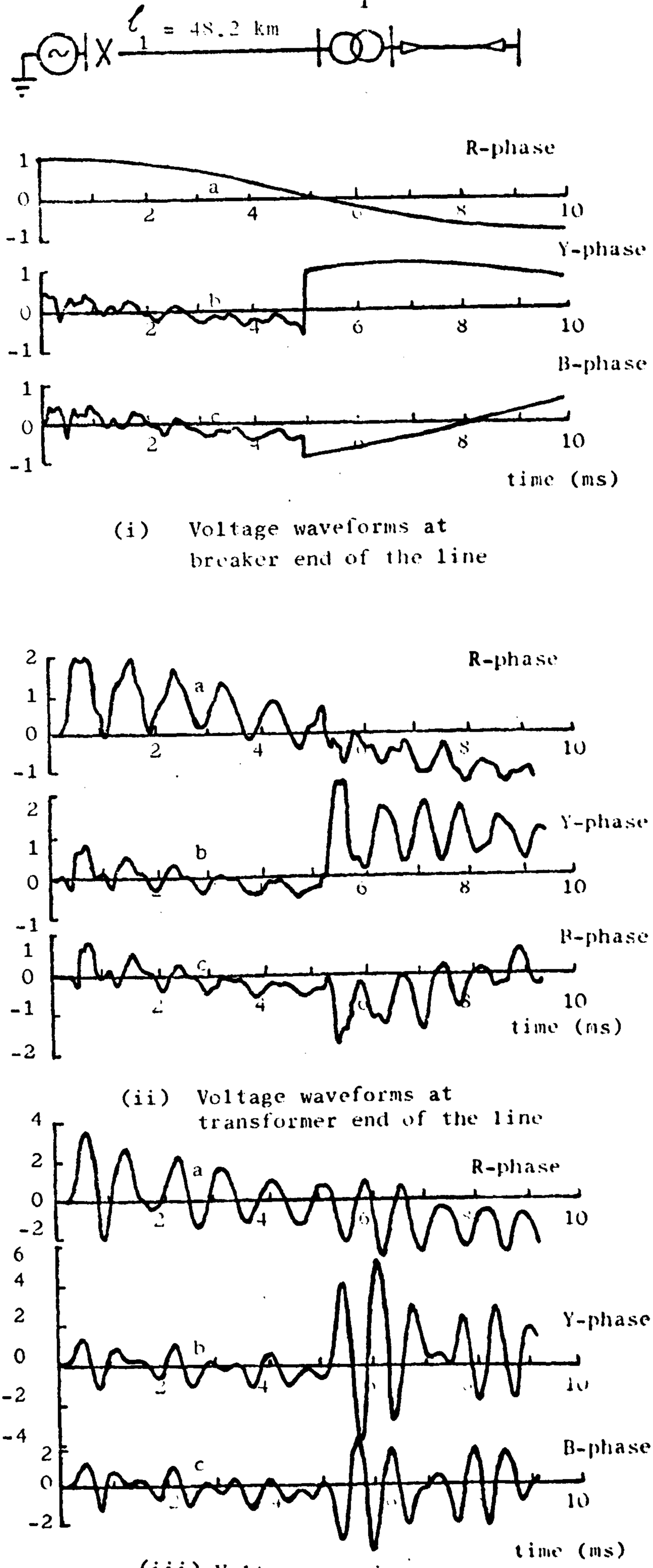

(i) Voltage waveforms at breaker end of the line

(ii) Voltage waveforms at transformer end of the line

(iii) Voltage waveforms at the transformer secondary

Fig.8.6 T.N.A. waveforms for sequential closure (R = 0^0 Y - 90^0, B = 90^0)

magnitude exceeding the initial step voltage launched on phase R. The voltage on the unenergised phases consists of electrostatic and electromagnetic components of induced voltage referred to in section 8.4.1. In this case, superposition of these components is such that a significant negative voltage exists on the Y phase immediately prior to it being closed while the system voltage is close to a positive maximum.

Examination of curve ii of Fig.8.6 will show that the voltage initially coupled to the unenergised phases is of opposite polarity to the surge on the closed phase. This short negative voltage swing may be explained in terms of differences in the propagation velocities of the line-to-line and the line-to-neutral voltage components of the surge. The initial coupled voltage steps at the sending end of the floating conductors are reflected initially as negative steps due to the delay in arrival of the earth mode.

Further voltage oscillogram traces are shown on Fig.8.7 for different closing instants of the second and third phases to close. The waveforms of curve (i) show an overvoltage of -5.4 p.u. when the Y and B phases are closed 10 and 20 degrees respectively after closure of phase R. It results from the large voltage existing across the poles of the B-phase breaker when this phase is switched. The point-on-wave settings resulting in the waveforms of curve (ii) (phases R,Y,B closed at 0,10 and 60 degrees respectively) yield the most severe recorded overvoltage on the transformer secondary (6.0 p.u.) Phase B is closed when its system voltage is a negative peak and the breaker line side terminal is precharged to a positive peak. The waveforms for zero pole span are shown on curve (iii) for comparison.

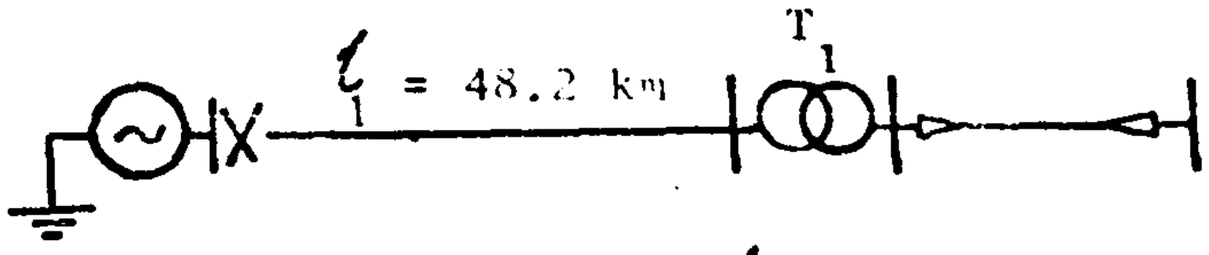

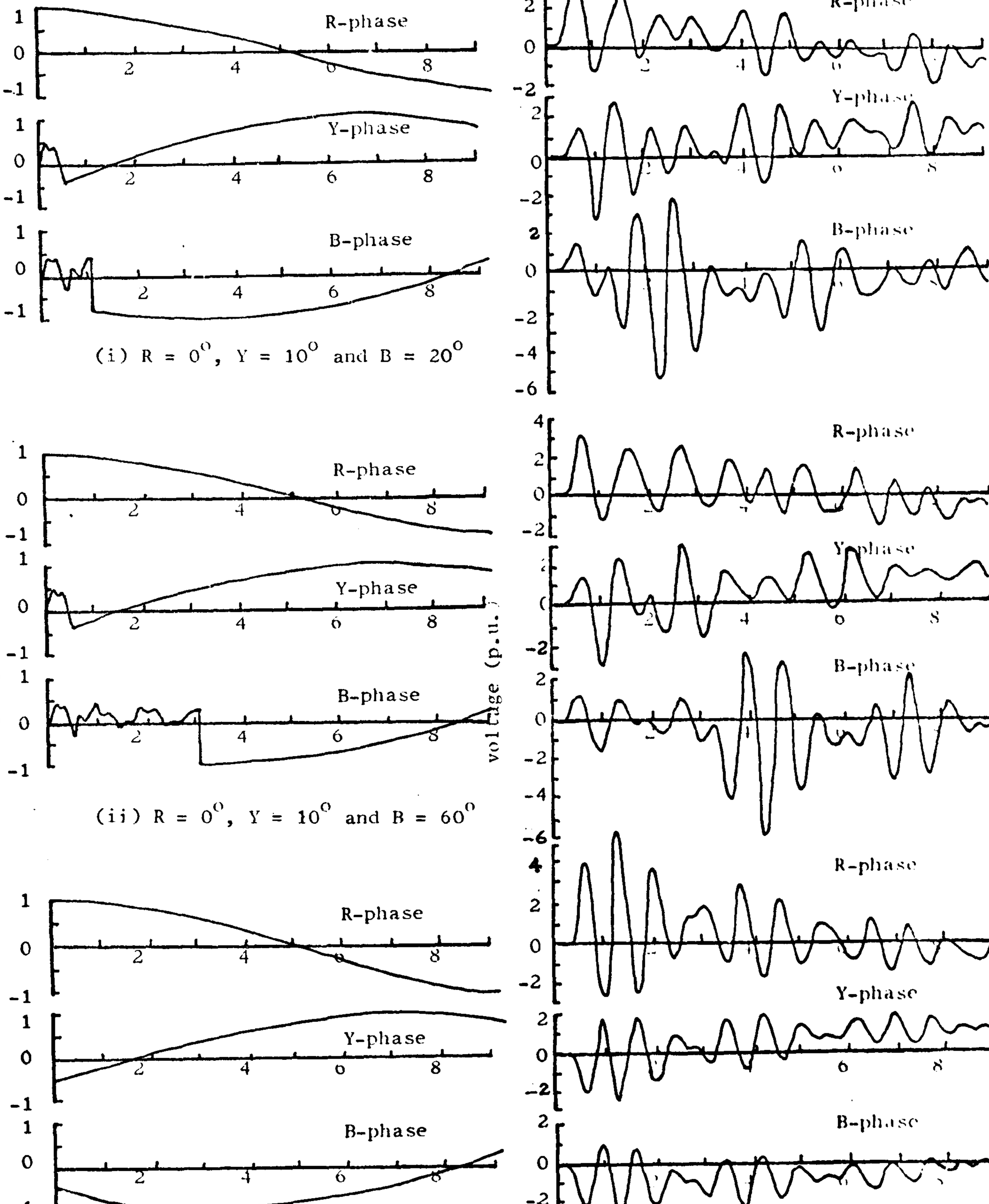

(i) R = 0^{o}, Y = 10^{o} and B = 20^{o}

(ii) R = 0^{o}, Y = 10^{o} and B = 60^{o}

(iii) simultaneous closure

Fig.8.7 T.N.A. waveforms at the transformer for sequential closure at the different settings

In order to identify the point-on-wave settings likely to produce excessive overvoltages, within a total time span of 5 ms, a topological search covering the entire spectrum of variation was made. This involved 1083 voltage peak measurements on the T.N.A. Phase R is the first to close at peak system voltage and its closing angle is maintained constant throughout this investigation. The Y - phase closing angle is varied in fixed steps of 5 degrees up to a quarter cycle of the system voltage. Within each 5 degrees interval of the B - phase switching angle, its point-on-cycle setting was adjusted to maximise the overvoltage for each phase. The transformer secondary overvoltages produced by such controlled pole switching of the Y and B phases are tabulated in Table 8.2. The phase on which the maximum overvoltage occurs for each setting is also given. The entries enclosed in heavy lines indicate maximum voltages which exceed the overvoltage at zero pole span.

It may be seen from Table 8.2 that peak voltages associated with simultaneous sparkover of two poles of the breaker (R and Y or R and B) almost always occur on phase R, and are very little influenced by the point-on-wave at which the third pole closes. Examination of the Table will show that certain conditions tend to favour the occurrence of overvoltages which exceed the overvoltage at zero pole span. These are:

(a) Phase Y closes such that the voltage across its breaker contacts is relatively small at the time it closes, as is the case 10 to 15 degrees after phase R closure (see Fig. 8.7). The dominant surge on this phase will therefore be that coupled from phase R. Since the surges on the two closed

Y-Phase delay / B-phase delay angle (°)	0	5	10	15	20	25	30	35	40	45	50	55	60	65	70	75	80	85	90
0 - 5	5.2 R	4.6 R	-4.6 B	4.6 R	4.5 R	4.4 R	4.4 R	4.4 R	4.4 R	4.4 R	4.4 R	4.4 R	4.3 R	4.4 R	4.3 R	4.2 R	4.3 R	4.3 R	4.3 R
5 - 10	-4.5 Y	4.5 R	3.8 R	4.3 R	-3.9 B	4.1 R	-3.9 B	-3.9 B	-3.9 B	-3.8 B	-3.8 B	-3.8 B	-3.7 B	-3.7 B	+4.1 Y	4.0 Y	-3.9 B	-3.7 B	5.0 Y
10 - 15	4.5 R	3.8 R	-4.1 B	-3.8 B	-3.8 B	-4.0 B	-3.9 B	-3.9 B	-3.8 B	-3.8 B	-3.8 B	-3.8 B	-3.7 B	-3.6 B	-3.6 B	4.2 Y	3.9 Y	+3.7 B	5.0 Y
15 - 20	4.5 R	-4.8 B	-5.3 B	-5.3 B	-4.4 B	-5.0 B	-4.9 B	-4.9 B	-4.9 B	-4.8 B	-4.8 B	-4.8 B	-4.7 B	-4.7 B	-4.7 B	-4.6 B	-4.7 B	-4.7 B	-4.7 B
20 - 25	4.3 R	4.5 R	-5.4 B	-5.3 B	-4.5 B	-5.0 B	-4.9 B	-4.8 B	-4.6 B	-4.7 B	-4.6 B	-4.7 B	-4.6 B	-4.3 B	-4.6 B	-4.5 B	-4.4 B	-4.5 B	-4.6 B
25 - 30	4.3 R	4.3 R	-4.3 B	-3.8 B	4.6 Y	3.6 R	3.8 R	4.0 R	4.0 R	4.0 R	4.1 R	4.1 R	4.0 R	4.0 R	4.5 Y	4.0 R	4.0 R	4.0 R	4.9 Y
30 - 35	4.3 R	4.3 R	-4.2 B	-4.3 B	4.1 R	-4.8 B	-4.6 B	-4.3 B	-4.1 B	-4.0 B	-4.5 B	-4.5 B	-3.8 B	-4.1 B	4.3 Y	4.3 Y	-4.4 B	-4.1 B	4.7 Y
35 - 40	4.3 R	-4.4 B	-4.9 B	-4.3 B	-4.2 B	-5.0 B	-5.0 B	-4.8 B	-4.6 B	-4.3 B	-4.6 B	-4.8 B	-4.4 B	-4.4 B	-4.3 B	-4.4 B	-4.5 B	-4.4 B	-4.4 B
40 - 45	4.3 R	-4.4 B	-5.0 B	-4.7 B	-3.9 B	-4.1 B	-4.6 B	-4.6 B	-4.4 B	-4.0 B	-3.6 B	-3.9 B	3.9 B	-4.0 B	-3.5 B	-4.0 B	-3.6 B	-3.8 B	-4.0 B
45 - 50	4.3 R	4.3 R	-4.5 B	-4.6 B	-3.9 B	-4.2 B	-4.3 B	-4.0 B	-3.9 B	-3.9 B	-4.0 B	-3.7 B	-3.9 B	-3.6 B	4.9 Y	3.7 Y	3.7 Y	-3.6 B	4.7 Y
50 - 55	4.3 R	4.3 R	-3.9 B	-3.6 B	-3.7 B	-3.8 B	-3.8 B	-3.7 B	-3.6 B	-3.6 B	-3.7 B	-3.6 B	-3.5 B	-3.6 B	4.9 Y	-4.1 B	4.0 Y	3.7 Y	4.6 Y
55 - 60	4.3 R	-4.9 B	-5.3 B	-4.8 B	-4.7 B	-5.0 B	-5.0 B	-4.6 B	-4.5 B	-4.6 B	-4.6 B	-4.7 B	-4.9 B	-4.0 B	-4.0 B	-4.5 B	-4.0 B	-4.0 B	4.4 Y
60 - 65	-4.4 B	-5.0 B	-6.0 B	-5.1 B	-4.7 B	-5.0 B	-5.0 B	-4.8 B	-4.6 B	-4.6 B	-4.6 B	-4.6 B	-4.7 B	-4.3 B	-3.8 Y	-4.3 B	-4.4 B	-3.9 B	-4.0 B
65 - 70	4.3 R	4.3 R	-4.8 B	-4.4 B	-3.5 B	-3.9 B	-4.1 B	-4.1 B	-4.0 B	-3.6 B	-3.3 B	-3.7 B	-3.5 B	-3.7 B	4.7 Y	3.8 R	[illegible] Y	4.2 Y	4.9 Y
70 - 75	4.3 R	4.3 R	-3.7 B	-3.7 B	3.5 R	-3.8 B	-3.8 B	-3.7 B	-3.6 B	-3.8 B	-3.8 B	-3.9 B	-3.8 B	-3.9 B	4.8 Y	-4.7 B	+3.8 Y	4.2 Y	4.9 Y
75 - 80	4.3 R	4.3 R	-4.0 B	-3.7 B	-3.8 B	-4.1 B	-4.2 B	-4.0 B	-3.9 B	-4.1 B	-3.8 B	-4.1 B	-4.2 B	-3.9 B	4.1 Y	-4.7 B	-4.9 B	4.0 Y	4.4 Y
80 - 85	4.3 R	-4.4 B	-4.4 B	-4.3 B	-3.9 B	-4.1 B	-4.3 B	-4.0 B	-4.0 B	-4.1 B	-3.7 B	-4.1 B	-4.2 B	-4.2 B	-3.8 B	-3.8 B	-4.3 B	+4.4 Y	4.2 Y
85 - 90	4.3 R	4.3 R	-4.5 B	-4.4 B	-3.9 B	-3.9 B	-3.7 B	-3.9 B	-3.7 B	-3.7 B	-3.5 B	-3.4 B	-3.6 B	-40. B	4.1 Y	-3.6 B	4-4 Y	4.5 Y	5.5 Y
90 - 95	4.3 R	4.3 R	-3.4 B	-3.3 R	-3.5 B	-3.5 B	-3.5 B	3.3 R	3.3 R	3.3 R	3.3 R	-3.4 B	3.2 R	3.2 R	3.6 Y	-3.8 B	-3.8 B	3.5 Y	5.5 Y

TABLE 8.2 : Maximized phase-to-earth overvoltages at the transformer secondary as a function of phases Y and B delay angles relative to phase A closure (T.N.A.)

phases will have the same polarity, they will induce voltage components which tend to reinforce each other on the still open phase B. Consequently, significant positive voltage oscillations will be generated on phase B as indicated on Fig.8.7. If the B phase closes onto a positive peak of these oscillations (e.g. between the ranges 15-25, 35-45 and 55-75 degrees), large overvoltages are produced at the transformer secondary. This is particularly the case when the system voltage at the time of closure is near a negative peak (e.g. 60 degrees after phase R closure).

(b) The second and third phases close at or near 90 degrees after phase R closure. The waveform of Fig.8.6 (i) shows that such a closing sequence is likely to generate a large voltage step on phase Y when its system voltage is approaching a positive peak. Another contributory factor to this large step is the electromagnetic transference of surges between phases in the transformer which, in this case, tend to cause a sag in voltage oscillations on phase Y.

8.4.4. Open phase conductors

It is sometimes possible for one or two poles of the breaker to remain in the open position for a period exceeding half a cycle at system frequency. Such a condition may result from one or two poles of the breaker being mechanically stuck in the open position, even when pressurised-head breakers are used.

Fig.8.8 (i) (ii) and (iii) shows the voltage waveforms at the transformer on the first phase to close (R) for single-pole, 2-pole and 3-pole operation respectively. The overvoltages at the transformer secondary are lower when at least one pole remains in the open position, than those relating to simultaneous closure. Over-voltages of 3.2, 4.3 and 5.2 p.u. were recorded during 1-pole, 2-pole and 3-pole operation respectively. These differences in oscillation magnitudes may be explained in terms of energy considerations. The energy required to establish a precharge in the floating conductors and sustain the transformer secondary oscillations on the unenergised phases is drawn from the phase or phases already closed. When only one phase is closed, energy drains to the two open phases, whereas in 2-pole operation only one phase is supplied with energy. Hence the transformer oscillation magnitudes will be lower in the former case.

8.4.4 Inter-phase overvoltages

Although this investigation is essentially a study of phase-earth overvoltages, a limited number of results pertaining to voltages occurring between phases when a condition of resonance exists are included for the sake of completeness.

In this study, it is assumed that the system parameters are such that a condition of resonant excitation of the transformer exists. The influence of pole scatter, within the postulated maximum pole span of 5 ms, in modifying the overvoltages between phases at the transformer is determined. The first phase to close (R) does so at maximum system voltage. The inter-phase voltage magnitudes are expressed in per unit of the steady-state peak phase-to-earth voltage.

Fig.8.9 (i and ii) shows inter-phase voltage waveforms at the transformer when the three poles close simultaneously. The

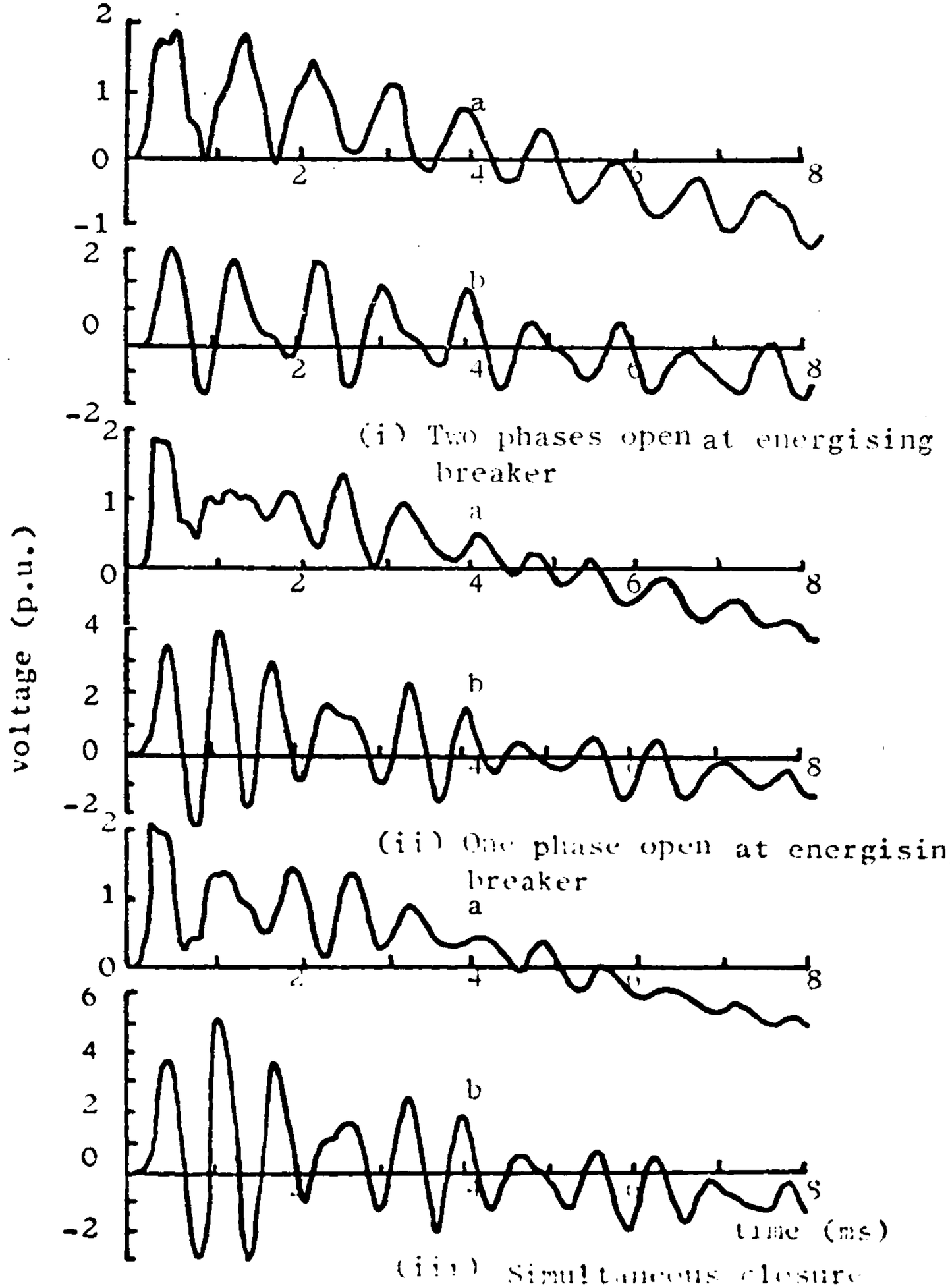

(i) Two phases open at energising breaker

(ii) One phase open at energising breaker

(iii) Simultaneous closure

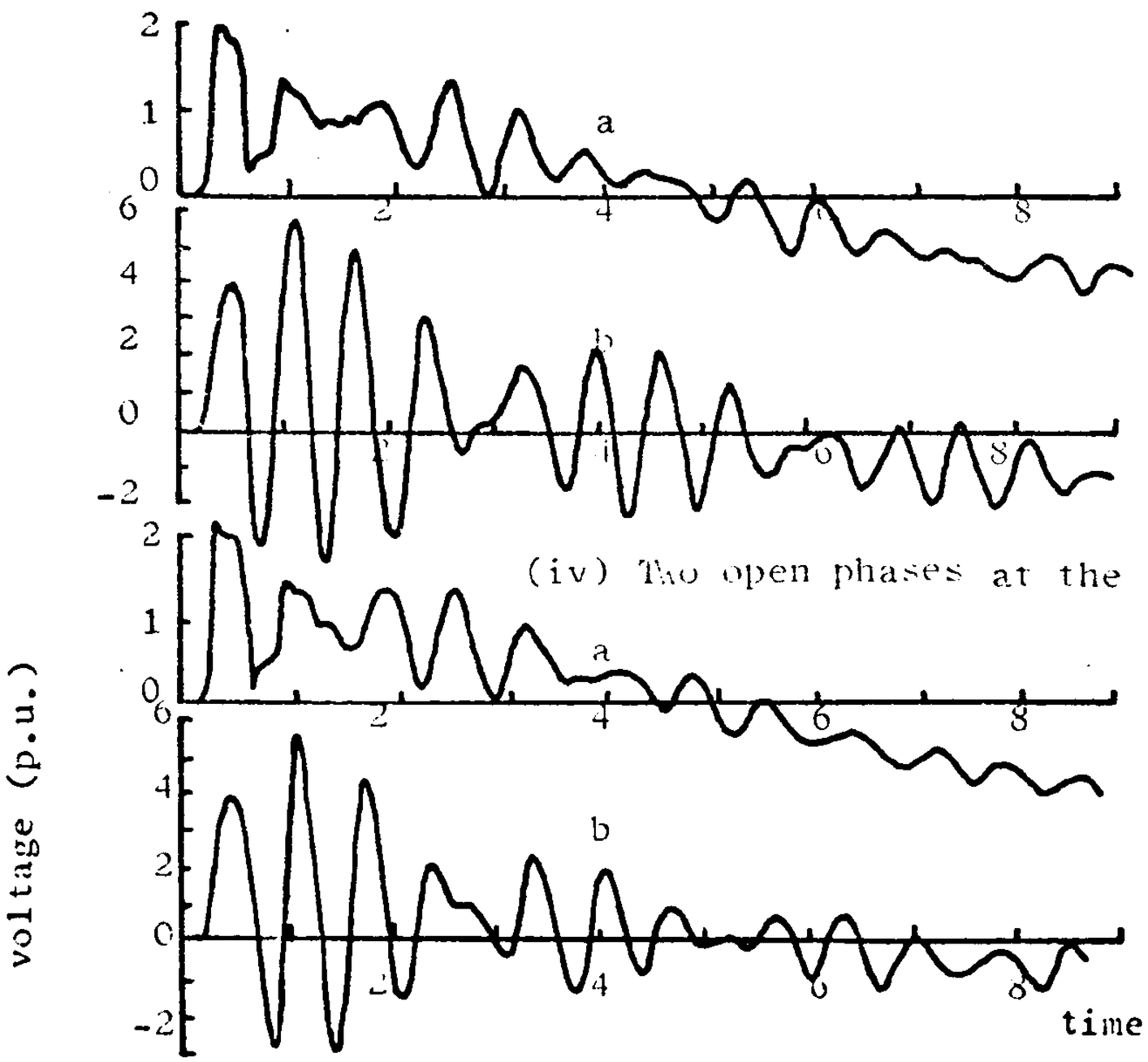

(iv) Two open phases at the transformer

(v) One open phase at the transformer

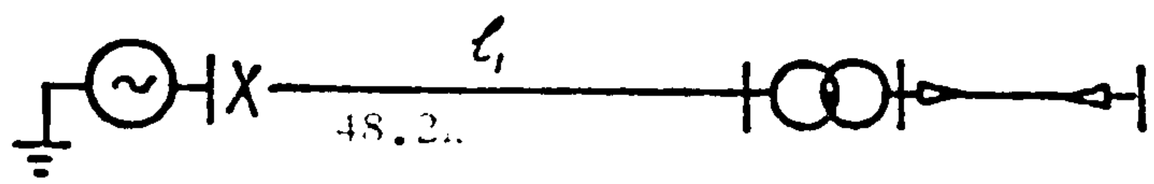

Fig.8.8 Voltage waveforms for open conductors.
(a) Transformer line side waveforms (b) Transformer secondary waveforms

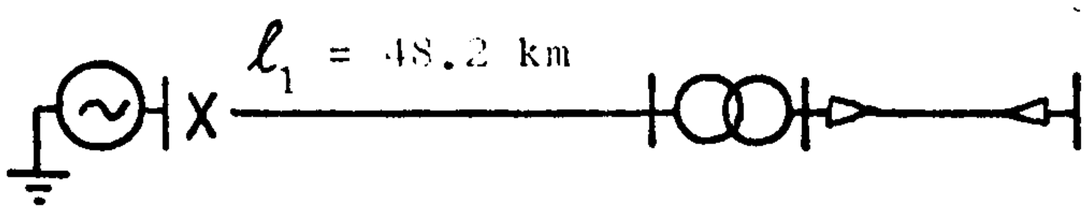

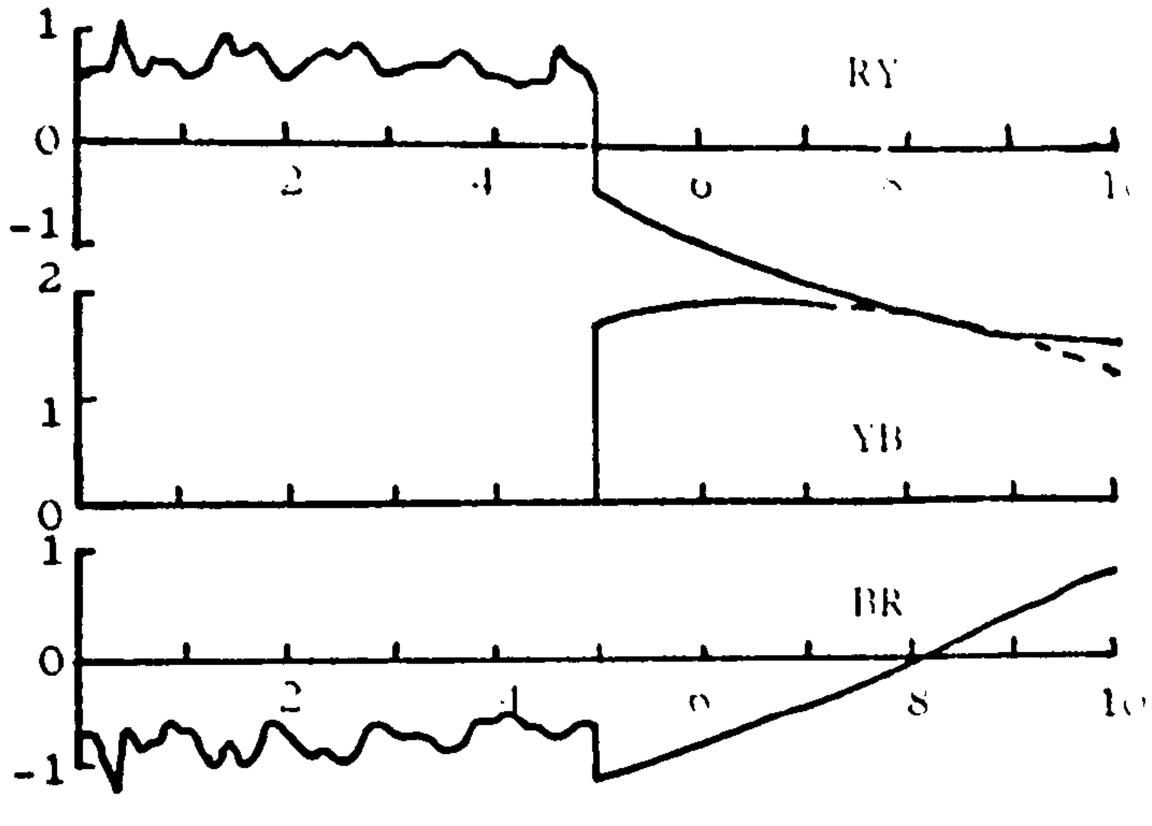

(iii) time (ms)

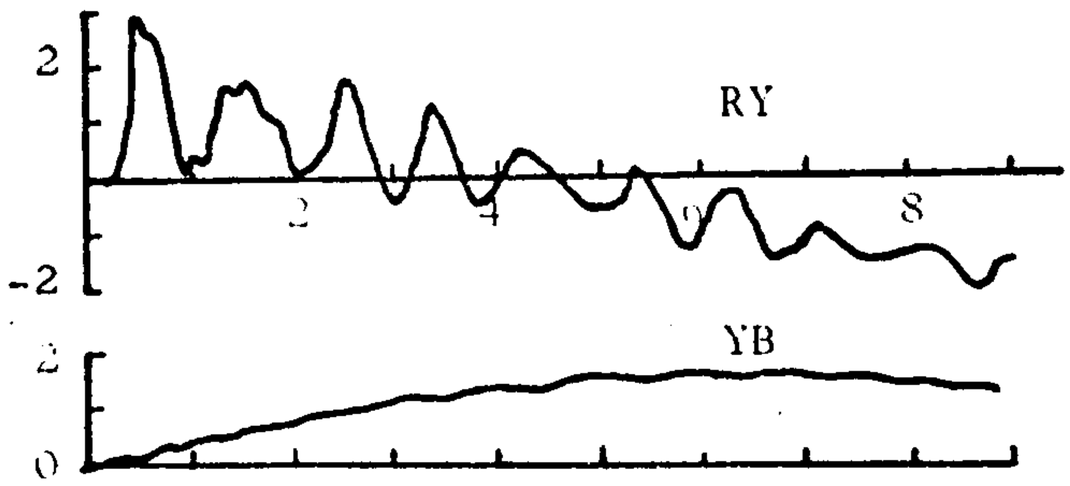

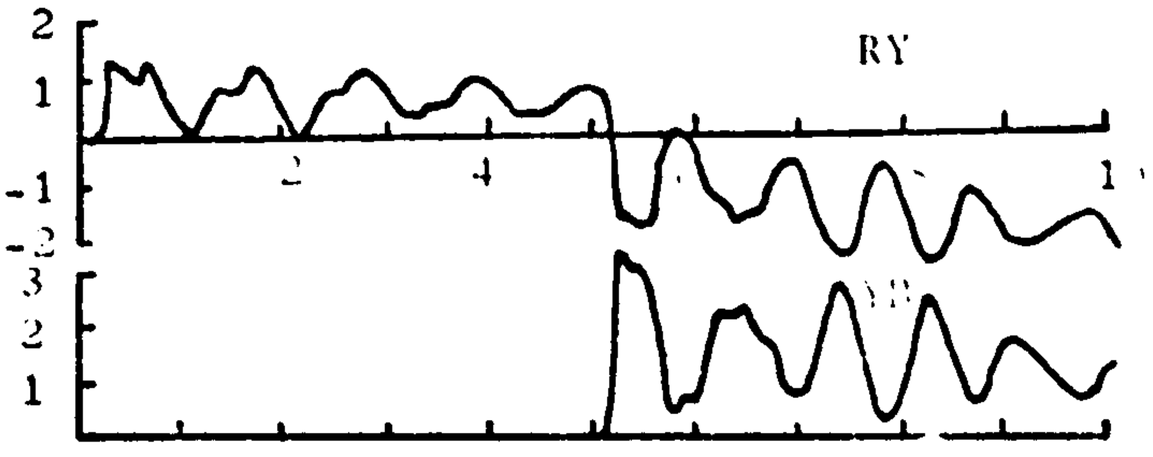

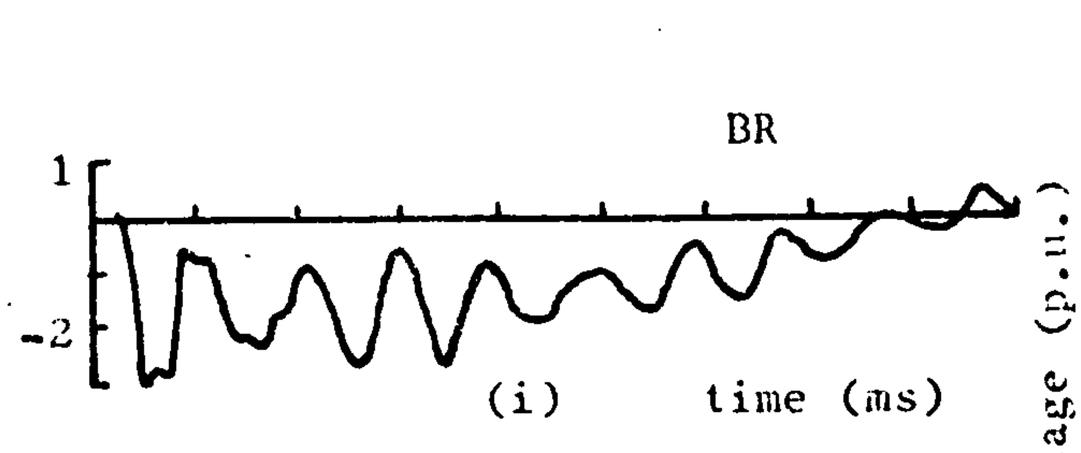

(i) time (ms)

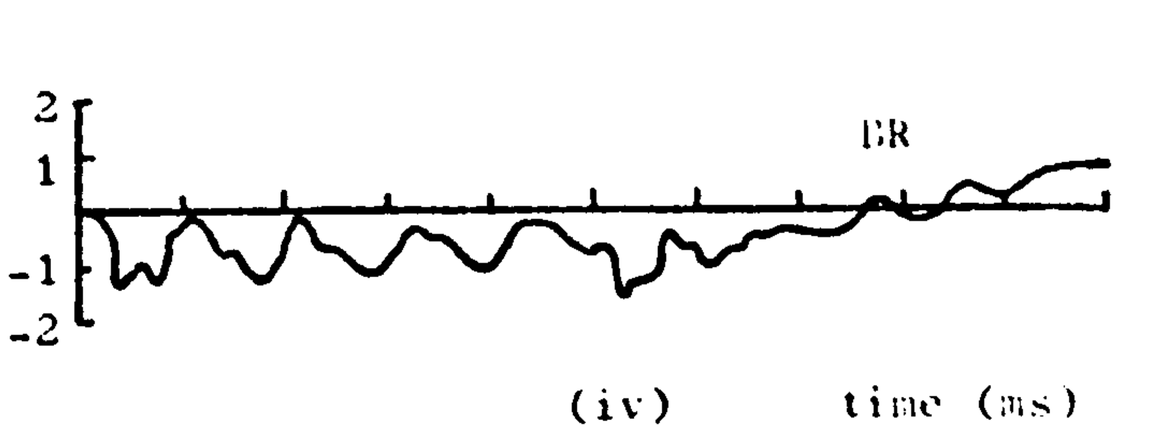

(iv) time (ms)

voltage (p.u.)

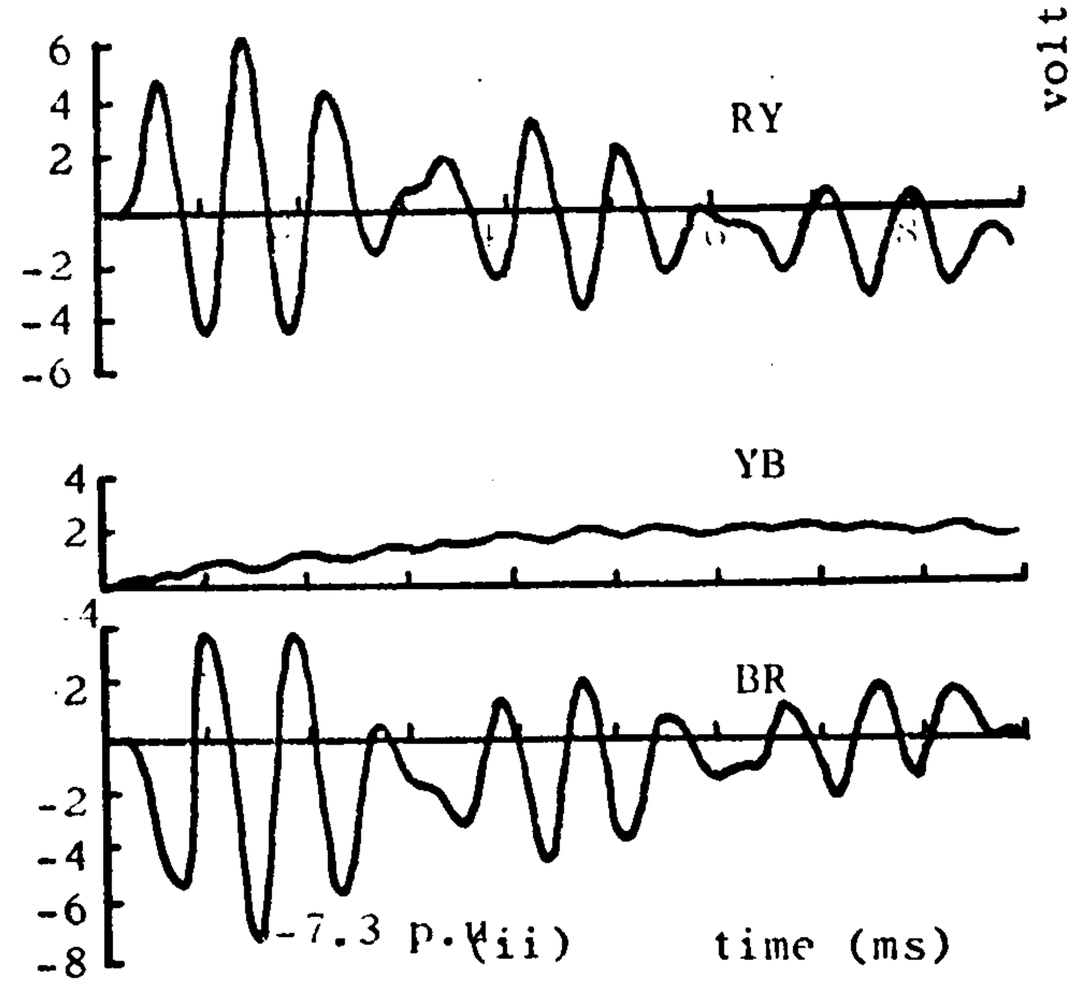

(ii) time (ms)

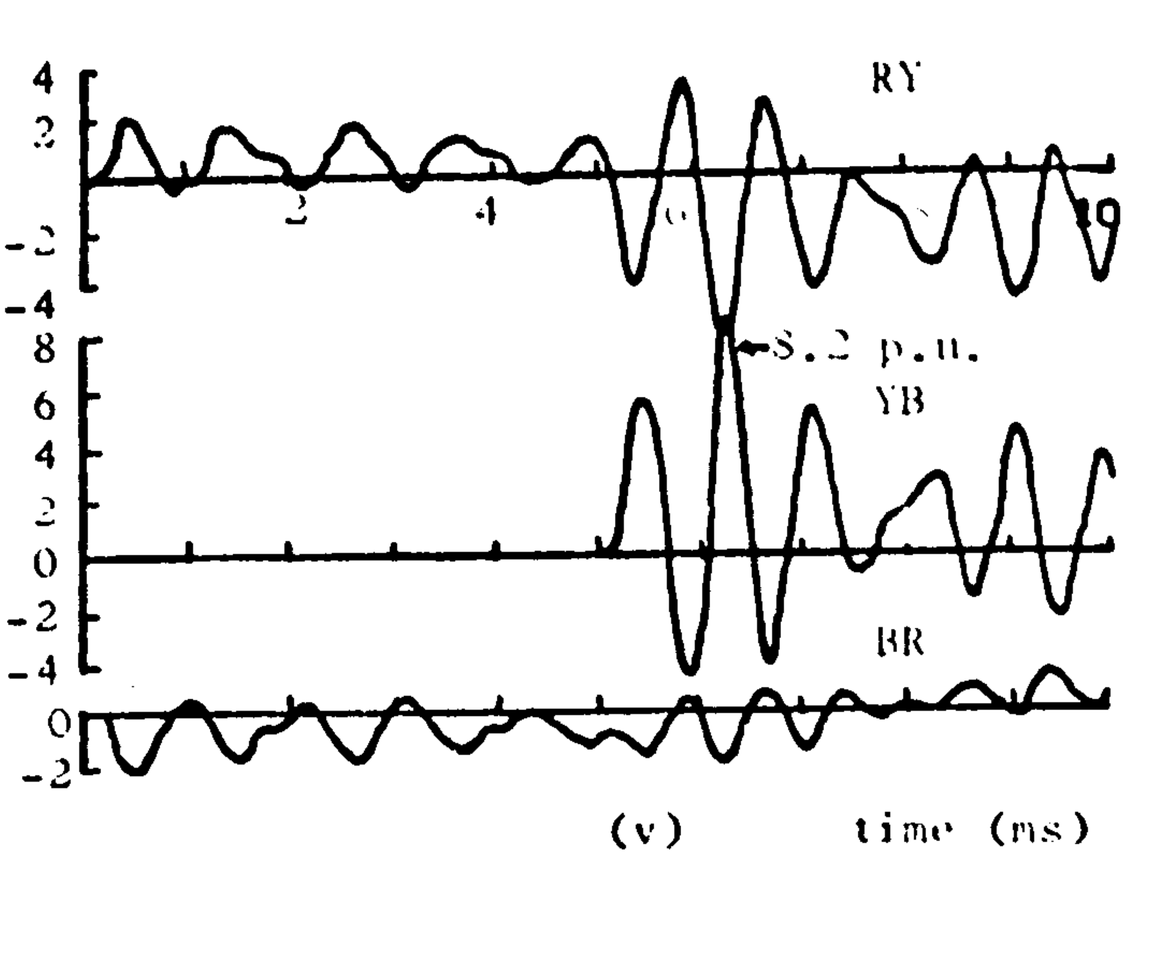

(v) time (ms)

Fig.8.9 TNA inter-phase voltage waveforms. Simultaneous closure waveforms at (i) the transformer line side terminal, (ii) the transformer secondary
Non-simultaneous closure waveforms at
(iii) the source-side of the line, (iv) the transformer end of the line, (v) the transformer secondary.

absence of oscillations between phases Y and B is due to the fact that the initial voltages launched into these phases are identical in magnitude and phase. The maximum overvoltage at the transformer secondary (-7.3 p.u.) occurs between the B and R phases because the steady state voltage between these phases, which forms the axis of the oscillations, is increasing while that between R and Y is decreasing in magnitude.

Simultaneous closure of the Y and B phases 90 degrees after phase R is energised produces the waveforms displayed in Fig.8.9 (iii),(iv) and (v). This closing sequence was found to produce the most onerous inter-phase overvoltage (8.2 p.u.). The large voltage step between phases Y and B is due to the substantial voltages of opposite polarity existing between the breaker poles of these phases prior to their energisation. The voltage surges coupled from the energised phase R before the other two phase close are identical. Hence zero voltage exists between the Y and B phases before they are closed.

Conditions under which Table 8.3 was compiled are similar to those pertaining to Table 8.2. Concerning the pole closing sequence and timing producing transformer secondary inter-phase overvoltages which exceed those obtaining when all poles close simultaneously (7.3 p.u), the following observations may be made from the Table.

(i) The location of the heavy lined boxes (indicating voltages in excess of those at zero pole span) above the 0,0 and 90, 90 degrees diagonal on the Table indicates that the B phase must close before Y in order to generate significantly high overvoltages. This is because the 50Hz voltage between R and B increases until it peaks 30 degrees later, while that between

Y-phase delay angle (°) / B-phase delay angle (°)	0	5	10	15	20	25	30	35	40	45	50	55	60	65	70	75	80	85	90
0 - 5	-7.3 BR	-7.3 BR	-7.6 BR	-7.5 BR	-7.5 BR	-7.7 BR	-7.7 BR	-7.7 BR	-7.6 BR	-7.6 BR	-7.6 BR	-7.5 BR	-7.5 BR	-7.7 BR	-7.9 BR	-8.0 BR	-7.9 BR	-7.8 BR	-7.9 BR
5 - 10	7.0 RY	3.7 YB	-4.0 BR	4.3 RY	-5.5 BR	-4.7 BR	-5.0 BR	-4.4 BR	-5.2 BR	-4.7 BR	-5.3 BR	-4.6 BR	-3.9 BR	-4.5 BR	5.6 YB	6.4 YB	-5.0 BR	-4.5 BR	5.7 YB
10 - 15	7.0 RY	-6.0 BR	-4.8 BR	-6.1 BR	-5.0 BR	-6.3 BR	-4.9 BR	-4.9 BR	-5.3 BR	-5.6 BR	-5.5 BR	-5.9 BR	-6.2 BR	-6.6 BR	-5.5 BR	6.4 YB	-6.5 BR	-6.1 BR	5.6 YB
15 - 20	7.0 RY	-7.1 BR	-6.5 BR	-7.3 BR	-7.1 BR	-7.5 BR	-7.5 BR	-7.4 BR	-7.3 BR	-7.3 BR	-7.3 BR	-7.3 BR	-7.3 BR	-7.5 BR	-7.6 BR	-7.8 BR	-7.6 BR	-7.5 BR	-7.7 BR
20 - 25	7.0 RY	-6.4 BR	-6.7 BR	-6.9 BR	-7.1 BR	-7.4 BR	-7.4 BR	-7.3 BR	-7.3 BR	-7.2 BR	-7.2 BR	-7.2 BR	-7.1 BR	-7.4 BR	-7.6 BR	-7.8 BR	-7.5 BR	-7.3 BR	-7.7 BR
25 - 30	7.0 RY	4.9 YB	-4.9 BR	6.0 YB	6.5 YB	-5.3 BR	-5.4 BR	-5.3 BR	-5.2 BR	-5.1 BR	-5.1 BR	-5.1 BR	-5.2 BR	-5.3 BR	-5.5 BR	-5.7 BR	-5.3 BR	-5.3 BR	7.2 YB
30 - 35	7.0 RY	-5.8 BR	-3.8 BR	-5.6 BR	5.6 YB	5.3 YB	-5.0 BR	-5.2 BR	-5.2 BR	-5.3 BR	-5.5 BR	-6.0 BR	-5.7 BR	-6.6 BR	-5.8 BR	-6.1 BR	-6.3 BR	-6.8 BR	6.8 YB
35 - 40	7.0 RY	-6.3 BR	6.6 YB	5.9 YB	-6.3 BR	-6.8 BR	-7.1 BR	-7.1 BR	-7.3 BR	-7.1 BR	-7.2 BR	-7.3 BR	-7.3 BR	-7.4 BR	-7.6 BR	-7.6 BR	-7.5 BR	-7.5 BR	-7.7 BR
40 - 45	7.0 RY	6.3 YB	6.8 YB	6.1 YB	6.4 YB	-6.5 BR	-7.1 BR	-7.0 BR	-7.2 BR	-7.1 BR	-7.1 BR	-7.1 BR	-7.0 BR	-7.0 BR	-7.5 BR	-7.3 BR	-6.3 BR	-7.1 BR	-7.5 BR
45 - 50	7.0 RY	5.7 YB	-6.0 BR	-5.6 BR	-5.5 BR	5.9 YB	-6.0 BR	6.0 YB	6.2 YB	-5.4 BR	-5.3 BR	-5.2 BR	-5.1 BR	-5.2 BR	-5.9 BR	6.0 YB	-5.1 BR	5.9 YB	7.1 YB
50 - 55	7.0 RY	-5.1 BR	4.9 YB	-5.5 BR	-5.7 BR	5.5 YB	-5.5 BR	-5.4 BR	-5.4 BR	-5.9 BR	-5.7 BR	-5.9 BR	-5.5 BR	-6.0 BR	7.0 YB	-6.1 BR	-6.2 BR	-5.9 BR	7.2 YB
55 - 60	7.0 RY	6.6 YB	6.0 YB	-5.0 BR	6.5 YB	6.3 YB	6.0 YB	5.9 YB	-5.3 BR	-5.9 BR	-6.7 BR	-6.1 BR	-6.1 BR	-6.4 BR	7.0 YB	6.8 YB	-6.5 BR	-6.2 BR	7.2 YB
60 - 65	7.0 RY	6.6 YB	6.9 YB	6.8 YB	6.6 YB	6.5 YB	6.3 YB	6.2 YB	-5.7 BR	6.1 YB	-6.5 BR	-6.0 BR	-5.9 BR	7.0 YB	-6.3 BR	6.8 YB	6.3 YB	-5.9 BR	6.4 YB
65 - 70	7.0 RY	-5.9 BR	6.3 YB	-6.6 BR	-6.0 BR	5.8 YB	6.0 YB	6.1 YB	5.9 YB	5.9 YB	6.2 YB	-5.5 BR	5.8 YB	7.6 YB	7.5 YB	-5.3 BR	5.9 YB	6.6 YB	7.1 YB
70 - 75	7.0 RY	-4.8 BR	5.0 YB	-5.7 BR	6.1 YB	4.9 YB	4.6 YB	4.7 YB	49. YB	4.6 YB	5.0 YB	-4.9 BR	-4.3 BR	-6.1 BR	7.5 YB	7.4 YB	4.8 YB	6.6 YB	7.9 YB
75 - 80	7.0 RY	5.7 YB	5.8 YB	5.7 YB	6.2 YB	5.9 YB	5.7 YB	5.9 YB	5.9 YB	5.6 YB	5.9 YB	6.1 YB	5.8 YB	6.6 YB	-7.0 BR	7.8 YB	7.8 YB	6.9 RY	7.9 YB
80 - 85	7.0 RY	5.8 YB	6.4 YB	5.9 YB	6.1 YB	6.3 YB	6.2 YB	6.3 YB	6.4 YB	6.2 YB	6.0 YB	6.1 YB	5.9 YB	7.2 YB	7.0 YB	-6.6 BR	8.0 YB	7.7 YB	-7.6 RY
85 - 90	7.0 RY	5.5 YB	6.2 YB	6.0 YB	6.2 YB	5.9 YB	6.1 YB	6.0 YB	6.0 YB	6.1 YB	5.9 YB	5.4 YB	5.9 YB	6.2 YB	7.0 YB	-6.1 BR	6.1 YB	8.1 YB	-6.5 BR
90 - 95	7.0 RY	4.9 YB	5.6 YB	5.7 YB	4.7 YB	4.3 YB	4.7 YB	-4.7 BR	-4.8 BR	4.7 YB	4.3 YB	4.3 YB	4.3 YB	4.9 YB	5.0 YB	5.8 RY	4.3 YB	6.8 YB	8.4 YB

TABLE 8.3 : Maximized phase-to-phase overvoltages at the transformer secondary as a function of phase Y and B delay angles relative to phase A closure (T.N.A.)

R and Y is decreasing. If the B-pole closes near its negative peak voltage at the instant when the surge reflected from the R-phase breaker terminal is positive, a large voltage step between the B and R phases will be initiated. This is confirmed by Table 8.3 where it may be seen that the maximum over-voltages occur between B and R for B-phase closing angles up to 45 degrees. Subsequently the Y-B 50Hz inter-phase voltage increases until it reaches a positive maximum at 60 degrees. Hence the maximum overvoltages tend to occur between Y and B around the 60 degrees B-pole closing angle. As the B-phase closing angle approaches 90 degrees, the phase relation-ship of the R and Y phases tend to favour excessive overvoltages between these phases.

(ii) A 2-pole prestrike of the R and Y phases always produces maximum overvoltages while the overvoltage of 7.0 p.u. is not affected by simultaneous closure of the R and B phases.

(iii) Closure of the B and Y phases instantaneously produces large overvoltages as seen from the concentration of the heavy-ruled boxes along the 0,0 and 90, 90 degrees closing angles diagonal on Table 3.

(iv) Comparison of Tables 2 and 3 will show that the areas of phase-to-earth peak overvoltages do not always correspond to regions of maximum overvoltages between phases.

An alternative method of presenting the results of Table 3

is given in Fig.8.10. It is a topographical view of the maximum overvoltages in three-dimensional space. The several layers denote surfaces of constant overvoltage magnitude. This contour representation is amenable to interpolation of overvoltage magnitudes for any closing instants of the last two phases to be energised. The several areas of localised peaks and troughs are simply illustrated. These enable an easier identification of regions likely to generate significantly high overvoltages to be made. It must be emphasised, however, that this contour format is applicable only to the system studied.

The horizontal disposition of the contour lines, particularly for B-pole closing angles up to about 45 degrees, indicates that variations in the Y-pole closing instants has little significance in the overvoltage magnitudes. On the other hand, for Y-phase closing angles less than about 5 degrees, changes in the instants of closing the B-phase do not materially alter the overvoltage magnitudes. This is illustrated by the contour lines running parallel to the B-phase axis in this region. The inclination of the contour lines observed when the closing angles of the last two phases approach 90 degrees, indicates that significant overvoltages would result in this region when the two poles close nearly at the same instant.

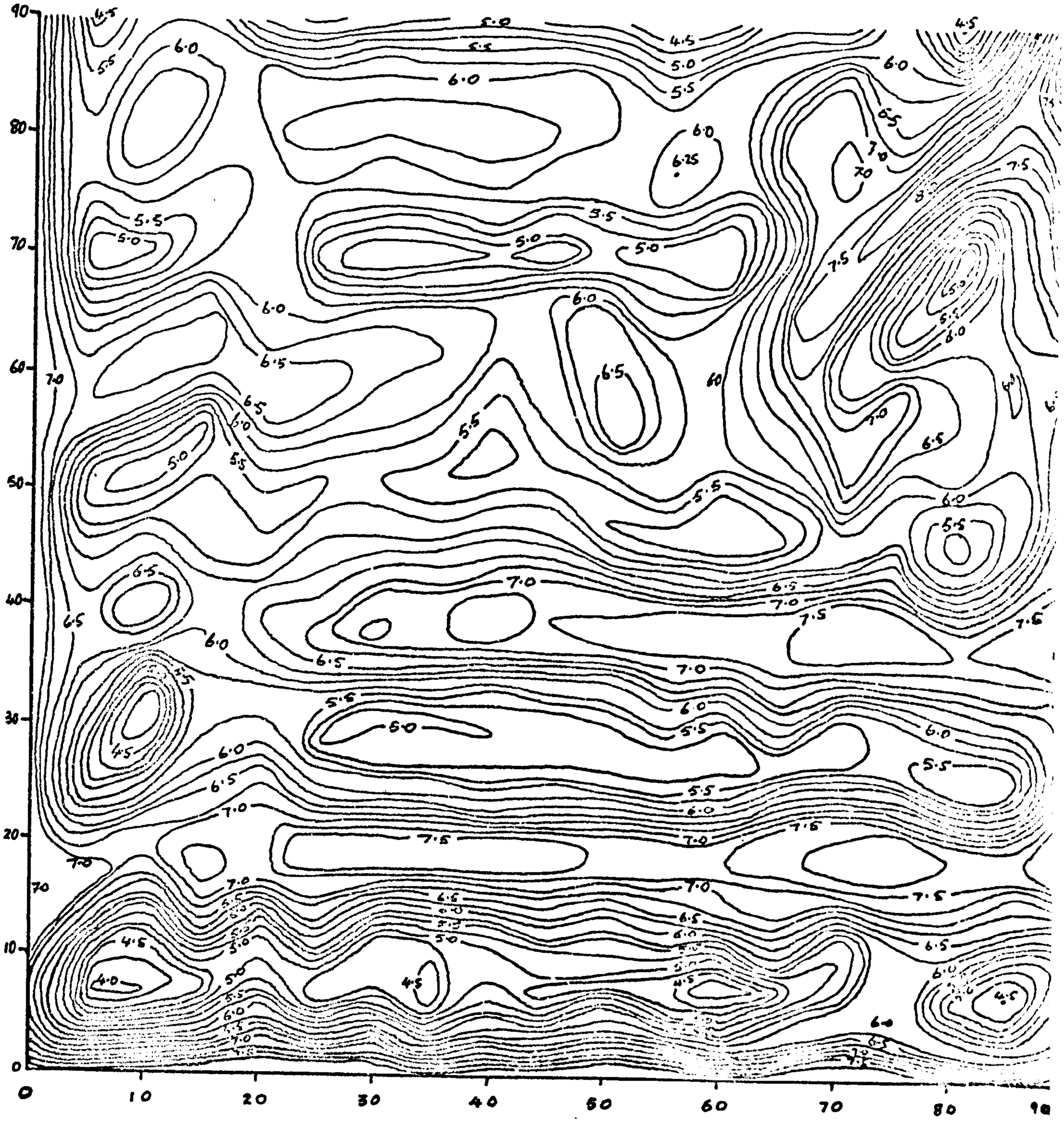

Fig. 8.1) Inter-phase overvoltage contours for sequential pole closure.

8.5 Methods of reducing resonance overvoltages

It has been shown in Chapters 5,6 and the present chapter, that the magnitude of the overvoltages at the transformer secondary when a resonance condition exist , depends on:

(i) circuit parameters

(ii) system configuration, and

(iii) performance characteristics of the energising circuit breaker.

Consequently, all these factors have to be taken into account when seeking remedial action to prevent or limit the magnitudes of these oscillations below the insulation level of the transformer secondary. Reduction of these overvoltages may be effected by employing the following measures:

(a) Methods which inhibit the development of resonant overvoltages by ensuring that the system conditions are such that the resonant phenomenon will not occur.

(b) Methods which will limit the magnitudes of resonant oscillations where these already exist.

8.5.1 Circuit parameters and operational restrictions

The most effective measure of eliminating excessive voltages due to resonance is to ensure that the transformer frequency differs appreciably from the natural frequency of the line. It was shown in Chapter 5 that this can be achieved by simply detuning the circuit by any of the following actions:

(a) Varying the line frequency by changing its length.

(b) Varying the transformer frequency by changing either its leakage reactance or the length of the cable on

the secondary circuit.

(c) Addition of sufficient capacitance on the secondary circuit by installing shunt capacitors.

Factors (a) and (b) may be impracticable since transmission distances are dictated by the geographical layout of the rest of the interconnected network and the transformer impedances are determined by other considerations. Factor (c) may prove to be too expensive.

In Chapter 6, it was shown that the voltage waveform which excites the transformer is dependent on the circuit configuration of the network as seen from the terminals of the transformer. The effects of the physical layout of the feeder, the type of source from which it is energised and the relative position and length of intermediate sections of cable, were investigated. It was found that certain circuit arrangements, which are summarised below, obviate the development of excessive overvoltages:

(i) Energising the circuit from a breaker adjacent to the terminating transformer.

(ii) The presence of another line tee-ed together with the feeder at the transformer line side terminal, and having a length close to an odd multiple of the length of feeder being energised.

(iii) A tee-off line connected along the feeder whose length is close to an odd multiple of the feeder length.

(iv) Feeder energised from a source containing several generators.

(v) A line on the source side of the breaker of a length nearly equal to an odd multiple of the feeder length.

(vi) A short length of cable interposed between the line being energised and the transformer.

It should be pointed out that implementation of these measures can only be realised in practice at the planning stage of the system network.

8.5.2 Synchronous switching and closing resistors

It has been shown in this chapter that the magnitude of the transformer secondary oscillations are somewhat related to the amplitude of the exciting surge. Any measures taken to reduce the line oscillation amplitudes will, to some extent, be useful in reducing the secondary overvoltages. In this context, therefore, all the methods used to limit overvoltages in unterminated transmission lines (see section 1.9) may be of some value when transformers are connected at the end of the feeder. These measures include the following:

(a) Damping resistors

If a closing resistor of optimum value is used (typically half to twice the line surge impedance) lower amplitude line oscillations result. Further reductions may be achieved by using multiple step closing resistors. In addition, these resistors, when present during the opening of the switch contacts, will assist the transformer in reducing the residual charge on the line. This will alleviate the otherwise onerous circumstance of re-energising on a line pre-charged with a significant voltage.

(b) Controlled point-on-wave switching

Closing of the breaker poles at the instant when the

voltage difference is zero can significantly reduce the line oscillations. This method is, however, fraught with severe technical problems since stringent accuracy of the switching angle of each pole has to be observed. The results of the pole scatter study show that the secondary phase-to-phase and phase-to-earth overvoltages can be significantly reduced by a judicious choice of closing angle settings.

The methods discussed above will limit the line oscillation amplitudes if the surges originate from the energising breaker. If the cause of the line oscillations is a line flashover near the breaker end of the feeder which, by collapsing the peak line system voltage, produces waves of similar amplitude and frequency, neither the synchronous switching nor the damping resistors will be effective.

8.5.3 Surge diverters

At present, the usual practice is to install surge diverters on the transformer line side terminal where they are normally required for lightning and switching surge protection. If a resonance condition exists, however, the voltage magnitudes at the transformer primary are, in most cases, below the diverter protective level. Hence, in this position the diverters will be ineffective in limiting those overvoltages occurring on the secondary circuit. Where resonance already exists, it may be necessary to install additional surge diverters at the secondary terminals. In comparison with the previously mentioned overvoltage controlling measures, this method does not suffer from the disadvantage of being ineffective when voltage surges are initiated by line conductor flashover.

8.6 Conclusion

Results have shown that for the relatively short period under investigation, the transient oscillations at the transformer secondary are insensitive to the non-linearity of the saturation characteristics of the transformer if the breaker poles close at the same instant. This is true for the 3-limb star-star connected transformer with both neutrals solidly earthed. In general, the effect of the transformer on the oscillations at the secondary is therefore the same as that of an inductance equal to the short circuit inductance of the transformer. Results of the single phase studies of Chapters 5 and 6 will be valid for a balanced symmetrical three phase system. This is the case when the breaker pole span is zero and there is no pre-charge on the transposed line prior to energisation.

In the case of sequential closure, computed waveforms have shown that the influence of saturation characteristics in modifying the voltage waveforms at the transformer increases with time.

In non-simultaneous closure of the breaker poles, the over-voltages at the transformer are largely dependent on the time displacement between the closing of the three poles. The instant at which a pole closes is governed by the mechanism of closure of the circuit breaker poles and the premature flashover across the closing contacts. The increase of the amplitude of oscillations at the transformer secondary can be directly related to the increase in the magnitude of the line oscillations caused by closing onto a coupled surge. Maximum over-voltages occur on one phase when closing near to a peak of surge coupled from the energised phase or phases which is in phase opposition to a system voltage of large value on this phase.

Recent studies have demonstrated that flashover between

phases during switching surges may be an important consideration in dimensioning inter-phase insulation. This is particularly true during sequential closure under resonance conditions.

In this Chapter, only single circuit feeders have been considered. The next Chapter will deal with linear resonance phenomena associated with double-circuit feeders.

C H A P T E R 9

INDUCED RESONANT OSCILLATIONS ON DOUBLE CIRCUIT FEEDERS

9.1 Introduction

By virtue of the close electrostatic coupling which exists between the individual circuits of a double circuit line, induced voltages will be present on one of the circuits if it is de-energised while the other circuit on the same towers remains energised. Apart from considerations of workmen's safety when one of the circuits is taken out of service for maintenance purposes, these voltages will be harmless. If the circuit being dropped is terminated in a transformer directly connected to the feeder, with a compensating reactor at its tertiary winding terminals, the possibility of a resonance condition being excited exist. Excessive overvoltages would result.

This chapter will examine, with the aid of a computer program outlined in Chapter 7, the linear resonant oscillations which appear on the de-energised circuits. Ferroresonant oscillations appropriate to double-circuit feeders will be the subject of the next Chapter. It will be shown in this Chapter that the oscillations developed at the transformer terminating the dead circuit are attributable to unbalanced capacitive coupling which exist between the phases of the live and de-energised circuits. If two or more circuits are supported on the same tower or are in sufficiently close proximity for the entire or part of their length, mutual electrostatic coupling will exist between the circuits. Usually the zero sequence coupling predominates while the positive and negative sequence coupling are so small that they could be neglected.

The amplitude of the oscillations excited on the circuit being dropped depend largely on the following factors:-

(i) the length of the line being de-energised;

(ii) the degree of compensation;

(iii) the transformer leakage reactance between the primary and tertiary windings;

(iv) the physical configuration and characteristics of the lines;

(v) the residual charge voltage left on the line being dropped and their phase relationship to the coupled voltages; and

(vi) the losses inherent in the system.

The effects of line losses, which in practice are relatively small in such closely coupled low loss systems, and the losses inherent in the transformer and reactor, have been ignored in this study. The main objective in this Chapter is to derive simplified expressions which could be used to predict whether a resonance condition would exist given certain parameters of the double circuit line and terminating reactances.

9.2 System studied

The circuit diagram of the system studied is shown on Fig. 9.1 (i). Transmission lines of two different constructions as detailed in Chapter 7 will be used. These are:

(i) Twin 0.4 sq. in. 275kV lines with zero earth resistivity, and

(ii) Quadruple 0.4 sq. in. 400kV lines with earth resistivity equal to 30 ohm-metre.

One circuit which is energised is of infinite length and the other, of finite length, is terminated in a transformer and reactor unit. An infinite line is chosen so as to eliminate the line frequency oscillations which would otherwise be superimposed on the source frequency voltage. The transformer and feeder combine is isolated from the rest of the system by opening the circuit breakers shown at both ends. The reactances of the 275/132/33kV 240MVA auto-transformer are given in Fig. 9.1 (ii). The 30/60 MVAr shunt compensating reactor is connected to the 33kV tertiary terminals of the transformer.

9.3 Equivalent reactive termination

In this study, the transformer magnetising reactance has been neglected since it is considered infinite in comparison with the sum of leakage reactance between the primary and tertiary windings and that of the compensating reactor. Its omission only has a minor order effect on the accuracy of the results. The leakage reactance between the primary and tertiary of the transformer is given by

$$X_{TR} = 45\% \times \frac{(kV)^2}{MVA} \qquad \text{where } kV = 275 \text{ and } MVA = 240$$

$$= 141.8 \text{ ohms}$$

$$\text{i.e } L_{TR} = 0.45H$$

The reactance of the compensating reactor, referred to the 275kV system, may be calculated as follows:

$$X_R = \frac{(kV)^2}{MVAr} \times \left(\frac{275}{33}\right)^2 \qquad \text{where } kV = 33 \text{ and } MVAr = 30$$

$$= 2520.8 \text{ ohms}$$

$$\text{i.e. } L_R = 8.03H$$

It is assumed that the zero sequence inductance of the reactor is equal to that of the positive sequence . The equivalent shunt inductance terminating the compensated circuit is therefore given by :

$$L_T = L_{TR} + L_R$$

$$= 8.48H$$

For the 60 MVAr reactor the equivalent inductance is 4.465H.

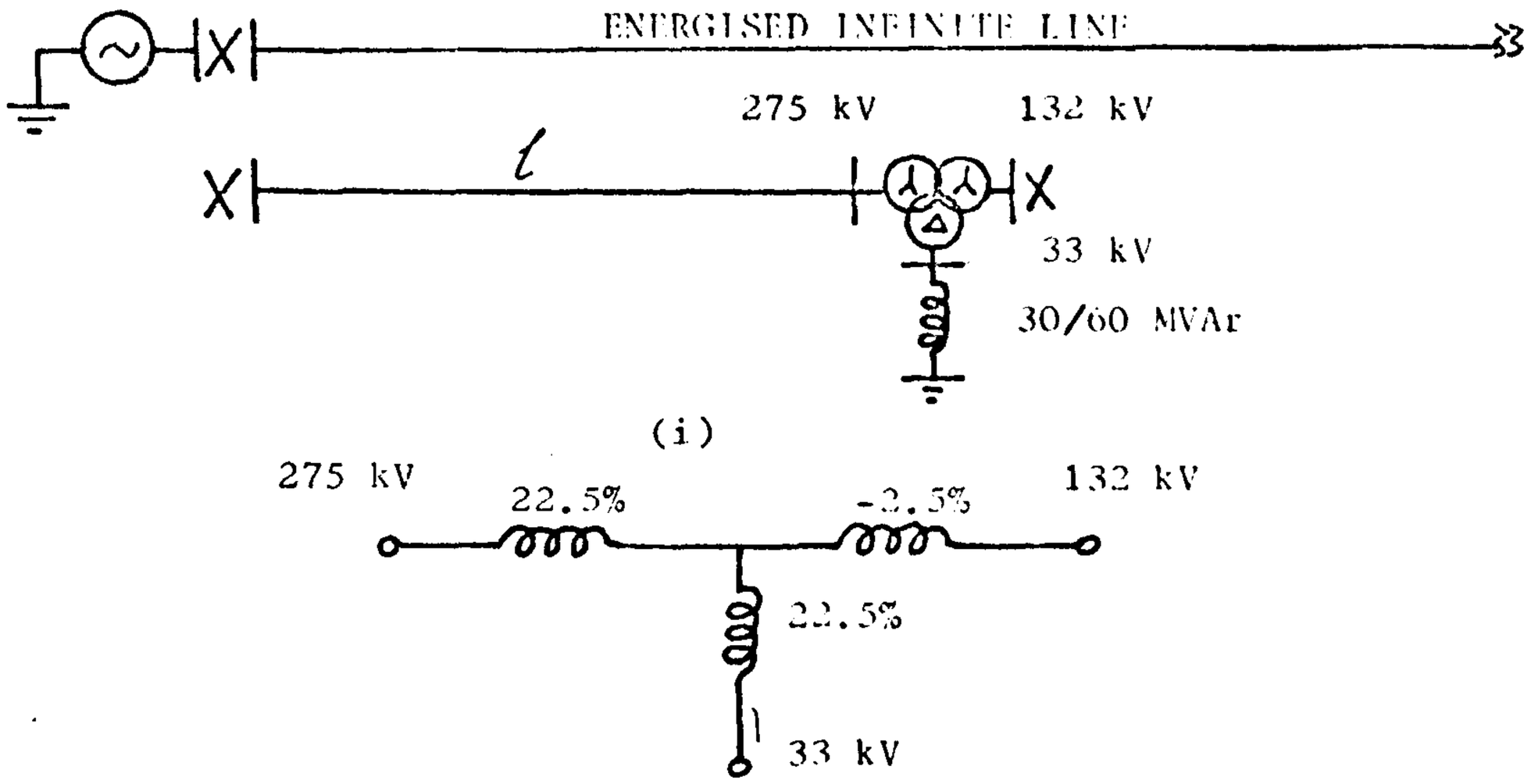

Fig. 9.1 (i) Single line diagram of double circuit feeder
(ii) Transformer equivalent cirucit
(iii) Line electrostatic equivalent circuit
(iv) Reduced circuit relating to (iii)
(v) Simplified circuit illustrating voltage induction.

9.4 Capacitance equivalent circuit

The analysis that follows ignores the electromagnetic coupling between the circuits since this forms a negligible fraction of the total coupled voltage. Fig. 9.1 (iii) shows the lumped electrostatic equivalent circuit of a double circuit line[61]. The symmetrical component susceptances per unit length are derived from the shunt reactance matrix, $\left[X_{SH}\right]$, obtained from a computer program referred to in Chapter 7. From a knowledge of physical dimensions of the conductor configuration, this program calculates, using potential coefficients, the shunt reactances for each conductor in the array, including the effects of earth wires and bundled conductors, if present. Both the earth wires and bundled conductors are eliminated from the shunt reactance matrix. This reduced matrix, $\left[X_{SH}\right]$, is inverted in order to find the array elements ($B_{i,k}$, where i, k = 1 to 6) required for determining the symmetrical component sequence susceptances (i.e. $\left[B\right] = \left[X_{SH}\right]^{-1}$)

The susceptances per phase of an overhead line are defined as:

$$\left[B\right] = 2\pi f \left[C\right] \quad \mu S/km \ (\mu S = \text{micro-Siemens}) \qquad 9.1$$

where $\left[C\right]$ = Maxwell's coefficients defined as phase capacitance to neutral in F/km, and

f = frequency in Hz.

The self and mutual positive and zero sequence susceptances are defined by the following relations[61,62] (the suffix T relates to twin conductor lines and Q to quadruple conductor lines):

Positive sequence self susceptance:

$$B_1 = \tfrac{1}{3} \left(B_{11} + B_{22} + B_{33} - B_{12} - B_{23} - B_{13}\right) \qquad 9.2$$

i.e. $B_{1(T)} = 3.644\ \mu S/km$

$B_{1(Q)} = 4.138\ \mu S/km$

Zero sequence self susceptance:

$$B^1_o = \tfrac{1}{3}\left[B_{11} + B_{22} + B_{33} + 2(B_{12} + B_{23} + B_{31}) \right] \qquad 9.3$$

i.e. $B^1_{o(T)} = 2.274\ \mu S/km$

$B^1_{o(Q)} = 2.515\ \mu S/km$

Zero sequence mutual susceptance:

$$B^1_{mo} = \tfrac{1}{3}\ (B_{14} + B_{15} + B_{16} + B_{24} + B_{25} + B_{26} + B_{34} + B_{35} + B_{36}) \qquad 9.4$$

i.e. $B^1_{mo(T)} = -\ 0.679\ \mu S/km$

$B^1_{mo(Q)} = -\ 0.680\ \mu S/km$

The zero sequence component values as calculated above relate to a delta configuration of the equivalent circuit in the zero sequence network. In order to obtain the equivalent star circuit appropriate to the circuit shown on Fig 9.1 (iii), a delta/star transformation has to be made. This transformation may be achieved by inverting the symmetrical susceptance matrix relating to the zero sequence equivalent circuit given by:

$$\begin{bmatrix} B^1_o & B^1_{mo} \\ B^1_{mo} & B^1_o \end{bmatrix} \qquad 9.5$$

to obtain the following reactance matrix:

$$\begin{bmatrix} X_o & X_{mo} \\ X_{mo} & X_o \end{bmatrix} \qquad 9.6$$

The matrix (9.6) corresponds to a star configuration of the equivalent circuit. The reciprocal of the self term in this matrix ($1/X_o$) gives the zero sequence self susceptabce of each circuit, (B_o), and the reciprocal of the mutual term ($1/X_{mo}$) represents the mutual zero sequence susceptance between circuits, (B_{mo}). In relation to the twin and quadruple transmission lines simulated,

$B_{o(T)}$ = 2.071 μS/km and $B_{o(Q)}$ = 2.332 μS/km

$B_{mo(T)}$ = 6.937 μS/km and $B_{mo(Q)}$ = 8.631 μS/km

These values are identical to those given in the C.E.G.B. Design No. T787 (dated 20th January 1965) for the twin and quadruple double circuit lines.

The value of B_A in Fig. 9.1 (iii) is obtained as follows:-

$$B_A = \frac{1}{\frac{1}{B_{pp}} - \frac{1}{B_{cc}}} \qquad 9.7$$

where B_{pp} = interphase mutual susceptance

$$= \frac{3}{\frac{1}{B_o} - \frac{1}{B_1}} \qquad 9.8$$

and B_{cc} = inter-circuit mutual susceptance

$$= 3\ B_{mo} \qquad 9.9$$

$$\text{i.e. } B_A = \frac{3B_oB_1B_{mo}}{B_{mo}(B_1-B_o) - B_oB_1} \qquad 9.10$$

9.5 Induced Voltage

The susceptance equivalent circuit of Fig. 9.1 (iii) is reducible to a simplified single phase form shown on Fig.9.1 (iv). The positive sequence voltage on the energised line, E , (assuming balanced conditions) is represented as a voltage source applied to a circuit similar to a voltage divider feeding a series capacitor-inductor circuit. The divider voltage across B_{cc} may be calculated as follows:-

$$V_{cc} = \frac{B_s}{B_{cc} + B_s} E_o \qquad 9.11$$

where $B_{cc} = 3B_{oo}$, and

$$B_s = \frac{B_1 B_A}{B_1 + B_A}$$

$$= \frac{3B_o B_1 B_{mo}}{2B_o B_{mo} + (B_{mo} - B_o) B_1} \qquad 9.12$$

i.e. $B_{s(T)} = 3.380$ μS/km

and $B_{s(Q)} = 3.767$ μS/km

$$V_{cc} = \frac{B_o B_1}{B_{mo}(2B_o + B_1)} E \qquad 9.13$$

This represents the open circuit or Thevenin voltage at the end of the de-energised line. Fig 9.2 shows computed open circuit phase-to-earth voltage waveforms at the end of the de-energised circuit. It will be seen that the peak amplitudes of the voltage on the three phases of the twin transmission lines are 0.08, 0.10 and 0.12 p.u. These amplitudes are somewhat lower than the value calculated from equation 9.13(i.e 0.14 p.u.), mainly due to the partial cancellation of voltages induced separately by the energised phase conductors. With regard to the quadruple conductor line, the computed peak voltages on the three

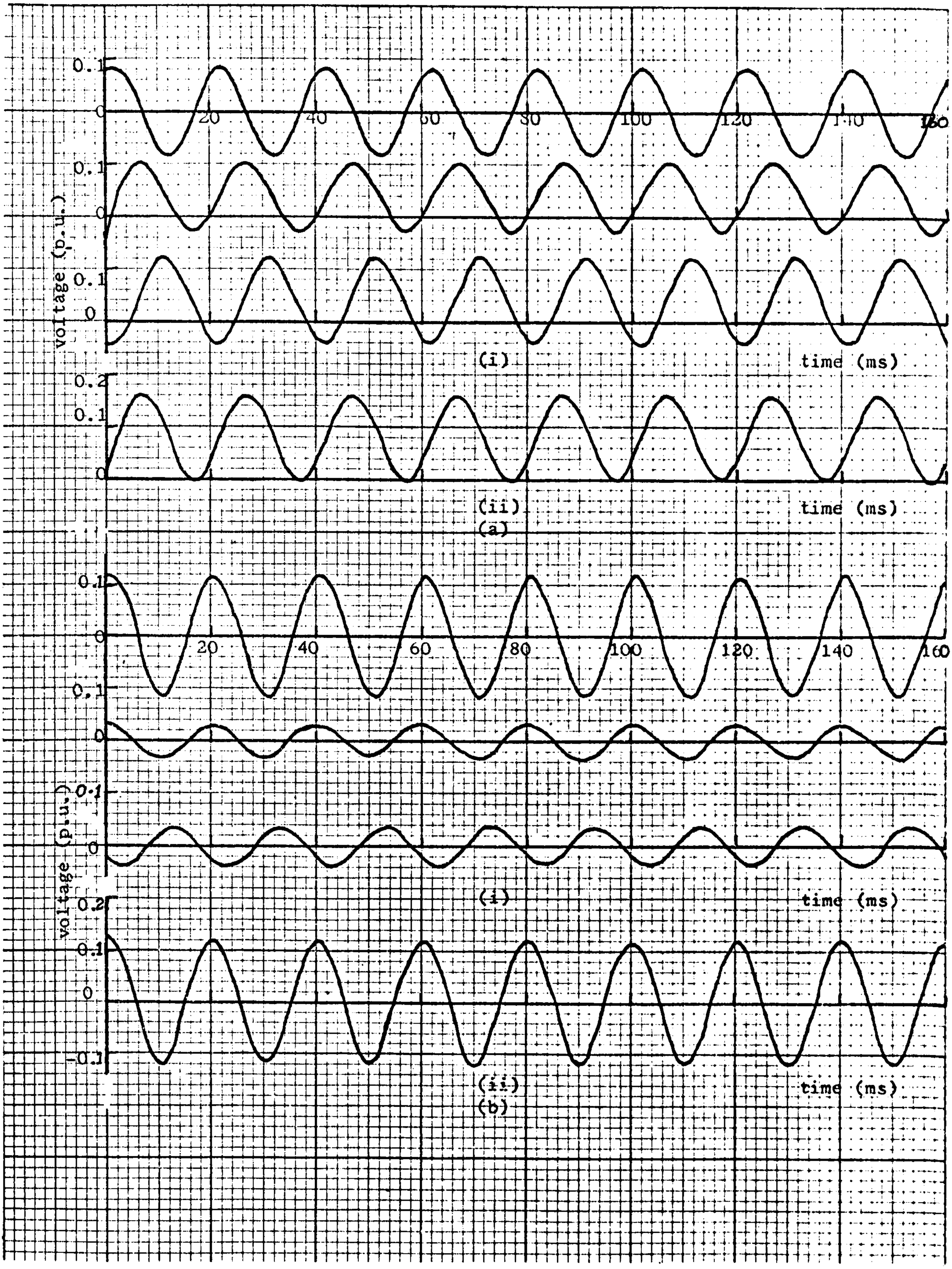

Fig. 9.2 Induced open-circuit voltages on the de-energised circuit

a) Twin conductor line
b) Quadruple conductor line
   (i) voltage waveforms on each phase
   (ii) vector sum of voltages

phases are 0.12, 0.03 and 0.04 p.u. The peak voltage on phase 1 conductors which occupy the upper position on the tower is close to the value predicted from equation 9.13 (i.e. 0.13 p.u). The reduced magnitude of the coupled voltage on the two bottom phase conductors is attributed mainly to the following factors:

a) The separation between corresponding phase conductors of the two circuits is much larger for phases 2 and 3 than it is for phase 1 conductors, and consequently coupling will be weaker.

b) Partial cancellation of the induced voltages due to phase differences of these voltages is more pronounced on the two lower phase conductors. This is because the quadruple configuration used is such that the distances from each of the two lower conductors to the three energised phases of the other circuit are nearly equal.

9.5.1 Induced zero sequence voltage

Fig. 9.2 also shows the vector sum of the induced voltages, demonstrating the presence of a relatively large component of zero sequence voltage. The calculated peak amplitudes of the induced sinusoidal zero sequence voltages per phase are 0.027 and 0.040 p.u. for the twin and quadruple conductor lines respectively. The latter is symmetrical about the zero line whereas the former exhibits a fully asymmetric voltage (i.e. it is offset from the zero line by an amplitude equal to its sinusoidal peak value).

A close approximation of this zero sequence component of induced voltage could be predicted from the symmetrical component format of the shunt susceptance matrix. Hesse and Wilson[35] have shown that, based on certain assumptions, the sequence susceptance matrix defined by:

$$\begin{bmatrix} I_o \\ I_1 \\ I_2 \\ I'_o \\ I'_1 \\ I'_2 \end{bmatrix} = j \begin{bmatrix} B_{00} & B_{01} & B_{02} & B_{00'} & B_{01'} & B_{02'} \\ B_{10} & B_{11} & B_{12} & B_{10'} & B_{11'} & B_{12'} \\ B_{20} & B_{21} & B_{22} & B_{20'} & B_{21'} & B_{22'} \\ B_{0'0} & B_{0'1} & B_{0'2} & B_{0'0'} & B_{0'1'} & B_{0'2'} \\ B_{1'0} & B_{1'1} & B_{1'2} & B_{1'0'} & B_{1'1'} & B_{1'2'} \\ B_{2'0} & B_{2'1} & B_{2'2} & B_{2'0'} & B_{2'1'} & B_{2'2'} \end{bmatrix} \cdot \begin{bmatrix} E_o \\ E_1 \\ E_2 \\ E'_o \\ E'_1 \\ E'_2 \end{bmatrix} \quad 9.14$$

is reducible to the simpler form

$$\begin{bmatrix} I_1 \\ I'_0 \end{bmatrix} = j \begin{bmatrix} B_{11} & 0 \\ B_{0'1} & B_{0'0'} \end{bmatrix} \cdot \begin{bmatrix} E_1 \\ E'_0 \end{bmatrix} \quad 9.15$$

where the primed quantities relate to the de-energised circuit.

For a symmetrical double circuit transmission line,

$B_{11'} = B_{11}$ = positive sequence self susceptance

i.e $B_{11(T)} = 3.644$ μS/km

and $B_{11(Q)} = 4.138$ μS/km

$B_{0'0'} = B_{00}$ = zero sequence self susceptance (Delta configuration)

i.e $B_{0'0'(T)} = 2.274$ μS/km

and $B_{0'0'(Q)} = 2.515$ μS/km

$B_{0'1}$ = the mutual susceptance between the positive sequence voltages on the energised circuit and the zero sequence currents on the de-energised circuit.

$$= \tfrac{1}{2}(B_{14} + B_{15} + B_{16} - B^1_{mo}) + j\,\sqrt{3}/6\,(B_{34}+B_{35}+B_{36}) - B_{24} - B_{25} - B_{26}) \quad 9.16$$

where B^1_{mo} is as defined by equation 9.4

i.e $B_{0'1(T)} = (-0.02581 + j\,0.04844)$ μS/km

and $B_{0'1(Q)} = (-0.10780 + j\,0.02142)$ μS/km

The reduction of the equivalent circuit defined by equations 9.14 to the simpler form described by equations 9.15 is based on the following assumptions:-

(i) only positive sequence voltages are applied to the energised circuit, and consequently the zero and negative sequence voltages available for coupling to the de-energised circuit are relatively negligible.

(ii) the off-diagonal terms of the sequence susceptance matrix ($B_{i,k}$ where $i \neq k$) are small in comparison with the diagonal terms, with the exception of the zero sequence inter-circuit mutual susceptance $B_{00'}$, and could therefore be neglected, and

(iii) products of low order terms are neglected.

Fig. 9.1 (v) shows the equivalent circuit corresponding to the reduced matrix representation of the system sequence susceptances. It demonstrates the manner in which the positive sequence voltages on the energised circuit are coupled to the'dead' circuit. Using this simplified circuit, the open circuit zero sequence voltage on the compensated circuit could be estimated as follows:

$$V_{OC} = \frac{|B_{0'1}|}{B_{0'0'}} E \qquad 9.17$$

i.e. $V_{OC(T)} = 0.025\ E$

and $V_{OC(Q)} = 0.044\ E$

The agreement between these values and the computed sinusoidal open circuit zero sequence voltage amplitudes per phase (0.027 and 0.040 respectively as shown on Fig. 9.2), is very close.

Both equations used for calculating induced voltages (equations 9.13 and 9.17) show the independence of these voltages on the length of the de-energised circuit. It should be noted that the effects of trapped charge and losses on the phase conductors have not been taken into account.

9.6 Resonance Conditions

Fig. 9.1 (iv) reflects the possibility of resonant oscillations being excited due to the oscillatory circuit formed by the effective series capacitance, $C_s = B_s/\omega$ ($\mu F/km$), and the total linear reactance of the transformer and compensating reactor combination $L_T(H)$. This condition exists if the natural frequency of the circuit formed by C_s and L_T is close to the frequency of the induced voltages, f_s

$$\text{i.e } f_s = \frac{10^3}{2\pi \sqrt{L_T C_s \times \ell}} \qquad 9.18$$

Where ℓ is the length of the de-energised line (km). Hence, ignoring system losses, the length of line at which a condition of exact resonance would occur is given by

$$\ell = \frac{10^6}{4\pi^2 f_s^2 L_T C_s} \text{ km} \qquad 9.19$$

$$= \frac{1.195}{C_s} \text{ km} \qquad \text{for } L_T = 8.48 \text{ H}$$

For the twin and quadruple conductor lines used, the length of line is estimated as 111 and 100 km respectively.

Computed voltage waveforms shown on Figs. 9.3 and 9.4 for the twin and quadruple conductor line, respectively, illustrate the build-up of resonant system frequency voltage oscillations to excessive levels. The amplitude of these oscillations exceed normal system voltage after only four or five cycles. The predicted values of lengths of line at which resonance occurs have been validated (i.e 111 and 100km for the twin and quadruple conductor lines respectively). The total zero sequence voltage waveforms also shown on these figures, do not exhibit any build-up of oscillations in this mode. This indicates that, in this case, the phenomenon of resonance

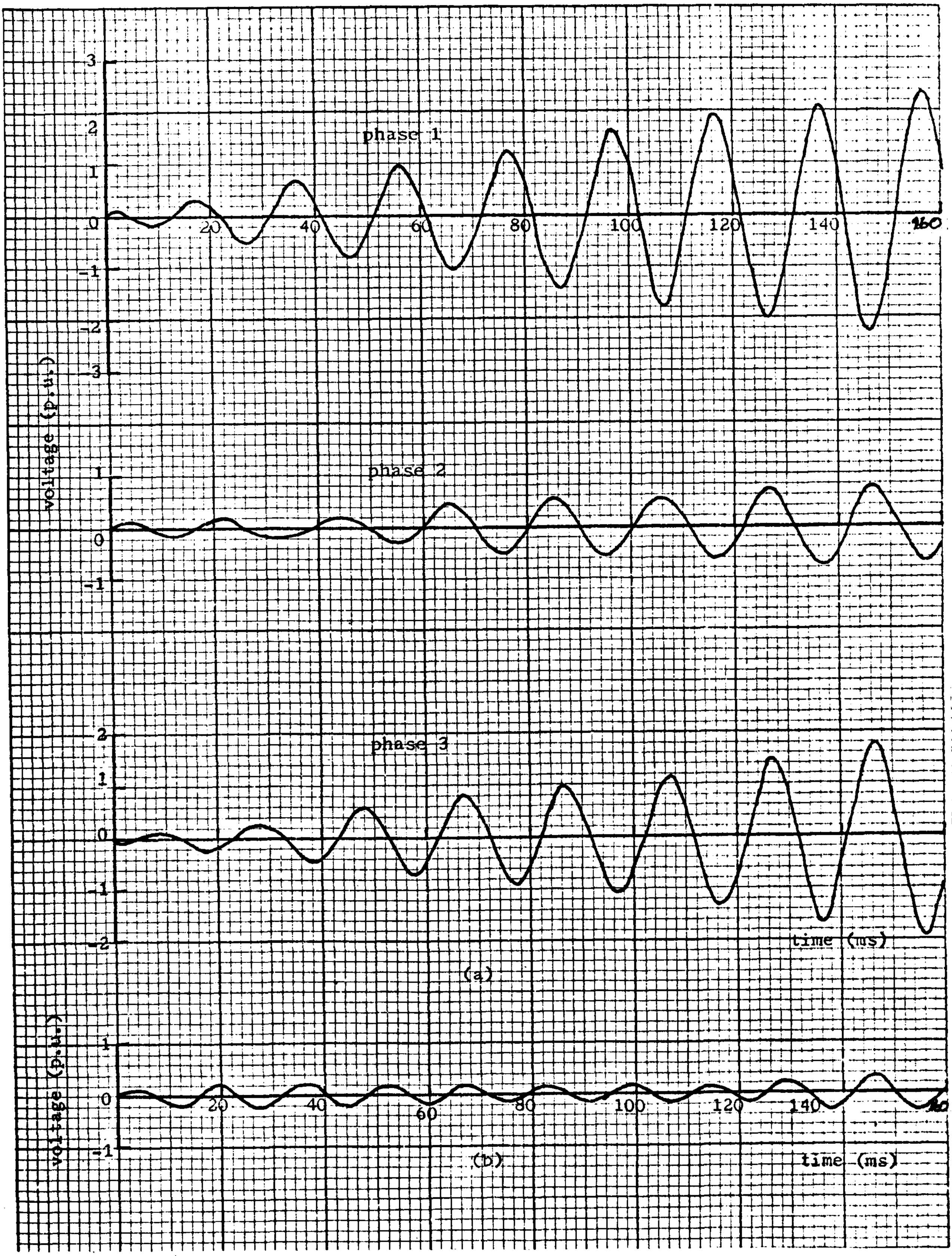

Fig. 9.3 Induced resonant oscillations at the transformer terminating a 111km twin-conductor line (L_T= 8.48H)
a) voltage waveforms on each phase
b) vector sum of voltages.

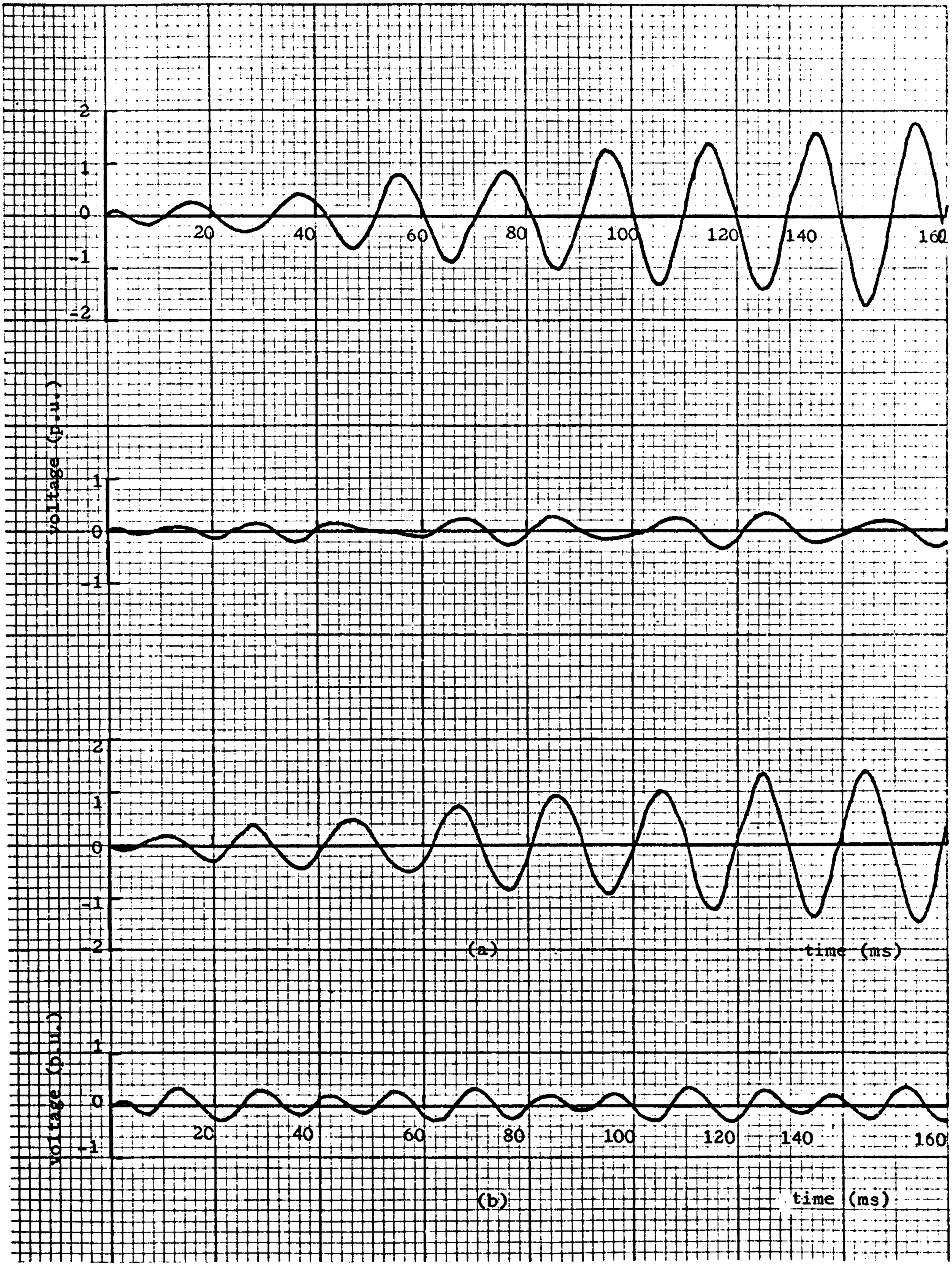

Fig. 9.4 Induced resonant oscillations at the transformer terminating a 100km quadruple-conductor line (L_T= 8.48H)
a) voltage waveforms on each phase

b) vector sum of voltages

occurs primarily in the positive sequence or balancedmode.

Figs 9.5 and 9.6 show maximum overvoltages (within 160 msec. of energising the first circuit) on each of the transformer phases, as a function of line length, for the twin and quadruple conductor lines respectively. Excessive overvoltages in the neighbourhood of the predicted lengths of line at resonance are clearly indicated. This close correlation verifies the analysis based on the simplified equivalent circuit. The overvoltages on the phase conductor occupying the middle position are in both cases less than those on the other phases.

Further increase of the length of line beyond the values predicted above reveals another region of resonance with maximum amplitudes somewhat reduced. Resonance phenomenon in this case occurs predominantly in the zero sequence mode. This is confirmed by the waveforms of Fig 9.7 relating to a 180km twin-conductor line. While there is a steady build-up of the oscillations on the three phases, their vector sum, which is a measure of the zero sequence component of voltage, reveals a rapid intensification of overvoltages.

If the reactor is connected to provide 60MVAr compensation (i.e L_T= 4.465H) instead of 30 MVAr, similar predictions will show that the length of line at resonance is given by

$$l = \frac{2.270}{C_s} \text{ km}$$

This relation gives line lengths of 210.9 and 189 km for the twin and quadruple conductor lines used, respectively. Voltage waveforms relating to the twin conductor line are given on Fig 9.8. Again, resonant oscillations in the positive sequence mode obtain. This is demonstrated by comparison of the constant amplitude zero sequence oscillations with the increasing amplitudes of the voltages on each phase.

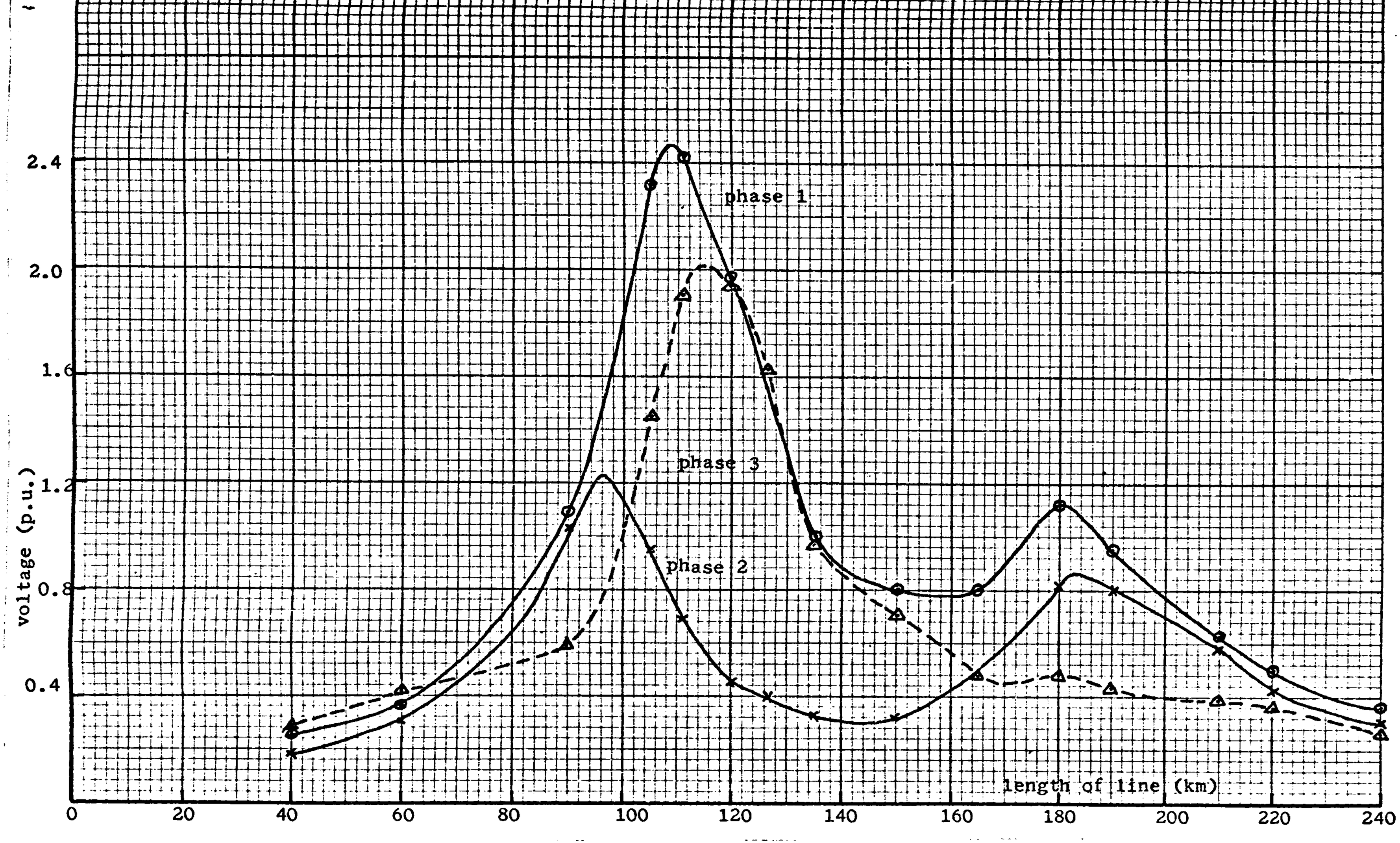

Fig. 9.5 Maximum overvoltages within 160msec as a function of line length for a twin-conductor line (L_T = 8.48H)

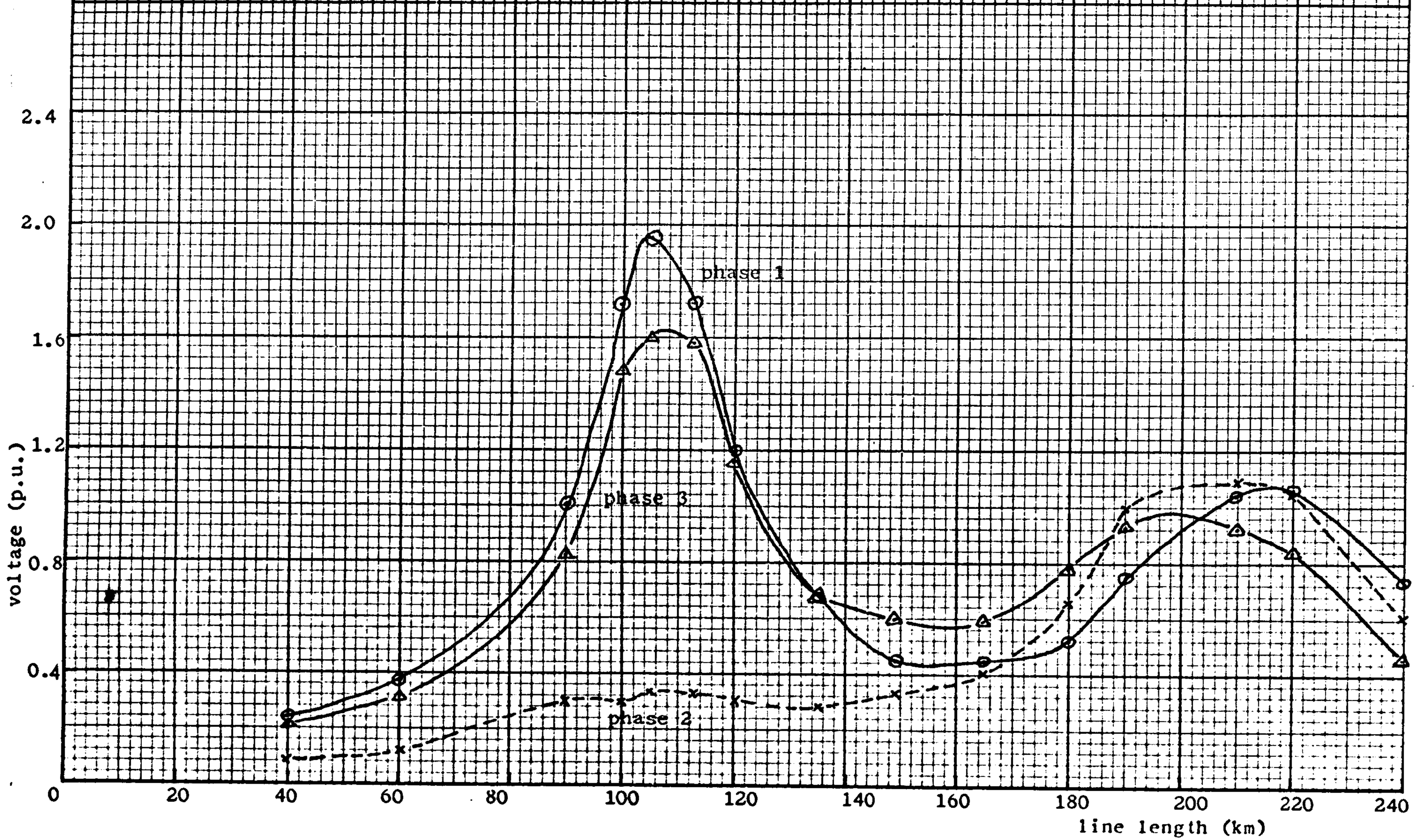

Fig 9.6. Maximum overvoltages within 160 msec as a function of line length for a quadruple-conductor line (L_T = 8.48H)

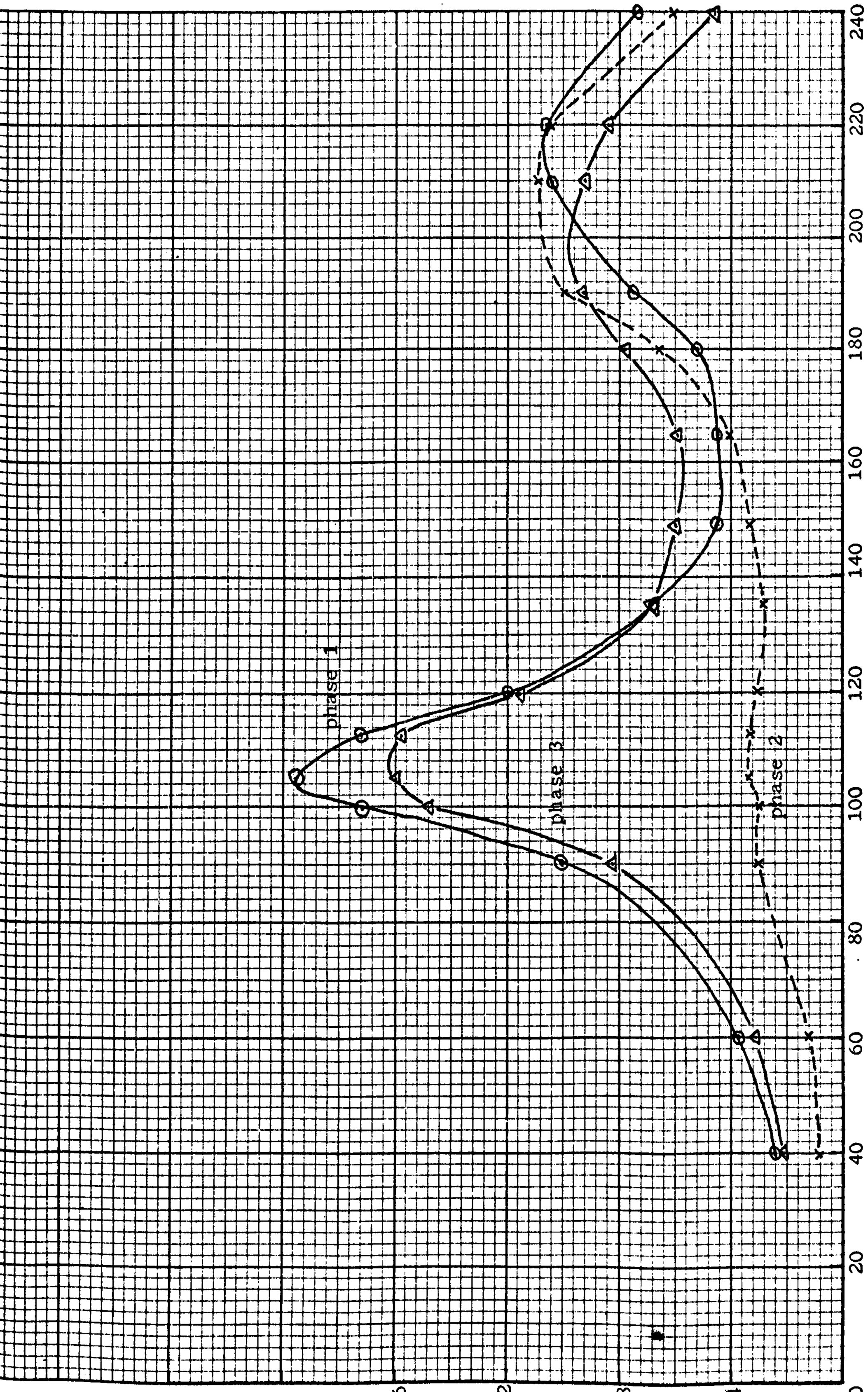

Fig 9.6. Maximum overvoltages within 160 msec as a function of line length for a quadruple-conductor line (L_T = 8.48H)

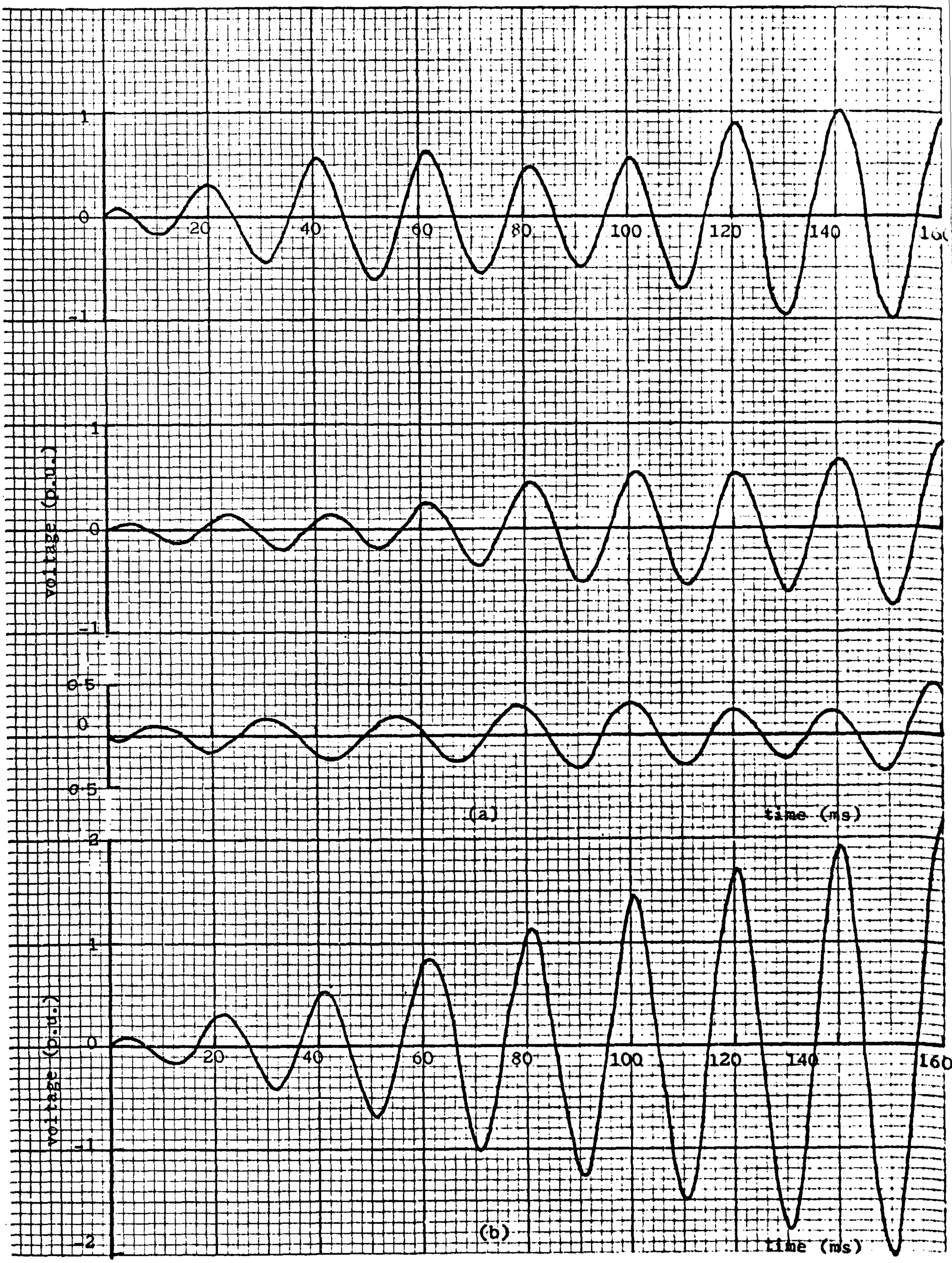

Fig. 9.7 Induced resonant oscillations at the transformer terminating a 180km twin-conductor line (L_T=8.48H)
a) voltage waveforms on each phase
b) vector sum of voltages.

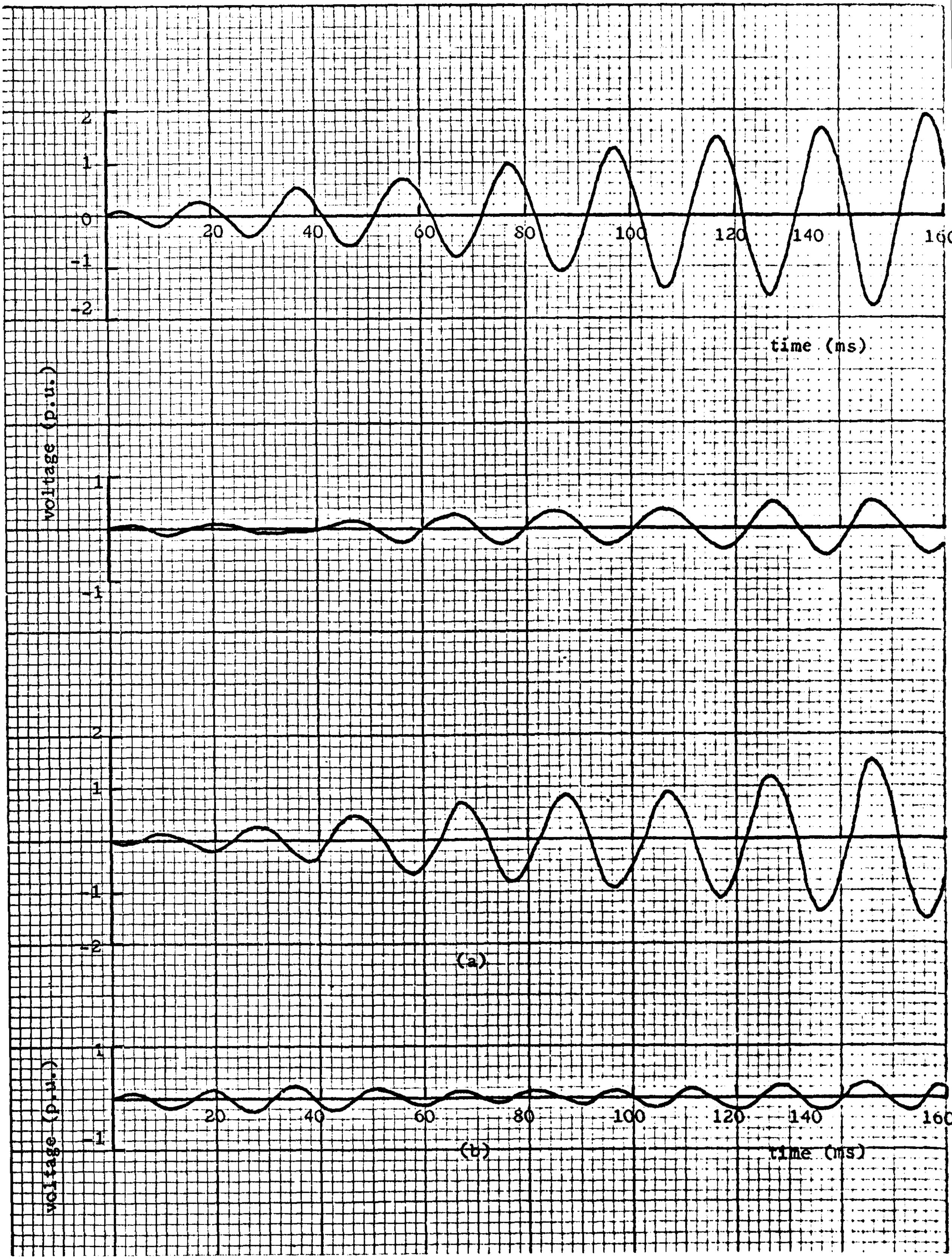

Fig. 9.8 Induced resonant oscillations at the transformer terminating a 210.9km twin-conductor line (L_T= 4.465H)

a) voltage waveforms on each phase

b) vector sum of voltages.

9.7 Residual charge voltage

The resonant oscillations previously analysed could be made more severe if trapped charge voltage is present on the compensated line following its isolation from the system. Depending on the phase displacement between the two circuits, the oscillations excited by the induced voltages could be compounded with the trapped charge voltages to produce severe oscillations.

When the load is dropped from the compensated circuit, the remaining system reactances normally permit the flow of current in the lines leading the voltage by approximately 90 elec. deg. This is the case if the inductive reactance of the termination exceeds the line capacitive reactance. Subsequently, when the circuit breaker contacts at the source-end open at successive current zeros to isolate the line from the system, voltages close to peak system voltages of either polarity will be trapped on the line. The point-on-wave at which the contacts begin to open determines the distribution of the positive and negative polarity voltages trapped on the lines. The decay of this voltage during the breaker clearing time will be ignored.

It can be shown that there are only six different combinations in which the positive and negative polarity voltages are trapped on the individual phases of the line. These are indicated on the first six rows of Table 9.1. Also shown are the resultant phase angle differences between the two circuits, taking the first circuit as reference. It will be noted that the maximum overvoltages obtained for these combinations are most severe when there is 120 elec.deg. phase difference between the circuits, for both the twin and quadruple conductor lines. By comparison of these overvoltages with those obtained without any trapped voltage on the compensated circuit (row 7), it will

TABLE 9.1

Maximum overvoltage as a function of the phase angle advance of the compensated circuit with respect to the energised circuit.

Phase difference between circuits (elec.deg.)	Trapped Charge voltage (p.u.)			Maximum overvoltage within 160 msec.(p.u.)					
				Twin-conductor line . (ℓ=111km; L_T=8.48H)			Quadruple-conductor line (ℓ =100km; L_T = 8.48H)		
	Phase 1	Phase 2	Phase 3	Phase 1	Phase 2	Phase 3	Phase 1	Phase 2	Phase 3
0	1	-1	1	2.58	1.34	-2.27	2.41	-1.66	-2.14
60	1	-1	-1	2.87	-1.26	3.12	-2.68	-1.02	2.86
120	1	1	-1	-3.82	-1.89	-2.30	-3.17	-1.60	2.34
180	-1	1	-1	2.92	-2.25	-2.08	-2.00	-1.83	-2.14
240	-1	1	1	2.10	-1.47	1.47	-1.66	-1.27	-1.41
300	-1	-1	1	-1.98	-1.40	-1.71	1.41	-1.20	1.53
-	0	0	0	2.42	-0.69	-1.90	1.72	-0.30	-1.48

be seen that, in some cases, the residual charge exacerbate the overvoltage magnitudes.

If, instead, the phase difference between the circuits is varied by advancing the phase angles of the energised circuit while keeping the trapped charge voltages on the compensated circuit constant at 1, -1 and 1 p.u. on phases 1, 2 and 3 respectively, curves of maximum overvoltages shown on Fig. 9.9 are obtained. For the twin-conductor line, peak overvoltages occur when the phase difference is 120 elec. deg. on phases 1 and 2, and 270 elec. deg. on phase 3. Corresponding values for the quadruple-conductor line are approximately 90 and 240 elec. deg.

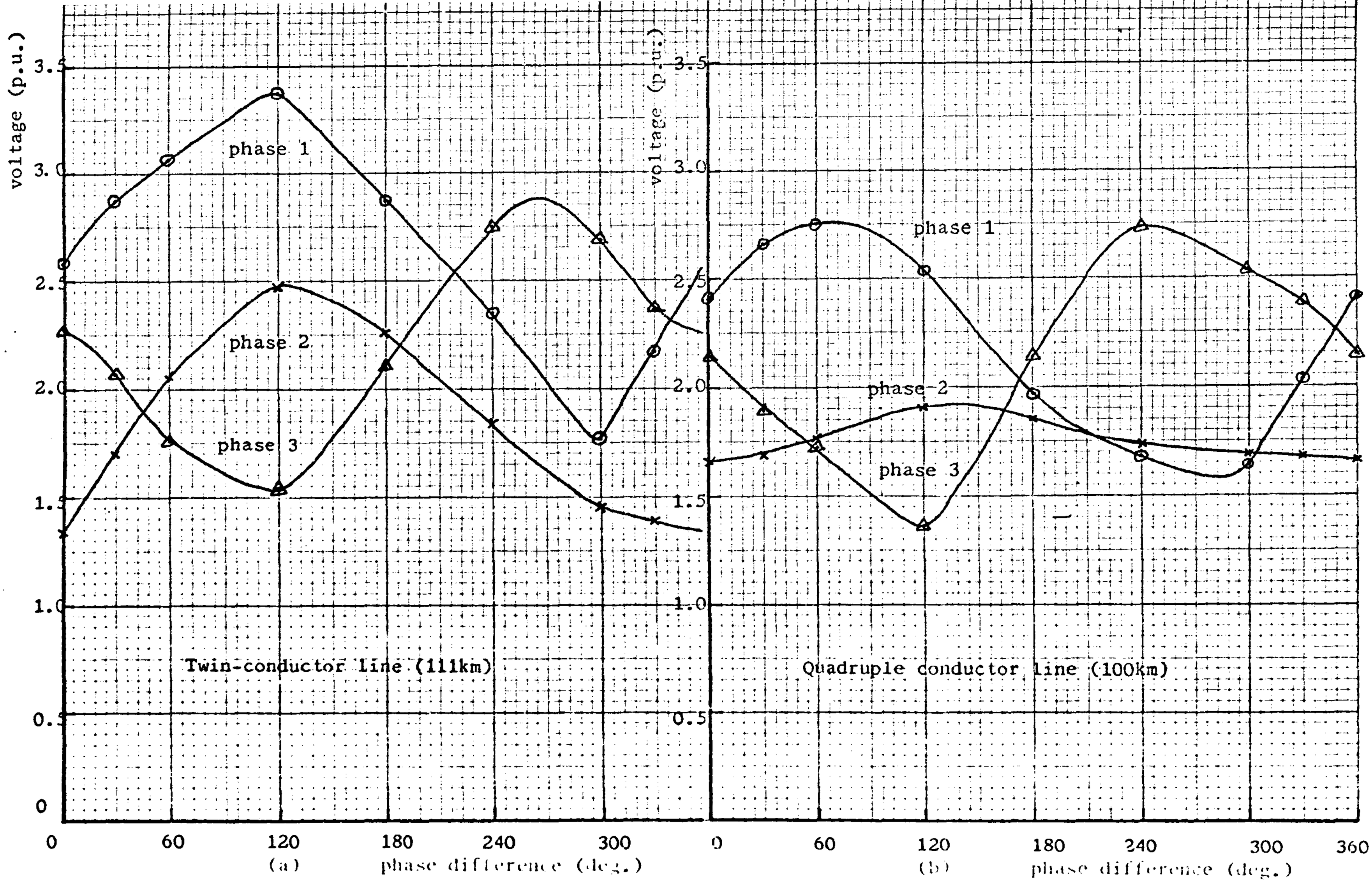

Fig. 9.9 Variation of overvoltages at the transformer with phase difference between circuits (Maximum trapped charge voltage assumed on the compensated circuit and L_T= 8.48H)

9.8 Preventive measures

9.8.1 Line transposition

It is evident from the preceding sections that voltage oscillations on the compensated circuit are attributable to unbalanced electrostatic coupling between the circuits. Consequently, any means of minimising the coupling would be desirable. Transposition of the phase conductors within each circuit and between the two circuits reduces the magnitude of the coupled voltages by effecting a reduction in the electrostatic unbalance which would otherwise be present. Chaston[36] has investigated the effects of various schemes of transposition on voltage oscillations in a near resonant condition . He has shown that, for relatively small shunt reactor ratings, transposition reduces the amplitude of the oscillations substantially. The reduction is not as profound, however, when a resonance condition exists. The oscillations, in this case, although somewhat less severe, would still be excessive.

9.8.2 De-tuning

Since the resonance phenomenon investigated here is primarily linear in nature, the possibility exists of de-tuning the system by ensuring that the natural frequency of the oscillatory circuit is not close to system frequency. Such action, however, may be impractical. This is because the transformer and reactor parameters and location are set by several other considerations such as the degree of compensation, voltage stabilisation and system load requirements.

If the shunt reactors are connected to the tertiary windings by means of low voltage circuit breakers, these reactors may be switched out of the system when the compensated circuit is de-energised, and only re-connected when they are required to provide

compensation for line charging MVA under light load operation . If such operating restrictions are observed, the problem of excessive voltage oscillations could be completely eliminated.

9.8.3 Damping

Introduction of additional losses in series with the transformer and reactor windings to assist in attenuating the oscillations is not desirable on account of the accompanying increase in system losses under normal operating conditions. Insertion of resistors of suitable value between the reactor neutral and earth would not, however, materially affect system losses when the system is operating normally. But since the phenomenon under investigation is essentially in balanced mode for certain lengths of line with relatively small reactor neutral current, inserting a neutral resistor in the zero sequence path would not exert any significant influence on these resonant oscillations. The predominantly zero sequence oscillations arising when longer lengths of line are involved could, however, be damped in this manner. Resistors of a suitable value connected in the delta tertiary windings could provide the necessary losses to damp the oscillations.

9.9 Conclusions

The computer calculations presented in this chapter give somewhat more pessimistic results, since mitigating factors such as system losses and corona, which are inherently present in an actual physical system, have been disregarded. The objective of the investigation was, however, to derive some analytical methods of accurately predicting whether resonant oscillations are likely to be produced, from the knowledge of physical dimensions of the transmission line conductor configuration and the reactive termination parameters. Simple equations which make it possible to identify the potentially dangerous combination of system parameters, have been presented. The validity of predictions made from these equations has been demonstrated by computer analysis of the system. It is shown that, if the reactance of the transformer and reactor units is such that resonance occurs with the effective series coupling capacitance between the circuits at a frequency close to system frequency, voltage oscillations build up to excessive levels. If a reclosing operation on the compensated circuit is activated during this voltage build-up, large switching surges would result.

Resonant oscillations are found to occur in both the balanced and the zero sequence mode, the latter producing somewhat less severe overvoltages.

When residual charge voltages are considered, the phase difference between the two circuits has a dominant influence on the resulting oscillations. These overvoltages tend to be less severe when the two circuits operate in phase.

Transposition of the phase conductors within each circuit and between circuits reduces the coupled voltages. But under conditions of near resonance transposition is not very effective. In

addition, it may not be acceptable as a solution on economic grounds. Insertion of neutral resistors at the reactor for oscillation damping purposes has been found ineffective in some cases. Additional losses introduced in the delta tertiary winding could, if acceptable, assist in damping the oscillations. Total de-tuning could be achieved by providing means of switching the reactors out during the period when the oscillations are likely to develop. If circuit breakers, switching isolators or air disconnect switches are available on the line side of the transformer, this phemomenon could be eliminated by switching off the transformer and reactor unit immediately following de-energisation of the compensated line.

C H A P T E R 1 0

FERRORESONANCE IN E.H.V. DOUBLE CIRCUIT FEEDERS

10.1 Introduction

An extensive literature exists on the subject of ferro-resonance, particularly in single phase circuits. The enormous complexity of the problem has, however, confined previous attempts at a mathematical analysis to some grossly oversimplified circuits. The system is usually reduced to a simple equivalent circuit comprising a single non-linear inductor and one or two capacitors in order to make the mathematics involved less complicated. This does not in any way underestimate the valuable contributions of those who have addressed themselves to this problem in the past, notably Rudenberg [17, 63], Hayashi [64], and Wright [65, 66] among others. The simplified treatment is essential to the understanding of the fundamental concepts and mechanisms relating to ferroresonance in three phase circuits and is also amenable to solution by simple analytical techniques [38, 39]. Due to the fact that ferroresonance in practice may occur under widely varying system constants and conditions, there is a need to develop more general methods to simulate in more detail various pertinent aspects of power systems.

In the context of a practical three phase system where the single capacitance normally used in simplified circuits corresponds to a complex structure of distributed capacitance to earth, between phases and between circuits, and the single non-linear inductance is replaced by a multi-winding auto-transformer with its interacting electrical and magnetic complexities, simplified equivalent circuits are inadequate in reproducing realistic system response. For such a complex problem, the development of fast

digital computers has made possible a more comprehensive and rigorous analysis of ferroresonance.

In this Chapter, ferroresonance in double circuit feeder circuits will be analysed with the aid of a computer program presented in Chapter 7. The program will be used to examine the effects of those parameters of the transmission line and the transformer which influence the ferro-oscillations produced at the transformer. This investigation is by no means an exhaustive study of all aspects associated with ferroresonance in double circuit feeders. It is more an attempt to demonstrate the potential applications of the new method presented in Chapter 7 in assessing the significance of system parameters on the occurrence of ferroresonance. Some examples of the ferro-oscillations will be presented. Table 10.1 contains all the pertinent details of the waveforms presented in this Chapter.

Fig. No.	Number of Transformer Core Limbs	Line Length (km)	Line Conductor Construction Code *	Delta tertiary Winding Code **	System Voltage %	Code for Initial Voltages on phases 1, 2 & 3 ***
10.3	3	45	4	1	100	1
10.4	5	45	4	1	100	1
10.5	3	150	4	1	100	1
10.6	5	150	4	1	100	1
10.7	3	45	4	0	100	1
10.8	5	45	4	0	100	1
10.9	3	45	4	2	100	1
10.10	5	45	4	2	100	1
10.11	3	150	4	2	100	1
10.12	3	45	4	1	75	1
10.13	5	45	4	1	75	1
10.14	3	45	4	1	125	1
10.15	5	45	4	1	125	1
10.16	5	45	4	3	100	1
10.17	3	45	2	1	100	1
10.18	5	45	2	1	100	1
10.19	3	150	2	1	100	1
10.20	5	150	2	1	100	1
10.21	3	45	4	1	100	0
10.22	5	45	4	1	100	0
10.23	3	7.5	4	1	100	1
10.24	5	30	4	1	100	1
10.25	5	15	4	1	100	1
10.26	5	7.5	4	1	100	1

* 2 = twin
4 = quadruple

** 0 = open delta winding
1 = closed delta winding
2 = reduced delta winding impedance
3 = 2 p.u. resistor in each delta winding phase

*** 1 = 1, 1 and -1 p.u.
2 = 0.5, 0.5 and -0.5 p.u.

Table 10.1 : Pertinent details of the ferroresonance waveforms

10.2 System studied

Only one aspect of the transient ferroresonant oscillations in double circuit feeders is being investigated in this Chapter. Particular interest in this phenomenon arises from recent reports of its existence in H.V. systems operated by the Bonneville Power Administration (BPA) in Oregon [38, 39], the South of Scotland Electricity Board (SSEB) and the Central Electricity Generating Board (CEGB) in Britain, and also in the State Electricity Commission's distribution system in Victoria, Australia [66]. The sequence of events which led to the incidence of ferroresonance involved the disconnection of one transformer feeder circuit from its source after its load had been shed. The other circuit, in close proximity to it for the whole of its length, remained énergised. The consequences were overheating and gassing of the transformer in cases where the ferro-oscillations are sustained.

The transmission lines simulated on the computer model consists of the twin and quadruple conductor double circuit lines described in Chapter 7. Details of the auto-transformer terminating one of the circuits and its comprehensive mathematical model are also included in that Chapter.

10.3 Basic features of ferroresonance

The fundamental elements in a ferroresonant circuit are a capacitance and a non-linear inductance connected either in series or in parallel, and a source of energy. The capacitance could be that of a capacitor deliberately connected to the transformer terminals, or it could be the distributed capacitance of transmission lines or cables feeding the transformer. The non-linearity of the inductance constitutes the essential difference between this circuit and that corresponding to a linear resonance condition discussed in Chapter 9. One practical aspect of such an inductor is a transformer where the flux path is formed predominantly by the iron core. In this case the inductance varies in a manner which is dependent on the current and flux linkages as characterised by the B/H curve. This relationship between the flux density B, and field strength H, is multi-valued and is dependent on previous magnetic history. In this study, however, a single-valued B/H curve is used since the effects of hysteresis do not have a profound influence on the essential features of the type of ferroresonance being investigated[67].

The B/H characteristics of transformers normally exhibit three main regions :

(i) a region of high permeability of the iron core associated with the unsaturated condition;

(ii) a region of wide variation of permeability signifying saturation of the iron and dependent on the time integral of the applied voltage waveform; and

(iii) a region where the permeability of the iron approximates that of the air, indicating a severely saturated condition.

10.3.1 Mechanism of ferro-oscillations in double-circuit feeders

The mechanism of ferroresonance in double circuit feeders will be explained with the aid of a simplified single-phase circuit shown in Fig. 10.1 (ii), where X_T represents the effective non-linear reactance of the unloaded transformer. This circuit is similar to that shown on Fig. 9.1 (v) of Chapter 9, and is equivalent to the system shown on Fig. 10.1 (i). The lumped electrostatic delta circuit isobtained by a process of approximations from the complete capacitive equivalent circuit of the double circuit line, as described in section 9.4. The susceptances of the line were defined as follows :

B_{11} = positive sequence self susceptance

$B_{0'0'}$ = zero sequence self susceptance

$B_{0\ 1}$ = mutual susceptance between the positive sequence voltage on the energised circuit and the zero sequence currents in the de-energised circuit

The first circuit which is energised is represented by a voltage source (E) and the transformer (X_T) is connected at the end of the de-energised circuit.

Depending on the previous history of the system, a voltage having an amplitude up to normal peak system voltage may be trapped on the capacitance represented by $B_{0'0'} + B_{0'1}$ at the instant when the circuit is de-energised by opening the circuit breakers at both ends of the feeder. Due to the high permeability of the iron corresponding to the unsaturated core, this voltage will remain approximately constant for as long as the core remains unsaturated. The flux linkages defined by the time integral of the voltage applied to the transformer would then begin to increase until the region of saturation is reached. At this point, the permeability of the iron

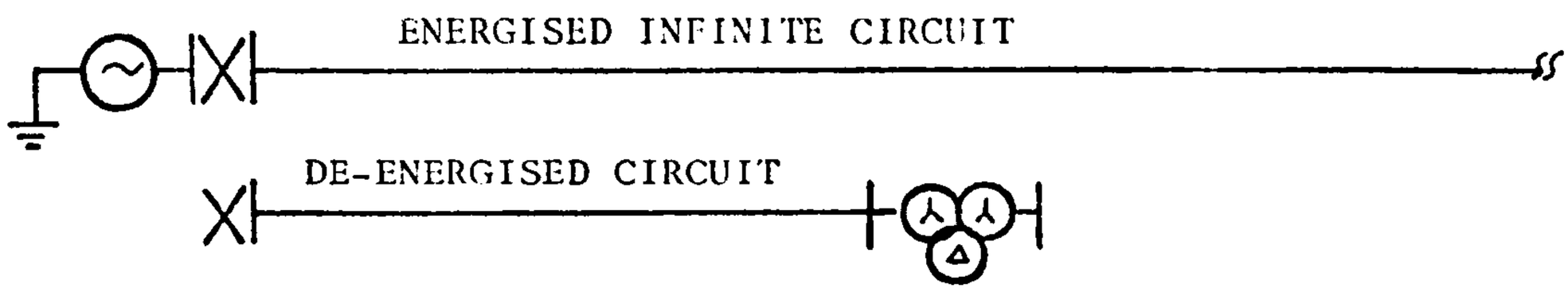

(i)

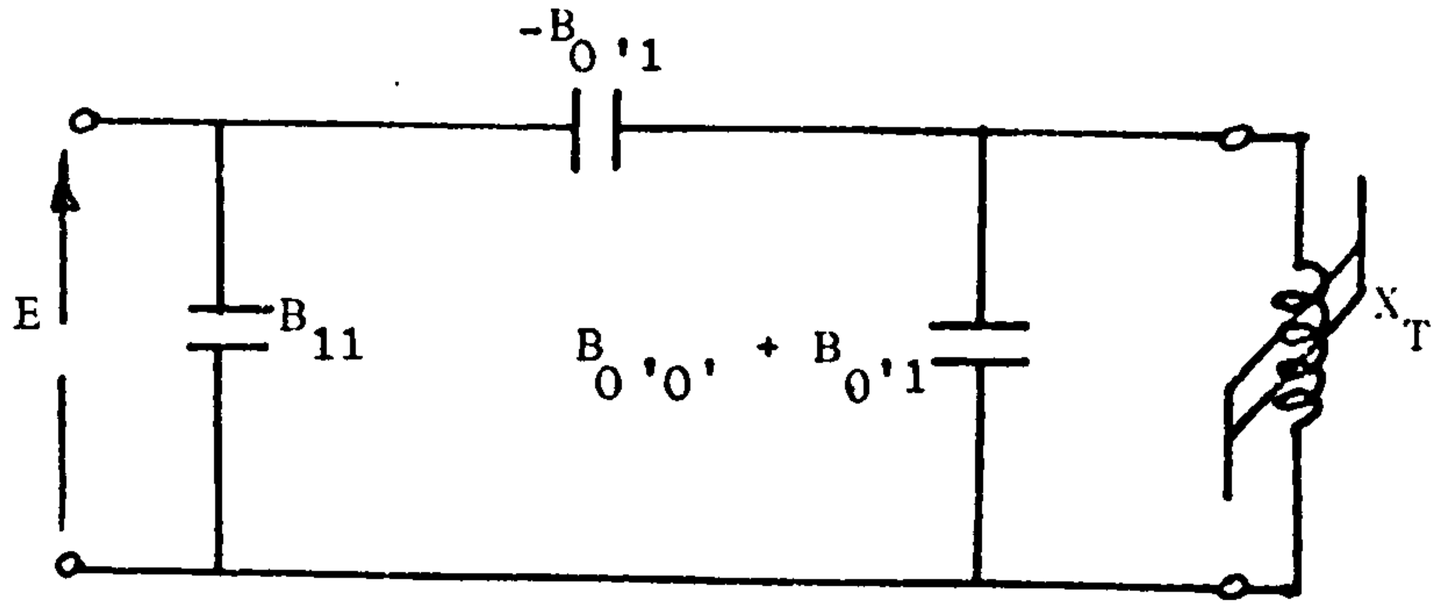

(ii)

Fig. 10.1 (i) Double circuit system studied
(ii) Equivalent circuit

drops drastically and a large current pulse will be driven into the transformer due to the low value of inductance obtaining. As the energy previously embodied in the electrostatic field drains into the transformer magnetic field, the voltage collapses to zero and the current attains its peak value. At this instant, the energy in the magnetic field will be transformed back into the electrostatic field of the lines and the equivalent capacitance ($B_{0,0'} + B_{0',1}$) will be charged with opposite polarity voltage until a voltage peak is reached. At the same time the current decays to a relatively small value. Due to voltage of opposite polarity being applied to the transformer, the flux linkages will be driven towards zero. This state will persist until the flux linkages in the core have reached saturation level in the reverse direction. The sequence of events will then be repeated.

10.3.2 Characteristics of waveforms

The current waveforms will be characterised by large saturation current pulses and the flux linkages in the core will vary in a somewhat triangular fashion. The voltage waveforms will consist of trapezoidal pulses decaying in a manner dictated by system losses. If, however, the energy dissipated in the transformer is made good by dynamic induction from the adjacent energised circuit through the sequence coupling capacitance represented by $-B_{0',1}$, the oscillations may persist. The concept of the natural frequency of an oscillatory circuit has no meaning in this case, however, as this frequency varies in accordance with the magnetic state of the transformer core. This causes the oscillatory circuit to have a broad band of tuning.

Since the flux linkages required to saturate the core are constant, the area under the voltage curve, which is a measure of this quantity, will be approximately constant over the duration of

the transient ferro-oscillations. Hence regions of amplitude associated with lower values of inductance will correspond to higher frequencies while low amplitude oscillations will be characterised by lower frequencies due to the higher effective values of inductance. As the amplitude of the transient ferro-oscillations decays in an exponential manner determined by system losses and the amount of energy replenished from the energised circuit, its period will decrease with time proportionately. During this variation of trapped voltage oscillation frequency, there is a possibility of these oscillations being 'locked-in' at the frequency of the induced voltages. In this case, ferroresonance will be sustained. If, however, the difference between the two frequencies is relatively small, the waveforms will be characterised by alternating regions of high amplitude at the average frequency, and low amplitude at the difference frequency, exhibiting a beating phenomenon characteristic of resonance in linear circuits.

10.3.3 Superharmonic oscillations

In addition to the fundamental and subharmonic modes of oscillations referred to above, superharmonic components of voltage and current are also present in the waveforms. These components, which are essentially zero sequence quantities, originate from the free oscillations which exist between the transmission line zero sequence susceptance ($B_{0'0'} + B_{0'1}$) and the effective zero sequence reactance of the transformer, X_0. The frequency of the natural oscillations is given by these circuit constants and the losses inherent in the system which also dictate the rate at which the oscillations decay. If the ohmic resistance representing series and parallel losses in the transformer is small in comparison with the oscillation resistance given by $\sqrt{X_0/(B_{0'0'} + B_{0'1})}$, as is normally

the case, the frequency could closely be approximated by $1/2\pi\sqrt{L_0(C_{00'} + C_{0'1})}$. These components are capable of effecting substantial distortion of the transformer voltage waveform.

10.3.4 Linear resonance

Prolonged fundamental frequency resonance is possible between the effective inductance of the transformer when it is not in a highly saturated state, and the capacitive reactance of the lines. Conditions conducive to such a phenomenon arise if the effective capacitance shunting the transformer is relatively small such that the trapped charge is not sufficient to subject the transformer to severe saturation. Consequently, the effective inductance would be relatively large with a low degree of non-linearity, and could resonate with the line capacitance at system frequency. Sustained oscillations could result.

10.3.5 Factors affecting ferroresonance

The character of the ferroresonant oscillations is a function of several system constants and conditions. These are :

(i) initial conditions of the system as specified by the trapped voltage and the residual flux in the core,

(ii) saturation characteristics of the core,

(iii) geometrical form of the core,

(iv) transformer windings connection and presence of a delta tertiary winding,

(v) the capacitance distribution of the transmission circuit as determined by the line physical construction, configuration and dimensions, and

(vi) the energy losses inherent in the systems.

In the subsequent sections of this Chapter, the effects of some of these factors in modifying the ferro-oscillations will be assessed.

10.4 Effects of ferroresonance

Although ferro-oscillations may not have severe consequences with regard to voltage insulation levels of the system, they do cause overheating of the transformer which could reach proportions sufficient to damage its insulation. The superharmonic currents generated cause interference with neighbouring communications circuits which may reach unacceptable levels.

10.4.1 Thermal effects

During the periodic saturation of the core while the transformer is in a state of ferroresonance, the permeability of the iron is substantially reduced to the same order of magnitude as that of the surrounding air. The resulting high values of flux linking adjacent metal parts generates heat in the tank and core clamping structures. If ferroresonance is sustained, the elevated temperatures could create localised hot spots leading to a rapid deterioration of the insulation. Overheating is further accentuated by the presence of relatively large zero sequence components of current. Associated with this heating phenomenon is the problem of gassing caused largely by the decomposition of oil or solid insulation. The incidence of such overheating and gassing has been reported in the literature [38, 39] under conditions similar to those being investigated in this Chapter. These consequences reportedly occurred nine minutes after the circuit feeding the transformer was de-energised. Hence the problem arises only when the ferro-oscillations are sustained.

Depending on the duration and mode of the ferro-oscillations, overheating of the transformer windings and degradation of its associated insulation may be attributed to high current pulses

drawn by the transformer during severe saturation of the core. The magnitude of these saturation currents could be several times greater than the normal magnetising currents. Depending on the duration of the phenomenon, the heat generated mainly by ohmic-losses and stray losses within the winding conductors and between conductor strands may be severe.

10.4.2 Insulation co-ordination

Under conditions where ferroresonant voltages oscillate at or near system frequency, voltage magnitudes marginally higher than normal system voltage could develop. This does not pose severe problems as far as system insulation is concerned if both lines operate at the same voltage level. If, however, the voltage level of the de-energised circuit is much lower than that of the live circuit, the magnitude of the coupled voltages could form a significant fraction of the normal voltage on the de-energised circuit. In such a case, the high frequency trapped charge voltage oscillations will be exaggerated, and the insulation of this circuit could be considerably stressed.

Re-energisation of the circuit while it is in a state of ferro-resonance could increase the initial voltages injected into the line. Consequently, large transient voltage surges will oscillate in the lines.

10.4.3 Inductive interference

Although the amplitudes of the superharmonic zero sequence components of current are small relative to system voltage, the inductive effects of these components on communication circuits parallel to the power lines may be objectionable. Since these currents are in time phase, the flux linkages which they produce separately with neighbouring communications circuits are additive.

This, together with the relatively high frequencies of the zero sequence currents, could cause such interference as to adversely affect the proper operation of the communication circuits.

10.5 Induced voltages

In Chapter 9, open circuit voltages coupled on to a de-energised circuit from a live circuit were investigated analytically. The existence of a prominent zero sequence component on the induced voltage waveforms was established. Results of a similar computation, with the exception that the de-energised circuit is now terminated in a five-limb transformer with a closed delta winding, are presented in Fig. 10.2. The transmission line in this case is of quadruple construction and is 45 km long. Since the induced voltages are independent of the length of the de-energised circuit if it is coupled to the energised circuit for the whole of its length the waveforms of Fig. 10.2 will apply irrespective of line length. The waveforms relate to a steady state condition where any residual voltage which may have been trapped on the line at the instant of dropping the circuit has completely decayed.

Comparison of the induced voltage waveforms of Fig. 10.2 with the open-circuit voltage waveforms shown on Fig. 9.2 indicates differences which are attributable to the impedance of and magnetic coupling within the transformer. In particular, the finite loading by the transformer zero sequence impedance reduces the vector sum of the transformer voltages from a peak value of 0.12 p.u. to 0.05 p.u. The peak voltages in each phase are 0.08, 0.02 and 0.08 p.u. of normal line-to-earth voltages, having a total phase displacement of 122 deg. The zero sequence components are caused by the unbalance existing in the electrostatic coupling between circuits and the magnetic coupling between the phases of the transformer.

Examination of the line currents reveals the predominance of the zero sequence components. All these currents are equal in magnitude (1.3 A peak) and time phase, and their amplitudes depend on the effective zero sequence impedance of the transformer.

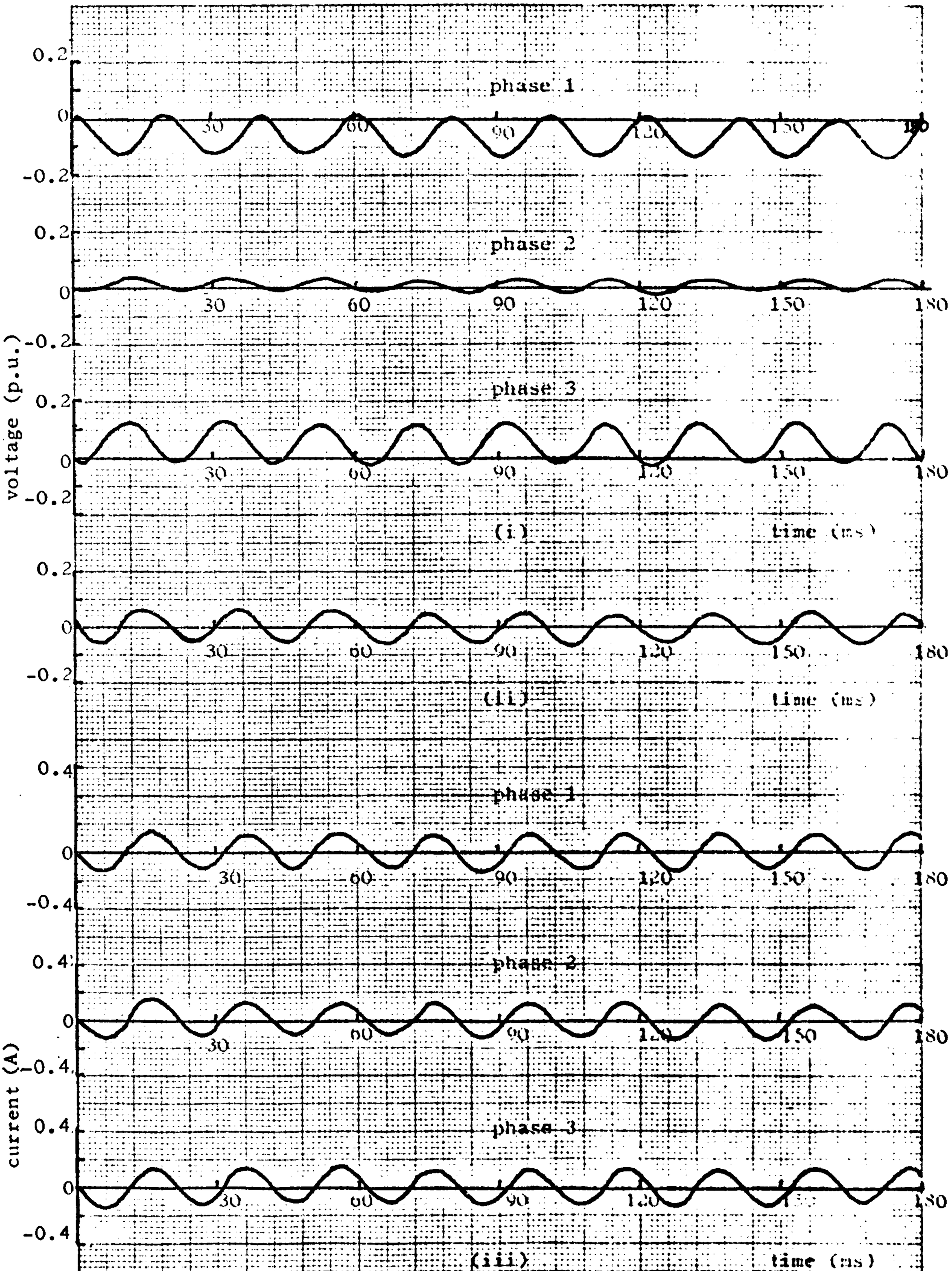

Fig. 10.2 Induced voltages and currents on the de-energised circuit phases terminated in a five-limb transformer with a delta tertiary winding
(i) Transformer primary voltage waveforms
(ii) Vector sum of transformer primary voltages
(iii) Transformer current waveforms

10.6 Transformer design parameters

The design parameters of the transformer have a profound influence on the magnitude and waveshapes of the ferro-oscillations, the most significant being the core saturation characteristics and the transformer zero sequence impedance. The former is governed by the characteristics of the iron comprising the magnetic circuit while the latter is dependent on the following factors :

(i) the geometry and type of the core,

(ii) the manner in which the windings are connected and the method of earthing the transformer neutral,

(iii) the physical arrangement of the windings on the core, and

(iv) the impedance of the delta tertiary windings, if present.

These transformer characteristics, together with the initial conditions and system losses are the critical features which govern the character of the widely divergent oscillations pertaining to the ferroresonance phenomenon. In the following sections, results of computer studies showing the effects of some of these parameters will be presented. Except where otherwise stated, it will be assumed that the delta tertiary winding is closed and the trapped voltages left on the phase conductors (phases 1, 2 and 3) at the time of de-energising the circuit are 1, 1 and -1 p.u. respectively, with a phase difference of 120 deg. between normal system voltages on the two circuits prior to de-energisation. Core losses are simulated by a resistance shunting the magnetising impedance and energy dissipation in the windings is simulated by resistances in series with the leakage reactances.

There are two primary sources of zero sequence

quantities in the circuit studied. These are :

(a) system frequency zero sequence currents produced by induction from the energised circuit voltages, whose amplitude is determined by the zero sequence impedances of the transformer and transmission line. These currents produce zero sequence component of voltage at the transformer whose magnitude depends on the sequence currents permitted to flow.

(b) superharmonic zero sequence currents caused by the free oscillations between the feeder and transformer zero sequence impedances. These currents produce zero sequence voltages at the transformer terminals whose frequency depends on the circuit constants and losses. The voltage amplitude is governed by the initial conditions, sequence component parameters and the ohmic losses in the system.

10.6.1 Transformer geometry

Transformers and auto-transformers of a composite core structure are almost universally used in H.V. systems in Britain in preference to banks of three single phase units. The most common forms are the three- and five-limb types which have been described in Chapter 7. These two types differ significantly in the impedance they present to zero sequence currents. Garin [68, 69] has not only demonstrated the dissimilarities between the zero sequence characteristics of these two types, but also the wide variation which may exist between these characteristics and those pertaining to the corresponding positive sequence impedances. These differences may be explained in terms of the behaviour of the flux linkages in the interlinked magnetic core of the three- and five-limb transformers when the unit is excited by the various sequence voltages.

The transformer zero sequence impedance is a major factor influencing the ferro-oscillations and their duration. The widely varying waveforms yielded by the two types of core used in this study are mainly attributable to the manner in which the two transformers behave in the zero sequence mode.

In a three-limb transformer, the zero sequence flux linkages in each limb are at every instant the same in magnitude and direction and the return is through the high reluctance non-magnetic air path. The resulting zero sequence impedance is therefore appreciably reduced and the flux linkages between windings on different limbs is negligible when the transformer is excited by zero sequence quantities. This is at variance with the positive and negative sequence fluxes which have a closed magnetic circuit through the iron core. Consequently, a three-limb transformer exhibits an open circuit zero sequence impedance which is much lower than the positive sequence impedance and also much less subject to saturation.

In a five-limb transformer, on the other hand, the zero sequence fluxes return primarily through the outer core legs. Due to the essentially independent magnetic circuits for each phase, the transformer behaves in a similar manner as a bank of three single phase units in respect of zero sequence components. Since the flux is confined almost entirely within the iron, the zero sequence impedance is relatively large in comparison with the positive sequence impedance and with the zero sequence impedance of a three-limb transformer. In addition, the core is easily saturated even at relatively low values of zero sequence voltages, producing an impedance varying widely with voltage. However, the presence of a delta-connected tertiary winding which provides a finite impedance

to zero sequence quantities tends to reduce the wide variation, since it effectively appears in parallel with the open circuit zero sequence impedance.

10.6.1.1 Three-limb transformer

Fig. 10.3 shows voltage and current waveforms for the three-limb transformer. In this case, the length of the quadruple conductor line is 45 km. Examination of this Figure will show that, for a three-limb transformer, the trapped voltage oscillations having a frequency near the fundamental system frequency, persist for about 13 cycles before the waveforms degenerate into lower amplitude sub-harmonic oscillations. Voltage amplitudes up to 1.4 p.u. are obtained. The first 13 cycles are also characterised by large amplitude currents during saturation of the core. Subsequently, the saturation currents are greatly reduced during the subharmonic oscillations. The superharmonic oscillations which are super-imposed on the voltage and current waveforms are in time phase and hence constitute zero sequence quantities. As explained in section 10.3, the frequency of this component (400 Hz) is related to the zero sequence impedances of the line and the transformer. Neglecting system losses, the equation for the natural frequency of oscillations shows that the effective zero sequence inductance of the transformer is approximately 0.5 H.

The near coincidence of the system and the trapped charge oscillation frequency during the first 13 cycles is indicated by the low beat frequency of about 7 Hz, which is evident on both the voltage and current waveforms.

In spite of the unbalanced voltages initially trapped on the lines, the effectiveness of the delta tertiary winding in balancing subsequent oscillations is demonstrated. The system

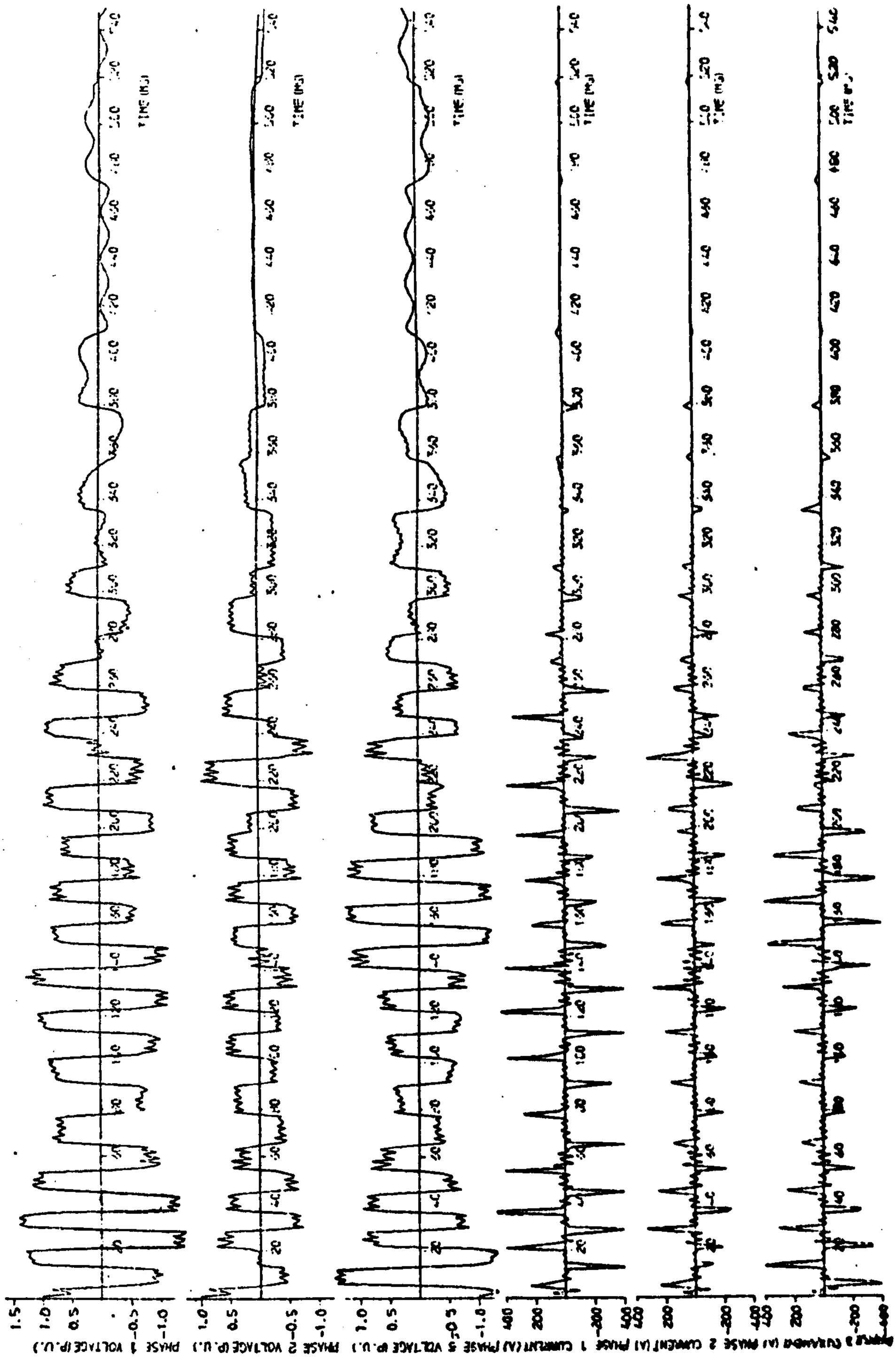

Fig. 10.3 : 45 km quadruple conductor line terminated in a 3-limb transformer with closed delta winding

frequency voltages coupled from the energised circuit became more evident during the subharmonic mode of oscillations. The relatively low value of the transformer zero sequence impedance permits sufficient energy transfer from the energised circuit to neutralise to some extent the effects of losses, and limits the amplitude of the superharmonic voltage oscillations superimposed on the transformer voltage waveforms.

10.6.1.2 Five-limb transformer

The voltage waveforms of Fig. 10.4 relating to a five-limb transformer exhibit highly damped trapped charge oscillations. Due to the relatively high zero sequence impedances, the energy induced from the energised line is not sufficient to sustain these oscillations and the delta tertiary winding losses become more effective in damping these oscillations.

A notable and typical feature of the voltage waveforms is the initially large amplitude of the high frequency oscillations - approximately 50 per cent of the magnitude of the trapped voltage. The zero sequence voltage drop across the transformer impedance due to the superharmonic current oscillations is amplified by the relatively large transformer zero sequence impedance. The effective zero sequence inductance of the transformer, derived from the line zero sequence capacitance and oscillation frequency (225 Hz), is approximately 1.6H, if losses are ignored. This value is more than three times larger than that relating to the three-limb transformer.

10.6.1.3 Effect of line length

Waveforms similar in character to those shown on Figs. 10.3 and 10.4 are presented in Figs. 10.5 and 10.6 for the three- and five-limb transformers respectively and for a line length of 150 km. The increased line length has the effect of reducing the frequency and increasing the amplitude of the superharmonic current

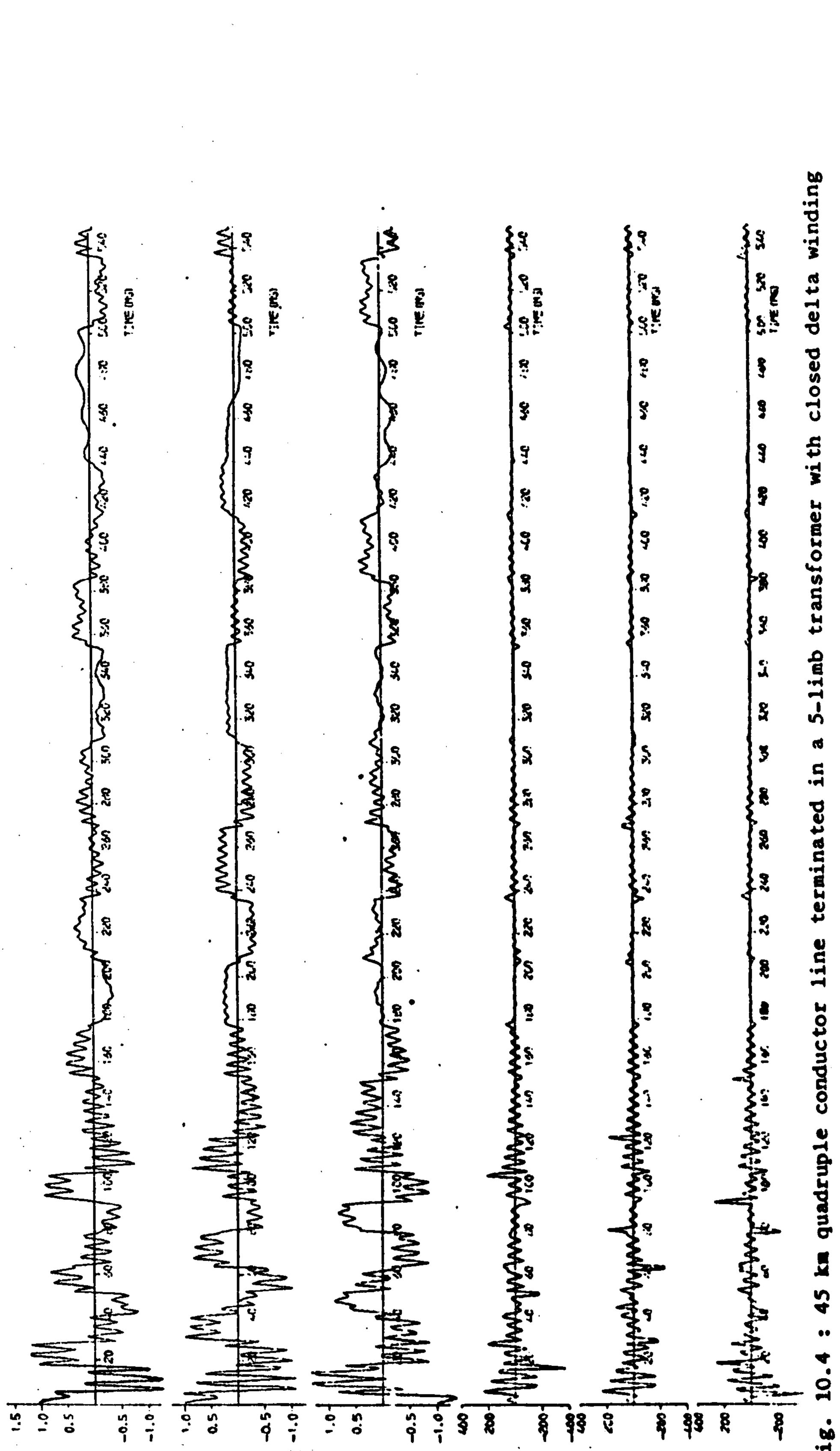

Fig. 10.4 : 45 km quadruple conductor line terminated in a 5-limb transformer with closed delta winding

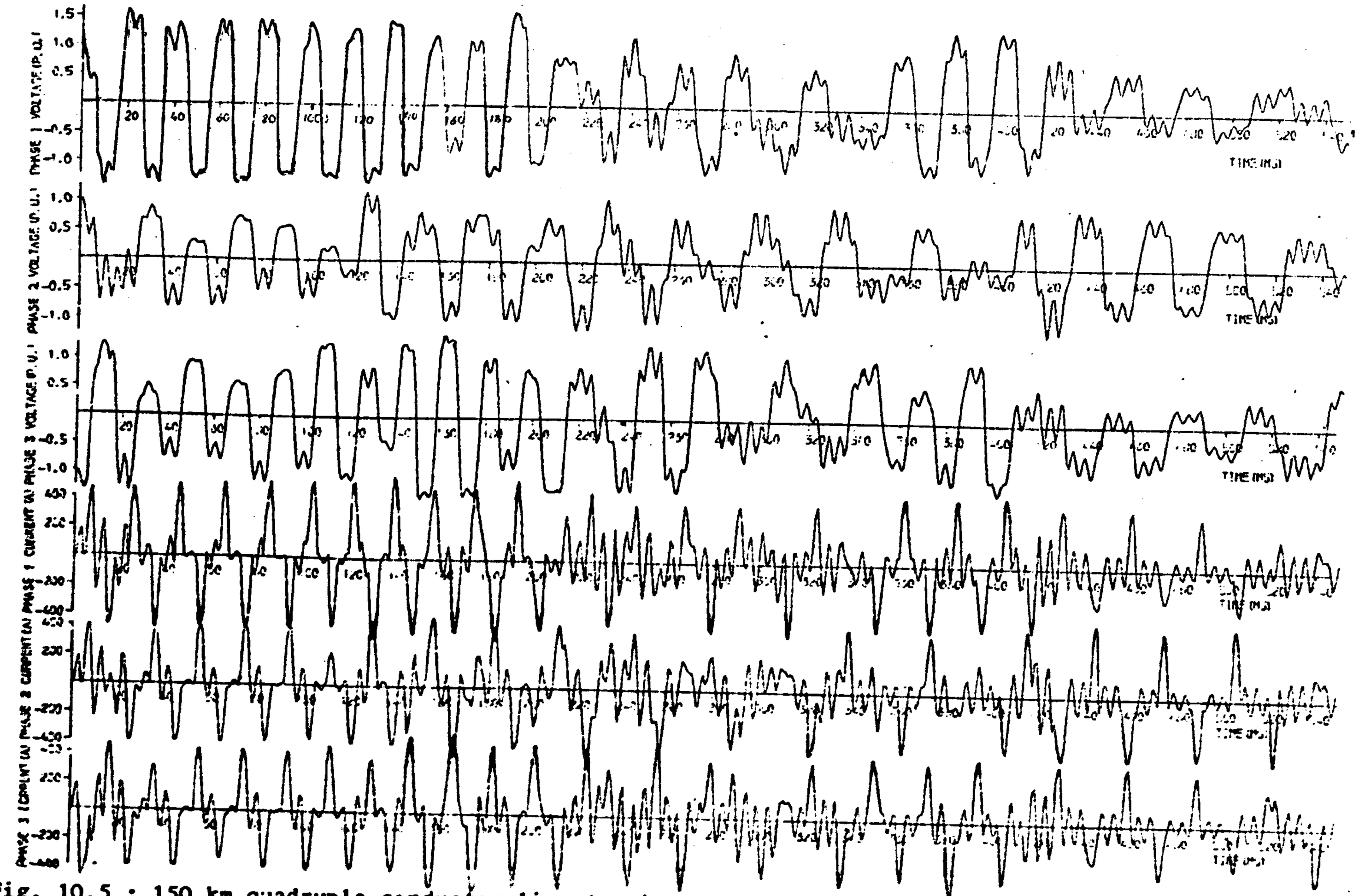

Fig. 10.5 : 150 km quadruple conductor line terminated in a 3-limb transformer with closed delta winding

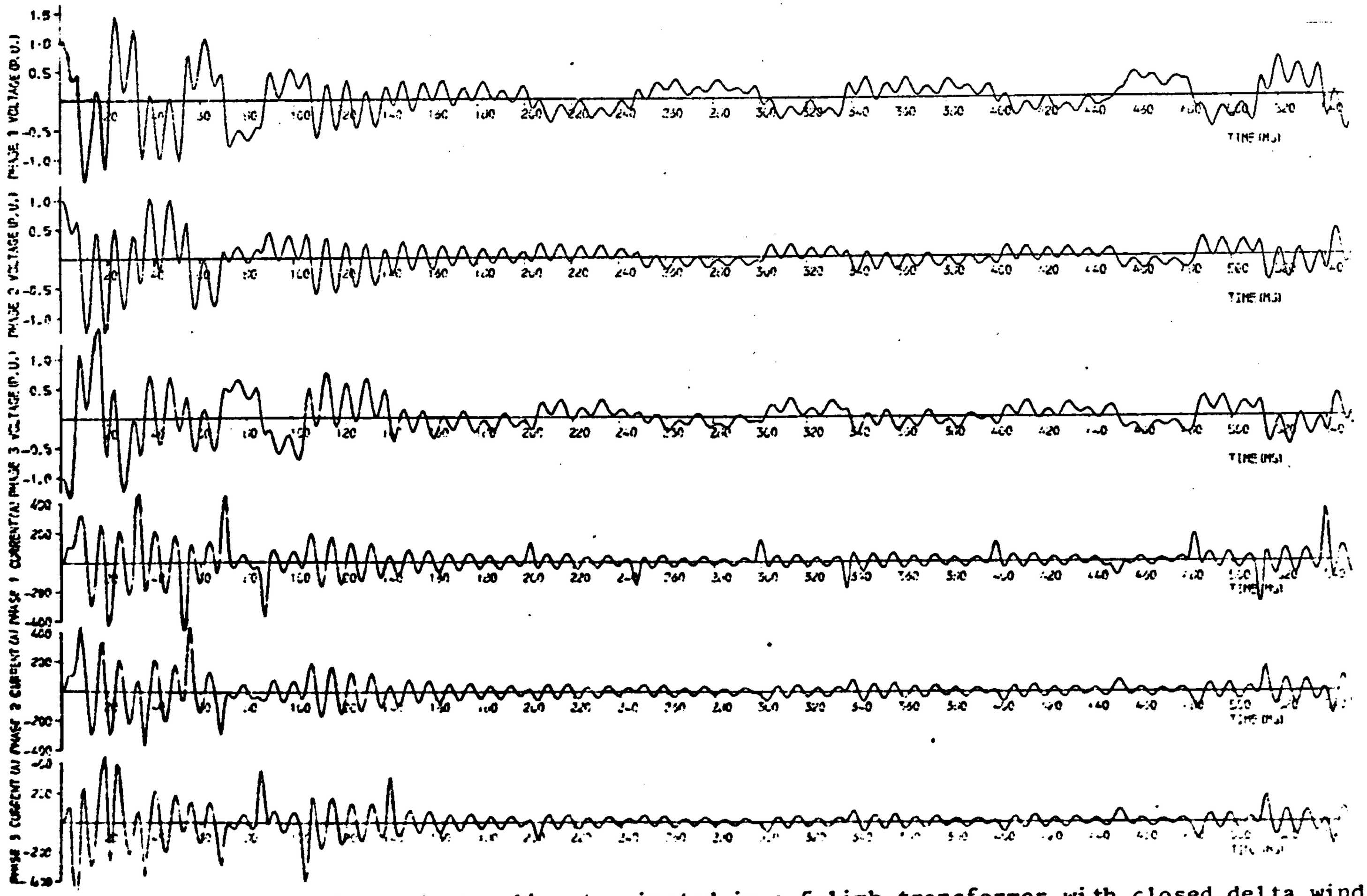

Fig. 10.6 : 150 km quadruple conductor line terminated in a 5-limb transformer with closed delta winding

oscillations. This will be discussed further in section 10.7.3. Examination of the waveforms of Fig. 10.5 again illustrates the near coincidence of the trapped voltage oscillation frequency with system frequency as demonstrated by the low modulation frequency shown on the voltage and current waveforms.

10.6.2 Delta tertiary winding

Normal practice in Britain is to provide a delta tertiary winding for auto-transformers with solidly earthed neutrals. This additional winding is normally required for such purposes as :

(i) to suppress the flow of third harmonic currents in the transmission lines and stabilise the system neutral,

(ii) to provide connection for synchronous or static condensers or shunt reactors for reactive compensation, and

(iii) to provide power for station services and local loads.

A delta-connected tertiary winding has a significant effect on the transformer zero sequence impedance and on the duration of the ferro-oscillations. By furnishing a low impedance shunt path to the flow of zero sequence currents which circulate in its winding, it reduces appreciably the zero sequence component of voltage at the transformer. Depending on its impedance in relation to the transformer magnetising impedance and line reactances, it provides damping for the trapped charge oscillations.

The generally accepted view that the presence of a delta tertiary winding negates the persistence of ferro-oscillations is not always true, particularly when three-limb transformers are involved. Certain system conditions exist under which the trapped charge oscillations may 'lock-in' at or near system frequency,

producing sustained oscillations. In general, however, the damping effect of the delta winding accelerates the progression of the voltage oscillations into lower harmonic modes, depending on the energy transferred from the energised circuit.

Comparison of Figs. 10.3 and 10.7 demonstrates the effect of a closed delta tertiary winding in a three-limb transformer. In the absence of a tertiary winding (Fig. 10.7), the high amplitude trapped charge oscillations persist for a much longer period, indicating a low decrement. It will be observed that the oscillations appear balanced in spite of the delta winding being open due to the finite open circuit zero sequence impedances inherent in the interlinked magnetic circuit of a three-limb transformer. This interlinkage is in effect equivalent to a high reactance delta winding.

The regularity of the alternating current pulses of opposite polarity, which generally characterise waveforms relating to a transformer with a closed delta tertiary winding, is not evident. Successive current pulses of the same polarity frequently occur.

The superharmonic current oscillations are intensified by the absence of a delta winding shunt path to assist in damping. The unidirectional nature of the oscillations on the three phases arises from the relatively low zero sequence impedance of a three-limb transformer due to its interlinked magnetic circuit. From the line zero sequence capacitance and the oscillation frequency (360 Hz) the transformer zero sequence inductance is estimated as 0.6 H. As shown in section 10.6.1, the presence of a closed delta tertiary winding reduces this value to 0.5 H.

Owing to the relatively high zero sequence impedance associated with a five-limb transformer, waveforms obtained with and

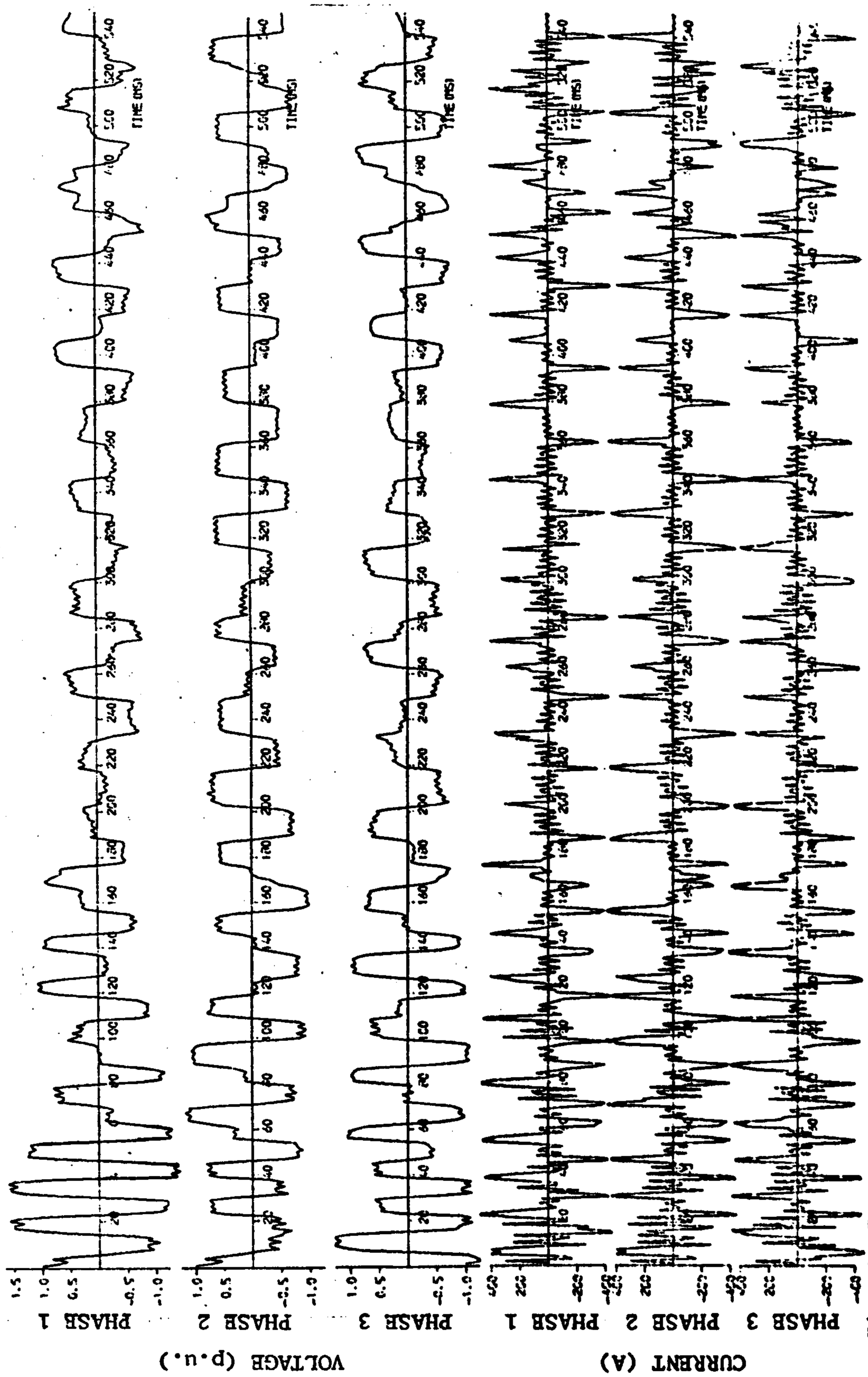

Fig. 10.7 : 45 km quadruple conductor line terminated in a 3-limb transformer with open delta winding

without the delta-connected winding (Figs. 10.4 and 10.8 respectively) differ fundamentally in character. With the delta winding open, the voltage oscillations are greatly distorted, unbalanced and highly damped. They show no discernible regular pattern or periodic behaviour. Since only a high impedance path is available through the transformer for the flow of zero sequence currents, these components are suppressed and the zero sequence voltages appearing at the transformer terminals are intensified. The current pulses during core saturation are aperiodic and have a much larger amplitude than the corresponding waveforms obtained with the delta closed.

10.6.2.1 Delta tertiary winding impedance

A reduction of the delta tertiary winding impedance by a factor of three gives the three-and five-limb transformer waveforms of Figs. 10.9 and 10.10, respectively, for comparison with corresponding curves of Figs. 10.3 and 10.4. In terms of design practice, such a low leakage impedance obtains if the tertiary conductors are wound close to the core extending over a greater portion of the core limbs. The direct effect of this reduction is to decrease further the effective zero sequence impedance of the transformer. As a consequence, the trapped charge oscillations become more persistent as the circuit impedance permits more energy transfer from the energised circuit to sustain the oscillations.

Comparison of the waveforms of Fig. 10.9 with those of Fig. 10.3 indicates the intensification of the ferro-oscillations when the tertiary winding impedance is reduced in a three-limb transformer. A similar tendency is observed in relation to the five-limb transformer by comparing waveforms of Fig. 10.10 with those of Fig. 10.4. A peculiar feature of the wave forms resulting from a

Fig. 10.8 : 45 km quadruple conductor line terminated in a 5-limb transformer with open delta winding

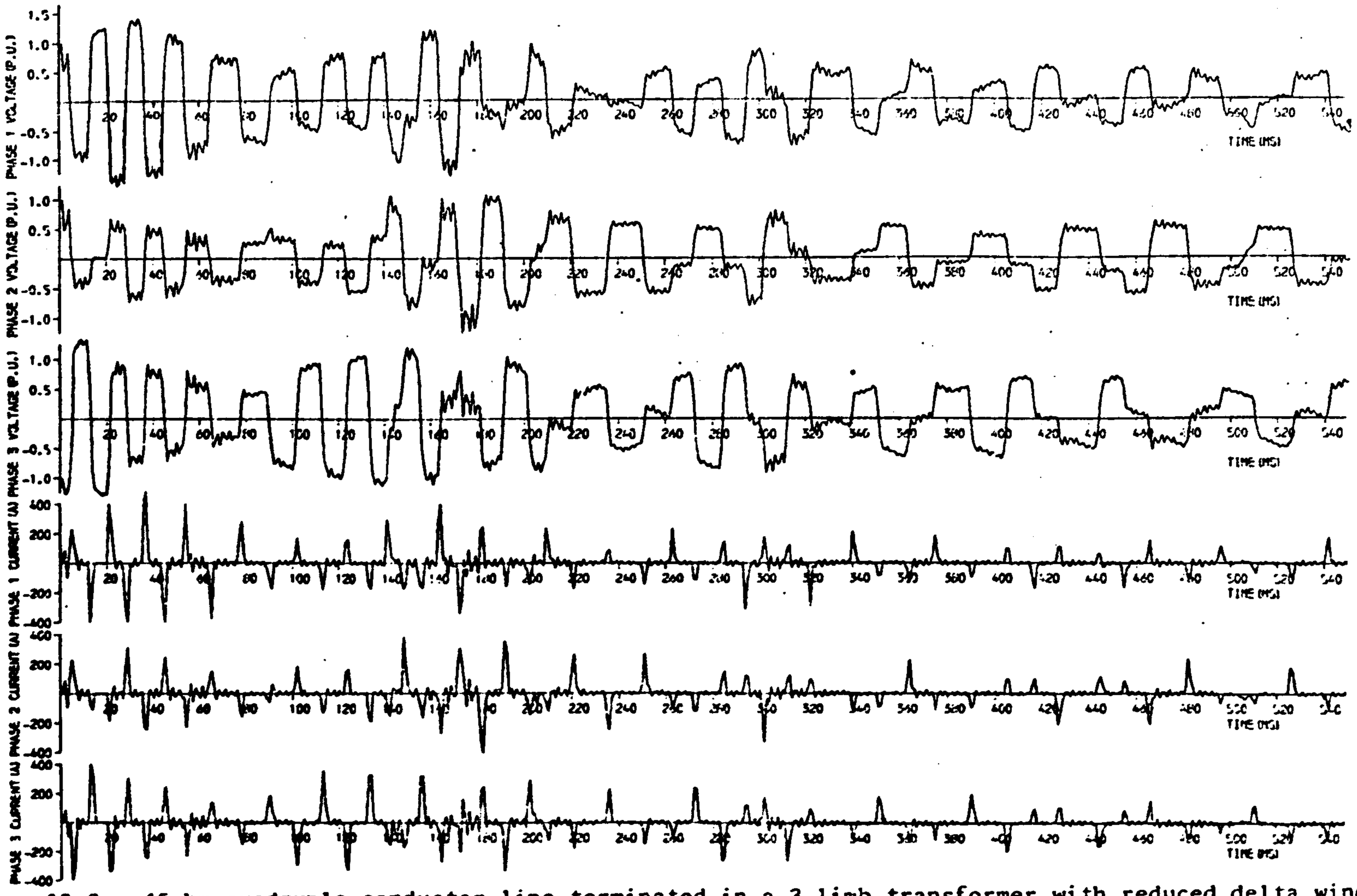

Fig. 10.9 : 45 km quadruple conductor line terminated in a 3-limb transformer with reduced delta winding impedance

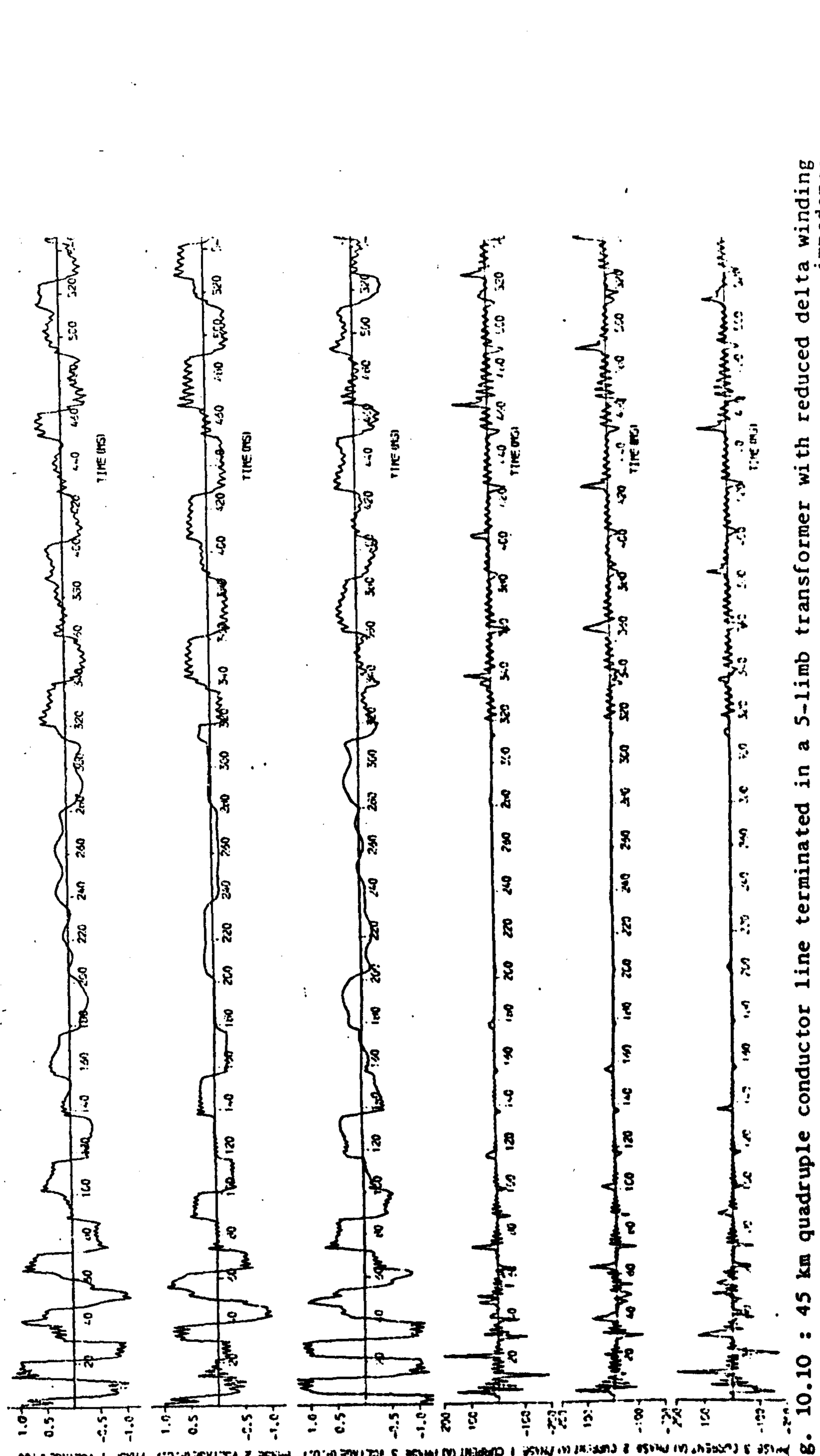

Fig. 10.10 : 45 km quadruple conductor line terminated in a 5-limb transformer with reduced delta winding impedance

reduced tertiary winding impedance (Fig. 10.10) is the sudden jump into oscillations of a higher subharmonic mode following a period of lower frequency harmonic oscillations, accompanied by the reappearance of superharmonic zero sequence oscillations. This modulation of the amplitude by a low frequency waveform is not apparent on the waveforms of Fig. 10.4. With both types of transformer cores, the increased diversion of zero sequence current into the low impedance delta winding leakage paths causes some reduction of the zero sequence voltage induced at the transformer terminals.

The prolongation of the high amplitude ferro-oscillations due to a reduction in the tertiary winding leakage impedance is again illustrated by waveforms of Fig. 10.11 relating to a three-limb transformer terminating a 150 km line. By comparison with waveforms of Fig. 10.5 obtained with a higher tertiary winding impedance, these high amplitude oscillations prevail over a period nearly thrice as long, and contain smaller amplitudes of the zero sequence component of voltage.

10.6.3 System voltage relative to saturation knee

The instigation of a ferroresonant state depends to a great extent on whether the magnitude and duration of the voltage applied at the transformer are sufficient to drive the core into saturation. Once this phenomenon is initiated, its persistence will be governed, among other things, by the applied voltage amplitude in relation to the core saturation threshold level as defined by the knee of the B/H characteristics.

A decrease in system voltage would have the same effect as raising the knee of the saturation characteristics. Conversely, increasing system voltage is tantamount to lowering the knee by

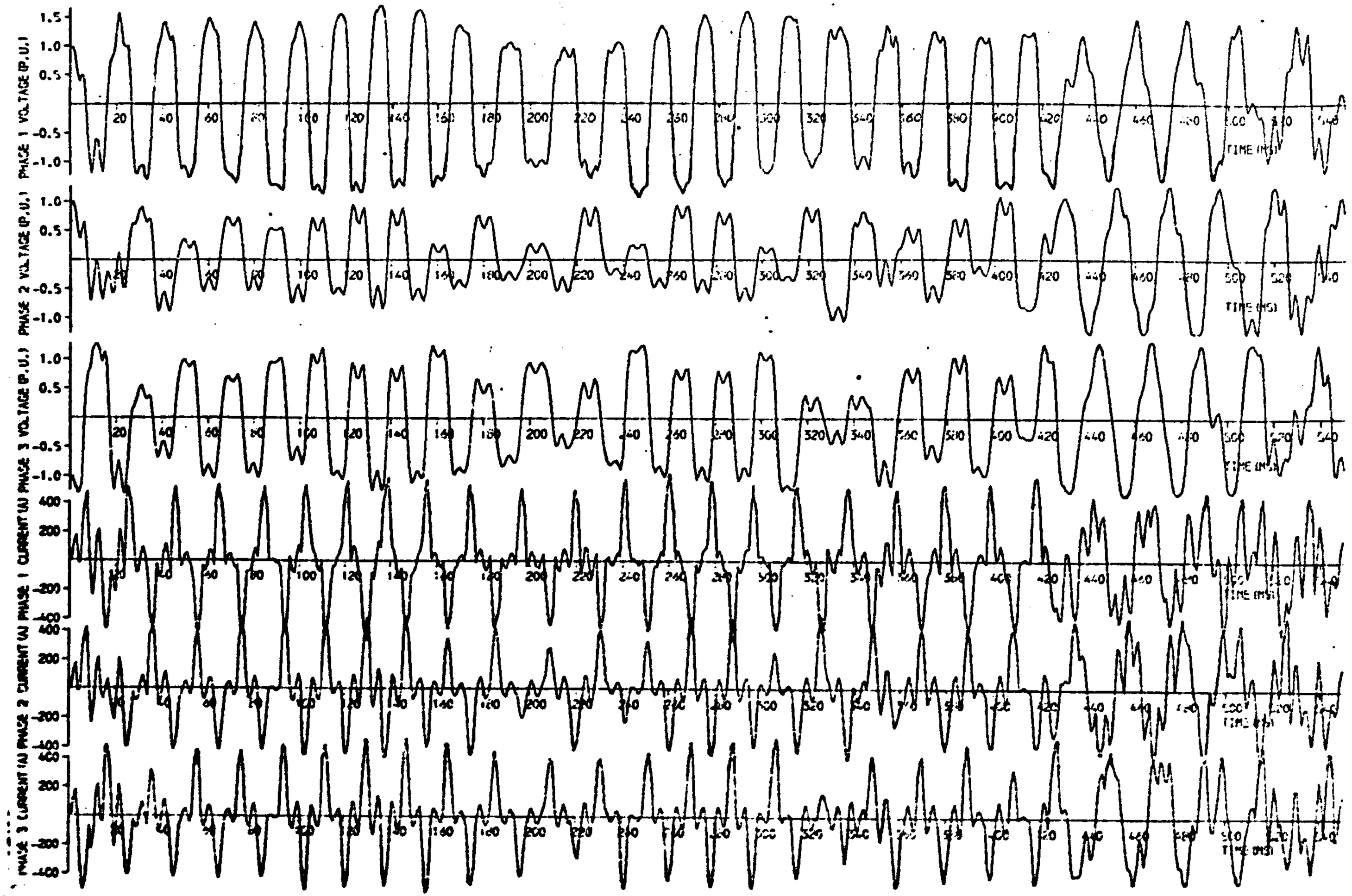

Fig. 10.11 : 150 km quadruple conductor line terminated in a 3-limb transformer with reduced delta winding impedance

reducing saturation flux density. Hence, variation of system voltage for the same magnetisation characteristics could be regarded as equivalent to variation of the relative point of saturation. It should be noted that per unit voltage in this case is given in terms of the operating system voltage chosen.

A 25 per cent reduction in system voltage gives waveforms of Figs. 10.12 and 10.13 for the three- and five-limb transformers respectively. The 1 p.u. trapped charge voltage is equivalent to 75 per cent of the initial voltage assumed for the curves of Figs. 10.3 and 10.4 respectively. Fig. 10.12 shows that oscillations close to fundamental frequency do not persist beyond the third cycle. Subsequently, there is a steady progression to lower subharmonic oscillation modes. These voltage oscillations are amplitude modulated by a very low subharmonic frequency of nearly 2 Hz decaying rapidly with time. The current waveforms are indicative of moderate saturation of the core during the higher amplitude oscillations. The reduction in system voltage does not alter the frequency of the superharmonic components for both the three- and five-limb transformers.

When the system voltage is increased by 50 per cent, the three- and five-limb transformer waveforms are shown on Fig. 10.14 and Fig. 10.15, respectively. The high amplitude trapped charge oscillations are intensified in respect of magnitude and duration than in the case when normal system voltages are applied. This is due to the combined effects of increases in the trapped charge voltage and energy transferred from the energised circuit as a result of higher system voltages.

It will be seen that, in general, the trapped charge voltage takes longer to saturate the core when the transformer is

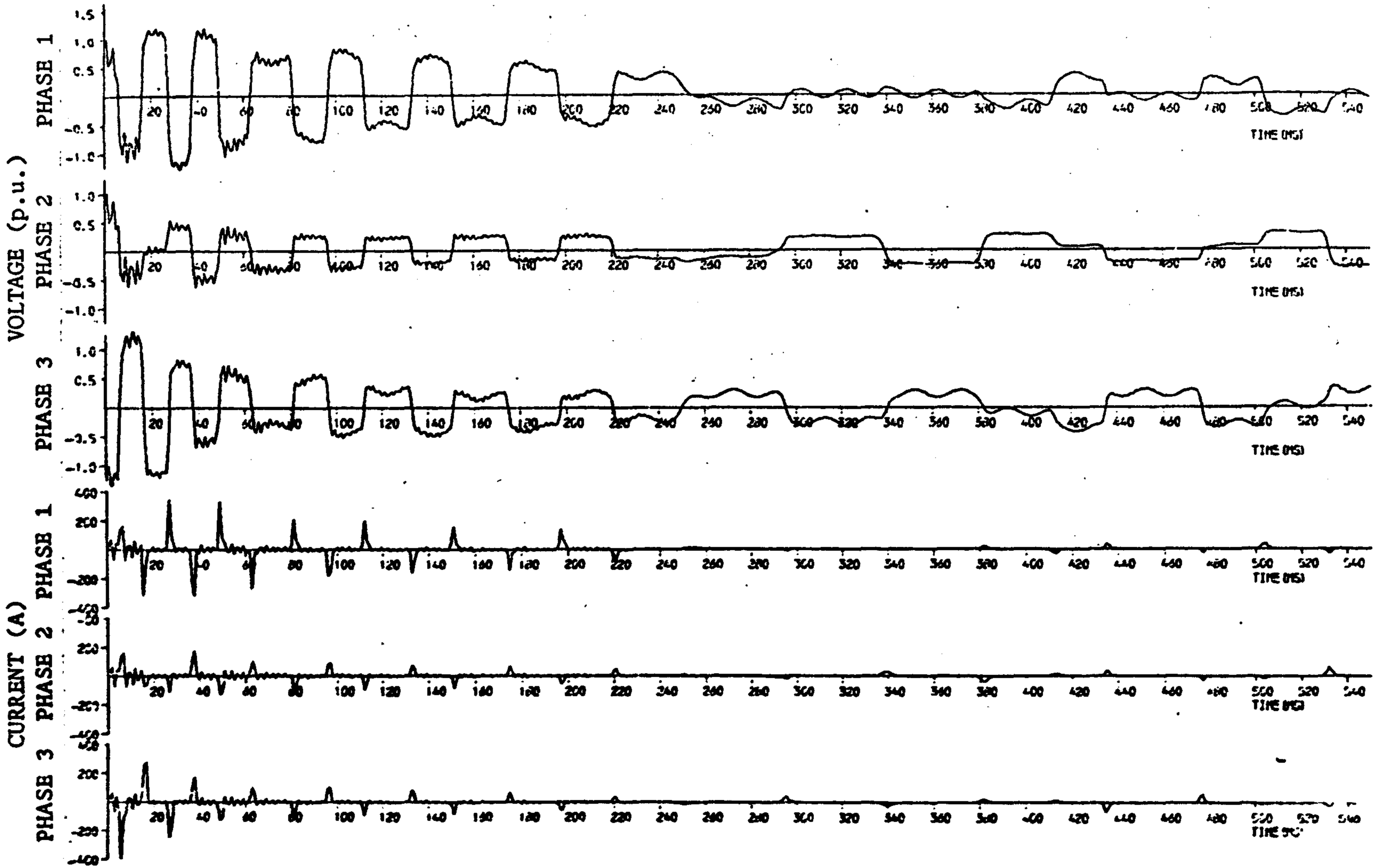

Fig. 10.12 : 45 km quadruple conductor line terminated in a 3-limb transformer with closed delta winding (75% system voltage)

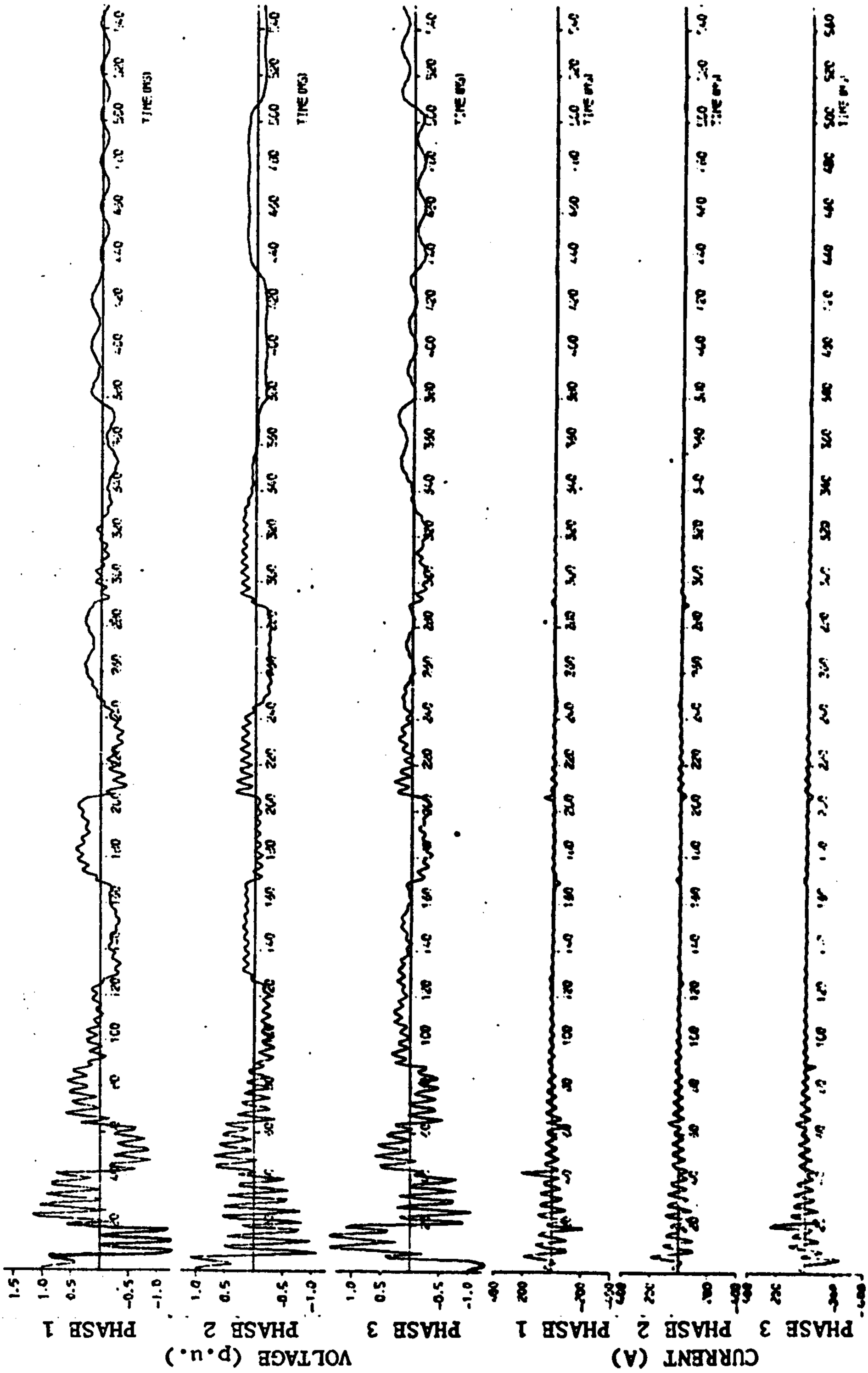

Fig. 10.13 : 45 km quadruple conductor line terminated in a 5-limb transformer with closed delta winding (75% system voltage)

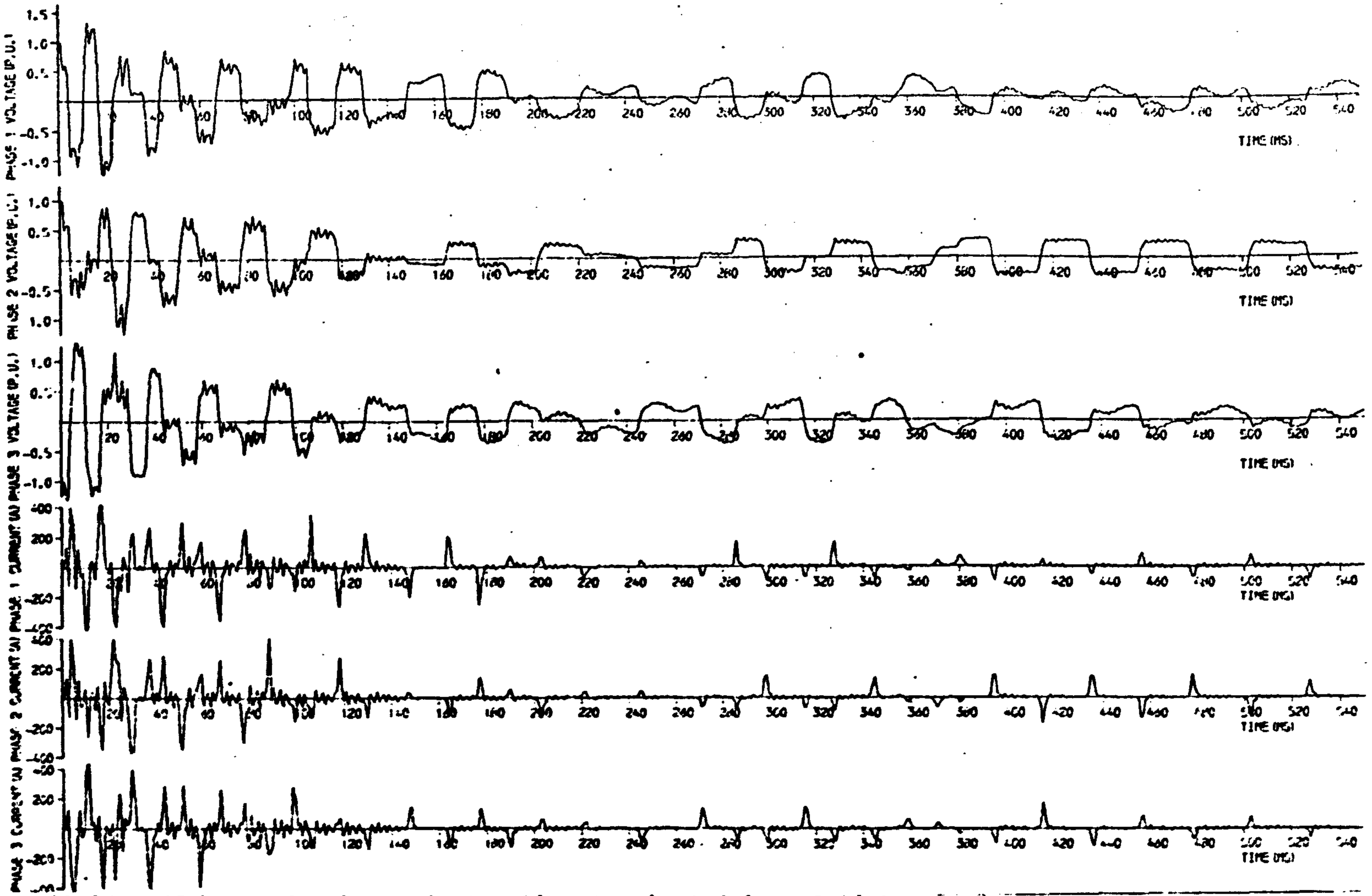

Fig. 10.14 : 45 km quadruple conductor line terminated in a 3-limb transformer with closed delta winding (125% system voltage)

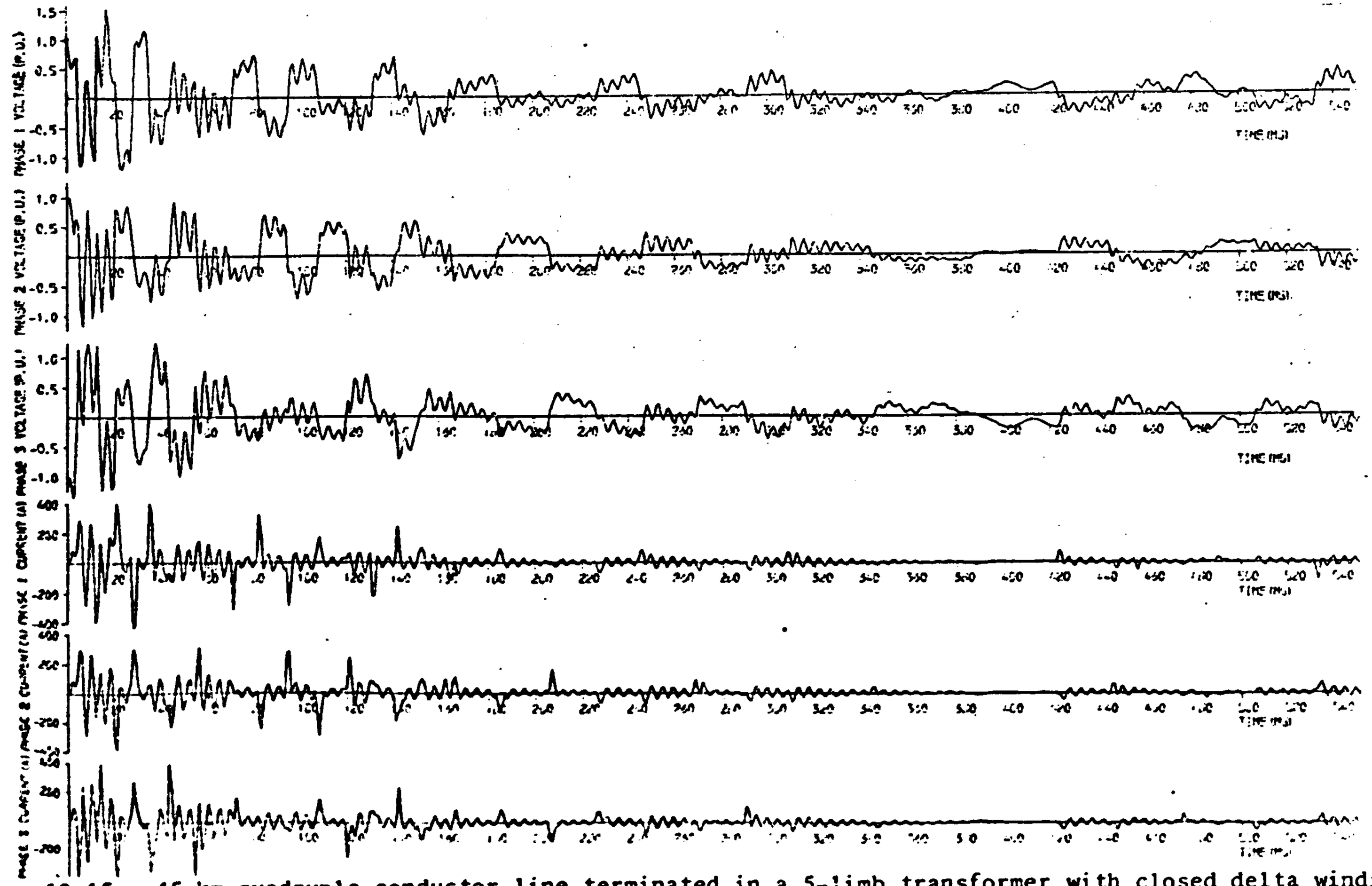

Fig. 10.15 : 45 km quadruple conductor line terminated in a 5-limb transformer with closed delta winding (125% system voltage)

being worked well below the knee of its saturation characteristics, than is the case when system voltage is increased. The frequency of the subharmonic oscillations therefore tend to be lower in the former case.

10.6.4 Transformer losses

Energy losses in the transformer mainly consist of resistive losses in the windings and losses associated with the core. Ferro-oscillation damping could be increased further by connecting resistors in the tertiary delta or primary windings, in the neutral terminal, or loading the secondary windings resistively. Only the effects of resistance in the delta winding were investigated.

Fig. 10.16 shows that for a five-limb transformer, a 2 p.u. resistor (based on 1000 MVA 275 kV ratings) connected in each phase of the delta winding practically eliminates the periodic oscillations about 300 msec. after initiation. Reference to waveforms of Fig. 10.4 obtained without the additional resistor will show that these oscillations persist throughout the time interval investigated (540 msec.). The subharmonic oscillations of Fig. 10.16 are characterised by alternating periods of the third and seventh subharmonic modes.

The superharmonic oscillations decay much faster than in the case when there is no additional tertiary resistor due to increased damping.

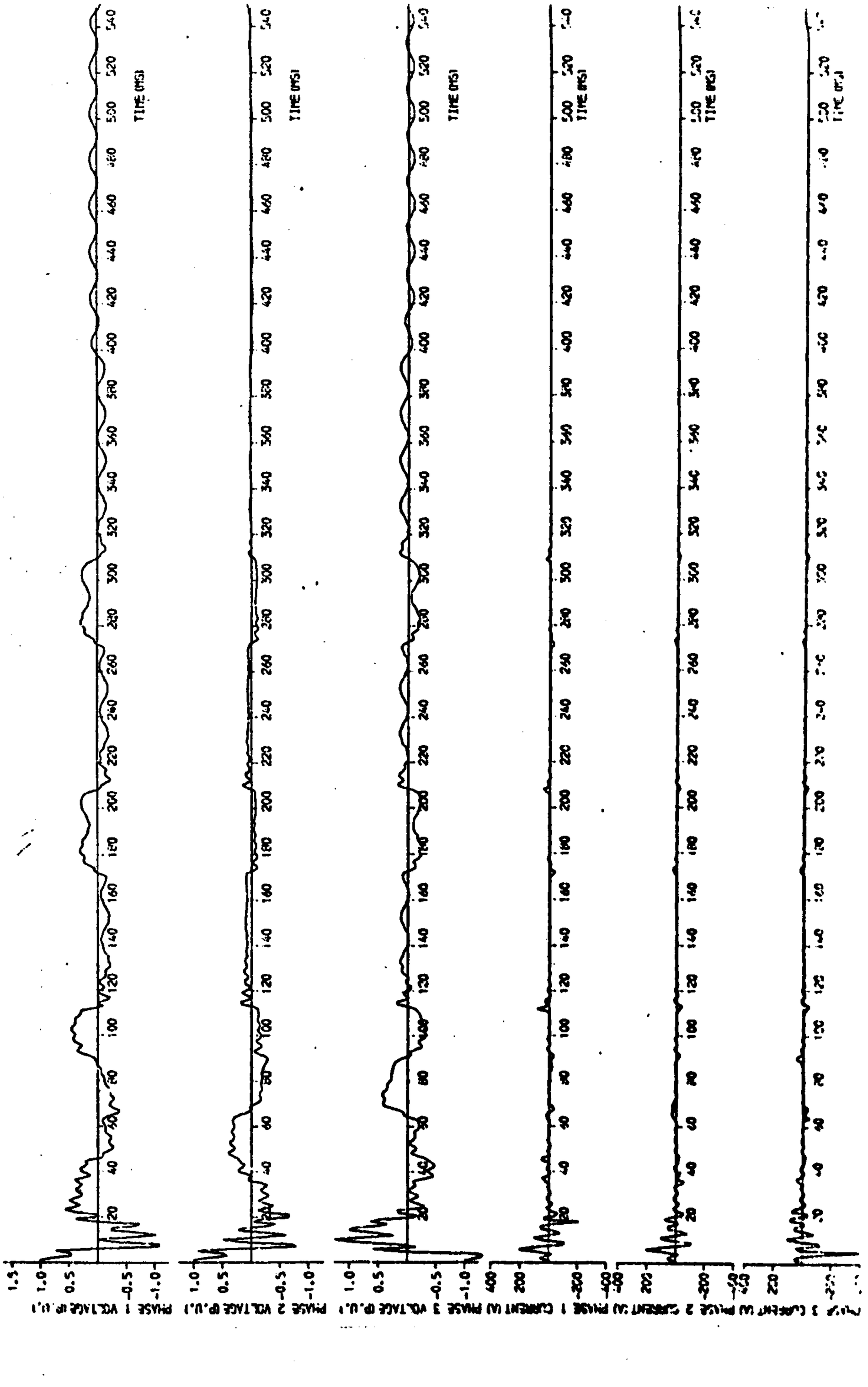

Fig. 10.16 : 45 km quadruple conductor line terminated in a 2 p.u. resistor in each delta winding phase

10.7 Transmission line parameters

The length of the de-energised line and its physical configuration have a crucial effect on both the initiation and duration of the ferro-oscillations. It dictates the amount of residual trapped charge on the line when the load is shed from the feeder. If this charge is sufficient to saturate the core, ferro-resonant oscillations would result. The line configuration mainly determines the degree of energy coupling from the energised circuit. This energy is necessary to compensate the losses in the system if ferroresonance is to be sustained.

Almost the entire H.V. double circuit feeder lines in Britain consist of either two or four conductors bundled in close proximity in each phase. In addition to increasing the current carrying capacity of the lines, the bundling of conductors reduces corona loss and radio interference level by decreasing the radial voltage gradient, and reduces line series reactance. These benefits increase in proportion to the number of conductors bundled together. For voltage levels between 200 and 400 kV, lines of twin conductor construction predominate, while for voltages in excess of 400 kV, quadruple conductor lines are preferred. Under heavy loading conditions, however, lines of quadruple conductors are normally used even at voltage levels less than 400 kV.

10.7.1 Line configuration

The particulars of the twin and quadruple conductor lines used in this investigation have been presented in Chapter 7, and the effects of line configuration on the coupled voltages and currents have been assessed in Chapter 9 and in Section 10.5 of this Chapter. It was evident that the zero sequence impedance of the circuit and the mutual impedance between the sequence equivalent

circuit were major factors in determining the degree of coupling between circuits due to electrostatic unbalance. Both these factors are related to the following :

(i) the physical dimensions of the transmission line geometry,

(ii) the number of conductors bundled together in each phase,

(iii) the location and characteristics of the ground wires,

(iv) the irregularity of the terrain and the composition of the earth path, and

(v) the method of transposition used (if any) to minimise electrostatic unbalance.

One of the consequences of bundling conductors is an increase in the line capacitances, depending on the number and dimensions of spacings between conductors in each phase. For the line configurations used, sequence component values derived in section 9.4 show that the quadruple-conductor line gives positive and zero sequence capacitances some 13 per cent larger than those of the twin-conductor lines. The sequence capacitance between the positive sequence voltages on the energised line and the zero sequence currents in the transformer circuit is nearly doubled. As a result, the energy transferred from the energised circuit and the charge initially stored in the line capacitance are somewhat less when conductors of twin construction are used instead of the quadruple type. However, examination of the open circuit coupled voltages (Fig. 9.2) will show that the vector sum of coupled voltages in twin-conductor lines contain an offset voltage of the same amplitude as the induced system frequency voltage. This voltage off-set is not present when quadruple conductor lines are used. The voltage biasing

effect renders the transformer terminating a twin-conductor line more susceptible to saturation. Consequently, the duration of the high amplitude trapped charge oscillations would tend to be more prolonged.

Figs. 10.17 and 10.18 present computed waveforms relating to the 45 km twin-conductor lines for the three- and five-limb transformers, respectively, for comparison with corresponding quadruple-conductor line results shown on Figs. 10.3 and 10.4. One significant difference between the voltage waveforms of the three-limb transformers is the longer duration of the high amplitude oscillations obtaining in twin-conductor lines. This may be attributable to the zero-sequence voltage biasing effect already referred to. The unequal amplitude of the positive and negative saturation current pulses observed on the current waveforms of Fig. 10.17 is evidence of this offset voltage. The differences between the waveforms relating to the five-limb transformer are not as striking since the high amplitude trapped voltage oscillations decay very rapidly.

If the length of line is increased to 150 km, differences between waveforms similar to those outlined above could be discerned by comparison of Figs. 10.19 and 10.20 (twin-conductor lines) with Figs. 10.5 and 10.6 (quadruple-conductor lines) for the three- and five-limb transformers respectively. In the case of the five-limb transformer, the trapped charge oscillations persist much longer when lines of twin conductor construction are used. The voltage waveforms of Fig. 10.19 relating to a three-limb transformer terminating a twin-conductor line exhibit a sustained component of oscillations in the second subharmonic mode.

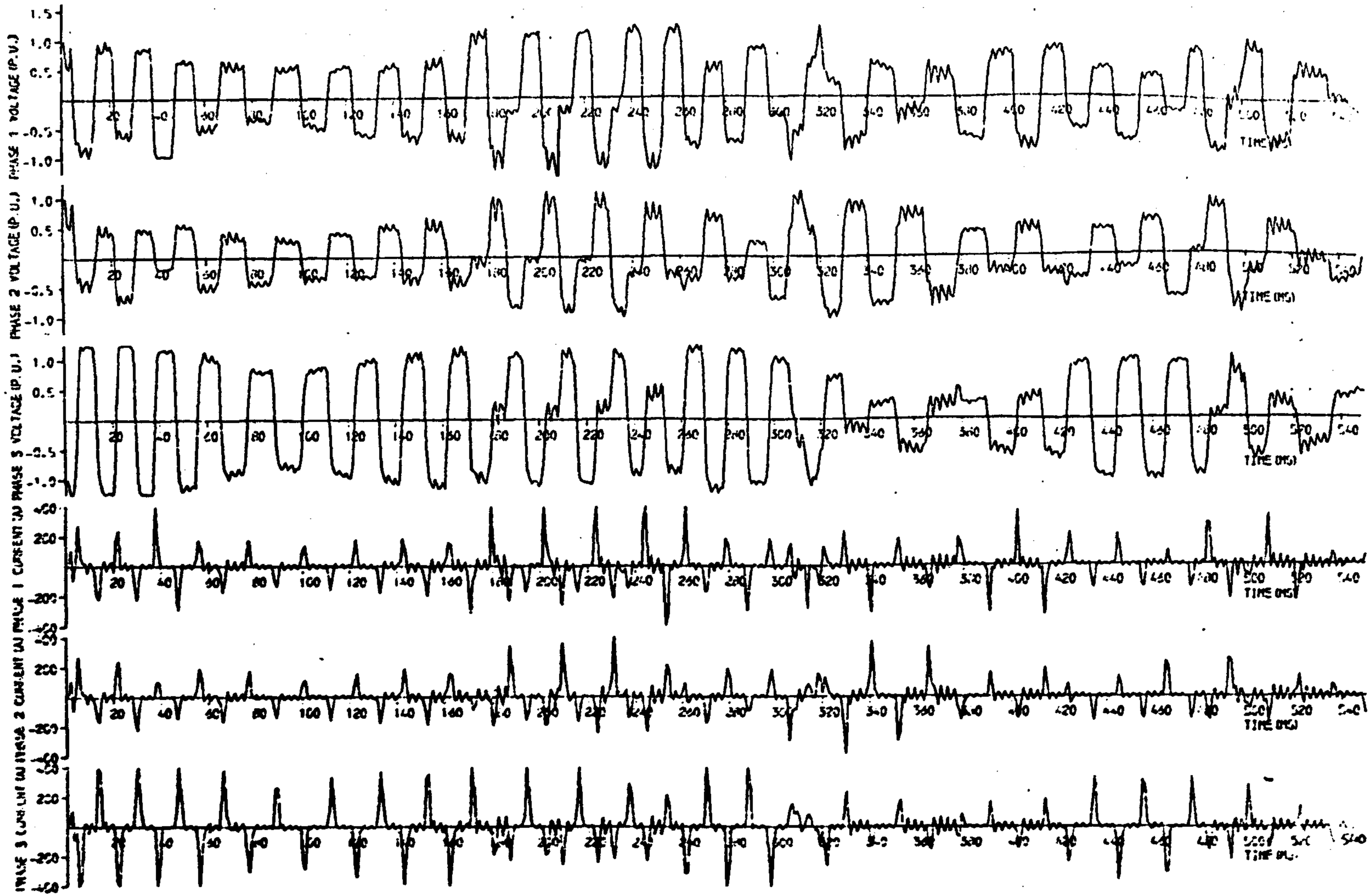

Fig. 10.17 : 45 km twin conductor line terminated in a 3-limb transformer with closed delta winding

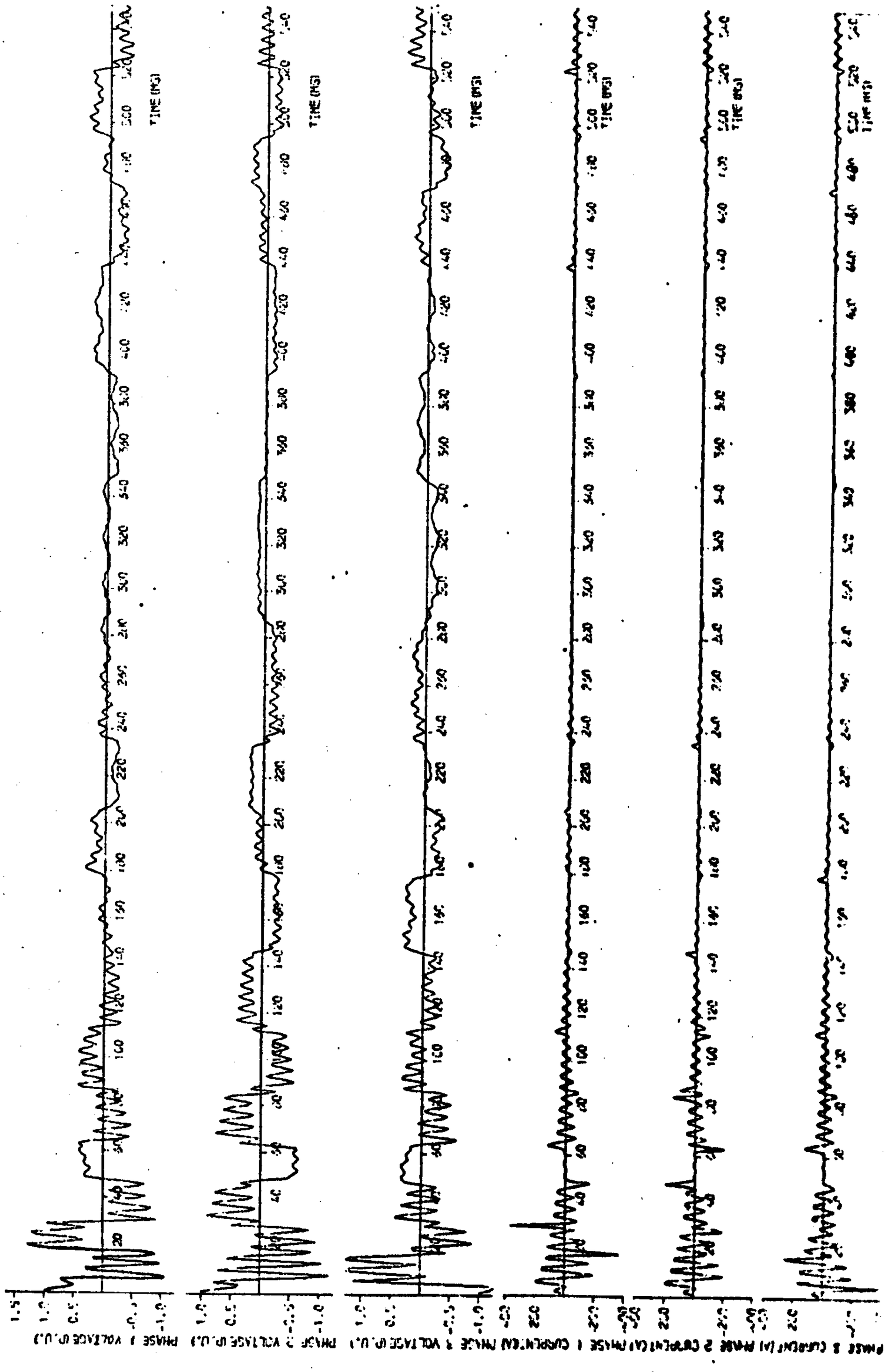

Fig. 10.18 : 45 km twin conductor line terminated in a 5-limb transformer with closed delta winding

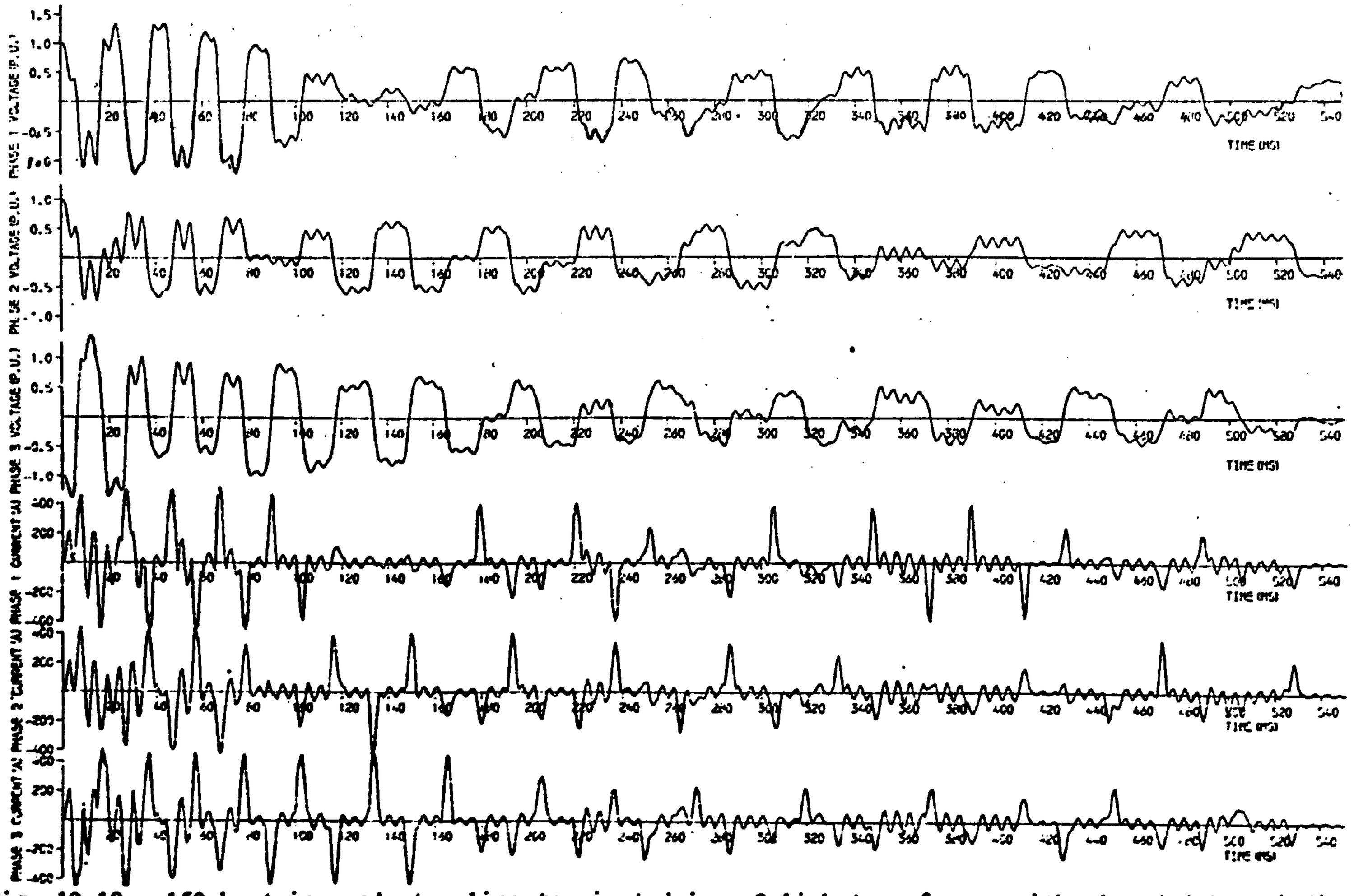

Fig. 10.19 : 150 km twin conductor line terminated in a 3-limb transformer with closed delta winding

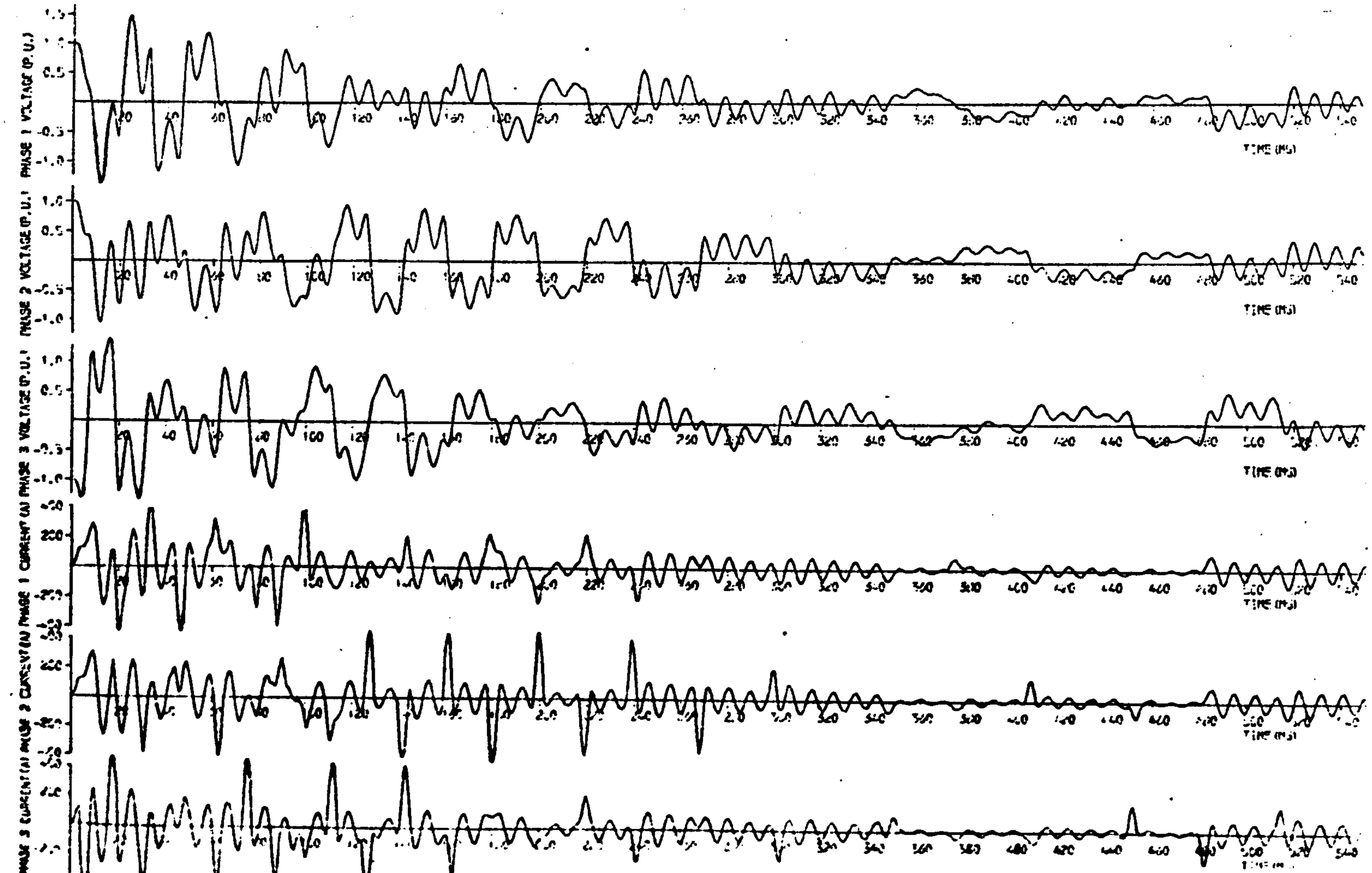

Fig. 10.20 : 150 km twin conductor line terminated in a 5-limb transformer with closed delta winding

10.7.2 Initial conditions

The voltage conditions existing immediately following de-energisation of the transformer-terminated circuit are of paramount importance in determining the character of the resulting transformer current and voltage waveforms. The energy coupled from the energised line is not sufficient on its own to initiate ferro-resonance, as illustrated by waveforms of Fig. 10.3. An additional requirement for the existence of ferro-oscillations is that a certain amount of trapped charge be present on the lines. This charge largely depends on the procedure used to isolate the line from the system. If this charge is sufficient to drive the core flux beyond the point of saturation, relatively stable trapped charge oscillations could result. The transformer voltage-time capability has to be exceeded before the transformer voltage decays to zero through damping if the oscillations are to persist.

When the circuit is de-energised, there exists a finite combination of residual voltages trapped on the three phases of the line, depending on the sequence of operations and on the point-on-wave at which the circuit breaker poles of the first phase to clear begin to open. In practice, the normal sequence of operations is as follows :

(i) the circuit is first unloaded by opening the circuit breaker located on the transformer secondary, leaving the transformer-terminated line energised from the source, and

(ii) the circuit is subsequently isolated from the system by opening the circuit breakers at the source end.

If the unsaturated magnetising reactance of the transformer exceeds the capacitive reactance of the line, as is normally

the case, a charging current leading the voltage by approximately 90 elec. deg. would flow in the lines following load shedding. This means that at the zero crossing of the line current wave, the transformer magnetising current and core flux would be relatively small. Subsequent interruption of line current at successive current zeros on each phase would therefore favour conditions of minimal residual flux density in the core and a voltage of magnitude near system voltage being trapped on the phases of the line being dropped. For the purpose of this study, it is assumed that during the time span of this operation (120 elec. deg.), this voltage remains constant and all the trapped charge remains entirely in the electrostatic field. The validity of this assumption would, in practice, depend on :

(i) the relative magnitudes of the line and transformer reactances,

(ii) the relative point of transformer core saturation,

(iii) the decay rate and the natural frequency of the trapped charge, and

(iv) the operating characteristics of the breaker.

Use of the computer program to establish exact initial conditions by opening the circuit breaker at the source end at successive current zeros when steady-state conditions prevail, revealed that the error in assuming one per unit trapped voltage was less than 5 per cent.

As it was shown in section 9.7 of Chapter 9, there are six different combinations in which the one per unit trapped charge of either polarity is distributed among the three phases of the line. In that section, it was also demonstrated that the combination producing the most severe resonant voltage oscillations is +1, +1 and -1 per unit voltage on phases 1, 2 and 3, situated at

the top, middle and bottom positions of the line circuit, respectively. The phase displacement between the two circuits is 120 elec. deg. Phase 3 is connected to the transformer phase winding on the centre limb. On account of the severity of such conditions, only this phase distribution of voltage was investigated.

The effects of reducing the trapped charge voltage to 50 per cent is demonstrated by comparison of the waveforms shown on Figs. 10.21 and 10.22 with those of Figs. 10.3 and 10.4 for the three- and five-limb transformers respectively. The salient point of interest is that the subharmonic oscillations relating to a three-limb transformer (Fig. 10.21) show no indication of decaying during the time of observation. Even at this moderate voltage level, the voltage-time capabilities of the transformer are exceeded. The frequency of the superharmonic oscillations is reduced to 200 Hz due to the higher zero sequence transformer impedance arising from reduced voltage level.

Comparison of the five-limb transformer waveforms will show that the oscillations die away much faster when the trapped charge voltage is reduced to 0.5 p.u.

10.7.3 Line length

Variation of line length determines not only the amount of charge initially stored in the electrostatic field of the line, but also the subsequent modes of oscillations. With other appropriate conditions prevailing, the system can enter into a ferroresonant state only if the transformer becomes saturated by the energy transferred from the line. Hence longer lines are more susceptible to ferro-oscillations, particularly of the type involving large amplitude and high frequency, than lines with relatively small capacitance. Since for large values of capacitance the initial

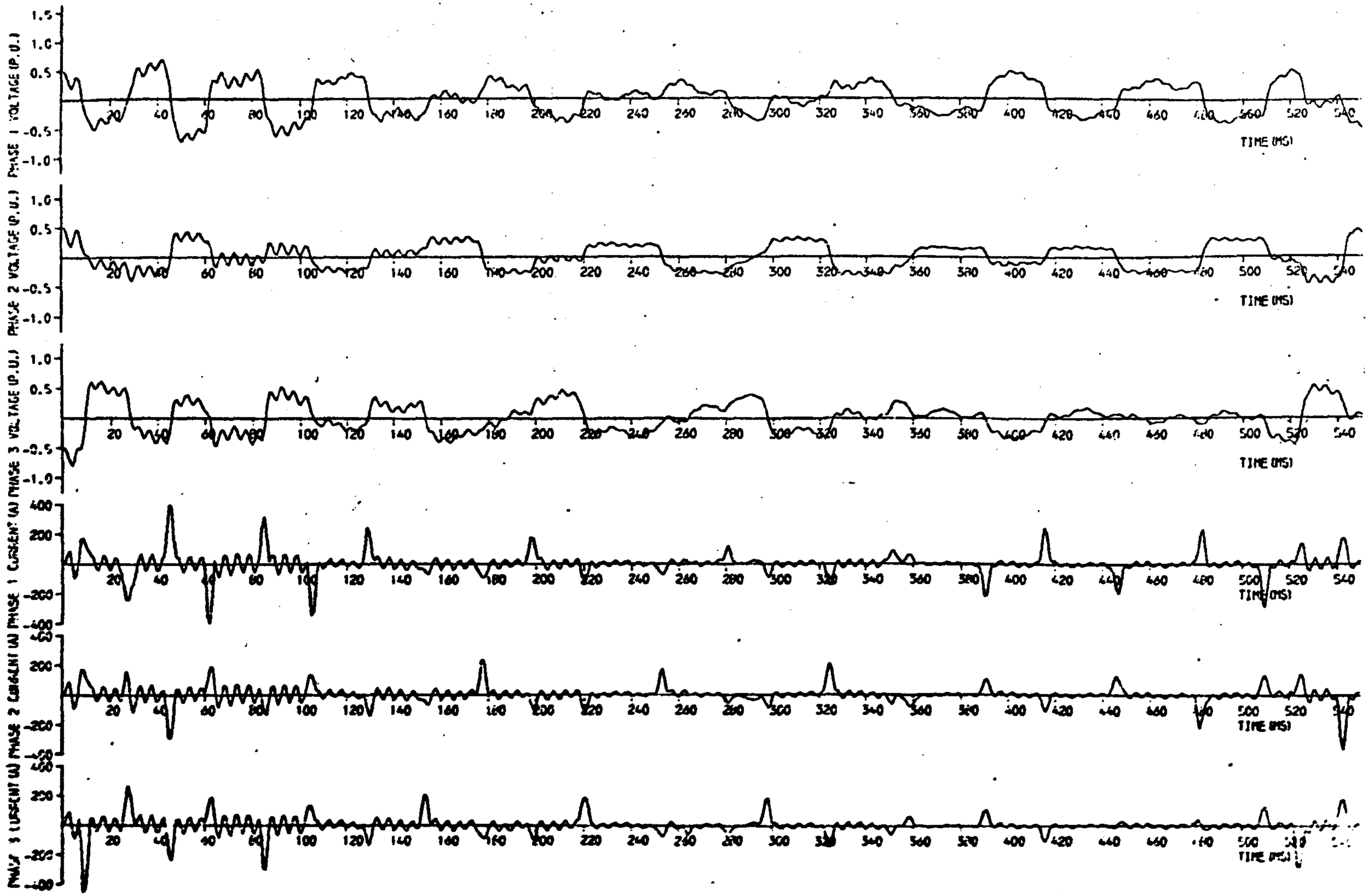

Fig. 10.21 : 45 km quadruple conductor line terminated in a 3-limb transformer with closed delta winding (0.5 p.u. trapped charge voltage)

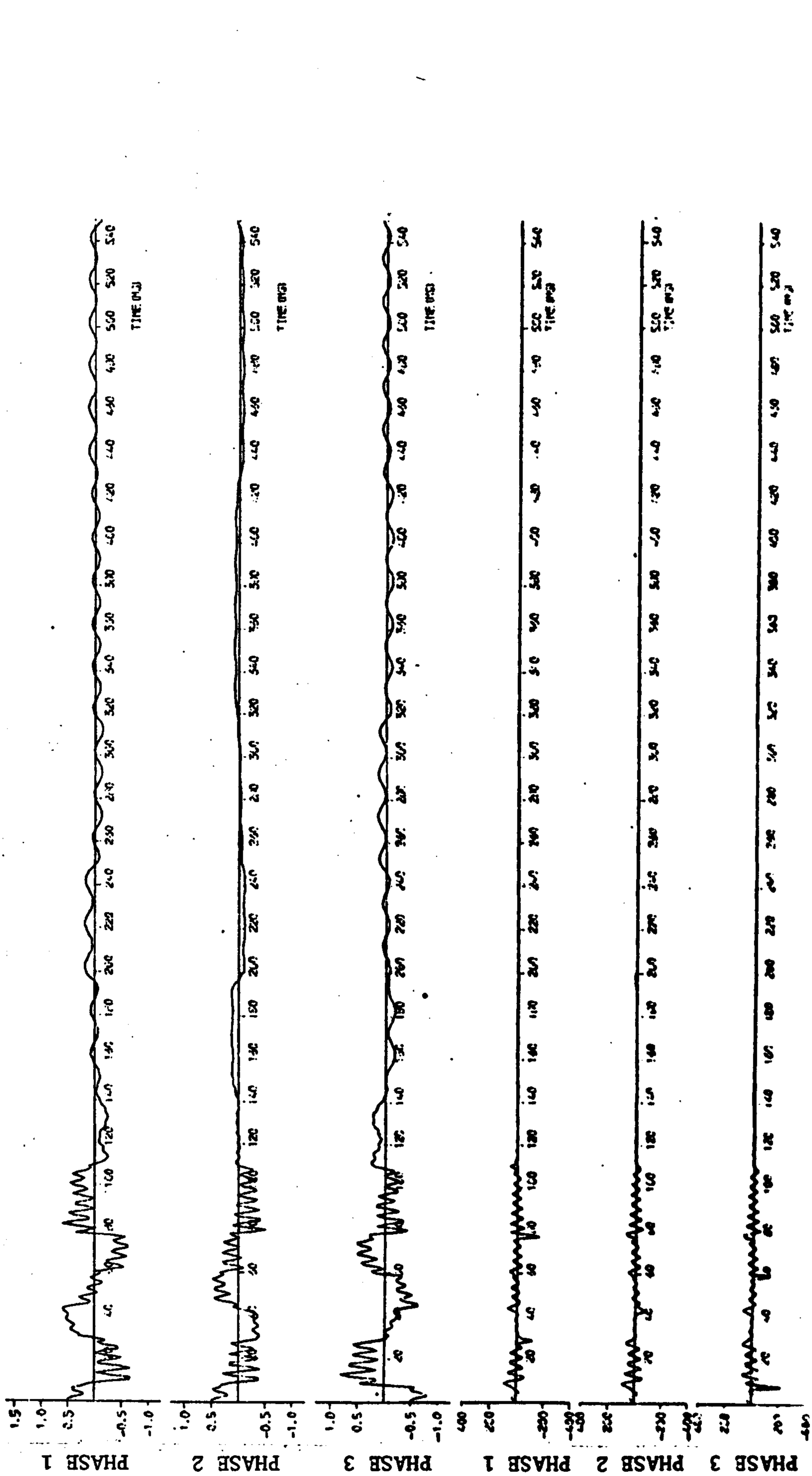

Fig. 10.22 : 45 km quadruple conductor line terminated in a 5-limb transformer with closed delta winding (0.5 p.u. trapped charge voltage)

charge stored is large, the time interval for the energy to decay due to losses to a level at which the transformer fails to saturate is longer. Hence the high amplitude oscillations would tend to persist much longer. However, due to the increased line and delta winding currents, the resultant damping may be of such a value as to negate the persistence of the oscillations.

Reducing the capacitive reactance of the lines in relation to the transformer zero sequence inductive reactance increases the amplitude and reduces the frequency of the zero sequence super-harmonic voltages at the transformer. The associated currents are amplified due to the reduction in the oscillation resistance of the oscillatory circuit.

The effect of increasing the length of line from 45 to 150 km for a three-limb transformer is demonstrated by comparison of the waveforms shown on Figs. 10.3 and 10.5 respectively. It will be observed that the larger capacitance associated with the longer line produces more severe voltage waveforms in terms of amplitude and duration. The saturation currents are greatly exaggerated by the transformer being severely saturated, and have a longer duration of discharge as evidenced by the wider current pulses.

A reduction of the length of line to 7.5 km gives waveforms shown on Fig. 10.23. The waveform in this case shows that the trapped charge voltage oscillations 'lock-in' at the fundamental system frequency. This is in spite of the presence of factors such as a closed delta winding and system losses which militate against the oscillations being sustained. This behaviour is contrary to the generally held view that ferro-oscillations cannot be sustained in the presence of a closed delta tertiary winding. Due to the high capacitive reactance of the line, the zero sequence component of current and voltage are imperceptible on the waveforms.

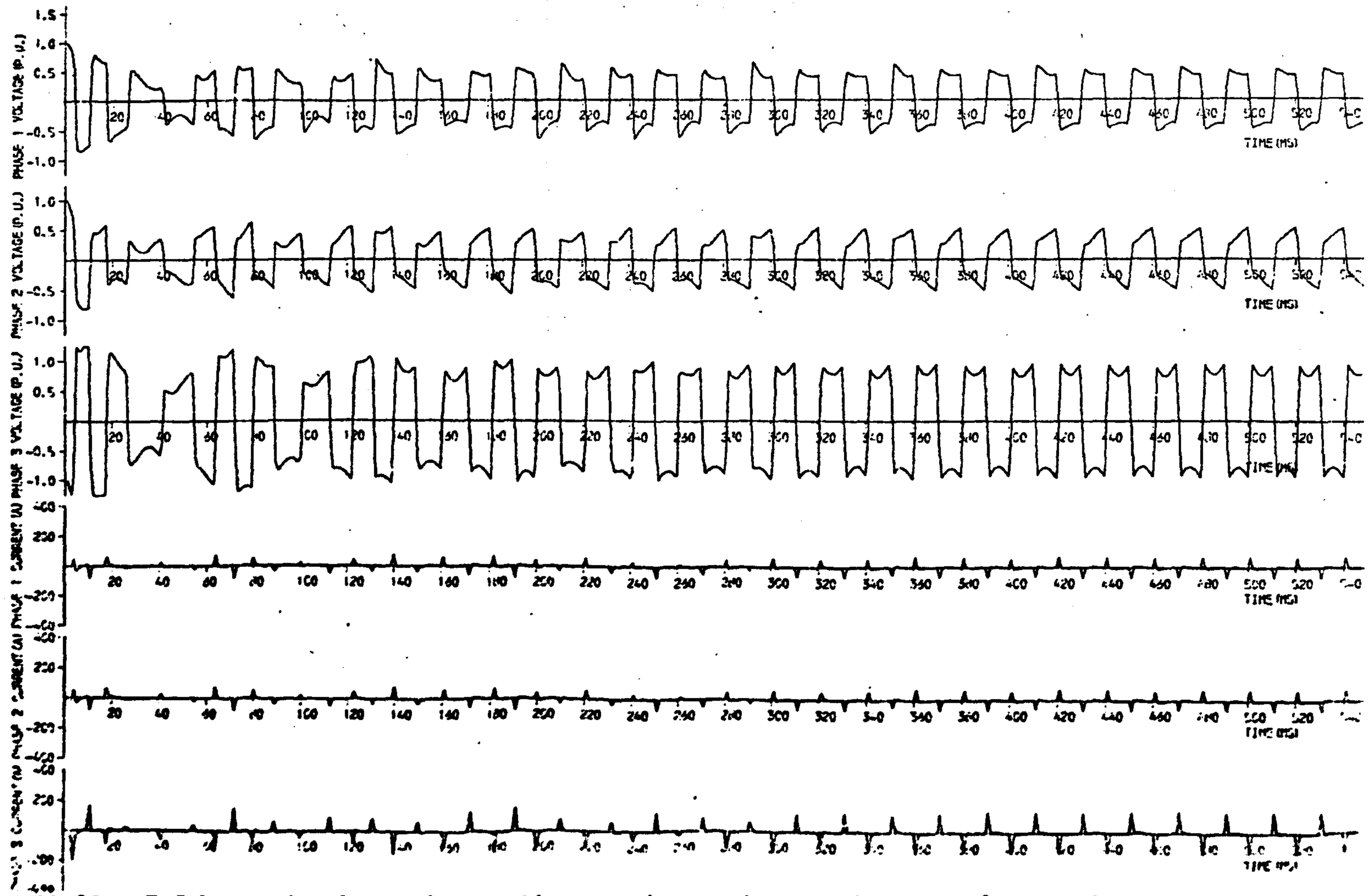

Fig. 10.23 : 7.5 km quadruple conductor line terminated in a 3-limb transformer with closed delta winding

Figs. 10.6, 10.4, 10.24, 10.25 and 10.26 show waveforms obtained for the five-limb transformer with line lengths of 150. 45, 30, 15 and 7.5 km respectively. As the length of line is reduced, the waveforms show a progressive decrease in the amplitude of the zero sequence components of current and voltage, and increase in their frequency. With all line lengths, the trapped voltage oscillations decay rapidly.

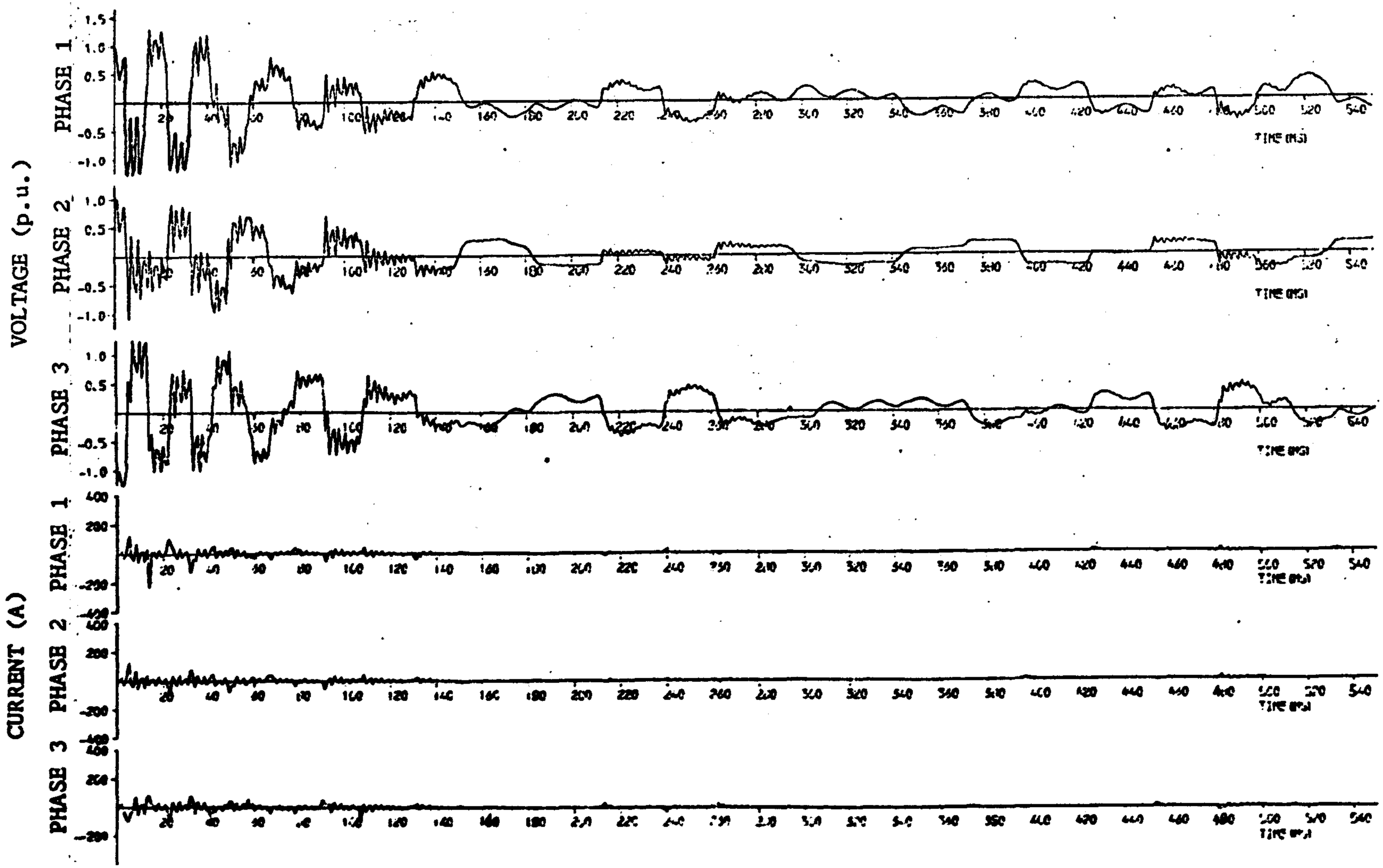

Fig. 10.24 : 30 km quadruple conductor line terminated in a 5-limb transformer with closed delta winding

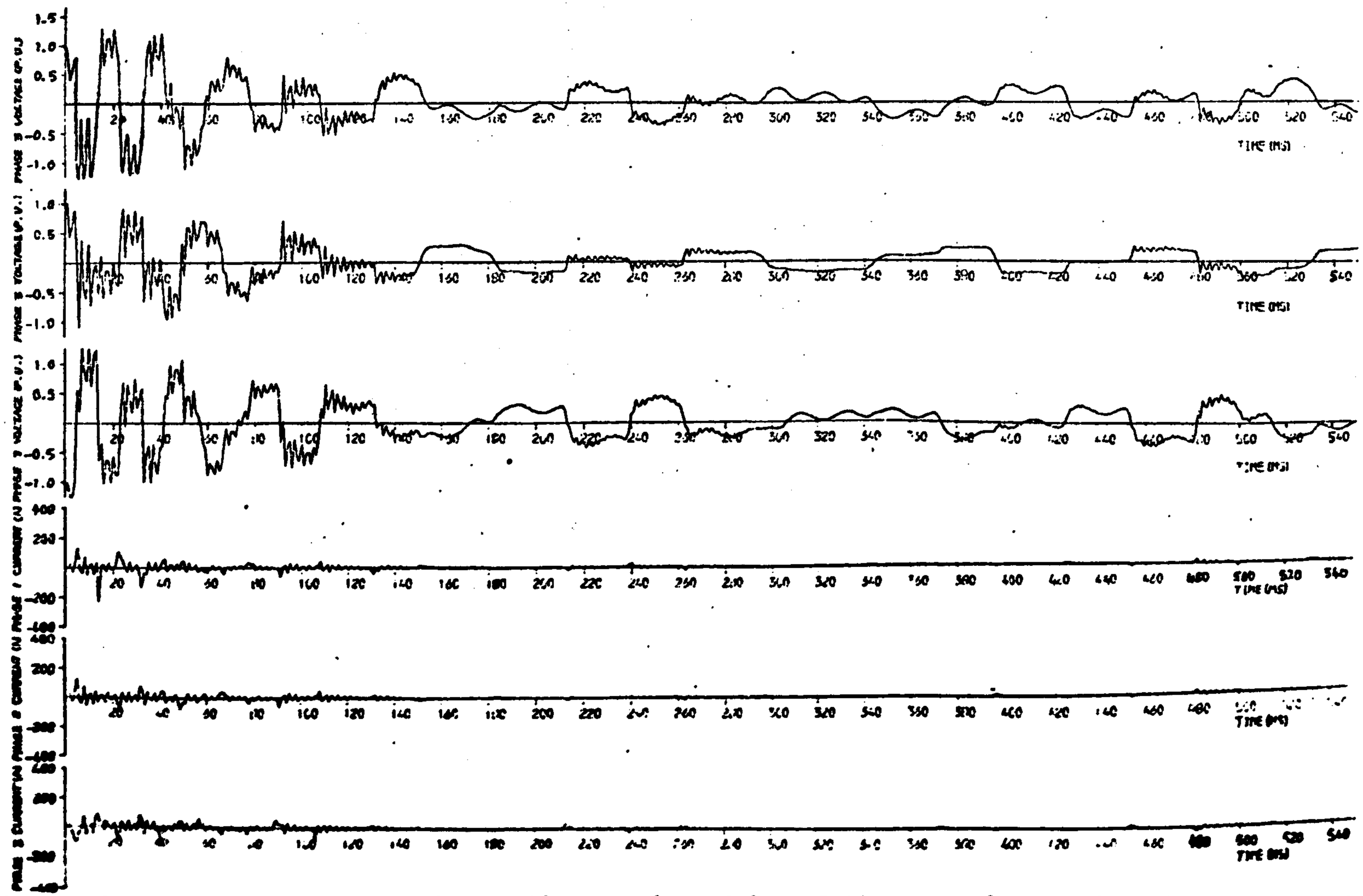

Fig. 10.25 : 15 km quadruple conductor line terminated in a 5-limb transformer with closed delta winding

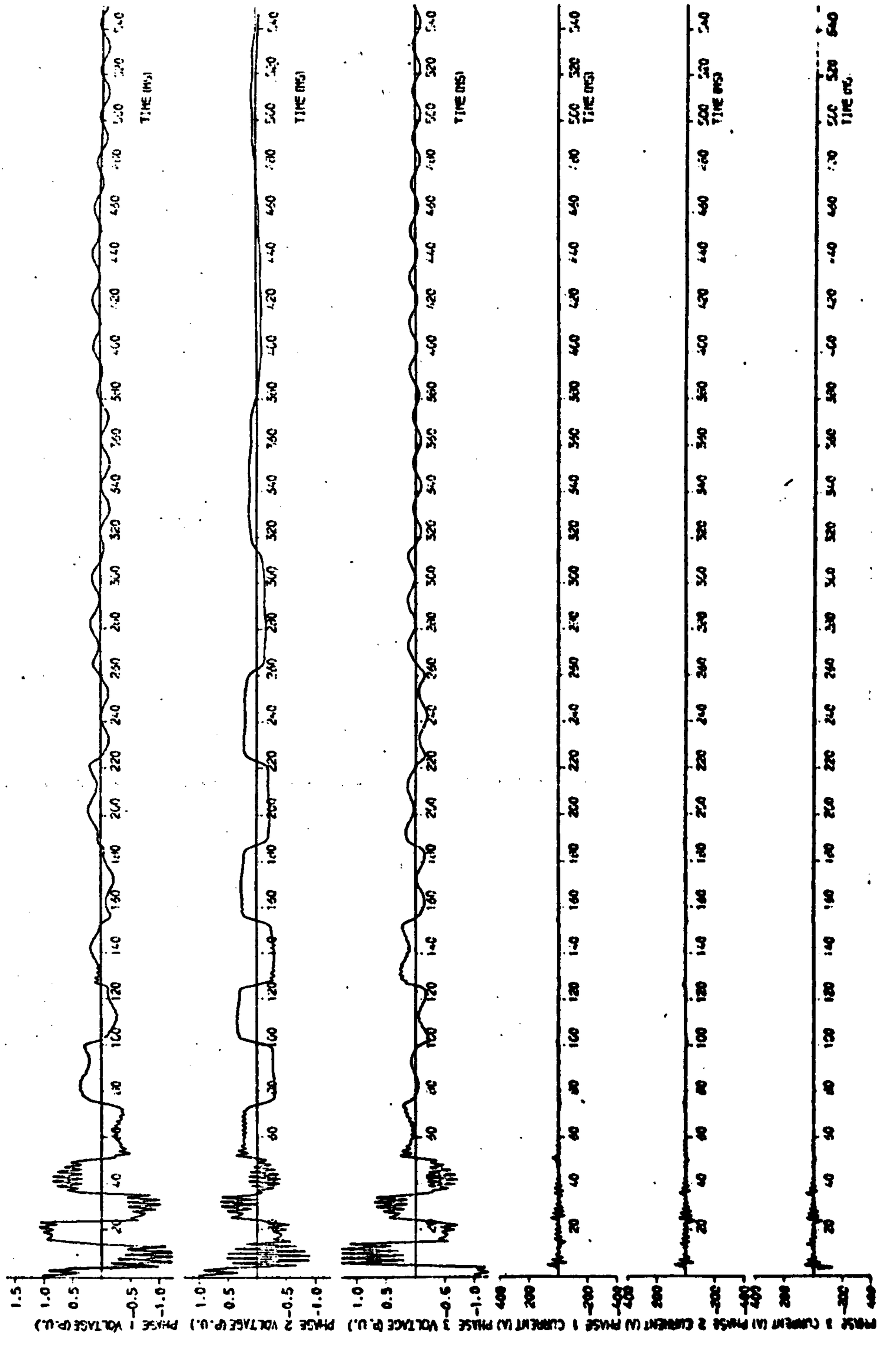

Fig. 10.26 : 7.5 km quadruple conductor line terminated in a 5-limb transformer with closed delta winding

10.8 Preventive measures

The consequences of ferro-oscillations when one circuit of a double-circuit system is dropped could be serious enough to warrant particular consideration to ensure that these oscillations are rendered harmless in terms of workmen's safety and transformer overheating. The measures which are effective in either preventing ferroresonance or minimising its effects involve the avoidance of system parameters and configurations, and operating conditions under which the system may enter into a ferroresonant state.

10.8.1 System constants and configuration

Due to the wide variation of the natural frequency of the circuit involving the non-linear reactance of the transformer, the concept of detuning the circuit by ensuring that the frequency of the oscillatory circuit differs from that of the exciting wave-form is not strictly applicable. Although in some cases, fundamental frequency oscillations may not be possible when certain circuit constants are used, subharmonic modes of oscillations may be excited. The measures outlined below do, however, assist in suppressing the oscillations with varying degrees of effectiveness.

10.8.1.1 Transposition

Transposition of phase conductors within each circuit and between the two circuits of a double circuit line minimises the effects of electrostatic coupling and hence materially reduces the magnitude of the induced voltages. Consequently, the induced energy may not be sufficient to sustain the ferro-oscillations. This method, although generally not economically acceptable, can readily be employed in cases where tee-off connections are made along the length of the circuit by transposing both the conductors and the circuits at these locations. The impact of transposition on induced

voltages is, however, minimal in the case when resonance conditions exist. Outside the region of resonance, transposition could be quite effective. Chaston [36] has shown that for relatively low values of reactive compensation, a reduction in the magnitude of induced voltages by up to 40% could be achieved if the phase conductors within the individual circuits are transposed. If, in addition, the two circuits are themselves transposed, a reduction factor of up to 70% could be obtained.

10.8.1.2 Relative point of saturation

It has been shown in section 10.6.3 that using a lower operating flux density helps to reduce the possibility of high amplitude trapped charge oscillations persisting and reduces the amplitude and frequency of the superharmonic voltage oscillations. This method is expensive since it requires the use of more iron in the core to ensure that the operating point is far below the knee of the saturation curve.

10.8.1.3 Delta tertiary winding

A closed delta tertiary winding decreases the effective zero sequence impedance of the transformer and provides additional damping. As a result, a relatively fast decay of the trapped voltage oscillations generally occurs. Since present day transformers and auto-transformers are normally provided with delta tertiary windings required for other purposes, no additional expense is involved. The decrement in the ferro-oscillations could further be increased by connection of resistors in the delta tertiary windings. The effectiveness of this method cannot, however, be guaranteed since certain circuit conditions exist under which sustained steady-state ferro-oscillations are excited, as shown in section 10.7.3.

10.8.2 Operating Conditions

By far the most effective and the most economic method of aborting the ferro-oscillations is to isolate the transformer from the feeder immediately following the line dropping operation using switching isolators normally provided between the feeder and the transformer in the absence of circuit breakers. The switching isolators used must be capable of making or breaking the transformer magnetising currents which would follow load rejection. A rapid collapse of the voltage would follow as the arc drawn by the opening isolator contacts introduces additional damping.

10.9 Conclusion

Ferroresonance in double circuit feeders can occur under widely varying circuit constants, and contains several frequency modes depending on initial conditions, circuit impedances, transformer characteristics and energy transferred from the energised circuit. Once initiated, the trade-off between energy losses and energy supplied through the line coupling capacitances would dictate the duration of the oscillations.

The transformer zero sequence impedance is one of the most crucial factors influencing the character of the ferro-oscillations. The three- and five-limb transformers, which differ significantly in their zero sequence characteristics, yield waveforms which vary widely. The inherently low zero sequence impedance of the three-limb type tends to favour high amplitude trapped voltage oscillations of a relatively long duration which could, in certain cases, be sustained. On the other hand, the higher zero sequence impedance of the five-limb transformer tends to preclude prolonged high amplitude oscillations due in part to the increased effectiveness of the delta winding in damping the oscillations.

The delta tertiary winding furnishes damping and lowers the zero sequence impedance of the transformer by providing a low impedance path to the flow of zero sequence current. The circuit becomes, in general, less conducive to prolonged trapped charge oscillations, and the zero sequence component of voltage at the transformer is considerably reduced. Further reduction of the zero sequence impedance by decreasing the tertiary winding leakage impedance tends to intensify the ferro-oscillations by permitting increased transfer of energy from the energised line. The

mitigating effects of a closed delta winding could, however, be nullified when relatively short lengths of line terminate in a three-limb transformer.

The degree of imbalance inherent in the line electrostatic circuit, which depends largely on the line physical constants and dimensions, determines, in conjunction with the transformer zero sequence impedance, the energy transferred from the live circuit. A long line associated with a transformer with a low zero sequence impedance involves relatively large amount of energy oscillating between the line and the transformer. Consequently, the trapped charge voltage oscillations tend to be prolonged. The fully asymmetric zero sequence voltage produced by the line configuration with twin conductor construction provides a biasing effect on the saturation curve. The transformer is therefore more susceptible to severe saturation. This increases the probability of the trapped charge oscillations being prolonged.

The main effects of sustained ferroresonance are transformer overheating, communications interference and the possibility of large re-energisation transients being excited. The simplest and most economic method of minimising these effects is to isolate the transformer from its feeder by means of switching isolators normally provided, immediately following line dropping.

The results have demonstrated the potential usefulness of the method of analysis presented in Chapter 7. The waveforms obtained are similar in character to those obtained in practice. Discrepancies which may exist between the predicted and the actual system ferroresonant behaviour are attributable mainly to how closely the transformer model resembles the actual transformer it

simulates. In particular, accuracy would depend on the degree of correlation achieved between the saturation characteristics of the transformer and its model. Realistic data on these characteristics is not readily available. As a result, ideal characteristics for the material had to be used. The inability to corroborate the theoretical results with field tests relating to the system simulated arises also from lack of knowledge of the precise initial conditions prevailing immediately after the line is dropped. The validity of the model used has been established, however, by systematically assembling the model from sections which have separately been verified by comparison with known system behaviour. The model is unique in that it portrays the travelling wave phenomena in transmission lines as well as the electrical and magnetic interactions within the transformer.

C H A P T E R E L E V E N

CONCLUSIONS

This thesis is concerned mainly with transient resonance and ferroresonance phenomena initiated by certain switching operations in high voltage transformer-terminated feeders. An extensive survey of overvoltages generated in transmission lines is included in the introductory chapters as background material. In certain cases, these overvoltages may be accentuated due to resonance effects involving the inductive reactances of the transformer terminating the feeder and the capacitive reactances associated with lines, cables and the transformer. The ability to predict such resonance conditions is therefore of critical importance to the system planning engineer. This is particularly so at the higher transmission system voltages where economic dictates necessitate a reduction in both the overvoltage factor and the system insulation level.

The main emphasis of this research effort has been directed towards

(i) identification of circuit arrangements and operational conditions likely to produce resonant overvoltages;

(ii) application of appropriate and sufficiently accurate methods to analyse the behaviour of the network over a wide range of realistic system constants;

(iii) derivation of simple mathematical expressions for predicting potentially onerous overvoltage conditions; and

(iv) determination of measures effective in suppressing the overvoltages or protecting system equipment from their effects.

Although the oscillations relating to a ferroresonant condition are usually not severe in terms of voltage magnitudes, they do have adverse effects on neighbouring communication circuits and on the transformer in respect of excessive heat and noise generation as well as insulation degeneration. A prediction of this phenomenon is not possible due to the multiplicity of factors on which it depends and the wide range of system constants under which it can occur.

This thesis can be resolved into the following three distinct categories :

(i) methods of analysis;

(ii) resonance phenomena; and

(iii) ferroresonance phenomena.

Most of the available mathematical methods of analysing transients were found inadequate when applied to transformer-feeder circuits. These circuits consist of elements with distributed and lumped constants, including non-linear saturation properties. Although high accuracy can be achieved if these methods are applied separately to either the lumped or distributed parameter elements, a significant reduction in accuracy results when the transformer feeder is considered as a unit. In such a case, the need for an efficient method capable of high accuracy in respect of both the transformer and the feeder has been met by the proposed compensation method. The method utilises the compensation theorem to permit the application of an established, simple and fast lattice diagram technique to distributed-parameter sub-networks, and the use of a method best suited for solution of complex and non-linear lumped-parameter sections.

A comprehensive model of the terminating network has been presented. In this model, the equations describing the transformer electrical characteristics are compounded with the equations representing the magnetic interactions within a geometrically composite core. The non-linear saturation properties are simulated by an exponential series truncated at the fourth term. This representation is sufficiently accurate in respect of both the flux density and differential permeability over the practical operating range of field strength. The resultant non-linear differential equations are solved by a step-by-step Runge-Kutta numerical integration technique, using an efficient inversion routine suitable for ill-conditioned matrices.

Linear resonance phenomena in single circuit feeders arises from resonant excitation of the terminating circuit by line oscillations set up when the composite feeder is energised as a unit. Near coincidence of the natural frequencies relating to the feeder (or its odd harmonic) and the terminating network produces excessive voltage oscillations at the transformer secondary. The effects of a wide range of system constants on the magnitudes of these overvoltages have been investigated using analogue and digital computer models of the system on a single-phase basis. A study of three-phase effects revealed that sequential closure of the circuit breaker poles and associated mutual interactions within the transformer could further exacerbate these overvoltages. The effects of two transformers terminating the feeder have also been considered together with the attributes of an interconnected network which are likely to influence the magnitude and frequency of the oscillations exciting the termination. These factors include the characteristics of the

source network from which the feeder is energised, the relative arrangement of mixed line and cable feeder sections and the topological layout of lines connected to the feeder. Analysis of the frequency spectrum of the open-circuit line oscillations has been found to provide sufficient information from which a resonance condition may be predicted.

Linear resonance can also be excited in a reactively compensated circuit of a double circuit arrangement. This occurs when the compensated circuit is isolated from the system while the other circuit remains energised and acts as a source of induced voltages. For certain constants of the line, transformer and reactor connected to its tertiary terminals, power frequency oscillations could build up to excessive levels. Analytical relations for determining the lengths of feeder likely to produce this condition have been derived.

The problem of ferroresonance has for many decades been subjected to a close scrutiny. This phenomenon has many and varied manifestations. A particular facet which has only recently come to light is that associated with ferro-oscillations in a transformer terminating a double-circuit feeder. The switching sequence leading to these oscillations is similar to that producing the linear resonance conditions referred to above. This aspect of the problem has been investigated by applying the compensation method described to the detailed system model.

The study is confined mainly to transformers of a geometrically composite core structure incorporating delta tertiary windings. An attempt has been made to identify those constants of the system which have a significant influence on the character of the

transient ferro-oscillations. In this respect, the transformer zero sequence impedance, which largely depends on the core geometry and winding connections, constitutes a dominant factor. Although a closed delta winding negates the development of sustained ferro-oscillations, there are certain circuit constants which could lead to prolonged and essentially linear system frequency oscillations of relatively large amplitude. Short lengths of feeder are found to be prone to such a phenomenon involving only moderate saturation of the transformer core.

The ferroresonance voltage waveforms are characterised by three distinct frequency components. These are :

(i) high amplitude trapped charge oscillations;

(ii) subharmonic oscillations of decreasing amplitude; and

(iii) superharmonic oscillations which are zero sequence quantities.

In most cases, these oscillations decay with a decrement depending on the excess of system losses over the energy supplied from the live circuit. The latter depends on the physical constants and dimensions of the double-circuit line. If, however, the transformer normally operates close to the knee of the saturation curve, or if excessive voltages are initially trapped in the electrostatic field of the line, the resultant ferro-oscillations may be intensified in respect of both amplitude and duration. The most effective and economical means of suppression is to isolate the transformer from the feeder immediately following dropping the composite feeder unit from the system. This may be effected by means of switching isolators normally provided on the transformer high voltage side.

Although an attempt has been made where possible to generalise the results in such a manner that they are applicable to most practical systems, certain networks with peculiarities not

considered in this thesis may, however, require an individual study. The mathematical method of analysis presented, although limited to certain transformer-feeder arrangements, may be extended to cope with any network configuration. Such a general purpose method could incorporate facilities which would permit simulation of the following system aspects :

(i) more than one transformer at the same or at different locations;

(ii) transformers comprising a bank of three single-phase units;

(iii) transformers with a delta primary or secondary winding;

(iv) multi-valued core saturation characteristics;

(v) transmission line frequency-dependent parameters; and

(vi) appropriate initial conditions relating to residual flux in the core and voltage trapped in the line electro-static field.

It should be noted, however, that an accurate simulation incorporating most of these factors relies to a great extent on the availability of appropriate and accurate system data. Any effort to extend the analysis in this direction should therefore be made consistent with data availability.

Although confidence in the validity of the mathematical method has largely been established by a systematic validation of the various components which make up the method, and by comparison with a limited amount of field results, there is clearly a need to obtain extensive field test data relating to the phenomena studied, so that a conclusive corroboration may be made.

C H A P T E R 1 2

APPENDICES

12.1 Transient Overvoltages at Resonance

The square wave voltage appearing at the end of the feeder remote from the circuit breaker when the feeder is energised from an infinite source, may be synthesised by the sum of a series of Heaviside functions,

$$H\,(t - nT) \quad \text{for } t \geqslant nT$$

where T is the travel time of the line and n = 0, 1, 2, 3, ...

This function, H(t - nT) is equal to H(t) delayed by a time nT. It therefore takes account of the delay due to the wave travelling the length of the line. If the apparent surge impedance of the termination is assumed infinite and losses are neglected, the receiving end voltage may be represented by

$$V_R(t) = 2E \cdot \Big[H(t-T) - H(t-3T) + H(t-5T) + ... + (-1)^{m+1} \cdot H(t-mT) + ... \Big] \qquad 12.1$$

where E = step voltage applied.

In effect, the square wave voltage has been resolved into an infinite number of positive and negative step functions displaced from one another in time of origin.

Written concisely,

$$V_R(t) = 2\,E \cdot \sum_{n=1}^{\infty} \Big\{ H\big[t-(2n-1)T\big] \Big\} \cdot (-1)^{n+1} \qquad 12.2$$

where $t \geqslant (2n-1)T$ always.

Heaviside Shifting Theorem relates to the Laplace Transformation of functions delayed by time τ, and is given symbolically as follows :

$$\text{If } \mathcal{L}\left[H(t)\right] = \int_0^\infty \exp(-pt).H(t)dt = f(p)$$

$$\text{then } \mathcal{L}\left[H(t-\tau)\right] = \exp(-p\tau).\ f(p)$$

where $p = \frac{d}{dt}$.

The term by term Laplace transform of the voltage expression (12.2) is then given by

$$V_R(p) = \frac{2E}{p} \cdot \sum_{n=1}^{\infty} \left[\exp(1-2n)pT\right] \cdot (-1)^{n+1} \qquad 12.3$$

Using Thevenin's Theorem, an equivalent circuit of the network may be formed. It will consist of a generator, having an internal voltage given by equation 12.3 and an internal impedance Z, representing the line surge impedance (Z_L), applied to the terminating series Land C circuit. It will be appreciated that the resulting equivalent circuit is an approximation. It is implicit in this circuit that energy will be expended in a resistance of the same value as the surge impedance of the line. In practice, this is not the case. The energy apparently dissipated is in fact embodied in the surges oscillating along the line. This energy is comparatively small, however, because of the relatively high surge impedance of the transformer. Moreover, the error introduced is, to a large extent, counterbalanced by the error due to neglecting system losses.

Solution of the equivalent circuit for the secondary voltage of the transformer gives

$$V_C(p) = \frac{1/pC}{pL + 1/pC + Z_L} \cdot \frac{2E}{p} \cdot \sum_{n=1}^{\infty} \left[\exp(1-2n)pT\right] \cdot (-1)^{n+1}$$

where L is the transformer leakage inductance, and C, the equivalent secondary capacitance, referred to the primary side.

$$V_C(p) = \frac{1}{LC\left[(p + \frac{Z_L}{2L})^2 + (\frac{1}{\sqrt{LC}} - \frac{Z_L^2}{4L})^2\right]} \cdot \frac{2E}{p} \cdot \sum_{n=1}^{\infty} \left[e^{-(2n-1)pT}\right] \cdot (-1)^{n+1}$$

Consideration of normal practical constants shows that

$$1/LC \gg Z_L^2/4L^2$$

i.e. if $Z_L/2L = \alpha$ and $1/\sqrt{LC} = \omega_T$, then $\omega_T^2 \gg \alpha^2$

$$\therefore V_C(p) = \frac{\omega_T^2}{(p + \alpha)^2 + \omega_T^2} \cdot \frac{2E}{p} \cdot \sum_{n=1}^{\infty} \left[\exp(1-2n)pT\right] \cdot (-1)^{n+1} \quad 12.4$$

To obtain the actual secondary voltage, a term by term inverse transform is applied to the expression given by 12.4.

$$\text{i.e. } V_C(t) = 2E\omega_T^2 \cdot \sum_{n=1}^{\infty} \left[K + A \exp\left\{-\alpha\left[t-(2n-1)T\right]\right\} \cdot \sin\left\{ \omega_L \left[t-(2n-1)T\right] + \phi \right\}\right]$$

$$\cdot H\left[t - (2n-1)T\right] \cdot (-1)^{n+1} \quad 12.5$$

where $A = 1/(\omega_T\sqrt{\omega_r^2 + \alpha^2})$,

$K = 1/(\alpha^2 + \omega_T^2)$,

and $\phi = -\tan^{-1}(-\omega_T/\alpha)$

But by assumption

$$\omega_T^2 \gg \alpha^2$$

$$\left.\begin{aligned} \therefore A &= 1/\omega_T^2 = K \\ \text{and } \phi &= -\frac{\pi}{2} \end{aligned}\right\} \quad 12.6$$

approximately.

Substituting the relation

$$\sin\left\{\omega_T\left[t-(2n-1)T\right] - \frac{\pi}{2}\right\} = -\cos\omega_T\left[t-(2n-1)T\right]$$

and equations 12.6 in 12.5.

$$V_C(t) = 2E \cdot \sum_{n=1}^{\infty} \left[1 - \exp\left\{ -\alpha\left[t-(2n-1)T\right]\right\}\cos\ \omega_T\left[t - (2n-1)T\right]\right]$$

$$\cdot\ H\left[t - (2n-1)T\right] \cdot (-1)^{n+1} \qquad 12.7$$

When a resonance condition exists, the natural frequency of the line given by $f_L = 1/4T$, equals the natural frequency of the oscillatory circuit.

$$\therefore\ \omega_T = \pi/2T$$

Substituting for ω_T in 12.7

$$V_C(t) = 2E. \sum_{n=1}^{\infty} \left[1 - \exp\left\{ -\alpha\left[t-(2n-1)T\right]\right\}\cos\ \frac{\pi}{2T}\left\{ t-(2n-1)T\right\}\right]$$

$$.\ H\left[t - (2n-1)\ T\right] .\ (-1)^{n+1} \qquad 12.8$$

By equating the derived series of equation 12.8 to zero, the times at which the voltage peaks occur may be found. Thus the mth peak will occur when the following relation holds :

$$\sum_{n=1}^{m} \tan\ \frac{\pi}{2T}\left[t - (2n-1)T\right] \cdot (-1)^{n+1} = \frac{-\alpha}{\omega_T} \qquad 12.9$$

where $t \gg (2n-1)T \quad (n = 1, 2, 3....)$

Since $\omega_T \gg \alpha$, each term of the series given by 12.9 must be identically zero. Hence the time at the mth peak is

$$t = (2m + 1)\ T \qquad 12.10$$

(since at t = T, the voltage is zero).

From 12.8 and 12.10, the mth voltage peak is derived as

$$\hat{V}_m = 2 \cdot \sum_{n=1}^{m+1} \left[1 - (-k)^{m-n+1}\right] \cdot (-1)^{n+1} \qquad 12.11$$

where $k = \exp(-2\ \alpha\ T)$

and E = 1 p.u.

i.e. $$\hat{V}_1 = 2\ (1 + k)$$

$$\hat{V}_2 = -2\ (k + k^2)$$

$$\hat{V}_3 = 2\ (1 + k + k^2 + k^3)$$

$$\hat{V}_4 = -2\ (k + k^2 + k^3 + k^4)$$

Since the value of k is always less than 1, the geometric series contained on the r.h.s. of the above equations will converge with a sum given by :

$$\left.\begin{aligned} \hat{V}_m &= 2\ \left(\frac{1 - k^{m+1}}{1 - k}\right) \text{ if m is odd and } k \neq 1 \\ &= -2\ \left(\frac{k - k^{m+1}}{1 - k}\right) \text{ if m is even and } k \neq 1 \end{aligned}\right\} \quad 12.12$$

Equation 12.12 shows that, at resonance, the successive peaks of the secondary oscillation depend on the value of k where

$$k = \exp\ (-Z_L T/L) = \exp\ (-Z_L/Z_T .\ \pi/2) \qquad 12.13$$

where $Z_T = \sqrt{L/C}$ is the apparent surge impedance of the transformer.

The above expressions for k demonstrate that, at resonance, the rate of increase in and the value of the magnitudes of successive voltage peaks is related to system parameter values.

12.2 Formulation of transformer state equations

12.2.1 Transformer voltage equations

The voltage equations describing the electrical characteristics of each winding of a five-limb three-winding transformer are an extension of the equations 4.3 and 4.4 of Chapter 4. Using the same symbols described in section 4.2.2, and the diagram shown on Fig. 7.2 (ii), the equations may be written as follows :

$$V_A = R_A i_A + L_A p i_A + M_1 p i_1 \qquad 12.15$$

$$V_B = R_B i_B + L_B p i_B + M_2 p i_2 \qquad 12.16$$

$$V_C = R_C i_C + L_C p i_C + M_3 p i_3 \qquad 12.17$$

$$V_a = R_a i_a + L_a p i_a + M_1 p i_1 \qquad 12.18$$

$$V_b = R_b i_b + L_b p i_b + M_2 p i_2 \qquad 12.19$$

$$V_c = R_c i_c + L_c p i_c + M_3 p i_3 \qquad 12.20$$

$$V_\alpha = R_\alpha i_\alpha + L_\alpha p i_\alpha + M_1 p i_1 \qquad 12.21$$

$$V_\beta = R_\beta i_\beta + L_\beta p i_\beta + M_2 p i_2 \qquad 12.22$$

$$V_\gamma = R_\gamma i_\gamma + L_\gamma p i_\gamma + M_3 p i_3 \qquad 12.23$$

where subscripts A, B, C relate to the primary winding turns, a, b, c to the secondary, and α, β, γ to the tertiary. The inductances M_1, M_2 and M_3 are defined by the corresponding flux paths shown on Fig. 7.2 (ii). The equations relate to a star/star/delta transformer with the primary neutral earthed and provide for secondary winding loading.

12.2.2 Magnetic circuit equations

The magnetic circuit equations, obtained by applying the magnetic circuit law $\Sigma \phi = 0$ at the junctions between the three winding limbs and the yoke, are as follows :

$$0 = \phi_1 - \phi_4 - \phi_6 - \phi_9 \qquad 12.24$$

$$0 = \phi_2 - \phi_5 - \phi_7 - \phi_{10} \qquad 12.25$$

$$0 = \phi_3 + \phi_4 + \phi_5 - \phi_8 \qquad 12.26$$

By substituting $\phi = \mu HA$

$$= \mu \frac{NIA}{\ell}$$

multiplying equations 12.24, 12.25 and 12.26 by N and differentiating, these magnetic circuit equations may be written as :

$$0 = M_1 pi_1 - M_4 pi_4 - M_6 pi_6 - M_9 pi_9 \qquad 12.27$$

$$0 = M_2 pi_2 - M_5 pi_5 - M_7 pi_7 - M_{10} pi_{10} \qquad 12.28$$

$$0 = M_3 pi_3 + M_4 pi_4 + M_5 pi_5 - M_8 pi_8 \qquad 12.29$$

where $M = \frac{N^2 A \mu}{\ell}$ is expressed in dimensions of inductance. Since there are 19 unknown currents and only 12 voltage and magnetic circuit equations, a further 7 equations are required. These equations are obtained by application of the magnetic circuit law

$$N I = \oint H.dl \qquad 12.30$$

to any 7 flux path loops as follows :

$$i_1 = i_A + i_a + i_\alpha - i_6 \qquad 12.31$$

$$i_2 = i_B + i_b + i_\beta - i_7 \qquad 12.32$$

$$i_3 = i_C + i_c + i_\gamma - i_8 \qquad 12.33$$

$$i_4 = i_6 - i_8 \qquad 12.34$$

$$i_5 = i_7 - i_8 \qquad 12.35$$

$$i_9 = i_6 \qquad 12.36$$

$$i_{10} = i_7 \qquad 12.37$$

The voltages V_A, V_B and V_C are excitation voltages, and the secondary load voltages, V_a, V_b and V_c are expressed by the

product of corresponding currents and load impedances as explained in section 4.2.2. In the case of unloaded delta tertiary winding, the tertiary voltage equations expressed by 12.21, 12.22 and 12.23 may be combined by summation into a single equation as follows :

$$-i_d(R_\alpha + R_\beta + R_\gamma) = (L_\alpha + L_\beta + L_\gamma)\, pi_d + M_1 pi_1 + M_2 pi_2 + M_3 pi_3 \quad 12.38$$

Substituting equations 12.31 to 12.37 into the voltage and magnetic circuit equations, the matrix equations shown on Table 12.1 results.

Table 12.1 : Transformer state equations

$V_A - i_A R_A$	$L_A + M_1$			$-M_1$			M_1			M_1		pi_A
$V_B - i_B R_B$		$L_B + M_2$			$-M_2$			M_2		M_2		pi_B
$V_C - i_C R_C$			$L_C + M_3$			$-M_3$			M_3	M_3		pi_C
0	$-M_1$			$M_1 + M_4 + M_6 + M_9$		$-M_4$	$-M_1$			$-M_1$		pi_6
0		$-M_2$			$M_2 + M_5 + M_7 + M_{10}$	$-M_5$		$-M_2$		$-M_2$		pi_7
0			$-M_3$	$-M_4$	$-M_5$	$M_3 + M_4 + M_5 + M_8$			$-M_3$	$-M_3$		pi_8
$V_a - i_a R_a$	M_1			$-M_1$			$L_a + M_1$			M_1		pi_a
$V_b - i_b R_b$		M_2			$-M_2$			$L_b + M_2$		M_2		pi_b
$V_c - i_c R_c$			M_3			$-M_3$			$L_c + M_3$	M_3		pi_c
$-i_d (R_\alpha + R_\beta + R_\gamma)$	M_1	M_2	M_3	$-M_1$	$-M_2$	$-M_3$	M_1	M_2	M_3	$M_1 + M_2 + M_3 + L_\alpha + L_\beta + L_\gamma$		pi_d

12.3 Transformer phase leakage inductance

The magnetic phase leakage flux paths (ϕ_6, ϕ_7 and ϕ_8 on Fig. 7.2(ii)) are mainly in air, and the associated inductances are essentially constant. By definition, the phase leakage inductance associated with ϕ_6 for example is given by

$$M_6 = N^2 A_6 \mu_o / \ell_6 \qquad 12.39$$

where A_6 and ℓ_6 are the effective area and length of the phase leakage flux paths, N the number of turns and μ_o, the permeability of free space. Since the dimensions, A_6 and ℓ_6, are not clearly defined, it is necessary to translate these quantities into measurable ones, using the reluctance of the phase leakage path given by

$$\overline{R}_6 = \frac{\ell_6}{\mu_o A_6}$$

$$= \frac{\ell_6 H_6}{\phi_6} \qquad 12.40$$

(using $B_6 = \phi_6 \quad A_6 = \mu_o H_6$)

Applying the magnetic circuit law $NI = \oint H.d\ell$ around the closed loop denoted by flux paths ϕ_1 and ϕ_6 (see Fig. 7.2 (ii)), the following relation for an unloaded transformer is obtained :

$$N(i_A + i_d) = H_1 \ell_1 + H_6 \ell_6 \qquad 12.41$$

where i_A and i_d are the primary and delta tertiary winding currents, respectively. During the studies reported in reference 56, it was found that, normally $H_6 \ell_6 \gg H_1 \ell_1$

Hence

$$\overline{R}_6 = \frac{N (i_A + i_d)}{\phi_6}$$

and $$M_6 = \frac{N^2}{\overline{R}_6} = \frac{N\phi_6}{i_A + i_d} \qquad 12.42$$

In equation 12.42, the phase leakage inductance has been expressed in

terms of measurable quantities. Similarly,

$$M_7 = \frac{N\phi_7}{i_B + i_d}$$

$$\text{and } M_8 = \frac{N\phi_8}{i_C + i_d}$$

R E F E R E N C E S

1. Glavitsch, J. : 'Power frequency overvoltages in e.h.v. systems', Brown Boveri Review, Vol. 51, No. 1/2, 1964, pp. 21-32.

2. Peterson, H.A. : 'Transients in power systems', John Wiley and Sons, New York, 1951.

3. Hauspurg, A., Vassell, G.S., Stillman, G.I., Charkow, J.H., and Haahr, J.C. : 'Overvoltages on the AEP 765 kV system', IEEE Trans., Vol. PAS-88, No. 9, pp. 1329-1342.

4. Thanawala, H.L., and Young, D.J. : 'Saturated reactors - some recent applications in power systems', Energy International, Vol. 7, No. 11, Nov. 1970.

5. 'Insulation coordination', International Electrochemical Commission, Publication 71-1, 1976.

6. 'Specification for surge diverters for alternating current power circuits', B.S. 2914 : 1972.

7. Kimbark, E.W. and Legale, A.C. : 'Fault surge versus switching surge - a study of transient voltages caused by line to ground faults', IEEE Trans., Vol. PAS-87, No. 8, Sept. 1968, pp. 1762-1769.

8. Clerici, A. and Taschini, A. : 'Overvoltages due to line energisation versus overvoltages caused by faults and fault clearing', IEEE Trans., Vol. PAS-89, No. 5/6, May/June 1970, pp. 932-941.

9. Bickford, J.P. and El-Dewieny, R.M.K. : 'Energisation of transmission lines from inductive sources', Proc. IEE, Vol. 120, No. 8, Aug. 1973, pp. 883-889.

10. Bickford, J.P. and El-Dewieny, R.M.K. : 'Energisation of transmission lines from mixed sources', Proc. IEE, Vol. 121, No. 5, May 1974, pp. 355-359.

11. Bickford, J.P. : 'Composite feeder switching', Symposium on power system overvoltages, 1974, University of Manchester Institute of Science and Technology, Manchester, England.

12. Bolton, E., Ehrenberg, A.C., Hamilton, F.L., Hawkins, A.G., Matravers, F.P. and Thomas, J.A. : 'British investigation of short-line fault phenomena', CIGRE, Paris, Reports 109, 109(a), 1964.

13. Flugum, R.W., Kalb, J.W. : 'Operation of surge arresters on low surge impedance circuits', IEEE paper, T74-198-8. Winter Power Meeting, Jan. 30, 1974.

14. Maury, E. : 'Synchronous closing of 525 and 765 kV circuit breakers', CIGRE 1966, Report No. 143.

15. AIEE Committee Report : 'Switching surges, I-phase-to-ground voltages', AIEE Trans., Vol. 80, 1961, pp. 240-256.

16. Barthold, L.O., Johnson, I.B. and Schultz, A.I. : 'Overvoltages following secondary switching of transformers connected to high-voltage lines', AIEE Trans., Vol. 77, pt. III, 1958, pp. 1492-1501.

17. Rudenberg, R. : 'Transient performance of electric power systems', McGraw-Hill, New York, 1950.

18. McElroy, A.G., Price, W.C., Smith, H.M. and Shankle, D.F., : 'Field measurements of switching surges as modified by unloaded 345 kV transformers', IEEE Trans., Vol. PAS-82, Aug. 1963, pp. 500-520.

19. Shankle, D.F. and Taylor, E.R. : 'Transmission line switching surges as modified by transformer impedances and arrester operation', AIEE Trans., Vol. 77, pt. III, 1958, pp. 1596-1604.

20. Johnson, I.B. and Schultz, A.J. : 'Switching surges on energising a transformer-terminated line', AIEE Trans., Vol. 79, pt. III, June 1960, pp. 241-245.

21. Wilson, D.D. : 'Phase-phase switching surges on 500 kV transformer-terminated lines, Part I : 500 kV circuit-breaker operation', IEEE Trans., Vol. PAS-89, No. 5/6, May/June, 1970, pp. 685-690.

22. Johnson, I.B., Silva, R.F. and Wilson, D.D. : 'Phase-to-phase switching surges on line energisation (transformer terminated)', AIEE Trans., Vol. 81, pt. III, 1962.

23. White, E.L. : 'Switching surges on a 275/132 kV auto-transformer', Electrical Research Association, S/T 111, 1961.

24. Czuros, L., Foreman, K.F. and Glavitsch, H. : 'Energisation over-voltages on transformer feeders', Electra No. 18, July 1971, pp. 83-105.

25. Czuros, L., and Foreman, K.F. : 'Energisation overvoltages on transformer feeder circuits', Electrical Times, 31st August 1972, pp. 37-40.

26. Toland, H. : '132 kV transformer feeder overvoltages', S.S.E.B. Report No. RD 26/69, 1969.

27. Toland, H. : 'Investigation into a transformer rod-gap flashover at Wishaw', S.S.E.B. Report No. RD 28/69, 1969.

28. Heaton, A.G. and Reid, I.A. : 'Transient overvoltages and power line terminations', IEE Proc., Vol. 113, No. 3, 1966, pp. 461-470.

29. Hopkinson, R.H. : 'Ferroresonant overvoltage control based on TNA tests on three-phase delta-wye transformer banks', IEEE Trans., Vol. PAS-86, No. 10, Oct. 1967, pp. 1258-1263.

30. Hopkinson, R.H. : 'Ferroresonant overvoltage control based on TNA tests on three-phase wye-delta transformer banks', IEEE Trans., Vol. PAS-87, No. 2, Feb. 1968, pp. 352-361.

31. Clarke, E., Peterson, H.A. and Light, P.H. : 'Abnormal voltage conditions in three-phase systems produced by single-phase switching', AIEE Trans., Vol. 60, 1941, pp. 329-339.

32. Young, F.S., Schmid, R.L. and Fergestad, P.I. : 'A laboratory investigation of ferro-resonance in cable-connected transformers', IEEE Trans., Vol. PAS-87, No. 5, May 1968, pp. 1240-1248.

33. Swift, G.W. : 'An analytical approach to ferroresonance', IEEE Trans., Vol. PAS-88, No. 1, Jan. 1969, pp. 42-46.

34. Pickett, M.J., Manning, H.L. and Van Geem, H.N. : 'Near resonant coupling on ehv circuits : I - Field Investigations', IEEE Trans., Vol. PAS-87, No. 2, Feb. 1968, pp. 322-325.

35. Hesse, M.H. and Wilson, D.D. : 'Near resonant coupling on ehv circuits : II - Methods of analysis', IEEE Trans., Vol. PAS-87, No. 2, Feb. 1968, pp. 326-334.

36. Chaston, A.N. : 'Ehv ac parallel transmission line calculations with application to the near resonance problem', IEEE Trans., Vol. PAS-88, No. 5, May 1969, pp. 627-635.

37. Welle, D.H., Hedin, R.A., Burkhard, L.A., Thomas, C.H., Kilgour, A.E. and Lund, W.R. : 'Parallel ehv untransposed transmission lines studied for overvoltages due to switching surges and resonance', IEEE Trans., Vol. PAS-91, Jan/Feb. 1972, pp. 190-194.

38. Dolan, E.J. and Kimbark, E.W. : 'Ferroresonance in a transformer switched with ehv line', IEEE Trans., Vol. PAS-91, No. 3, May/June, 1972, pp. 1273-1280.

39. Wale, G.D. : 'Ferroresonance in a disconnected ehv power system', GEC Journal of Science and Technology, Vol. 40, No. 2, 1973, pp. 79-86.

40. Thomas, C.H. and Hedin, R.A. : 'Switching surges on transmission lines studied by differential analyser simulation', IEEE Trans., Vol. PAS-88, No. 5, May 1969, pp. 636-645.

41. Pender, J.T. : 'A combined steady-state and transient a.c. network analyser', Internation Journal of Electrical Engineering Education, Vol. 6, 1968, pp. 353-361.

42. Abetti, P.A. : 'Transformer models for the determination of transient voltages', AIEE Trans., June 1963, pp. 468-480.

43. Moss, D.W. : 'Transient analyser', Associated Electrical Industries Report No. TPE20, 614/1, 1970.

44. Battison, M.J., Day, S.J., Mulliineux, N., Parton, K.C. and Reed, J.R. : 'Calculation of switching phenomena in power systems', Proc. IEE, Vol. 114, No. 4, 1967, pp. 478-486.

45. Bickford, J.P., Mullineux, N. and Reed, J.R. : 'Computation of power system transients', IEE Monograph Series 18, Peter Peregrinus Ltd., England 1976.

46. Uram, R. and Miller, R.W. : 'Mathematical analysis and solution of transmission - line transients I - Theory', Trans., IEEE, Vol. PAS-83, Nov. 1964, pp. 1116-1123.

47. Frey, W. and Althammer, P. : 'The calculation of electromagnetic transients on lines by means of a digital computer', Brown Boveri Review, Vol. 48, No. 5/6, May/June, 1961, pp. 344-355.

48. Dommel, H.W. : 'Digital computer solution of electromagnetic transients in single- and multiphase networks', Trans., IEEE, Vol. PAS-88, No. 4, April 1969, pp. 388-399.

49. Bewley, L.V. : 'Travelling waves on transmission systems', Dover, New York, 1963.

50. Bickford, J.P. and Doepel, P.S. : 'Calculation of switching transients with particular reference to line energisation', Proc. IEE, Vol. 114, No. 4, April 1967, pp. 465-477.

51. Barthold, L.O. and Carter, G.K. : 'Digital travelling wave solutions', Trans., AIEE, Vol. 80, Part III, 1961, pp. 812-820.

52. McElroy, A.J. and Porter, R.M. : 'Digital computer calculation of transients in electric networks', Trans. IEEE, Vol. PAS-82, 1963, pp. 88-96.

53. Wedepohl, L.M. : 'Application of matrix methods to the solution of travelling wave phenomena in polyphase systems', Proc. IEE, Vol. 110, No. 12, 1963, pp. 2200-2212.

54. Hedman, D.E. and Mountford, J.D. : 'Travelling wave terminal simulation by equivalent circuit', Trans. IEEE, Vol. PAS-90, Nov/Dec. 1971, pp. 2451-2459.

55. Tinney, W.F. : 'Compensation methods for network solutions by triangular factorisation', Proc. Power Industry Computer Applications Conference, Boston, Mass. May 24-26, 1971.

56. Macfadyen, W.K., Simpson, R.R.S., Slater, R.D. and Wood, W.S., : 'Method of predicting transient-current patterns in transformers', Proc. IEE, Vol. 120, No. 11, Nov. 1973, pp. 1393-1396.

57. Rudenberg, R. : 'Electrical shock waves in power system', Howard University Press, 1968.

58. Christoffel, M. : 'The effect of power cables on over-voltages in high and medium-voltage transmission system', Brown Boveri Review, Vol. 51, No. 6, June, 1964, pp. 31-38.

59. Macfadyen, W.K., Simpson, R.R.S., Slater, R.D. and Wood, W.S. : 'Representation of magnetisation curves by exponential series', Proc. IEE, Vol. 120, No. 8, August 1973, pp. 902-904.

60. Brameller, A., John, M.N. and Scott, M.R. : 'Practical diakoptics for electrical networks', Chapman and Hall Ltd., London, 1969.

61. Galloway, R.H., Shorrocks, W.B. and Wedepohl, L.M. : 'Calculation of electrical parameters for short and long polyphase transmission lines', Proc. IEE, Vol. III, No. 12, Dec. 1964, pp. 2051-2059.

62. Clarke, E. : 'Circuit analysis of a-c power systems, Vol. I - Symmetrical and related components', John Wiley and Sons, New York, 1943.

63. Rudenberg, R. : 'Non-harmonic oscillations as caused by magnetic saturation', AIEE Trans., Vol. 68, 1949, pp. 676-685.

64. Hayashi, C. : 'Nonlinear oscillations in physical systems', McGraw-Hill, New York, 1964.

65. Wright, I.A. and Morsztyn, K. : 'Subharmonic oscillations in power systems - Theory and practice', Trans., IEEE, Vol. PAS-89, No. 8, Nov/Dec. 1970, pp. 1805-1815.

66. Wright, I.A. : 'Three-phase subharmonic oscillations in symmetrical power systems', Trans., IEEE, Vol. PAS-90, No. 3, May/June, 1971, pp. 1295-1304.

67. Teape, J.W., Slater, R.D., Simpson, R.R.S. and Wood, W.S. : 'Hysteresis effects in transformers, including ferro-resonance', Proc. IEE, Vol. 123, No. 2, Feb. 1976, pp. 153-158.

68. Garin, A.N. : 'Zero-phase-sequence characteristics of transformers', Part I, General Electric Review, Vol. 43, No.3, March 1940, pp. 131-136.

69. Garin, A.N. : 'Zero-phase-sequence characteristics of transformers', Part II, General Electric Review, Vol. 43, No.4, April 1940, pp. 174-177.